METHODS IN MOLECULAR MEDICINE™

Angiotensin Protocols

Edited by

Donna H. Wang

Humana Press

1

Historical Perspective of the Renin–Angiotensin System

John E. Hall

> "To understand a science it is necessary to know its history."
>
> Auguste Comte, 1798–1857

The renin–angiotensin system (RAS) is now recognized as the body's most powerful hormone system for controlling sodium balance, body fluid volumes, and arterial pressure. It is mainly for this reason that researchers continue to be fascinated with this system more than 100 years after its discovery. With the development of drugs that effectively block different components of the RAS, the therapeutic advantages of inhibiting this system in hypertension, heart failure, diabetes, and other pathophysiological states have become apparent. Yet, as our knowledge of the physiology and molecular biology of this system continues to accelerate, it is also obvious that there is still much to learn and that many talented scientists will continue to devote their careers to understanding how the RAS functions in health and disease.

This brief review summarizes a few of the many milestones that have paved the way for our current understanding of the RAS. I have focused mainly on discoveries during the first 80 years and have not attempted to review the explosion of molecular biology literature during the past several years; much of this information can be found in other chapters of this volume. Other historical perspectives of the RAS are presented in several excellent reviews ***(1–7)***.

1. Tigerstedt's Discovery of Renin

The birth of research on the RAS was in 1898 when Finnish physiologist Robert Tigerstedt of the Karolinska Institute in Stockholm and his student Per Gunnar Bergman published a landmark paper ***(8)*** entitled "Niere Uud Kreislauf" ("Kidney and Circulation") in *Skandinavisches Archiev für Physiologie*. Their

From: *Methods in Molecular Medicine, vol. 51: Angiotensin Protocols*
Edited by: D. H. Wang © Humana Press Inc., Totowa, NJ

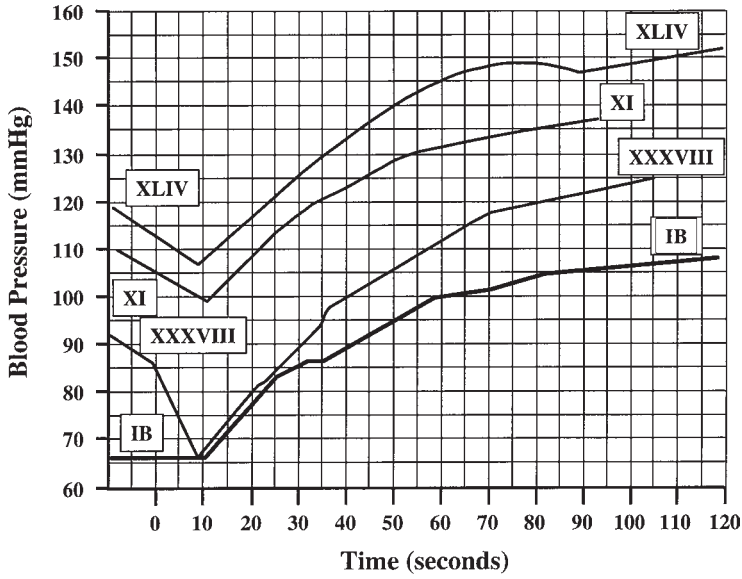

Fig. 1. Tigerstedt and Bergman's experiments demonstrating a pressor effect of crude saline extracts injected into four rabbits. Notice that the blood pressure response was biphasic, with a short-lived decrease and then an increase in blood pressure that was maximal at about two minutes. (Redrawn from data in **ref. *8***.)

meticulous experiments documented the long-lasting pressor effects of renal cortex extracts and they named the substance *renin* (**Fig. 1**). Extracts of the renal medulla did not contain the active substance and transection of the spinal cord to remove the effects of sympathetic activation did not influence the pressor effects of renal extract injections, leading them to conclude that the blood pressure effects of renin depended upon stimulation of "peripheral vascular centres." Tigerstedt further speculated that increased renin production might be important for the cardiac hypertrophy often observed in kidney diseases.

It is not entirely clear why Tigerstedt decided to study the blood pressure effects of renal extracts, although work by Richard Bright in the 1830s pointed out the potential importance of renal disease as a cause of hypertension. Tigerstedt may also have been influenced by the French physiologist Brown-Sequard's discovery of an adrenal hormone that stimulated the search for new hormones in research centers throughout the world. According to Mattias Aurell ***(4)***, another factor that may have led Tigerstedt to perform these experiments is that he "needed a paper" to present at the International Congress of Medicine in Moscow, Russia during summer 1897. This may explain why all 50 experiments described in Tigerstedt's landmark paper were conducted

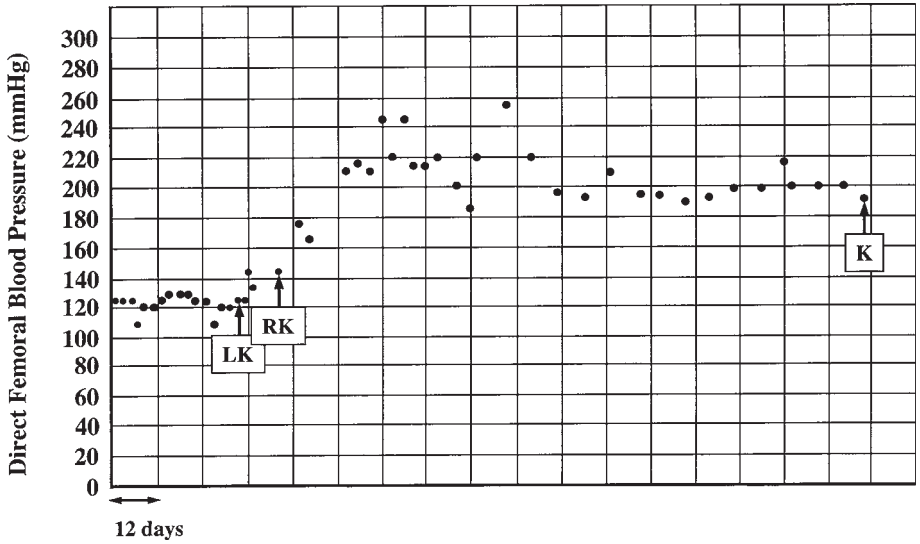

Fig. 2. Goldblatt's experiment demonstrating that moderate constriction of the left renal artery (LK) followed by moderate constriction of the right renal artery (RK) cause sustained hypertension in a dog. (Redrawn from **ref. *5***.)

between November 1896 and May 1897, with a few additional experiments conducted in autumn 1897. Tigerstedt did not continue his studies after he returned in 1901 to his native Finland where he became deeply involved in the administration of a new institute of physiology in Helsinki, and his discovery was not initially given much recognition.

2. The Goldblatt Experiments—A New Paradigm for Hypertension

The period from Tigerstedt and Bergman's discovery until the 1930s is often referred to as the "dormant period" for the RAS, although there were several unsuccessful attempts to verify their experiments. Also, Janeway ***(9)*** demonstrated in 1909 that ligation of one of the renal artery branches and removal of the contralateral kidney caused a 13–33 mmHg rise in blood pressure in three dogs. However, there was very little interest in renin until the 1930s when Harry Goldblatt and his colleagues of Case Western University in Cleveland, Ohio demonstrated in dogs that constriction of the renal arteries with silver clamps consistently produced chronic hypertension ***(10)*** (**Fig. 2**).

This discovery was perhaps the greatest single advance in producing an experimental model of hypertension that resembled human hypertension. It also spawned a wave of studies examining the mechanisms of what became known as "Goldblatt hypertension" and renewed interest in the nature of the

pressor substance released by the kidney. As a pathologist, Goldblatt observed that hypertensive patients almost always had arteriosclerosis of the kidney. He reasoned that placing a clamp on the renal artery would mimic the ischemia produced by arteriosclerosis of renal blood vessels. Goldblatt was convinced that his dog models were paradigms not only of human renovascular hypertension, but also of essential hypertension.

In a series of elegant experiments sometimes forgotten by modern physiologists, Goldblatt and his colleagues demonstrated that adrenalectomy, section of the renal nerves, spinal cord section, and other maneuvers designed to block the sympathetic nervous system did not significantly modify hypertension induced by renal artery stenosis. They also showed that constricting the aorta above the kidneys caused hypertension, whereas aortic constriction below the kidneys had little chronic effect on arterial pressure. Goldblatt's experiments, which continue to be confirmed to the present day, paved the way for identifying the renal pressor system. The similarities of the pathologic changes produced in Goldblatt's experimental model with those found in human essential hypertension also led to the concept that the kidneys play a central role in the etiology of hypertension; this contrasted with the prevailing view that renovascular disease was primarily a consequence, rather than a cause of hypertension.

Goldblatt did not initially consider renin to be a primary candidate in mediating hypertension caused by renal artery constriction, although he believed that a humoral substance was involved. Later experiments confirmed Goldblatt's suspicion that the RAS was only a partial explanation of the mechanisms of Goldblatt hypertension.

3. Discovery of the Angiotensins

The failure to demonstrate involvement of the nervous system in Goldblatt hypertension supported the concept that a humoral mechanism was involved, but as Goldblatt stated,

> the view that in the pathogenesis of hypertension due to renal ischemia, a humoral mechanism involving a hypothetical effective substance of renal origin plays a part of primary importance is based almost entirely upon indirect evidence.

Thus, the search for the elusive pressor substance released from the kidney was renewed. Harrison et al. ***(11)*** and Prinzmetal and Friedman ***(12)*** in 1937 showed that saline extracts from ischemic kidneys of hypertensive animals raised blood pressure, although the results were sometimes inconsistent. Several other investigators also obtained negative results.

In 1938, Juan Carlos Fasciolo, working on his doctoral thesis in the laboratory of the great Argentine physiologist Bernardo Alberto Houssay, demonstrated the presence of a humoral pressor substance by grafting an ischemic

kidney to the neck circulation in dogs. In these experiments, the ischemic kidney released a substance that produced hypertension in the recipient dog ***(13)***. Further evidence that the ischemic kidneys from hypertensive dogs secreted a vasopressor substance came from the experiments of Houssay and Taquini in 1938 ***(14)*** who demonstrated that blood drawn from the renal vein of hypertensive dogs caused intense vascular constriction in the hind leg of toads.

The idea that renin was not a constrictor itself, but rather acted as an enzyme to produce a pressor substance, was proposed in 1938 by Kohlsteadt et al. ***(15)*** working with Irving Page's group in Indianapolis (and later at the Cleveland Clinic) and in 1939 by Mua-aoz et al. working with Braun-Menendez in Buenos Aires, Argentina ***(16)***. Thus, two laboratories separated by great distance embarked on a series of experiments to identify the pressor substance released from underperfused kidneys. Although the two groups followed different paths, they discovered almost simultaneously the substance in plasma that is now called *angiotensin*. Kohlstaedt, Helmer, and Page, while attempting to purify renin in 1938, found that the preparation had greater blood pressure effects when assayed in cats and dogs in vivo than in the isolated dog tail perfused with Ringer's solution ***(15)***. Something in the blood appeared to enable renin to exert its pressor action, and when they added small amounts of blood to Ringer's solution containing the purified renin, the solution elicited powerful vasoconstriction in the perfused dog tail. They gave the name "renin activator" to the putative plasma protein responsible for activation of renin.

In 1940, Page and Helmer ***(17)*** isolated a pressor substance formed by the interaction of renin and renin activator and named it *angiotonin*. That same year Braun-Menendez et al. ***(18)*** found that the renal venous blood contained a substance that could be extracted in acetone, was thermostable, produced a sharp rise in blood pressure that lasted only 3–4 min, and they named this new substance *hypertensin*. It was soon recognized that hypertensin and angiotonin were the same substance, and for the next 18 yr, both terms were used, although hypertensin was probably more popular because it was chosen by Ciba Pharmaceuticals for their synthetic and commercially available angiotensin II preparation. In 1958, Braun-Menendez and Page ***(19)*** agreed to name the pressor substance *angiotensin*; by extension the substrate from which angiotensin is released was called *angiotensinogen*.

During the 1950s, there were amazing advances in the biochemistry of the RAS, with Leonard Skeggs and his colleagues at the Case Western Reserve University leading the way (*see* **Table 1**). Skeggs' group purified angiotensin in 1954 and discovered that it existed in two different forms, a decapeptide called *angiotensin I* (Ang I), and an octapeptide called *angiotensin II* (Ang II), derived from the cleavage of a dipeptide from Ang I ***(20,21)***. In 1956, Skeggs' group discovered angiotensin-converting enzyme (ACE) and published the

Table 1
Milestones In Renin–Angiotensin System (RAS) History

1898	Tigerstedt and Berman discover that an extract from rabbit kidney cortex increases blood pressure (**ref. *8***).
1934	Goldblatt induces hypertension in dogs by renal artery constriction (**ref. *10***).
1939–1940	Braun-Menendez et al. (**refs. *16,18***) and Page et al. (**refs. *15,17***) discover hypertensin and angiotonin (later known as angiotensin).
1954	Skeggs et al. purify angiotensin and discover that it exists in two forms, angiotensin I and II, and predict the presence of ACE (**refs. *20,21***).
1954	Elliot and Peart (**ref. *24***) and Skeggs et al. (**ref. *23***) report amino acid sequence of angiotensin II.
1956	Skeggs partially purifies renin substrate (angiotensinogen) and its N-terminal part (**ref. *25***).
1957	Bumpus et al. (**ref. *26***) and Rittel et al. (**ref. *27***) synthesize angiotensin II, which is widely distributed to researchers by Ciba Pharmaceuticals.
1958	Gross (**ref. *28***) articulates the hypothetical relationship between angiotensin II and aldosterone.
1959–1961	Davis et al. (**ref. *29***), Laragh et al. (**ref. *30***) Genest et al. (**ref. *31***), and Ganong and Mulrow (**ref. *32***) demonstrate that angiotensin II regulates aldosterone secretion.
1968	Bradykinin-potentiating factor, described in 1965 by Ferreira (**ref. *59***) is shown by Bahkle (**ref. *60***) to inhibit the conversion of AI to AII.
1969	Radioimmunoassay methods for renin are introduced (**refs. *53,54***).
1969–1971	Peptide antagonists of angiotensin II are developed (**refs. *55,56***).
1971	Elucidation of structure and synthesis of bradykinin-potentiating peptide (teprotide) (**ref. *61***).
1977	Ondetti, Rubin, and Cushman describe a novel class of orally active ACE-inhibitors (captopril) (**ref. *62***).
1982–1988	Orally active, nonpeptide blockers of the AII type I receptor are described (**refs. *63,64***).

amino acid sequence of the octapeptide Ang II ***(23)***. At about the same time, Elliott and Peart ***(24)*** in England also published the amino acid sequence of angiotensin. Skeggs' group published papers in 1956 and 1957 that showed the active part of angiotensinogen is a 14-amino acid sequence ***(25)***. This period of rapid progress culminated in 1957 with the synthesis of Ang II by Bumpus et al. ***(26)*** at the Cleveland Clinic in the United States and by Rittel et al. ***(27)*** in Switzerland.

The brilliant discoveries of the biochemical components of the RAS, the successful synthesis of Ang II, and the distribution of synthetic Ang II (Hypertensin) by Franz Gross and his colleagues at Ciba Pharmaceuticals paved the

way for physiological studies of the RAS in the 1960s and 1970s. Also, the development of sensitive methods to measure plasma renin activity (PRA) and Ang II concentration in the late 1960s made it possible to examine the feedback systems that regulate activity of the RAS and to differentiate between pharmacological and physiological actions of Ang II.

4. Role of Ang II in Control of Aldosterone Secretion

For most of the 1930s until the 1950s, research on the RAS was directed toward its pathogenic significance in hypertension. In the 1950s Gross and colleagues began to investigate the physiological relationships between adrenal hormones and the RAS in their laboratory in Heidelberg, Germany. Gross reviewed their observations in 1958, clearly articulating their finding that changes in sodium balance caused parallel changes in the RAS and aldosterone secretion and proposing that Ang II was an important regulator of aldosterone secretion ***(28)***. Although Gross did not have techniques available in his laboratory to measure aldosterone secretion, he generously supplied synthetic Ang II (Hypertensin) to several researchers, including John Laragh, Jacques Genest, James O. Davis, and Francis Ganong and Patrick Mulrow who, although working in different laboratories, proved almost simultaneously that Ang II was a powerful stimulator of aldosterone secretion.

Between 1958 and 1961, Davis and colleagues demonstrated, with an elegant series of experiments in dogs, the presence of an unidentified aldosterone-stimulating hormone, that the source of the hormone was the kidney, and that infusion of synthetic Ang II stimulated aldosterone secretion ***(29)***. In 1960, Laragh and colleagues ***(30)*** showed that Ang II infusion raised plasma aldosterone in human volunteers and that same year Genest et al. ***(31)*** reported that Ang II increased urinary aldosterone excretion. Ganong and Mulrow ***(32)*** demonstrated in 1961 that an aldosterone-stimulating substance was released by the kidney during hemorrhage and confirmed that Ang II administration stimulated aldosterone secretion in dogs. These observations were the starting point for investigations of the physiology of the renin–angiotensin–aldosterone axis and the concept that blood pressure control by Ang II is closely interrelated to its renal sodium-retaining actions. Moreover, these studies provided a new focus on physiologic regulation of sodium and water balance and its major role in blood pressure regulation.

Elucidation of Ang II's role in regulating aldosterone secretion was preceded by identification of the steroid structure of aldosterone in 1952 and development of physicochemical methods for its detection by Simpson and Tait ***(33)***; several other laboratories were busy developing reliable methods for measurement of aldosterone in urine with bioassay, chemical, and isotope methods. With improved methods to measure aldosterone in urine and plasma

in the 1960s and with the development of specific Ang II antagonists and ACE inhibitors, the importance of Ang II in controlling aldosterone secretion was gradually revealed.

5. Role of Ang II in Controlling Renal Function

One of the first studies to examine the role of the RAS in controlling renal function was in 1939 by Merrill et al. ***(34)*** who reported that injections of kidney cortex extracts decreased renal blood flow, increased blood pressure and urine excretion, and caused the kidneys to swell. He speculated that renin in the extracts caused contraction of the efferent glomerular vessels. This is in contrast to other pressor substances such as tyramine, which also decreased renal blood flow, but caused shrinkage of the kidney, decreased urine volume, and presumably contraction of afferent glomerular vessels. In 1940, Corcoran and Page ***(35)*** demonstrated in conscious dogs that iv infusion of the newly discovered angiotensin elicited essentially the same renal responses as observed with infusions of renal extracts—reduced renal blood flow and increased GFR and urine volume.

With the widespread availability of synthetic Ang II, there were many studies of the effects of Ang II infusion on kidney function in the 1960s, but their physiological relevance was uncertain because of the inability to accurately measure Ang II concentrations or to block the physiological actions of Ang II. A major advance toward understanding the physiology of the RAS came with the development of specific Ang II antagonists and ACE inhibitors. These new compounds allowed, for the first time, physiological and clinical studies aimed at the role of *endogenous* Ang II in controlling kidney function and arterial pressure. With the availability of effective blockers of the RAS in the early 1970s, it became apparent that even normal levels of Ang II have a tonic vasoconstrictor effect on the kidney.

5.1. The RAS and Macula Densa Feedback Control of GFR

Goormaghtigh ***(36)*** speculated in 1937 that the juxtaglomerular cells of the afferent arterioles were the source of renin and that these cells might play a role in linking tubular and vascular functions of the kidney. This concept remained largely dormant until 1963 when Guyton ***(37)*** proposed, on the basis of a computer model, that the juxtaglomerular apparatus (JGA) played a major role in the feedback control of GFR. Less than a year later Thurau ***(38)*** proposed a similar idea and suggested that intrarenally formed Ang II was the mediator of this feedback; according to this hypothesis, increased sodium chloride delivery to the macula densa stimulates renin release and causes constriction of afferent arterioles, thereby returning GFR toward normal. Although the existence of macula densa feedback control of GFR was later verified when

micropuncture methods became available, there were two aspects of this hypothesis that proved incorrect: (1) increased sodium chloride delivery was shown in 1964 by Vander and Miller ***(39)*** to *decrease* rather than increase renin secretion; and (2) Ang II was found to constrict the *efferent* arterioles to a greater extent than the *afferent arterioles* ***(40)***, an action that had been suggested by earlier studies of the renal effects of Ang II.

5.2. Blockade of Ang II Protects Against Hemodynamic Injury in Overperfused Nephrons

When nephrons are overperfused and renin release is not appropriately suppressed, as occurs in certain types of renal disease or diabetes, blockade of Ang II formation, by decreasing efferent arteriolar resistance and glomerular hydrostatic pressure, protects the glomeruli from hemodynamic injury. Anderson et al. ***(41)*** were the first to demonstrate in a series of experiments in rats with partial renal ablation that blockade of the RAS was more effective in slowing glomerular injury than other antihypertensive agents. Later studies in humans with diabetes and renal disease confirmed these early observations in rats.

Although the beneficial effects of Ang II blockers and ACE inhibitors in slowing renal disease are now well established, the mechanisms involved are still debated. In vitro studies have shown than Ang II in high concentrations can promote vascular smooth muscle growth, increased collagen formation, and proliferation of extracellular matrix, particularly by mesangial cells. These findings have led to the hypothesis that blockade of the RAS protects the kidney from injury via nonhemodynamic mechanisms. However, an observation that is difficult to reconcile with this concept is that physiological activation of the RAS, by sodium depletion or renal artery stenosis, is not associated with vascular, glomerular, or tubulointerstitial injury as long as the kidney is not overperfused or exposed to high blood pressure. This suggests that the hemodynamic effects of Ang II, particularly efferent arteriolar constriction and increased arterial pressure, are necessary for many of the glomerular, tubular, and interstitial cell proliferative and phenotypic changes that occur when Ang II levels are excessively increased. Resolution of this controversy will await new experimental tools and novel approaches.

5.3. Intrarenal Actions of Ang II Control Sodium Excretion

Early observations that acute infusions of large amounts of renin or kidney extracts often caused natriuresis and diuresis led to the notion that the main direct effects of Ang II on the kidney were vasoconstriction and a direct *inhibitory* effect on renal tubular sodium transport. When purified Ang II became widely available for studies in humans and experimental animals in the 1960s, Ang II was demonstrated to reduce sodium excretion by stimulating aldoster-

one secretion. However, several groups also found that infusion of physiological doses of Ang II caused rapid antinatriuresis that could not be attributed entirely to stimulation of aldosterone, followed by an "escape" from sodium retention as hypertension developed. Laragh's group ***(42)*** made the key observation that Ang II, in contrast to other vasoconstrictors such as norepinephrine, not only caused sodium retention, but also elicited a gradual increase in blood pressure that could be sustained with decreasing amounts of Ang II. Thus, sodium retention appeared to enhance the blood pressure effects of Ang II.

What was not clear from these studies, however, was the relative importance of the direct renal actions of Ang II, compared to its indirect effects mediated by aldosterone in causing sodium and water retention and elevated blood pressure. When peptide antagonists of Ang II became available to block the actions of endogenous Ang II, Freeman et al. ***(43)*** reported in 1972 that iv infusion of an Ang II antagonist increased renal blood flow, but had virtually no role in controlling sodium excretion, independent of aldosterone. However, Ang II blockade also caused large reductions in blood pressure that were not taken into account in analyzing the changed in kidney function in these studies. Studies in our laboratory ***(40,44)*** and by Kimbrough et al. ***(45)*** avoided the effects of changes in arterial pressure or aldosterone by blocking Ang II intrarenally and demonstrated that Ang II has important direct effects on sodium reabsorption independent of aldosterone. In addition, intrarenal Ang II blockade also greatly enhanced renal-pressure natriuresis ***(40)***, an effect which proved to be important in mediating the long-term effect of Ang II blockers to lower blood pressure ***(46)***. However, these studies did not determine the mechanism by which Ang II increased sodium reabsorption because Ang II blockade also caused renal hemodynamic changes.

5.4. Ang II Directly Stimulates Renal Tubular Sodium Reabsorption

In 1977, Harris and Young ***(47)***, using micropuncture methods, demonstrated that Ang II at low physiologic concentrations (10^{-13} to $10^{-10}M$) stimulated proximal tubular reabsorption, whereas higher concentrations ($10^{-9}M$) inhibited tubular reabsorption. Similar conclusions were reached by Schuster ***(48)*** using isolated perfused tubules to conclusively demonstrate a direct stimulatory effect of Ang II on renal sodium reabsorption. These studies also explained why many previous investigators either failed to find a stimulatory effect of Ang II on sodium reabsorption, or actually observed inhibition of tubular transport; in most of the earlier studies, supraphysiologic concentrations of Ang II were used that resulted in inhibition of sodium reabsorption.

With the development of cellular and molecular methods, the mechanisms by which Ang II increases proximal tubular reabsorption were extensively studied in the 1980s and 1990s. Ang II is now recognized to increase sodium trans-

port at the luminal and basolateral membranes of the proximal tubule. On the luminal side, Ang II stimulates the sodium-hydrogen antiporter and on the basolateral membrane, Ang II stimulates the sodium-potassium pump as well as sodium-bicarbonate cotransport. At least part of the stimulatory effect of Ang II on proximal sodium reabsorption is coupled to inhibition of adenylyl cyclase and stimulation of phospholipase C activity. Ang II also increases reabsorption of the loop of Henle, distal tubule, and possibly the collecting tubules, although the regulatory role of Ang II in these nephron segments is just beginning to be investigated. Thus, current available evidence indicates that Ang II has multiple intrarenal and actions that increase sodium reabsorption and that these effects provide the basis for a powerful role of the RAS in long-term control of body fluid volumes and arterial pressure.

6. Ang II and Long-Term Blood Pressure Regulation—Dominant Role of Renal Actions

Although many studies in the 1940s through the 1960s examined the acute effects of renin or Ang II on the kidney or on blood pressure, the dominant role of the renal actions of Ang II in long-term blood pressure regulation was not appreciated until the 1960s when Arthur Guyton and colleagues began to develop theoretical analyses and experimental evidence supporting a powerful renal-body fluid feedback for blood pressure regulation. Prior to that time, the RAS was believed to control blood pressure mainly through its peripheral vasoconstrictor effects or through stimulation of aldosterone, a hypothesis that some still embrace. Guyton and Coleman ***(49)*** developed a simple, but elegant, computer model incorporating cardiovascular concepts advanced by the great English physiologist Ernest Starling ***(50)*** and the pressure natriuresis mechanism described by Goll ***(51)*** in 1854 working in Carl Ludwig's laboratory and again by Ewald Selkurt in 1949 ***(52)***. Guyton and Coleman's model predicted that Ang II (or any other blood pressure control system) could not change arterial pressure chronically unless it also altered the set-point of renal-pressure natriuresis. Without a shift of pressure natriuresis, increased blood pressure could not be sustained because it would also provoke an increase in sodium excretion and a decrease in extracellular fluid volume until blood pressure returned to normal.

Guyton's and Coleman's prediction was confirmed in a series of studies that demonstrated that Ang II has important acute and chronic effects on pressure natriuresis. Blockade of Ang II formation greatly increased the ability of the kidney to excrete sodium, so that sodium balance could be maintained at lower blood pressures and Ang II infusion shifted pressure natriuresis to higher blood pressures ***(46)***. It is now clear that long-term control of arterial pressure by the RAS is closely intertwined with volume homeostasis and

with the renal actions of Ang II, mediated by stimulation of aldosterone and by direct intrarenal effects, such as stimulation of tubular transport or efferent arteriolar constriction.

7. Measuring Activity of the Renin–Angiotensin System

Much of the early work on the RAS, especially on the pressor effects of renin, was conducted using bioassay techniques and semipurified renin. When the link between the RAS and aldosterone was discovered in the 1960s, more refined techniques for assaying renin and measuring its secretion rate were needed. Several groups developed renin assays that depended on extracting renin from plasma and incubating it under standard conditions either with fixed amounts of renin substrate or with the substrate available in plasma. The rate of Ang generation in the incubation medium was assumed to be proportional to the concentration or activity of renin enzyme present and was initially measured with bioasssay methods.

By the late 1960s, more precise radioimmunoassay methods for measuring renin activity or renin concentration were introduced by Haber et al. ***(53)*** and Boyd et al. ***(54)***. Despite the different methods used for renin assays, there was remarkable agreement of results from many studies that determined the factors controlling renin secretion. These methods became widely available, were used in laboratories throughout the world, and are still being used today. Although assays for plasma Ang II concentrations were developed as early as the 1950s, Ang II is not routinely determined even at the present time because of the demanding methodology required for accurate measurements.

8. Blockade of the Renin–Angiotensin System as a Therapeutic Approach

The development of blockers of the RAS in the 1970s provided novel research tools that opened a new era of rapid advances in our understanding of the physiological and clinical significance of the RAS. The first substances used to block the RAS were polypeptide analogs of Ang II with amino acids substituted in various positions, enabling them to competitively inhibit Ang II binding to its receptor. Numerous analogs of this type were developed by Bumpus and colleagues at the Cleveland Clinic ***(55)***. However, the compound that was used most extensively was *saralasin*, developed by Pals et al. in 1971 ***(56)*** by substituting sarcosine in position 1 and alanine in position 8 of bovine Ang II. When this compound became available, it was widely used to investigate the multiple physiologic actions of Ang II. Clinical studies were also conducted by Gavras and Brunner, working in Laragh's group in New York, to elucidate the role of Ang II in hypertension and congestive heart failure ***(57,58)***. However, the analog antagonists of Ang II had significant agonist activity,

which led to an underestimate of the potential importance of Ang II in regulating blood pressure and sodium balance, particularly in subjects with normal or reduced renin activity. Also, these peptides were not orally active and did not provide a practical means for treating chronic cardiovascular disorders such as hypertension. Nevertheless, their importance in demonstrating the potential therapeutic value of blocking the RAS cannot be overstated.

In the late 1970s, the development of ACE inhibitors provided another important tool for investigating the physiology of the RAS. The first ACE inhibitor, *teprotide* (SQ20881), was a nonapeptide isolated from the venom of the Brazilian snake, *Bothrops jararaca*. Interest in this peptide initially stemmed from the observation of Brazilian scientist Sergio Ferreira that it inhibited kinin-destroying enzymes; for this reason it was first named *bradykinin-potentiating peptide (BPP)* ***(59)***. It was then discovered that ACE and plasma kininase II are the same enzyme and that BPP was effective in inhibiting the conversion of Ang I to Ang II ***(60)***. Elucidation of the structure of BPP (teprotide) and its synthesis was performed by researchers at the Squibb Institute for Medical Research in Princeton, NJ, who also made this compound available for basic and clinical research ***(61)***.

An advantage of teprotide, compared to the Ang II antagonists, was that it did not have agonist activity. A disadvantage, however, was that it also inhibited the degradation of bradykinin and for many years investigators debated the relative importance of these two actions in mediating the blood pressure and renal effects of ACE inhibition. Although teprotide was used for experimental studies in humans, it had to be given parenterally or intravenously and was not practical for routine therapy of hypertension or congestive heart failure.

The synthesis of the first orally active ACE inhibitor, *captopril*, by Ondetti, Rubin, and Cushman at Squibb in 1977 was a major therapeutic advance, as well as a model of successful drug design ***(62)***. In 1978, researchers at Merck Laboratories synthesized *enalapril*, the first orally active ACE inhibitor lacking a sulfhydryl group. The ready availability of captopril and enalapril permitted long-term blockade of the studies RAS which, in turn, led to an explosion of experimental and clinical studies and the development of many new ACE inhibitors.

The development of specific, nonpeptide orally active Ang II antagonists that selectively block the AT_1-type receptor represents one of the most important recent advances in cardiovascular therapy ***(63,64)***. One advantage of these drugs is that they inhibit the AT_1-receptor mediated actions of Ang II, but do not directly influence kinin formation. Therefore, they do not have some of the common side effects that ACE inhibitors such as cough, angioedema, and exaggerated allergic reactions that are believed to be mediated by increased levels of bradykinin.

Over the past 20-plus years, the efficacy of RAS blockers in treating hypertension, heart failure, and renal disease has gradually unfolded. The success of this therapeutic approach is also evident from the tremendous proliferation of ACE inhibitors, renin inhibitors, and orally active Ang II type 1 receptor AT_1 antagonists, and their effectiveness in reducing blood pressure even in patients who do not have increased Ang II formation. This further highlights the powerful role that the RAS plays in normal cardiovascular and renal function.

9. The Molecular Era and Beyond

It is difficult to determine precisely when the "molecular era" began, but important contributions in the biochemistry and cell biology of the RAS have played a key role in advancing knowledge of this system throughout its history. The purification of renal renin in the 1970s by the laboratories of Inagami ***(65)***, Corvol ***(66)***, and others, the production of specific antibodies to renin, the pharmacologic characterization of Ang II receptors, and other developments paved the way for the explosion of molecular work that began in the 1980s.

Molecular biology and genetics have provided powerful tools that have led to DNA cloning of various components of this system, including the genes for the Ang II type 1 (AT_1) and type 2 (AT_2) receptors, and the renin and angiotensinogen genes in humans and experimental animals. Multiple studies have examined genetic upregulation or downregulation of RAS components in response to a wide variety of physiologic and pathophysiologic conditions. Recombinant DNA technology has made it possible to characterize naturally occurring mutations that affect gene regulatory elements and to construct hybrid genes in which specific mutations can be made in order to examine their biochemical, structural, and physiological consequences. Gene deletions have been performed for various components of the RAS, such as the AT_1 receptor, demonstrating a major role for Ang II in the development, as well as physiological function of the kidney and cardiovascular system. The ability to insert renin or angiotensinogen genes into the germ lines of rats and mice has provided new models of experimental hypertension. Although altered function of RAS genes have not been established as being causally connected to human essential hypertension or other cardiovascular diseases, the promise of genetic manipulation of the RAS as a therapeutic tool remains attractive to many scientists.

The RAS has, for most of its history, been considered mainly as a circulating hormone system. However, in recent years, there has also been an explosion of work on the role of local tissue RAS's in contributing to a multitude of functions, including normal organ development, as well as pathophysiologic changes associated with cell hypertrophy or mitogenesis in diseases such as hypertension and heart failure. Our understanding of the role of local Ang II

formation in tissues other than the kidney is still very limited, although the application of molecular and genetic techniques will likely help to unravel many unanswered questions about this powerful regulator of cardiovascular and renal function in the future.

The vast array of genetic, molecular, cellular, and physiological methods described in this chapter not only demonstrates the rapid progress that has been made in developing new techniques, but also the potential for a better understanding of how the RAS functions in health and disease. As pointed out by Ruskin ***(67)***, there has been an exponential increase in the rate of major discoveries and a marked compression of the time span over which discoveries are made in fields such as hypertension. It took over 50 years after the discovery of renin before an elementary understanding of the biochemistry of the RAS was achieved. Discovery and development now proceed at a much more rapid pace. For example, the first description of the vasoconstrictor peptide endothelin and its amino acid sequence were published in the same paper ***(68)*** in 1988 and within a few years pharmacological antagonists of this system were developed. As noted by Swales ***(69)***, the multiplicative growth of knowledge is "*like a reproducing colony of bacteria*." The reason for this is obvious—scientific discovery is based on previous work, and each new observation or new method spawns more research, more publications, and so forth.

Our challenge for the next millennium will be to effectively utilize the technological advances that are taking place in virtually all areas of science. This will require more than developing and implementing new methods. It will also require parallel integration of the vast amounts of information into new conceptual frameworks. Living systems are much more than the sum of their individual parts, and understanding the complexity of the human body will require integrative, as well as reductionism intellectual efforts. Sometimes, new technology keeps us so busy collecting data and reducing biological systems to their constituent physicochemical parts that we do not devote sufficient time to the less obvious, but equally important, aspect of discovery—integrative thinking.

> Discovery consists of seeing what everybody has seen and thinking what nobody has thought.
>
> Albert Szent-Gyorgyi

Acknowledgments

The author wishes to acknowledge, with great appreciation, the many investigators whose pioneering work he was unable to reference because of space limitations. This research was supported by a grant from the National Heart, Lung and Blood institute (PO1 HL 51971).

References

1. Aurell, M. (1998) The renin-angiotensin system—the centenary jubilee. *Blood Pressure* **7,** 71–75.
2. Page, I. H. (1987) *Hypertension Mechanisms.* Grune & Stratton, Orlando, FL.
3. Robertson, J. I. S. (1993) Renin and angiotensin: an historical review, in *The Renin–Angiotensin System* (Robertson, J. I. S. and Nicholls, M. G., eds.), Gower, London, pp. 1–18.
4. Aurell, M. (1998) Robert Tigerstedt—scientist, teacher and critic, in *Renin–Angiotensin* (Ulfendahl, H. R. and Aurell, M., eds.), Portland Press, London, pp. 1–12.
5. Skeggs, L. (1986) Current concepts and historical perspectives of renal pressor mechanisms. *J. Hypertens.* **4,** s3–s10.
6. Pickering, G. W. (1982) Systemic arterial hypertension, in *Circulation of the Blood—Men and Ideas* (Fishman, A. P. and Richards, D. W., eds.), The American Physiological Society, Waverly Press, Baltimore, MD, pp. 487–541.
7. Inagami, T. (1998) A memorial to Robert Tigersteadt—the centennial of renin discovery. *Hypertension* **32,** 953–957.
8. Tigerstedt, R. and Bergman, P. G. (1898) Niere und Kreislauf. *Skand. Arch. Physiol.* **8,** 223–271.
9. Janeway, T. C. (1909) Note on the blood pressure changes following reduction of the renal arterial circulation. *Proc. Soc. Exp. Biol. Med.* **109,** 5,6.
10. Goldblatt, H., et al. (1934) Studies on experimental hypertension. I. The production of persistent elevation of systolic blood pressure by means of renal ischemia. *J. Exp. Med.* **59,** 347–380.
11. Harrison, T. R., Blalock, A., and Mason, M. F. (1937) Effect on blood pressure of injection of kidney extracts of dogs with renal hypertension. *Proc. Soc. Exp. Biol.* **35,** 38.
12. Prinzmetal, M. and Friedman, B. (1937) Pressor effects of kidney extracts from patients and dogs with hypertension. *Proc. Soc. Exp. Biol.* **35,** 122.
13. Fasciolo J. C., et al. (1938) The blood pressure raising secretion of the ischemic kidney. *J. Physiol.* **94,** 281–290.
14. Houssay, B. A. and Taquini, A. C. (1938) Acción vasoconstrictora de la sangre venosa del riñon isquemiado. *Rev. Soc. Argent. Biol.* **14,** 5.
15. Kohlstaedt, K. G., Helmer, O., and Page, I. H. (1938) Activation of renin by blood colloids. *Proc. Soc. Exp. Biol. Med.* **39,** 214,215.
16. Muá-áoz, J. M., et al. (1939) Hypertensin: the substance causing renal hypertension. *Nature* **144,** 980.
17. Page I. H. and Helmer, O. H. (1940) A crystalline pressor substance (angiotonin) resulting from the interaction between renin and renin-activator. *J. Exp. Med.* **71,** 29–42.
18. Braun-Menéndez, E., et al. (1940) The substance causing renal hypertension. **98,** 283–298.
19. Braun-Menéndez, E. and Page I. H. (1958) Suggested revision of nomenclature—angiotensin. *Science NE* **127,** 242.

20. Skeggs. L. T., Marsh, W. H., Kahn, J. R., and Shumway, N. P. (1954) The purification of hypertension I. *J. Exp. Med.* **100,** 363.
21. Skeggs, L. T., Marsh, W. H., Kahn, J. R., and Shumway, N. P. (1954) The existence of two forms of hypertensin. *J. Exp. Med.* **29,** 275.
22. Skeggs, L. T., et al. (1956) Preparation and function of the hypertensin-converting enzyme. *J. Exp. Med.* **103,** 295–305.
23. Skeggs, L. T., Lentz, K. E., Kahn, J. R., Shumway, N. P., and Woods, K. R. (1956) The amino acid sequence of hypertensin II. *J. Exp. Med.* **104,** 193–197.
24. Elliott, D. F. and Peart, W. S. (1956) Amino acid sequence in a hypertensin. *Nature* **177,** 527–528.
25. Skeggs, L. T., Kahn, J. R., Lentz, K. E., and Shumway, N. T. (1957) The preparation, purification, and amino acid sequence of a polypeptide renin substrate. *J. Exp. Med.* **106,** 439–453.
26. Bumpus, F. M., Schwarz, H., and Page, I. H. (1957) Synthesis and pharmacology of the octapeptide angiotonin. *Science* **125,** 3253.
27. Rittel, W. B., Iselin, B., Kappeler, H., Riniker, B., and Schwyzer, R. (1957) Synthese eines hochwirksamen hypertensin II-amids (L-asparagynl-L-arginyl-L-valyl-L-tyrosyl-L-isoleucyl-L-histidyl-L-prolyl-L-phenylalanin). *Helv. Chim. Acta* **40,** 614–624.
28. Gross, F. (1958) Renin und Hypertensin: physiologische oder pathologische Wirkstroffe? *Klinische Wochenschrift* **36,** 693–706.
29. Davis, J. O. (1959) Discussion. *Recent Prog. Hormone Res.* **15,** 298–303.
30. Laragh, H. H., Angers, M., Kelly, W. G. and Lieberman, S. (1960) Hypotensive agents and pressor substances: The effect of epinephrine, norepinephrine, angiotensin II, and others on the secretory rate of aldosterone in man. *JAMA* **174,** 240–243.
31. Genest, J., Nowaczynski, W., Noiw, E. Sandor, T., and Biron, P. (1960) Adrenocortical function in essential hypertension, in *Essential Hypertension* (Bock, K. D. and Cottier, P. T., eds.), Springer-Verlag, Berlin, pp. 126–146.
32. Mulrow, P. J. and Ganong, W. R. (1961) Stimulation of aldosterone secretion by angiotensin II. *Yale J. Biol. Med.* **33,** 386–395.
33. Simpson, S. A. S. and Tait J. F. (1953) Physiochemical methods of detection of a previously unidentified adrenal hormone. *Mem. Soc. Endocrinol.* **2,** 9–24.
34. Merrill, A., Williams, R. H., and Harrison, T. R. (1938) The effects of a pressor substance obtained from the kidneys on the renal circulation of rats and dogs. *Am. J. Med.* **96,** 240–246.
35. Corcoran, A. C. and Page, I. H. (1940) The effects of angiotensin on renal blood flow and glomerular filtration. *Am. J. Physiol.* **130,** 335–339.
36. Goormaghtigh N. (1937) L'Appareil neuromyartériel juxtaglomérulaire du rein: ses reactions en pathologie et ses rapports avec le tube urinefére. *C. R. Soc. Biol. (Paris)* **124,** 293–296.
37. Guyton, A. C. (1963) Theory for autoregulation of glomerular filtration rate and blood flow in each nephron by the juxtaglomerular apparatus. *The Physiologist* **6,** 194.
38. Thurau, K. (1964) Renal hemodynamics. *Am. J. Med.* **36,** 698–719.

39. Vander, A. and Miller, R. (1964) Control of renin secretion in the anesthetized dog. *Am. J. Physiol.* **207,** 537–546.
40. Hall, J. E., Guyton, A. C., Jackson, T. E., Coleman, T. G., Lohmeier, T. E., and Trippodo, N. C. (1977) Control of glomerular filtration rate by renin-angiotensin system. *Am. J. Physiol.* **233,** F366–F372.
41. Anderson, S, Rennke, H. G., and Brenner B. M. (1986) Therapeutic advantage of converting enzyme inhibitors in arresting progressive renal disease associated with systemic hypertension in the rat. *J. Clin. Invest.* **77,** 1993–2000.
42. Ames, R. P., Borkowski, A. J., Sicinski, A., and Laragh, J. H. (1965) Prolonged infusions of angiotensin II and norepinephrine and blood pressure, electrolyte balance, and aldosterone and cortisol secretion in normal man and in cirrhosis with ascites. *J. Clin. Invest.* **44,** 1171–1185.
43. Freeman, R. H., Davis, J. O., Vitale, S. J., and Johnson, J. A. (1973) Intrarenal role of angiotensin II. homeostatic regulation of renal blood flow. *Circ. Res.* **32,** 692–698.
44. Hall, J. E., Guyton, A. C., Trippodo, N. C., Lohmeier, T. E., McCaa, R. E., and Cowley, A. W., Jr. (1977) Intrarenal control of electrolyte excretion by angiotensin II. *Am. J. Physiol.* **232,** F538–F544.
45. Kimbrough, H. M., Jr., Vaughn, E. D., Jr., Carey, R. M., and Ayers, C. R. (1977) Effect of intrarenal angiotensin II blockade on renal function in conscious dogs. *Circ. Res.* **40,** 174–178.
46. Hall, J. E., Guyton, A. C., Smith, M. J., Jr., and Coleman, T. G. (1980) Blood pressure and renal function during chronic changes in sodium intake: role of angiotensin. *Am. J. Physiol.* **239,** F271–F280.
47. Harris, P. J. and Young, J. A. (1977) Dose-dependent stimulation and inhibition of proximal tubular sodium reabsorption by angiotensin II in the rat kidney. *Pflugers Arch.* **367,** 295–297.
48. Schuster, V. L., Kokko, J. P., and Jacobson, H. R. (1984) Angiotensin II directly stimulates sodium transport in rabbit proximal convoluted tubules. *J. Clin. Invest.* **73,** 507–515.
49. Guyton, A. C. and Coleman, T. G. (1969) Quantitative analysis of the pathophysiology of hypertension. *Circ. Res.* **24(Suppl I),** 1–19.
50. Starling, E. H. (1909) The fluids of the body, in *The Herter Lectures*. Keever, Chicago, IL.
51. Goll, R. (1854) Ueber den Einfluss des Blutdrucks auf die Harnabsonderung. *Z. Nat. Med.* **4,** 78.
52. Selkurt, E. E., Hall, P. W., and Spencer, M. P. (1949) Effect of graded arterial pressure decrement on renal clearance of creatinine, P-amino hippurate and sodium. *Am. J. Physiol.* **159,** 369–384.
53. Haber, E., Koerner, T. Page, L. B., Kliman, B., and Purnode, A. (1969) Application of a radioimmunoassay for angiotensin I to the physiologic measurements of plasma renin activity in normal human subjects. *J. Clin. Endocrinol. Metab.* **29,** 1349–1355.

54. Boyd, G. W., Adamson, A. R., Fitz, A. E., and Peart, W. S. (1969) Radio-immunoassay determination of plasma-renin activity. *Lancet* **1,** 213–218.
55. Khairallah, P. A., Toth, A., and Bumpus, F. M. (1970) Analogs of angiotensin II. Mechanism of receptor interactions. *J. Med. Chem.* **13,** 181.
56. Pals, D. T., Masucci, F. D., Sipos, F., and Denning, G. S. (1971) Specific competitive antagonists of the vascular action of angiotensin II. *Circ. Res.* **29,** 664–672.
57. Brunner, H. R., Gavras, H., Laragh, J. H., and Keenan, R. (1973) Angiotensin-II blockade in man by SAR^1-Ala^8-angiotensin II for understanding and treatment of high blood-pressure. *Lancet* **1,** 1945–1948.
58. Gavras, H., Brunner, H. R., Vaughn E. D., Jr., and Laragh, J. H. (1973) Angiotensin-sodium interaction in blood pressure maintenance of renal hypertensive and normotensive rats. *Science* **180,** 1369–1372.
59. Ferreira, S. H. and Rocha e Silva, M. (1965) Potentiation of bradykinin and eledoisin by BPF (bradykinin-potentiating factor) from *Bothrops jararaca* venom. *Experientia* **21,** 347–349.
60. Bahkle, Y. S. (1968) Conversion of angiotensin I to angiotensin II by cell–free extracts of dog lung. *Nature* **220,** 919–921.
61. Ondetti, M. A., Williams, N. J., Sabo, E. F., Pluscec, J., Weaver, E. R., and Kocy, O. (1971) Angiotensin-converting enzyme inhibitors from the venom of *Bothrops jararaca*. Isolation, elucidation of structure and synthesis. *Biochemistry* **10,** 4033–4039.
62. Ondetti, M. A., Rubin, B., and Cushman, D. V. (1977) Design of specific inhibitors of angiotensin converting enzyme: new class of orally active antihypertensive agents. *Science* **196,** 441–444.
63. Furukuwa, Y., Kishimoto, S., and Nishikawa, K. (1982) hypotensive imidazole derivatives. US Patent 4,340,598 issues to Takeda Chemical Industries, Ltd., Osaka, Japan.
64. Wong, P. C., Chiu, A. T., Price, W. A., Thoolen, J. M. C., Carini, D. J., Johnson, A. L., et al. (1988) Nonpeptide angiotensin II receptor antagonists. I. Pharmacological characterization of 2-n-butyl-4-chloro-1-(2-chlorobenzyl) imidazole-5-acetic acid, sodium salt (S-8307). *J. Pharmacol. Exp. Ther.* **247,** 1–7.
65. Inagami, T. and Murakami, K. (1977) Pure renin: isolation from hog kidney and characterization. *J. Biol. Chem.* **252,** 2978–2983.
66. Corvol, P., Devaux, C., Ito, T., Sicard, P., Duclous, J., and Menard, J. (1977) Large scale purification of hog renin. *Circ. Res.* **41,** 612–622.
67. Ruskin, A. (1956) *Classics in Arterial Hypertension.* Thomas, Springfield, IL, pp. ix–x.
68. Yanigisawa, M., Kurihara, H., Kimura, S., Tomobe, Y., Kobayishi, M., Mitsui, Y., et al. (1988) A novel potent vasoconstrictor peptide produced by vascular endothelial cells. *Nature* **332,** 411–415.
69. Swales, J. D. (1994) Hypertension: the past, the present and the future, in *Textbook of Hypertension* (Swales, J. D., ed.), Blackwell Scientific, Oxford, pp. 1–7.

2

Three Angiotensin Paradigms in One Patient

Etiology of Hypertension, Glomerular Hemodynamics, and Long-Term Glomerular Protection

Cheryl L. Laffer and Fernando Elijovich

1. Introduction

This chapter on new methods of molecular biology applied to the investigation of the renin–angiotensin system (RAS) contains a description of a clinical case in its first section. There are two reasons for this. First, the case will illustrate the importance of increased understanding of the RAS, because of research by basic scientists, for clinical scientists, clinicians, and human health. Second, and more importantly, describing the applicability of scientific advances in the understanding of RAS to a particular patient is a fitting tribute to two remarkable clinician scientists, Irvin Page and Eduardo Braun Menendez, the co-discoverers of angiotensin II (Ang II) in the United States and Argentina, respectively ***(1,2)***. Their insurmountable curiosity was driven by a desire to help patients, at a time at which human hypertension was an untreatable and devastating problem.

2. The Etiological Role of Angiotensin II in a Case of Human Hypertension

2.1. Initial Medical History

R. Y. is a 77-yr-old African-American man who developed hypertension at age 68. At the time of diagnosis, he already had evidence for vascular disease in the iliofemoral arteries (the symptom of intermittent claudication and the physical finding of bruits on these arteries). In addition to a family history positive for hypertension, coronary artery disease, and diabetes, the patient was a current smoker and was known to have high cholesterol. Approximately

From: *Methods in Molecular Medicine, vol. 51: Angiotensin Protocols*
Edited by: D. H. Wang

in 1993, his hypertension, previously well controlled with a simple medication regimen (prazosin and the diuretic combination HCTZ-amiloride), became refractory to treatment. A renal scan, before and after captopril showed normal uptake of the isotope by both kidneys, with captopril-induced bilateral slowing of excretion. His physician considered that this test was equivocal for diagnosis of renal artery stenosis and renovascular hypertension and decided not to perform an angiogram, considering this test too invasive in view of the perceived low diagnostic yield. The patient was, therefore, maintained on multiple antihypertensive medications, including the angiotensin-converting enzyme (ACE) inhibitor, benazepril, which only produced a modest reduction of blood pressure (BP) when added to other agents.

Two years later, the patient consulted us at the Hypertension Clinic of the University of Texas Medical Branch. His BP was elevated at 202/88 mmHg, his physical exam was characterized by the previously noted arterial bruits, which could now be heard from the epigastrium down to the level of the aortic bifurcation and in both flanks and lower abdominal quadrants. An echocardiogram disclosed left atrial enlargement and concentric left ventricular hypertrophy. The most important finding in his laboratory data was a deterioration of renal function (serum creatinine 206 μmol/L) without proteinuria in the urinalysis.

Serum creatinine values starting in 1975 were retrieved from old records. The plot of the inverse of serum creatinine over time (**Fig. 1**) demonstrated a clear change in slope (steeper downward) starting in early 1993. The refractoriness of the hypertension, the smoking and hypercholesterolemia, the presence of obvious peripheral vascular disease, and the deterioration of renal function, made it likely that the patient had developed renal artery stenosis with its two clinical manifestations, renovascular hypertension and ischemic nephropathy. An abdominal angiogram confirmed this suspicion, showing bilateral, severely stenotic renal arteries (both >90%, **Fig. 2**), with systolic BP gradients across the stenoses of 130–140 mmHg.

2.2. Goldblatt Hypertension in Humans

In the 1950s and 1960s, most clinicians thought of renovascular stenosis as a potentially reversible cause of hypertension in the young, because of one of the forms of congenital fibrous or fibromuscular dysplasia of the renal arteries ***(3)***. With the exception of progression to renal artery occlusion in the rare form of intimal hyperplasia, the clinical problem of these patients was exclusively that of potentially curable hypertension. Repercussion on renal function was either nil or modest. The marked improvement in survival of the elderly over the last four decades, particularly those with cardiovascular disease, has radically changed this issue. Atherosclerosis of the renal arteries is now the most common cause of renal artery stenosis ***(4)***. Its progression is such an important

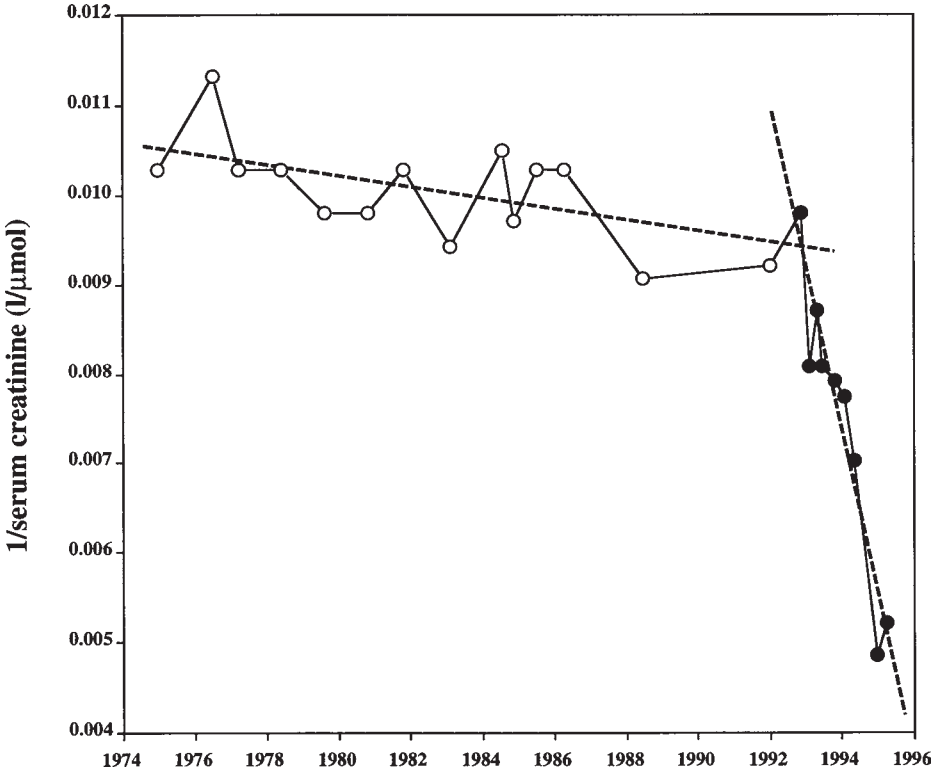

Fig. 1. Plot of the inverse of serum creatinine from 1974 until the time of the angiogram. The open symbols depict slow progression of renal dysfunction over the course of eighteen years, probably because of aging and essential hypertension. The closed circles indicate a 2-yr period of acceleration of renal dysfunction, presumably caused by superimposed, hemodynamically significant, bilateral renal artery stenoses (see discussion in text). The regression lines for both periods are shown. The choice of the cutoff point between the two periods was arbitrary, by inspection of the plot.

cause of renal dysfunction in the elderly that nephrologists have coined the specific term "ischemic nephropathy" to designate this entity ***(5)*** and differentiate it from renovascular hypertension, the other consequence of stenoses of the renal arteries.

Normal subjects start losing glomerular filtration rate (GFR) at about age 35 and at a rate of 1 mL/min/yr ***(6)***. The rate of loss of GFR with aging is increased in nonmalignant essential hypertension, because of arteriolar nephrosclerosis ***(7)***. This process exhibits large interindividual variability, probably due to differences in genetic susceptibility to renal disease ***(8,9)***. However, in uncomplicated essential hypertension, serum creatinine rarely reaches the levels we saw

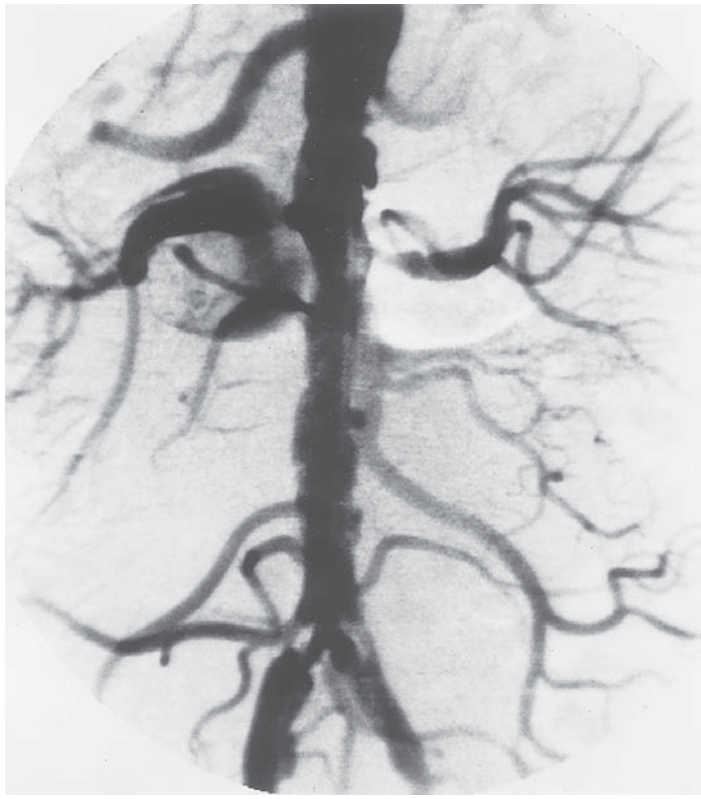

Fig. 2. Aortogram depicting a markedly irregular atherosclerotic abdominal aorta and obvious stenoses of both renal arteries, extending from their origins for approximately 2 cm. Poststenotic dilatation of the renal arteries and involvement of the iliac arteries in the atherosclerotic process are also visible.

in our patient at his age. Furthermore, he had an abrupt change in the rate of loss of GFR (**Fig. 1**). This finding, if not explained by intercurrent illness, nephrotoxic medications, or acceleration of essential hypertension, must trigger the clinician's suspicion of atherosclerotic involvement of the renal arteries.

The Goldblatt experiment was a paradigmatic demonstration of the existence of a condition in which renin and angiotensin had a definite effect on regulation of BP. However, it was not until Gavras' seminal experiments in the 1970s that it was understood that the dependence of BP on renin in Goldblatt hypertension was contingent upon the existence of an uninvolved contralateral kidney, capable of undergoing pressure-induced natriuresis when exposed to the hypertension. Hence, in the rat with two kidneys and one clip (2K1C model), the clipped kidney secretes renin, producing BP elevation that leads to

pressure-induced natriuresis by the unclipped kidney. Maintenance of normal (or slightly contracted) plasma volume by this natriuresis perpetuates stimulation of renin secretion by the stenosed kidney. The resulting hypertension is, therefore, renin-dependent in sustained manner and pharmacologic blockade of the RAS reduces BP in its early and late stages ***(10)***. In contrast, in the rat with a clipped single kidney (1K1C), the entire renal mass is affected by hypoperfusion; therefore, pressure-induced natriuresis is impaired. Sodium retention and plasma volume expansion shut off the initial hypersecretion of renin produced by the clipping of the solitary renal artery. In its maintenance phase, this model becomes a sodium/volume-dependent form of Goldblatt hypertension which does not exhibit significant antihypertensive responses to antagonists of the RAS ***(11)***. In humans, occurrence of the "1K1C model" requires that atherosclerotic lesions of both renal arteries be not only present (which is common), but also hemodynamically significant on both sides (much less common) ***(12)***.

In our patient, several findings supported the diagnosis of hemodynamically significant bilateral renal artery stenoses before this was actually documented by the angiogram. First, the apparently "false" negative results of the renal scan. This test utilizes the fact that Ang II is predominantly a constrictor of the efferent glomerular arteriole ***(13)***. Pharmacologic blockade of the RAS will, therefore, increase "run-off" of blood flow to the distal nephron, with consequent decreases in glomerular capillary pressure and filtration fraction. In normal human beings, GFR is not decreased because of concomitant increase in renal blood flow. Renal artery stenosis precludes the increase in renal blood flow, therefore, the decrease in filtration fraction results in actual decrease of GFR. This is visualized as a captopril-induced decrease in the excretion of a radioisotopic compound in the scan. Hence, a "true positive" test depends on captopril-induced worsening of GFR in the affected kidney, as compared to the unaffected one. Bilateral hemodynamically significant lesions make this comparison unreliable and constitute a well-recognized cause of "false negatives" for this test ***(14)***.

Second, addition of an ACE inhibitor had very little effect on BP. This finding resembles the situation observed in the 1K1C model, hence, suggesting hemodynamically significant bilateral stenoses. It was noteworthy, however, that the poor response to benazepril was observed despite concomitant use of diuretics, a maneuver that may restore renin-dependency of the hypertension in the 1K1C rat by producing natriuresis ***(11)***.

Finally, a creatinine of 206 μmol/L indicated that more than 50% of GFR had been compromised by the pathologic process. Even if one of the renal arteries were totally occluded, an explanation was needed to account for decreased GFR in the contralateral kidney. Hypertensive nephrosclerosis in

the kidney with a patent renal artery, i.e., exposed to the hypertension, could have been the explanation *(15)*. However, the lack of an episode of accelerated hypertension to account for severe arteriolar disease of the nonstenosed kidney, and the other elements of the history made it very likely that the marked decrease in GFR was because of involvement of both renal arteries in the atherosclerotic process.

3. The Role of Angiotensin II in the Regulation of Glomerular Hemodynamics

3.1. Therapy and Initial Clinical Course

Percutaneous transluminal balloon angioplasty was carried out on both renal arteries immediately after the diagnostic angiogram. The gradients across both stenoses were successfully abolished. The patient experienced a transient slight increase in creatinine (**Fig. 3**). This was attributed to dye-induced nephrotoxicity because there was no evidence (e.g., eosinophilia or eosinophiluria) for renal cholesterol embolism, the other relatively common complication of revascularization procedures on the renal arteries. Successful angioplasty decreased, but did not normalize BP completely. Approximately half the previous medications were needed to achieve a BP of 138/62 mmHg. At the time of addition of benazepril (which was required to successfully correct the hypertension), there was a striking increase in serum creatinine (**Fig. 3**).

3.2. Glomerular Hemodynamics in Hypertension

The characteristic histologic abnormality of nonmalignant essential hypertension is benign arteriolar nephrosclerosis, involving predominantly the afferent arteriole. In a kidney biopsy specimen, the distribution of this lesion is heterogeneous. Glomeruli with severe afferent arteriolar narrowing coexist with others minimally affected and still others without any lesion whatsoever *(16)*. It has been hypothesized that this morphologic heterogeneity leads to functional heterogeneity of the RAS. According to this hypothesis, the ischemic hypoperfused glomeruli hypersecrete renin in an attempt to constrict the efferent arteriole for maintenance of GFR. In contrast, glomeruli with normal afferent arterioles sustain hypertensive hyperfiltration, leading to initial high-distal delivery of sodium to the macula densa, with suppression of renin secretion. The plasma renin activity resulting from the different secretion by these two populations of nephrons averages out to normal values. This results in inadequate compensation of reduced GFR in the ischemic glomeruli, and in inappropriate, excessive renin concentration reaching the hyperfiltering glomeruli.

In the ischemic glomeruli, persistent reduction of GFR with consequent reduction in distal delivery of sodium leads to antinatriuresis and sustained hypersecretion of renin by the macula densa/JGA. In the hyperfiltering glom-

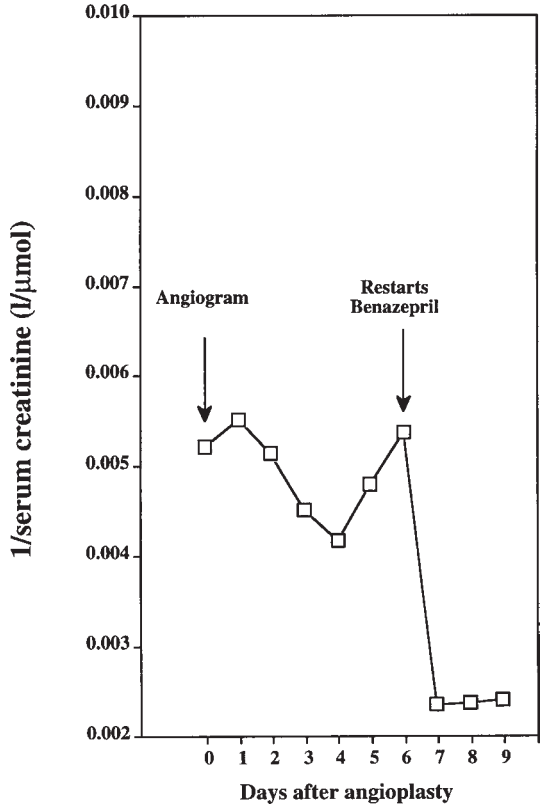

Fig. 3. Plot of the daily inverses of serum creatinine after the angiogram and after resumption of therapy with the ACE inhibitor benazepril (arrows). The angiogram produced a mild, 5-day deterioration of renal function, probably because of the contrast dye (*see text*). Administration of benazepril normalized blood pressure, but led to sudden marked deterioration of renal function. It is apparent from the graph that 1 and 2 days after this complication, there was evidence for minimal, but unequivocal, recovery of renal function. Therefore, benazepril was continued *(see text)*.

eruli, tubulo-glomerular feedback, and the direct action of Ang II on sodium reabsorption at the proximal tubule also lead to antinatriuresis. These changes result in a sodium-retaining state that is inappropriate to the hypertension. Furthermore, this sodium-retaining state fails to completely suppress plasma renin activity, which is continuously driven by afferent arteriolar "stenoses" ***(17)***.

In addition to the anatomical abnormality of hypertensive nephrosclerosis (a combination of smooth muscle hypertrophy and fibrosis of the afferent arteriole), there is also superimposed afferent arteriolar vasoconstriction during severe hypertension ***(18)***, in part mediated by circulating vasoconstrictors and

also because of tubulo-glomerular feedback. As a consequence of this, autoregulation of renal blood flow is altered in hypertension and reduction of BP may lead to significant worsening of GFR. This is true for BP reduction of any magnitude, produced by any antihypertensive drug, but the severity of the phenomenon increases with the degree of preexisting BP elevation and involvement of the renal vasculature. For example, in accelerated or malignant hypertension, normalization of BP may lead to elevations of creatinine indistinguishable from those of acute renal failure. However, resetting of the autoregulatory curve by correction of the hypertension leads to a progressive decrease in serum creatinine over the ensuing 6–12 wk, until a plateau (indicating the degree of residual renal dysfunction because of "scarring" of the fibrinoid necrosis) is reached ***(19)***. Although the deterioration of GFR by BP reduction is independent of the type of agent utilized, efferent arteriolar dilatation by ACE inhibitors will tend to exaggerate it beyond what would be expected from BP reduction alone. An analogous mechanism explains the reports on ACE inhibitor-induced acute renal failure in bilateral renal artery stenosis, a situation in which both kidneys are unable to compensate for the decrease in filtration fraction with an increase in renal blood flow, not due to a problem with autoregulation, but to the stenoses of the main renal arteries themselves ***(20)***.

Our patient most likely had essential hypertension preceding the establishment of renal artery stenoses, as supported by lack of "cure" of the hypertension by the angioplasty. Therefore, he most likely had hypertensive nephrosclerosis preceding the period of hemodynamic "protection" of his glomeruli by the trans-stenotic gradients. Once the latter were abolished by the angioplasty, his compromised renal arterioles were exposed to a systemic BP that had been normalized by drugs. This most likely accounted for the period of nonoliguric acute renal failure that followed administration of benazepril. Although he had tolerated ACE inhibitors before the revascularization procedure (i.e., with bilateral renal artery stenoses), it is conceivable that part of his renal dysfunction was because of their use. The reason by which GFR was more profoundly altered during exposure of afferent arterioles to normal systemic pressure (i.e., abnormal autoregulation after angioplasty) than during the period of bilateral artery stenoses when the glomerular vessels were exposed to even lower (postgradient) pressures, remains unresolved, but may be linked to transient, concomitant, dye-induced tubulointerstitial damage.

4. The Role of Angiotensin II in the Long-Term Protection of Glomerular Function

4.1. Long-Term Follow-Up and Outcomes

In view of the fact that abrupt deterioration of renal function by use of benazepril and normalization of BP was expected, and because of confirma-

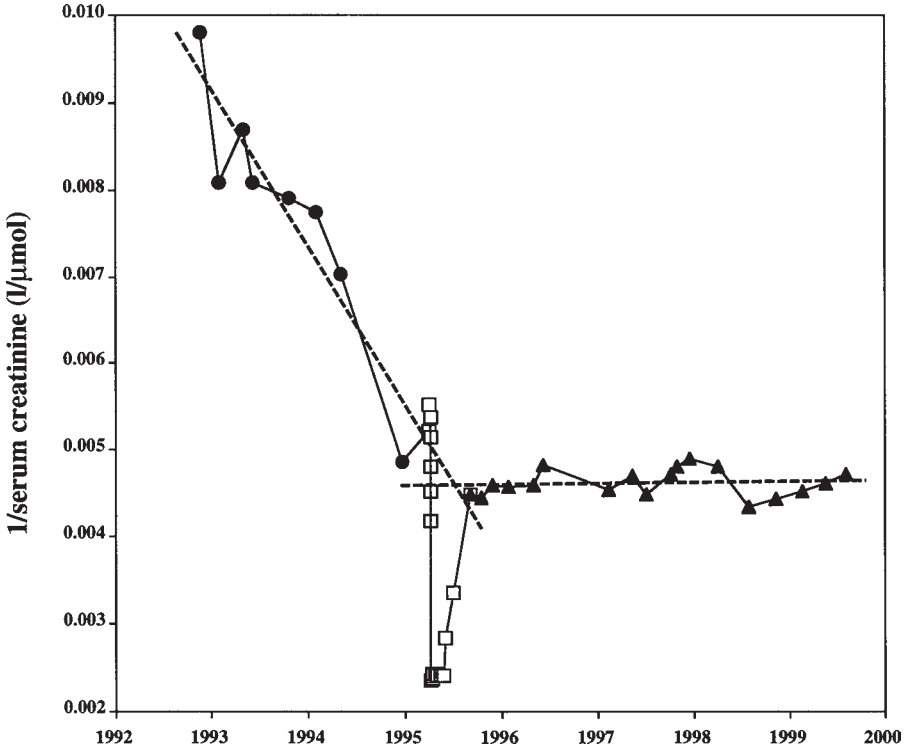

Fig. 4. Data from previous figures (filled circles = spontaneous progression of renal dysfunction before therapy, and open squares = detrimental effects of the angiogram and benazepril on renal function) are followed by the long-term course of renal function until the present (filled triangles). In addition to the arrest of the progression of renal dysfunction (abolition of the slope of 1/serum creatinine over time), the graph depicts the point of intersection between the predicted (before intervention) and actual (long-term after intervention) regression lines, which occurred in early July 1995. This demonstrates that despite the complications of therapy, and soon after them, the patient's renal function was better than it would have been if left to its spontaneous progressive deterioration. This observation supports an aggressive approach to the management of ischemic nephropathy, as advocated by many.

tion of some improvement of serum creatinine over the next few days (**Fig. 3**), we did not decrease dosages or change antihypertensive medication. **Figure 4** shows that this led to progressive improvement of renal function, to the level before angioplasty. More importantly, the long-term progression of renal dysfunction was arrested, as shown by the zero (i.e., horizontal) slope adopted by the line depicting inverse of serum creatinine over time, once maximum improvement was achieved. The dotted line, extrapolating the previous slope

(i.e., loss of renal function before therapy) crosses the actual line in early July 1995, indicating that soon after the abrupt, but transient, deterioration of renal function by the angiogram and the ACE inhibitor, the patient was better off than he would have been left to his spontaneous course. This arrested progression of renal dysfunction has now lasted 4 yr. Thus, aggressive management of the problem, despite its risks (i.e., cholesterol embolism due to angioplasty, dye-induced nephrotoxicity, and ACE inhibitor-induced decompensation of glomerular hemodynamics), was well warranted and resulted in long-term benefit retarding the functional consequences of progressive hypertensive nephrosclerosis. The patient leads an active productive life and his BP remains well controlled on the benazepril-containing regimen. There has been no evidence for restenosis, a relatively frequent phenomenon after angioplasty, and one that has made primary stenting of the renal arteries the currently preferred method of treatment in many medical centers ***(21)***.

4.2. Progression of Glomerular Dysfunction and Its Prevention in Experimental and Human Renal Disease

It has long been known that glomerular damage of any cause, with significant loss of renal mass, leads to inexorable progression of renal dysfunction despite resolution of the initial etiologic factor. Hyperperfusion and increased pressure in the remnant, unaffected nephrons, are thought to have a major role in this progression. Among all experimental models in which this has been tested, perhaps the most important one is the rat with surgically induced renal mass reduction. In this model, hyperperfusion of the remnant glomeruli is produced by 5/6 nephrectomy; therefore, no other factor (e.g., inflammatory or metabolic) but redistribution of renal blood flow to a reduced remnant renal mass may be invoked in the causation of progressive renal dysfunction ***(17)***.

ACE inhibitors, by dilating preferentially the efferent arteriole and thus reducing intraglomerular pressure, slow down the progression of renal dysfunction in rats with reduced renal mass, independent of or beyond the effect that can be obtained by reducing arterial pressure with an agent that does not preferentially dilate the efferent arteriole ***(22)***. This observation has been replicated in many other experimental models of renal damage, where the noxious stimulus was of immunologic, metabolic, or hypertensive nature ***(23,24)***.

Investigation of the mechanisms by which glomerular hypertension ultimately leads to mesangial proliferation and glomerular sclerosis, the anatomic hallmarks of progression of renal dysfunction of any cause, led to the unraveling of another role for Ang II in the progression of renal disease. Hence, it became apparent that this peptide acts as a growth factor, with mitogenic effects resulting in glomerular endothelial and mesangial proliferation ***(25,26)***, and gene-stimulatory effects leading to fibroblast and mononuclear cell activation.

The latter effect leads to increased deposition of collagen I and III, fibronectin, vitronectin, and laminin ***(24)***, and other components of intercellular matrix. Multiple intracellular mediators for these actions of Ang II have been uncovered, such as TGF-beta ***(27)***, PDGF ***(28)***, nuclear factor-kappa B ***(29)***, and VEGF ***(30)***. Actions of Ang II or smaller angiotensin peptides on the coagulation cascade (e.g., stimulation of PAI-1) may also contribute via local thrombosis of the microcirculation ***(31)***. MAP kinase signal transduction pathways and overexpression of proto-oncogenes ***(32)*** participate in Ang II-stimulation of glomerular cell growth and proliferation.

All the actions of Ang II as a growth factor are mediated by its AT1 receptor and are, therefore, amenable to pharmacologic manipulation by means of either ACE inhibitors or the newer angiotensin AT1-receptor blockers (ARBs). In contrast to decreased generation of Ang II caused by ACE inhibitors, ARBs produce feedback increases in circulating Ang II, while blocking its actions on the AT1 receptor. Whether increased Ang II by ARBs confers an advantage to these agents by stimulation of the spared AT2 receptor (putatively involved in vasodilation and antiproliferation) is yet to be proved.

The theoretical advantages of pharmacologic interruption of the RAS in hypertensive or normotensive renal disease with threatened progression of renal dysfunction have been explored by clinical trials in humans. There is little doubt that ACE inhibitors retard the progression of renal disease in normotensive diabetic patients with microalbuminuria ***(33)***. A specific role for these agents in improving progression of renal disease in hypertensive diabetic patients is somewhat more controversial ***(34)***, perhaps because of the important independent role of systemic BP in determining the course of renal disease in these patients. In primary, severe ***(35)*** or mild ***(36)*** glomerulopathies, therapy with ACE inhibitors also slows the rate of progression of renal dysfunction. In contrast, there is not yet incontrovertible evidence for renal protection by pharmacological interruption of the RAS in hypertensive nephrosclerosis. Proof may emerge from ongoing trials such as the NIDDK-sponsored African American Study of Kidney Disease and Hypertension (AASK), which will compare the renal protective effects of different antihypertensive drug classes, or the industry-sponsored RENAAL, which assesses the effect of the ARB losartan on renal protection in hypertension. In the absence of a definitive clinical trial, but taking into consideration that the mechanisms involved in progression of renal damage seem to be common to all etiologies, we extrapolated the knowledge obtained in diabetic and other glomerulopathies to the aggressive approach we employed in our patient. The excellent result we obtained is hopefully a preview of the results to be obtained in the clinical trials testing for the effects of pharmacologic interruption of the RAS in human hypertensive nephrosclerosis.

5. Conclusion

Understanding of the role of the RAS in the causation of unilateral and bilateral renovascular hypertension in humans, knowledge about the role of Ang II as a regulator of acute glomerular hemodynamic changes, and information about the hemodynamic and tissue (growth factor) roles of Ang II in determining long-term progression of glomerular damage, allowed for the therapeutic decisions that led to a successful outcome in the complex hypertensive patient presented here.

A myriad of other patients are already deriving benefit from other aspects of research in the renin–angiotensin field. Examples include prolongation of survival in congestive heart failure and secondary prevention of coronary artery disease ***(37,38)***, and arrest or improvement in the progression of renal damage in diabetic ***(33)*** and nondiabetic glomerulopathies ***(35,36)***. Ongoing studies are also exploring effects of ACE inhibition on primary prevention of myocardial infarction ***(39)***, ARBs on regression of hypertensive left ventricular hypertrophy ***(40)***, and also ARBs on reduction of overall cardiovascular morbidity-mortality in unselected but complicated hypertensive patients ***(41)***. These studies, as well as the AASK study on progression of hypertensive nephrosclerosis in African Americans, may further extend the payoff of research in the field of RAS for the benefit of human cardiovascular disease prevention and therapy.

References

1. Page, I. H. and Helmer, O. M. (1939) A crystalline pressor substance, angiotensin, resulting from reaction of renin and renin activator. *Proc. Soc. Clin. Invest.* **12,** 17.
2. Munoz, M. J., Braun-Menendez, E., Fasciolo, J. D., and Leloir, L. F. (1939) Hypertensin: the substance causing renal hypertension. *Nature* **144,** 980.
3. Maxwell, M. H., Bleifer, K. H., Franklin, S. S., and Varady, P. D. (1972) Cooperative study of renovascular hypertension: demographic analysis of the study. *JAMA* **220,** 1195–1204.
4. Working Group on Renovascular Hypertension. Detection, evaluation and treatment of renovascular hypertension. (1987) *Arch. Intern. Med.* **147,** 820–829.
5. Dean, R. H., Tribble, R. W., Hansen, K. J., O'Neil, E. A., Craven, T. E., and Redding, J. F. (1991) Evolution of renal insufficiency in ischemic nephropathy. *Ann. Surg.* **213,** 446–456.
6. Davies, D. F. and Shock, N. W. (1950) Age changes in glomerular filtration rate, effective renal plasma flow, and tubular excretory capacity in adult males. *J. Clin. Invest.* **29,** 496.
7. Lindeman, R. D., Tobin, J. D., and Shock, N. W. (1984) Association between blood pressure and the rate of decline in renal function with age. *Kidney Int.* **26,** 861–868.

8. Levy, S. B., Talner, L. B., Coel, M. N., Holle, R., and Stone, R. A. (1978) Renal vasculature in essential hypertension: racial differences. *Ann. Intern. Med.* **88,** 12–16.
9. Bell, E. T. (1953) Renal vascular disease in diabetes mellitus. *Diabetes* **2,** 376.
10. Gavras, H., Brunner, H. R., Thurston, H., and Laragh, J. H. (1975) Reciprocation of renin dependency with sodium volume dependency in renal hypertension. *Science* **188,** 1316–1317.
11. Gavras, H., Brunner, H. R., Vaughan, E. D., and Laragh, J. H. (1973) Angiotensin-sodium interaction in blood pressure maintenance of renal hypertensive and normotensive rats. *Science* **180,** 1369–1372.
12. Mann, S. J. and Pickering, T. G. (1992) Detection of renovascular hypertension: state of the art, 1992. *Ann. Intern. Med.* **117,** 845–853.
13. Myers, B. D., Deen, W. M., and Brenner, B. M. (1975) Effects of norepinephrine and angiotensin II on the determinants of glomerular ultrafiltration and proximal fluid reabsorption in the rat. *Circ. Res.* **37,** 101–110.
14. Mann, S. J., Pickering, T. G., Sos, T. A., Uzzo, R. G., Sarkar, S., Friend, K., et al. (1991) Captopril renography in the diagnosis of renal artery stenosis: accuracy and limitations. *Am. J. Med.* **90,** 30–40.
15. Tullis, M. J., Zierler, R. E., Caps, M. T., Bergelin, R. O., Cantwell-Gab, K., and Strandness, D. E., Jr. (1998) Clinical evidence of contralateral renal parenchymal injury in patients with unilateral atherosclerotic renal artery stenosis. *Ann. Vasc. Surg.* **12,** 122–127.
16. Castleman, B. and Smithwick, R. H. (1943) The relation of vascular disease to the hypertensive state based on a study of renal biopsies from one hundred hypertensive patients. *JAMA* **121,** 1256.
17. Brenner B. M., Meyer T. W., and Hostetter T. H. (1982) Dietary protein intake and the progressive nature of kidney disease: the role of hemodynamically mediated glomerular injury in the pathogenesis of progressive glomerular sclerosis in aging, renal ablation, and intrinsic renal disease. *New Engl. J. Med.* **307,** 652–659.
18. Hollenberg, N. K., Adams, D. F., Solomon, H., Chenitz, W. R., Burger, B. M., Abrams, H. L., et al. (1975) Renal vascular tone in essential and secondary hypertension: hemodynamic and angiographic responses to vasodilators. *Medicine* **54,** 29–44.
19. Lawton, W. J. (1982) The short-term course of renal function in malignant hypertensives with renal insufficiency. *Clin. Nephrol.* **17,** 277–283.
20. Textor, S. C., Novick, A. C., Tarazi, R. C., Klimas, V., Vidt, D. G., and Pohl, M. (1985) Critical perfusion pressure for renal function in patients with bilateral atherosclerotic renal vascular disease. *Ann. Intern. Med.* **102,** 308–314.
21. Tuttle, K. R., Chouinard, R. F., Webber, J. T., Dahlstrom, L. R., Short, R. A., Henneberry, K. J., et al. (1998) Treatment of atherosclerotic ostial renal artery stenosis with the intravascular stent. *Am. J. Kidney Dis.* **32,** 611–622.
22. Ots, M., Mackenzie, H. S., Troy, J. L., Rennke, H. G., and Brenner, B. M. (1998) Effects of combination therapy with enalapril and losartan on the rate of progression of renal injury in rats with 5/6 renal mass ablation. *J. Am. Soc. Nephrol.* **9,** 224–230.

23. Goyal, R. K., Satia, M. C., Bangaru, R. A., and Gandhi, T. P. (1998) Effect of long-term treatment with enalapril in streptozotocin diabetic and DOCA hypertensive rats. *J. Cardiovasc. Pharmacol.* **32,** 317–322.
24. Nakamura, T., Obata, J., Kimura, H., Ohno, S., Yoshida, Y., Kawachi, H., et al. (1999) Blocking angiotensin II ameliorates proteinuria and glomerular lesions in progressive mesangioproliferative glomerulonephritis. *Kidney Int.* **55,** 877–889.
25. Wolf, G., Ziyadeh, F. N., Zahner, G., and Stahl, R. A. (1996) Angiotensin II is mitogenic for cultured rat glomerular endothelial cells. *Hypertension* **27,** 897–905.
26. Weiss, R. H. and Ramirez, A. (1998) TGF-beta- and angiotensin-II-induced mesangial matrix protein secretion is mediated by protein kinase C. *Nephrol. Dialysis Transplant.* **13,** 2804–2813.
27. Ruiz-Ortega, M. and Egido, J. (1997) Angiotensin II modulates cell growth-related events and synthesis of matrix proteins in renal interstitial fibroblasts. *Kidney Int.* **52,** 1497–510.
28. Hanada, M., Saito, E., Kambe, T., Hagiwara, Y., and Kubo, T. (1999) Evidence for the involvement of platelet-derived growth factor in the angiotensin II-induced growth of rat vascular smooth muscle cells. *Biol. Pharm. Bull.* **22,** 137–141.
29. Ruiz-Ortega, M., Bustos, C., Hernandez-Presa, M. A., Lorenzo, O., Plaza, J. J., and Egido, J. (1998) Angiotensin II participates in mononuclear cell recruitment in experimental immune complex nephritis through nuclear factor-kappa B activation and monocyte chemoattractant protein-1 synthesis. *J. Immunol.* **161,** 430–439.
30. Gruden, G., Thomas, S., Burt, D., Zhou, W., Chusney, G., Gnudi, L., et al. (1999) Interaction of angiotensin II and mechanical stretch on vascular endothelial growth factor production by human mesangial cells. *J. Am. Soc. Nephrol.* **10,** 730–737.
31. Wilson, H. M., Haites, N. E., and Booth, N. A. (1997) Effect of angiotensin II on plasminogen activator inhibitor-1 production by cultured human mesangial cells. *Nephron* **77,** 197–204.
32. Hamaguchi, A., Kim, S., Yano, M., Yamanaka, S., and Iwao, H. (1998) Activation of glomerular mitogen-activated protein kinases in angiotensin II-mediated hypertension. *J. Am. Soc. Nephrol.* **9,** 372–380.
33. Ravid, M., Lang, R., Rachmani, R., and Lishner, M. (1996) Long-term renoprotective effect of angiotensin-converting enzyme inhibition in noninsulin-dependent diabetes mellitus: a 7-year follow-up study. *Arch. Intern. Med.* **156,** 286–289.
34. UK Prospective Diabetes Study Group. (1998) Efficacy of atenolol and captopril in reducing risk of macrovascular and microvascular complication in type 2 diabetes: UKPDS 39. *Brit. Med. J.* **7160,** 713–720.
35. Ruggenenti, P., Perna, A., Gherardi, G., Gaspari, F., Benini, R., and Remuzzi, G. [on behalf of Gruppo Italiano di Studi Epidemiologici in Nefrologia (GISEN)]. (1998) Renal function and requirement for dialysis in chronic nephropathy patients on long-term ramipril: REIN follow-up trial. *Lancet* **352,** 1252–1256.
36. Ruggenenti, P., Perna, A., Gherardi, G., Garini, G., Zoccali, C., Salvadori, M., et al. (1999) Renoprotective properties of ACE-inhibition in non-diabetic nephropathies with non-nephrotic proteinuria. *Lancet* **354,** 359–364.

37. The SOLVD Investigators. (1991) Effect of enalapril on survival in patients with reduced left ventricular ejection fractions and congestive heart failure. *New Engl. J. Med.* **325,** 293–302.
38. Pfeffer, M. A., Braunwald, E., Moye, L. A., Basta, L., Brown, E. J., Jr., Cuddy, T. E., et al., on behalf of the SAVE Investigators. (1992) Effect of captopril on mortality and morbidity in patients with left ventricular dysfunction after myocardial infarction. Results of the survival and ventricular enlargement trial. *New Engl. J. Med.* **327,** 669–677.
39. Lees, R. S., Pitt, B., Chan, R. C., Holmvang, G., Dinsmore, R. E., Campbell, L. W., et al. (1996) Baseline clinical and angiographic data in the Quinapril Ischemic Event (QUIET) Trial. *Am. J. Cardiol.* **78,** 1011–1016.
40. Dahlof, B., Devereux, R. B., Julius, S., Kjeldsen, S. E., Beevers, G., de Faire, U., et al. [for the LIFE study group]. (1998) Characteristics of 9194 patients with left ventricular hypertrophy: the LIFE study. Losartan Intervention For Endpoint Reduction in Hypertension. *Hypertension* **32,** 989–997.
41. Mann, J. and Julius S. (1998) The Valsartan Antihypertensive Long-term Use Evaluation (VALUE) trial of cardiovascular events in hypertension. Rationale and design. *Blood Pressure* **7,** 176–183.

3

Production and Use of Chimeric Mice

Junji Takaya, Taiji Matsusaka, and Iekuni Ichikawa

1. Introduction

The gene-targeting technology allows complete and selective inactivation of a specific gene to study the consequence of total absence of the gene product. The availability of such null-mutant mice enables investigators to identify the biological function of the gene product in physiological or pathophysiological conditions. This technology, popularly known as "gene knockout," can also induce more subtle mutations at the targeted site of the genome.

Using this technology over the last decade, we and other investigators have produced more than ten strains of mice deficient or in excess of a specific gene within the renin–angiotensin (Ang) system, including angiotensinogen ***(1,2)***, Ang II type 1A (AT1A) receptor ***(3,4)***, Ang II type 1B (AT1B) receptor ***(5)***, Ang II type 2 (AT2) receptor ***(6)***, and angiotensin I converting enzyme ***(7)***. Detailed examination of these mutant mice not only confirmed the well-known blood pressure raising action of Ang II, but also revealed several important biological functions of Ang that had not been recognized before.

Of note, the conventional targeting methods described above is not different from pharmacological Ang II inhibition, and cannot distinguish the role of direct vs blood pressure-mediated or indirect effect of endogenous Ang II on the end-organ tissue. In this regard, the revised method or "conditional gene targeting" more recently established by Rajewsky et al. ***(8)*** allows targeting of a gene of interest in a tissue- and/or time-specific manner. The revised method involves, in addition to the conventional gene targeting, a genome manipulation to incorporate a specific DNA recombinase that acts on the targeted gene at the specific tissue and time of investigators' choice. However, as described elsewhere ***(9)***, the method is currently highly limited for its practical use in specifying the site.

From: *Methods in Molecular Medicine, vol. 51: Angiotensin Protocols*
Edited by: D. H. Wang

Assuming that further technological advancement lets investigators freely target genes in a specific tissue of their choice, "the conditional gene targeting" is still not ideal to investigate the specific issue that we have, direct vs indirect effect of Ang II on the tissue. Hypothetically, if an Ang receptor gene is selectively targeted in the heart, and the cardiac tissue architecture is modified, can we conclude that the receptor's function is direct in achieving and maintaining normal cardiac architecture? The authors think otherwise. The reason being such architectural changes will affect cardiac function and hence, systemic hemodynamics and other organ functions so that blood pressure and the humoral environment harboring the heart is affected. Under this circumstance, we cannot conclude that the cardiac architectural changes reflect only the direct tissue effect of Ang II (*see* **Fig. 1**).

A different approach has, therefore, been used by us to address the issue ***(3)***. The method, called "regional gene targeting," involves generation of chimeric mice, which are made up of two clones of cells, one with wild-type genome and the other with genome targeted, for example, for an Ang II receptor gene. In such mice, the cardiac architecture and function are likely affected, and the systemic milieu harboring the heart is also altered. Of note, however, the altered milieu affects equally these two clones of cells in each organ so that any difference in behavior between the two clones of cells within a given organ must be attributed to the presence vs absence of Ang receptor, hence to the direct tissue receptor effect of Ang II.

The "regional knock out" mouse should be distinguished from the "heterozygous" mouse produced by the conventional gene targeting as, in the latter, all cells have a single intact allele and, hence, have the potential to express the angiotensin receptor. To identify targeted cells in chimeric mouse tissues microscopically, *lacZ* or other reporter gene can be incorporated into the targeted cells or wild-type cells.

1.1. Chimera Generated from Two Embryos or ES Cells and Embryos

Chimeric mice can be generated by combining either two embryos or ES cells and embryos. The advantage of the former is that establishment of a new ES cell line is not necessary. Any type of strains, i.e., wild-type mice, natural mutants, transgenic mutants, can be combined. However, especially when the homozygous mutant mice are lethal or not reproducible, the strain need to be maintained by mating heterozygous mice, and only a quarter (if the gene is located on an autosomal chromosome) of chimeric mice generated carry homozygous mutation. On the other hand, in the latter method, once an ES cell line carrying the mutation of interest is established, it can be expected that the mouse line does not need to be established. This is a great merit especially

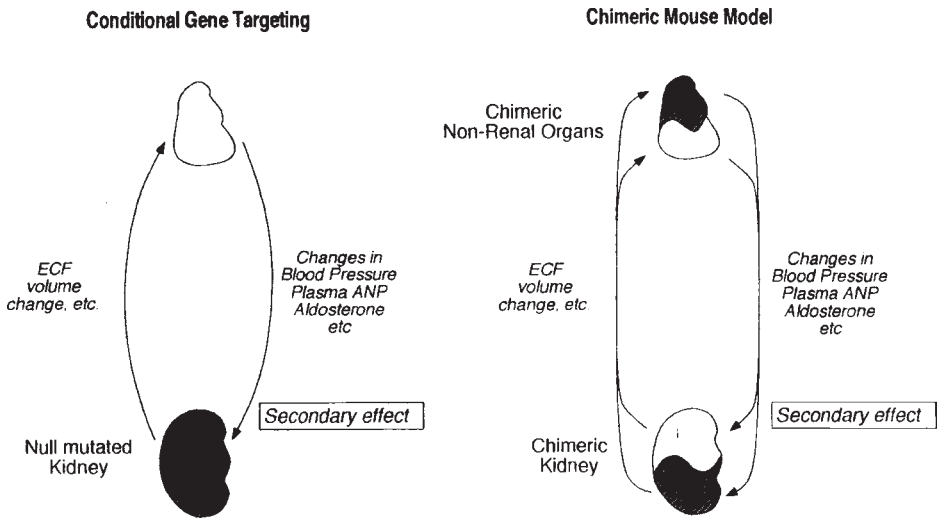

Fig. 1. Studies of local renal tissue effect of a specific gene product that is normally expressed in the kidney by cell-type specific gene targeting vs chimeric mouse. Cell-type specific gene targeting, if successfully performed, can selectively inactivate a gene of interest in the kidney, and not in other organs. However, some abnormal phenotypes in the kidney can change the environment surrounding the kidney via ECF volume change, and so on, and, hence, blood pressure and so on, which in turn secondarily induces other abnormal phenotypes within the kidney. It is then not possible to distinguish between the primary vs local tissue effect of angiotensin within the kidney. In chimeric mouse models, portions of nonrenal, as well as renal, organs are expected to carry inactivated gene, hence causing changes in blood pressure and/or other systemic environment. However, because such altered milieu affects both wild-type and null mutant cells equally, any difference in behavior between the two clones of renal cells are attributed to a reflection of the intact vs null-mutated gene.

when the homozygous mutant mice are lethal or not reproducible. In many cases, the abnormal phenotype of a mutant gene is apparent only when the mutation is homozygous. In that case, ES cells homozygous for the mutation should be established.

For this purpose, there are four methods:

1. *De novo* establishment of ES cells from homozygous blastocysts
2. Introduction of additional mutation in the intact allele of heterozygous ES cells
   a. by increasing the concentration of G418 ***(10,11)***
   b. by using another selection gene, such as hygromycin resistant gene.
   c. by removing *neo* gene using Cre-loxP system, and targeting again with the same targeting vector ***(8)***.

Methodologically, two embryos are combined by aggregation, and ES cells and embryos are combined either by aggregation ***(12–14)*** or by injection. For injection, equipment for the microinjection, i.e., microscope, manipulators, injector, pooler, and so on is necessary. For aggregation, no special equipment other than dissection microscope is necessary.

We generated chimeric mice that are made up with wild-type cells and cells homozygous for AT1A gene mutation *(Agtr1a–/–)*. We used the embryo-aggregation methods in our recent studies. This method is technically easy and can be easily applied to study other genes. Therefore, in the following section, we will describe this method in detail. We also used injection methods. We will briefly write about this method focusing on specific matters for making chimeric mice with homozygous mutations.

2. Materials

2.1. Aggregation of Wild-Type and Agtr1a–/– Embryos

1. Mice used for embryo donors. We used *Agtr1a–/–* mice without the *lacZ* gene. They had a mixed genetic background of C57BL/6 and 129 strains. To distinguish cell types in the chimeric tissue, we used ROSA26 transgenic mice for wild-type embryo donors. ROSA26 mice, originally generated by Soriano et al. ***(15,16)***, are available from Jackson laboratory. This transgenic strain intensely expresses *lacZ* gene in most types of cells. We used ROSA26 mice with a mixed genetic background of C57BL/6, 129 and ICR.

   Pseudopregnant ICR mice are prepared by mating females with vasectomized males on the day of aggregation.
2. Hormones
   a. Gonadotropin from pregnant mares' serum (PMS) (Sigma, Cat. No. G4877)
   b. Human chorionic gonadotropin (Sigma, Cat. No. C1063)

   They are both diluted in 0.9% NaCl at 500 IU/mL, aliquoted, and stored at –20°C. Before use, they are diluted 10 times by 0.9% NaCl.
3. M2 medium: 94.66 m*M* NaCl, 4.78 m*M* KCl, 1.71 m*M* $CaCl_2$, 1.19 m*M* KH_2PO_4, 1.19 m*M* $MgSO_4$, 4.15 m*M* $NaHCO_3$, 20.95 m*M* HEPES, 23.28 m*M* CL-Na lactate, 0.33 m*M* Na pyruvate, 5.56 m*M* D-glucose, 4 mg/L BSA, 0.01 g/L phenol red.
4. M16 medium: 94.66 m*M* NaCl, 4.78 m*M* KCl, 1.71 m*M* $CaCl_2$, 1.19 m*M* KH_2PO_4, 1.19 m*M* $MgSO_4$, 25 m*M* $NaHCO_3$, 23.28 m*M* DL-Na lactate, 0.33 m*M* Na pyruvate, 5.56 m*M* D-glucose, 4 mg/L BSA, 0.01 g/L phenol red.
5. Acidified Tyrode's solution: 137 m*M* NaCl, 2.7 m*M* KCl, 1.6 m*M* CaCl $2H_2O$, 0.5 m*M* $MgCl_2$, 5.6 m*M* glucose, 0.4% polyvinylpyrrolidone.
   These are available from Sigma (Cat. No. M7167, M7292, T1788)
6. Light mineral oil (Sigma Cat. No. M-8410)
7. 3.5-mm Petri dish for bacterial culture (Falcon Cat. No. 1008): Note that embryos are very sticky, and tissue-culture dish is not suitable after removal of zona pellucida.

8. Aggregation needle (Biological Lab Tool Maintenance and Service Plc, H-1165 Budapest, ZsÇlyi A. u. 31. Hungary)
9. Micropipets: We made them by pulling out siliconized 100-µL glass micropipets (MICROPET, Clay Adams, Cat. No. 4625) in a gas burner flame. We made three sizes of pipets: thin (inner diameter (id) less than 125 µm), medium (125–150 µm), and thick (around 150 µm). Thin pipets were used for transferring embryos into acidic Tyrode's solution, medium ones were used for general purposes, and the thick ones were flame polished at the end and used for transferring embryos into the uterus. These pipets were sterilized by heating at 200°C for 2 h.
10. Dissection microscope.
11. Light source.
12. Humidified 37°C incubator with an atmosphere of 5% CO_2 and 95% air.

3. Methods

3.1. Aggregation of Wild-Type and Agtr1a*–/– Embryos*

1. Superovulation: 5 IU of PMS is intraperitoneally injected into females 48 h before mating. 5 IU of hCG was intraperitoneally injected just before mating. Superovulated females are mated with males (at 1:1 or 2:1 ratio). The number of mice necessary for one experiment depends on the age and genetic background of the female mice. We used about 20 *Agtr1a–/–* and 10 ROSA females for one experiment. In the next morning, the females are checked for the presence of a copulation plug in the vagina.
2. Collecting embryos: Around 56 h postcoitum, females with a plug are sacrificed and the abdominal cavity is opened up. The upper end of an uterine horn is grasped with forceps and gently lifted up. The mesometrium attached is gently removed and the uterus at about 5 mm from the oviduct-uterus junction and the portion between the oviduct and the ovary are dissected. The dissected oviducts are temporally stored in M2 medium in a 35-mm dish. Under a dissecting microscope, the oviduct is placed on an empty 35-mm dish. The end of the oviduct, or infundibulum is detected by gently touching with fine forceps. A blunted 30-gage needle attached to a 1-mL syringe containing M2 medium is inserted in the infundibulum. The infundibulum and the needle are fixed with forceps, and M2 medium (about 0.2 mL) is flushed (**Fig. 2**). Three to five oviducts can be flushed in a dish. Embryos are harvested, washed in M2 medium and then in M16 medium, and cultured in microdrops of M16 medium covered with paraffin oil at 37°C in 5% CO_2 until the next step.
3. Removal of zona pellucida: Embryos are packed in a fine glass pipet and transferred in acidic Tyrode's solution in a 35-mm dish. The dish is gently stirred. After 15 to 20 s, the zona pellucida disappears (**Fig. 3**). Immediately, embryos are transferred into M2 medium, washed there, and then in M16 medium. Up to 30 embryos can be handled at a time. The most important point in this step is that the medium carried into the Tyrode's solution should be minimized, otherwise the local pH increases and the zonae are not dissolved at the same time. Prolonged incubation in Tyrode's solution causes damage to embryos, even if the embryos appear normal.

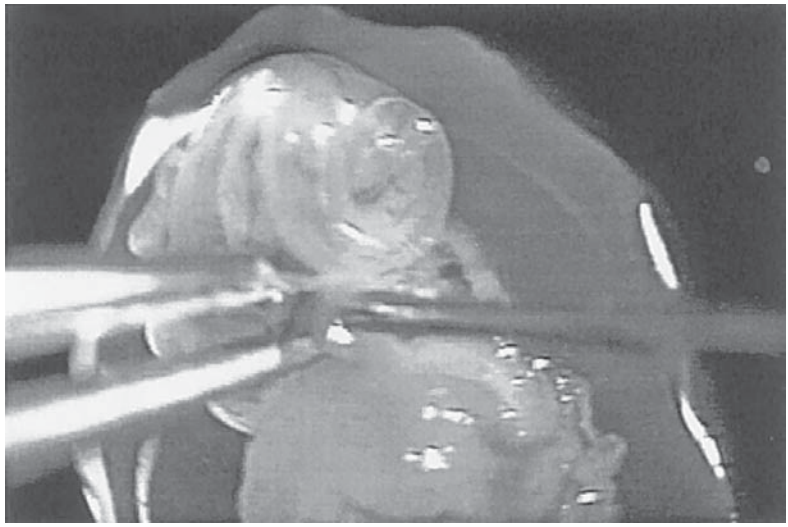

Fig. 2. Flushing oviduct.

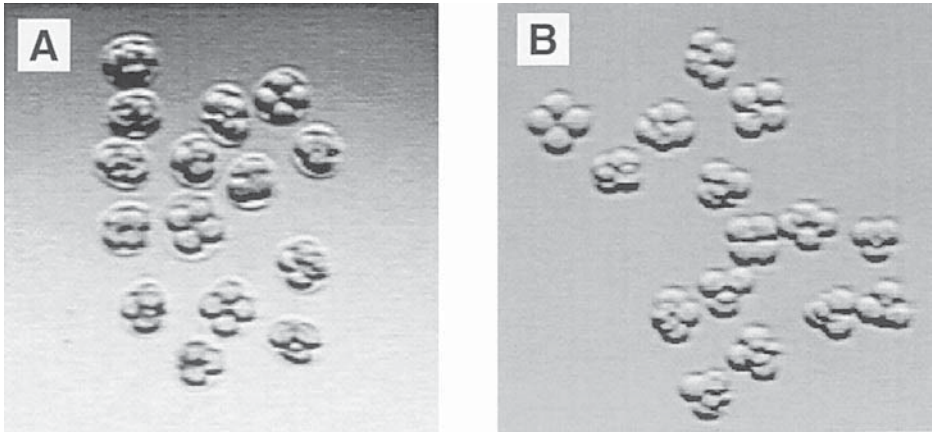

Fig. 3. Embryos. **(A)** before, and **(B)** after removing zona pellucida.

4. Aggregation: Small depressions are made with an aggregation needle in M16 microdrops on a 35-mm Petri dish. We make 5 to 25 microdrops in a dish and two depressions in a drop. Embryos in pairs or triplets are placed in the depressions, so that embryos contact each other. During incubation in a CO_2 incubator, embryos in each microwell are fused to each other, forming a single morula, which is matured into a blastocyst (**Fig. 4**). To monitor culture condition, several untreated embryos are cultured.

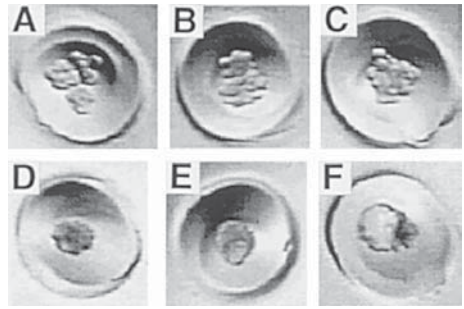

Fig. 4. Embryos during aggregation. **(A)** 0 h. **(B)** 12 h. **(C)** 24 h. **(D)** 36 h. **(E)** 48 h. **(F)** 60 h after starting aggregation.

5. Embryo transfer: After 58 h of culture, chimeric blastocysts are transferred into the uteri of pseudopregnant ICR females (2.5 d.p.c). Under the anesthesia of pentobarbital (0.6 mg/10g of body weight), the back skin is shaved and sterilized. Two small incisions are made in the skin above the ovaries. The ovary and fat around it are visible through the translucent muscle layer. An incision is made in muscle layer over the ovary. The fat pad around the ovary is pulled out so that the ovary, oviduct, and uterine horn are exposed and placed on the back. These are fixed by clamping the fat with a clip (serrefine). A small hole is made in the uterine wall with a 26-gage needle. A transfer pipet, in which 10 to 15 blastocysts are packed with a minimum volume of M2 medium, is inserted through the hole, and the embryos are transferred into the uterine cavity (**Fig. 5**). The process is repeated for the remaining uterine horn.
6. Efficiency: About 10 and 5 embryos are obtained from one ROSA and one *Agtr1a–/–* mouse with vaginal plugs, respectively. More than 90% of aggregated embryos develop into mature blastocysts. About 20–40% of mice are born. The ratio of ROSA cells are determined from coat color ranged from 0 to 99%. The mice, whose coat color ratio of ROSA is less than 30%, are suitable for analysis.

3.2. Findings

3.2.1. Studies on the Heart

Both myocytes and fibroblasts independently form areas that are randomly integrated into the heart. In the heart of *Agtr1a–/–↔ROSA* chimeric mice, each myocyte and vascular smooth muscle cell was either clearly stained for *lacZ* or completely negative. Fibroblasts are less clearly stained. The clonal distribution of myocytes and fibroblasts was independent. The distribution of AT1 receptor depicted by binding autoradiography using radiolabeled Ang II was coincided completely with that of ROSA myocytes. This indicates that most cardiac AT1 receptors reside in myocytes, not in fibloblasts, which is contrary to the previous in vitro findings ***(17)***.

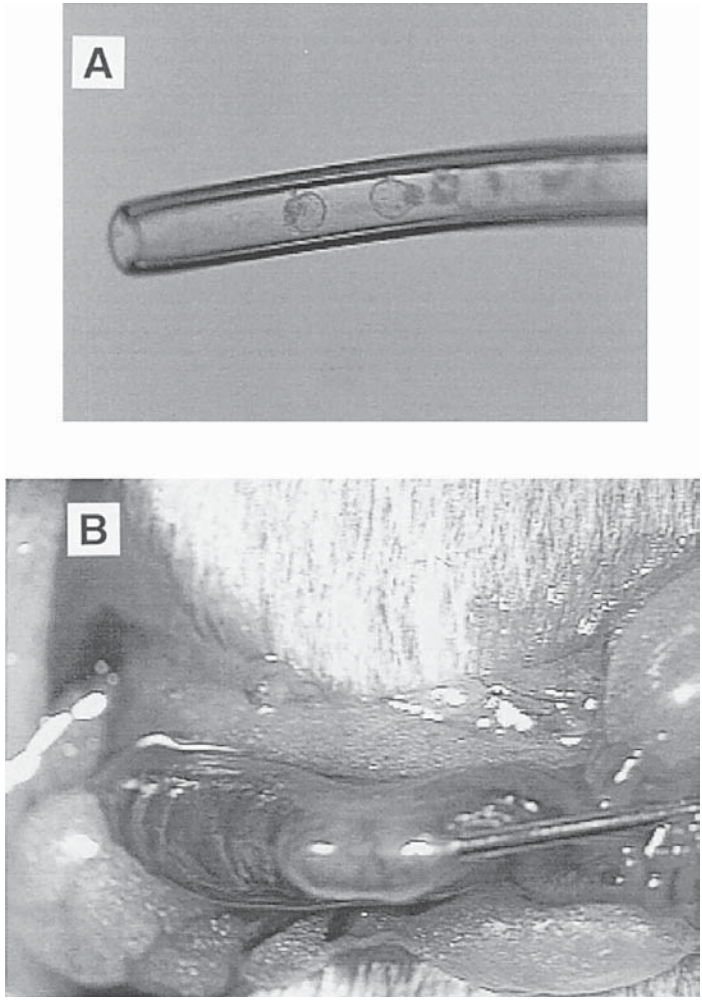

Fig. 5. Embryo transfer. **(A)** Embryos packed in a transfer pipet. **(B)** Making a small hole in uterine wall with a needle.

We next infused chronically Ang II (1 ng/min/g) for 2 wk using miniosmotic pumps. With the same treatment, wild-type mice or ROSA26 transgenic mice developed severe hypertension and extensive cardiac fibrosis, accentuated in perivascular regions, although *Agtr1a–/–* mice showed no hypertension and fibrosis. *Agtr1a–/–↔ROSA* showed mild to severe hypertension, depending on the ratio of ROSA cells. In most hearts, cardiac fibrosis was not observed, although ROSA fibroblasts were present in adjacent sections. To detect more subtle cardiac remodeling, proliferating fibroblasts were identified by bromo-

deoxyuridine (BrdU) staining. The BrdU incorporation was present predominantly in the areas adjacent to ROSA myocytes. This phenomenon was not observed in control chimeric mice *(Agtr1a+/+↔ROSA)*, which were made up of wild-type and ROSA cells, i.e., both carrying intact *Agtr1a*. These indicate that in response to Ang II, cardiac fibroblasts proliferate through the function of both *local* and *systemic* Ang II. Importantly, the local mechanism acting on fibroblasts is mediated by the AT1 receptor of neighboring *cardiomyocytes*, indicating that a communication between myocytes and fibroblasts plays an important role during Ang II-dependent cardiac remodeling ***(18)***.

3.2.2. Studies on the Vasculature

We analyzed the aortic vascular smooth muscle cells (VSMCs) of the same chimeric mice used in the above experiment. The BrdU incorporation in VSMCs was very low (3.5 ± 2.3%) in the mice with mild hypertension ($n = 3$), and high (26.0 ± 6.5%) in the moderately hypertensive mice ($n = 3$). Importantly, when *Agtr1a–/–* and ROSA VSMCs were compared within the same chimeric mouse, BrdU incorporation was not different. In control chimeric mice *(Agtr1a+/+↔ROSA)*, which developed severe hypertension, BrdU incorporation in VSMCs were high (28.0 ± 10.3%). Among all chimeric mice, i.e., both *Agtr1a–/–↔ROSA* and *Agtr1a+/+↔ROSA*, BrdU positivity ratio in VSMCs of the thoracic aorta was correlated with blood pressure ($R = 0.767$, $p < 0.01$).

Therefore, local stimulation of AT1 receptor by systemic Ang II induces no DNA synthesis in VSMCs. Instead, systemic factor(s) have a major role for VSMC proliferation induced by chronic exposure to systemic Ang II.

3.2.3. Studies on the Adrenal Gland

We also studied the adrenal gland in chimeric mice infused with Ang II. Previously, it was understood that Ang II increases both aldosterone synthesis, the enzyme catalyzing the rate-limiting step for aldosterone synthesis, and induces mitogenesis in zona glomerulosa (ZG) cells. When *Agtr1a–/–* and ROSA in ZG cells were compared within the same chimeric mice, BrdU incorporation is suppressed specifically in ROSA cells. In separate wild-type mice, Ang II given chronically was shown to suppress BrdU incorporation in a dose-dependent manner. During dietary sodium restriction, plasma aldosterone level increased and the number of ZG cells dramatically increased over time. Thus, ZG cells markedly proliferate over time during chronic ECF volume depletion. The direct effect of Ang II on ZG cell proliferation during this time frame is inhibitory. The results attest to the functional significance of non-Ang II mechanisms for the enhancement of aldosterone secretion during the transition from acute to chronic phase of ECF volume depletion.

4. Generation of *Agtr1a–/–↔+/+* Chimeric Mice by Injecting *Agtr1a–/–* ES Cells into Agtr1a+/+ Blastocysts

4.1. Materials

1. *Agtr1a*+/– ES cells
2. Hygromycin resistant feeder cells; NHL-7 (kind gift from Dr. H. Kondo, Osaka University, Osaka, Japan; **ref. *19***)
3. An *Agtr1a* targeting vector containing the hygromycin resistant gene *(Hgr)*.
4. Hygromycin B (Sigma Chemical Co.)
5. Geneticin (Sigma Chemical Co.)
6. Gancyclovir (Syntex Inc., Palo Alto, CA)
7. ES cell medium [Dulbecco's modified Eagle's medium (DMEM) supplemented with 17% fetal calf serum (Gibco-BRL Products)]
8. The system for microinjection
   a. Micromanipulators
   b. Inverted fixed-stage microscope
   c. Cooling stage and injection chamber for microscope
9. Blastocysts of C57BL/6 strain
10. Pseudopregnant ICR females

4.2. Method

1. Introducing a second mutation in *Agtr1a*+/– ES cells: We constructed a second *Agtr1a* targeting vector containing *Hgr*. In this second construct, a reporter gene, *LacZ*, was also incorporated so that the mutated cells with *Agtr1a* promoter activity can be identified. One clone of *Agtr1a*+/– ES was expanded, electropolated with the second targeting vector, selected in medium containing hygromycin B (0.1 mg/mL), gancyclovir (2 μ*M*), and geneticin (0.4 mg/mL) for 9 d on the layer of irradiated NHL-7 cells.
2. Blastocyst injection: The *Agtr1a–/–* ES cells obtained were injected into blastocysts from wild-type C57BL/6 mice. The efficiency of generating Agtr1a–/–↔+/+ chimeric mice was similar to that for Agtr1a–/+↔+/+ chimeric mice. Also, the degree of chimerism determined by coat color similarly ranged from 0 to 99%. Both mutations were transmitted to germline. Chimeric mice obtained are subjected to the experiments, and the germline transmission of the mutant genes is not necessary.

4.3. Findings

The renin–angiotensin system is under the control of a negative-feedback regulation that involves the renin-secreting cells of juxtaglomerular (JG) apparatuses. Because JG cells are rich in AT1 receptors, it is believed that the feedback is driven, among others, by a direct angiotensin-AT1 receptor interaction at the level of JG cells. Although results from in vitro studies are consistent with this hypothetical local mechanism, its significance in vivo has not been validated.

The JG cells of *Agtr1a–/–* mice were markedly enlarged with intense expression of renin mRNA and protein. Within a given chimeric *Agtr1a–/–*↔*+/+* mouse, the expression of renin mRNA and the protein was similar between *Agtr1a+/+* and *Agtr1a–/–* JG cells, which were distinguished by the lacZ gene expression. In *Agtr1a–/–*↔*+/+* with small contribution of *Agtr1a–/–* cell, which were hypotensive, both types of JG cells were hypertrophic. The quantity of renin mRNA and protein was comparable between these two clones of cells even in animals placed on low sodium diet, a condition known to increase renin. These results indicate that the local interaction between And II and AT1 receptors on the JG cells in vivo has little functional contribution to the feedback regulation of JG renin synthesis.

Acknowledgments

The authors thank Mary Lee Jones and Dr. Toshio Homma for editorial assistance.

References

1. Niimura, F., Labosky, P. A., Kakuchi, J., Okubo, S., Yoshida, H., Oikawa, T., et al. (1995) Gene targeting in mice reveals a requirement for angiotensin in the development and maintenance of kidney morphology and growth factor regulation. *J. Clin. Invest.* **96,** 2947–2954.
2. Okubo, S., Niimura, F., Nishimura, H., Takemoto, F., Fogo, A., Matsusaka, T., and Ichikawa, I. (1997) Angiotensin-independent mechanism for aldosterone synthesis during chronic extracellular fluid volume depletion. *J. Clin. Invest.* **99,** 855–860.
3. Matsusaka, T., Nishimura, H., Utsunomiya, H., Kakuchi, J., Niimura, F., Inagami, T., et al. (1996) Chimeric mice carrying 'regional' targeted deletion of the angiotensin type 1A receptor gene. *J. Clin. Invest.* **98,** 1867–1877.
4. Tsuchida, S., Matsusaka, T., Chen, X., Okubo, S., Niimura, F., Nishimura, H., et al. (1998) Murine double nullizygotes of the angiotensin type 1A and 1B receptor genes duplicate severe abnormal phenotypes of angiotensin nullizygotes. *J. Clin. Invest.* **101,** 755–760.
5. Chen, X., Li, W., Yoshida, H., Tsuchida, S., Nishimura, H., Takemoto, F., et al. (1997) Targeting deletion of angiotensin type 1B receptor gene in the mouse. *Am. J. Physiol.* **272,** F299–304.
6. Ichiki, T., Labosky, P. A., Shiota, C., Okuyama, S., Imagawa, Y., Fogo, A., et al. (1995) Effects on blood pressure and exploratory behaviour of mice lacking angiotensin II type-2 receptor. *Nature* **377,** 748–750.
7. Esther, C. R., Jr., Howard T. E., Marino, E. M., Goddard, J. M., Capecchi, M. R., and Bernstein, K. E. (1996) Mice lacking angiotensin-converting enzyme have low blood pressure, renal pathology, and reduced male fertility. *Lab. Invest.* **74,** 953–965.
8. Gu, H., Marth, J. D., Orban, P. C., Mossmann, H., and Rajewsky, K. (1994) Deletion of DNA polymerase β gene segment in T cells using cell type-specific gene targeting. *Science* **265,** 103–106.

9. Rajewsky, K., Gu, H., Kühn, R., Betz, U. A. K., Müller, W., Roes, J., and Schwenk, F. (1996) Molecular medicine in genetically engineered animals. Conditional gene targeting. *J. Clin. Invest.* **98,** 600–603.
10. Mortensen, R. M., Conner, D. A., Chao, S., Geisterfer, L. A., and Seidman J. G. (1992) Production of homozygous mutant ES cells with a single targeting construct. *Mol. Cell. Biol.* **12,** 2391–2395.
11. Mortensen, R. M. and Seidman J. G. (1994) Inactivation of G-protein genes: double knockout in cell lines. *Methods Enzymol.* **237,** 356–366.
12. Wood, S. A., Allen, N. D., Possant, J., Auerbach, A., and Nagy, A. (1993) Non-injection methods for the production of embryonic stem cell-embryo chimaeras. *Nature* **365,** 87–89.
13. Wood, S. A., Pascoe, W. S., Schmidt, C., Kemler, R., Evans, M. J., and Allen, N. D. (1993) Simple and efficient production of embryonic stem cell-embryo chimeras by coculture. *Proc. Natl. Acad. Sci. USA* **90,** 4582–4585.
14. Pirity, M., Hadjantonakis, A., and Nagy, A. (1998) Embryonic stem cells: creating transgenic animals. *Methods Cell Biol.* **57,** 279–293.
15. Friedrich, G. and Soriano, P. (1991) Promoter traps in embryonic stem cells: a genetic screen to identify and mutate developmental genes in mice. *Genes Dev.* **5,** 1513–1523.
16. Zambrowicz, B. P., Imamoto, A., Fiering, S., Herzenberg, L. A., Kerr, W. G., and Soriano, P. (1997) Disruption of overlapping transcripts in the ROSA beta geo 26 gene trap strain leads to widespread expression of beta-galactosidase in mouse embryos and hematopoietic cells. *Proc. Natl. Acad. Sci. USA* **94,** 3789–3794.
17. Villarreal, F. J., Kim, N. N., Ungab, G. D., Printz, M. P., and Dillmann, W. H. (1993) Identification of functional angiotensin II receptors on rat cardiac fibloblasts. *Circulation* **88,** 2849–2861.
18. Matsusaka, T., Katori, H., Inagami, T., Fogo, A., and Ichikawa, I. (1999) Communication between myocytes and fibroblasts in cardiac remodeling in angiotensin chimeric mice. *J. Clin. Invest.* **103,** 1451–1458.
19. Sawai, S., Shimono, A., Hanaoka, K., and Kondoh, H. (1991) Embryonic lethality resulting from disruption of both N-myc alleles in mouse zygotes. *New Biol.* **3,** 861–869.

4

Genetic Manipulation of the Renin–Angiotensin System Using Cre-loxP-Recombinase

Curt D. Sigmund and David E. Stec

1. Introduction

The advent of gene-targeting technology in embryonic stem cells has provided an important tool for the dissection of complex biological systems by allowing investigators to generate germ line mutations in selected genes. Since the introduction of this technology in the early 1980s, hundreds of genes have been targeted for systemic deletion (knocked out), including each gene of the renin–angiotensin system (RAS). Although the technique is very powerful, there are weaknesses that limit its usefulness for studying the RAS. For example, systemic deletion of several of the RAS genes leads to a phenotype, of varying severity depending on the gene in question, in which the mice succumb to severe renal lesions and ultimately die before the age of weaning. This is observed in angiotensinogen (Agt–/–), angiotensin-converting enzyme (ACE–/–), and combined angiotensin receptor subtype 1A and 1B (At1a–/–, At1b–/–) deficient "knockout" mice ***(1–5)***. Mice deficient in At1a, but wild type at the At1b locus, are phenotypically normal on mixed genetic backgrounds, but exhibit the same renal lesions and reduced mortality when bred onto "pure" genetic backgrounds, suggesting that renal morphology in response to Ang-II may be under some complex genetic control ***(6)***. Presumably, Ang-II is required during the early neonatal period for the continued development of the kidney, and the mice die if they are unable to either generate or utilize Ang-II during this period.

An additional complication of classical gene targeting is that even if the mice survive, the observed phenotype is caused by the loss of gene function in

From: *Methods in Molecular Medicine, vol. 51: Angiotensin Protocols*
Edited by: D. H. Wang

every cell of the body. In the case of angiotensinogen, a gene expressed in a variety of different cell types of diverse embryonic origin, it can be difficult to assess the physiological significance of its expression in a specific cell and tissue when the gene is eliminated from all cells and tissues. In cases like this, the generation of a cell-specific knockout would become very attractive. A cell-specific knockout of angiotensinogen would provide an ideal opportunity to assess its physiological function in specific cell types, such as renal proximal tubule cells, hepatocytes, adipocytes, glia, and neurons *(7,8)*.

1.1. Introduction to the Cre-loxP Recombinase System

Generating a loss of function knockout relies on recombination between two segments of DNA and results in the replacement or deletion of a critical portion of the gene, rendering it nonfunctional. This type of recombination can occur by two means: (1) homologous recombination; or (2) site-specific recombination. Although traditional gene targeting utilizes the former, tissue-specific knockouts use the latter. Site-specific recombination relies upon the integration of recognition sites for a sequence-specific recombinase enzyme within the gene of interest. Two such recombinase systems, Cre-loxP and Flp-frt, have been described in detail *(9)*. We will only discuss the cre-loxP system herein.

Cre-recombinase is a 38,500-Da protein capable of catalyzing site-specific recombination at 34 bp DNA sequences termed loxP (locus of recombination), and does not require cofactors or other bacterial proteins. It is derived from the bacteriophage P1, which uses the system during DNA replication and packaging. When two loxP sites are present in circular DNA, cre-mediated recombination results in the formation of two separate circles, each containing a single loxP site (**Fig. 1**). One circle contains the DNA outside the loxP sites, whereas the second circle contains the DNA lying between the loxP sites. When two loxP sites are present in genomic DNA, cre-mediated recombination results in a deletion of DNA lying between two loxP sites and the formation of a circular intermediate containing one loxP site and the intervening sequence (**Fig. 1B**). Because these circles lack an origin of replication, they are either lost when the cell replicates and divides, or are degraded, leaving behind only the altered genome.

The generation of a tissue-specific knockout requires two general steps. The first is to "flox," or introduce loxP sites, into a gene of interest. This is accomplished by gene targeting in embryonic stem cells using methodology similar to that required for a systemic knockout *(10)*. The loxP sites are strategically placed into introns surrounding an exon encoding an important region of the protein (as in **Fig. 1B**). Consequently, in the absence of cre-recombinase, the gene will be transcribed and translated normally. However, in the presence of cre-recombinase, a deletion will occur in genomic DNA thus eliminating the

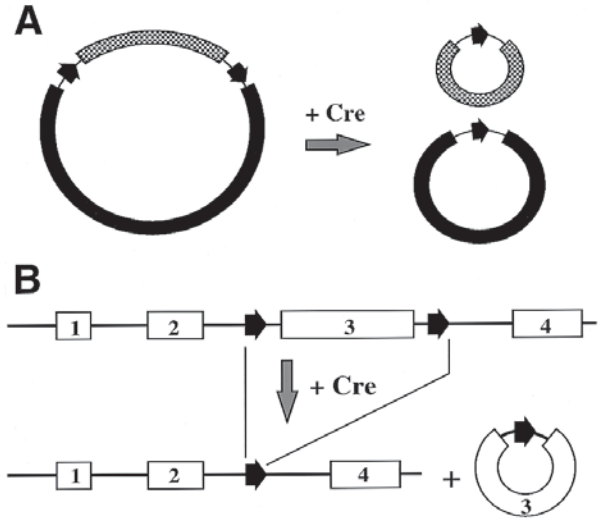

Fig. 1. Function of Cre-recombinase. Cre-recombinase catalyzes the recombination between two loxP sites. When present in circular DNA, cre-recombinase resolves the structure into two separate circles **(A)**. When present in linear DNA, cre-recombinase resolves the structure into a linear, internally deleted DNA and a circular intermediate which will be lost **(B)**.

critical exon and its protein coding potential. We will not discuss the specific details of gene targeting in ES cells as excellent reviews on the subject are available ***(11,12)***.

The second step requires the expression of Cre-recombinase in a tissue-specific manner. Generally, this is accomplished by expressing cre-recombinase from a tissue- and cell-specific promoter in transgenic mice. Numerous cre-recombinase mice have been generated or are in the process of being generated, and a database of these mice is accessible over the internet (http://www.mshri.on.ca/nagy/Cre.htm). An animal containing both a floxed gene and tissue-specific cre-recombinase will exhibit tissue-specific recombination and a deletion of DNA lying between the loxP sites (**Fig. 2**). We have recently reported some of the technical details on generating a cell-specific knockout in the kidney ***(8)***. The use of a cell-specific promoter provides an element of spatial control over cre-recombinase expression that is critical in cell-specific knockout experiments. In addition, some element of cell-specificity or region-specificity can be obtained by delivery of cre-recombinase using viral vectors ***(13–15)***. For example, we and others have reported that adenoviral delivery of cre-recombinase is very effective for generating a liver-specific deletion *(see below)* ***(7,16)***.

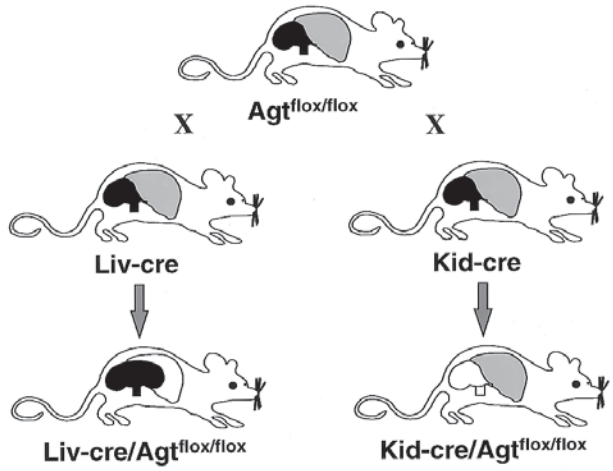

Fig. 2. Generation of experimental models. In this example, a floxed angiotensinogen gene ($AGT^{flox/flox}$) is bred with a mouse expressing cre-recombinase from a liver-specific promoter (Liv-cre) or a kidney-specific promoter (Kid-cre). Expression of Agt in the liver and kidney is normal in the starting $AGT^{flox/flox}$ or Liv-cre and Kid-cre mice. However, there is no Agt expression in the liver of the Liv-cre/$AGT^{flox/flox}$ mice and no expression in the kidney of the Kid-cre/$AGT^{flox/flox}$ mice. Agt expression in the liver and kidney is indicated by the gray and black shading, respectively.

1.2. Applications of the Cre-loxP Recombinase System

The Cre-loxP recombinase system has been used as an effective tool to target tissue-specific genetic alterations in vivo that result in either gene activation or inactivation. An investigator may employ a gene activation strategy when early expression of the gene product of interest causes developmental defects, lethality, or some other unwanted phenotype, or if a genetic time course experiment is desired. In gene activation, a transgene is designed in which a gene is placed under the control of a tissue-specific promoter. However, between the promoter and gene is a sequence termed "STOP," which contains transcriptional termination signals (**Fig. 3**). The STOP signal is surrounded by loxP sites. In the absence of cre-recombinase, transcripts initiating at the promoter are terminated before entering the protein coding portion of the construct. In the presence of cre-recombinase, the STOP signal is eliminated and the transgene is activated. This type of temporal control over gene activation was employed by Lakso et al. ***(17)*** to study tumorigenesis in the lens of the eye. Other examples of cre-mediated gene activation have been reported ***(18)***. It is important to stress that in this model, gene activation mediated by cre-recombinase is essentially irreversible and therefore a permanent alteration.

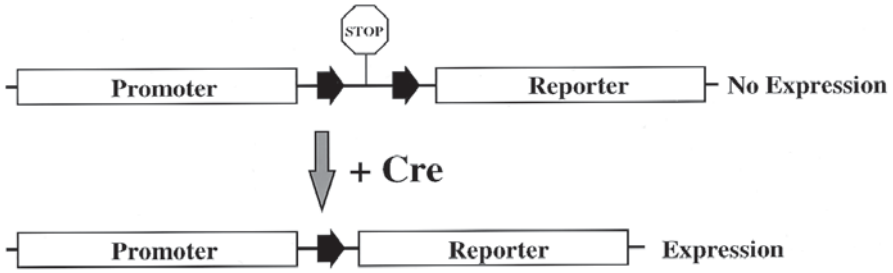

Fig. 3. Schematic of Cre-recombinase-mediated gene activation. The top construct diagrams the expression of a reporter construct such as β*gal* or luciferase under the control of a cell-specific promoter. Transcripts initiating at the promoter are blocked by the "STOP" sequence. In the presence of cre-recombinase, the STOP signal is deleted and expression of the construct is induced.

Gene activation via cre-recombinase also forms the basis for a variety of cre-reporter systems that have been recently developed to provide a rapid and easy screen for cell-specific expression and function of cre-recombinase. In one example, expression of a floxed β-*gal* gene is under the control of a ubiquitous promoter that is active in all cell types, and expressed both throughout development and in adults ***(19)***. Upon exposure to cre-recombinase, the first reporter gene, β-*gal*, is deleted and replaced with a second reporter gene, human alkaline phosphatase. The precise spatial- and temporal-expression of cre-recombinase can be determined by breeding a cre-containing mouse with the double reporter-containing mouse. Both expression and the recombination function of cre-recombinase can then be easily scored by comparing the cell-specific expression of β-*gal* and alkaline phosphatase in a tissue. Other reporter systems based on similar construct designs have been reported ***(20)***.

The second and most popular use of the cre-loxP recombinase system for generating mouse models is cell-specific gene inactivation. The first reported cre-mediated cell-specific knockout was of the DNA polymerase β gene in T cells ***(10)***. Since then, the system has seen increasing use as a genetic tool to dissect complex biologic systems in vivo. Indeed, gene knockouts have been generated specifically in the pyramidal cells of the hippocampus ***(21)***, pancreatic β-cells ***(22)***, skeletal muscle ***(23)***, hepatocytes ***(7,16)***, and cardiac ventricular myocytes ***(24)***. A system to generate an inducible liver-specific knockout has also been described ***(25)***.

1.3. Using the Cre-loxP Recombinase System to Study the RAS

We previously described a mouse model of hypertension in which the human renin and human angiotensinogen genes are coexpressed in a double transgenic

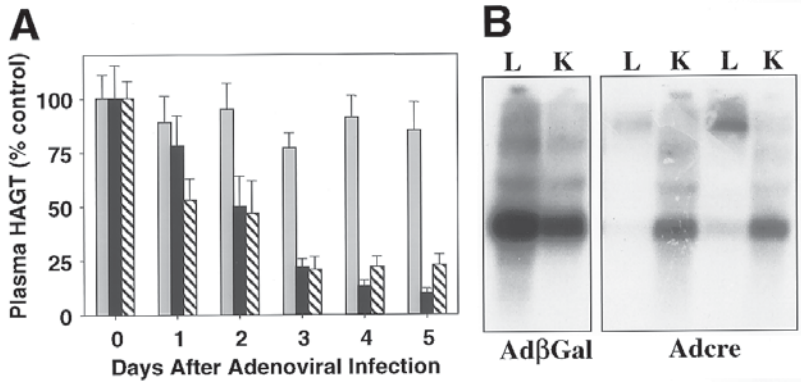

Fig. 4. Liver-specific knockout of a floxed human AGT transgene. **(A)** Levels of circulating human AGT protein (as % of control) before (day 0) or 1–5 d after infection with Adβ*gal* (gray bars) or Adcre (filled and crosshatched bars). The filled and crosshatched bars represent two different lines of human AGT^{flox} mice. **(B)** Expression of human AGT was scored in the liver (L) and kidney (K) by Northern blot in human AGT^{flox} mice infected with either Adβ*gal* or Adcre.

mouse ***(26)***. Recent genetic and pharmacologic studies revealed that activation of the RAS in the kidney and central nervous system may participate in the pathogenesis of hypertension in this model ***(27,28)***. To begin to dissect the contribution of tissue RAS systems in the pathogenesis of hypertension, we generated a new transgenic mouse model containing a human angiotensinogen genomic construct in which exon II, encoding the Ang-I and Ang-II peptides, is flanked by loxP sites ***(7)***. Expression of this transgene is essentially identical to the expression of a native human angiotensinogen transgene lacking loxP sites ***(29)***. Two lines of mice, one with modest levels (11 ± 2 μg/mL) and one with high levels (237 ± 18 μg/mL) of circulating human angiotensinogen were studied in detail. In order to deliver Cre, we constructed an adenoviral vector expressing Cre-recombinase from a strong viral promoter. Reduced levels of circulating human angiotensinogen protein (**Fig. 4A**), hepatic human angiotensinogen mRNA (**Fig. 4B**) and protein, and a marked blunting of the pressor response to infused human renin was observed in all mice that received the cre-containing adenovirus ***(7)***. All the data are consistent with the liver-specific pattern of cre-expression observed after systemic adenoviral infection. These data have provided the important proof-of-principle that the cre-loxP recombinase system can be used to study the importance of the renin–angiotensin system and experiments are in progress to express cre-recombinase specifically in the kidney, vasculature and central nervous system, among other tissues. In addition, experiments are now in progress to flox the endogenous

mouse angiotensinogen gene to assess its role in the regulation of organ development and baseline arterial pressure.

2. Materials

2.1. Floxing the Target Gene

1. Cell lines: Embryonic stem cells and neomycin resistant embryonic fibroblasts isolated from neomycin transgenic mice (The Jackson Laboratory, Bar Harbor, ME).
2. Cell culture reagents ***(30)*** including G418 (Gibco, Grand Island, NY) and gancyclovir (University of Iowa Hospital Pharmacy).
3. Plasmid vectors and reagents for standard recombinant DNA manipulations.
4. LoxP sites either present in a plasmid vector or cloned using oligonucleotides. The sequence of the loxP site is: ATAACTTCGTATAATGTATGCTATACGAAGTTAT.
5. Standard reagents for PCR and Southern blot analysis ***(31)***.

2.2. Generation of Cre Transgenic Mice

1. Cre-recombinase constructs ***(10,32)***.
2. Cell-specific promoter(s).
3. Tetracycline or ecdysone inducible promoter systems (Clontech, Palo Alto, CA and Stratagene, La Jolla, CA).

2.3. Development and Characterization of Cre-loxP Models

1. Gene$^{flox/+}$ mice from **step 2.1.**
2. Cell-specific promoter–cre-recombinase transgenic mice from **step 2.2.**
3. Equipment and reagents for PCR, Southern blots, and assays of gene and protein expression.

3. Methods

3.1. Floxing the Target Gene

A discussion of each aspect of ES cell culture and manipulation are beyond the scope of this chapter and are described in detail elsewhere ***(30)***. Instead, we will focus on technical details that distinguish standard gene targeting approaches for generation of a knockout with those required for the cre-loxP system.

1. The first step in generating a cell-specific knockout by the cre-loxP system is to "flox" the gene of interest. In other words, insert loxP sites surrounding an important coding exon(s) of the gene. In the case of angiotensinogen, the second exon was chosen because it encodes the translation initiation codon, the secretory peptide, the Ang I and Ang II peptides, and most of the remaining coding region. In other genes, exactly which exon or exons are chosen will depend upon the protein in question. However, it may be attractive to try to identify a region of the protein that is critical for its function and flox the exons encoding that region. Such motifs may include those signaling secretion or intracellular trafficking, interactions with other proteins or DNA, membrane spanning domains, and active sites of enzymes (*see* **Note 1**).

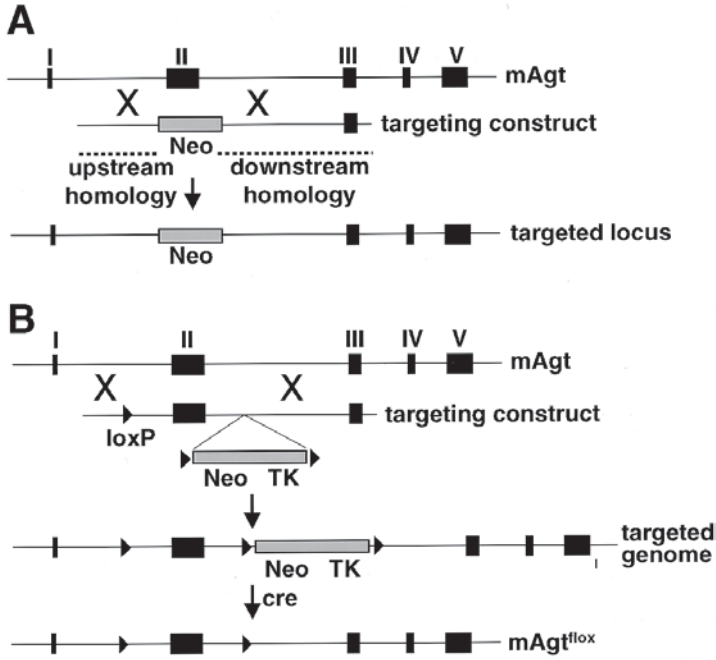

Fig. 5. Schematic of targeting vectors. A schematic representation of a standard targeting **(A)** or floxing **(B)** vector is shown. The selection cassettes are indicated by the gray boxes, exons by black boxes, and introns by thin black lines.

2. Arguably the most important step in any gene targeting experiment is the design and construction of the targeting construct. All gene-targeting constructs consist of: (1) an upstream homology; (2) a selectable marker (generally the neomycin resistance gene); and (3) a downstream homology (**Fig. 5A**). The upstream and downstream homologies provide the anchor sequences necessary for a successful recombination event to occur in ES cells, and the selectable marker is used for selection of transformants. It is critical to recognize that a classical knockout essentially renders the gene inactive in all cells, whereas in a tissue-specific knockout, the target gene must remain fully functional (in the absence of cre-recombinase). Therefore, there are some characteristic differences in the targeting construct used for these purposes. In addition to the elements discussed above, a floxing construct must contain two additional segments. First, it is necessary to insert, between the upstream homology and selection cassette, the actual region of the gene to be floxed (*see* **Fig. 5B**). The second is an expansion of the selectable marker cassette to include both a positive selection for transformants (as above), and also a second gene designed for negative selection (discussed below) (*see* **Note 2**).
3. The final targeting construct is linearized and transfected into ES cells via electroporation as described in detail elsewhere ***(30)***. Transformants are selected

for resistance to G418 (neomycin selection) and are then screened for homologous recombination at the target locus using PCR or Southern blots. It is often attractive to screen a large number of colonies first by PCR and then confirm appropriate gene targeting by Southern blot analysis. Correctly targeted clones have the exon of choice flanked by loxP sites, but also contain the selection cassette. Because the selection cassette can ultimately effect the expression of the target gene, it must be removed. This can be accomplished by transient transfection with a cre-recombinase expression vector and using the second marker for selection. Most often, this selectable marker is the herpes simplex virus thymidine kinase (TK) gene, which renders the cells sensitive to the antiviral agent gancyclovir. Cells retaining the selection cassette will be killed by gancyclovir (selected against) while these eliminating the cassette will grow in its presence. It is important to recognize that the final targeted locus looks identical to the starting locus except for the insertion of loxP sites (**Fig. 5B**) (*see* **Note 3**).

4. The final targeted ES cells are microinjected into mouse blastocysts for the generation of a chimeric mice as described elsewhere ***(30)***. The characterization of the chimera, germ line transmission, and establishment of transgenic lines is the same as a classical knockout experiment and therefore will not be described further (*see* **Note 4**).

3.2. Generation of Cre Transgenic Mice

1. The spatial- and temporal-selectivity of the cre-recombinase reaction is controlled by the generation of transgenic mice expressing cre-recombinase from a promoter with the appropriate cell-specific and temporal expression characteristics. Standard recombinant DNA methodology is used to generate a fusion construct consisting of the selected cell-specific promoter and cre-recombinase. Two "flavors" of cre-recombinase are commonly available. The first is the wild-type P1 phage cre-recombinase originally developed by Dr. Brian Sauer and the second is a modified form of the protein including a nuclear targeting signal designed to increase transport to the nucleus, the intracellular site of action of cre-recombinase ***(10,32)***.
2. The choice of promoter used to drive expression of cre-recombinase will depend upon the desired cell type to be targeted. In this regard, appropriate consideration must be paid to the spectrum of cells where the promoter is active, and the time during development, neonatal life, or adulthood when the promoter is activated. For example, if a cell-specific knockout is desired to avoid a lethal phenotype caused by the absence of the gene product during development, one must choose a promoter that is not expressed until that "temporal window" has passed. The development of inducible and ligand-regulated promoter systems also provides an element of temporal and spatial control over cre-recombinase expression ***(25,33–36)***.
3. A database of transgenic mice expressing cre-recombinase in a tissue-specific and cell-specific fashion is accessible over the internet (http://www.mshri.on.ca/nagy/Cre.htm) and some cre mice are available from the Jackson Laboratory Induced Mutant Resource (http://www.jax.org/resources/documents/imr/).

3.3. Development and Characterization of Cre-loxP Models

1. The next step is to combine the above mice into a single model. This is most easily accomplished by breeding the mice containing the floxed gene with mice expressing cre-recombinase. The compound heterozygotes (gene$^{flox/+}$ X promoter-cre) can then either be interbred or backcross bred back to the floxed mice to obtain the final model (gene$^{flox/flox}$ X promoter-cre). These mice should exhibit a cell-specific knockout of the floxed gene based on the cell-specific and temporal characteristics of the promoter chosen to drive cre-recombinase (*see* **Note 5**).
2. Before assessing the pathophysiological characteristics of the mice, they should be analyzed to assess the efficiency of the cell-specific knockout. This is a critical step as some promoters, although able to target a specific type of cell, will exhibit a mosaic or "variegated" pattern of expression. Variegation occurs when the promoter targets expression of cre-recombinase to the correct cell types, but not to 100% of those cells. The cells lacking cre-recombinase would not undergo a recombination event and therefore would still express the floxed gene. Because of this, it is attractive to first breed the cre-recombinase mice with one of the reporter systems aforementioned above to determine the level of variegation exhibited by the promoter ***(19,20)***. Presumably, variegated activity of the promoter is caused by the absence of some important regulatory elements controlling expression of the gene. To avoid this, Chen et al. ***(24)*** used a gene-targeting knock-in procedure to insert the cre-recombinase gene downstream of the MLC-2v promoter in the genome. They did this assuming that all regulatory elements needed for correct targeting of ventricular myocytes would be present if cre-recombinase were inserted directly into the genome downstream of the promoter. Although the strategy requires an additional gene-targeting step, it has the advantage of not requiring experimental data on the location of elements required for appropriate promoter function.
3. Determining the efficiency of cell-specific recombination can be accomplished using a host of standard assays of gene expression. Expression of the mRNA can be scored by Northern blot, RNase protection, RT-PCR, or *in situ* hybridization, whereas the presence of the protein can be scored by Western blot, enzymatic assay, or immunohistochemistry, among many others. The efficiency of recombination at the tissue level can also be determined by Southern blot analysis. We used each of these methods to demonstrate the high efficiency of liver-specific knockout caused by expression of cre-recombinase after adenoviral infection with Adcre ***(7)***.

4. Notes

1. Technically, the main problems encountered are in floxing the target gene. Manipulations in ES cells can be tricky and some loci in the genome are easier to target than others.
2. The absence of a negative selection in the initial transfection step may require the screening of many G418 resistant colonies. In the initial transfection, sufficient numbers of clones should be analyzed to increase the chances of detecting a homologous recombination event.

3. A difficulty may arise when removing the selection cassette from the targeted locus. Because the genome has three loxP sites (two surrounding the floxed portion of the gene, and two surrounding the selection cassette) it can be difficult to obtain the final targeted locus as transfection with cre-recombinase may cause an elimination of both segments (**Fig. 5**). A PCR-based or Southern blot strategy should be designed to distinguish between a complete deletion (of both floxed segments) and a deletion of the selection cassette alone.
4. It is important to note that ES cells that contain a deletion of both segments can be used to generate a complete null mutation for the gene in all tissues and cells.
5. Tissue-specific gene targeting requires a highly efficient cell-specific removal of the floxed gene by cre-recombinase. As aforementioned, this reaction is not always 100% efficient because of variegated expression of cre-recombinase. When using mice homozygous for the floxed allele ($gene^{flox/flox}$), two independent recombination events must occur per cell to generate a homozygous knockout ($gene^{-/-}$). The efficiency may be improved by requiring only a single recombination event per cell. This can be achieved by using mice containing one floxed allele and one null allele ($gene^{flox/-}$). This mouse can be generated by altering the breeding scheme discussed above by breeding the $gene^{flox/+}$ with $gene^{+/-}$. The null allele can be obtained by standard gene targeting or by using the null ES cells obtained after transfection with cre-recombinase. Of course, it remains possible that deletion of even a single copy of a gene will have some detrimental phenotype.

References

1. Kim, H. S., Krege, J. H., Kluckman, K. D., Hagaman, J. R., Hodgin, J. B., Best, C. F., et al. (1995) Genetic control of blood pressure and the angiotensinogen locus. *Proc. Natl. Acad. Sci. USA* **92,** 2735–2739.
2. Davisson, R. L., Kim, H. S., Krege, J. H., Lager, D. J., Smithies, O., and Sigmund, C. D. (1997) Complementation of reduced survival, hypotension and renal abnormalities in angiotensinogen deficient mice by the human renin and human angiotensinogen genes. *J. Clin. Invest.* **99,** 1258–1264.
3. Niimura, F., Labosky, P. A., Kakuchi, J., Okubo, H., Yoshida, T., Oikawa, T., et al. (1995) Gene targeting in mice reveals a requirement for angiotensin in the development and maintenance of kidney morphology and growth factor regulation. *J. Clin. Invest.* **96,** 2947–2954.
4. Tsuchida, S., Matsusaka, T., Chen, X., Okubo, S., Niimura, F., Nishimura, H., et al. (1998) Murine double nullizygotes of the angiotensin type 1A and 1B receptor genes duplicate severe abnormal phenotypes of angiotensinogen nullizygotes. *J. Clin. Invest.* **101,** 755–760.
5. Oliverio, M. I., Kim, H. S., Ito, M., Le, T., Audoly, L., Best, C. F., et al. (1998) Reduced growth, abnormal kidney structure, and type 2 (AT2) angiotensin receptor-mediated blood pressure regulation in mice lacking both AT1A and AT1B receptors for angiotensin II. *Proc. Natl. Acad. Sci. USA* **95,** 15,496–15,501.
6. Oliverio, M. I., Best, C. F., Smithies, O., and Coffman, T. M. (1997) A severe kidney phenotype in AT1A receptor-deficient mice. *J. Am. Soc. Nephrol.* **8,** 406A (Abstr.).

7. Stec, D. E., Davisson, R. L., Haskell, R. E., Davidson, B. L., and Sigmund, C. D. (1999) Efficient liver-specific deletion of a floxed human angiotensinogen transgene by adenoviral delivery of cre-recombinase in vivo. *J. Biol. Chem.* **274,** 21,285–21,290.
8. Stec, D. E. and Sigmund, C. D. (1998) Modifiable gene expression in kidney: kidney-specific deletion of a target gene via the cre-loxP system. *Exp. Nephrol.* **6,** 568–575.
9. Kilby, N. J., Snaith, M. R., and Murray, J. A. H. (1994) Site-specific recombinases: tools for genome engineering. *Trends Genet.* **9,** 413–421.
10. Gu, H., Marth, J. D., Orban, P. C., Mossman, H., and Rajewsky, K. (1994) Deletion of a DNA polymerase beta gene segment in T cells using cell type-specific gene targeting. *Science* **265,** 103–106.
11. Bronson, S. K. and Smithies, O. (1994) Altering mice by homologous recombination using embryonic stem cells. *J. Biol. Chem.* **269,** 27,155–27,158.
12. Capecchi, M. R. (1989) Altering the genome by homologous recombination. *Science* **244,** 1288–1292.
13. Wang, Y., Krushel, L. A., and Edelman, G. M. (1996) Targeted DNA recombination in vivo using an adenovirus carrying the cre recombinase gene. *Proc. Natl. Acad. Sci. USA* **93,** 3932–3936.
14. Anton, M. and Graham, F. L. (1995) Site-specific recombination mediated by an adenovirus vector expressing the Cre recombinase protein: a molecular switch for control of gene expression. *J. Virol.* **69,** 4600–4606.
15. Lee, Y. H., Sauer, B., Johnson, P. F., and Gonzalez, F. J. (1997) Disruption of the c/ebp alpha gene in adult mouse liver. *Mol. Cell. Biol.* **17,** 6014–6022.
16. Chang, B. H., Liao, W., Li, L., Nakamuta, M., Mack, D., and Chan, L. (1999) Liver-specific inactivation of the abetalipoproteinemia gene completely abrogates very low density lipoprotein/low density lipoprotein production in a viable conditional knockout mouse. *J. Biol. Chem.* **274,** 6051–6055.
17. Lakso, M., Sauer, B., Mosinger, B., Lee, E. J., Manning, R. W., Yu, S.-H., et al. (1992) Targeted oncogene activation by site-specific recombination in transgenic mice. *Proc. Natl. Acad. Sci. USA* **89,** 6232–6236.
18. Drago, J., Padungchaichot, P., Wong, J. Y., Lawrence, A. J., McManus, J. F., Sumarsono, S. H., et al. (1998) Targeted expression of a toxin gene to D1 dopamine receptor neurons by cre-mediated site-specific recombination. *J. Neurosci.* **18,** 9845–9857.
19. Lobe, C. G., Koop, K. E., Kreppner, W., Lomeli, H., Gertsenstein, M., and Nagy, A. (1999) Z/AP, a double reporter for cre-mediated recombination. *Dev. Biol.* **208,** 281–292.
20. Mao, X., Fujiwara, Y., and Orkin, S. H. (1999) Improved reporter strain for monitoring cre recombinase-mediated DNA excisions in mice [In Process Citation]. *Proc. Natl. Acad. Sci. USA* **96,** 5037–5042.
21. Tsien, J. Z., Chen, D. F., Gerber, D., Tom, C., Mercer, E. H., Anderson, D. J., et al. (1996) Subregion- and cell type-restricted gene knockout in mouse brain. *Cell* **87,** 1317–1326.

22. Postic, C., Shiota, M., Niswender, K. D., Jetton, T. L., Chen, Y., Moates, J. M., et al. (1999) Dual roles for glucokinase in glucose homeostasis as determined by liver and pancreatic beta cell-specific gene knock-outs using Cre recombinase. *J. Biol. Chem.* **274,** 305–315.
23. Bruning, J. C., Michael, M. D., Winnay, J. N., Hayashi, T., Horsch, D., Accili, D., et al. (1998) A muscle-specific insulin receptor knockout exhibits features of the metabolic syndrome of NIDDM without altering glucose tolerance. *Mol. Cell* **2,** 559–569.
24. Chen, J., Kubalak, S. W., and Chien, K. R. (1998) Ventricular muscle-restricted targeting of the RXRalpha gene reveals a non-cell-autonomous requirement in cardiac chamber morphogenesis. *Development* **125,** 1943–1949.
25. Kuhn, R., Schwenk, F., Aguet, M., and Rajewsky, K. (1995) Inducible gene targeting in mice. *Science* **269,** 1427–1429.
26. Merrill, D. C., Thompson, M. W., Carney, C., Schlager, G., Robillard, J. E., and Sigmund, C. D. (1996) Chronic hypertension and altered baroreflex responses in transgenic mice containing the human renin and human angiotensinogen genes. *J. Clin. Invest.* **97,** 1047–1055.
27. Davisson, R. L., Ding, Y., Stec, D. E., Catterall, J. F., and Sigmund, C. D. (1999) Novel mechanism of hypertension revealed by cell-specific targeting of human angiotensinogen in transgenic mice. *Physiol. Genomics* **1,** 3–9.
28. Davisson, R. L., Yang, G., Beltz, T. G., Cassell, M. D., Johnson, A. K., and Sigmund, C. D. (1998) The brain renin-angiotensin system contributes to the hypertension exhibited by mice containing both human renin and human angiotensinogen transgenes. *Circ. Res.* **83,** 1047–1058.
29. Yang, G., Merrill, D. C., Thompson, M. W., Robillard, J. E., and Sigmund, C. D. (1994) Functional expression of the human angiotensinogen gene in transgenic mice. *J. Biol. Chem.* **269,** 32,497–32,502.
30. Joyner, A. L. (1993) *Gene Targeting: A Practical Approach.* IRL Press, Oxford.
31. Ausubel, F. M., Brent, R., Kingston, R. E., Moore, D. D., Seidman, J. G., Smith, J. A., and Struhl, K. (1989). *Current protocols in Molecular Biology.* Wiley, New York.
32. Sauer, B. and Henderson, N. (1988) Site-specific DNA recombination in mammalian cells by the Cre recombinase of bacteriophage P1. *Proc. Natl. Acad. Sci. USA* **85,** 5166–5170.
33. Furth, P. A., St. Onge, L., Böger, H., Gruss, P., Gossen, M., Kistner, A., et al. (1994) Temporal control of gene expression in transgenic mice by a tetracycline-responsive promoter. *Proc. Natl. Acad. Sci. USA* **91,** 9302–9306.
34. Gossen, M., Freundlib, S., Bender, G., Muller, G., Hillen, W., and Bujard, H. (1995) Transcriptional activation by tetracyclines in mammalian cells. *Science* **268,** 1766–1769.
35. St-Onge, L., Furth, P. A., and Gruss, P. (1996) Temporal control of the Cre recombinase in transgenic mice by a tetracycline responsive promoter. *Nucleic Acids Res.* **24,** 3875–3877.
36. No, D., Yao, T. P., and Evans, R. M. (1996) Ecdysone-inducible gene expression in mammalian cells and transgenic mice. *Proc. Natl. Acad. Sci. USA* **93,** 3346–3351.

5

Systemic Delivery of a Transgene in Intact Animals by a Retroviral Vector

Michael J. Katovich, Hong-Wei Wang, Craig H. Gelband, and Mohan K. Raizada

1. Introduction

Essential hypertension is a chronic cardiovascular disease that effects over 50 million people in the United States. It is a complex pathophysiological state that is primarily characterized by a sustained elevation in blood pressure (BP). If untreated, this chronically elevated BP can affect major target organs of the body including the heart, kidney, brain, and vascular system. As a consequence of the sustained high BP, there is an increased risk of mortality and morbidity that is characterized by myocardial infarction, congestive heart failure, stroke, end-stage renal failure, and peripheral vascular disease ***(1–3)***. Because hypertension is basically an asymptomatic disease, it confounds effective treatment and makes compliance a major issue in the treatment of this disease. Pharmacological agents currently utilized have to be administered daily in an attempt to control BP, and there are no agents available to cure essential hypertension. Thus, more effective therapeutic intervention is required in order to have a significant impact in alleviating this chronic disease and its lethal cardiovascular sequel.

The renin–angiotensin system (RAS) has been implicated in the development and maintenance of essential hypertension ***(2,4–7)***. Major drug classes that inhibit components of the RAS have been effective in reducing BP in hypertensive patients and in reducing the incidence of the cardiovascular complications associated with the disease of hypertension ***(1,5,6,8)***. The RAS is somewhat unique as an endocrine system because it is composed of not only its systemic endocrine aspects, but also is characterized by specific tissue paracrine and autocrine effects. Thus, it has important roles in both the increase in BP and organ dysfunction. The endocrine RAS is characterized by the circu-

From: *Methods in Molecular Medicine, vol. 51: Angiotensin Protocols*
Edited by: D. H. Wang

lating angiotensin II (Ang II). It has been suggested that the short-term effects of Ang II, such as arteriolar vasoconstriction, sodium and water reabsorption, renal hemodynamics, aldosterone and ADH release, cardiac ionotropic effects, and regulation of the central sympathetic activity are mediated by the circulating Ang II. In contrast, the tissue RAS ***(9)*** mediates the long-term effects of Ang II. These actions include regulation of cardiac hypertrophy and vascular remodeling. Therefore, the coordinated action of the tissue and circulating RAS are important in the regulation of BP and alterations in this system have been implicated in the development and establishment of hypertension and its related complications. Targeting this system with effective therapeutic intervention should have far-reaching consequences in the management and potential cure of hypertension.

Traditional agents designed to inhibit the formation of Ang II (renin and angiotensin-converting enzyme [ACE] inhibitors) or to inhibit the actions of Ang II (AT_1-receptor blockers) are reliable and successful in the treatment of hypertension; however, there are major limitations with the use of these conventional agents. These effects are short-lived and, therefore, the agents need to be administered daily. Additionally, some of these agents have side effects, which complicates the compliance issue. Although these agents effectively reduce BP, not all of these agents are effective in reducing or preventing other morphological complications associated with hypertension. Finally, these agents hold little promise in curing this disease. Recent advances in the field of gene delivery and gene transfer have been used to improve the treatment of various disease states. In the area of hypertension, both an antisense and sense approach have been effectively used to lower blood pressure in animal models of hypertension ***(10–14)***. These studies have used a variety of gene delivery techniques, which have resulted in a significant lowering of blood pressure ranging from 3 to 30 d following a single delivery of the agent. We have been successful in delivering in vivo to the spontaneously hypertensive rat (SHR) antisense to the angiotensin II-type 1 receptor (AT_1R). A single injection of this AT_1R-AS by a retroviral-mediated delivery approach has completely prevented the development of hypertension in these animals and prevented the morphological and pathophysiological cardiovascular complications normally associated with this hypertensive state ***(15–18)***. This approach has been successful in preventing the development of the offspring of the treated rat suggesting that the antisense is permanently incorporated in the genome ***(19)***. This chapter will describe the techniques we have developed for an effective antisense approach for the long-term management and possible cure for hypertension. A schematic (**Fig. 1**) describes the process by which antisense to the angiotensin II-type 1 receptor is delivered and incorporated into cells to reduce the formation of AT_1R, which leads to the prevention of hypertension and cardiovascular sequel

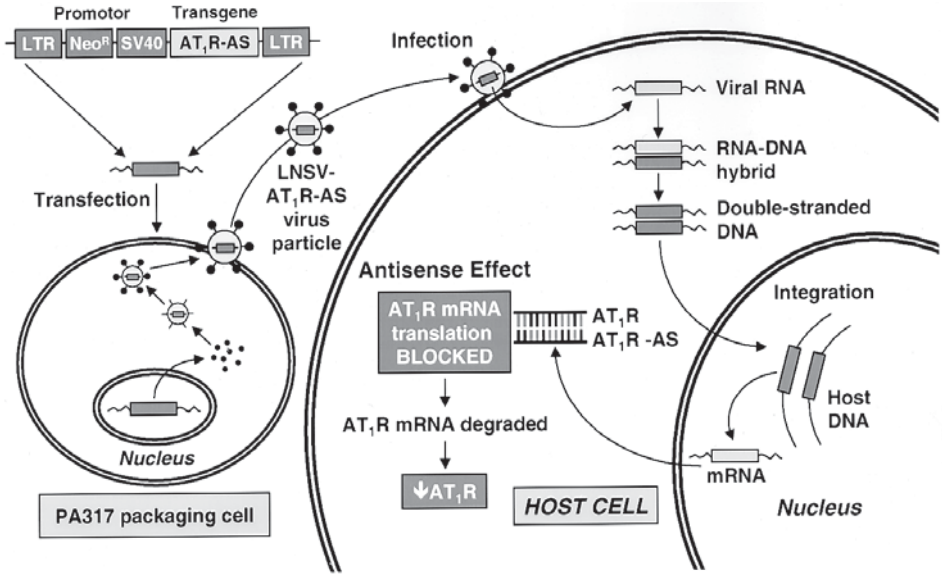

Fig. 1. Schematic of proposed transgene transfection, infection, and integration into host cell with subsequent antisense action in the tissue.

in the spontaneously hypertensive rat (SHR). The methods will describe the preparation of the retroviral particles containing the AT_1R-AS, transfection of the PA 317 cells with the LNSV-AT_1R-AS, concentration of the LNSV-AT_1R-AS, injection of the antisense into the animal, and methodologies of assessment of the effectiveness of the AT_1R-AS in vivo. LNSV = *l*ong terminal repeats, *n*eomycin selection, and *s*imian *v*irus promoter.

2. Materials

2.1. Cell Culture and Virus Preparation

This subheading lists the cell lines and reagents needed for cell culture and virus preparation and the sources of these materials. Specific concentrations and usage of these agents are described in **Subheading 3.**

1. The PA317 packaging cell line (ATCC # CRL 9078) and the NIH 3T3 cell line (ATCC # CRL 1658), were purchased from American Type Culture Collections (Rockville, MD).
2. Dulbecco's modified Eagle's medium (DMEM), LIPOFECTIN reagent, Genetcin (G418 sulfate), and Hank's balance salt solution (HBSS) were all obtained from Life Technologies (Grand Island, NY).
3. Fetal bovine serum (FBS) and calf serum were purchased from Biocell (Rancho Dominguez, CA).

4. Trypsin was obtained from Worthington Biochemical Corporation (Freehold, NJ).
5. Polybrene was obtained from Sigma (St. Louis, MO).

2.2. Solutions for Transcript Determinations

This subheading lists the solutions needed for transcript determination. The uses of the agents are described in **Subheading 3.**

1. Plasmid purification kits, *Taq* DNA polymerase, dNTP, Oligo-$(dT)_{15}$ restriction enzyme, and T_4ligase, were obtained from Promega (Madison, WI).
2. Trizol reagent, SUPERSCRIPT™ II RNase H^- Reverse Transcriptase was purchased from Life Technologies.
3. Ampicillin was obtained from Sigma.

2.3. Animal Supplies

1. The inhalant anesthesia used for injection was methoxyflurane (Metofane, Mallinckodt Veterinary, Inc., Mundelein, IL).
2. Silicone elastomer catheter (Helix Medical) and PE-50 catheter (Clay Adams) and heparin solution (10 U/mL, Elkins-Sinns, Inc., Cherry Hill, NJ) were used for the cannulation of the animal for direct measurement of BP and the iv administration of agents to the animal.
3. In the study described, animals (SHR) were purchased from Harlan Sprague Dawley (Indianapolis, IN).
4. During injection, animals were placed on deltaphase isothermal pads (Braintree Scientific, Inc., Braintree, MA) to maintain normal body temperature during the procedure.
5. Injections were made with a microfine needle, 0.5 cm^3, 100 U insulin syringes (Becton Dickinson, Franklin Lakes, NJ).

3. Methods

3.1. Preparation of Retroviral Particles Containing AT_1R-AS

Construction and recombination of retroviral vector, LNSV-AT_1R-AS. A pair of specific primers containing a *Hin*dIII restriction site at the 5' end is used to generate AT_1B-R cDNA by RT-PCR. These primers are: sense 5' – CCA AGC TTG TGT CAG AGA GCA ATT CAC CTC ACC – 3', and antisense 5' – CCA AGC TTG GTA GTG AGT GAG CTG CTT AGC CCA – 3'. The procedures are described below:

1. Five μg of total RNA from rat hypothalamus brainstem neuronal cells or rat adrenal gland are subjected to reverse transcript reaction using SUPERSCRIPT II. Five μg of total RNA and 1 μL oligo $(dt)_{15}$ (500 μg/mL) are mixed and the volume is brought up to 12 mL with sterile, distilled water.
2. The mixture is heated to 70°C for 10 min and quickly chilled on ice. The contents of the tube is collected after a brief centrifugation and 4 μL 5X first strand buffer, is added with 2 μL 0.1 *M* dithiothreitol (DTT), 1 μL of 10 m*M* dNTP, and 100 U of SUPERSCRIPT II.

3. The mixtures are subjected to incubation for 50 min at 42°C and inactivated by heating the mixture to 70°C for 10 min.
4. One unit of *Escherichia coli* RNase H is added and incubated at 37°C for 20 min to remove the RNA complimentary to the cDNA.
5. The polymerase chain reaction (PCR) contains 20 pmol AT_{1B}-R sense and antisense primers. PCR of 35 cycles [94°C for 1 min, 58°C for 1 min, 72°C for 1 min] is performed by a standard protocol ***(20–22)*** using 10 m*M* Tris-HCl, pH 9.0 at 25°C, 50 m*M* KCL, 0.1% Triton®X-100, 200 μ*M* each of dNTP, 1.5 m*M* $MgCl_2$, and 1 U *Taq* DNA polymerase.
6. The PCR mixture is electrophoresed on 1% low melting agarose gel and the band of 1.26 kb is excised and purified by using QIAEX II gel extraction kit.
7. Further characterization of the 1.26 kb AT_{1B} PCR product is carried out by *Cla*I and *Fok*I restriction enzyme analysis and sequencing. The identity of the AT_{1B} cDNA should correspond to nt –132 to +1228 of the coding region of the AT_{1B} R. With the 95–98% homology between AT_{1A} and AT_{1B} receptor subtypes the transcriptional expression of either would be obtained with our proposed antisense technique.

LNSV is a retroviral vector of 6234 bp, derived from $pLNL_6$, and contains long terminal repeat promoter, which can drive neomycin-resistance selection gene, and an internal simian virus 40 promoter that controls the expression of the transgene. The 1.26-kb AT_1R-cDNA is cloned into the LNSV by using a T_4 ligase by the following steps:

1. 50 ng of the LNSV and 100 ng of the 1.26 Kb AT_1R-cDNA are digested with *Hin*dIII followed by isolation and purification by using the QIAEX II gel extraction kit.
2. The fragments are then mixed with 1 X standard ligase buffer [50 m*M* Tris-HCl, pH 7.5; 7 m*M* $MgCl_2$; 1 m*M* DTT; 1 m*M* adenosine triphosphate (ATP)] and 5 U of bacteria T_4 ligase.
3. This mixture is incubated at 12°C overnight.
4. The recombinant DNA from the ligation is transformed into competent HB101 bacterial cells by a heat pulse of 42°C for 45 s and the AT_1R-AS colonies are selected.
5. To select AT_{1B}R positive recombinants more than 20 bacterial colonies are picked from a transformed LB plate and grown in LB medium with ampicillin (100 μg/mL).
6. The recombinant DNA is purified with a plasmid purification kit according to the protocol provided by the company.
7. Control LNSV is processed the same way except for the introduction of the 1.26 kb AT_{1B} R-cDNA.
8. AT_1R recombinant and its antisense orientation essentially are characterized by restriction enzyme analysis as previously described ***(20)***. Hind III digestion gives the anticipated 1.26-kb band that corresponds to nt –132 to +1128 in the AT_{1B} –R sequence as previously described ***(20)***. *Fok*I digestion of the 1.26-kb band results in two bands of 952 bp and 308 bp. A *Cla*I digestion will give two bands of 536 bp and 7090 bp for AT_{1B} –AS. *Cla*I/*Sal*I digestion should result in two bands of

1171 bp and 536 bp, which would be consistent with their restriction sites. Further characterization of individual bands could be determined by sequence analysis.

3.2. Transfection of Cells PA317 with the LNSV-AT$_1$R-AS

This transfection is a 4-d process.

Day 1:

1. Plate 2×10^5 PA317 cells in a 60-mm diameter culture dish and culture in DMEM containing 25 m*M* glucose and 10% FBS.
2. Allow the cells to grow in 5% CO_2 at 37°C for 24 h.

Day 2:

1. Mix 3–5 μL LIPOFECTIN Reagent with 100 μL serum-free DMEM.
2. Dilute 3 μg LNSV-AT1R-AS recombinant DNA into 100 μL serum-free DMEM.
3. Allow mixtures to stand at room temperature for 45 min.
4. Both solutions are then mixed gently and incubation is continued for an additional 15 min.
5. Add 1.8 mL of serum free DMEM into the LIPOFECTIN-DNA mixture and gently overlay the mixture onto PA 317 cells.
6. The PA317 cells medium is aspirated and rinsed by serum-free medium once before this mixture is added.
7. The cells are then incubated (at 37°C, in 5% CO_2) with this mixture for 12 h.

Day 3:

1. Replace the LIPOFECTIN-DNA containing medium with 4 mL of DMEM containing 10% FBS.
2. Incubate this mixture for 24 h at 37°C in 5% CO_2.

Day 4:

1. Subculture PA317 cells at a 1:10 or 1:20 ratio into the selection medium (DMEM + 10% FBS containing 800 μg/mL G418) for 10–14 d.

The selection medium is then changed every 3 d to remove the dead cells. After 10 more days of selection, the G418 resistant colonies can be observed. They are then chosen and are transferred into multiple six-well dishes with the same selection medium as aforementioned. These cells are grown for 3–5 d for cells to reach confluence. The duration is dependent on the rate of different G418 resistant colonies. Before the cultures become confluent, the medium is changed with normal DMEM+10% FBS medium. The supernatant is harvested and filtered through a 0.45-μm filter. This material is used to determine the titer.

3.3. Preparation of High-Titer Particles Containing AT$_1$R-AS

3.3.1. Viral Titration

NIH 3T3 cells are used to determine the concentration of viral particles as follows:

Day 1:

1. Plate NIH 3T3 cells at 1×10^5 cells in a 60-mm diameter culture dish in DMEM + 10% calf serum.

Day 2:

1. Replace the medium with 2 mL of DMEM + 10% calf serum containing 8 μg/mL polybrene.
2. One or 0.1 μL of media containing virus particles is added to each dish. This is done in duplicate.
3. The cultures are mixed carefully and incubated for 2.5 h at 37°C.
4. Next, add 2 mL of fresh DMEM +10% calf serum in each dish. The final concentration of polybrene is 4 μg/mL.

Day 3:

1. The virus containing medium is replaced with 4 mL fresh DMEM + 10% calf serum and incubation is continued for an additional 24 h at 37°C.

Day 4:

1. Subculture infected NIH 3T3 cells at a 1:10 or 1:20 dilution into 800 μg/mL G418 selection medium for 10–14 d.

Selection medium is changed every 3 d. The G418 resistant colonies are then counted before they spread. The titer is calculate as follows:

G418-R cfu/mL = no. of colonies/virus volume (mL) X dilution number

Select 2–4 colonies of the highest titer (10^5–10^6 cfu/mL). These are subcultured once, and store in 10 vials (1- to 2-mL aliquots) in 10% dimethylsulfoxide (DMSO) in liquid nitrogen.

3.3.2. Concentration of Viral Vector Before Use

Prior to injection into the animal, the viral vector needs to be concentrated to >10^8 cfu/mL. The viral vector need not be concentrated for in vitro usage. The method used to concentrate the viral vector is ultracentrifugation (*see* **Note 1**). The following steps are followed in order to achieve successful concentration of the viral vector.

1. The stored AT_1R-AS virus-producing cells usually yield a titer of about 10^5–10^6 cfu/mL.
2. The virus medium is harvested every 24 h for 3 d after cell confluence reaches 75–80%.
3. Centrifuge tubes (thick walled polypropylene) are filled with 25 mL virus medium (0.45-μm filtered) and the tubes are carefully balanced into rotor buckets (Beckman SW 28) *see* **Note 2**.
4. Pellet the viral in an ultracentrifuge at 50,000*g* for 2 h at 4°C.
5. The supernatant is decanted and the virus suspended in 100 μL HBSS overnight.

6. Repeat **steps 3–5** and dissolve the virus pellet using virus suspensions harvested in **step 5** from day 1 (*see* **Note 3**).
7. Virus suspensions are dialyzed for 4 h in 1X PBS at 4°C. The virus suspensions are collected and placed into the dialyzed Spectra/Por® molecularporous membrane (Spectrum Laboratories, Inc.). The membrane needs to be treated in double-distilled water at least 4 h before use (*see* **Note 4**).

3.4. Infection of Ang II Target Cells In Vitro

Vascular smooth muscle cells (VSMC) and astroglia brain cells are well-established Ang II target tissues ***(20,22)***. Thus, we can demonstrate the efficiency of transduction of AT_1R-AS in vitro by utilizing VSMC and astroglial cell cultures. The following is the protocol used for infecting astroglia/VSMCs.

1. Day 1: Plate 5×10^5 cells/100-mm dish in DMEM + 10% FBS for VSMC and DMEM + 10% horse serum. Grow the cells for 48 h at 37°C in 5% CO_2:95% O_2.
2. Day 2: Replace media with DMEM + 10% FBS containing 5×10^5 cfu/mL LNSV-AT1R-AS or LNSV and allow the incubation for 24 h at 37°C in 5% CO_2.
3. Day 3: Replace medium with the selection medium (DMEM + 10% FBS + 800 μg/mL G418 or DMEM + 10% HS + 800 μg/mL G418).
4. Day 4: Grow cells in selection medium for 10–14 d. Subculture G418 resistant cells until confluent and subjected to isolate genomic DNA and total RNA.

PCR and RT-PCR are performed to measure the transduction efficiency of the culture as previously reported ***(20,23)***. In our hands, this protocol results in >70% of the cells expressing the AT_1R-AS transcript.

3.5. In Vivo Transduction of AT_1R-AS

Once the antisense virus is concentrated, 5-d-old SHRs are removed from the mother and anesthetized with methoxyflurane. The SHR is utilized because this rat model spontaneously develops an increase in BP with age without any other interventions. This increase in BP is dependent on actions of the RAS.

1. The animals are injected with the either the LNSV- AT_1R-AS or the control LNSV in a volume of 20–50 μL/rat. The virus preparation is injected directly into the heart (*see* **Notes 5** and **6**).
2. After injection, the animals are appropriately tagged so that they can be identified as they grow. We currently take a small clip off the top of the right ear in the LNSV- AT_1R-AS treated animals. If other controls are used, or other doses administered, tags could be placed on the other ear or the ears can be notched or left intact. Thus several different groups can be identified at this 5-d interval.
3. As the animals recover from the anesthesia, they are lightly coated with peanut oil before being returned to their mothers. This final maneuver appears to increase the mother's acceptance of their offspring after the injection procedure. The survivability after the animals are returned to the mother is about 96% (*see* **Note 7**).

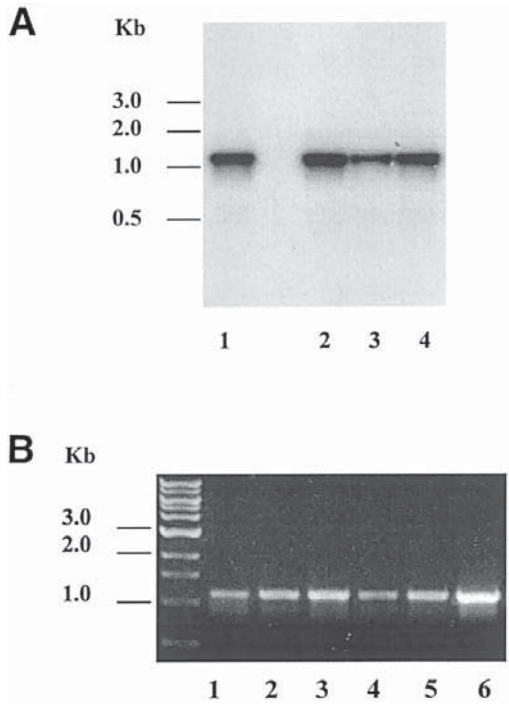

Fig. 2. **(A)** Representative Southern blot demonstrating the presence of the LNSV-AT_1R-AS in the SHR. Specific PCR products were amplified and subjected to Southern blotting as previously described ***(20,21)***. AT_1R-AS generated by Cla I and Sac I restriction enzyme treatment of the LNSV-AT_1RAS vector was used as the probe. The fragment (approx 1 Kb) was randomly labeled with ^{32}P-dCTP and used for hybridization by the standard protocol ***(21)***. Lane 1, PA317 cells; Lane 2, Liver; Lane 3, heart; Lane 4, adrenal. **(B)** Representative RT-PCR demonstrating the expression of AT_1R-AS transcript in various tissues of LNSV-AT_1R-AS treated SHR. Total RNA was isolated from tissues obtained from adult rats treated neonatally with LNSV-AT_1R-AS . The RNA was subjected to RT-PCR with the use of specific primers to detect AT_1R-AS ***(21)***. Lane 1, adrenal; Lane 2, kidney; Lane 3, lung; Lane 4, heart; Lane 5, liver; Lane 6, spleen.

4. Animals are then allowed to grow normally and are weaned at the normal day 21. Microchips can be inserted, subcutaneously, for subsequent identification after weaning. Other marking methods can be substituted for microchips.
5. As the animal grows, viral vector integration into the genome needs to be determined. This is accomplished by sacrificing the animal at various ages and harvesting the cardiovascular relevant tissues for conduction of Southern analysis ***(20,21)*** (*see* **Notes 8** and **9**). A representative experiment from adult rat tissues is shown in **Fig. 2**. This demonstrates that the viral vector containing the AT_1R-AS is integrated into the genome.

6. Another method is to confirm the expression of AT_1R-AS mRNA. Standard RT-PCR ***(20–23)*** was performed to show that AT_1R-AS mRNA is abundantly expressed in several tissues.

We have previously reported that adrenal, mesenteric tissue, kidney, and heart express the AT_1R-AS mRNA as early as 3 d after the initial injection ***(15)*** and is still present in adult animals. The expression of the AT_1R-AS transcript is associated with an attenuation of the high BP exclusively in the SHR and a reduction in the physiological responsiveness of treated animals to exogenous Ang II ***(15–18)***.

Indirect BPs were performed in awake animals as early as 40 days of age. A variety of instruments can be used to make this assessment using the tail cuff methodology ***(15,16)***. Basically, the animals are placed in a mild heat stress to increase blood flow to the tail (*see* **Note 10**). A BP cuff is placed on the tail and inflated. Mean BP can be determined both during the inflation and deflation periods by this method. Usually three to four repeated determinations are obtained and averaged. Effective treatment with the AT1 R-AS in the SHR will result in a BP that is significantly lower than that of the control (LNSV) - treated SHR and similar to that of a normotensive WKY control (**Fig. 3**). Blood pressures are not altered in normotensive animals ***(15–18)***. We have observed a significant decrease in BP in the SHR as early as 39 days of age ***(15)*** and in excess of 210 days of age ***(18)***.

To further determine the effectiveness of the AT_1 R-AS in vivo, we challenged the animal with Ang II and determine the physiological effects with respect to the control animal. One noninvasive test we performed in the animal was the dipsogenic response to exogenous Ang II ***(24)***. The protocol is as follows:

1. Animals are housed in individual cages and a calibrated water bottle is affixed to the cage.
2. After a 1-h control period, Ang II (150 μg/mL) is administered subcutaneously and water intake is determined at 30-min intervals.
3. Water intake can be calculated by subtracting the difference in bottle weight or volume and standardized by dividing by the body weight of the animal.

Ang II results in a significant increase in water intake that was completely restored to control values in the AT_1R-AS-treated animals. One hour water intake in saline-treated animals was 3.7 ± 2.4 mL/kg compared to 14.2 ± 3.9 mL/kg in the Ang II-treated rat. This water intake was significantly reduced to 5.0 ± 3.1 in the AT_1R-AS treated rat administered Ang II, demonstrating a complete blockage of the Ang II-induced dipsogenic response in AT_1R-AS treated rats. This test is a rapid and reliable noninvasive test of Ang II responsiveness. We have demonstrated that this dipsogenic response to Ang II can is normalized in AT_1R-AS –treated rats as early as 40 d after treatment and is maintained in

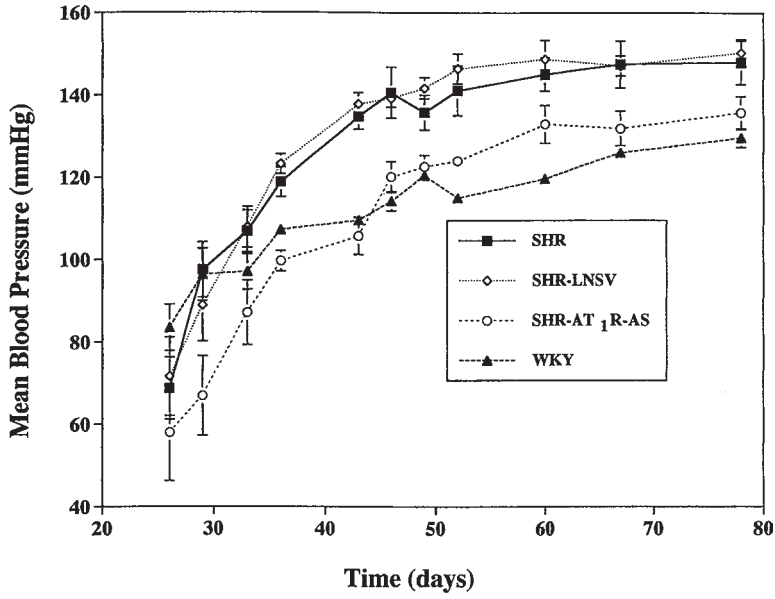

Fig. 3. Indirect BPs of untreated SHR, LNSV-treated SHR, LNSV-AT_1R-AS-treated SHR and untreated WKY over time. Treatment was initiated at 5 d of birth. Time is age of the animals. There are 6–8 animals/group at each time-point.

adulthood ***(16)***. This noninvasive test can be performed as early as 1 mo of age. Refer to **Note 11** for possible complications.

Another in vivo determination of the effectiveness of AT_1R-AS is the assessment of direct blood pressure, which is assessed in the animals after a surgical intervention.

1. A cannula is inserted into the aorta (any number of arteries can be utilized).
2. The cannula is exteriorized to an external blood pressure transducer.
3. Direct BP (and heart rate) is then recorded in free moving, unanesthetized animals ***(15,16)***.

Alternatively, to avoid any handling of the animals, direct BP can be continuously monitored by a telemetry transducer, which is placed in the abdomen of the animal. Another measurement of the effectiveness of the AT_1R-AS treatment is to measure the pressor response to exogenous Ang II in unanesthetized animals. This can be accomplished by the addition of a venous catheter placed in the animal (jugular or femoral vein). You then can administer Ang II through the venous catheter while measuring BP in the arterial catheter. Thus, the pressor response to exogenous Ang II can be utilized as an in vivo assessment of the effectiveness of the AT_1R-AS treatment. Using this methodology we have

demonstrated that direct BP is reduced in the SHR treated neonatally with AT_1R-AS ***(15–19)*** and the pressor responsiveness to exogenous angiotensin (0.005 μg/kg to 0.32 μg/kg, iv) is significantly reduced in AT1R-AS- treated animals ***(15,16)***.

Depending on the experimental question, other measures of assessment of Ang II responsiveness can be determined in vivo or in vitro in this animal model. We have determined the vascular smooth muscle responsiveness in several vascular beds demonstrating a reduced responsiveness to Ang II and a normalization of vascular alterations associated with hypertension in the SHR ***(15,17)***. In addition, the pathophysiological responses related to calcium ***(18)*** or histological alterations in vascular tissue ***(17)*** have been assessed in this model in our lab to confirm the long-lasting beneficial effects of this therapeutic intervention. Also, we have challenged animals with losartan, the Ang II receptor antagonist, and demonstrated that no further reduction in BP is apparent in the AT_1R-AS-treated animals compared to the LNSV animals ***(15,16)***. This further demonstrated that the mechanism by which our AT_1 R-AS mediated its effect was through the AT_1 R and was as effective as utilizing the pharmacological antagonism of the same receptor. However, the effects were more permanent with the AT_1 R-AS treatment compared to the actions of losartan, which were absent within 24 h ***(16)***. We have further determined that AT_1R, but not AT_2R, mRNA is reduced in the adult AT_1R-AS-treated animals ***(15,16)***. Thus, introduction of AT_1 R-AS via a retroviral carrier system in intact animals can be assessed for its effectiveness in vivo, both with invasive and noninvasive techniques. This gene therapy approach is effective in preventing the development of hypertension in a genetic hypertensive animal model and can be used in other models of hypertension. In addition, other gene delivery vectors can be used to improve upon these results and revolutionarize the way hypertension is treated in the future.

4. Notes

1. When AT_1R-AS virus medium is prepared, it should be subjected to ultracentrifugation and then used or stored at –80°C before concentration for use at a later time. The frozen medium can be thawed quickly by shaking the container in a 37°C water bath (*see* **Subheading 3.3.2.**).
2. The centrifuge tubes and rotor should sit in ice during the preparation of the concentrated virus (*see* **Subheading 3.3.2.3.**).
3. When using the HBSS solution to dissolve the viral pellet, pipet the material gently to avoid forming any bubbles (*see* **Subheading 3.3.2.6.**).
4. The concentrated virus cannot be stored at 0–4°C for more than 2 d before use. (*See* **Subheading 3.3.2.7.**)
5. Prior to use in animals, one must ensure that the final concentration of polybrene is not greater than 6 μg/mL. Higher concentrations can be toxic to the animal (*see* **Subheading 3.5.1.**).

6. Young animals have a problem thermoregulating, thus care should be taken to keep the animals warm while under anesthesia (*see* **Subheading 3.5.1.**).
7. The animals should also be mechanically stimulated to hasten recovery after anesthesia (*see* **Subheading 3.5.3.**).
8. During the measurements of indirect BP in the animals, heating is used to increase blood flow through the tail that is used to determine BP. This can be considered a stress and may artificially elevate blood pressure. One should ensure that the animals are not overheated and that they go through the procedure on several occasions prior to the collection of data. If animals are routinely handled, this should reduce the possible effects of stress on the BP measurements. Alternatively, if the animals are instrumented with a telemetry device at an early age, the BP obtained will also be "stress-free" (*see* **Subheading 3.5.**).
9. Ensure that the titer is correct before proceeding too far into the animal studies. It may take a couple of days to check the titer, but it should be done with each batch (*see* **Subheading 3.5.5.**).
10. It is also prudent to check for incorporation of the antisense in tissues from the animal (say, 4 to 10 days after injection) before carrying out animal studies for a protracted period of time (*see* **Subheading 3.5.5.**).
11. For all the in vivo studies assessing the responsiveness of exogenous Ang II, one must be aware that the estrous cycle can modify the responsiveness to Ang II ***(25)***. Therefore, it is prudent to either determine the stage of the estrus cycle, or ovariectomize all female rats to eliminate the estrous cycle. Conversely, just use male rats for these determinations (*see* **Subheading 3.5.**).

References

1. Kang, P. M., Landau, A. J., Eberhardt, R. T., and Fishman, W. H. (1994) Angiotensin II receptor antagonists: a new approach to blockade of the renin angiotensin system. *Amer. Heart J.* **127,** 1388–1401.
2. Whelton, P. K. (1994) Epidemiology of hypertension. *Lancet* **334,** 101–106.
3. Stamler, J., Stamler R., and Neaton, J. D. (1993) Blood pressure, systolic and diastolic and cardiovascular risks: US population data. *Arch. Intern. Med.* **153,** 598–615.
4. Brunner, H. R., Nussberger, J., and Waeber, B. (1993) Angiotensin II blockade compared with other methods of inhibiting the renin-angiotensin system. *J. Hypertens.* **11,** 553–558.
5. Parmley, W. W. (1998) Evolution of angiotensin-converting enzyme inhibition in hypertension, heart failure, and vascular protection. *Am. J. Med.* **105,** 27s–31s.
6. Pitt, B. (1998) Regression of left ventricular hypertrophy in patients with hypertension: blockade of the renin-angiotensin-aldosterone system. *Circulation* **98,** 1987–1989, 1998.
7. Jeunemaitre, X., Soubrier, F., Kotelevtsev, Y. V., Lifton, R. P., Williams, C. S., Charru, A., et al. (1992) Molecular basis of human hypertension: role of angiotensinogen. *Cell* **71,** 169–180.
8. Vogt, M., Motz W. H., Schwartzkopf, B., and Strauer, B. E., (1993) Pathophysiology and clinical aspects of hypertensive hypertrophy. *Eur. Heart J.* **14,** 2–7.

9. Dzau, V. (1993) Tissue renin-angiotensin system in myocardial hypertrophy and failure. *Arch. Intern. Med.* **153,** 937–942, 1993.
10. Chao, J., Zhang, J. J., Lin, K. F., and Chao, L. (1998) Human kallikrein gene delivery attenuates hypertension, cardiac hypertrophy, and renal injury in Dahl salt-sensitive rats. *Hum. Gene Ther.* **9,** 21–31.
11. Lin, K. F., Chao, J., and Chao, L. (1995) Human atrial natriuretic peptide gene delivery reduces blood pressure in hypertensive rats. *Hypertension* **26,** 847–853.
12. Makino, N., Sugano, M., Ohtsuka, S., and Sawada, S. (1998) Intravenous injection with antisense oligonucleotides against angiotensinogen decreases blood pressure in spontaneously hypertensive rats. *Hypertension* **31,** 1166–1170.
13. Phillips, M. I., Mahuczy-Dominiak, D., Coffey, M., Galli, S. M., Kimura, B., Wu, P., and Zelles, T. (1997) Prolonged reduction of high blood pressure with an in vivo, nonpathogenic, adeno-associated viral vector delivery of AT_{1R} mRNA antisense. *Hypertension* **29,** 374–380.
14. Tomita, N., Morishita, R., Higaki, J., Aoki, M., Nakamura, Y., Mikami, H., et al. (1995) Transient decrease in high blood pressure by in vivo transfer of antisense oligodeoxynucleotides against rat angiotensinogen. *Hypertension* **26,** 131–136.
15. Iyer, S. N., Lu, D., Katovich, M. J., and Raizada, M. K. (1996) Chronic control of high blood pressure in the spontaneously hypertensive rat by delivery of angiotensin type 1 receptor antisense. *Proc. Natl. Acad. Sci. USA* **93,** 9960–9965.
16. Lu, D., Raizada, M. K., Iyer, S., Reaves, P., Yang, H., and Katovich, M. J. (1997) Losartan versus gene therapy: chronic control of high blood pressure in spontaneously hypertensive rats. *Hypertension* **30,** 363–370.
17. Martens, J. R., Reaves, P. Y., Lu, D., Berecek, K. H., Bishop, S. P., Katovich, M. J., et al. (1998) Prevention of renovascular and cardiac pathophysiological changes in hypertension by angiotensin II type 1 receptor antisense gene therapy. *Proc. Natl. Acad. Sci. USA* **95,** 2664–2669.
18. Gelband, C. H., Reaves, P. Y., Evans, J., Wang, H., Katovich, M. J., and Raizada, M. K. (1999) Angiotensin II type 1 receptor antisense gene therapy prevents altered renal vascular calcium homeostasis in hypertension. *Hypertension* **33,** 360–365.
19. Reaves, P. Y., Wang, H-W., Yang, H., Katovich, M. J., Berecek, K., and Raizada, M. K. (1999) Permanent prevention of hypertension by angiotensin type 1 receptor antisense gene therapy in the SHR. *FASEB J.* **13,** A776.
20. Lu, D., Yu. K., and Raizada, M. K. (1995) Retrovirus-mediated transfer of an angiotensin type 1 receptor (AT1-R) antisense sequence decreases AT_1RS and angiotensin action in astroglia and neuronal cells in primary culture. *Proc. Natl. Acad. Sci. USA* **92,** 1162–1166.
21. Ausubel, F. M., Brent, R., Kingston, R. E., Moore, D. D., Seidman, J. G., Smith, J. A., and Struhl, K. (1992) *Short Protocols in Molecular Biology.* Green Publishing Associates and Wiley, New York.
22. Raizada, M. K., Lu, D., Yang, H., Richards, M., Gelband, C. H., and Summers, C. (1999) *Advances in Molecular and Cellular Endocrinology* (Le Roith, D., ed.), vol. 3, JAI, Stamford, CT, pp. 75–101.

23. Lu, D. and Raizada, M. K. (1995) Delivery of angiotensin II type 1 receptor antisense inhibits angiotensin action in neurons from hypertensive rat brain. *Proc. Natl. Acad. Sci. USA* **92,** 2914–2918.
24. Iyer, S. N., Wright, B. E., Strubbe, G., Hanely, K., and Katovich, M. J. (1995) Chronic losartan treatment blocks isoproterenol-induced dipsogenesis. *Physiol. Behav.* **58,** 283–286.
25. Findlay, A. L. R., Fitzsimons, J. T., and Kucharczyk, J. (1979) Dependence of spontaneous and angiotensin-induced drinking in the rat upon the oestrous cycle and ovarian hormones. *J. Endocrinol.* **82,** 215–225.

6

Antisense Inhibition of the Renin–Angiotensin System

Dagmara Mohuczy and M. Ian Phillips

1. Introduction

Antisense inhibition has been developed, particularly in cell-culture applications, to the point where it is being tested in clinical trials for HIV and cancer ***(1,2)***. The pros and cons of its use have been reviewed elsewhere ***(3)***. Before 1992, however, antisense (AS) had not been applied in vivo with any success. There was much concern about the efficiency of cellular uptake of oliogodeoxynucleotides (ODNs). During 1992–1993, a few laboratories simultaneously and independently designed AS-ODNs and tested them in the brain ***(4–8)***. Cellular uptake was not a limiting factor in the central nervous system.

AS-ODNs have many potential attractive features as a new class of therapeutic agents to inhibit the renin–angiotensin system (RAS) ***(9)***. The role of the components of RAS in a disease state has been described in many previous publications ***(10–15)***. The first demonstration of antisense for reducing hypertension was the use of antisense to angiotensinogen mRNA and angiotensin II type 1 receptor (AT_1–R) mRNA in the brain ***(8)***. To prolong the effect of antisense inhibition for weeks or months, DNA (partial or full-length) can be inserted in the antisense direction in viral vectors.

1.1. Antisense Oligonucleotides

1.1.1. Ideal Antisense Molecules

Table 1 lists the characteristics of AS-ODNs that need to be incorporated into their design and use.

AS-ODNs have several potential sites of action. AS-ODNs inhibit translation by hybridizing to the specific mRNA that they are designed for and the

From: *Methods in Molecular Medicine, vol. 51: Angiotensin Protocols*
Edited by: D. H. Wang

Table 1
Characteristics of Ideal Antisense ODNs

1. The DNA sequence is specific and unique
2. Uptake into cells is efficient
3. The effect in cells is stable (for long-term treatment) or transient (for short-term treatment)
4. There is no nonspecific binding to protein
5. Hybridization of the ODN is specific for the target DNA
6. The targeted protein and/or mRNA level is reduced
7. The ODN is not toxic
8. No inflammatory or immune response is induced
9. The ODN is more effective than appropriate sense and mismatch ODN controls

hybridization prevents either ribosomal assembly or ribosomal sliding along the mRNA ***(16)***. This kind of action assumes that AS-ODNs are acting in the cytosol and do not affect measurable mRNA levels. Indeed, there are several articles reporting antisense effects without detectable change in target mRNA levels ***(6)***.

The general principles we follow in the design of the antisense are described in the following protocol.

1.1.2. Stability of Oligonucleotides

Oligonucleotides in their natural form as phosphodiesters are subject to rapid degradation in the blood, intracellular fluid, or cerebrospinal fluid by exo- and endonucleases.

The most widely used modified ODNs are phosphorothioates, where one of the oxygen atoms in the phosphodiester bond between nucleotides is replaced with a sulfur atom. These phosphorothioate ODNs have greater stability in biological fluids than normal oligos. The half-life of a 15-mer phosphorothioate ODN is 9 h in human serum, 14 h in tissue-culture medium, and 19 h in cerebrospinal fluid ***(17)***.

1.1.3. Cellular Uptake of Oligonucleotides

In order to hybridize with the target mRNA, AS-ODNs have to cross the cell membrane. Saturable uptake of ODNs reaches a plateau within hours, occurs rapidly, and, depending on the cells, can be efficient ***(18–20)***. Uptake is faster for shorter ODNs than for longer ones.

1.1.4. Pharmacology of AS-ODNS

Antisense inhibition can be considered pharmacologically as a drug–receptor interaction, where the oligonucleotide is the drug and the target sequence is

the receptor. Binding between the two affinity is provided by hydrogen bonding between the Watson-Crick basepairs and basestacking in the double helix that is formed. In order to achieve pharmacological activity, a minimum number of 12–15 bases can provide the minimum level of affinity ***(20)***.

Increasing the length of the ODN should result in higher level of specificity, but it also decreases its uptake into cells ***(17)***. With viral vectors, however, the length problem is overcome because the virus enters cells by binding to viral receptors on cell membranes. Therefore, in a viral vector, a full-length DNA-AS sequence can be used. The mechanism of action of antisense DNA differs from that of the AS-ODN. The AS-DNA produces an antisense mRNA that competes negatively with the cell's own mRNA.

1.1.5. Toxicity

AS-ODNs can inhibit protein synthesis in cultured cells in nmol/L doses. The therapeutic window for AS-ODNs is rather narrow: when testing for the optimal dose, small increments in the high nmol/L range should be tested ***(20,21)***. High concentrations may produce nonspecific binding to cytosolic proteins and give misleading results.

Phosphodiester ODNs are degraded to their naturally occurring nucleotide building blocks relatively quickly, therefore no toxic reaction is expected from even high doses of phosphodiester. Studies on phosphorothioated ODNs rats show that following intravenous (iv) injection, phosphorothioated ODNs are taken up from plasma mainly by the liver, fat, and muscle tissues. Phosphorothioate ODNs are excreted through the urine in 3 d, mainly in their original form. An apparently mild increase in plasma lactate dehydrogenase (LDH) and, to a lesser extent, indicators of a possible transient liver toxicity with very high doses of phosphorothioated ODN was observed ***(22)***. Whole new classes of ODN backbone modification are being developed to avoid the possible liver toxicity in humans with phosphorothioates ***(1–7,21)***.

1.1.6. Delivery of Antisense as a Naked ODNs

Direct injection of the AS-ODN to inhibit RAS has been used in the experiments described below ***(23–25)***. For injections into the brain, ODNs appear to be very successful. In a number of studies, using different antisense ODNs, there has been efficient uptake and effective reduction in protein, as well as inhibition of the physiological parameters studied. Uptake is so efficient that one difficulty with intracerebroventricular injections is that the ODN tends to be taken up close to the site of injection and not to spread to other parts of the brain. Whereas this has little impact for hypertension therapy, it is an important consideration in antisense strategies for the treatment of brain diseases, such as Parkinson's disease, thalamic pain, Alzheimer's disease, and gliomas.

1.1.7. Liposomes

Liposomes are self-assembling particles of bilipid layers that have been used for encapsulating antisense ODN for delivery in blood and cell culture ***(26–29)***. Antisense, directed to angiotensinogen mRNA in liposomes has had successful results.

Tomita et al. ***(28)*** used liposome encapsulation of angiotensinogen antisense and a Sendai virus injected into the portal vein. Blood pressure decreased for several days. However, they did not compare their results with the effects of naked ODN. Wielbo et al. ***(29)*** compared liposome-encapsulated antisense and naked ODN given intra-arterially. They found that liposome encapsulation was effective, whereas naked ODN was not, under the same conditions. Twenty-four hours after injection of 50 μg of liposome-encapsulated antisense ODN, blood pressure decreased by 25 mmHg. Neither empty liposome, liposome-encapsulated scrambled ODN, nor unencapsulated antisense ODN had a significant effect on blood pressure. Confocal microscopy of rat liver tissue 1 h after intra-arterial injection of 50 μg of unencapsulated fluorescein isothiocyanate (FITC) antisense, or liposome-encapsulated FITC-conjugated antisense, showed intense fluorescence in liver tissue sinusoids with the liposome-encapsulated ODN. Levels of protein (angiotensinogen and angiotensin II in the plasma) were significantly reduced in the liposome-encapsulated ODN group. Antisense alone, lipids alone, and scrambled ODN in liposomes had no effect on protein levels ***(29)***. The short, single-stranded antisense ODNs are not, in fact, encapsulated, but complexed with bilamellar vesicles by electrostatic interactions. Liposome development with cationic lipids also allows high transfection efficiency of plasmid DNA.

1.2. Plasmid Vectors

Partial or full-length cDNA of the gene of interest can be subcloned in antisense orientation under chosen promoter in a plasmid vector. Antisense mRNA is then expressed and completes with host sense mRNA for translation machinery. Plasmid vectors cause a relatively small immune response and can deliver long DNA sequences. Current limitations, however, are of a low efficiency of gene transfer and poor long-term expression.

We subcloned full-length angiotensinogen (AGT) cDNA in antisense orientation under the cytomegalovirus (CMV) promoter. This plasmid vector was used for transient transfection of hepatoma cells H4-IIE. Antisense expression was detected from 2 h after transfection and caused 50% reduction in AGT level secreted by the cells ***(30)***. Also, we injected AGT-AS plasmid (3 mg/kg body weight) intravenously to adult spontaneously hypertensive rats (SHR) and observed maximum decrease in the blood pressure of –22 mmHg, as compared to sense or saline-injected animals, lasting up to 6 d ***(31)***. For the local

Table 2
Features of the Perfect Viral Vector

1. It is safe, so if it is known to cause disease, it must be reengineered to be harmless.
2. Does not elicit an immune or inflammatory response
3. Does not integrate into the genome randomly, as this would risk disrupting other cellular genes and mutagenesis
4. Is replication-deficient so that it will not spread to other tissues or infect other individuals.
5. It delivers a defined gene copy number into each infected cell.
6. Is efficiently taken up by the target tissue, therefore, infects the target cells with high efficiency
7. Has high capacity so it can accommodate the gene of interest, along with its regulatory sequences
8. The recombinant DNA is packaged with high efficiency into the viral capsid.
9. It is easy to manipulate and produce in pure form.

effect, the most frequently used route of administration for plasmid DNA is probably intramuscular (im) injection.

Generally, use of plasmid DNA is considered to be safer than viral vectors, but expression is less efficient and shorter lasting, therefore, is useful when the transient effect is sufficient.

1.3. Viral Vectors for Antisense DNA Delivery

1.3.1. Perfect Viral Vector

There are several viruses that have been tested for gene delivery, and each has its advantages, but does not fit perfectly to the description of the "ideal viral vector." To be the perfect vector, a virus should fulfill all of the following criteria listed in **Table 2**.

1.3.2. Retroviruses

These have been used primarily because of their high efficiency in delivering genes to dividing cells ***(32)***. Retroviruses permit insertion and stable integration of single-copy genes. Although effective in cell-culture systems, they randomly integrate into the genome, which raises concerns about their safety for practical use in vivo. Because retroviruses can only act in dividing cells, they are ideal for tumor therapy, but less desirable where other cells are dividing that need to be protected.

In hypertension research, retroviruses are being investigated in treating developing SHR. Our colleagues at the University of Florida delivered retrovirus vector (LNSV) containing an antisense DNA to $AT_{1\text{-}B}$ receptor mRNA ***(33)***. Injections in the heart of 5-day-old SHR resulted in effective,

long-term inhibition of AT_1 receptor mRNA and significant inhibition of the development of hypertension. Several measures indicated that the treatment reduced responsiveness of AT_1-R in vessels to angiotensin II stimulation ***(33)***.

1.3.3. Adenoviruses

Adenovirus vectors have been tested successfully in their natural host cells, the respiratory endothelia, as well as other tissues such as vascular smooth and striated muscle, and brain ***(34–36)***.

Adenovirus is a double-stranded DNA with 2700 distinct adenoviral gene products. It infects many mammalian cell types because most cells have membrane receptors. The viruses enter the cell by receptor-induced endocytosis and translocate to the nucleus. Most adenovirus vectors in their current form are episomal, that is, they do not integrate into the host DNA. They provide high levels of expression, but the episomal DNA will invariably become inactive after some time. In some species, e.g., mice, this time may be long, relative to their life-span, but in humans it is a limitation of the virus as a vector. Repeated infections result in an inflammatory response with consequent tissue damage. This is because the adenovirus expresses genes that lead to immune cell attacks. This further limitation makes current recombinant adenovirus unsuitable for long-term treatment, thus, several gene therapy trials using adenovirus vectors have failed to produce acceptable results. Preliminary studies with adenovirus vectors for delivery of AT_1-R mRNA antisense have been tested in rats and reduced developing hypertension in SHR ***(37)***. The adenovirus is easy to produce and, therefore, useful for animal studies of mechanisms. However, the adenovirus as a vector has too many limitations at present to be successful in human gene therapy. Further engineering of the adenovirus may eventually avoid these limitations. Promising results have been obtained by Burcin et al. ***(38)*** who used adenovirus devoid of all viral coding sequences ***(39)***.

1.3.4. Adeno-Associated Virus (AAV)

The AAV has been gaining attention because of its safety and efficiency ***(40)***. It has been successfully used for delivering antisense RNA against alpha-globin ***(41)*** and HIV LTR ***(42)***, and it is our vector of choice for delivering antisense targeted to the RAS in hypertensive animal models.

AAV is a parvovirus, discovered as a contamination of adenoviral stocks. It is widespread (it is estimated that antibodies are present in 85% of people in the United States) and has not been linked to any disease. Its replication is dependent on the presence of a helper virus, such as adenovirus or herpes virus. Five serotypes have been isolated, of which AAV-2 is the best characterized. AAV has a single-stranded linear DNA that is encapsidated into capsid proteins VP_1, VP2, and VP3 to form an icosahedral virion of 20–24 nm in diameter ***(40)***.

Table 3
Features of AAV as a Vector

Benefits	Drawbacks
1. Nonpathogenic	1. Capacity up to 4.4. kb
2. Very broad host range ***(46)***	2. Complex packaging requires helper virus and helper plasmids with *rep* and *cap* genes
3. Virus sequences limited to ITRs (290 bp), therefore, does not evolve an inflammatory response	3. Multistep purification method
4. Long-lasting expression	

The AAV DNA is approx 4.7-kb long. It contains two open reading frames and is flanked by two inverted terminal repeats (ITRs). There are two major genes in the AAV genome: *rep* and *cap*. *Rep* codes for proteins responsible for viral replications, whereas *cap* codes for capsid proteins VP1–3. Each ITR forms a T-shaped hairpin structure. These terminal repeats are the only *cis*-components of the AAV necessary for packaging. Therefore, the AAV can be used as a vector with all viral coding sequences removed and replaced by the cassette of genes for delivery. Three viral promoters have been identified and named *p5*, *p19*, and *p40*, according to their map position. Transcription from *p5* and *p19* results in production of *rep* proteins, whereas transcription from *p40* produces the capsid proteins ***(40)***. For more powerful expression, we have inserted a cytomegalovirus (CMV) promoter. For expression in a particular tissue, there is an option of local injection or use tissue-specific promoters.

Upon infection of a human cell, the wild-type AAV integrates into the q-arm of chromosome 19 ***(43,44)***. Although chromosomal integration requires the terminal repeats, the viral components responsible for site-specific integration have been recently targeted to the *rep* proteins ***(45)***. With no helper virus present, AAV infection remains latent indefinitely. Upon superinfection of the cell with helper virus, the AAV genome is excised, replicated, packaged into virions, and released to the extracellular fluid. This fact is the basis of recombinant AAV production for research.

Several factors prompted researchers to study the possibility of using recombinant AAV as an expression vector. Benefits and drawbacks of using AAV are listed in **Table 3**.

The advantages, particularly its safety, make AAV appear to be one of the best candidates for delivery of genes for long-term therapy. Recently, Flotte and colleagues ***(47)*** have established gene-therapy Phase I trials for cystic fibrosis using AAV gene delivery in patients.

The general concept for antisense gene delivery in the AAV vector and the steps involved are shown in **Fig. 1**. To illustrate these steps, a brief

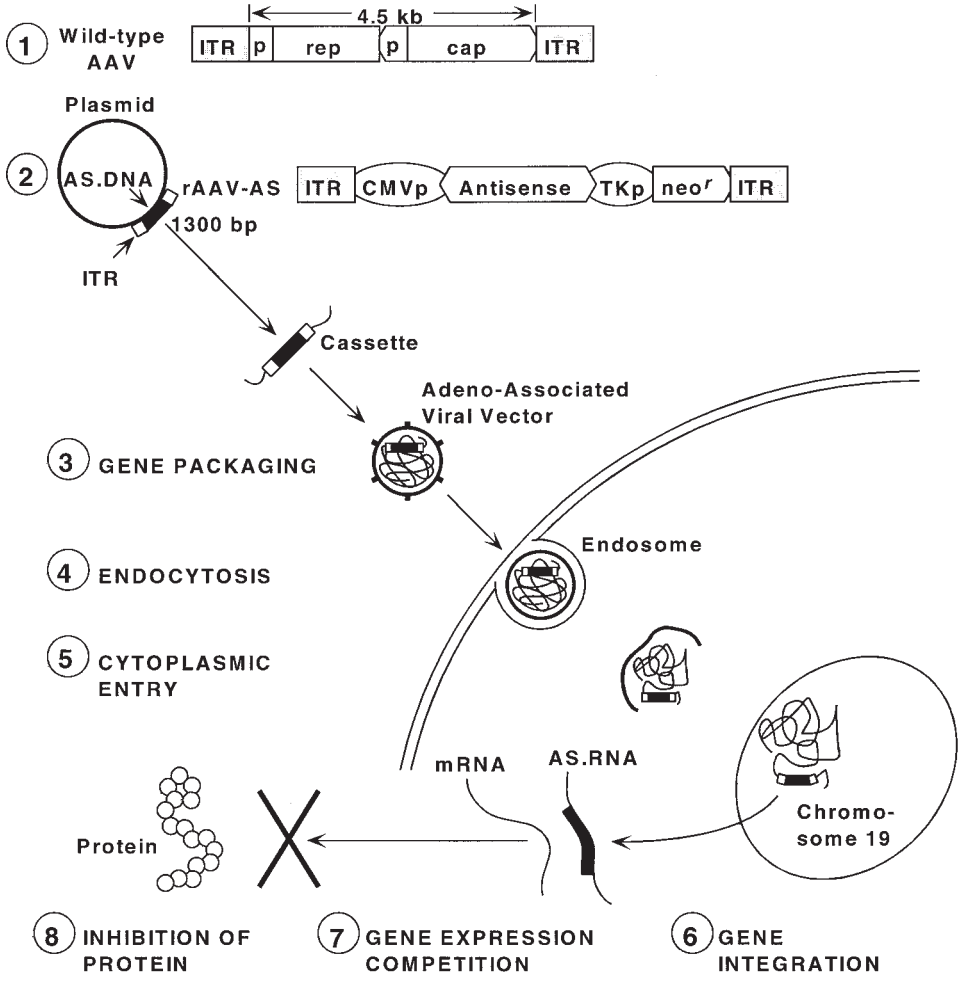

Fig. 1. Gene delivery of antisense DNA (AS-ODN) with adeno-associated viral vector (AAV). 1. Wild-type AAV (simplified): terminal repeats (STR), native promoters (p), genes necessary for replication (rep) and capsid (cap). 2. AAV-based plasmid: the plasmid contains the inverted terminal repeats (ITR) characteristic of AAV. A casette contains CMV promoter-driven antisense and TK promoter-driven *neo^r* gene for selection by G418 (geneticin). 3. Virus packaging: the packaging cell line is transfected with AAV-based plasmid and helper plasmid with *rep* and *cap* genes, and transduced with adenovirus as a helper virus. 4. Endocytosis: the viral vector fuses with the cell membrane by binding to adhesion molecules and becomes an endosome within the bilipid layer. 5. Cytoplasmic entry: the vesicle "opens" in the cytoplasm, releasing the vector that is transported to, and enters the nucleus. 6. Gene integration: AAV integrates with chromosome 19. It is not known if the addition of foreign DNA interferes with this integration. 7. Gene expression competition: Genomic DNA in chro-

description is given that is applicable to the RAS. Further details are presented in ***(47)***.

2. Materials

2.1. Large-Scale Plasmid Purification

1. J2-HS centrifuge with JA-20.1 and JA-14 rotors (Beckman) or equivalent.
2. Ultracentrifuge with NVT90 rotor (Beckman) or equivalent.
3. 250-mL polypropylene centrifuge bottles.
4 50-mL polypropylene centrifuge bottles.
5. 30-mL Corex tubes or equivalent.
6. 4.9-mL Optiseal centrifuge tube (Beckman) or equivalent.
7. 3-mL syringe with an 18-gage needle.
8. LB (Luria-Bertani) medium with 100 μg/mL ampicillin.
9. Lysozyme buffer (25 m*M* Tris pH 7.5, 10 m*M* ethylenediamine tetracetic acid (EDTA), 15% sucrose or glucose).
10. Lysozyme (12 mg/mL in lysozyme buffer).
11. 0.2 *N* NaOH-1% SDS.
12. 3 *M* sodium acetate, pH 4.8–5.2.
13. Chloroform.
14. 40% PEG 8000.
15. 5.5 *M* LiCl.
16. Isopropanol.
17. TE pH 7.4 (10 m*M* Tris-Cl with 1 m*M* EDTA).
18. Cesium chloride.
19. Isoamyl alcohol.
20. Ethanol, 100% and 75%.
21. Phenol:chloroform (25:24, v/v).

2.2. Preparation of Recombinant Adeno-Associated Virus (rAAV)

1. Cell-culture incubator with the temperature 37°C and 5% CO_2.
2. Cell-culture hood.
3. Inverted microscope.
4. 15-cm cell-culture plates.
5. Sonicator.
6. Ultracentrifuge with SW41 rotor.
7. Syringe (6 mL).
8. Centricon-30 tubes (Amicon).

---

mosome 19 produces an antisense RNA (AS-RNA). This competes with the natural mRNA and prevents it from producing its product. 8. Inhibition of protein synthesis: a binding of antisense RNA to the mRNA prevents sliding through the ribosomal assembly to produce protein. The result of this gene delivery system should be reduction in the amount of protein, specifically targeted by the antisense.

9. HEK293 cells grown in DMEM with 10% heat-inactivated FBS and penicillin/streptomycin.
10. Plasmid to be transfected, purified as described in **Subheading 3.2.**
11. Helper plasmid containing *rep* and *cap* genes.
12. 0.1 × TE (1 m*M* Tris-Cl, 0.1 m*M* EDTA pH 8.0).
13. HBS, pH 7.4.
14. 2 × HBS pH 7.05 (280 m*M* NaCl, 10 m*M* KCl, 1.5 m*M* $Na_2HPO_4 \cdot 2H_2O$, 12 m*M* dextrose and 50 m*M* HEPES).
15. 2 *M* $CaCl_2$.
16. Tris-Cl (50 m*M*, pH 8.4) with 150 m*M* NaCl.
17. Ammonium sulfate pH 7.0, saturated at 4°C.
18. Cesium chloride, solid and solutions of density 1.5 and 1.39 g/mL.
19. Phosphate-buffered saline (PBS).
20. 0.05% porcine trypsin with 0.02% EDTA.

2.3. Identifying Fractions Containing rAAV

1. Dot-blot apparatus and vacuum pump.
2. Nylon membrane.
3. Whatman 3MM filter paper.
4. Microwave oven.
5. Autoradiography film.
6. 20X SSC (3 *M* NaCl, 0.3 *M* sodium citrate pH 7.0).
7. 10% SDS.
8. 0.5 *M* NaOH with 1.5 *M* NaCl.
9. 0.5 *M* Tris-HCl pH 7.2 with 1.5 *M* NaCl.
10. [^{32}P]dCTP-labeled AAV probe, labeled by random priming using a kit.
11. 50X Denhardt's reagent (5 g Ficoll 400, 5 g polyvinylpyrrolidone, 5 g bovine serum albumin fraction V in 500 mL water).
12. Prehybridization buffer (5X Denhardt's solution diluted from 50X concentrate in 6X SSC, 0.5% SDS, 100 μg/mL denatured, fragmented salmon sperm DNA).
13. Hybridization buffer (6X SSC, 0.5% SDS, 100 μg/mL denatured, fragmented salmon sperm).
14. Washing buffer (2X SSC with 0.1% SDS).

2.4. Infectious Virus Assay

1. Cell-culture incubator with the temperature 37°C and 5% CO_2.
2. Cell-culture hood.
3. Inverted microscope.
4. 24-well cell-culture plate.
5. Vacuum pump.
6. HEK293 cells.
7. 0.05% porcine trypsin with 0.02% EDTA.
8. Adenovirus.
9. Wild-type and recombinant AAV.
10. PBS.

11. Nylon filter presoaked in PBS.
12. Whatman 2MM paper soaked in 0.5 *N* NaOH with 1.5 *M* NaCl.
13. Whatman paper soaked in 1 *M* Tris-HCl pH 7.0 with 2X SSC.
14. ^{32}P-labeled probe specific for the gene of interest (labeled by random priming using a kit).

3. Methods

3.1. Method for Design of Antisense Oligonucleotides

1. Check GenBank for mRNA sequence of the target protein in the species to be studied. If there is more than one lab cloning the same protein, compare the homology of different reports. These sequences will point out the controversial bases, which can be caused by natural mutations in variant strains of the same species or sequencing errors. Try to avoid these debatable regions. Target the ODN to the identical regions, which ensures reliability of the sequence being used. The best targets for designing effective AS-ODNs are the 5' *cap* region, the AUG translation initiation codon and the 3' untranslated region of the mRNA ***(48–50)***.
2. Choose the length of the antisense. The AS-ODNs we are using are 15–20 bases long, but longer or full-length cDNA in the antisense direction is used in plasmid or viral vectors. When designing antisense molecules, one has to consider two antagonistic factors: the affinity of oligonucleotide to its target sequence, which is dependent on the number and composition of complementary bases, and the availability of the target sequence, which is dependent on the folding of the mRNA molecule ***(51–53)***.
3. Check if antisense sequence is unique using Blast Search. Antisense sequence should be unique and specific for the target mRNA.
4. Avoid antisense with complicated secondary structure and self-dimerizing. Complicated secondary structures like loops and hairpins in the antisense sequence and self-dimerization prevent degradation, but also make hybridization with target mRNA more difficult. We are using phosphorothioated antisense, which is much more resistant to degradation than natural phosphodiester, therefore, it is more important to facilitate interaction with target mRNA. To check the presence of the secondary structure, we use a program for designing PCR primers.

3.2. Method for Preparation of pAAV-AT$_1$R-AS

The 749-bp fragment of the AT$_1$-R cDNA (-183 to 566) was amplified using polymerase chain reaction (PCR) and ligated to an AAV-derived vector (**Fig. 2**) in the antisense orientation, in place of *gfp*. The resulting plasmid vector (pAAV-AT$_1$R-AS) contained adeno-associated virus terminal repeats (TR), a cytomegalovirus promoter (Pcmv), the DNA encoding AT$_1$ receptor mRNA in the antisense orientation, and a *neo*mycin resistance gene *(neo^r)* (**Fig. 3**). *Escherichia coli* bacteria (Sure II, Stratagene) were transformed with the plasmid according to the manufacturer protocol. The plasmid DNA was purified on CsCl gradient, as described in **Subheading 3.3.**

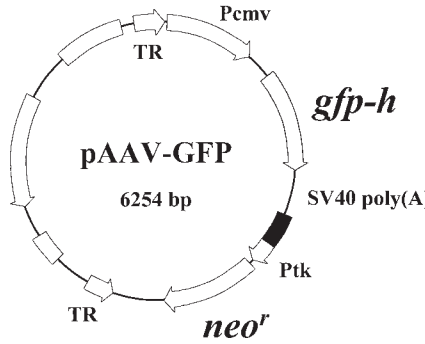

Fig. 2. Schematic diagrams of recombinant AAV vector containing the *gfp* gene. In the recombinant AAV-*gfp* vector almost all of the parental wild-type AAV genome (except the terminal repeats-TR) has been deleted and replaced with humanized *gfp*, the *Aequorea Victoria* green fluorescent protein gene, driven by a CMV promoter (Pcmv). The *neo*mycin resistance (*neo*^{r}) gene is under the control of thymidine kinase promoter (Ptk). The *gfp* serves as a reporter gene in vitro or in vivo, and the *neo*^{r} serves for selection in vitro.

3.3. Method for Large-Scale Plasmid Preparation

After subcloning the target gene into AAV-based vector with chosen promoter, highly purified plasmid is needed for virus packaging. To reach this goal, we recommend the protocol as follows.

1. Grow bacteria containing the appropriate plasmid in 1 L of LB (Luria-Bertani) medium with 100 μg/mL ampicillin.
2. Pellet bacteria at 3000*g* at 4°C for 15 min.
3. Resuspend bacteria in 20 mL of lysozyme buffer.
4. Add 4 mL of lysozyme (12 mg/mL in lysozyme buffer), mix.
5. Place on ice for 5 min until the mixture becomes viscous.
6. Add 48 mL of 0.2 *N* NaOH-1%SDS. Mix using a glass pipet as a stirring rod.
7. Place on ice for 5–10 min.
8. Add 36 mL of 3 *M* sodium acetate, pH 4.8–5.2; mix with the same pipet.
9. Add 0.2 mL of chloroform; mix.
10. Place on ice for 20 min.
11. Spin at 3000*g* at 4°C for 20 min.
12. Transfer supernatant into a fresh bottle.
13. Add 33 mL of 40% PEG8000, mix, and incubate on ice for 10 min.
14. Spin at 14,000*g* at 4° for 10 min.
15. Discard supernatant, dissolve pellet in 10 mL of sterile water, then add 10 mL of 5.5 *M* LiCl.
16. Place on ice for 10 min.
17. Spin at 14,000*g* at 4°C for 10 min.

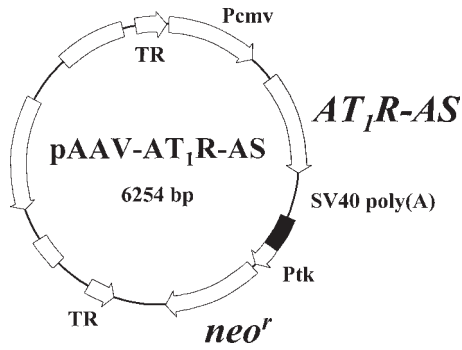

Fig. 3. Plasmid vector pAAV-AT_1R-AS contains a 750-bp fragment of the AT_{1A} receptor cDNA in antisense orientation. Abbreviations: TR, AAV terminal repeat; Pcmv, human cytomegalovirus early promoter; SV40 poly (A), polyadenylation signal from simian virus; Ptk, thymidine kinase promoter; *neo*^{r}, *neo*mycin phosphotransferase gene from Tn5. Other promoters have been substituted for CMV, including the arginine vasopressin (AVP), neuron specific enolase (NSE), and glial fibrillary acid protein (GFAP) promoters.

18. Save supernatant, transfer equal amounts (each 10 mL) into two 30-mL Corex (or plastic) tubes, add 6 mL of isopropanol to each tube; mix.
19. Incubate at room temperature (RT) for 10 min.
20. Spin at 10,000*g* at room temperature for 10 min.
21. Dissolve each pellet in 3.7 mL of TE pH 7.4.
22. Add 4.2 g of cesium chloride to each tube, mix and dissolve, add 0.24 mL of ethidium bromide (10 mg/mL), mix.
23. Transfer the solution in each tube into a 4.9-mL Optiseal centrifuge tube
24. Spin in NVT90 rotor (Beckman) at 484,500*g*, 15°C for 4 h.
25. After centrifugation, you will see three bands: the upper one contains protein, the middle one is nicked and linear DNA, and the lowest one is closed circular plasmid DNA. Carefully remove the plasmid band using a 3-mL syringe with a 18-gage needle and transfer it into Eppendorf tubes (two tubes, each about 0.5 mL).
26. Extract 3 to 4 times with an equal volume of isoamyl alcohol, discarding the organic phase (top layer) every time until all pink color is removed.
27. Transfer into one 30-mL Corex or plastic tube, add 2.5 vol (2.5 mL) of water, mix and add two combined volumes of ethanol (7 mL).
28. Place on ice for 30 min.
29. Pellet plasmid DNA at 12,000*g* for 15 min at 4°C.
30. Discard supernatant, dissolve pellet in 500 μL of TE (pH 7.4).
31. Transfer into Eppendorf tube, add 500 μL of phenol:chloroform (25:24, v/v), vortex, spin for 2 min at top speed in a microcentrifuge.
32. Save the top aqueous layer and transfer into a fresh Eppendorf tube.
33. Add 50 μL of 3 *M* sodium acetate buffer, pH 4.8–5.2 and mix; add 1 mL ethanol, mix.

34. Pellet the plasmid DNA at top speed in microcentrifuge for 5 min at 4°C.
35. Discard the supernatant, wash the pellet with 75% ethanol, and vacuum dry.
36. Dissolve the pellet in 1 mL of TE.

We constructed plasmids for both AT_1 receptor antisense and angiotensinogen antisense in the AAV-derived expression vector. Initially, we used a plasmid containing AAV genome and 750 bp cDNA inserted into the AAV in the antisense direction downstream from the AAV promoter. The NG108-15 cells or hepatoma H4 cells were transfected with AT_1-R-AS or AGT-AS plasmid, respectively, using lipofectamine ***(54,55)***. In both cases, there were significant reductions in the appropriate proteins, namely AT_1-R and angiotensinogen. To test that the cells expressed AAV, we used the *rep* gene product as a marker. Immunocytochemical staining with a rep protein antibody showed that the majority of cells in culture expressed the vector. A further development of the AAV was the insertion of more powerful and specific promoters than the p40 promoter. AAV with CMV promoter and *neo*mycin resistance (*neo*^{r}) gene as a selectable marker is now being used in our current experiments. The AAV cassette contained a marker, either the *gfp* gene, which encodes the green fluorescent protein (**Fig. 2**, **ref. *56***) or *lac*Z gene ***(57)***. NG108-15 cells transfected with AAV plasmid containing the *gfp* and *neo*^{r} genes were selected by antibiotic, G418 (600 μg/mL), and the selected clones viewed for *GFP* expression. Very few cells died during selection. Two weeks after transfection, all of the cells were expressing *GFP*. The transfection efficiency of this pAAV-*gfp* construct in different cell lines, including ATt20 (mouse pituitary cells), L929 (mouse fibroblasts), HEK293 (human embryonic kidney cells), and NG108-15 was over 50% ***(58)***.

Plasmid pAAV-AT_1R-AS was tested for AT_1 receptor inhibition in vitro, using NG108-15 ***(59)*** and vascular smooth muscle cells ***(60)***. The cells had a significant ($p < 0.01$) decrease in angiotensin II AT_1 receptors number comparing with the control cells. No effect was seen on the AT_2 receptors.

3.4. Method to Prepare rAAV

To prepare rAAV, HEK293 cells are transfected with plasmid vector containing gene of interest in antisense orientation and AAV terminal repeats (pAAV-AS), together with helper plasmid delivering *rep* and *cap* genes (necessary for AAV replication) in *trans* using calcium phosphate method. Eight hours after transfection, helper virus is added at a multiplicity of infection (MOI) of 5. Details are described below.

1. Split low-passage number HEK293 cells grown in DMEM with 10% heat-inactivated FBS and 100 μg/mL penicillin and 100 μg/mL streptomycin onto 15-cm cell-culture plates, so they are about 70% confluent the following day.

2. For each plate, mix 20 μg of your plasmid, and 20 μg of helper plasmid (containing *rep* and *cap* genes) in a final volume 876 μL of 0.1X TE
3. Add 1 mL of 2X HBS and mix.
4. Dropwise, and with mixing, add 124 μL of 2 *M* $CaCl_2$.
5. Incubate 15–20 min at RT to form precipitate, mix once by pipeting.
6. Add 2 mL of mixture to the plate of cells, swirl gently, and return cells to the incubator.
7. Eight h after transfection, replace medium with fresh medium and add adenovirus at an MOI of 5.
8. When cytopathic effects are observed (usually 2–3 d) harvest cells in own medium, using a rubber policeman, and place in centrifuge bottles.
9. Centrifuge cell suspension at 900*g* at 4°C for 15 min.
10. Resuspend the cell pellet in 1 mL multiplied by the initial amount of plates of 50 m*M* Tris-Cl pH 8.4 with 150 m*M* NaCl and freeze-thaw three times.
11. Sonicate cell suspension for 30 s three times on ice.
12. Spin down cell debris by centrifugation at 2000*g* at 4°C for 10 min. Transfer the supernatant to a new tube.
13. Repeat freezing-thawing, sonicating, and spinning down the pellet once. Combine supernatants.
14. Calculate 33% of the volume of supernatant, slowly, and with continuous mixing, add this volume of ammonium sulfate pH 7.0, saturated at 4°C, and incubate slurry at 4°C for 15 min.
15. Spin the sample at 8000*g*, 4°C for 15 min. Transfer the supernatant to a new tube.
16. Dropwise, and with mixing, add 67% of the initial volume of supernatant of ammonium sulfate pH 7.0, saturated at 4°C.
17. Incubate on ice for 20 min. Centrifuge the solution at 17,500*g* at 4°C for 20 min. Discard supernatant and turn the tube upside down on a paper towel to make sure that all fluid is removed.
18. Dissolve the pellet from 10 plates in 8.5 mL of HBS, pH 7.4.
19. Mix with 5.5 g of solid CsCl and transfer to centrifuge tubes (density should be 1.39 g/mL).
20. Underlay with 1 mL of CsCl solution of 1.5 g/mL density; use a marker pen to mark the level of the cushion on the outside of the tube.
21. Spin the sample in SW41 rotor at 274,400*g* at 18°C for 40 h. You will see a white diffuse band of proteins at the top and a sharp white band of adenovirus below.
22. Using a 6-mL syringe, pull out the fluid that lies from about one-third of the way up the tube to about 2-mm below adenovirus band.
23. Mix the sample with 1.39 g/mL CsCl and spin in an SW41 rotor at 274,400*g* at 18°C for 40 h.
24. Gently, without disturbing the CsCl gradient, place a needle in an upper part of the tube, tape it (so you can control speed of the fluid dripping later on), puncture the bottom of the tube with a needle and start to collect fluid. Collect five 1-mL fractions, then ten 0.5-mL fractions.
25. Check these fractions for AAV using hybridization with [^{32}P]dCTP-labeled random primed AAV probe using dot-blot apparatus (*see* **Subheading 3.5.**)

3.5. Method to Identify Fractions Containing rAAV

1. Assemble dot-blot apparatus with Whatman 3MM paper filter under a nylon filter presoaked in distilled water and then 20X SSC.
2. Add 200 μL of 20X SSC per well and apply slow vacuum to remove the fluid.
3. Add 5-μL aliquots of each fraction from CsCl gradient and apply a slow vacuum to remove the fluid
4. Remove the nylon filter from the manifold, place on Whatman 3MM paper filters soaked as follows: 10% SDS for 3 min, 0.5 *M* NaOH with 1.5 *M* NaCl for 5 min, 0.5 *M* Tris-HCl pH 7.2 with 1.5 *M* NaCl for 5 min. Air-dry filter for 10 min, briefly wash in 4X SSC for 10 s and air-dry for 10 min. Microwave the filter for 4 min with 0.5 L of water in the beaker placed nearby.
5. Radiolabel the probe using random-primed labeling kit to specific radioactivity 10^9 cpm/μg or greater.
6. Incubate the wet filter in prehybridization buffer for 1 h at 65°C.
7. Remove prehybridization buffer and replace with hybridization buffer.
8. Denature radiolabeled probe (1–2 ng/mL) by heating for 5 min at 100°C and rapidly cooling in ice water.
9. Add probe to the hybridization buffer and incubate overnight at 65°C.
10. Wash filter in a washing buffer 2–3 times, 10 min each time at RT.
11. Expose the filter to autoradiography film at –80°C. The packaged AAV virions should be present near the middle of the gradient.
12. Combine positive fractions, concentrate virus by using Centricon-30 (Amicon) at 4350*g* for 30 min at 4°C.
13. Overlay the filter with concentrated virus with 0.5 mL of PBS and spin again for 2 min at 500*g*. Collect the virus.

To determine the titer of the rAAV one can use infectious particles titer assay described in **Subheading 3.6.**

3.6. Infectious Virus Titer Assay

The titer of the virus is assayed using HEK293 cells, wild-type AAV, and adenovirus.

1. Seed 5×10^4 cells in each well of a 24-well plate and incubate 24 h.
2. Infect all, but one, well with adenovirus at an MOI of 20.
3. Infect all, but one, well (a different one from that in **step 2**) with wild-type AAV at an MOI of 4.
4. Make serial fivefold dilutions of the recombinant AAV in PBS and infect 8–10 wells, which contain already adenovirus and wild-type AAV. Inject well without adenovirus or without wild-type AAV with undiluted rAAV. Incubate cells for 24 h.
5. Spin down the media, discard supernatant, combine pellet with prewashed and trypsinized cells from the plate (100 μL trypsin-EDTA per well), add 10 mL of PBS and disperse into single-cell suspension.

6. Transfer cell suspension onto nylon filter presoaked in PBS and apply low vacuum.
7. Place filter on Whatman 2MM paper soaked in 0.5 *N* NaOH with 1.5 *M* NaCl for 5 min at RT.
8. Transfer filter to the top of Whatman paper soaked in 1 *M* Tris/HCl pH 7.0 with 2X SSC for 5 min at room temperature.
9. Air-dry the filter.
10. Hybridize the filter with ^{32}P-labeled probe specific for your gene of interest (random primed according to the kit instruction)—*see* **Protocol 3.**
11. Expose the filter to autoradiography film at –80°C. Count the spots and multiply by the dilution factor for each well. Wells without adenovirus detect contamination with adenovirus and wells without wild-type AAV detect contamination with wtAAV in rAAV.

In our studies, recombinant AAV-AT_1R-AS was tested for AT_1 receptor inhibition in vitro, using vascular smooth muscle cells ***(60)***. Transduced cells, without G418 selection, expressed the transgene for at least 8 wk, had a decreased number of AT_1 receptors and reduced calcium response to angiotensin II stimulation.

Expression in vivo was tested first by direct injection into the brain. An AAV with an arginine vasopressin promoter (AVP) to drive a *lac*Z reporter gene was constructed. The vector expressed β-galactosidase in neurons of the paraventricular nucleus and supraoptic nucleus. The expression was in magnocellular cells that normally express AVP ***(57)***. The expression was observed at 1 d, 1 wk, and after 1 mo with no diminution of signal. This is an example of how AAV can be developed for specific tissue and/or cell gene expression and shows that AAV vectors can deliver foreign genes into an adult brain for long periods of time.

Next, to test for effectiveness in vivo, rAAV-AT_1R-AS was microinfused into the lateral ventricles of adult male SHR. Control rats received AAV with *gfp* reporter gene, but without the AS gene ("mock" vector), in vehicles that was artificial cerebrospinal fluid. Blood pressure was measured by tailcuff method. There was a significant decrease in systolic blood pressure (SBP) in one group of rats, which received the rAAV-AS vector. No effect was observed in the controls. SBP decreased by 23 ± 2 mmHg in the first week after administration. This drop in blood pressure was prolonged in four rats for 9 wk, whereas controls had no reduction in blood pressure ***(61)***. This was considerably longer than the longest effect observed with AS-ODN. Recombinant AAV-*gfp* expression in hypothalamus of the control rat group was detectable by RT-nested PCR 11 mo after injection. Further, intracardiac injection of rAAV-AS in SHR, significantly reduced blood pressure and slowed the development of hypertension for several weeks ***(61,62)***. This result demonstrates that rAAV-AS in a single application, is effective in chronically

inhibiting RAS. This encourages further research on gene regulation in cardiovascular diseases and to explore the most effective routes of delivery applicable to humans.

Acknowledgments

This work has been supported by NIH (MERIT) grant HL23774 and grants from the American Heart Association, Florida Affiliate. Thanks to Nick Muzyczka, Ed Meyer, Allyson Peele, Birgitta Kimura, Leping Shen, and Sara Galli for help in developing these methods and to Gayle Butters for word processing.

References

1. Wagner, R. W. (1994) Gene inhibition using antisense oligodeoxynucleotides. *Nature* **372,** 333–335.
2. Crooke, S. T. (1992) Therapeutic applications of oligonucleotides. *Annu. Rev. Pharmacol. Toxicol.* **32,** 329–376.
3. Stein, C. A. and Cheng, Y.-C. (1993) Antisense oligonucleotides: is the bullet really magical? *Science* **261,** 1004–1012.
4. Chiasson, B. J., Hooper, M. L., Murphy, P. R., and Robertson, H. A. (1992) Antisense oligonucleotide eliminates *in vivo* expression of c-fos in mammalian brain. *Eur. J. Pharmacol.* **277,** 451–453.
5. Wahlestedt, C., Pich, E. M., Koob, G. F., Yee, F., and Heilig, M. (1993) Modulation of anxiety and neuropeptide Y-Y1 receptors by antisense oligodeoxynucleotides. *Science* **259,** 528–531.
6. Wahlestedt, C., Golanov, E., Yamamoto, S., Yee, F., Ericson, H., Yoo, H., et al. (1993) Antisense oligonucleotides to NMDA-R1 receptor channel protect cortical neurons from excitotoxicity and reduce focal ischemic infarctions. *Nature* **363,** 260–263.
7. McCarthy, M. M., Masters, D. B., Rimvall, K., Schwartz-Giblin, S., and Pfaff, D. W. (1994) Intracerebral administration of antisense oligodeoxynucleotides to GAD65 and GAD67 mRNAs modulates reproductive behavior in the female rat. *Brain Res.* **636,** 209–220.
8. Gyurko, R., Wielbo, D., and Phillips, M. I. (1993) Antisense inhibition of AT_1 receptor mRNA and angiotensinogen mRNA in the brain of spontaneously hypertensive rats reduces hypertension of neurogenic origin. *Regul. Pept.* **49,** 167–174.
9. Phillips, M. I. (1997) Antisense inhibition and adeno-associated viral vector delivery for reducing hypertension. *Hypertension* **29,** 177–187.
10. Junemaitre, X., Soubrier, F., Kotelvtsev, Y. V., Lifton, R. P., Williams, C. S., Charru, A., et al. (1992) Molecular basis of human hypertension: role of angiotensinogen. *Cell* **71,** 169–180.
11. Kim, H. S., Krege, J. H., Kluckman, K. D., Hagaman, J. R., Hodgin, J. B., Best, C. F., et al. (1995) Genetic control of blood pressure and the angiotensinogen locus. *Proc. Natl. Acad. Sci.* **92,** 2735–2739.

12. Tanimoto, K., Sugiyama, F., Goto, Y., Ishida, J., Takimoto, E., Yagami, K., et al. (1994) Angiotensinogen-deficient mice with hypotension. *J. Biol. Chem.* **269,** 31,334–31,337.
13. Phillips, M. I., Mann, J. F. E., Haebara, H., Hoffman, W. E., Dietz, R., Schelling, P., and Ganten D. (1977) Lowering of hypertension by central saralasin in the absence of plasma renin. *Nature* **270,** 445–447.
14. Nazarali, A. J., Gutkind, J. S., Correa, F. M., and Saavedra, J. M. Decreased angiotensin II receptors in subfornical organ of sponta*neo*usly hypertensive rats after chronic antihypertensive treatment with enalapril. *Am. J. Hyperten.* **3,** 59–61.
15. Phillips, M. I. and Kimura, B. (1988) Brain angiotensin in the developing spontaneously hypertensive rat. *J. Hypertens.* **6,** 607–612.
16. Simons, R. W. (1998) Naturally occurring antisense RNA control—a brief review. *Gene* **72,** 35–44.
17. Campbell, J. M., Bacon, T. A., and Wickstrom, E. (1990) Oligodeoxynucleotide phosphorothioate stability in subcellular extracts, culture media, ser and cerebrospinal fluid. *J. Biochem. Biophys. Methods* **20,** 259–267.
18. Li, B., Hughes, J. A., and Phillips, M. I. (1997) Uptake and efflux of intact antisense phosphorthioate deoxyoligonucleotide directed against angiotensin receptors in bovine adrenal cells. *Neurochem. Int.* **31,** 393–403.
19. Iversen, P. L., Zhu, S., Meyer, A., and Zon, G. (1992) Cellular uptake and subcellular distribution of phosphorothioate oligonucleotides into cultured cells. *Antisense Res. Dev.* **2,** 211–222.
20. Loke, S. L., Stein, C. A., Zhang, X. H., Mori, K., Nakanishi, M., Subasinghe, C., et al. (1989) Characterization of oligonucleotide transport into living cells. *Proc. Natl. Acad. Sci. USA* **86,** 3474–3478.
21. Wagner, R. W., Matteucci, M. D., Lewis, J. G., Gutierrez, A. J., Moulds, C., and Froehler, B. C. (1993) Antisense gene inhibition by oligonucleotides containing C-5 propyne pyrimidines. *Science* **260,** 1510–1513.
22. Iversen, P. L., Mata, J., Tracewell, W. G., and Zon, G. (1994) Pharmacokinetics of an antisense phosphorothioate oligodeoxynucleotide against rev from human immunodeficiency virus type 1 in the adult male rat following single injections and continuous infusion. *Antisense Res. Dev.* **4,** 43–52.
23. Phillips, M. I., Wielbo, D., and Gyurko, R. (1994) Antisense inhibition of hypertension: a new strategy for renin-angiotensin candidate genes. *Kidney Int.* **46,** 1554–1556.
24. Ambuehl, P., Gyurko, R., and Phillips, M. I. (1995) A decrease of angiotensin receptor number in rat brain nuclei by antisense oligonucleotides against the angiotensin AT_{1A} receptor. *Regul. Pept.* **59,** 171–182.
25. Wielbo, D., Sernia, C., Gyurko, R., and Phillips, M. I. (1995) Antisense inhibition of hypertension in the sponta*neo*usly hypertensive rat. *Hypertension* **25,** 314–319.
26. Morishita, R., Gibbons, G. H., Kaneda, Y., Ogihara, T., and Dzau, V. J. (1994) Pharmacokinetics of antisense oligodeoxyribonucleotides (cyclin B1 and CDC 2 kinase) in the vessel wall *in vivo*: enhanced therapeutic utility for restenosis by HVJ-liposome delivery. *Gene* **149,** 13–19.

27. Colige, A., Sokolov, B. P., Nugent, P., Baserge, R., and Prockop, D. J. (1993) Use of an antisense oligonucleotide to inhibit expression of a mutated human procollagen gene (COL1A1) in transfected mouse 3T3 cells. *Biochemistry* **32,** 7–11.
28. Tomita, N., Morishita, R., Higaki, J., Kaneda, Y., Mikami, H., and Ogihara, T. (1994) *In vivo* transfer of antisense oligonucleotide against rat angiotensinogen with HVJ-liposome delivery resulted in reduction of blood pressure in SHR. *Hypertension* **24,** 397.
29. Wielbo, D., Simon, A., Phillips, M. I., and Toffolo, S. (1996) Inhibition of hypertension by peripheral administration of antisense oligodeoxynucleotides. *Hypertension* **28,** 147–151.
30. Mohuczy, D., Tang, X. P., Kimura, B., and Phillips, M. I. (1999) Adeno-associated virus-based vector with angiotensinogen cDNA is effective in rat hepatoma cells. *FASEB J.* **13,** A484 (abstr.).
31. Tang, X. P., Mohuczy, D., Zhang, Y., Kimura, B., Galli, S. M., and Phillips, M. I. (1999) Intravenous angiotensinogen antisense in AAV-based vctor decreases hypertension. *Am. J. Physiol.* 277 (*Heart Circ. Physiol.* 46), H2392–H2399.
32. Mulligan, R. C. (1993) The basic science of gene therapy. *Science* **260,** 926–932.
33. Iyer, S. N., Lu, D., Katovich, M. J., and Raizada, M. K. (1996) Chronic control of high blood pressure in sponta*neo*usly hypertensive rat by delivery of angiotensin type 1 receptor antisense. *Proc. Natl. Acad. Sci. USA* **93,** 9960–9965.
34. Brody, S. L., Jaffe, H. A., Eissa, N. T., and Daniel, C. (1994) Administration of an adenovirus containing the human CFTR cDNA to the respiratory tract of individuals with cystic fibrosis. *Nat. Genet.* **8,** 42–51.
35. Quantin, B., Perricaudet, L. D., Tajbakhsh, S., and Mandel, J.-L. (1992) Adenovirus as an expression vector in muscle cells *in vivo*. *Proc. Natl. Acad. Sci USA* **89,** 2581–2584.
36. Le Gal La Salle, G., Robert, J. J., Berrard, S., Ridoux, V., Stratford-Perricaudet, L. D., Perricaudet, M., and Mallet, J. (1993) An adenovirus vector for gene transfer into the neurons and glia in the brain. *Science* **259,** 988–990.
37. Lu, D., Yang, H., and Raizada, M. K. (1998) Attenuation of Ang II actions by adenovirus delivery of AT_1 receptor antisense in neurons and SMC. *Am. J. Physiol.* **274,** H719–H727.
38. Burcin, M. M., Schiedner, G., Kochanek, S., Tsai, S. Y., and O'Malley, B. W. (1999) Adenovirus-mediated regulable target gene expression *in vivo*. *Proc. Natl. Acad. Sci. USA* **96,** 355–360.
39. Kochanek, S., Clemens, P. R., Mitani, K., Chen, H. H., Chan, S., and Caskey, C. T. (1996) A new adenoviral vector: replacement of all viral coding sequences with 28 kb of DNA independently expressing both full-length dystrophin and beta-galactosidase. *Proc. Natl. Acad. Sci. USA* **93,** 5731–5736.
40. Muzyczka, N. and McLaughin, S. (1988) Use of adeno-associated virus as a mammalian transduction vector, in *Current Communications in Molecular Biology: Viral Vectors* (Gluzman, Y. and Hughes, S. H., eds.), Cold Spring Harbor Laboratory Press, Cold Spring Harbor, NY, pp. 39–44.
41. Ponnazhagan, S., Nallari, M. L., and Srivastava, A. (1994) Suppression of human a-globin gene expression mediated by the recombinant adeno-associated virus 2-based antisense vectors. *J. Exp. Med.* **179,** 733–738.

42. Chatterjee, S., Johnson, P. R., and Wong, K. K. (1992) Dual-target inhibition of HIV-1 *in vitro* by means of an adeno-associated virus antisense vector. *Science* **258,** 1485–1488.
43. Muzyczka, N. (1992) Use of adeno-associated virus as a general transduction vector for mammalian cells, in *Current Topics in Microbiology and Immunology*, vol. 158, Springer-Verlag, Berlin, pp. 97–129.
44. Samulski, R. J., Zhu, X., Xiao, X., Brook, J. D., Housman, D. E., Epstein, N., and Hunter, L. A. (1991) Targeted integration of adeno-associated virus (AAV) into human chromosome 19. *EMBO J.* **10,** 3941–3950.
45. Linden, R. M., Winocour, E., and Berns, K. I. (1996) The recombination signals for adeno-associated virus site-specific integration. *Proc. Natl. Acad. Sci. USA* **93,** 7966–7972.
46. Lebkowski, J. S., McNally, M. M., Okarma, T. B., and Lerch, B. (1988) Adeno-associated virus: a vector system for efficient introduction and integration of DNA into a variety of mammalian cell types. *Mol. Cell. Biol.* **8,** 3988–3996.
47. Flotte, T. R., Carter, B., Conrad, C., Guggino, W., Reynolds, T., Rosenstein, B., et al. (1996) A phase I study of an adeno-associated virus-CTFR gene vector in adult CF patients with mild lung disease. *Hum. Gene Ther.* **7,** 1145–1159.
48. Bennett, C. F., Condon, T. P., Grimm, S., Chan, H., and Chiang, M. Y. (1994) Inhibition of endothelial cell adhesion molecule expression with antisense oligonucleotides. *J. Immunol.* **152,** 3530–3540.
49. Bacon, T. A. and Wickstrom, E. (1991) Walking along human c-myc mRNA with antisense oligonucleotides: maximum efficacy at the 5' *cap* region. *Oncogene Res.* **6,** 13–19.
50. Cowsert, L. M., Fox, M. C., Zon, G., and Mirabelli, C. K. (1993) *In vitro* evaluation of phosphorothioate oligonucleotides targeted to the E2 mRNA of papillomavirus: potential treatment for genital warts. *Antimicrob. Agents Chemother.* **37,** 171–177.
51. Lima, W. F., Monia, B. P., Ecker, D. J., and Freier, S. M. (1992) Implication of RNA structure on antisense oligonucleotide hybridization kinetics. *Biochemistry* **31,** 12,055–12,061.
52. Sczakiel, G., Homann, K., and Rittner, K. (1993) Computer-aided search for effective antisense RNA target sequences of the human immunodeficiency virus type 1. *Antisense Res. Dev.* **3,** 45–52.
53. Jaroszewski, J. W., Syi, J. L., Ghosh, M., Ghosh, K., and Cohen, J. S. (1993) Targeting of antisense DNA: comparison of activity of anti-rabbit beta-globin oligodeoxyribonucleoside phosphorothioates with computer predictions of mRNA folding. *Antisense Res. Dev.* **3,** 339–348.
54. Gyurko, R. and Phillips, M. I. (1995) Antisense expression vector decreases angiotensin receptor binding in NG108-15 cells. *Exp. Biol.* #1915 (abstr.).
55. Gyurko, R., Wu, P., Sernia, C., Meyer, E., and Phillips, M. I. (1994) Antisense expression vector decreases angiotensinogen synthesis in H-4 hepatoma cells. *American Heart Assoc. 48th Ann. Council for High Blood Pressure*, (abstr.).
56. Zolotukhin, S., Potter, M., Hauswirth, W. W., Guy, J., and Muzyczka, N. (1996) A "humanized" green fluorescent protein cDNA adapted for high-level expression in mammalian cells. *J. Virol.* **70,** 4646–4654.

57. Wu, P., Du, B., Phillips, M. I., Bui, J., and Terwilliger, E. F. Adeno-associated viral vector mediated transgene integration in non-dividing cells. *J. Virol*. **72,** 5919–5926.
58. Mohuczy, D. and Phillips, M. I. (1996) Adeno-associated virus vector as a highly efficient transporter of exogenous DNA into cells. *FASEB J.* **10,** A447 (abstr.).
59. Zelles, T., Mohuczy, D., and Phillips, M. I. (1996) Inhibition of angiotensin receptor (AT_1) expression in NG108-15 cells transfected with AT_1 receptor antisense in an adeno-associated viral vector. *Soc. Neurosci.* #41.18, 83 (abstr.).
60. Mohuczy, D., Gelband, C., and Phillips, M. I. (1999) Antisense inhibition of AT_1 receptor in vascular smooth muscle cells using adeno-associated virus-based vector. *Hypertension* **33,** 354–359.
61. Phillips, M. I., Mohuczy-Dominiak, D., Coffey, M., Wu, P., Galli, S. M., and Zelles, T. (1997) Prolonged reduction of high blood pressure with an *in vivo*, nonpathogenic, adeno-associated viral vector delivery of AT_1-R mRNA antisense. *Hypertension* **29,** 374–380.
62. Kimura, B., Mohuczy, D., and Phillips, M. I. (1998) Injection of AT_1 receptor antisense in adeno-associated virus (AAV) attenuates hypertension in the spontaneously hypertensive rat (SHR). *FASEB J.* **12,** #522, A90, (abstr.).

7

Analysis of Transcriptional Control Mechanisms I

Techniques for Characterization of cis*-Regulatory Elements*

Christopher T. Sherman and Allan R. Brasier

1. Introduction

Transcriptional control, the process controlling when and how much RNA is produced from a DNA template, is a major determinant of gene expression in eukaryotic cells. This process, intensely studied over the last few decades, is under control of specific DNA sequences (*cis* elements) that function by virtue of their ability to be recognized by sequence-specific DNA-binding proteins (*trans*-acting elements). Both of these elements function in concert to control the rate and location of RNA transcript formation. Therefore, identification of these *cis*- and *trans*-acting elements provides important mechanistic insight into gene expression control. These studies are relevant to understanding aspects of the renin–angiotensin system. For example, a large body of evidence has shown that angiotensinogen (AGT) is a highly inducible gene, regulated by a variety of physiological hormone systems. Because AGT circulates close to its Michaelis–Menten constant (K_m) for renin, changes in AGT concentration influence the long-term activity of the RAS [Reviewed in ***(1)***].

In the next two chapters, we will introduce methodology for identification of *cis*- (Chapter 7) and *trans*- (Chapter 8) acting factors in control of gene expression. For example, using these techniques, it has been possible to make insight into how AGT is inducible by diverse hormonal mediators including steroid hormones [glucocorticoids ***(2–8)***], cytokines [interleukin 1 (IL-1) ***(9)***, tumor necrosis factor-α ***(10–12)***] and intravascular angiotensin II ***(13)***. The techniques are written generically for application to any gene promoter in the renin–angiotensin system.

From: *Methods in Molecular Medicine, vol. 51: Angiotensin Protocols*
Edited by: D. H. Wang

1.1. General Strategy

The mapping of *cis*- promoter elements typically begins after a statistically significant increase in mRNA levels of the gene of interest has been shown by Northern-blot analysis following treatment of cells with cytokine, growth factor, hormone, and so on. At this point, a region of the promoter of the gene of interest is cloned and ligated upstream of a reporter gene for use in transient transfection assays. Examples of reporter genes include growth hormone, firefly luciferase, and chloramphenicol acetyl-transferase (CAT). A discussion of the relative merits of these, and other reporter gene systems, is given in **Subheading 3.** They all follow a similar concept: that induction of the promoter ligated upstream of the reporter gene will cause an increase in the message for that particular reporter gene, which is subsequently translated into a protein, that can be quantitated directly (e.g., growth hormone) or a protein with enzymatic activity which can be quantitated (e.g., luciferase).

In addition to choosing a reliable reporter gene, the boundaries of the promoter region that one wishes to ligate upstream of the reporter gene, must also be chosen carefully. This region should be large enough to contain all possible response elements as well as the transcription initiation site. One must take care not to include any intron/exon splice sites when a boundary far downstream of the transcription initiation site has been chosen. Subjecting the basepair sequence of the promoter region to a computer search of transcription factor binding sites may aid one's choice of boundaries. Such analysis programs are available through the NIH web site (www.nih.gov/). Additionally, one may want to search the literature for previously described response element sequences known to be utilized by the factor which one has found through Northern-blot analysis to induce the gene of interest. Armed with this knowledge, a search for such sequences can then be performed on the promoter of interest manually or with the aid of a computer. One must also keep in mind the effects of enhancer elements far removed from the promoter region of a gene that may influence native gene expression. The effects of enhancer elements as well as the chromatin structure may cause differences in the degree of activation observed during Northern-blot analysis of a gene vs that observed during a transient transfection assay. The effects of chromatin structure on promoter activation can often be accounted for through the use of cells stably transfected with the reporter gene (*see* **Notes**).

The approach our laboratory typically takes when cloning a promoter region is to design polymerase chain reaction (PCR) primers which incorporate a restriction enzyme digestion site into the PCR product. Typically, the upstream gene-specific primer has a *Bam*HI site at the 5' end of the primer and the downstream primer has a *Hin*dIII site. Additionally, five to six basepairs are added 5' of the restriction site on each primer such that the site-specific restric-

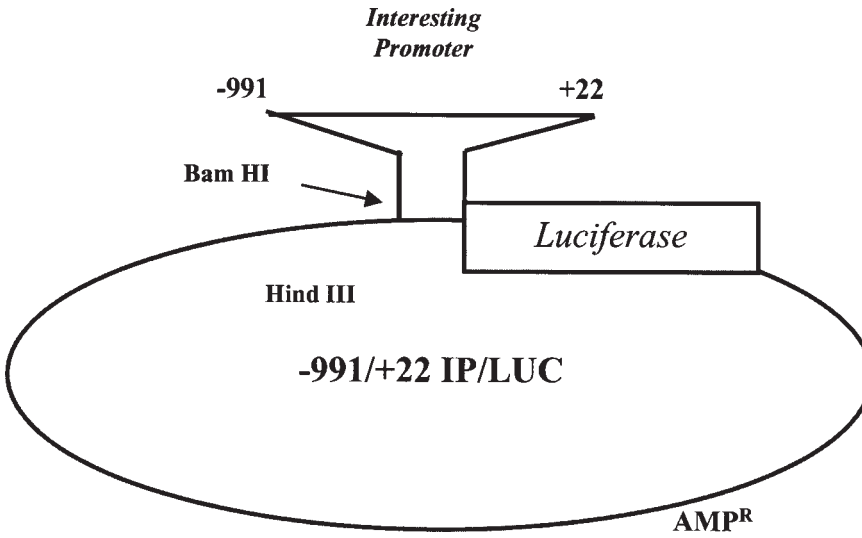

Fig. 1. Example of reporter gene construct. Here, a region from 991 basepairs upstream to 22 basepairs downstream of the transcription initiation of an interesting promoter (IP) are ligated upstream of a plasmid containing the firefly luciferase reporter. Note that any reporter gene can replace the luciferase reporter described above. I will use the luciferase reporter throughout my promoter analysis example figures because it is the reporter system with which I am most familiar.

tion enzyme, which requires approx 4 nonspecific basepairs flanking the specific restriction site, can cleave the purified PCR product producing sticky ends. This approach not only simplifies cloning, but also ensures ligation of the PCR product into the luciferase reporter plasmid in the correct orientation. **Figure 1** gives an example of a reporter gene construct that utilizes luciferase in schematic form. A real example can be found in ***(13)***. Genomic DNA, typically from the cells/cell line used in Northern-blot analysis, is the target of these primers. The PCR reaction is then fractionated on an agarose gel and products having the correct size are gel purified, subjected to restriction digest with *Bam*HI and *Hin*dIII, and then ligated into a purified reporter gene plasmid also cleaved with *Bam*HI and *Hin*dIII. The reporter plasmid with which our laboratory has the most experience is termed poLUC. It is a modified luciferase reporter plasmid ***(12)***.

Once the construct has been cloned and its sequence verified, it is ready for transfection studies. Our laboratory has utilized three methods of transfection: cationic liposomes, electroporation, and calcium phosphate coprecipitation. All have worked efficiently in our hands, but must be empirically applied to each new cell type to determine the optimal method of gene transfer. For example,

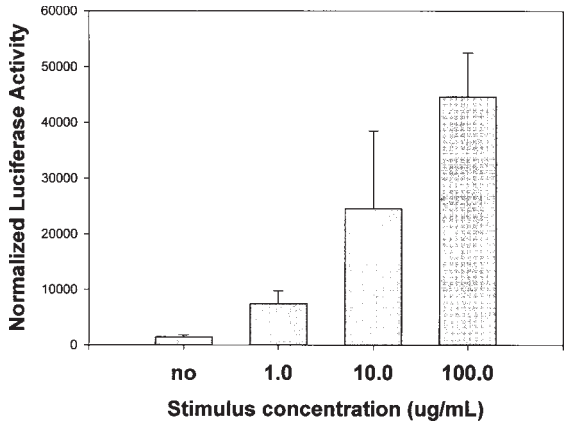

Fig. 2. Dose response curve of –991/+22 IP/LUC. –991/+22 IP/LUC and internal control alkaline phosphatase reporter plasmids were transfected into cell line by cationic liposomes (DOTAP). Twenty-four hours following transfection, cells were stimulated for 24 h with the indicated doses of stimulus and assayed for luciferase and alkaline phosphatase activity. Normalized activity is plotted as the mean ± S.D. of triplicate plates.

in investigating a new cell line, we will introduce a positive control plasmid, such as SV2-LUC [luciferase driven by the SV40 early region promoter ***(12)***] by all techniques in separate plate. We then select the technique that gives the highest luciferase reporter activity. As a general rule, cationic liposomes are most effective and work in a wide range of cell types, including HepG2, Hep3b, HeLa, A549, K562, and many others. Because the commercial sources of cationic liposomes are typically expensive, we have found a simple and reliable technique for producing our own supply at a fraction of the cost. It is described later in this chapter. In addition to the reporter gene, a second internal control plasmid is usually cotransfected into the cells during transient transfection studies in order to determine transfection efficiency. Our laboratory primarily uses an expression vector for alkaline phosphatase ***(10,14)***, but plasmids that express β-galactosidase have also been used and are described in ***(10,15)***. After harvest, reporter gene activity levels for each plate are standardized against alkaline phosphatase levels for the same plate to correct for plate-to-plate variability in transfection efficiency.

1.2. Identification and Analysis of Inducible cis*-Regulatory Elements*

Time and dose responses with a stimulus initially used in Northern-blot analysis are typically performed to determine if the promoter region is capable of responding to stimulus but also to optimize for future *cis*-response element mapping. **Figures 2** and **3** exemplify arbitrarily the type of results

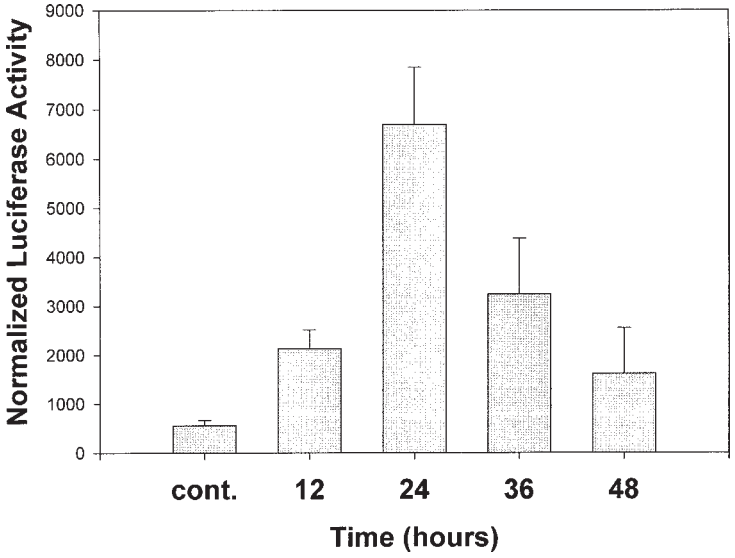

Fig. 3. Time-course of –991/+22 IP/LUC induction. –991/+22 IP/LUC was transfected as in **Fig. 2**. Cells were stimulated with 10 μg/mL stimulus for indicated times prior to simultaneous harvest and reporter gene assay. Normalized activity is plotted as the mean ± S.D. of triplicate plates.

one would expect from a time- and dose-response for the imaginary reporter gene –991/+22 IP/LUC. At least three separate experiments should be performed in order to establish statistical significance. **Figures 2** and **3** exemplify single transient transfection assays in which each vertical bar represents the average activity of triplicate plates.

1.3. 5'-Deletional Analysis

Once stimulus conditions have been optimized (the dose and time of stimulus exposure required for maximal effect), 5' deletions of the promoter can then be constructed to grossly map the region of stimulus response. In our laboratory, 5' deletions are typically constructed through the use of several promoter-specific PCR primers each of which are 100–150 basepairs closer to the TATA box or transcription initiation site. Each primer, as described earlier, has a *Bam*HI site at the 5' end to aid in cloning of the PCR product. The downstream primer is the same one used to construct the full-length PCR product having a *Hin*dIII site at its 5' end. Instead of genomic DNA, the full-length reporter gene construct can be used in this PCR reducing nonspecific bands. The left panel of **Fig. 4** shows schematically several 5'-deletion constructs of –991/+22 IP/LUC. The smallest construct should be a minimal promoter, containing the TATA box and little else. The right panel of **Fig. 4** shows

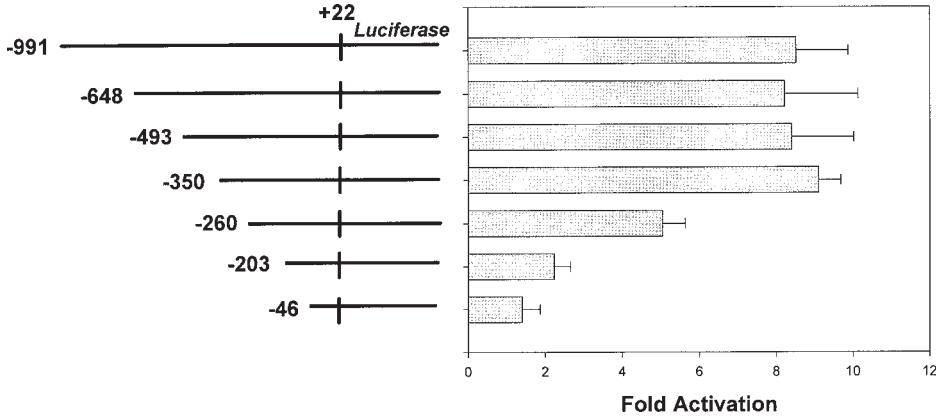

Fig. 4. 5' deletions of the stimulus response domain. Serial 5' deletions of the –991/+22 IP/LUC reporter plasmid were generated by PCR and cotransfected as in **Fig. 2**. Twenty-four hours following transfection cells were stimulated with 10 μg/mL stimulus for 24 h. Data are mean ± S.D. of three independent transient transfection assays.

the ideal result one would expect from this type of experiment. Note that the minimal promoter is not inducible. The results shown here would be derived through the transfection of several (typically, six 60-mm plates) plates with each 5'-deletion construct alone. Half of the plates for each construct are left untreated, the other half treated with stimulus. The fold activation (treated activity/untreated activity) is then determined and plotted in graphical form as shown. At least three separate experiments are performed in order to establish statistical significance. In this example, a biphasic response element is described because there are two falls in the fold-activation: the first from –350 to –260 and the second from –260 to –203. An example of real 5'-deletion results can be found in **refs.** ***(2,14)***.

1.4. 3'-Deletional Analysis

Once the 5' boundary of the response element has been grossly mapped, the 3'-stimulus response boundary can be mapped through the employment of 3'-internal deletions. The left panel of **Fig. 5** shows schematically several 3'-deletion constructs of –350/+22 IP/LUC. In our laboratory, these internally deleted constructs are synthesized again using PCR primers that sequentially move upstream from the transcription initiation site. The 5' end of these primers, however, have a *Bgl* II restriction site (5'-GATC-3' overhang). The upstream primer for each construct typically is the 5'-deletion primer, which produces a construct that still contains full stimulus inducibility (in this example the primer

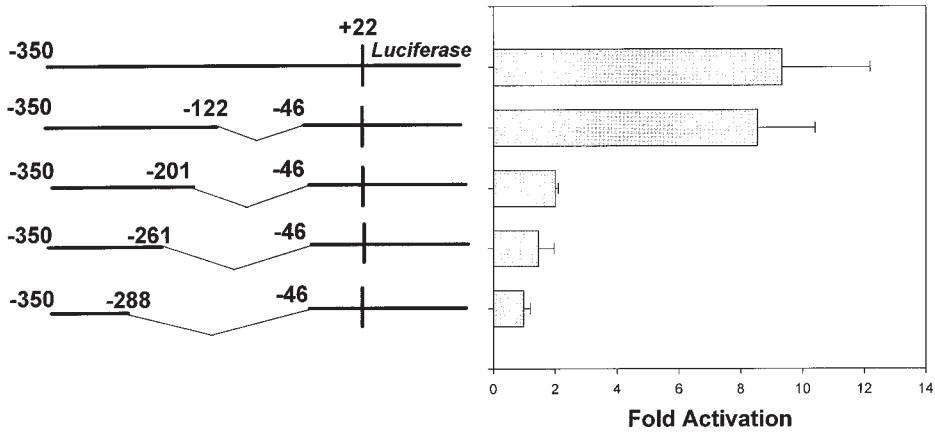

Fig. 5. 3' deletions of the stimulus response region. Internal deletions of the IP/LUC promoter fixed at 5' end (nucleotide –350) were generated and cloned upstream of the –46/+22 minimal promoter. Cells were transfected and stimulus measured as in **Fig. 2**. Data are mean ± S.D. of three independent transient transfection assays.

is –350 from **Fig. 4**). Again, the template DNA for this PCR is the full-length promoter construct. Once the various PCR products have been produced and cleaved with *Bam*HI and *Bgl*II, they are ligated into the minimal promoter (–46/+22 IP/LUC, **Fig. 4**) that has been cut with *Bam*HI alone. Sequence verification is important here. Again, each construct is transfected into several (six 60-mm) plates, of which half are left untreated and, the other half are treated with stimulus. The right panel of **Fig. 5** shows the ideal results of such an experiment. In this case, the region between –122 and –201 contains a stimulus response element because there is such a significant loss in luciferase activity. Based on the imaginary result of **Figs. 4** and **5**, the stimulus response region spans a region from –350 to –122 of the IP promoter. An example of 3' deletions can be found in **ref.** ***(2)***.

1.5. Promoter Mutational Analysis (Site Mutations)

At this point, fine mapping of promoter-response elements begins. Typically, a protein-DNA binding assay (footprinting) is employed to determine regions of stimulus inducible protection in the stimulus responsive region. Described in the next chapter, DNase I footprinting and methylation interference can be used for this purpose. Alternatively, genomic footprinting can also be employed [*see* ***(24,25)***; examples are found in ***(14,26)***]. Once regions of inducible protection have been ascertained, site-directed mutagenesis of the sites can be performed on the reporter-gene construct in order to determine the

effect of such mutations of promoter activity. A description of site-mutant reporter-gene construction and analysis is to follow.

As an alternative to footprinting, although not as scientifically rigorous, one can subject the basepair sequence of the stimulus response region to a computer algorithm that would identify potential transcription factor binding sites. One could limit this search to include only those transcription factors known to be activated by the stimulus in question. Because of their rigidity, however, it is often better to search the literature for known stimulus response element consensus sequences and manually search the promoter for sites bearing homology or semihomology to these consensus sequences. The human mind is much better at this type of analysis than a computer and it will pick up sites that would otherwise be missed by a machine. Once one or many stimulus response elements have been identified, these sites can then be subjected to site-directed mutagenesis. In our laboratory, this is typically done using sense and antisense PCR primers which change critical binding site basepairs from pyrimidines to purines or vice-versa. PCR SOeing ***(2,14,27)*** has been the approach that has yielded greatest success in the production of mutants in our laboratory. Here, two PCR reactions are set up. In the first reaction, an upstream promoter-specific sense primer is used with an antisense mutant primer. In the second reaction, a downstream promoter-specific antisense primer is used with a sense mutant primer. Both reactions are fractionated on an agarose gel and products having the correct size are purified. These purified products then serve as templates for a third PCR reaction that contains the upstream promoter-specific sense primer and downstream promoter-specific antisense primer. During this PCR, the template strands melt and anneal to one another at the overlapping mutant site. DNA polymerase then uses the 3' ends of this overlap to fill-in basepairs making a full-length double-stranded mutant product. The promoter-specific primers then amplify the full-length mutant product with each cycle. This reaction is then fractionated on an agarose gel, purified, subjected to restriction digestion, and ligated into the reporter-gene plasmid. We have had success using the full-length wild-type reporter-gene construct (–991/+22 IP/LUC, in this example) and its specific primers in the synthesis of site mutants (the first two PCR reactions described). One must be careful, however, because stimulus response elements upstream of the 5' stimulus response region boundary (–350 in the example) may compensate for sites mutated within the stimulus response region (–350 to –122). If you believe this might be a problem then use the 5' deletion primer that contains full-stimulus inducibility in place of the upstream full-length promoter primer (–350 in this example, **Fig. 4**). The left panel of **Fig. 6** shows schematically several site mutant constructs. In this example, three stimulus response elements are present in the stimulus response

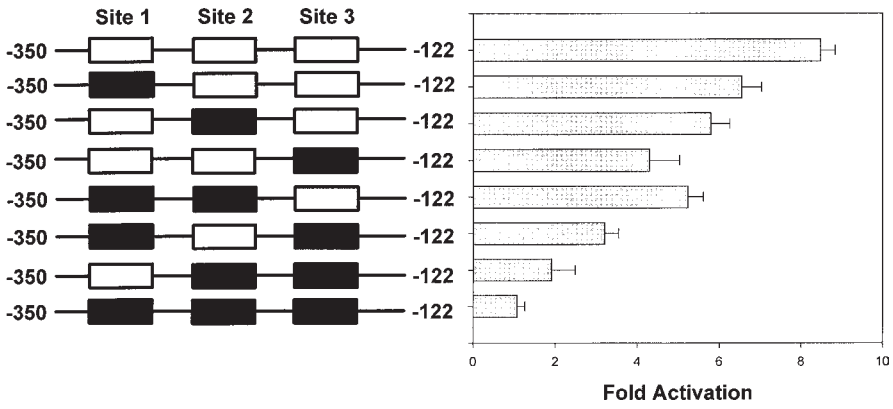

Fig. 6. Site mutants of stimulus response elements in full-length –991/+22 IP/LUC promoter. Site mutation of the three stimulus response elements were generated in series and in combination using PCR and the full-length –991/+22 IP/LUC reporter plasmid. Note that only the stimulus response region (–350 to –122) is shown in the figure. Darkened boxes represent mutated response elements. Wild-type and mutant plasmids were cotransfected with internal control alkaline phosphatase reporter plasmid into cell line and stimulated with 10 μg/mL stimulus for 24 h. X-axis represents fold induction of stimulated cells over unstimulated controls. Data are mean ± S.D. of three independent transient transfection assays.

region (–350 to –122). Systematic site mutation of each is shown. The right panel of **Fig. 6** shows ideal results for these site mutant reporter gene constructs. An actual example of such an experiment can be found in **refs.** ***(2,13,28)***.

1.6. Functional Analysis of Individual Enhancer Elements

Once one has established the stimulus response elements, multimerization of one (or each) response element is often used to further confirm it stimulus responsiveness. **Figure 7** shows an example of multimerization of the site 1 stimulus response element from the IP promoter. Multimerization of a response element is typically done in our laboratory by having an oligonucleotide synthesized containing the stimulus response element as well as eight to ten of its flanking basepairs. The sense and antisense oligos are synthesized containing 5' overhangs typically having the sequence: 5'-GATC-3'. These overhang aid ligation of double-stranded oligomers to one another and ligation into a minimal promoter. The sense and antisense oligos are phosphorylated and then annealed to one another. Ligation of the double-stranded oligonucleotides is then performed and the reaction is then fractionated on a sodium dodecyl sulfate-polyacrylamid gel electrophoresis (SDS-PAGE) gel along with a lane con-

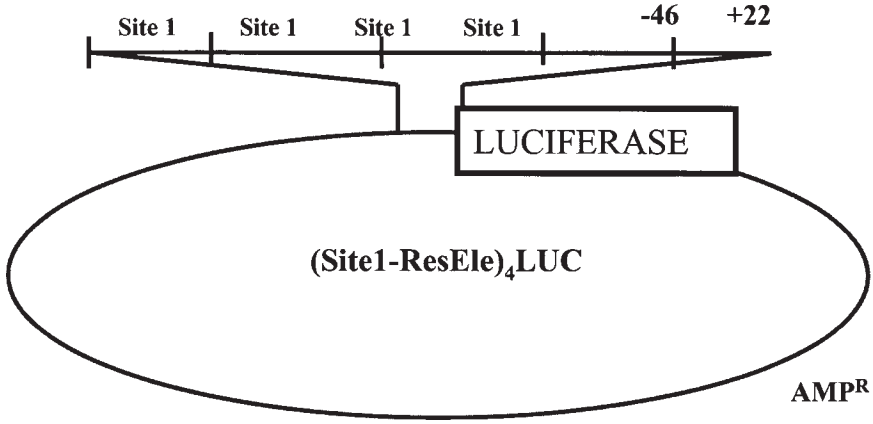

Fig. 7. Example of multimerized response element from –991/+22 IP/LUC stimulus response region. In this example, the most upstream response element (Site 1 from **Fig. 6**) is multimerized. This construct is termed (Site1-ResEle)$_4$LUC.

taining unligated (single-) double-stranded oligomer. After ethidium bromide staining, the gel is put under a an ultraviolet (UV) light and bands that appear to have three to four oligomers are cut out and purified. The purified multimer is then ligated into a minimal promoter reporter-gene construct that has been cut with *Bam* HI (creating 5'-GATC-3' sticky ends). Sequencing this construct is important in order to determine the number of oligomers present and their orientation. The orientation of each oligomer, however, does not appear to affect its transcriptional activating ability. Additionally, this process must be performed with synthesized oligomers that contain a mutated stimulus response site. Our laboratory mutates critical binding site pyrimidines to purines and vice versa. This construct will serve as a site-specific control to the wild-type multimer. Once constructed, the wild-type and mutant multimers are transfected into cells and stimulated. **Figure 8** exemplifies the ideal result in which stimulation of a wild-type multimer is compared to the mutant multimer. The mutant multimer should not be responsive to stimulus. Such an experiment strongly supports the response element as the *cis*-regulatory element for the stimulus in question. Once sequence specificity of the wild-type multimer has been confirmed, then characterization of its properties can then be done (dose- and time-response). **Figures 2** and **3** exemplify the experimental approach. Typically, the fold activation is much higher for the multimer than the full-length promoter (–991/+22 IP/LUC in this case), but the dose-response and time of maximal activation remain similar. An example of a multimeric luciferase reporter gene construct can be found in **ref.** ***(13)***.

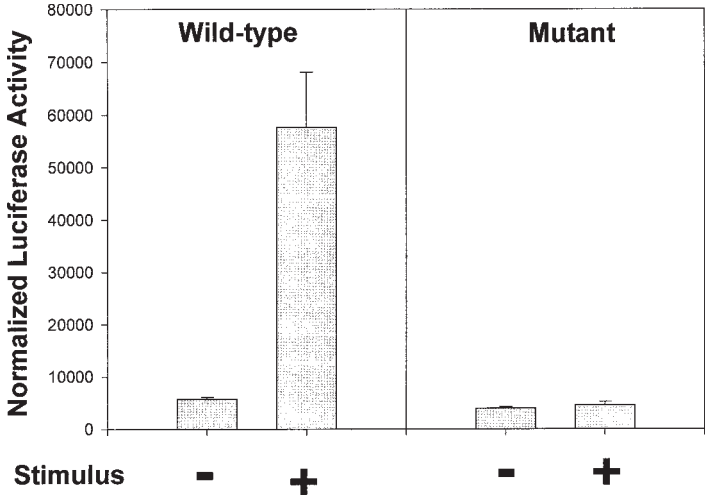

Fig. 8. Stimulus induction of Site1-ResEle luciferase reporter is sequence specific. $(Site1\text{-}ResEle)_4LUC$, indicated as "wild-type," and its site mutation, indicated as "mutant," were transfected into cell line along with internal control alkaline phosphatase reporter plasmid. Twenty-four hours following transfection, cells were stimulated with 10 μg/mL stimulus for 24 h. Data is mean ± S.D. of triplicate plates.

2. Materials

2.1. Preparation of DOTAP Liposomes by Alcohol Injection

1. Sterile DOTAP buffer. Prepare as follows:
   a. Autoclave ddH_2O in 10 m*M* HEPES, pH 7.4. After solution has cooled to room temperature, add ascorbic acid [in sterile H_2O or phosphate-buffered saline (PBS)] to a final concentration of 1 m*M*.
   b. Dry down 714 μL of DOTAP (N-[1-(2,3,-Dioleoyloxy)propyl]-N,N,N-trimethylammmonium methylsulfate, 20 mg/mL in chloroform, Avanti Polar lipids) under gaseous nitrogen.
   c. Dissolve in 1 mL of 100% ethanol (ETOH).
   d. Pipette 50 μL into 1 mL of sterile aqueous buffer (while rapidly vortexing for 10 s in DOTAP buffer (10 m*M* HEPES, pH 7.4, sterilized by autoclaving).
   e. Add (after cooling DOTAP buffer to room temperature) a final concentration of 1 m*M* ascorbic acid (in sterile H_2O or PBS).
   f. Overlay with gaseous N_2.
   g. Aliquot into 1.2-mL sterile Revco freezing vials purged with gaseous N_2.
   h. Label, date, and store at 4°C (the preparation is stable for several months).
2. Ca^{++}/Mg^{++} free PBS: For 8 L, add 64 g NaCl, 1.6 g KCl, 9.2 g $Na_2HPO_4 \cdot 7H_2O$, 1.6 g KH_2PO_4, 7.5 L of ddH_2O. Adjust the pH to 7.4 with 1 *N* NaOH. Add ddH_2O to a final volume of 8 L.

3. Sterile 20 m*M* HEPES, pH 7.8. For 500 mL, add 2.83 g of HEPES to 400 mL ddH_2O. Adjust the pH to 7.8 with 1 NaOH. Add ddH_2O to a final volume of 500 mL. Aliquot 50 mL into glass bottles and autoclave. Allow aliquots to cool to room temperature before use.

2.2. Calcium Phosphate Transfection

1. 2X HEPES-buffered saline (HBS). For 500 mL, add 8 g NaCl, 0.37 g KCl, 0.1 g Na_2HPO_4 (anhydrous), 1 g dextrose, 5 g HEPES to 450 mL ddH_2O. Adjust to pH 7.1 with addition of NaOH and add ddH_2O until the volume is 500 mL. Sterilize solution by passing through 0.22-μ*M* filter and store at room temperature. The solution is stable for months.
2. 2 *M* $CaCl_2$ in ddH_2O. Sterilize solution by passing through 0.22-μ*M* filter and store at –20°C.

3. Methods

3.1. DOTAP DNA Transfection

1. Pass HepG2 cells into appropriate number of 60-mm plates 4–20 h prior to addition of DNA.
2. Add 20 μg of Qiagen-or Cesium chloride purified reporter DNA (to be divided into triplicate 60-mm plates) into a sterile Falcon 5-mL Falcon snap-cap tube. If appropriate, include 5 μg of internal control plasmid and or 1–5 μg expression plasmid.
3. Adjust volume to 400 μL with 20 m*M* HEPES, pH 7.8.
4. Add 100 μL of DOTAP (stock DOTAP is @ 1 mg/mL). Mix gently. The DNA should turn slightly cloudy or milky colored.
5. Incubate at room temperature for 15 min.
6. Wash HepG2 cells with 1X sterile PBS (PBS; without calcium or magnesium).
7. Add 165 μL of DOTAP:DNA mixture to each plate. Gently rock plate back and forth to ensure even distribution of mixture over cells.
8. Incubate at room temperature under the tissue culture hood for 5 min.
9. Add 3 mL of growth medium (containing serum) and return to incubator.
10. Next morning, change the medium to fresh growth medium.
11. Incubate for a total of approx 48 h (because of the addition of the liposome). Hormonal stimulations are done during this time and timed to be harvested simultaneously (*see* **Subheading 3.4.2.**).

3.2. Transfection by Calcium Phosphate Coprecipitation

1. In a sterile 5-mL Falcon snap-cap tube, add 31 μL of 2 *M* $CaCl_2$, and 20 μg of purified DNA. Add sufficient sterile ddH_2O to achieve a final volume of 250 μL.
2. Add 250 μL of 2X HBS, gently mix and allow the DNA to form a precipitate at room temperature for 15 min.
3. Wash cells in 1X PBS twice and aspirate to dryness.
4. Add 166 μL of the calcium phosphate-DNA mixture dropwise to each of three 60-mm tissue-culture plates.
5. Gently rock the plate back and forth to allow even distribution of the precipitate.

6. Incubate at room temperature for 10–15 min in the tissue culture hood with occasional rocking.
7. Add 3 mL of growth medium and return cells to the incubator.
8. Next morning, change medium with fresh growth medium.

3.3. Electroporation

1. Harvest cells with trypsin and gently pipet to make sure the cells are evenly dispersed.
2. Wash the cell pellet twice with 1X PBS by centrifugation (40*g* × 2–4 min).
3. Suspend cells in 1X PBS at a density of 2×10^7 cells/250 μL volume.
4. Add 250-μL cell suspension to electroporation cuvette (Bio-Rad Gene pulser cuvet).
5. Add plasmid DNA in electroporation cuvet (30 μg reporter).
6. Incubate on ice for 15 min.
7. Electroporate in Bio-Rad Gene Pulser cuvet at settings of 960 μF; 200–250 V.
8. Afterward, check time constant (should be approx 50).
9. Incubate in cuvet on ice for an additional 15 min.
10. Add prewarmed complete medium to plates (60 mm).
11. Add a 250-μL prewarmed medium to cuvet and gently aspirate cell with a wide-mouth pipet. Transfer to plates. Discard clumps of dead cells.
12. Return cells to incubator.
13. Change medium the next day to remove dead cells. There should be 10–50% viable cells remaining.

3.4. Reporter Gene Assays

3.4.1. Reporter Gene Selection

Several reviews of the advantages of various reporter genes are found in ***(15,16)***. Additionally, a comparison of the strengths and weaknesses of different reporter systems can be found in ***(16)***, p. 9.6.8–9.6.9). We and others have extensively relied on the measurement of firefly luciferase activity as an indicator of the kinetics of gene expression. Parallel nuclear run on transcription assays and analysis of reporter activity following gene activation have shown that firefly luciferase is rapidly turned over and a fairly accurate measurement of changes in endogenous gene expression ***(14,17)***. The assay for firefly luciferase is linear over six orders of magnitude and can detect $1 - 3 \times 10^5$ molecules of luciferase, a detection limit of 2–3 orders of magnitude more sensitive than the measurement of chloramphenicol acetyl transferase [CAT, ***(15)***]. Moreover, CAT assays take much longer to complete, are nonlinear, and require the use of long-lived radioactive compounds. The drawback of luciferase, as well as CAT, is that it is a cytoplasmic protein and transfected cells have to be lysed in order to determine its activity. This complicates kinetic studies in which one is attempting to determine reporter-gene activity sequentially over a period of time. Reporter genes, such as growth hormone [*see* ***(18)***], which is secreted from the cell, and secreted alkaline phosphatase [*see* ***(19,20)***] circumnavigate

this problem. Growth hormone can be assayed simply through use of commercially available radioimmunoassay or enzyme-linked immunosorbent assay (ELISA) techniques. Commercially available assays for secreted alkaline phosphatase are also available that utilize chemiluminescent technology making quantitation of this reporter gene simple as well ***(21)***. Green fluorescent protein [described in ***(22,23)*** also can be quantitated simply by fluorescence microscopy, flow cytometry, or Western immunoblotting techniques. This reporter also has the advantage of being able to be measured sequentially in living cells on a sequential basis. The following section describes the lysis and assay for commonly used reporter-genes luciferase, CAT, and alkaline phosphatase.

3.4.2. Firefly Luciferase Reporter Assay

Prepare the following buffers:

3.4.2.1. Luciferase Lysis Buffer

1. 3.125 mL Tris-phosphate pH 7.8 (1 *M* stock).
2. 2.5 mL CDTA (100 m*M* stock).
3. 1.25 mL Triton-X 100.
4. 12.5 mL 100% glycerol.
5. Add double-distilled water to a final volume of 125 mL. Luciferase lysis buffer is stable indefinitely at room temperature.
6. Immediately prior to use, aliquot 10 mL of buffer per 24 60-mm plates when cells are ready to harvest and add 10 µL of 1 *M* dithiothreitol (DTT, final concentration of 1 m*M*). Unused reconstituted lysis buffer is discarded.

3.4.2.2. Luciferase Reagent Buffer

1. 1.79 g Tricine (final conc, 20 m*M*).
2. 0.26 g $(MgCO_3) \cdot 4\ Mg(OH)_2 \cdot 5H_2O$ (final conc., 1.07 m*M*).
3. 0.161 g $MgSO_4$ (final conc., 2.67 m*M*).
4. 0.0146 g ethylenediaminetetraacetic acid (EDTA)—disodium salt—(final conc., 0.1 m*M*).
5. Add double-distilled water to a final volume of 500 mL.
6. The solution is stable at room temperature indefinitely.

3.4.2.3. Luciferase Assay Buffer

Mix the following reagents on ice

1. 4 mL reagent buffer.
2. 1 mL luciferin (D-luciferin, 10 mg, Sigma cat. no. L-9504, dissolved in 15 mL of reagent buffer). The final concentration of luciferin in assay buffer is 470 µ*M*).
3. 50 µL of coenzyme A (Sigma, 25-m*M* stock solution). The final concentration in Assay Buffer is 270 µ*M*.
4. 13 µL adenosine triphosphate (ATP) (0.2 *M* stock solution in H_2O). The final concentration in assay buffer is 530 µ*M*.

5. 167 μL 1 *M* DTT. The final concentration in assay buffer is 33.3 m*M*.
6. The sample is stored on ice protected from light for immediate use. Following use, it is frozen at –20°C protected from light.

3.4.2.4. Cell Harvest and Luciferase Reporter Assay

1. Wash cells 2X with 1X PBS.
2. Add 250-μL lysis buffer (with added DTT) per 60-mm plate.
3. Allow to stand at RT for 15 min.
4. Scrape cells in a microcentrifuge tube and keep on ice.
5. Spin at 8500*g* for 1 min at RT.
6. Pipet supernatant to a new microcentrifuge tube and discard pellet.
7. Measure luciferase activity of the supernatant using 20–100 μL of sample, 5 mL of assay buffer per 24–60-mm plates, and a luminometer. Include three tubes, which contain 20–100 μL of lysis buffer to serve as blanks (background activity of lysis buffer).
8. Measure alkaline phosphatase activity with 50–100 μL of sample (*see* **Subheading 3.4.4.**).
9. Calculation of results: The three values for the blanks (lysis buffer only) are averaged and subtracted from the raw luciferase value for each 60-mm plate. This number is then divided by the alkaline phosphatase measurement for the same plate. The now normalized values for a triplicate set are averaged. The average value of stimulated triplicate plates is divided by the average value of the unstimulated triplicate plates. The resulting number is the fold induction over unstimulated controls.

3.4.3. CAT Assay

3.4.3.1. Reagents

1. 0.25 *M* Tris-Cl, pH 7.5 in ddH_2O (solution is stable indefinitely at RT).
2. 4.4 m*M* acetyl CoA in 0.25 *M* Tris, pH 7.5 (Sigma, A-2056, 10 mg into 3.2 mL). Freeze in small aliquots at –20°C.

3.4.3.2. Cell Lysis

1. Wash transfected cells with 1X PBS. Scrape and briefly spin in an Eppendorf microfuge tube.
2. Add 250 μL 0.25 *M* Tris-Cl, pH 7.5, and resuspend pellet.
3. Freeze/thaw three times. [Occasionally, it is necessary to use 0.1% (v/v) Nonidet P-40 (NP40) for cell disruption; if this is employed, do not use more.]
4. Spin out cell debris. Measure protein concentration by Bio-Rad Protein Reagent or measurement of protein absorbance at 280 nm (A_{280}).

3.4.3.3. CAT Assay

1. Add 75 μL 0.25 *M* Tris, pH 7.5, 4 μL 1,2 ^{14}C-chloramphenicol (CAT assay grade), 50 μL extract, and 20 μL acetyl CoA (4.4 m*M*)*.

*Or, make a reaction assay pot (for *n* assays) containing: 0.25 *M* Tris: 75 × *n* μL; ^{14}C chloramphenicol: 4 × *n* μL; Acetyl Co A 20 × *n* μL; add 99 μL of the pot to each tube.

2. Incubate at 37°C, 1 h.
3. Spin tubes. Add 500 µL ethylacetate to each tube.
4. Vortex, spin down, and transfer supernatant to fresh Eppendorf tube.
5. Speed-vac dry.
6. Add 20-µL ethyl acetate to resuspend and spot onto thin-layer chromatography (TLC) plate. Chromatograph on TLC plate in preequilibrated chamber with 95:5 chloroform:methanol for approx 1 h, or until solvent front reaches top of plate.
7. Air-dry. Expose to film. Quantitate by exposure to Molecular Dynamics Phosphorimager cassette.

3.4.4. Alkaline Phosphatase Assay

We use alkaline phosphatase for determining the transfection efficiency in individual plates. For information on secreted alkaline phosphatase as a reporter gene *see* **refs.** ***(19–21)***.

Prepare the following.

3.4.4.1. DEA Buffer (1 L)

1. 105.4 g/L diethanolamine (MW 105.4; 1 *M* final conc.).
2. Add 800 mL of ddH_2O.
3. 16.36 g/L NaCl (MW 58.44; 0.28 *M* final conc.).
4. 0.102 g/L $MgCl_2$ $6H_2O$ (MW 203.3; 0.5 m*M* final conc.).
5. pH to 9.85 with concentrate HCl.
6. Bring volume to 1 L with ddH_2O.
7. Store at 4°C.

3.4.4.2. p-Nitro-Phenyl Phosphate (PNPP, Sigma 104 Phosphatase Substrate)

1. Make 0.1 *M* solution of PNPP (MW 371) in diethylamino (DEA) buffer.
2. Store frozen (–20°C), in 1-mL aliquots, shield from light.

3.4.4.3. Alkaline Phosphatase Assay

1. Mix 1 vol PNPP and 19 vol DEA buffer.
2. Add 0.9-mL assay buffer to spectrophotometer cuvet for each sample.
3. Add 100 µL of each sample to each cuvet.
4. Make a blank by mixing 100-µL lysis buffer and 0.9-mL assay buffer.
5. Incubate at RT until color turns light yellow.
6. Read absorbance at 405 nm (A_{405} nm) using lysis buffer as the blank. (Absorbance valve should be >0.1, but <1.1.)

4. Notes

1. A number of problems may lead to low or undetectable reporter-gene activity. It is often the result of poor transfection efficiency and may mean that another method of transfection must be utilized. Antimycotic agents, such as Fungizone,

which punches holes in the plasma membrane, can lead to a decrease in transfection efficiency with cationic liposomes such as DOTAP. The purity of the transfected DNA can also be a factor when using electroporation. Although, we typically use Qiagen-purified DNA (by anion exchange), occasionally impurities result in extensive cell death or poor transfection efficiency. In this case, we will purify the DNA by cesium chloride gradient centrifugation. Also, it is important to recognize that not all cells handle firefly luciferase reporter activity equally well. We, and others, have found that certain cell lines target luciferase enzyme to lysosomal structures and degrade the reporter activity. For example, rat pancreatic cells (RIN series) degrade luciferase rapidly. In this case, a different species of luciferase or other reporter gene must be selected.

In the study of inducible control elements, an additional problem is a lack of stimulus activity. A first consideration is whether the promoter region under study contains the stimulus response element(s) within its boundaries. Cellular response can be tested by repeating Northern blot or nuclear run-on analysis. This will reassure the investigator that the hormone and cells are active and responding appropriately. There are numerous potential problems that results in variability of promoter activity in transient transfection assays. These include variability in transfection efficiency and growth state of the transfected cells. Variability in transfection efficiency can be partially remedied by cotransfecting cells with an internal control plasmid. An example is an SV40-driven alkaline phosphatase expression vector (SV40-PAP) cotransfected with a test luciferase reporter ***(10,14)***. In this situation, we generally transfect 15 μg of luciferase with 5 μg of SV40-PAP. These internal control plasmids allow one to correct for plate-to-plate variation in transfection efficiency in an individual experiment but interassay variation still is a problem. Before using alkaline phosphatase as an internal control reporter, however, it is wise to check to ensure that the cells do not express endogenous alkaline phosphatase activity. If significant background alkaline phosphatase activity is detected, we will use β-galactosidase as our next choice for internal control.

Transient transfection procedures, such as calcium phosphate, cation lipids (DOTAP), or electric shock stress cultured cells which may alter the transcriptional activity of the promoter of interest. These variables are difficult to control and ultimately may result in significant interassay variation. Stable transfections overcome many of these problems. In this situation, DNA containing a promoter/reporter construct and a selectable marker is introduced into cells (conferring neomycin or hygromycin resistance) and cells expressing the transfected DNA is selected by resistance to the selection antibiotic. An important advantage of stable transfectants is that the DNA is ordered within chromatin, a feature not shared with transient transfectants ***(10)***. Although stable transfectants are advantageous because all of the cells now express the transgene, the disadvantage of stable transfection is the length of time it takes to select a cell line. This presents a very real obstacle to deletion or mutational analysis of the target promoter.

Acknowledgments

This work was supported by grants from NHLBI (1R01 55630, A.R.B.), and NIEHS (P30 ES06676, R.S. Lloyd, UTMB). A.R. Brasier is an Established Investigator of the American Heart Association.

References

1. Corvol, P. and Jeunemaitre, X. (1997) Molecular genetics of human hypertension: role of angiotensinogen. *Endocr. Rev.* **18,** 662–677.
2. Brasier, A. R., Ron, D., Tate, J. E. and Habener, J. F. (1990) Synergistic enhansons located within an acute phase responsive enhancer modulate glucocorticoid induction of angiotensinogen gene transcription. *Mol. Endocrinol.* **4,** 1921–1933.
3. Kalinyak, J. E. and Perlman, A. J. (1987) Tissue-specific regulation of angiotensinogen mRNA accumulation by dexamethasone. *J. Biol. Chem.* **262,** 460–464.
4. Brasier, A. R., Philippe, J., Campbell, D. J., and Habener, J. F. (1986) Novel Expression of the Angiotensinogen gene in a rat pancreatic islet cell line: transcriptional regulation by glucocorticoids. *J. Biol. Chem.* **261,** 16148–16154.
5. Campbell, D. J. and Habener, J. F. (1986) Angiotensinogen gene is expressed and differentially regulated in multiple tissues of the rat. *J. Clin. Invest.* **78,** 31–39.
6. Klett, C., Hellmann, W., Hackenthal, E., and Ganten, D. (1993) Modulation of tissue angiotensinogen gene expression by glucocorticoids, estrogens, and androgens in SHR and WKY rats. *Clin. Exp. Hypertens.* **15,** 683–708.
7. Coezy, E., Bouhnik, J., Clauser, E., Pinet, F., Philippe, M., Menard, J., and Corvol, P. (1984) Effects of glucocorticoids and antiglucocorticoids on angiotensinogen production by hepatoma cells in culture. *In Vitro* **20,** 528–534.
8. Gordon, M. S., Chin, W. W., and Shupnik, M. A. (1992) Regulation of angiotensinogen gene expression by estrogen. *J. Hypertens.* **10,** 361–366.
9. Brasier, A. R., Ron, D., Tate, J. E., and Habener, J. F. (1990) A family of constitutive C/EBP-like DNA binding proteins attenuate the IL-1 alpha induced, NF kappa B mediated trans- activation of the angiotensinogen gene acute-phase response element. *EMBO J.* **9,** 3933–3944.
10. Brasier, A. R., Li, J., and Wimbish, K. A. (1996) Tumor necrosis factor activates angiotensinogen gene expression by the Rel A transactivator. *J. Hypertens.* **27,** 1009–1017.
11. Han, Y. and Brasier, A. R. (1997) Mechanism for biphasic Rel A:NF-kB1 nuclear translocation in tumor necrosis factor α-stimulated hepatocytes. *J. Biol. Chem.* **272,** 9823–9830.
12. Brasier, A. R. and Ron, D. (1992) Luciferase reporter gene assay in mammalian cells. *Methods Enzymol.* **216,** 386–397.
13. Li, J. and Brasier, A. R. (1996) Angiotensinogen gene activation by AII is mediated by the Rel A (NF-kB p65) transcription factor: One mechanism for the renin angiotensin system (RAS) positive feedback loop in hepatocytes. *Mol. Endocrinol.* **10,** 252–264.

14. Brasier, A. R., Jamaluddin, M., Casola, A., Duan, W., Shen, Q., and Garofalo, R. (1998) A promoter recruitment mechanism for TNFα-induced IL-8 transcription in type II pulmonary epithelial cells: Dependence on nuclear abundance of Rel A, NF-kB1 and c-Rel transcription factors. *J. Biol. Chem.* **273,** 3551–3561.
15. Alam, J. and Cook, J. L. (1990) Reporter genes: Application to the study of mammalian gene transcription. *Anal. Biochem.* **188,** 245–254.
16. Brasier, A. R. (1990) Reporter system using firefly luciferase, in *Current Protocols in Molecular Biology* (Ausubel, F. M., ed)., Wiley, New York, pp. 9.6.10–9.6.13.
17. Brasier, A. R. and Ron, D. (1991) Use of firefly luciferase reporter gene to study angiotensinogen acute phase response element, in *Methods in Neurosciences* (Conn, P. M., ed.), Academic, San Diego, CA, pp. 108–123.
18. Selden, R. F., Howie, K. B., Rowe, M. E., Goodman, H. M., and Moore, D. D. (1986) Human growth hormone as a reporter gene in regulation studies employing transient gene expression. *Mol. Cell. Biol.* **6,** 3173–3179.
19. Berger, J., Hauber, J., Hauber, R., Geiger, R., and Cullen, B. R. (1997) Secreted alkaline phosphatase: a powerful new quantitative indicator of gene expression in eukaryotic cells. *Gene* (Amsterdam) **66,** 1–10.
20. Kain, S. R. (1997) User of secreted alkaline phosphatase as a reporter of gene expression in mammalian cells. *Methods Mol. Biol.* **63,** 49–60.
21. Yang, T. T., Sinai, P., Kitts, P. A., and Kain, S. R. (1997) Quantification of gene expression with a secreted alkaline phosphatase reporter system. *Biotechniques* **23,** 1110–1114.
22. Tsien, R. Y. (1998) The green fluorescent protein. *Ann. Rev. Biochem.* **67,** 509–544.
23. Chalfie, M. and Kain, S., eds. (1999) *Green Fluorescent Protein: Properties, Applications, and Protocols*, Wiley, New York.
24. Mueller, P. R. and Wold, B. (1991) Ligation-mediated PCR: applications to genomic footprinting. *Methods* **2,** 20–31.
25. Pfeifer, G. P., Steigerwald, S. B., Mueller, P. R., Wold, B., and Riggs, A. D. (1989) Genomic sequencing and methylation analysis by ligation mediated PCR. *Science* **246,** 810–813.
26. Patterson, C., Wu, Y., Lee, M., DeVault, J., Runge, M. S., and Haber, E. (1997) Nuclear protein interactions with the human KDR/flk-1 promoter in vivo. *J. Biol. Chem.* **272,** 8410–8416.
27. Horton, R. M., Cai, Z., Ho, S. N., and Pease, L. R. (1990) Gene splicing by overlap extension: tailor-made genes using the polymerase chain reaction. *Biotechniques* **8,** 528–535.
28. Ron, D., Brasier, A. R., Wright, K. A., and Habener, J. F. (1990) The permissive role of glucocorticoids on interleukin-1 stimulation of angiotensinogen gene transcription is mediated by an interaction between inducible enhancers. *Mol. Cell. Biol.* **10,** 4389–4395.
29. Archer, T. K., Lefebvre, P., Wolford, R. G., and Hager, G. L. (1992) Transcription factor loading on the MMTV promoter: a bimodal mechanism for promoter activation. *Science* **255,** 1573–1576.

8

Analysis of Transcriptional Control Mechanisms II

Techniques for Characterization of trans*-Acting Factors*

Allan R. Brasier, Christopher T. Sherman, and Mohammad Jamaluddin

1. Introduction

cis-Acting DNA control elements, enhancers and promoters, function to control gene expression by acting as targets for specific DNA-binding proteins (*trans*-acting factors). *trans*-acting factors are sequence-specific DNA-binding proteins that recognize specific signatures in base composition of the DNA, and upon binding, are able to influence transcriptional activity of the core promoter by multiple diverse mechanisms. These mechanisms include direct interaction with the preinitiation complex, recruitment of additional bridging proteins (coactivators), or induction of chromatin remodeling (such as altering nucleosomal phasing). These mechanisms are coordinated to result in changes in gene expression that control critical events in cellular differentiation and responses to extracellular signals or stressors.

The next step in analysis of an identified *cis* control element, through techniques described in the preceding chapter, is to identify the nature and potential mode of regulation of its cognate DNA-binding protein. For example, transcription factors can be constitutive or inducible. Inducible transcription factors have attracted much interest in the research community as these proteins respond to changes in cellular stimulation. Inducible proteins are functionally defined where DNA-binding activity increases following cellular stimulation. Mechanistically, inducible proteins can be regulated by changes in the rate of synthesis or by changes in nuclear translocation. Examples of changes in the rate of synthesis include the CCAAT/Box Enhancer binding proteins, DNA-binding proteins that bind to "CCAAT-like" sequences and whose synthesis can be altered by changes in cellular differentiation or extra-

From: *Methods in Molecular Medicine, vol. 51: Angiotensin Protocols*
Edited by: D. H. Wang

cellular stress. Conversely, entire families of inducible DNA-binding proteins can be kept in an inactive form in the cytoplasm, and upon cellular stimulation, can be induced to enter the nucleus to activate transcription from target genes. Examples of these proteins include Nuclear Factor-κB (NF-κB), a family of cytoplasmic transcription factors tethered to cytoplasmic inhibitory proteins [IκB; for reviews, *see* **refs.** ***(1–3)***]. NF-κB, important in cytokine activation of rat angiotensinogen gene, enters the nucleus following proteolysis of its inhibitor. The steroid receptors, such as the glucocorticoid receptor (GR), are inactivated in the cytoplasm by association with the heat shock proteins. The GR is activated by directly binding to cortisol, its ligand, allowing the activated GR to dissociate from heat shock protein, enter the nucleus and activate glucocorticoid responsive genes [reviewed in ***(4)***]. The signal transducers and activators of transcription (STAT) are cytoplasmic proteins associated with growth-factor related (tyrosine-kinase coupled) receptors. Following hormone binding, STATs are tyrosine phosphorylated, allowing the proteins to dimerize (acquires DNA-binding activity) and translocate into the nucleus [reviewed in **refs.** ***(5,6)***].

Using techniques described below, tentative identification of the DNA-binding protein, the DNA sequences to which it binds, and the potential nature of its regulation can be determined. Two general approaches can be made (in vitro vs in vivo). The most common approach, in vitro, refers to assays where nuclear protein from cell or tissue extracts is used to bind to labeled DNA in a test tube. Free (unbound) DNA can be fractionated from bound DNA in native polyacrylamide gels, such as the electrophoretic mobility shift assay (EMSA) or "gel shift assay." Larger pieces of DNA can be bound with protein, and the boundaries of the protein interaction can be determined by limited nuclease digestion in the DNase I footprinting assay. Likewise, the potential range of binding sites can be determined by a binding site selection assay (target detection assay), where random oligonucleotides are repeatedly bound to purified protein, eluted, and regenerated by polymerase chain reaction (PCR). More difficult, but sometimes more informative, is the in vivo assays, where the regions of protein-DNA interaction are determined in intact cells, such as the "genomic footprinting assay" [**refs.** ***(7–10)*** describe and utilize this technique]. This assay has received much attention because the effects of chromatin, which can control access of DNA-binding proteins to particular promoter sequences, cannot be accurately reproduced in a test tube.

2. Materials

2.1. Hepatocyte Cell Culture and Preparation of Cellular Extracts

1. Cell culture and treatment:
   a. The human hepatoblastoma cell-line HepG2 is a well-differentiated cell line that maintains its phenotype over numerous passages and is the reference cell line for hormone studies.

Table 1
20 mL Solution A (Low-Salt Buffer)

Components	Stock conc.	Working conc.	Vol. from stock
HEPES pH 7.9	1.0 *M*	50 m*M*	1 mL
KCl	2.0 *M*	10 m*M*	100 µL
EDTA pH 8.0	0.2 *M*	1 m*M*	100 µL
EGTA pH 8.0	0.2 *M*	1 m*M*	100 µL
DTT[a]	1.0 *M*	1 m*M*	20 µL
PMSF[a]	0.1 *M*	0.5 m*M*	100 µL
Pepstatin A	5 µg/µL	1 µg/µL	4 µL
Leupeptin	5 µg/µL	1 µg/µL	4 µL
STI	10 µg/µL	10 µg/mL	20 µL
Aprotinin	10 µg/µL	10 µg/mL	20 µL
Na_3VO_3	0.1 *M*	1 m*M*	200 µL
$Na_2P_2O_7$	0.1 *M*	1 m*M*	200 µL
NaF	0.5 *M*	20 m*M*	800 µL
NP-40 (Triton-X)	10%	0.5%	1 mL

Add ddH_2O to a final volume of 20 mL.
[a]The DTT and PMSF should be added immediately prior to use (DTT first, then PMSF) and vortex vigorously. The solution is kept on ice and stored at 4°C.

b. Other cell types, such as rat H4IIEC3 or human Hep3B cells are also interchangeable. All of these lines can be obtained from the American Type Culture Collection (ATCC, Rockville Pike, MD).
c. HepG2 cells are grown in Dulbecco's modified Eagle's medium (DMEM) (Gibco-BRL, Grand Island, NY) supplemented with 10% (v/v) heat-inactivated fetal bovine serum, 2 m*M* L-glutamine, 0.1 m*M* nonessential amino acids, 1 m*M* sodium pyruvate, and antibiotics (penicillin/streptomycin/fungizone) in a humidified atmosphere of 5% CO_2.
d. The cells are used in logarithmic phase of culture.

2. Nuclear and cytoplasmic extraction solutions:
a. The reagents indicated in **Tables 1–3** are dissolved in ddH_2O.
b. HEPES (N-2-Hydroxyethyl-piperzine-N'-2-ethansulfonic acid), adjusted to pH 7.9 at 25°C, potassium chloride (KCl), ethylenediaminetetraacetic acid (EDTA) (pH adjusted to 8.0 with NaOH), ethylene glycol-*bis* (β-aminoethyl ether) N,N,N',N' tetraacetic acid (EGTA), and Na_3VO_3, $Na_2P_2O_7$ and NaF are from Sigma and made in ddH_2O and stored at room temperature (RT).
c. The protease inhibitors, pepstatin A, leupeptin, soybean trypsin inhibitor (STI), and aprotinin, and the reducing agent dithiothreitol (DTT) are dissolved at the indicated stock concentrations in ddH_2O and stored frozen at –20°C.

Table 2
20 mL Solution B (Sucrose Cushion Buffer)

Dissolve 11.64 g sucrose in 20 mL Solution A (final volume) to a final concentration of 1.7 *M*.

d. The protease inhibitor, phenyl methyl sulfonyl fluoride (PMSF), is dissolved in isopropyl alcohol and stored at –20°C.
e. Nonidet P-40 (NP40) (Triton-X can be used as a substitute) is from Sigma and should be prepared as a 10% solution. This is added to Solution A (**Table 1**) at a final/working concentration of 0.5%.
f. Solution A (**Table 1**), Solution B (**Table 2**), and Solution C (**Table 3**) can be prepared in bulk without protease inhibitors (pepstatin A, leupeptin, STI, aprotinin, and PMSF), DTT, and NP-40 and stored at 4°C indefinitely. Immediately before use, an aliquot of each solution should be taken (typically 10 mL of Solutions A and B and 5 mL of Solution C) and the protease inhibitors, DTT, and NP-40 added to the working concentrations given in **Tables 1–3**.

2.2. Electrophoretic Mobility Shift Assays (EMSAs)

1. EMSA binding buffer:
   a. In ddH_2O, add 8% (v/v) glycerol, 100 m*M* NaCl, 5 m*M* $MgCl_2$, 5 m*M* DTT, and 0.1 μg/mL PMSF.
   b. Store at 4°C; stable for 1 wk.
2. 10X TBE: 10X TBE buffer:
   a. Add dry Tris base to a final concentration of 890 m*M*.
   b. Add dry boric acid to a final concentration of 890 m*M*.
   c. Add 500 m*M* EDTA, pH 8.0, to a final concentration of 20 m*M*.
   d. The pH of the final solution should be 8.3–8.6.
   e. Do not adjust the pH.
   f. The solution is stable at room temperature for months (with long storage the solution will begin to precipitate.

2.3. Microaffinity DNA-Binding Reactions

1. Binding buffer:
   a. Binding buffer is made in a buffer containing 8% (v/v) glycerol, 5 m*M* $MgCl_2$, 1 m*M* DTT, 60 m*M* KCl, 1 m*M* EDTA, and 12 m*M* HEPES, pH 7.8 in ddH_2O.
   b. This is stored at 4°C for 1 wk.
2. Prewashed streptavidin-agarose beads (Pierce).
   a. Prewash the streptavidin beads three times.
   b. For the prewashing, streptavidin beads are suspended as a slurry in binding buffer, briefly spun (5000 rpm for 60 s), the supernatant aspirated, and the pellet resuspended in binding buffer.
3. Electroblotting buffer:
   a. 1X CAPS (diluted from 10X CAPS buffer) with 10% (v/v) MEOH in ddH_2O.
   b. 10X CAPS buffer is made by dissolving 22.13 g CAPS (3-[cyclohexylamino]-1-propanesulfonic acid) in 900 mL ddH_2O.

Table 3
20 mL Solution C (High-Salt Buffer)

Components	Stock conc.	Working conc.	Vol. from stock
HEPES pH 7.9	1.0 *M*	50 m*M*	1 mL
KCl	2.0 *M*	400 m*M*	4 mL
EDTA pH 8.0	0.2 *M*	1 m*M*	100 µL
EGTA pH 8.0	0.2 *M*	1 m*M*	100 µL
DTT[a]	1.0 *M*	1 m*M*	20 µL
PMSF[a]	0.1 *M*	0.5 m*M*	100 µL
Pepstatin A	5 µg/µL	1 µg/mL	4 µL
Leupeptin	5 µg/µL	1 µg/mL	4 µL
STI	10 µg/µL	10 µg/mL	20 µL
Aprotinin	10 µg/µL	10 µg/mL	20 µL
NaF	0.5 *M*	20 m*M*	800 µL
$Na_2P_2O_7$	0.1 *M*	1 m*M*	200 µL
Na_3VO_3	0.1 *M*	1 m*M*	200 µL
Glycerol	100%	10%	2 mL

Add ddH_2O to a final volume of 20 mL.
[a]As above, DTT and PMSF should be added immediately prior to use. The buffer is stored at 4°C.

   c. Add approx 20 mL 2 *N* NaOH until pH is 11.0 at 25°C.
   d. Adjust volume to 1 L with ddH_2O; store at 4°C.
4. 1X Tris-buffered saline (TBS)-0.1% Tween:
   a. 1X TBS (diluted from 10X TBS buffer) with 0.1% (v/v) Tween in ddH_2O; store capped at RT.
   b. 10X TBS buffer is made by dissolving 24.2 gm TRIS (base) and 80 gm NaCl in 900 mL ddH_2O.
   c. The solution is then adjusted to pH 7.6 (25°C) by the addition of concentrated HCl (16 *N*).
5. Blotto:
   a. 8% (w/v) nonfat dry milk dissolved in TBS-0.1% Tween.
   b. Made fresh with each Western immunoblot.

2.4. DNase I Footprinting Assays

1. RNase-free DNase I (Calbiochem):
   a. Redissolve in buffer containing 10% glycerol, 1 m*M* DTT, and 20 m*M* HEPES, pH. 7.0 at a final concentration of 0.5 mg/mL DNase.
   b. DNase dilution buffer: 100 µg/mL BSA, 5 m*M* $MgCl_2$, and 1 m*M* DTT.
   c. 200 m*M* $MgCl_2$.

2.5. Target Detection Assay

1. Oligonucleotides:
   a. A random library of phosphoryl backbone oligonucleotides was synthesized by automated DNA synthesis.

b. This oligonucleotide is flanked by specific primer sequences and contains, in this case, a 22 basepair degenerate core that includes all four monomer bases of the oligonucleotide during the coupling of residues in a randomized segment.
c. The resulting library has potentially 4^{22} (10^{13}) different sequences.
d. The PCR primer segments at the 5' and 3' ends allows selected binding sequences to be replicated and amplified by *Taq* DNA polymerase (Amplitaq, Perkin Elmer), and contains suitable restriction sites for ease in subcloning.
e. The sequence used is:

5'-CAGTGCTCTAGAGGATCCGTGAC-N_{22}-CGAAGCTTATCGAT CCGAGCG-3'.

f. The sequence of upstream primer A is 5'-CAGTGCTCTAGAGGATCC GTGAC-3'. (*Xba*I restriction site is single underlined, *Bam*HI site double underlined.)
g. The sequence of downstream primer B is 5'-CGCTCGGATCGATAAGCTT CG-3'. (*Cla*I restriction site is single underlined, *Hin*dIII site is double underlined.)

2. Generating random phosphorothioate-modified library:
   a. The oligonucleotide library with phosphorothioate backbone substituted at dA positions was then synthesized by PCR amplification of the 66-mer template using commercially available *Taq* polymerase and using a mixture of dATP(αS), dTTP, dGTP, and dCTP as substrates (Pharmacia, Inc.).
   b. The PCR conditions for amplification of the starting random library includes 40 μ*M* each of dATP (αS), dTTP, dGTP, and dCTP, 500 μ*M* $MgCl_2$, 2.9 μ*M* 66-mer random template, 5 U *Taq* polymerase, and 400 n*M* each primer in a total volume of 100 μL. PCR was run for 25 cycles of 95°C/1 min, 55°C/1.5 min, 72°C/1 min.
   c. This polymerase is known to PCR amplify a phosphorothioate backbone template as long as the dNTP(αS)s are limited to no more than three different bases in the mixture.
   d. The PCR product is purified on 2% agarose minigel.
3. Filter elution buffer:
   a. Make 250 m*M* NaCl, 10 m*M* Tris-base, and 1 m*M* DTT, pH. 8.0 in ddH_2O.
   b. Store at 4°C for 1 wk.

3. Methods

3.1. Cytoplasmic and Nuclear Extract Preparation

1. In this technique, modified from a standard hypotonic/detergent lysis protocol, nuclear pellets are spun through a sucrose cushion to eliminate membrane contaminants from the nuclear pellets. We have found this additional step necessary in our analysis of inducible NF-κB and STAT binding activity following hormone treatment.
2. HepG2 cells are washed two times with calcium/magnesium-free PBS, and scraped with a rubber policeman in 1 mL of PBS.

3. The cell suspension is transferred to a 1.5-mL Eppendorf tube where the cells are briefly spun for 1 min at 3000 rpm in a microfuge tube.
4. The PBS is aspirated and the cell pellet is resuspended in Buffer A [**Table 1**; 50 m*M* HEPES (pH 7.4), 10 m*M* KCl, 1 m*M* EDTA, 1 m*M* EGTA, 1 m*M* DTT, 0.1 μg/mL PMSF, 1 μg/mL pepstatin A, 1 μg/mL leupeptin, 10 μg/mL soybean trypsin inhibitor, 10 μg/mL aprotinin, and 0.5% (v/v) NP40 in ddH_2O)] at 5-times the cell pellet volume.
5. After 10 min on ice, the lysates are centrifuged at 4000*g* for 4 min at 4°C and the supernatant collected and saved (the supernatant constitutes the cytoplasmic extract).
6. For the further purification of nuclei, nuclear pellets are purified through a sucrose cushion. This purification eliminates cytoplasmic contamination as measured by contaminating cytoplasmic proteins, such as β-actin. This technique has been optimized for hepatic cells; in the purification of nuclei form certain other cell types, the sucrose concentration may need to be modified. For example, in adipose cells, the nuclei do not pellet through this concentration of sucrose.
7. Nuclear pellets are resuspended in Buffer B [**Table 2**; 1.7 *M* sucrose, 50 m*M* HEPES (pH 7.4), 10 m*M* KCl, 1 m*M* EDTA, 1 m*M* EGTA, 1 m*M* DTT, 0.1 mg/mL PMSF, 1 μg/mL pepstatin A, 1 μg/mL leupeptin, 10 μg/mL soybean trypsin inhibitor, and 10 μg/mL aprotinin] at five times the pellet volume and centrifuged at 15,000*g* for 30 min at 4°C.
8. The supernatant is aspirated and the resultant nuclear pellets are resuspended and incubated in Buffer C [**Table 3**; 10% glycerol, 50 m*M* HEPES (pH 7.4), 400 m*M* KCl, 1 m*M* EDTA, 1 m*M* EGTA, 1 m*M* DTT, 0.1 mg/mL PMSF, 1 μg/mL pepstatin A, 1 μg/mL leupeptin, 10 μg/mL soybean trypsin inhibitor, and 10 μg/mL aprotinin] at two times the pellet volume with frequent vortexing for 30 min at 4°C.
9. The resuspended pellet is then subjected to centrifugation at 15,000*g* for 5 min at 4°C, the supernatant is saved for nuclear extract.
10. Both cytoplasmic and nuclear extracts are normalized for protein amounts determined by the Bradford assay using BSA as a standard (Bio-Rad, Hercules, CA).

3.2. Oligonucleotide and Plasmid Preparation

1. Sense and antisense oligonucleotides are synthesized commercially containing a GATC overhang, that is compatible with *Bam*H1 and *Bgl*II restriction endonuclease sites.
   a. These sequences allow for ligation of the duplex into reporter genes (*see* Chapter 7), or for radioactive labeling by Klenow fill-in reaction.
   b. The sequences of the APRE double-stranded oligonucleotides are:

```
APRE WT:  GATCCACCACAGTTGGGATTTCCCAACCTGACCA
                GTGGTGTCAACCCTAAAGGGTTGGACTGGTCTAG
APRE M6:  GATCCACCACAGTTGTGATTTCACAACCTGACCA
                GTGGTGTCAACACTAAAGTGTTGGACTGGTCTAG
APRE M2:  GATCCACCACATGTTGGATTTCCGATACTGACCA
                GTGGTGTACAACCTAAAGGCTATGACTGGTCTAG
APRE BPi: GATCCACCACAGTTGGGATTTCCCAACCTGACCA
                GTGGTGTCAACCCTAAAGGGTTGGACTGGTCTAG
```

2. To make duplex oligonucleotides:
   a. The DNA is supplied as a dried pellet following desalting (no additional purification is usually necessary for small [< 40 nucleotide-long oligomers]).
   b. The DNA is desalted and quantitated spectrophotometrically by absorbance at 260 nm (A_{260} nm).
   c. Equal numbers of picomoles are added to sterile ddH_2O in an Eppendorf tube. Typically, we find concentration of 25 picomoles/μL a convenient concentration for binding and competition assays.
   d. The tubes are capped and placed in a floater in 200 mL of 65°C H_2O.
   e. The tube is allowed to anneal overnight and is complete when the H_2O reaches room temperature.
   f. The oligonucleotides are stored frozen until use.
3. For modified oligonucleotides in the Microaffinity isolation assay:
   a. Duplex APRE WT oligonucleotides are chemically synthesized containing 5' biotin (Bt) on a flexible six-carbon linker. We have found the chemically synthesized oligonucleotide to be far superior than enzymatic incorporation, where >95% of the oligonucleotide is 5' biotinylated (compared to <50% achievable by enzymatic methods).
   b. The sense and antisense oligonucleotides are annealed as above and stored frozen.
   c. The biotin label is stable indefinitely.

3.3. Radiolabeling Oligonucleotide and Plasmid Fragments

1. For radiolabeling duplex oligonucleotides for gel shift or restriction fragments for DNase I footprinting assays, we use Klenow polymerase fill-in reaction. For this, assemble the following reaction components on ice in a 20-μL reaction volume:
   a. 10 pmol duplex oligonucleotide or plasmid fragment, 4 μL dNTP (-dA) mix (ultrapure, 25 m*M* stock of dTTP, dGTP, and dCTP in H_2O at pH 8.0), 4 μL α[^{32}P]dATP (>6000 Ci/mmol), 2 mL 10X reaction buffer (supplied commercially with the enzyme) and ddH_2O to make a reaction volume of 19 μL.
   b. Klenow polymerase is added (1 μL, U/μL), and the reaction is transferred to a 37°C water bath for 30 min.
   c. Following completion of the reaction, 75 μL TE (10 m*M* Tris, pH 8.0, 0.1 m*M* EDTA) buffer is added and the oligonucleotide is separated from the unincorporated radiolabel by centrifugation through a Sephadex G-50 column.
   d. Labeling efficiency is determined by counting the probe for β activity. We assume 100% recovery of the oligonucleotide.
   e. You should expect a yield of 10^7 cpm/μg oligonucleotide.
   f. The probe is stored in a lucite container at –20°C and is stable for 2 wk.

3.4. EMSAs

1. The electrophoretic mobility shift assay is a simple and sensitive assay for the detection of DNA binding proteins.

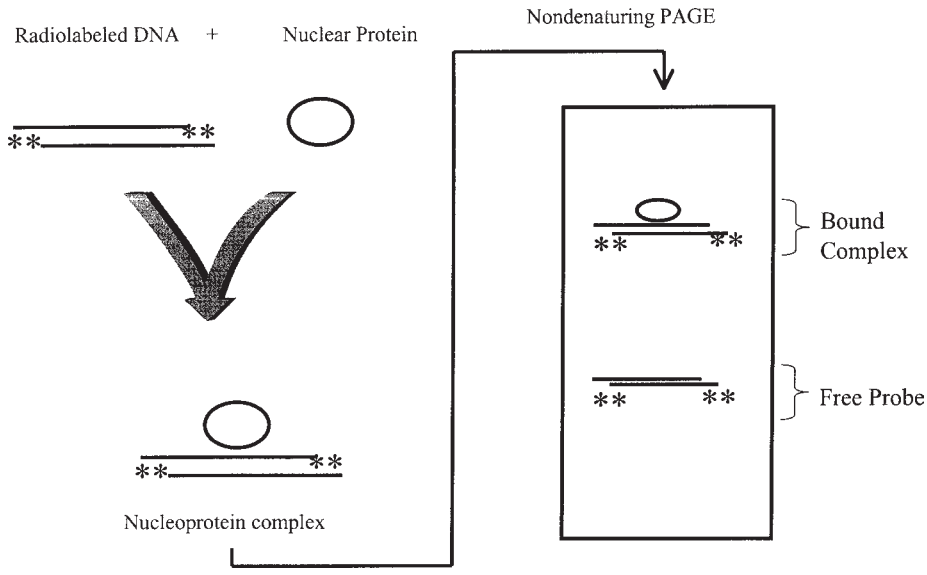

Fig. 1. Electrophoretic Mobility Shift Assay (EMSA). A labeled DNA fragment is incubated with nuclear protein in the presence of DNA carrier (to minimize nonspecific DNA binding). After the binding reaction reaches equilibrium, the reaction is fractionated on a nondenaturing (native) polyacrylamide gel and exposed for autoradiography. The nucleoprotein complex migrates more slowly than the free DNA allowing for their separate resolution and identification.

2. In this assay, radiolabeled DNA is incubated with nuclear protein as follows:
   a. Nuclear extracts (10 μg) are incubated with 40,000 cpm of ^{32}P-labeled APRE WT duplex oligonucleotide probe and 1 μg of poly (dA-dT) in a in a final volume of 20 μL of 1X EMSA Binding buffer.
   b. This binding reaction sample is then incubated for 15 min at RT.
   c. The binding reaction is then fractionated on a 6% native polyacrylamide gels run in 1X TBE, dried, and exposed to Kodak X-AR film at –70°C.
3. Free DNA migrates much faster than the DNA contained in a nucleoprotein complex.
4. The general strategy is displayed in **Fig. 1**.
5. **Figure 2** shows an example of the primary data generated by the EMSA. Additional examples of EMSA data can be found in **refs.** ***(10,11)***.

Information optimization of the binding reaction is contained in **Note 1**.

3.4.1. Competition in EMSA

1. Demonstration that bound complexes are binding in a sequence-specific manner requires either competing the binding proteins for binding the wild-type label with unlabeled wild-type and mutant competitors, or by demonstrating the complexes do not form on a radiolabeled mutant oligonucleotide.

Fig. 2. Data from EMSA. Radiolabeled angiotensinogen acute phase response element duplex oligonucleotide (APRE M6) was incubated with increasing concentrations of the recombinant transcription factor, nuclear factor for IL-6 (NF-IL6) ***(16)***. The bound and free complexes were fractionated by nondenaturing PAGE. Shown is an autoradiogram of the dried gel.

2. For most purposes, we have found that competing binding using unlabeled oligonucleotides is a reliable and economical way to demonstrate binding specificity.
3. To set up a competition assay, unlabeled wild-type and mutant oligonucleotide duplexes must be annealed.
4. The binding reaction is set up as aforementioned, omitting addition of the protein.
5. The protein is added after both the probe and a molar excess of unlabled competitor (usually 5–100-fold excess is used) are added and mixed.
6. The reactions are allowed to reach completion and the binding reactions are fractionated by nondenaturing polyacrylamide gel electrophoresis (PAGE).
7. Sequence-specific complexes are defined as those that are competed by wild type, but not by the mutant oligonucleotides.
8. An example of a competition assay in EMSA is shown in **Fig. 3**. Additional examples of competition assays can be found in **refs.** ***(10,11)***.

3.4.2. "Supershift" Assays

1. Antibody supershift assays take advantage of the specificity of antibodies to tentatively identify the presence of DNA binding proteins within a gel shifted complex.
2. In this assay, a standard gel shift binding reaction is set up.
3. Next, 1 μL of affinity-purified polyclonal antibodies (IgG fraction) is added and the samples incubated for 1 h on ice prior to fractionation by nondenaturing PAGE.
4. Controls include the addition of a similarly prepared IgG fraction from preimmune serum, or immune IgG that has been preadsorbed with the immunizing peptide. We prefer the use of affinity-purified IgG, as this minimizes nonspecific effects of serum in the EMSA.
5. The concept behind the supershifting assay is that an antibody binding to the nucleoprotein complex will produce a larger complex, further retarding its progression through the nondenaturing PAGE (producing a supershifted band).

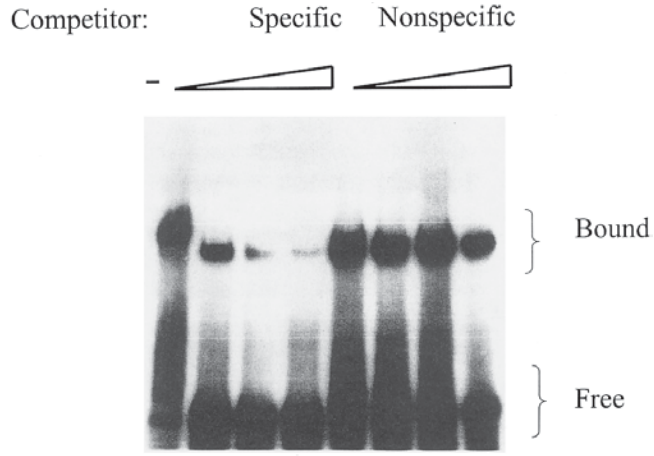

Fig. 3. DNA binding specificity assay. Radiolabeled angiotensinogen acute phase response element duplex oligonucleotide (APRE M6) was incubated with a fixed amount of DNA binding protein in the absence (–) or presence of increasing concentrations of specific (APRE WT) or nonspecific (APRE M2) duplex oligonucleotides. The ratio of unlabeled competitor spans from 10- to 1000-fold molar excess to that of the probe. The bound and free complexes were fractionated by nondenaturing PAGE. Shown is an autoradiogram of the dried gel. Increasing concentrations of the specific oligonucleotide competed for binding at concentrations where no competition by the nonspecific DNA was observed. Note that at high concentrations of DNA, even the nonspecific competitor competes for binding.

6. Sometimes, the presence of the antibody interferes with the binding of the target protein. This will result in an observation that no complex is formed; in this case, interpretation of the experiment is more difficult, as sometimes inhibition of nucleoprotein complex can also be a nonspecific effect (salt and detergent, for example will do the same thing) *see* **Note 2**.
7. Examples of supershift assay results can be found in **refs.** ***(10–12)***.

3.5. Microaffinity Purification of Acute-Phase Response Element (APRE)-Binding Proteins

1. Although in some instances the supershifting assay yields valuable information, for precise identification of individual protein components of a multiprotein family, such as our experience with the NF-κB and STAT protein families, the supershift assay is insensitive and unreliable.
2. We have recently developed a two-step biotinylated DNA-streptavidin capture assay that avoids many of these pitfalls.
3. In this assay, duplex APRE WT oligonucleotides chemically synthesized containing 5' biotin (Bt) on a flexible linker (*see* **Subheading 2.2.**) are incubated

with nuclear extract and binding proteins pulled down with the addition of streptavidin/agarose beads.
4. Following washing, the proteins are eluted from the beads and fractionated by denaturing sodium dodecyl sulfate (SDS)-PAGE.
5. The presence of proteins are then detected by Western immunoblot.
6. This is schematically diagrammed in **Fig. 4**.
7. An example of primary data generated by the Microaffinity purification assay is shown in **Fig. 5**.
8. An additional example of microaffinity purification assay data can be found in ***(10)***.

3.5.1. Microaffinity DNA-Binding Reactions

1. Binding Reaction:
   a. Add 1 mg of nuclear protein from control and hormone-stimulated extracts 50 pmoles Bt-APRE WT DNA in the presence of 12 μg poly dA-dT (as non-specific competitor) in binding buffer (500 μL total volume) at 4°C for 1 h.
   b. 100 μL of a 50 % (v/v) slurry of prewashed streptavidin-agarose beads was then added to the sample, and incubated at 4°C for an additional 20 min with shaking.
   c. Pellets were washed twice with 500 μL binding buffer, and then resuspended in 100 μL 1X SDS-PAGE buffer for analysis by Western immunoblot.
   d. Samples were boiled in 1X SDS-PAGE buffer and separated on 10% SDS-PAGE.
   e. For competition assays, a 10-fold molar excess of the indicated (nonbiotinylated) duplex DNA was added in the initial binding reaction.
   f. These controls establish DNA binding specificity (much as the competition assays in EMSA described above). **Ref.** ***(10)*** has an example of a microaffinity/competition assay result.

3.5.2. Western Immunoblots (for Detection of Affinity-Isolated DNA-Binding Proteins)

1. Transfer and Western Immunoblot:
   a. Following electrophoresis, the proteins are transferred to polyvinylidene difluoride (PVDF) membranes (purchased as Immobilon membranes, Millipore, Bedford, MA).
   b. To accomplish protein transfer, first soak the gel in Electroblotting buffer for 5–10 min at room temperature.
   c. While gel is soaking, prewet the PVDF membrane with 100% MEOH for 15–30 s in a stainless steel tray, rinse with ddH_2O for 2 min, then wash in Electroblotting buffer for 10–15 min.

Fig. 4. *(opposite page)* Microaffinity DNA binding assay. Schematic diagram for the microaffinity isolation/Western immunoblot assay for detection of inducible or constitutive proteins binding to target DNA sequence. Control or stimulated nuclear extracts are incubated with biotinylated DNA duplex. After the binding reactions reach equilibrium, the nucleoprotein complexes are captured by the addition of streptavidin beads and centrifugation. The proteins are subsequently eluted by denaturing SDS-PAGE buffer and fractionated on an SDS-PAGE for Western detection.

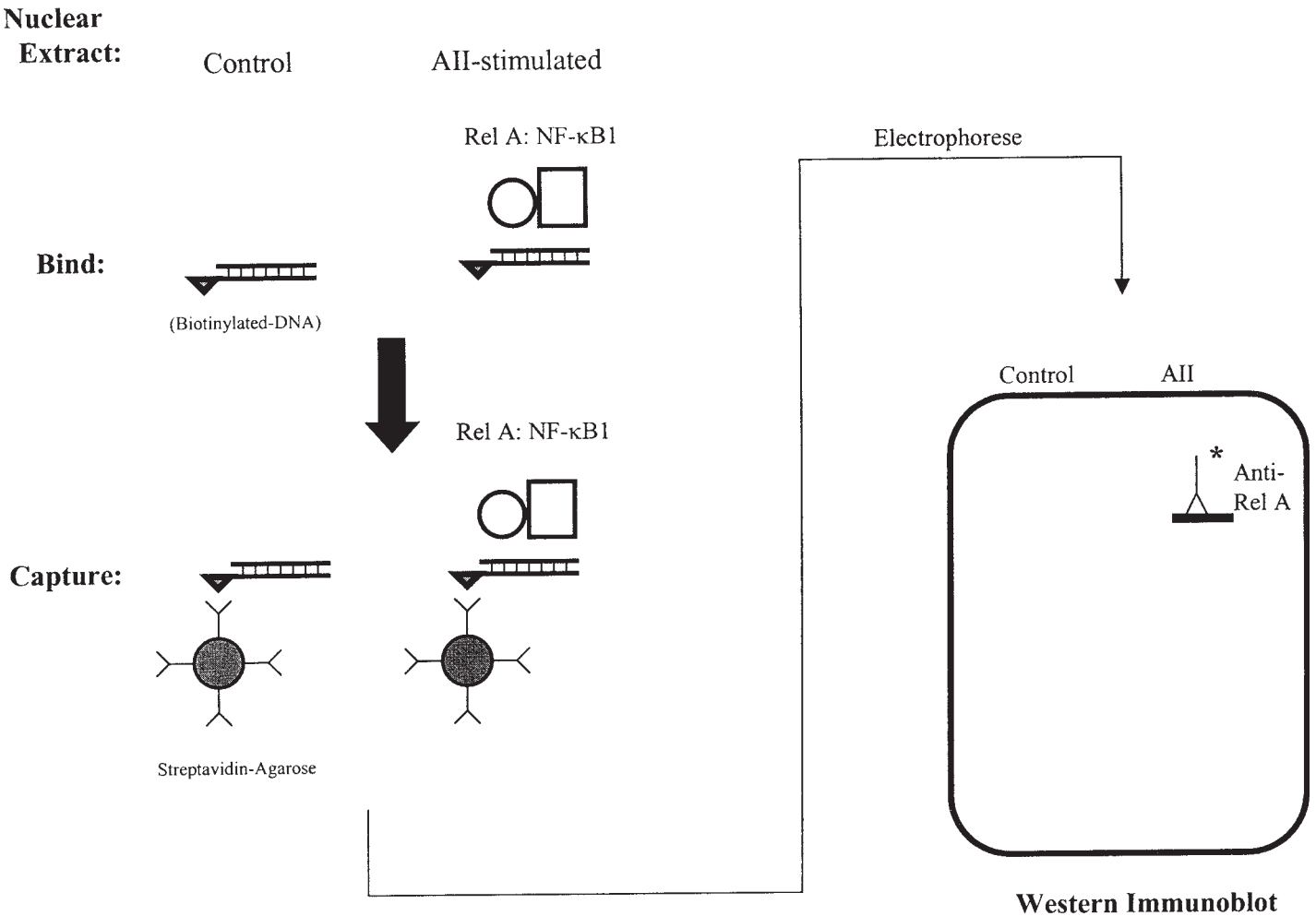
Nuclear Extract:
Control
AII-stimulated
Rel A: NF-κB1
Electrophorese
Bind:
(Biotinylated-DNA)
Control
AII
Rel A: NF-κB1
*
Anti-Rel A
Capture:
Streptavidin-Agarose
Western Immunoblot

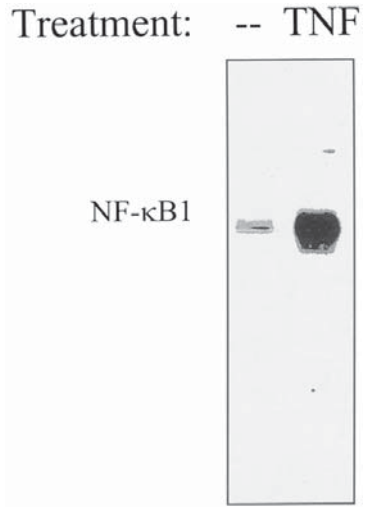

Fig. 5. Detection of NF-κB1 binding to angiotensinogen gene promoter. Nuclear extracts from control or stimulated HepG2 cells (15 min with 20 ng/mL TNFα) were incubated with biotinylated APRE WT DNA and processed as described in **Subheading 3.** for binding. After the nucleoprotein complexes were fractionated on SDS-PAGE, the Western immunoblot was performed using primary anti-NF-κB1 antibody. The immune complexes were then detected by enhanced chemiluminescence (ECL, Amersham International). The 50-kDa NF-κB1 protein binds in control extracts, but its abundance increases two-fold following TNF treatment.

d. Assemble the gel and PVDF membrane in a sandwich and electrotransfer the proteins at approx 50 V (100–170 mA) at room temperature for 30–90 min (depending on size of protein–the longer times are for large >100 kDa proteins).
e. To ensure that the proteins are transferred, we use prestained molecular weight markers (Bio-Rad) that are easily detected on the membrane.
f. Following transfer, the membranes are washed for 5 min in 1X TBS- 0.1% Tween. Membranes are then blocked in a premixed solution of Blotto for 1 h at room temperature.
g. The membranes are then blotted in 1:500–1:6000 (v/v) dilution of affinity-purified antibody in TBS-0.1% Tween for 2 h at room temperature or overnight at 4°C .
h. The dilution of antibody is determined empirically for each antibody type.
i. The membrane is then washed with 1X TBS-0.1% Tween three times, for 5 min. The membrane is then incubated with a 1:6000 (v/v) dilution of horse radish peroxidase (HRP) conjugated to donkey antirabbit IgG (Pierce, Rockford, IL) in 1X TBS-0.1% Tween for 1 h.
j. After incubation with secondary antibody, the membrane is washed with 1X TBS-0.1% Tween three times, 5 min each, and immune complexes detected

by enhanced chemiluminescence assay (ECL, Amersham International, Arlington Heights, IL) according to the manufacturer's recommendations.

k. Controls for the specificity of binding include loss of specific immunostaining upon preincubating with the immunizing peptide or absence of staining when using preimmune IgG in the primary antibody incubation step.

3.6. Methylation Interference Assay

1. Methylation interference assay is a powerful tool to identify individual guanosine contact points by proteins that bind to a specific region of a promoter of interest.
2. In this assay, uniquely end-labeled DNA is methylated at the N^6 position of guanosine residues by dimethyl sulfate (DMS). Guanosine residues that are necessary for protein-DNA interaction will interfere with DNA binding when methylated.
3. The probe is then incubated with nuclear protein extracts and fractionated into the "Free" and "Bound" components by EMSA.
4. The "Free" and "Bound" components of the binding reaction are then detected by autoradiography and excised from the PAGE.
5. We use electroelution into a salt buffer as this technique gives high yields of pure DNA.
6. Following cleavage of the methylated G residues in piperidine, the bound and free probes are fractionated by a denaturing (8 *M* Urea/polyacrylamide sequencing) gel.
7. The probes containing methylation at DNA contact sites will appear in the free DNA fraction, and be underrepresented in the bound fraction.
8. A schematic and example of this technique is shown in **Fig. 6**.
9. An example of real data obtained through use of this technique can be found in ***(10)***.
10. Detailed methodology is as follows:
    a. Purification of labeled DNA of promoter fragment:
        i. Cut plasmid containing sequence of choice with unique enzyme (150–300 bp is optimal).
        ii. Fill in label 10 μg of DNA with two labeled nucleoside triphosphates [α^{32}P dNTP] that are incorporated first into the overhang. (For *Bam* H1, as an example, yields an overhand of GATC. When labeling *Bam* H1 ends, use dGTP and dATP).
        iii. Following labeling reaction, chase with cold (other two) dNTPs to complete fill in reaction and generate a homogeneous length of DNA. This would be done by adding the other dNTPs in Klenow reaction buffer and some fresh Klenow.
        iv. Desalt labeling reaction with G-50 spin columns, ETOH-precipitate, and cut the downstream (nonlabeled boundary of promoter of interest) exhaustively.
        v. Separate the labeled insert from the labeled plasmid on a mininondenaturing (6–8%) PAGE gel.

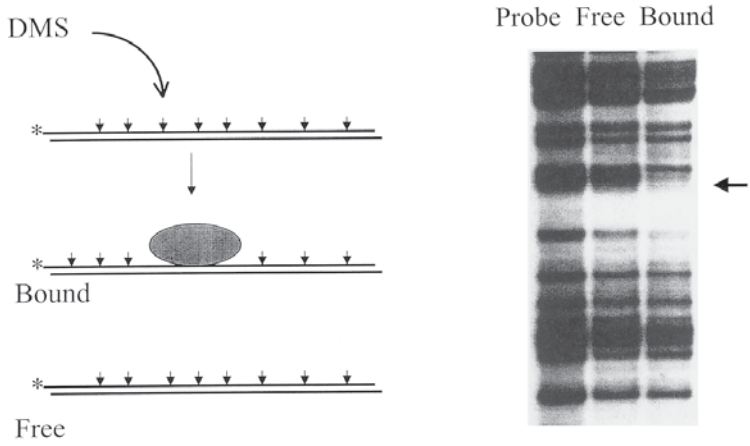

Fig. 6. Methylation interference assay. Left-hand panel is a schematic diagram of methylation interference assay. A uniquely end-labeled DNA fragment (indicated as *) is treated with limiting concentrations of DMS to methylate, on the average, one G residue per DNA fragment (modifications indicated as vertical arrows). After the DMS is inactivated, the methylated DNA is subjected to EMSA, where the bound and free complexes are separated, excised from the gel and the G residues cleaved by incubating in the presence of piperidine. The labeled DNA fragments are fractionated on an 8-*M* urea/8% polyacrylamide sequencing gel and the G ladder is detected by autoradiography (right panel). The absence of a G residue in the ladder indicates its methylation interferes with protein:DNA binding and hence is a site of contact.

vi. After electrophoresis, stain DNA with ethidium bromide in H_2O for 10 min at RT.
vii. Visualize the small band, excise, and electroelute DNA into NH_4OAc trap for 1.5 h at 100 V in 1X TBE.
viii. Follow disappearance of radioactivity using a handheld (Geiger) counter.
ix. Following electroelution, plug traps with 200-μL pipet tips, drain TBE buffer, and transfer the labeled fragment into an Eppendorf tube.
x. ETOH precipitate with glycogen, dry, and count dry tube.
xi. Adjust the probe to 100–500,000 cpm/μL with H2O.

b. Methylated DNA probe is generated by prereacting labeled DNA fragment with DMS.
i. Incubate 500,000 cpm of probe in 200 μL of ddH_2O.
ii. Add 1 μL of undiluted DMS, and incubate at RT for 3.5 min.
iii. Following incubation, add 50 μL of DMS stop buffer (1.5 *M* NaOAc, pH 7.0, 1.0 *M* 2-mercaptanethanol in H_2O), vortex.
iv. Add 25 μg of tRNA as carrier, 750 μL 100% ETOH, vortex, and spin in cold in microfuge.

v. Resuspend pellet in 250 μL of 0.3 *M* NaOAC, add 750 μL of 100% ETOH, and spin again.
vi. Rinse with 100% ETOH; Speed-Vac dry.
vii. Subject the labeled DNA fragment to EMSA (discussed earlier). After electrophoresis, disassemble the gel. Wrap the wet gel in Saran Wrap and expose the gel to Kodak X-AR film overnight at 4°C. Develop the film; align the film over the wet gel to identify the location of the radiolabeled DNA.
viii. Cut the free and bound bands, and electroelute the radiolabel. Ethanol precipitate using tRNA as a carrier. Rinse and dry.
ix. Resuspend pellet in 100 μL of 1.0 *M* Piperidine (work with 10 *M* stock solution under chemical hood). Heat at 65°C for 1 h. Following incubation, add 20 μL of 3 *M* NaOAC, 0.7 mL 100% ETOH, 20 μg tRNA, vortex, spin, and rinse with 100% ETOH. Dry.
x. Count dry tube and resuspend at the appropriate cpm in sequencing gel loading dye.

c. Electrophoresis:
i. Resolubilize the dry pellet with sequencing gel loading buffer (90% formamide and tracking dye). I add enough sequencing buffer to make each sample a constant cpm/μL (3000–7500 cpm/μL).
ii. To a prewarmed 7-8% denaturing sequencing gel, load a constant volume (5–10 μL) for each sample.
iii. In an adjacent lane, add 5000–10,000 cpm (total) of G ladder ***(13)***.
iv. Electrophorese/dry and expose as usual.
v. Additional information on methylation interference can be found in **refs.** ***(10,14)***.

d. *See* **Note 3** for additional information on optimizing this technique.

3.7. DNase I Footprinting Assays

1. DNase I footprinting is a technique to map the domains of a nucleoprotein complex over a region of the promoter of interest.
2. This technique provides important information on the boundaries required for protein–DNA interaction.
3. In this assay, uniquely end-labeled DNA is incubated with nuclear protein under conditions where 100% of the probe is bound.
4. As can be inferred in the schematic overview of the technique (**Fig. 7**), the technique will not work well if only a small population of the probe is bound.
5. In preliminary experiments, we frequently will use gel shift assays to determine the range of protein that will be required for footprinting.
6. We have had the most optimal results when using partly purified nuclear protein [this removes nonspecific DNA binding species from binding the probe ***(15,16)***].
7. Controls are digestions in the absence of nuclear protein (substitute equivalent amounts of BSA).
8. Usually, we use several different volumes of DNase I so that the amount of digestion in control samples will be matched with the digestion of samples containing nuclear protein.

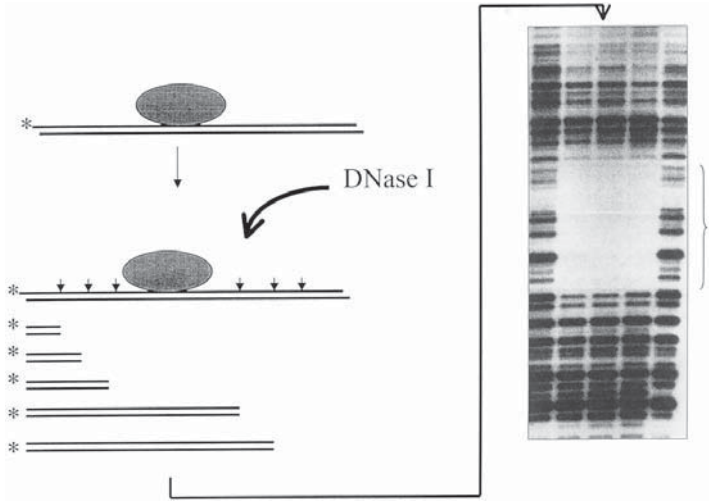

Fig. 7. DNase I footprint assay. Left-hand panel is a schematic diagram of DNase I footprint assay. A uniquely end-labeled DNA fragment (indicated as *) is incubated in the presence of nuclear protein. After binding equilibrium is reached, the nucleoprotein complex is treated with limiting concentration of DNase I. The presence of DNA binding protein protects the labeled DNA fragment. After deproteination and electrophoresis on a sequencing gel, the absence of cleavage in a region identifies the contacted region ("footprint", shown on right).

9. Frequently, more DNase I is required to digest probe in the presence of nuclear protein caused by contaminating nucleic acids and other interfering substances.
10. An example of data from a footprinting reaction is shown in **Fig. 7**.
11. An example of other data derived from this technique can be found in ***(15–17)***.
12. A detailed description of the methodology is as follows:
    a. Prepare/purify labeled DNA (as described in **Subheading 3.4.**).
    b. Dissolve RNase-free DNase I (Calbiochem) in a buffer of 10% glycerol, 1 m*M* DTT, 20 m*M* HEPES, pH 7.0 to a final concentration of 0.5 mg/mL.
    c. Set up a series of 50 µL binding assays using 1–2 µg poly dAdT, 10–100 µg nuclear protein, 200–500 K cpm of radiolabled probe.
    d. Dilute 0.5 mg/mL stock solution of DNase I 1:40 (v/v) in dilution buffer (100 µg/mL BSA, 5 m*M* $MgCl_2$, 1 m*M* DTT) at RT.
    e. To each binding assay, add 1.7 µL of 200 m*M* $MgCl_2$.
    f. Then to each tube, add 1–5 µL of diluted DNase I for exactly 1 min at RT. Mix gently.
    g. After exactly 1 min, stop reaction by adding 300 µL of 30 m*M* EDTA and 100 µL of 7.5 *M* NH_4OAc.
    h. Do one extraction with 100 µL of 1:1 (v/v) phenol/chloroform (a subsequent extraction with chloroform is not necessary), spin briefly 2–5 min, and transfer supernatant to a fresh tube.

i. Precipitate with the addition of 600 µL 100% ETOH and 20 µg of tRNA carrier. Vortex, incubate at –20°C for 10 min and spin at maximum in a microfuge for 10 min. The precipitates should be visible.
j. Rinse once with 100% ETOH and Speed-Vac dry. Count radioactivity in each dry tube.
k. Adjust the counts to an equal number of cpm/µL in Formamide loading dye. Load an equal volume (and number of cpm) for each lane.
l. Fractionate on sequencing gel, dry, and expose for autoradiography.
m. *See* **Note 4**.

3.7. Target Detection Assay

3.7.1. Empiric Determination of Nuclease-Resistant "Decoys"

1. A recent advance in combinatorial chemistry has been the ability to construct (and screen) large random-sequence nucleic acid libraries that specifically bind to target DNA-binding proteins.
2. Identifying the empiric binding sits is useful for two purposes.
   a. First, in the situation where a transcription factor with unknown DNA binding specificity has been cloned, identifying the types of high affinity DNA-binding sequences allows the investigator to generate hypothesis about potential target genes.
   b. Second, identification of nuclease-resistant high-affinity binding sites allows for the production of specific inhibitory molecules.
3. These aptamers, or "decoys," when added to cells or tissues, are taken up where they compete for the endogenous transcription factor to bind.
4. This reagent will then selectively block the activity of the target protein so that its function in complex biological systems can be determined.
5. In the target detection assay, a nucleic acid library containing a large number of potential DNA binding sites is incubated with the target protein.
6. After separating the bound from the unbound DNA, the bound fractions are amplified using the PCR.
7. This regenerated pool is incubated again with the protein for a second round of the screening process.
8. These iterations are repeated until the library is enhanced for high affinity binding sequences for the target protein.
9. A schematic diagram of the target detection assay is shown in **Fig. 8**.
10. Agents selected from combinatorial libraries of RNA and DNA have in the past had normal phosphate ester backbones and thus will generally be unsuitable drugs because of their nuclease susceptibility.
11. Although the effect of substituting of nuclease resistant thiophosphates into the DNA backbone will reduce nuclease sensitivity, this approach cannot be applied to known phosphoryl DNA-binding sites.
12. The sulfur substitution can lead to significantly decreased (or increased) binding to a specific protein.

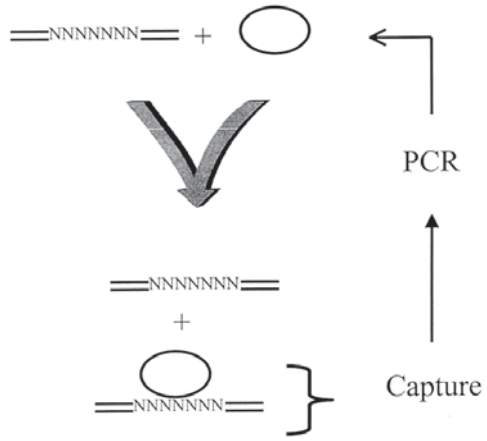

Fig. 8. Target detection assay. Schematic diagram of the target detection assay for empiric detection of protein–DNA interations. A degenerate library of duplex binding sites is incubated with protein. The bound complexes are captured on nitrocellulose filters, washed, and eluted from the filter. The PCR is used to regenerate the probe, and the cycle is repeated until high-affinity binding sites are selected.

13. We have recently developed and reported ***(18)*** a novel combinatorial approach involving the construction and screening of a phosphorothioate-modified DNA library.
14. This allows the empiric selection of high affinity, nuclease-resistant aptamers that can selectively target transcription factors.
15. More information on this technique can be found in ***(18–21)***.
16. A more detailed explanation of this technique is as follows:
    a. Anneal the purified phosphorothioate-modified library with 100 ng of purified transcription factor in 1X EMSA binding buffer (*see* **Subheading 3.1.1.**).
    b. Incubate 15 min at RT.
    c. Filter the binding reaction through Whatman filters.
    d. Wash with 1 mL 1X EMSA binding buffer.
    e. Remove, air-dry filters.
    f. Elute the DNA with 500 μL of filter elution buffer in 1.5-mL Eppendorf tube and agitation for 4 h.
    g. PCR amplify the eluted DNA using as a template 5 μL of the supernatant from the first binding reaction in the PCR reaction (described above).
    h. Gel purify the PCR reaction.
    i. Repeat **steps 1–8**, for 8–14 cycles.
    j. For sequence analysis, amplify the eluted DNA using conventional phosphoryl nucleotides, gel purify, and clone into TA cloning vector (Invitrogen) according to the manufacturer's recommendations.
    k. Align the binding sites and determine DNA binding site consensus sequence or synthesize the phosphorothioate modified decoy for introduction into cells.

4. Notes

1. Properly performed, the gel-mobility shift assay is a sensitive and specific assay for the identification of proteins that interact with individual *cis* elements under study. Widely applied in many labs, there have been a number of reported variations. Minor changes in the salt concentration, binding pH, and nonspecific DNA carrier are sometimes required for different DNA-binding species. Although we prefer the use of polydA-dT as a nonspecific carrier, some proteins are better identified using polydI-dC instead. Depending on the size of the nucleoprotein complex, the type of nondenaturing electrophoresis and polyacrylamide gel composition may need to be empirically adjusted as well. For example, although our conditions are adequate for NF-κB and NF-IL-6 DNA binding, they are not optimal for analysis of the TATA box binding protein, TBP. TBP is a large multiprotein complex that can only be resolved by a very "soft" PAGE (e.g., <4%).
2. The supershift assay is a specific assay for the detection of a particular protein within a nucleoprotein complex. However, the assay is not always sensitive, and frequently requires empiric determination of nuclear protein concentration, a probe labeled to a high specific-activity, and a high affinity antibody. Moreover, the supershift assay is sensitive to loss of epitopes. For example, if the antibody epitope is contained within the DNA-binding domain, the supershifting antibody will, at best, interfere with binding (or not bind at all). Although the supershift assay is a quick and easy assay to try, its interpretation in the case of loss of binding activity, or the probe precipitating in the EMSA well can produce difficulties. Importantly, a negative result in the supershifting assay cannot exclude the presence of the protein. For these reasons, we have developed the Microaffinity binding/Western immunoblot assay. Although frequently more nuclear protein is required for this latter assay, it avoids many of the potential pitfalls that arise in the supershifting assays.
3. Methylation interference is a very reliable assay for the determination of guanosine contacts by a particular transcription factor. The assay can be modified to also detect interactions with adenosines. We have used this assay to identify differences in base contacts within the same regulatory element ***(15)***. This has allowed the design of selective mutations that could be used in reporter assays to determine the individual roles of two binding proteins ***(15)***. The limitations of methylation interference assays, as well as for DNase I footprinting assays is the presence of a relatively purified source of nuclear protein. Crude nuclear extracts oftentimes contain nonspecific binding and interfering substances that prevent optimal results. Ion-exchange chromatography of nuclear proteins, assaying fractions by EMSA can be used to obtain partially purified extracts for contact and footprint analysis.
4. In the initial applications of DNase I footprinting assays, it is frequently useful to do dose outs of the diluted DNase I in the absence and in the presence of saturating concentrations of nuclear protein. This information will indicate what range of DNase I concentration will be required to produce an even footprint ladder. As shown in the example, we generally try to digest no more than 50% of the input probe.

5. New Frontiers

In Chapters 7 and 8, we have provided an overview of the current approaches for analyzing *cis* and *trans* regulatory elements important in the control of gene expression. Although we have largely focused on in vitro approaches to protein–DNA interaction, increasing appreciation is made to the effects of chromatin condensation and packing as an important controller of the activity of genes. Complete understanding of a target gene expression in any system occurs following analysis of protein–DNA interactions within its native chromatin context. Analysis of protein–DNA interactions within the native chromatin context can generate surprising information. For example, in a previous study ***(10)***, we described inducible TATA binding occurs following the cytokine activation of the interleukin-8 (IL-8) gene. In the uninduced state, there was no constitutive binding of the TATA box proteins to the promoter of IL-8. However, following translocation and binding of the upstream activator, NF-κB, TATA box binding was recruited to the IL-8 promoter. This is an example of gene activation being mediated through relief of chromatin-mediated repression. In this model, a gene promoter is condensed with histone H1 or nucleoprotein structures that prevent binding of the general transcription factors to the TATA box ***(22)***. In the absence of an upstream activator protein, the promoter is actively repressed as the consequence of a phased array of nucleosomes whose binding prevents the preinitiation complex from assembly onto the TATA box. In response to ligand-activated glucocorticoid receptor, a shift in the nucleosome array occurs, that opens up the previously occluded TATA sites for binding by their cognate ("constitutive") proteins ***(23,24)***. In this way, inducible transcription factors effect gene expression through a two-step mechanism: (1) to "derepress" promoters through nucleosome rearrangement; and (2) to "activate" their expression ***(22)***. This phenomenon has also been described as a mechanism for glucocorticoid regulation of the retrovirus, mouse mammary tumor virus (MMTV), a steroid hormone-inducible retrovirus [reviewed in ***(23)***]. Analysis of genomic footprinting techniques to inducible genes in the renin-angiotensin system may further reveal the complexities of cell specific and inducible gene expression regulation.

Acknowledgments

This work was supported by grants from NHLBI (1R01 55630-01A2, A. R. B.), and NIEHS (P30 ES06676, R.S. Lloyd, UTMB). A. R. B. is an Established Investigator of the American Heart Association. The authors also wish to acknowledge the efforts of our collaborators, David Gorenstein and David King, Sealy Center for Structural Biology, UTMB, for their efforts in developing the target detection assay.

References

1. Baeuerle, P. A. (1991) The inducible transcription activator NF-kappa B: regulation by distinct protein subunits. *Biochim. Biophys. Acta* **1072,** 63–80.
2. Siebenlist, U., Franzoso, G., and Brown, K. (1994) Structure, regulation and function of NF-κB. *Annu. Rev. Cell Biol.* **10,** 405–455.
3. Brasier, A. R. and Li, J. (1996) Mechanisms for inducible control of angiotensinogen gene transcription. *J. Hypertens.* **27(2),** 465–475.
4. Beato, M. (1989) Gene regulation by steroid hormones. *Cell* **56,** 335–344.
5. Heinrich, P. C., Behrmann, I., Muller-Newen, G., Schaper, F., and Graeve, L. (1998) Interleukin-6-type cytokine signalling through the gp130/Jak/STAT pathway. *Biochem. J.* **334,** 297–314.
6. Darnell, J. E., Jr. (1997) STATS and gene regulation. *Science* **277,** 1630–1635.
7. Mueller, P. R. and Wold, B. (1991) Ligation-mediated PCR: applications to genomic footprinting. *Methods* **2,** 20–31.
8. Pfeifer, G. P., Steigerwald, S. B., Mueller, P. R., Wold, B., and Riggs, A. D. (1989) Genomic sequencing and methylation analysis by ligation mediated PCR. *Science* **246,** 810–813.
9. Patterson, C., Wu, Y., Lee, M., DeVault, J., Runge, M. S., and Haber, E. (1997) Nuclear protein interactions with the human KDR/flk-1 promoter in vivo. *J. Biol. Chem.* **272,** 8410–8416.
10. Brasier, A. R., Jamaluddin, M., Casola, A., Duan, W., Shen, Q., and Garofalo, R. (1998) A promoter recruitment mechanism for TNFα-induced IL-8 transcription in type II pulmonary epithelial cells: dependence on nuclear abundance of Rel A, NF-κB1 and c-Rel transcription factors. *J. Biol. Chem.* **273,** 3551–3561.
11. Li, J. and Brasier, A. R. (1996) Angiotensinogen gene activation by AII is mediated by the Rel A (NF-κB p65) transcription factor: one mechanism for the renin angiotensin system (RAS) positive feedback loop in hepatocytes. *Mol. Endocrinol.* **10,** 252–264.
12. Garofalo, R., Sabry, M., Jamaluddin, M., Yu, R. K., Casola, A., Ogra, P. L., and Brasier, A. R. (1996) Transcriptional activation of the interleukin-8 gene by RSV infection in alveolar epithelial cells: Nuclear translocation of the Rel A transcription factor as a mechanism producing airway mucosal inflammation. *J. Virol.* **70,** 8773–8781.
13. Maxam, A. and Gilbert, W. (1980) Sequencing end-labeled DNA with base-specific chemical cleavages. *Methods Enzymol.* **65,** 499–560.
14. Hendrickson, W. and Scheif, R. (1985) A dimer of AraC protein contacts three adjacent major groove regions at the Ara I DNA site. *Proc. Natl. Acad. Sci. USA* **82,** 3129–3133.
15. Brasier, A. R., Ron, D., Tate, J. E., and Habener, J. F. (1990) A family of constitutive C/EBP-like DNA binding proteins attenuate the IL-1 alpha induced, NF kappa B mediated trans- activation of the angiotensinogen gene acute-phase response element. *EMBO J.* **9,** 3933–3944.
16. Brasier, A. R. and Kumar, A. (1994) Identification of a novel determinant for basic domain-leucine zipper (bZIP) DNA-binding activity in the acute-phase

inducible nuclear factor-interleukin 6 transcription factor. *J. Biol. Chem.* **269,** 10,341–10,351.
17. Ron, D., Brasier, A. R., Wright, K. A., Tate, J. E., and Habener, J. F. (1990) An inducible 50-kilodalton NF kappa B-like protein and a constitutive protein both bind the acute-phase response element of the angiotensinogen gene. *Mol. Cell Biol.* **10,** 1023–1032.
18. King, D. J., Ventura, D. A., Brasier, A. R., and Gorenstein, D. G. (1998) Novel combinatorial selection of phosphorothioate oligonucleotide aptamers. *Biochemistry* **37,** 16,489–16,493.
19. Pollock, R. and Treisman, R. (1990) A sensitive method for the determination of protein-DNA binding specificities. *Nucleic Acids Res.* **18,** 6197–6204.
20. Szostak, J. W. (1992) In vitro genetics. *Trends Biochem. Sci.* **17,** 89–93.
21. Thiesen, H.-J. and Bach, C. (1990) Target detection assay: a versatile procedure to determine DNA binding sites as demonstrated on SP1 protein. *Nucleic Acids Res.* **18,** 3203–3209.
22. Croston, G. E., Laybourn, P. J., Paranjape, S. M., and Kadonaga, J. T. (1992) Mechanism of transcriptional antirepression by GAL4-VP16. *Genes Dev.* **6,** 2270–2281.
23. Beato, M. (1996) Chromatin structure and the regulation of gene expression: remodeling at the MMTV promoter. *J. Mol. Med.* **74,** 711–724.
24. Cordingley, M. G., Riegel, A. T., and Hager, G. L. (1987) Steroid-dependent interaction of transcription factors with the inducible promoter of mouse mammary tumor virus in vivo. *Cell* **48,** 261–270.

9

Analysis of Cytosolic Proteins that Bind to the 5' Leader Sequence of the Angiotensin AT_1 Receptor by RNA Electromobility Shift Assay

Zheng Wu, Kamakshi Krishnamurthi, Koby Mok, and Kathryn Sandberg

1. Introduction

Electromobility shift assays (EMSAs) provide a way to study protein–nucleic acid interactions. This method is based on the observation that the electrophoretic mobility of nucleic acids through polyacrylamide gels is retarded when bound to proteins. The mobility of nucleic acid–protein complexes are thus "shifted" with respect to the free nucleic acids. Typically, the nucleic acids are labeled with ^{32}P. Once the nucleic acid–protein complexes are separated from free radiolabeled nucleic acids, the electrophoresis is terminated and the gel dried. The radiolabeled nucleic acids in their free and complexed forms are visualized and quantified by phosphor autoradiography or by X-ray autoradiography. DNA-binding proteins are commonly identified by EMSA. EMSA also works well for studying purified RNA-binding proteins ***(1–3)*** and this technique is currently being developed for identifying unknown RNA-binding proteins.

The 5' leader sequence (5'LS) of the type 1 angiotensin (AT_1) receptor mRNA has an unusually high GC content which is commonly found in RNA secondary structures ***(4)***. Furthermore, the Zuker algorithm ***(5)*** predicts that the 5'LS of the human AT_1 ***(6)*** and the rat AT_{1a} (rAT_{1a}) receptor ***(7)*** form highly stable ($\Delta G < -60$ kcal/mol) secondary structures such as hairpins, bulges, internal loops and junctions ***(8)*** (**Fig. 1**). Stabile RNA secondary structure in the 5'LS can provide a template for protein binding, which might regulate expression of the downstream open reading frame, as in the case of ferritin

From: *Methods in Molecular Medicine, vol. 51: Angiotensin Protocols*
Edited by: D. H. Wang

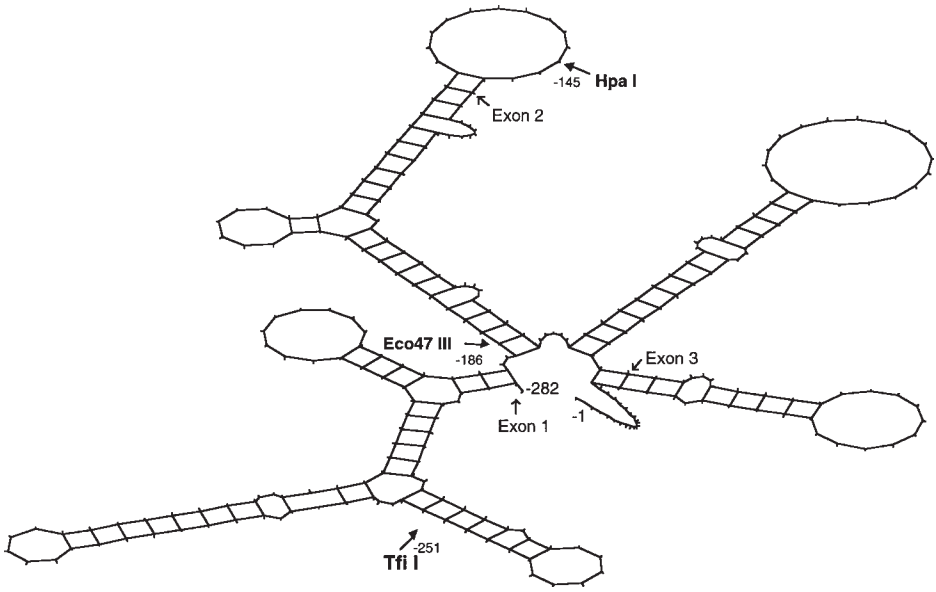

Fig. 1. Graphical representation of RNA secondary structure predicted by the StemLoop Program using the Zuker algorithm *(5)*. Arrows indicate the borders between exons 1–3 and restriction enzyme sites.

(9,10) and transforming growth factor β1 *(11)* by either modifying mRNA translation and/or mRNA stability. Using RNA EMSA, we have detected cytosolic proteins, which bind to the 5'LS of the rAT_{1a} receptor. Interestingly, the activities of these RNA-binding proteins are regulated in a manner that inversely correlates with changes in AT_1 receptor expression *(7,12)*. These findings suggest that 5'LS RNA-binding proteins are inhibitory to translation and/or mRNA stability. In this chapter, we describe an optimized RNA EMSA for measuring RNA-binding protein activity towards the 5'LS of the rAT_{1a} receptor mRNA.

2. Solutions and Materials

Common reagents for all three protocols.

1. DEPC-treated D&D water: In fume hood (*see* **Note 1**), add 100 μL of diethylpyrocarbonate (DEPC) (Sigma, cat. no. D-5758) to a prebaked (180°C for 12 h) 500 mL glass bottle (*see* **Note 2**) containing 500-mL of distilled and deionized (D&D) water. Shake thoroughly, then loosen cap and incubate for 2 h at 37°C. Autoclave for 15 min (at 15 lb/in.^{2}) on liquid cycle. Shake and then loosen cap in fume hood; wait at least 8 h before use in order to permit escape of trace DEPC (*see* **Note 3**). Store at room temperature.

2. Anhydrous ethyl alcohol (Warner Graham Co.; cat. no. 64-17-5). Store at room temperature.
3. 1 *M* Tris-HCl: Dissolve 121 g of Tris-base (Boehringer–Mannheim; cat. no. 1814273) in 800 mL of DEPC-treated D&D water. Adjust pH to 7.4 with 1 *N* HCl. Adjust final volume to 1 L. Autoclave and readjust final volume to 1 L with DEPC-treated D&D water, then store in 100-mL aliquots at room temperature.
4. 1 *M* dithiothreitol (DTT) (Sigma; cat. no. D9779). Dissolve 1.6 g in 10-mL DEPC-treated D&D water. Filter sterilize through a 0.2-μm filter; alternatively, purchase 100 m*M* DTT stock (Promega; cat. no. P1171). Store at –20°C in 100-μL aliquots.

2.1. Preparation of S100 Cytosolic Extract

2.1.1. Reagents and Solutions Required for Cytosolic Extract Preparation

1. Phosphate-buffered saline (PBS) [137 m*M* NaCl, 2.7 m*M* KCl, 10 m*M* Na_2HPO_4, 1.8 m*M* KH_2PO_4]: Dissolve 8 g of NaCl (Sigma; cat. no. S3014), 0.2 g of KCl (Sigma; cat. no. P9541), 1.44 g of Na_2HPO_4 (Sigma; cat. no. S3264) and 0.24 g of KH_2PO_4 (Sigma; cat. no. P9791) in 800-mL DEPC-treated D&D water. Titrate pH with 1 *N* HCl (Sigma; cat. no. 920-1) to 7.5 before adjusting final volume to 1 L. Store at 4°C.
2. 0.2 *M* Phenylmethylsulfonylfluoride (PMSF) (Sigma; cat. no. P7626): Dissolve 35 mg PMSF in 1 mL of anhydrous ethyl alcohol (*see* **Note 1**). PMSF can also be dissolved in anhydrous methyl or isopropyl alcohol. Store in 100-μL aliquots at –20°C.
3. 1 mg/mL leupeptin (Sigma; cat. no. L9783): Prepare a stock solution of 1 mg/mL in DEPC-treated D&D water. Store in 100-μL aliquots at –20°C.
4. 1 U/mL aprotinin (Sigma; cat. no. A6279): Prepare a stock solution of 1 U/mL in DEPC-treated D&D water. Store in 100-μL aliquots at –20°C.
5. 2 mg/mL antipain (Sigma; cat. no. A6191): Prepare a stock solution of 2 mg/mL in DEPC-treated D&D water. Store in 100-μL aliquots at –20°C.
6. 0.5 *M* ethylenediaminetetraacetic acid (EDTA) (Sigma; cat. no. E5134): Add 93 g of EDTA to 450 mL of DEPC-treated D&D water. Titrate pH to 8.0. Note that EDTA will not dissolve unless the pH is adjusted appropriately. After EDTA is dissolved, bring to a final volume of 500 mL. Autoclave and readjust final volume to 500 mL, then store in 100-mL aliquots at room temperature.
7. 1 *M* KCl (Sigma; cat. no. P9541): Dissolve 37 g of KCl in 400 mL of DEPC-treated D&D water. After dissolved, adjust final volume to 500 mL. Autoclave and readjust final volume to 500 mL, then store in 100-mL aliquots at room temperature.
8. Triton X-100 (Sigma; cat. no. X-100). Store at room temperature.
9. Homogenization buffer [25-m*M* Tris-HCl (pH 7.4), 0.1-m*M* EDTA (pH 8.0), 40 m*M* KCl, 1% Triton X-100]: Add 25 mL of 1 *M* Tris-HCl (pH 7.4), 0.2 mL of 0.5 *M* EDTA (pH 8.0), 40 mL of 1 *M* KCl and 10 mL of 100% Triton X-100 to DEPC-treated D&D water. Titrate pH with 1 *N* HCl to 7.4 and adjust final volume to 1 L. Store at 4°C.

10. 1 *M* $C_2H_3O_2K$ (Sigma; cat. no. P1190): Dissolve 49 g of $C_2H_3O_2K$ in 400 mL of DEPC-treated D&D water. After dissolved, adjust final volume to 500 mL. Autoclave and readjust final volume to 500 mL, then store in 100-mL aliquots at room temperature.
11. 1 *M* $Mg(C_2H_3O_2)_2$ (Sigma; cat. no. M5661). Dissolve 107 g of $Mg(C_2H_3O_2)_2$ in 400 mL of DEPC-treated D&D water. After dissolved, adjust final volume to 500 mL. Autoclave and readjust final volume to 500 mL, then store in 100-mL aliquots at room temperature.
12. 30% Sucrose cushion solution [10-m*M* Tris (pH 7.6), 1-m*M* $C_2H_3O_2K$, 1.5-mM $Mg(C_2H_3O_2)_2$ and 2-m*M* DTT]: Add 10 mL of 1 *M* Tris-HCl (pH 7.6), 1-mL 1 *M* $C_2H_3O_2K$, 1.5 mL of 1 *M* $Mg(C_2H_3O_2)_2$ and 2 mL of 1 *M* DTT to DEPC-treated D&D water. Titrate pH with 1 *N* HCl to pH 7.4 and adjust final volume to 1 L. Store at 4°C.
13. Bovine serum albumin (BSA) standard [0.5 mg/mL]: Dissolve 20-mg BSA (Sigma; cat. no. B2518) in 40-mL D&D water. Store in 500-µL aliquots at 4°C.
14. Bio-Rad protein dye (Bio-Rad; cat. no. 500-0006). Store at 4°C.

2.1.2. Equipment Required for S100 Cytosolic Extract Preparation

1. Heavy-duty aluminum foil.
2. Polytron homogenizer and 2 mm probe (Brinkmann Instruments; model nos. PT10/35 & PTA10TS).
3. Polytron generator (Brinkmann Instruments; model no. PTA-10TS).
4. Beckman centrifuge (Beckman; model no. GS-6R).
5. Sorvall centrifuge (Sorvall; model no. RC5C).
6. Sorvall rotor (Sorvall; model no. SS34).
7. Beckman ultracentrifuge (Beckman; model no. L8-M).
8. Sorvall swinging-bucket rotor (Sorvall; model no. AH-650).
9. Microplate reader (Dynatech Laboratories; cat. no. MR 600).

2.2. Preparation of Radiolabeled 5'LS

2.2.1. Reagents and Solutions Required for Radiolabeled 5'LS Preparation

1. 1-µg cDNA encompassing the entire 5'LS of the rAT_{1a} receptor (*see* **Note 4**) subcloned into the pCR3 vector *(7)* (**Fig. 2**) or other suitable transcription vectors. Store in 20-µL aliquots at 1–2 µg/µL at –20°C.
2. 10 U/µL Xho I with accompanying 10X Xho 1 buffer (New England Biolabs; cat. no. 146S) or other appropriate restriction enzyme (**Fig. 2**) (*see* **Note 4**). Store at –20°C in a nonfrost free freezer (*see* **Note 5**).
3. Agarose (Life Technologies; cat. no. 15510-027). Store at room temperature.
4. 10X TAE buffer [400-m*M* TRIS, 100-m*M* EDTA, pH 8.0]: Dissolve 48.4 g Tris base in 20 mL 0.5 *M* EDTA (pH 8.0) (*see* **Subheading 2.2.1.6.**), 11.4 mL glacial acetic acid (EM Science; cat. no. 64-19-7), and 800 mL DEPC-treated D&D water. Adjust final volume with DEPC-treated D&D water to 1 L. Store at room temperature.
5. 6X DNA loading dye [0.2% bromophenol blue, 0.2% xylene cyanol, 60% glycerol, and 60 m*M* EDTA] (included in GeneRuler DNA ladder). Store at –20°C.
6. GeneRuler DNA Ladder Mix (MBI Fermentas; cat. no. SM0331). Store at –20°C.

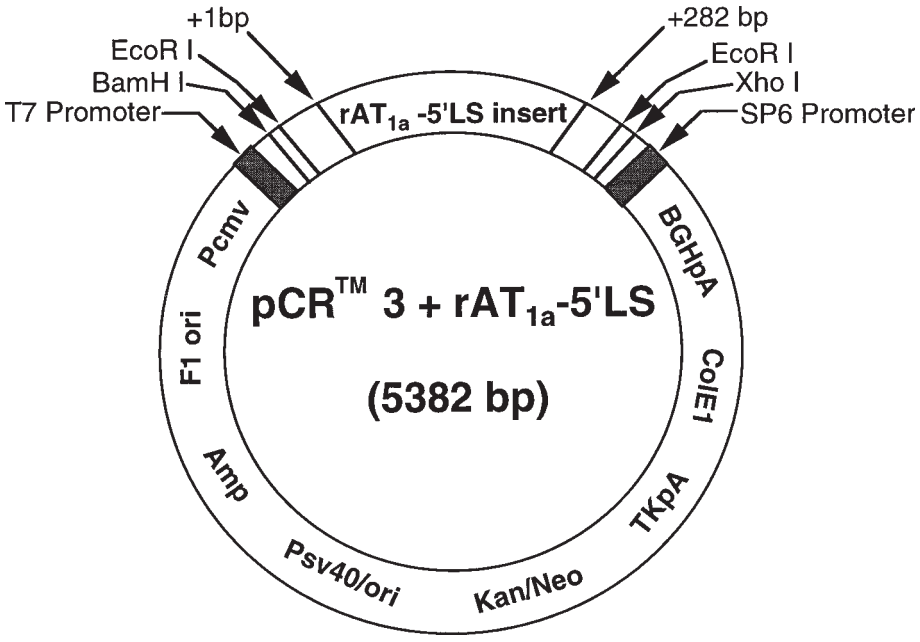

Fig. 2. 5'LS of the rAT_{1a} receptor in pCR3. The 5'LS (–282 to –1 nt) of the rat AT_{1a} receptor is subcloned into the TA cloning site in the pCR3 vector (Invitrogen). The restriction enzyme, *Xho*I, which is located 3' to the template DNA, is used to linearize the plasmid; there are no *Xho*I sites in the 5'LS cDNA.

7. PicoGreen DNA quantitation system (Molecular Probes; cat. no. R-P7589). Store at –20°C.
8. 1X TE buffer [10 m*M* TRIS, 1 m*M* EDTA, pH 8.0]: Combine 1 mL of 1 *M* Tris-HCl and 0.2 mL of 0.5 *M* EDTA in 88 mL of DEPC-treated D&D water. Autoclave and readjust final volume to 100 mL with DEPC-treated D&D water, then store in 10 mL aliquots at room temperature.
9. Lambda DNA standard [100 μg/mL in 1X TE] (included in the PicoGreen system): Dilute stock 1:50 to 2 μg/mL by mixing 40 μL of the 100 μg/mL stock with 1.96 mL of 1X TE buffer. Store in 40 μL aliquots at –20°C.
10. PicoGreen dsDNA quantitation reagent (included in the PicoGreen quantitation system). Store at –20°C.
11. Riboprobe in vitro transcription kit-T7 (Promega; cat. no. P1440). Store at –20°C.
12. 5X Transcription buffer (included in kit-T7).
13. 40 U/μL RNasin ribonuclease inhibitor (included in kit-T7 or purchase from Promega; cat. no. N2515).
14. ATP-CTP-UTP stock (2.5 m*M* each): Mix 100 μL of nuclease-free H_2O with 100 μL each of ATP, CTP, and UTP 10 m*M* stocks (included in kit-T7). Store in 40 μL aliquots at –20°C.

15. 100 μm GTP: Add 5 μL of 10 m*M* GTP stock (included in kit-T7) to 495 μL DEPC-treated D&D. Store in 10 μL aliquots in at –20°C.
16. 10 μCi/μL [α-^{32}P]GTP (New England Nuclear; cat. no. BLU 506X). Store at 4°C.
17. 20 U/μL T7 RNA polymerase (included in kit-T7).
18. 1 U/μL RQ1 RNase-free DNase (included in kit-T7).
19. LiCl precipitation solution [7.5 *M* lithium chloride, 75-m*M* EDTA] (Ambion; cat. no. 9480G). Store at –20°C.
20. 70% Ethyl alcohol. Mix 70 mL anhydrous ethanol with 30 mL DEPC-treated D&D water. Store at 4°C.
21. RNaseZap (Ambion; cat. no. 9780). Store at room temperature.
22. 30% Hydrogen peroxide (Fisher; cat. no. H325-500). Store at room temperature.
23. RNase away surface decontaminant detergent (Fisher; cat. no. 21-236-21). Store at room temperature.
24. Acetone (Sigma; cat. no. A4206). Store at room temperature.
25. Urea ultrapure MB grade (Ambion; cat. no. 9902). Store at room temperature.
26. Acrylamide (Bio-Rad; cat. no.161-0107). Store at room temperature.
27. N,N'-methylene-*bis*-acrylamide (Bio-Rad; cat. no.161-0201). Store at room temperature.
28. 10X TBE buffer [890-m*M* Tris-base, 890-m*M* boric acid, 20-m*M* EDTA]: Add 108 g of Tris base, 55 g of boric acid (Sigma; cat. no. B6768) and 40 mL of 0.5 *M* EDTA (pH 8.0) to 800 mL DEPC-treated D&D water. After reagents are dissolved, adjust final volume to 1 L. Autoclave and store at room temperature.
29. Ammonium persulfate (APS) powder (Bio-Rad; cat. no. 161-0700). Store at room temperature.
30. TEMED (Bio-Rad; cat. no. 161-0800). Store at room temperature.
31. RNA-loading buffer (Ambion; cat. no. 8546G). Store at –20°C.
32. ^{32}P-labeled RNA markers (Ambion; RNA Century Marker Plus Template Set, cat. no. 7782-5 μg). Store at –20°C.
33. Elution buffer [0.5 *M* ammonium acetate, 10 m*M* magnesium acetate, 1 m*M* EDTA and 0.1% sodium dodecylsulfate (SDS)]: Dissolve 7.708 g of ammonium acetate (Sigma; cat. no. A1542), 0.429 g magnesium acetate (Sigma; cat. no. M5661), 0.2 g SDS (Sigma; cat. no. L4509) and 0.4 mL 0.5 *M* EDTA (pH 8.0) to 180 mL DEPC-treated D&D water. Titrate pH to 7.5 with glacial acetic acid and adjust final volume to 200 mL. Store at room temperature.
34. Buffer-saturated phenol (Life Technologies; cat. no. 15513-039) (*see* **Note 1**). Store at 4°C.
35. Phenol-chloroform-isoamyl alcohol (25:24:1) (Life Technologies; cat. no. 15593-031). Store in 5 mL aliquots in glass tubes at 4°C (*see* **Note 1**).
36. 7.5 *M* Ammonium acetate (pH 6.0): Dissolve 115.62 g of ammonium acetate in 180 mL DEPC-treated D&D water. Titrate pH to 6.0 with 1 *M* acetic acid and adjust final volume to 200 mL. Store at room temperature.
37. Ultima Gold™ LSC cocktail (Packard; cat. no. 6013329).

2.2.2. Equipment Required for Radiolabeled 5'LS

1. Microfuge (Eppendorf; model no. 5415C).
2. 37°C cabinet incubator (Thelco; model no. 6DG).
3. Water bath (Equatherm; model no. 299-734).
4. Slab gel apparatus (Bio-Rad; cat. no. 165-2940).
5. Power supply (Bio-Rad; cat. no. 165-5056).
6. Film-processing system: transilluminator and camera (Fotodyne; model no. 3-3500).
7. Speed-Vac (Savant; model no. SVC100H).
8. 96-Well microplates (Fisher; cat. no. 07-200-38).
9. Fluorescent microplate reader (Millipore; model no. CytoFluor™ 2350).
10. Vertical electrophoresis apparatus (CBS Scientific Co.; model no. DASG-250).
11. Heat block (USA Scientific; cat. no. 2510-1102).
12. Kodak Biomax MS film (Fisher; cat. no. 05 728 1).
13. Kodak Biomax MS intensifying screen (Fisher; cat. no. 05 728 41).
14. Microhybridization oven (Bellco Glass; cat. no. #7930-00110)
15. Beckman multipurpose scintillation counter (Beckman; model no. LS6500).

2.3. 5'LS RNA EMSA

2.3.1. Reagents and Solutions Required for the RNA EMSA

1. RNaseZap (*see* **Subheading 2.2.1., step 21**).
2. 30% Hydrogen peroxide (*see* **Subheading 2.2.1., step 22**).
3. 10X TBE buffer (*see* **Subheading 2.2.1., step 28**). Store at room temperature.
4. 30% Acrylamide solution: Dissolve 29.5 g acrylamide (*see* **Subheading 2.2.1., step 26**) and 0.5 g *bis*-acrylamide (*see* **Subheading 2.2.1., step 27**) in 80 mL DEPC-treated D&D water. Adjust final volume to 100 mL and store at room temperature.
5. APS (*see* **Subheading 2.2.1., step 29**)
6. TEMED (*see* **Subheading 2.2.1., step 30**).
7. Glycerol (Sigma; cat. no. G6279). Autoclave and store in 10 mL aliquots at room temperature.
8. 100 m*M* DTT.
9. 40 U/μL RNasin ribonuclease (*see* **Subheading 2.2.1., step 13**).
10. 1 *M* HEPES (Sigma; cat. no. H0891). Dissolve 119 g of HEPES in 450 mL DEPC-treated D&D water. Adjust final volume to 500 mL. Filter sterilize through a 0.2-μm filter. Store in 100 mL aliquots at room temperature.
11. 1 *M* KCl (Sigma; cat. no. P9541). Dissolve 37 g KCl in 450 mL of DEPC-treated D&D water. Adjust final volume to 500 mL. Filter sterilize through a 0.2-μm filter. Store in 100 mL aliquots at room temperature.
12. 1 *M* $MgCl_2$ solution, molecular biology grade (Sigma; cat. no. M1028). Store in 100 mL aliquots at room temperature.
13. 10X Binding buffer [100 m*M* HEPES (pH 7.6), 400 m*M* KCl, 30 m*M* $MgCl_2$, and 50% glycerol]: Combine 10 mL of 1 *M* HEPES, 40 mL of 1 *M* KCl, 3 mL of 1 *M* $MgCl_2$, and 50 mL autoclaved 100% glycerol. Titrate pH to 7.6 with 1 *N* HCl and adjust final volume to 100 mL. Store at 4°C.

14. 1 U/μL T1 RNase [1359 U/μL] (Gibco-BRL Life Technologies; cat. no. 18030-015): Dilute to 1 U/mL in 1X binding buffer. Store in 40 μL aliquots at –20°C.
15. 100 μg/μL Heparin sulfate (Sigma; cat. no. H 3393): Prepare a stock solution of 100 μg/μL in DEPC-treated D&D water. Store at 4°C.
16. RNA EMSA loading dye [0.25% bromophenol blue, 0.25% xylene cyanole, 1 m*M* EDTA and 50% glycerol]: Prepare a 200-mL stock solution by adding 0.5 g bromophenol blue, 0.5 g xylene cyanole, 0.4 mL 0.5 *M* EDTA (pH 8.0), and 100 mL autoclaved 100% glycerol in 99.6 mL DEPC-treated D&D water. Store in 2 mL aliquots at room temperature.

2.3.2. Equipment Required for the RNA EMSA

1. Microfuge (*see* **Subheading 2.2.2., step 1**).
2. Vertical electrophoresis apparatus (*see* **Subheading 2.2.2., step 10**).
3. Power supply (*see* **Subheading 2.2.2., step 5**).
4. Water bath (*see* **Subheading 2.2.2., step 3**).
5. SpeedVac (*see* **Subheading 2.2.2., step 7**).
6. Heat block (*see* **Subheading 2.2.2., step 11**).
7. Gel dryer, model no. SG200-120 (Savant Instruments; cat. no. S200).
8. PhosphorImager (Molecular Dynamics; model no. Storm 840).
9. Kodak Biomax MS film (*see* **Subheading 2.2.2., step 12**).
10. Kodak Biomax MS intensifying screen (*see* **Subheading 2.2.2., step 13**).

3. Methods

3.1. Preparation of S100 Cytosolic Extract

3.1.1. S100 Cytosolic Extract Isolation

1. Sacrifice adult Sprague Dawley rats by decapitation and separate uterus from fat.
2. Wash off blood by passing tissue through three serial Petri dishes containing sterile ice-cold PBS set on an ice tray.
3. Transfer the tissue to a square of heavy-duty aluminum foil roughly 6 × 6 in.; wrap tissue securely and label (*see* **Note 6**). Immediately place wrapped tissue in liquid nitrogen or proceed immediately to **step 5** (*see* **Note 7**).
4. Add the following protease inhibitors to 10 mL homogenization buffer immediately before use: 5 μL PMSF (0.2 *M*), 100 μL leupeptin (1 mg/mL), 1 μL aprotinin (1 U/mL), and 50 μL antipain (2 mg/mL).
5. Place fresh or frozen tissue in 15 mL Falcon tube containing approx 2.5 vol of homogenization buffer per gram of tissue (*see* **Note 7**).
6. Homogenize the tissue on ice for 10 s on setting #10 using a 2-mm diameter probe. Immediately allow the tissue to incubate on ice for 20 s. Repeat homogenization procedure until tissue is completely homogenized (approx three times) (*see* **Notes 7** and **8**).
7. Centrifuge the homogenate at 300*g* for 10 min at 4°C in a Beckman GS-6R centrifuge using slow deceleration.

Table 1
Preparation of BSA Standard Curve and Sample Dilution

0.0 μg standard	0 μL BSA + 10 μL D&D water
0.5 μg standard	5 μL 0.1 mg/mL BSA + 5 μL D&D water
1.0 μg standard	10 μL 0.1 mg/mL BSA + 0 μL D&D water
2.0 μg standard	4 μL 0.5 mg/mL BSA + 6 μL D&D water
3.0 μg standard	6 μL 0.5 mg/mL BSA + 4 μL D&D water
5.0 μg standard	10 μL 0.5 mg/mL BSA + 0 μL D&D water
Unknown dilution 1	5 μL cytosolic extract (1:5 dilution)+ 5 μL D&D water
Unknown dilution 2	10 μL cytosolic extract (1:5 dilution) + 0 μL D&D water

8. Transfer the supernatant to an autoclaved 12 mL Sorvall tube and centrifuge at 20,000*g* for 20 min at 4°C in a Sorvall SS34 rotor with 15 mL adapters using slow deceleration.
9. Add 2.5 mL of ice-cold 30% sucrose cushion solution to sterile ultracentrifuge tubes.
10. Record the supernatant volume from **step 8**. Slowly layer the supernatant on top of the sucrose cushion. Be careful not to disturb the interface.
11. Centrifuge the samples at 230,000*g* for 3 h at 4°C in a Beckman L8-M ultracentrifuge using a Sorvall AH-650 rotor using slow deceleration.
12. Recover the supernatant (defined as cytosolic extract) above the sucrose cushion and aliquot in 80-μL quantities; freeze immediately in a dry ice-ethanol bath (*see* **Notes 6** and **7**). Store the extract at –80°C.

3.1.2. Protein Quantitation

1. Immediately, before use, dilute an aliquot of the uterus S100 cytosolic extract and the 0.5 mg/mL BSA stock 1:5 each. Prepare the standard curve and unknown samples according to **Table 1** in a 96-well microplate using a positive displacement pipettor (e.g., M-25 Microman positive pipettor; Rainin Instrument Co.; cat. no. M-25). Five different concentrations of BSA are prepared (0.5–5 μg) in addition to a blank (no protein). Prepare standards and samples in triplicate.
2. Prepare a 1:5 dilution of the Bio-Rad protein dye immediately before use. Add 200 μL of the diluted protein dye into each well using a repeat pipettor (e.g., Brinkmann Eppendorf Repeater Plus Pipettor; Fisher; cat. no. 21-380-8). Incubate at room temperature for 5 min.
3. Measure the absorbance of the standard curve and samples at a wavelength of 595 nm in a microplate reader.
4. Calculate the protein concentration of the unknown samples from the standard curve using linear regression analysis.

3.2. Preparation of Radiolabeled 5'LS

3.2.1. Plasmid Linearization

1. Dilute 5 μg 5'LS cDNA subcloned into the pCR3 plasmid (**Fig. 2**) in 17 μL DEPC-treated D&D water.

2. Add 2 µL 10X *Xho*I restriction enzyme buffer and vortex.
3. Add 1 µL *Xho*I enzyme and mix gently with a pipet tip; do not vortex (*see* **Notes 5** and **8**). Briefly spin tubes in microfuge for 5 s. Incubate at 37°C for 1 h.
4. Remove an aliquot to confirm plasmid linearization (*see* **Subheading 3.2.2.**).
5. Terminate reaction by precipitating the DNA. Add 100 µL of DEPC-treated D&D water and 0.1 vol (approx 12 µL) of LiCl precipitation solution ***(13)***. Centrifuge the mixture at 4°C for 30 min to pellet the DNA. Discard the supernatant and wash the DNA pellet twice by adding 1 mL 70% ethanol followed by a 30 min spin at 4°C (*see* **Note 9**). Briefly dry the final DNA pellet under vacuum (*see* **Note 9**). Resuspend the DNA in 20 µL DEPC-treated D&D water and store at –70°C.

3.2.2. Assessment of Plasmid Linearization

1. Assemble slab gel electrophoresis apparatus according to manufacturer's directions.
2. Prepare a 1% agarose gel by mixing 0.5 g of agarose with 50 mL 1X TAE buffer. Microwave the mixture just until the agarose dissolves completely into the solution. Be careful not to let the agarose boil over. Cool the agarose down to 55°C in a water bath. Pour the agarose onto the slab gel apparatus with care taken to avoid introducing air bubbles into the gel. Allow gel to polymerize (approx 20 min).
3. Mix 6.5 µL D&D water, 1 µL 10X TAE buffer and 1.5 µL 6X DNA loading dye with the following samples (1 µL at approx 250 ng each): digested plasmid; undigested plasmid; and DNA ladder mix size markers.
4. Briefly microfuge the samples, standard and control for 5 s and then load into the wells of the agarose gel. The samples are electrophoresed for 30–45 min at 100 V in 1X TAE buffer, until the bromophenol blue has migrated 75% of the length of the gel.
5. Visualize and photograph the DNA gel under UV-light using a transilluminator. If linearization is incomplete, repeat restriction enzyme digestion with fresh enzyme.

3.2.3. DNA Quantitation

1. Prepare a standard curve by diluting the lambda DNA stock (2 µg/mL) according to **Table 2** using a positive displacement pipettor. Five different concentrations of lambda DNA are prepared (20–100 ng/standard) in addition to a blank (no DNA). Prepare dilutions of the linearized 5'LS plasmid DNA similarly to the standards. Measure each standard and sample in triplicate (*see* **Note 10**).
2. Prepare a 1:200 dilution of the PicoGreen dsDNA reagent in 1X TE immediately before use. Add 100 µL of the diluted PicoGreen reagent (*see* **Note 10**) to each tube using a repeat pipetter. Vortex the samples and load 100 µL onto a 96-well microplate. Incubate at room temperature for 5 min.
3. Measure the fluorescence of the standard curve and samples at an excitation wavelength of 480 nm and an emission wavelength of 520 nm in a fluorescence measurement system. Read the sample within 1 h.
4. Calculate the DNA concentration of the unknown samples from the standard curve using linear regression analysis.

Table 2
Standard Curve for PicoGreen DNA Quantitation

Volume of TE (μL)	Volume (μL) of lambda DNA Standard (2 μg/mL)	Volume (μL) of 200-fold PicoGreen reagent	Final [DNA] (pg/μL)
0	100	100	1000
10	90	100	900
30	70	100	700
50	50	100	500
80	20	100	200
100	0	100	0

3.2.4. Radiolabeled RNA Synthesis

1. In a 1.5-mL microfuge tube at room temperature (*see* **Note 11**), combine 4 μL 5X transcription buffer, 2 μL 100 m*M* DTT, 0.5 μL RNasin inhibitor (at 40 units/μL), 4 μL ATP, CTP, UTP mixture (2.5 m*M* each), 2.4 μL 100 μ*M* GTP, 0.5–1.0 μg linearized 5'LS cDNA template and 50 μCi α-^{32}P-GTP (*see* **Note 12**); adjust volume to 19 μL using DEPC-treated D&D water. Mix gently with a pipet tip and then add 1 μL T7 RNA polymerase (20 U/μL). Mix gently again and briefly spin tubes in microfuge for 5 s. Incubate in a cabinet incubator at 37°C for 1 h (*see* **Note 11**).
2. Terminate the transcription reaction by adding 1 μL RQ1 RNase-free DNase (1 U/mg of template DNA) and incubate at 37°C for 15 min to digest the DNA template.
3. Add 20 μL of RNA gel loading buffer to the digestion reaction and prepare 40 μL of the radiolabeled RNA markers (approx 7000 cpm of the labeled RNA markers or approx 1000 cpm per band) in RNA gel loading buffer. Immediately proceed to **Subheading 3.2.5.**

3.2.5. Radiolabeled RNA Isolation

1. Treat glass plates with RNase Zap. Then, clean glass plates with RNase decontaminating detergent, rinse with DEPC-treated D&D water, then with ethanol/acetone mixture (1:1). Allow to air-dry. Touch plates only with gloved hands.
2. Assemble the vertical minigel apparatus according to the manufacture's instructions and prepare RNase free (*see* **Note 2**). A relatively thin (0.5–1 mm) gel is required for optimal conditions.
3. Prepare an 8-*M* urea-5% polyacrylamide (acrylamide: *bis*-acrylamide) gel in a Buchner flask by dissolving 9.6 g urea, 0.95 g acrylamide, 0.05 g N,N'-methylene-*bis*-acrylamide, and 2 mL 10X TBE buffer in 20 mL DEPC-treated D&D water. Degas the solution for 15 min by stirring under vacuum.
4. Add 120 μL 10% ammonium persulfate and 20 μL TEMED to the gel mixture (*see* **Note 13**). Gently mix the resolving mixture and slowly pour between the glass plates with care taken to avoid introducing air bubbles.

5. Carefully insert the Teflon comb into the gel with care taken to avoid bubble formation. Add more gel solution to completely fill the spaces of the comb. Allow gel to polymerize (approx 30 min).
6. Place the gel in the vertical minigel electrophoresis apparatus. Fill the bottom and top reservoirs of the minigel apparatus with 1X TBE buffer. After gently removing the combs from the gel, wash each well several times with 1X TBE buffer using a 25-gage needle and a 1-mL syringe (*see* **Note 14**).
7. Immediately before loading, heat the RNA sample at 85°C for 5 min and immediately chill on ice for 3 min (*see* **Note 15**). Load 40 µL of sample per lane (*see* **Note 16**). Electrophorese the samples at 420 V for approx 1.5 h until the front dye has run off the gel (*see* **Note 17**).
8. After the gel finishes running, carefully remove the top glass plate (*see* **Note 18**). Wrap the gel remaining on the bottom plate with Saran Wrap. Expose the gel to X-ray film for 30 s.
9. Align the gel with the developed film. Using a sterile razor blade, carefully excise the piece of gel wrapped in Saran Wrap that contains the 5'LS radiolabeled band. Proceed immediately to **Subheading 3.2.6.**

3.2.6. Elution of Radiolabeled RNA

1. Peel the slice of gel containing the RNA probe from the saran wrap and transfer the gel slice to a microfuge tube containing 600 µL elution buffer. Use a pipet tip to crush the gel against the wall of the tube.
2. Rotate the tube at 60°C for 1.5 h in a hybridization oven.
3. Transfer the elution buffer to a microfuge tube with care taken to leave behind the gel fragments. Extract the radiolabeled RNA probe twice with buffer saturated phenol, followed by one phenol/chloroform/isoamyl alcohol (25:24:1) extraction. Add an equal volume of phenol to the sample. Vortex the mixture at full speed for 5 s and separate the phases by centrifugation for 1 min at full speed in a microfuge. Transfer the aqueous (top) phase to a new tube containing an equal volume of phenol/chloroform/isoamyl alcohol. Again, vortex the mixture at full speed for 5 s and separate the phases by centrifugation for 1 min at full speed in a microfuge. Aliquot the aqueous (top) phase into fresh tubes at 200-µL per tube.
4. Precipitate the radiolabeled cRNA by adding 100 µL 7.5 *M* ammonium acetate and 1 mL 100% ethanol. Incubate at –20°C overnight ***(13)***.
5. Centrifuge in a microcentrifuge at 4°C for 20 min. Carefully pour off the supernatant and wash the pellet with 1 mL of 70% ethanol (*see* **Note 9**). Dry the pellet under vacuum and resuspend the pellet in 150 µL DEPC-treated D&D water (*see* **Note 9**). Count an aliquot of the radiolabeled RNA by adding 2 µL of ^{32}P-labeled 5'LS RNA to a 5-mL scintillation vial containing 4 mL scintillation cocktail. Count the sample in a scintillation counter.
6. Store the radiolabeled cRNA in 50 µL aliquots at –20°C (*see* **Note 19**).

3.2. 5'LS RNA-Electromobility Shift Assay

3.3.1. Gel Preparation

1. Treat glass plates with RNase Zap to remove RNases. Clean glass plates with RNase decontaminating detergent, rinse with DEPC-treated D&D water, then with ethanol/acetone mixture (1:1). Allow to air-dry. Touch plates only with gloved hands.
2. Assemble the vertical mini gel apparatus according to the manufacture's instructions and prepare RNase free (*see* **Note 2**). A relatively thin (0.5–1 mm) gel is required for optimal conditions.
3. Prepare a 4% polyacrylamide gel (acrylamide: *bis*-acrylamide) in a Buchner flask by mixing 15.3 mL of DEPC-treated D&D water, 2.7 mL of 30% acrylamide, 2 mL of 10X TBE buffer. Degass the solution for 15 min by stirring under vacuum.
4. Add 120 μL of 10% ammonium persulfate, 20 μL of TEMED (*see* **Note 13**), and 6 drops of glycerol to the gel mixture (*see* **Note 19**). The resolving mixture is then gently mixed and slowly poured between the glass plates, with care taken to avoid introducing air bubbles.
5. Carefully insert the teflon comb into the gel taking care to avoid bubble formation. More gel solution is added to completely fill the spaces of the comb. Allow gel to polymerize (approx 30 min).
6. Place the gel in the vertical mini gel electrophoresis apparatus. Fill the bottom and top reservoirs of the mini gel apparatus with the 1X TBE buffer. After gently removing the combs from the gel, wash each well several times with 1X TBE buffer using a 25-gage needle and a 1-mL syringe (*see* **Note 14**).
7. Prerun the gel at 150 V for 30 min.

3.3.2. Analysis of RNA Protein Complex Formation

1. Remove an aliquot of the S100 cytosolic extract and thaw it on ice.
2. Bring 10–30 μg of the S100 extract (*see* **Note 19**) up to 20 μL in homogenization buffer supplemented with protease inhibitors (*see* **Subheading 3.1.1., step 4**). Add 5–10 × 10^4 cpm ^{32}P–5' LS RNA, 2 μL 100 m*M* DTT, 2 μL RNAsin inhibitor (40 U/μL, and 4 μL 10X binding buffer (*see* **Note 19**). Include a zero protein control since the electromobility of the RNA protein complex is compared to the free radiolabeled RNA. Mix gently and incubate at 30°C for 20 min.
3. Add 4 μL of T1 RNase (1 U/mL) and 4 μL of heparin sulfate (100 μg/μL); incubate at 30°C for 15 min in a water bath (*see* **Note 19**).
4. Add 4 μL RNA EMSA loading dye. Wash the wells several times before loading the sample onto a 4% polyacrylamide gel (*see* **Note 14**). Electrophorese the samples at 200 V for 2 h in 1X TBE buffer until the bromophenol blue has migrated 75% of the length of the gel.
5. After the gel finishes running, carefully remove the top glass plate (*see* **Note 18**). Blot the gel onto a piece of Whatman 3MM filter paper that is approx 20% larger

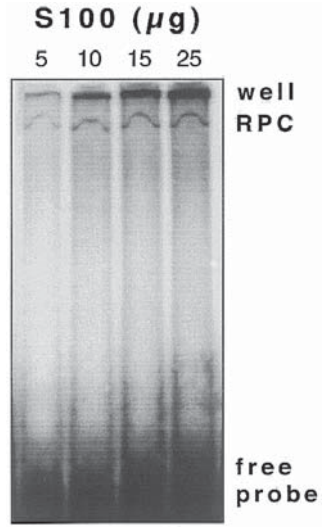

Fig. 3. Effect of increasing protein on RNA protein complex formation. Zero to 25 μg of uterus S100 cytosolic extract was incubated with 100,000 cpm [^{32}P]-5'LS cRNA at 30°C for 20 min followed by incubating with 4 μL T1 RNase and 4 μL heparin sulfate at 30°C for 15 min. RNA protein complex (RPC) formation was analyzed by RNA EMSA as described.

than the gel. After blotting the filter paper on three or four paper towels (*see* **Note 18**), wrap the gel with Saran Wrap and dry on a gel dryer at 80°C for 40 min.

6. Expose the dried gel for 1 h to a PhosphorImager screen for phosphor autoradiography followed by quantitation of the bands ([^{32}P]5'LS RNA protein complex) using ImageQuant (Macintosh version 1.2) software (**Figs. 3–5**) (*see* **Note 20**). Alternatively, expose the dried gel to Kodak Biomax MR film with a Biomax intensifying screen overnight at –70°C before developing the film.

4. Notes

1. DEPC, acrylamides, and formaldehyde are suspected carcinogens and thus are only used in the fume hood. When weighing out acrylamides, a charcoal face mask is worn for protection.
2. To obtain best results, RNase contamination must be avoided. RNases liberated during cell lysis are inhibited by inclusion of RNase inhibitors such as RNasin. Introduction of trace amounts of RNase from other sources in the laboratory must be prevented. RNases on laboratory glassware and metal are destroyed by heat inactivation; heat glassware and metal instruments such as forceps, spatulas, and razor blades at 180°C for 12 h before use. Sterile disposable plasticware (e.g., pipet tips and microfuge tubes) is essentially free of RNase contamination and is freshly autoclaved whenever possible. Rolls of aluminum foil and Saran Wrap

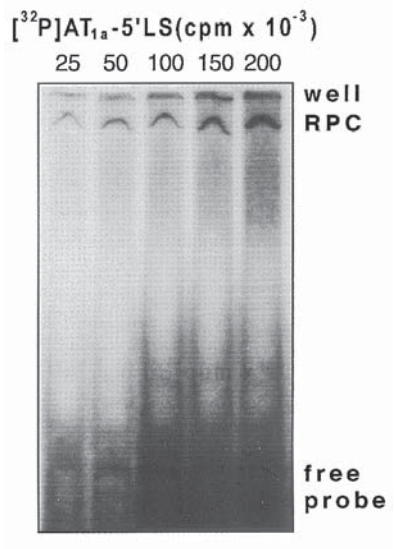

Fig. 4. Effect of increasing radiolabeled RNA on RNA protein complex formation. Twenty-five micrograms of uterus cytosolic extract was incubated with 50–400,000 cpm of [^{32}P]-AT$_{1a}$-5'LS RNA at 30°C for 20 min followed by incubating with 4 μL T1 RNase and 4 μL heparin sulfate at 30°C for 15 min. RNA protein complex (RPC) formation was analyzed by RNA EMSA as described.

are dedicated for RNA work only. These rolls are handled with fresh gloves and inner layers are taken for use in order to minimize possible RNase contamination. Likewise, bags of weigh boats are dedicated for RNA use only. All solutions are prepared using RNase-free glassware, DEPC-treated D&D water and chemicals reserved exclusively for RNA work. Reagents are aliquoted whenever possible to minimize crossover contamination should a stock solution become contaminated with trace amounts of RNase. Electrophoresis tanks are treated with a solution of 3% H_2O_2 for 20 min at room temperature followed by thoroughly rinsing with DEPC treated D&D water. Other cautions include using disposable sterile pipets and changing gloves frequently when working with RNA.

3. Autoclaving the DEPC-water removes trace DEPC. This step is necessary because DEPC is capable of modifying purine residues in RNA by carboxymethylation. Carboxymethylated RNA might interfere with RNA-protein binding reactions.
4. DNA templates are subcloned into appropriate plasmids containing bacteriophage promoters (e.g., CMV) and RNA polymerases (e.g., T7) upstream from the template DNA (e.g., 5'LS) (**Fig. 2**). Before in vitro transcription, plasmids are linearized with restriction enzymes (e.g., *Xho*I) that cut the plasmid 3' to the template DNA coding for the 5'LS RNA; however, if SP6 is used, the plasmid is left supercoiled because SP6-mediated transcription is more efficient using

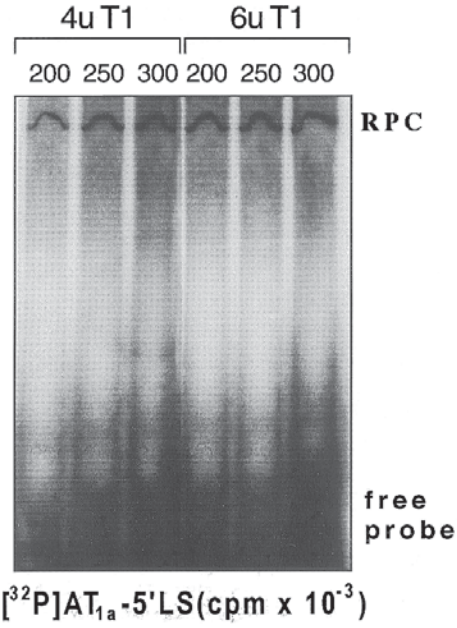

Fig. 5. Effect of T1 RNase concentration on RNA protein complex formation as a function of increasing radiolabeled RNA. In each lane, 25 μg uterus cytosolic extract was incubated with 200–300,000 cpm [^{32}P]-AT_{1a}-5'LS RNA followed by incubating for 15 min at 30°C with 4 μL heparin sulfate and 4 U or 6 U T1 RNase. RPC formation was analyzed by RNA EMSA as described.

supercoiled DNA. A runoff transcript is generated by in vitro transcription, which terminates downstream of the cloned sequence.

5. Enzymes are stored in a non-frost-free freezer; the temperature cycles in frost-free freezers. This temperature cycling denatures labile proteins such as enzymes and, thus is avoided. Likewise, solutions containing labile proteins are never vortexed because vortexing introduces air bubbles that denature proteins and thereby inhibit their activity. Instead solutions containing labile proteins are gently mixed by stirring with a pipet tip. Similarly, avoid repeated freeze thawing of reagents to minimize damage to the structure of molecules such as proteins and nucleic acids.
6. Some marking pens do not leave indelible marks on foil or microfuge tubes, if these samples are immersed in liquid nitrogen or a dry ice–acetone bath. Be sure to check the marking method before experimentation to avoid loss of labels.
7. Temperature is critical in preparation of cytosolic extracts. Samples should always remain on ice to reduce degradation caused by proteases. Performing procedures in the cold room that requires 4°C temperatures is strongly recommended. Homogenization can heat up tissues. Short pulses followed by cooling intervals

minimize over heating. Using fresh tissue can lessen the degree of protein degradation. If homogenization cannot be performed on the same day as tissue acquisition, tissues should be frozen in liquid nitrogen immediately and stored at –80°C. Three steps of centrifuge are performed in preparation of the S100 cytosolic extract. The first two lower-speed centrifugation steps remove nuclei, mitochondria, unbroken cells, and insoluble material such as connective tissue. Microsomes will be removed by the ultracentrifugation step. The cytosolic binding proteins remain in the second layer of the sucrose gradient suspension; the first layer contains floating fat.

8. Foaming should be minimized as it can cause protein denaturation through oxidation. This problem can be controlled by using the smallest possible tube for homogenization, which will reduce the volume of air above the liquid. Also, homogenize samples at low speed. For these same reasons, never vortex solutions containing enzymes such as polymerases and restriction enzymes. Instead, mix gently by stirring with a pipet tip.
9. When DNA and RNA are finally resuspended in DEPC-treated D&D water after an ethanol precipitation step, care is taken to ensure that no residual salts or ethanol are left in the sample because these contaminants inhibit enzymes such as polymerases. Place nucleic acid samples under vacuum for the minimum time necessary to remove trace ethanol (usually 5–10 min). Overdrying makes it difficult to resuspend the nucleic acids. Dissolve the nucleic acid-ethanol precipitates in DEPC-treated D&D water.
10. The tube containing the PicoGreen reagent is stored wrapped in aluminum foil and is diluted in the dark in order to minimize photodegradation caused by light exposure. Furthermore, the PicoGreen reagent is prepared in plastic vessels because it absorbs to glass. The diluted lambda DNA used for the standard curve is not stored and is diluted just before use. Approx 1.5 mL 1:200 diluted PicoGreen reagent is required per standard curve; 750 µL is required per sample.
11. Do not assemble the components of the transcription reaction on ice; assemble at room temperature in order to avoid precipitating the spermidine and consequently, the template DNA. Spermidine is used to stabilize the RNA polymerases ***(14)***. The RNA samples, however, are thawed on ice. Use a cabinet incubator to avoid condensation that occurs in heat blocks.
12. The 5'LS RNA is uniformly labeled to allow visualization of the RNA protein complex formation by incorporating [α-^{32}P]nucleoside triphosphates into the RNA during transcription. [α-^{32}P]CTP or [α-^{32}P]UTP exhibit the least radiolytic degradation in concentrated solutions and T7 RNA polymerase has lower Kms for both of these nucleosides than for GTP. However, labeling with ^{32}P-GTP resulted in radiolabeled 5'LS RNA with higher specific activity compared to ^{32}P-CTP and ^{32}P-UTP. Using ≥2 radioactive nucleosides in the same transcription reaction resulted in lower yields. Because the radiolabeled 5'LS RNA contains many labile ^{32}P-phosphodiesterase linkages, the probe should be used within 2 wk of synthesis.
13. Ammonium persulfate must be prepared fresh. When TEMED and ammonium persulfate are added together, the gel is poured within a few minutes (<5 min) to

avoid polymerization outside the glass plates. Minimize bubble formation by degassing before addition of ammonium persulfate and TEMED.

14. The wells are washed extensively to remove unpolymerized acrylamide, which will interfere with sample entering the gel.
15. Denature RNA at 85°C for 5 min and then place quickly on ice. This treatment breaks up aggregates and disrupts local regions of secondary structure, especially for GC rich mRNA ***(15)***.
16. Sample aggregation can be a significant problem by interfering with the sample from entering the gel. Methods to minimize aggregation problems include (1) filtering the running buffer before use, (2) washing the well thoroughly immediately before loading samples by using a 1-mL syringe filled with running buffer and a 25-gage needle. (3) increasing the amount of glycerol/sample (*see* **Note 19**), and (4) loading the gel while the current is running. In this case, be extremely careful not to touch the buffer in order to avoid receiving an electric shock.
17. Note that free radiolabeled 5'LS RNA migrates with the dye front. Therefore, the lower buffer chamber will be contaminated with ^{32}P if the dye front runs off the gel.
18. To easily remove the glass plates, a squirt bottle of buffer can be used to gently ease the gel off the top plate. Care is taken in lifting the top plate in order to avoid stretching the gel. Drying the gel on sufficient filter paper (two sheets) is important because ridges can develop on the autoradiogram from the gel drier, which can interfere with visualizing the radioactive bands.
19. Several variables contribute to the stability of the RNA protein complex including ionic strength, pH, time, temperature, presence of monovalent and divalent cations and glycerol. These elements were all empirically tested to determine the optimal conditions for RNA protein complex formation. The binding of protein to the 5'LS RNA is strongly affected by the ionic strength of the buffer, especially the presence of magnesium and the concentration of monovalent cations (e.g., potassium). Glycerol is added to the reaction to stabilize the proteins in the complex ***(16)***. Protein stability is a concern because RNA protein complexes will dissociate with time as proteins lose their activity through denaturation; this loss in protein stability is compounded by heat generated during electrophoresis. In a competition experiment, unlabeled competitor RNA should be incubated with the S100 extract 20 min at 30°C before the addition of ^{32}P-labeled 5'LS RNA followed by a second 20 min incubation at 30°C. Competition experiments with specific and nonspecific competitors typically require large amounts of unlabeled RNA. Transcription reaction systems are commercially available, which have been optimized to generate large amounts of unlabeled RNA (e.g., Ambion; mMessage system, cat. no. 1340). Increasing both the amounts of extract (**Fig. 3**) and radiolabeled 5'LS (**Fig. 4**) increased not only the RNA-complex formation, but also the background and, thus, optimal conditions involve a compromise between background and signal. Heparin sulfate inhibits nonspecific RNA protein complex formation; heparin sulfates are highly charged molecules and, thus, heparin competes for proteins that nonspecifically associate with any RNA because of the negatively charged nucleosides. T1 RNase degrades single

stranded RNA that is unprotected (i.e., RNA not bound to protein) after G residues and, thus, it reduces background associated with the radiolabeled probe. Note that 6 U of T1 RNase resulted in less background than 4 U when 300,000 cpm radiolabeled 5'LS was used in the EMSA (**Fig. 5**).

20. Alternatively to phosphorimaging, X-ray autoradiography can be performed. The advantage of phosphorimaging compared to X-ray autoradiography is that phosphorimaging is 10–250X more sensitive and 10X faster. Furthermore, phosphorimaging has a linear dynamic range of five orders of magnitude compared to less than 2 for X-ray film and, phosphorimaging can easily quantify the radioactivity in the individual bands.
21. If no detectable RNA protein complexes are observed, then several problems should be seriously considered. Some tissues contain high levels of proteases (e.g., the kidney) and some RNA binding proteins may be highly susceptible to protease degradation. In this case, freshly made extracts should be prepared and used immediately in RNA-EMSA. Different protease inhibitors should also be tested. RNase contamination is a constant problem. If contamination is suspected, rerun the radiolabeled probe on a denaturing gel to assess possible degradation. Increase the amounts of RNasin used in the reaction and prepare new stock solutions. Testing solutions for RNase activity (Ambion; RNase Alert™ kit, cat. no. 1960) is also an option.

References

1. Singh, R., Valcarcel, J., and Green, M. R. (1995) Distinct binding specificities and functions of higher eukaryotic polypyrimidine tract-binding proteins. *Science* **268,** 1173–1176.
2. Lynch, K. W. and Maniatis, T. (1996) Assembly of specific SR protein complexes on distinct regulatory elements of the Drosophila doublesex splicing enhancer. *Genes Dev.* **10,** 2089–2101.
3. Stebbins-Boaz, B., Hake, L. E., and Richter, J. D. (1996) CPEB controls the cytoplasmic polyadenylation of cyclin, Cdk2 and c-mos mRNAs and is necessary for oocyte maturation in Xenopus. *EMBO J.* **15,** 2582–2592.
4. Kozak, M. (1991) An analysis of vertebrate mRNA sequences: intimations of translational control. *J. Cell Biol.* **115,** 887–903.
5. Zuker, M. (1989) Computer prediction of RNA structure. *Methods Enzymol.* **180,** 262–288.
6. Curnow, K. M., Pascoe, L., Davies, E., White, P. C., Corvol, P., and Clauser, E. (1995) Alternatively spliced human type 1 angiotensin II receptor mRNAs are translated at different efficiencies and encode two receptor isoforms. *Mol. Endocrinol.* **9,** 1250–1262.
7. Krishnamurthi, K., Zheng, W., Verbalis, A. D., and Sandberg, K. (1998) Regulation of cytosolic proteins binding *cis* elements in the 5' leader sequence of the angiotensin AT_1 receptor mRNA. *Biochem. Biophys. Res. Commun.* **245,** 865–870.
8. Puglisi, E. V. and Puglisi, J. D. (1997) *RNA Structure,* Wiley-Liss, New York, pp. 1–22.

9. Klausner, R. D., Rouault, T. A., and Harford, J. B. (1993) Regulating the fate of mRNA: the control of cellular iron metabolism. *Cell* **72,** 19–28.
10. Melefors, O. and Hentze, M. W. (1993) Translational regulation by mRNA/protein interactions in eukaryotic cells: ferritin and beyond. *BioEssays* **15,** 85–90.
11. Romeo, D. S., Park, K. P., Roberts, A. B., Sporn, M. B., and Kim, S.-J. (1993) An element of the transforming growth factor-β1 5'-untranslated region represses translation and specifically binds a cytosolic factor. *Mol. Endocrinol.* **7,** 759–766.
12. Krishnamurthi, K., Verbalis, J. G., Zheng, W., Wu, Z., Clerch, L. B., and Sandberg, K. (1999) Estrogen regulates angiotensin AT1 receptor expression via cytosolic proteins that bind to the 5' leader sequence of the receptor mRNA. *Endocrinology* **140,** 5435–5438.
13. Sambrook, J., Fritsch, E. F., and Maniatis, T. (1989) *Molecular Cloning, A Laboratory Manual.* Cold Spring Harbor Press, Cold Spring Harbor, NY.
14. Davies, J. W., Aalbers, A. M., Stuik, E. J., and Van Kammen, A. (1977) Translation of cowpea mosaic virus RNA in a cell-free extract from wheat germ. *FEBS Lett.* **77,** 265–269.
15. Karr, S. R., Rich, C. B., Foster, J. A., and Przybyla, A. (1981) Optimal conditions for cell-free synthesis of elastin. *Coll. Relat. Res.* **1,** 73–81.
16. Andino, R., Rieckhof, G. E., and Baltimore, D. (1990) A functional ribonucleoprotein complex forms around the 5' end of poliovirus RNA. *Cell* **63,** 369–380.
17. Bonner, W. M. and Laskey, R. A. (1974) A film detection method for tritium-labeled proteins and nucleic acids in polyacrylamide gels. *Eur. J. Biochem.* **46,** 83–88.

10

In Vitro Translation of the Angiotensin AT_1 Receptor in Wheat-Germ Extracts

Hong Ji, Kamakshi Krishnamurthi, Zheng Wu, and Kathryn Sandberg

1. Introduction

In vitro translation is a powerful method for specifically investigating mRNA translation independently of transcription, post-translational processing, and protein trafficking. There are several well-characterized in vitro translation systems including mammalian cell extracts (e.g., HeLa cells and Chinese Hamster Ovary cells) ***(1,2)***, rabbit reticulocyte lysates ***(3,4)***, *Xenopus* egg extracts ***(5)***, rye embryo ***(6)***, and wheat germ ***(7,8)*** that efficiently and faithfully translate heterologous mRNAs. Our laboratory is interested in investigating translational control of the angiotensin AT_1 receptor. Thus, we need a cell-free system that efficiently translates the angiotensin AT_1 receptor.

Mori et al. ***(9)*** and Elton et al. ***(10)*** have successfully translated the rAT_{1a} and human AT_1 receptor cDNAs, respectively, in rabbit reticulocyte lysates using a coupled transcription–translation reticulocyte system. In this coupled system, the AT_1 receptors are subcloned into a plasmid containing a prokaryotic phage RNA polymerase promoter for initiation of transcription; however, translation is under eukaryotic control. Because transcription is incorporated directly into the translation mixture, the coupled system produces significantly (2–6X) more protein ***(11–13)***. However, it is not possible to distinguish changes in rates of transcription from rates of translation using this method and thus the trinitrotoluene (TNT)-coupled reaction system is not a useful method for studying translational control independently from transcription.

Previous studies by Curnow et al. ***(14)***, indicate that the human AT_1 receptor mRNA is poorly translated in a noncoupled rabbit reticulocyte lysate translation system. Another problem Curnow et al. ***(14)*** faced with rabbit reticulocyte

From: *Methods in Molecular Medicine, vol. 51: Angiotensin Protocols*
Edited by: D. H. Wang

lysates is that the translated reaction products are highly insoluble in SDS polyacrylamide gels caused by aggregation, even in the presence of 8 *M* urea. Our experience with the rat AT_{1a} (rAT_{1a}) receptor supports these findings ***(15)***. Although we tested a wide variety of experimental conditions (*see* **Note 1**), we never detected translation of the rAT_{1a} receptor in rabbit reticulocyte lysates, even under conditions in which the insolubility of the translation product was not a problem. Therefore, to circumvent the problems associated with rabbit reticulocyte lysates, we tested the ability of wheat-germ lysates to efficiently translate the AT_1 receptor.

A wide variety of viral prokaryotic and eukaryotic mRNAs are translated in vitro in cell-free wheat germ extracts ***(7,8,16–18)***. All of the cellular components necessary for protein synthesis (tRNA, ribosomes, initiation, elongation, and termination factors) are found in wheat-germ lysates. The extract is commercially available (e.g., Promega or Ambion). Alternatively, the lysate is simple to prepare and cost-effective. Basically, wheat germ is ground up and the cellular debris removed by centrifugation ***(7,19)***. Micrococcal nuclease is added to destroy endogenous mRNA. Phosphocreatine and phosphocreatine kinase are included to create an energy-generating system. The efficiency of chain elongation is increased by the addition of spermidine, which also inhibits premature termination and may stabilize long mRNAs ***(20)***.

Wheat-germ extract has several advantages over other translation systems. In contrast to rabbit reticulolysates and other cell-free mammalian expression systems that have high levels of endogenous mRNA, wheat-germ extract has low amounts ***(3)***. Even after nuclease treatment, significant levels of mRNA fragments remain in rabbit reticulolysates including sequences with initiation sites. Consequently, rabbit reticulolysate mRNAs compete with added mRNAs (like the AT_1 receptor) for ribosome binding resulting in less-efficient translation of exogenous mRNAs and especially weakly initiating mRNAs. The wheat-germ system more faithfully reflects the in vivo milieu because it efficiently translates weakly initiating mRNAs. One explanation for the poor translation observed in rabbit reticulolysates is the high abundance of hemoglobin mRNA, which markedly competes with the less-efficiently translated AT_1 receptor. The abundance of hemoglobin protein can also interfere with resolution of the AT_1 receptor on SDS gels by distorting the mobility of the AT_1-receptor protein.

Another advantage of wheat-germ extracts in contrast to rabbit reticulocyte lysates and other cell-free translation systems is that mRNA translation is not very sensitive to inhibition by oxidized thiols. After radiolabeling [^{35}S]methionine, ^{35}S degrades to sulfoxides with time. Thus, radiolabeled methionine has a more limited shelf-life if used in rabbit reticulocyte lysate and other translation systems compared to wheat-germ extracts ***(21)***. Another problem associated with

rabbit reticulolysates is sample smearing during electrophoresis when lanes are loaded with high concentrations of protein. Because the protein concentration is significantly less in wheat germ (30–50 μg/μL) than in rabbit reticulocyte (100–200 μg/μL) lysates, smearing during electrophoresis is not usually a problem.

In rabbit reticulolysates, a common background band resulting from a tRNA-dependent, but ribosome independent, addition of methionine to a preexisting protein is occasionally observed ***(22)***. This protein is 42–50 kDa and so its presence interferes with resolving the rAT_{1a} receptor on a SDS gel because the rAT_{1a} receptor before post-translational processing is 40,000 kDa in size. In this regard, wheat germ is the ideal system in which to study the characteristics of primary translated products (before post-translational modifications) because wheat-germ extracts lack processing capability ***(23)***. However, canine microsomal membranes can be added back to wheat-germ extracts to permit examination of cotranslational processing events such as signal peptide cleavage, membrane insertion, translocation, and core glycosylation ***(22)***.

Perhaps the most significant advantage of wheat-germ extracts is the lack of double-stranded RNA-dependent protein kinase R (PKR) ***(24)***. PKR is activated by double-stranded RNA and RNA with significant secondary structure ***(24)***. Activation of PKR inactivates eukaryotic initiation factor 2, which consequently inhibits mRNA translation. The 5' leader sequence of AT_1 receptor mRNAs are noted for their significant degree of highly stable secondary structure ***(14,25)***. Thus activation of PKR by AT_1-receptor RNA secondary structure is likely to play a major contributing role in the poor translatability of AT_1-receptor mRNAs in rabbit reticulocyte lysates. In this chapter, we describe an optimized in vitro translation assay in wheat-germ lysates that efficiently translates the rAT_{1a} receptor. Our success is most likely related to the reasons aforementioned.

2. Solutions and Materials

2.1. In Vitro Transcription

2.1.1. Reagents and Solutions Required for In Vitro Transcription

1. DEPC-treated D&D water: In fume hood (*see* **Note 2**), add 100 μL of diethylpyrocarbonate (DEPC) (Sigma, cat. no. D-5758) to a 500-mL glass bottle prebaked at 180°C for 12 h (*see* **Note 3**) containing 500 mL of distilled and deionized (D&D) water. Shake thoroughly, then loosen cap and incubate for 2 h at 37°C. Autoclave for 15 min (at 15 lb/in.^{2}) on liquid cycle. Shake and then loosen cap in fume hood; wait at least 8 h before use in order to permit escape of trace DEPC (*see* **Note 4**). Store at 4°C.
2. 1 μg rAT_{1a} receptor cDNA encompassing the entire coding region (*see* **Note 5**) subcloned into the pCR3 vector ***(25)*** (**Fig. 1**) or other suitable transcription vectors. Store in 20-μL aliquots at 1–2 μg/μL at –20°C.

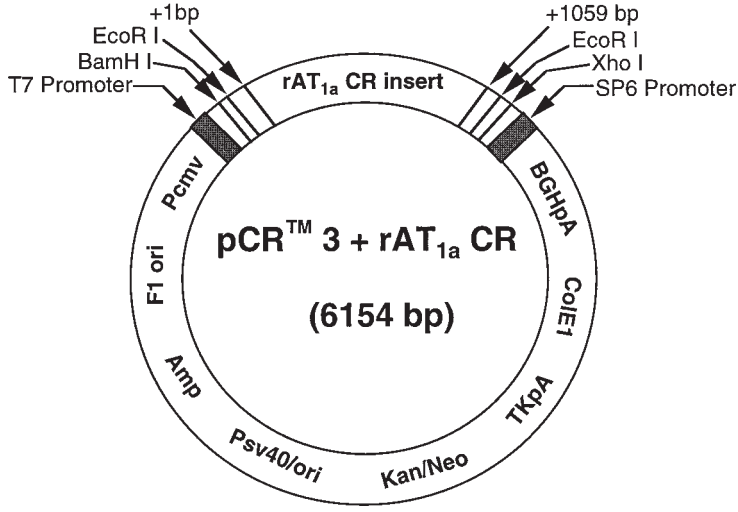

Fig. 1. rAT_{1a} receptor in pCR3. The coding region (1–1059 nt) of the rat AT_{1a} receptor is subcloned into the TA cloning site in the pCR3 vector (Invitrogen). The restriction enzyme, *Xho*I, which is located in the cloning site, is used to linearize the plasmid because there are no *Xho*I sites in the rAT_{1a} receptor cDNA.

3. 10 U/μL *Xho*I with accompanying 10X *Xho*I buffer (New England Biolabs; cat. no. 146S) or other appropriate restriction enzyme (**Fig. 1**) (*see* **Note 5**). Store at –20°C in a nonfrost-free freezer (*see* **Note 6**).
4. PicoGreen DNA quantitation system (Molecular Probes; cat. no. R-P7589). Store at –20°C.
5. Lambda DNA standard [100 μg/mL in 1X TE] (included in the PicoGreen system): Dilute stock 1:50 to 2 μg/mL by mixing 40 μL of the 100 μg/mL stock with 1.96 mL of 1X TE buffer. Store in 40 μL aliquots at –20°C.
6. 1:200 dilution of PicoGreen dsDNA quantitation reagent (included in the PicoGreen quantitation system): 100 μL of the PicoGreen reagent in dimethylsulfoxide is diluted in 19.9 mL of 1X TE immediately before use in the DNA quantitation assay.
7. Agarose (Life Technologies; cat. no. 15510-027). Store at room temperature.
8. 10X TE buffer [1 *M* Tris, 100 m*M* ethylenediaminetetraacetic acid (EDTA), pH 8.0] (included in the RiboGreen quantitation system). Store at room temperature.
9. 10X TAE buffer [400 m*M* Tris, 100 m*M* EDTA, pH 8.0]: Dissolve 48.4 g Tris base (Boehringer Mannheim; cat. no. 604-200) in 20 mL 0.5 *M* EDTA (pH 8.0), 11.4 mL glacial acetic acid (EM Science; cat. no. 64-19-7), and 800 mL D&D water. Adjust final volume with D&D water to 1 L. Store at room temperature.
10. 6X DNA loading dye [0.2% bromphenol blue, 0.2% xylene cyanol, 60% glycerol and 60 m*M* EDTA] (included in GeneRuler DNA ladder). Store at –20°C.

11. GeneRuler DNA Ladder Mix (MBI Fermentas; cat. no. SM0331). Store at –20°C.
12. mMessage mMachine system (Ambion; cat. no. 1340). Store at –20°C.
13. 5X transcription buffer (included in mMessage system). Store at –20°C.
14. Nucleic acid cocktail: ATP (15 m*M*), CTP (15 m*M*), UTP (15 m*M*), $M^7G(5')ppp(5')G$ (12 m*M*) (*see* **Note 7**) and GTP (3 m*M*) (included in mMessage system). Store in 40-µL aliquots at –20°C.
15. T7 RNA polymerase (40 U/µL) & RNase inhibitor (3 U/µL) cocktail (included in mMessage system). Store at –20°C (*see* **Note 6**).
16. 2 U/µL RNase-free DNase (included in mMessage system). Store at –20°C (*see* **Note 6**).
17. LiCl precipitation solution [7.5 *M* lithium chloride, 75 m*M* EDTA] (included in mMessage system). Store at –20°C.
18. 100% Anhydrous ethanol (Warner Graham Co.; cat. no. 64-17-5). Store at 4°C.
19. RiboGreen RNA quantitation system (Molecular Probes; cat. no. R-11490). Store at –20°C.
20. 16S Ribosomal RNA (included in the RiboGreen system): Dilute stock 1:50 to 2 µg/mL by mixing 40 µL of the 100 µg/mL 16S ribosomal stock with 1.96 mL 1X TE buffer. Store in 40 µL aliquots at –20°C (*see* **Note 6**).
21. 1:200 dilution of RiboGreen RNA quantitation reagent (included in the RiboGreen quantitation system): 100 µL of the RiboGreen reagent in dimethylsulfoxide is diluted in 19.9 mL of 1X TE immediately before use in the RNA quantitation assay.
22. 30% hydrogen peroxide (Fisher; cat. no. H325-500). Store at room temperature.
23. 37% formaldehyde solution (Fisher; cat. no. F79-500). Store at room temperature.
24. 10X MOPS [200 m*M* MOPS, 250 m*M* EDTA, 50 m*M* sodium acetate, pH 7.0]: Dissolve 41 g of MOPS (Gibco-BRL; cat. no. 11345022), 6.8 g of sodium acetate (Sigma; cat. no. S8625), and 93 g of EDTA in 800 mL DEPC-treated D&D water. Titrate the pH to 7.0 with sodium hydroxide pellets. Adjust final volume with DEPC-treated D&D water to 1 L. The solution is filter sterilized through a 0.2-µm filter and stored at room temperature in 100 mL aliquots.
25. RNA gel loading solution (Formaldehyde/MOPS) (Ambion; cat. no. 8552). Store in 50 µL aliquots at –20°C.
26. Low-range RNA markers (Life Technologies; cat. no. 15623-010). Store in 5 µL aliquots at –20°C (*see* **Note 6**).

2.1.2. Equipment Required for In Vitro Transcription

1. Microfuge (Eppendorf; model no. 5415C).
2. 37°C cabinet incubator (Thelco; model no. 6DG).
3. Speed-Vac concentrator (Savant; model no. SVC100H).
4. 96-Well microplates (Fisher; cat. no. 07-200-38).
5. Fluorescent measurement system (Millipore, CytoFluor™ 2350).
6. Water bath (Equatherm; model no. 299-734) is set at 55°C.
7. Slab gel apparatus (Bio-Rad; cat. no. 165-2940).

8. Power supply (Bio-Rad; cat. no. 165-5056).
9. Film processing system: transilluminator and camera (Fotodyne; model no. 3-3500).
10. Heat block (USA Scientific; cat. no. 2510-1102).

2.2. In Vitro Translation

2.1.2. Reagents and Solutions Required for In Vitro Translation

1. DEPC-treated D&D water (*see* **Subheading 2.1.1., step 1**).
2. Wheat-germ extract translation system (Promega; cat. no. L4330). Store at –80°C (*see* **Note 8**).
3. 1 m*M* amino acid mixture without methionine (included in wheat-germ translation system). Store in 40-µL aliquots at –20°C.
4. 1500 mCi/mmol; 10 mCi/mL L-[^{35}S]methionine (Amersham Life Science Inc.; cat. no. AG1594). Store at 4°C (*see* **Note 9**).
5. 40 U/µL RNasin (Promega; cat. no. N2515). Store at –20°C (*see* **Note 6**).
6. 10% SDS (Sigma; cat. no. 100146): Dissolve 10 g of SDS in 100 mL of D&D water to prepare a 10% SDS solution. Store at room temperature for up to 3 mo.
7. SDS-sample buffer: Mix 2 mL glycerol (Sigma; cat. no. G6279), 2 mL 10% SDS, 0.25 mg bromphenol blue (Sigma; cat. no. B5525), and 2.5 mL 4X stacking gel buffer in a tube. Add D&D water to a final volume of 9.95 mL. Store this solution at room temperature in 500 µL aliquots.
8. SDS-βME solution: 50 µL 100% β-mercaptoethanol (βME) (Sigma; cat. no. M3148) is added to 1 mL SDS sample buffer immediately before terminating the translation reaction.
9. 1 *M* NaOH/2%H_2O_2. Mix 100 mL 1N NaOH (Sigma, cat. no. 930-65) with 100 mL 2% H_2O_2. Store at room temperature.
10. 25% TCA/2% casamino acids. Dissolve 25 g trichloric acetic acid (TCA) (Sigma, cat. no. T6399) and 2 g casamino acids (Difco; cat. no. 0288-15-6) in 80 mL D&D water. Adjust final volume to 100 mL; 5% TCA. Dissolve 5 g TCA in 80 mL D&D water. Adjust final volume to 100 mL. Store at 4°C.
11. 30% Acrylamide solution: Dissolve 29 g of acrylamide (Bio-Rad; cat. no. 161-0107) and 1 g of *bis*-acrylamide (Bio-Rad; cat. no. 161-0201) in a total volume of 60 mL of D&D water. Heat the solution to 37°C to dissolve the acrylamides. Adjust the volume to 100 mL. The pH of the acrylamide solution must be ≤7 (*see* **Note 10**). Store the acrylamide solution at 4°C in a dark bottle or tightly wrap the bottle with aluminum foil (*see* **Note 10**).
12. 10% Ammonium persulfate (Bio-Rad; cat. no. 161-0700): Dissolve 0.1 g ammonium persulfate in 1 mL of D&D water. Use freshly prepared solutions; do not store (*see* **Note 11**).
13. TEMED (Bio-Rad; cat. no. 161-0800). Store in the dark at 4°C.
14. Low-range prestained sodium dodecyl sulfate-polyacrimide gel electrophoresis (SDS-PAGE) standards (Bio-Rad; cat. no. 161-0700) Store at –20°C.
15. 4X Stacking gel buffer: Dissolve 6 g of Tris base in 4 mL of 10% SDS solution. Adjust volume to 80 mL; Titrate pH to 6.8 with 12 *N* HCl (Sigma; cat. no. H7020)

and adjust final volume to 100 mL with D&D water. Store the 4X stacking gel buffer in 5-mL aliquots at room temperature.

16. 1.5 *M* Tris-HCl: Dissolve 182 g of Tris-HCl (Boehringer Mannheim; cat. no. 1814273) in 800 mL of D&D water. Titrate the pH to 6.8 with 12 *N* HCl. Adjust the final volume of the solution to 1 L with DEPC-treated water; 1 *M* Tris-HCl: dissolve 121 g of Tris-HCl in 800 mL of D&D water. Titrate the pH to 8.8 with 12 *N* HCl. Adjust the final volume of the solution to 1 L with D&D water. Store at room temperature.
17. 5X Tris-glycine buffer: Dissolve 15 g of Tris-base and 94 g of glycine (Sigma; cat. no. G7126) in 900 mL of D&D water. Add 50 mL of 10% SDS and adjust final volume to 1 L with D&D water; 1X Tris-glycine electrophoresis gel buffer: add 100 mL of 5X Tris-glycine electrophoresis buffer to 400 mL of D&D water. Store at room temperature.

2.2.2. Equipment Required for In Vitro Translation

1. Microfuge (*see* **Subheading 2.1.2., step 1**).
2. Water bath (*see* **Subheading 2.1.2., step 6**).
3. Heat block (*see* **Subheading 2.1.2., step 10**).
4. 37°C cabinet incubator (*see* **Subheading 2.1.2., step 2**).
5. Fluorescence measurement system (*see* **Subheading 2.1.2., step 5**).
6. Slab gel apparatus (*see* **Subheading 2.1.2., step 7**).
7. Power supply (*see* **Subheading 2.1.2., step 8**).
8. Film processing system: transilluminator and camera (*see* **Subheading 2.1.2., step 9**).
9. Brandel cell harvester (Brandel; model no. M-24).
10. Vertical Mini-Protean II gel apparatus (Bio-Rad; 165-2940).
11. Gel dryer (Savant; cat. no. S200).
12. Kodak Biomax Intensifying Screen (Fisher; cat. no. 0572841).
13. Film processing system (Kodak, model no. PRX-OMAT Processor, M6B).
14. Phosphorimager (Molecular Dynamics; model no. Storm 840).

3. Methods

3.1. In Vitro Transcription

3.1.1. Plasmid Linearization

1. Dilute 5 μg of the rAT_{1a} receptor cDNA subcloned into the pCR3 plasmid (**Fig. 1**) in 17 μL DEPC-treated D&D water.
2. Add 2 μL 10X *Xho*I restriction enzyme buffer and vortex.
3. Add 1 μL *Xho*I enzyme and mix gently with a freshly autoclaved pipet tip; do not vortex (*see* **Note 6**). Briefly spin tubes in microfuge for 5 s.
4. Incubate at 37°C for 1 h.
5. Precipitate the DNA by adding 100 μL of DEPC-treated D&D water, and 0.1 vol of LiCl precipitation solution (*see* **Note 12**) ***(26)***.

Table 1
Standard Curve for PicoGreen DNA Quantitation

Volume of TE (μL)	Volume (μL) of lambda DNA standard (2 μg/mL)	Volume (μL) of 200-fold PicoGreen reagent	Final [DNA] (pg/μL)
0	100	100	1000
10	90	100	900
30	70	100	700
50	50	100	500
80	20	100	200
100	0	100	0

3.1.2. DNA Quantitation

1. Quantify the linearized plasmid DNA by the PicoGreen fluorescent assay. To prepare the standard curve, the lambda DNA stock (2 μg/mL) is diluted according to **Table 1**. Five different concentrations of lambda DNA are prepared (20–100 ng/standard) in addition to a blank (no DNA).
2. Several dilutions (at least 3) of the linearized rAT_{1a} receptor plasmid DNA are prepared similarly to the standards. Measurement of each standard and sample is performed in triplicate (*see* **Note 13**).
3. 100 μL of the 200-fold diluted PicoGreen reagent (*see* **Note 13**) is added to the tubes containing lambda DNA and rAT_{1a} plasmid DNA samples. Vortex the samples and load 100 μL of the mixture per well onto a 96-well microplate. Incubate 5 min at room temperature.
4. Measure the fluorescence in a fluorescence measurement system. Read the sample within 1 h. The microplate reader is set to standard fluorescence wavelengths (excitation approx 480 nm and emission approx 520 nm). The concentration of unknown DNAs is calculated from the standard curve using linear regression analysis.

3.1.3. Assessment of Plasmid Linearization

1. Run restriction-enzyme-treated DNA samples on a 1% agarose gel to determine if linearization of the plasmid is complete. Assemble slab gel electrophoresis apparatus according to manufacturer's directions.
2. Mix 0.5 g of agarose with 50 mL 1X TAE. Microwave the mixture just until the agarose dissolves completely into the solution. Be careful not to let the agarose boil over. Cool the agarose down to 55°C in a water bath. Pour the agarose onto the slab gel apparatus with care taken to avoid introducing air bubbles into the gel. Allow gel to polymerize (approx 20 min).
3. Mix 1 μL of digested plasmid (approx 250 ng) with 7 μL D&D water, 1 μL 10X TAE buffer, and 1 μL 10X DNA loading dye. DNA markers are treated in the same way as is 250 ng of undigested plasmid (for a control).
4. The samples, standards, and control are briefly microfuged for 5 s and then loaded into the wells of the agarose gel. The samples are electrophoresed for 30–45 min

Table 2
Standard Curve for RiboGreen RNA Quantitation

Volume of TE (μL)	Volume (μL) of 16S RNA (2 μg/mL)	Volume (μL) of diluted RiboGreen reagent	Final [RNA] (pg/μL)
0	100	100	1000
20	80	100	800
40	60	100	600
60	40	100	400
80	20	100	200
100	0	100	0

at 100 V in 1X TAE buffer until the bromphenol blue runs 75% of the length of the gel.
5. Visualize and photograph the DNA gel under UV light using a transilluminator.

3.1.4. Capped RNA Synthesis

1. In a 1.5-mL microfuge tube at room temperature (*see* **Note 14**), add 2 μL of the 10X transcription reaction buffer, 10 μL of ribonucleotide mix (*see* **Note 15**), 1 μg of linearized DNA, and 2 μL of T7 RNA polymerase enzyme. Incubate in a cabinet incubator at 37°C for 2 h (*see* **Note 14**).
2. Add 1 μL RNase-free DNase to the 20 μL reaction, mix thoroughly, brief spin, and incubate at 37°C for 15 min.
3. Terminate the transcription reaction by adding 30 μL of DEPC-treated D&D water and 25 μL of LiCl precipitation solution.
4. Mix thoroughly and chill the reaction for at least 30 min or overnight at –20°C. Centrifuge the mixture at 4°C for 30 min to pellet the RNA. Discard the supernatant and wash the RNA pellet twice by adding 1 mL 70% ethanol followed by a 10-min spin at 4°C. Briefly dry the final RNA pellet under vacuum (*see* **Note 12**). Resuspend the RNA in 50 μL DEPC-treated D&D water and store in 10-μL aliquots at –70°C.

3.1.5. RNA Quantitation

1. Quantify the transcribed RNA by the RiboGreen fluorescent assay. To prepare the standard curve, the 16S ribosomal RNA stock (2 μg/mL) is diluted according to **Table 2**. Five different concentrations of ribosomal RNA are prepared (20–100 ng/sample) in addition to a blank (no RNA).
2. Several dilutions (at least 3) of the in vitro transcribed rAT_{1a}-receptor mRNA are diluted the same way as the standards. Each standard and sample is performed in triplicate.
3. 100 μL of the 200-fold diluted RiboGreen reagent (*see* **Note 13**) is added to the tubes containing ribosomal RNA and rAT_{1a}-mRNA samples. Vortex the samples and load 100 μL of the mixture per well onto a 96-well microplate. Incubate 5 min at room temperature.

4. Measure the fluorescence in a fluorescence measurement system. Read sample within 1 h. The microplate reader is set to standard fluorescence wavelengths (excitation at approx 480 nm and emission at approx 520 nm). The concentration of unknown RNAs is calculated from the standard curve using linear regression analysis.

3.1.6. RNA Quality Assessment

1. Run in vitro the transcribed RNA samples on a 1% formaldehyde denaturing agarose gel to check the quality of the RNA. Assemble slab gel electrophoresis apparatus according to the manufacturer's directions.
2. Mix 0.5 g agarose in 36 mL DEPC-treated D&D water. Add 5 mL 10X MOPS solution and microwave the mixture just until the agarose dissolves completely into the solution. Be careful not to let the agarose boil over. Cool the agarose down to 55°C in a water bath; add 9 mL of 37% formaldehyde solution to this mixture in the fume hood (*see* **Note 2**). Gently swirl the mixture to ensure mixing, then pour onto the slab gel electrophoresis apparatus (*see* **Note 3** for preparing apparatus RNase free). Take care to avoid introducing air bubbles into the gel. Allow gel to polymerize (approx 45 min).
3. Add 12 µL RNA loading buffer (3:1 dilution) to a 4-µL RNA sample. Heat mixture for 10 min at 70°C on a heat block. Immediately transfer the samples to ice and add 1 µL ethidium bromide (2 mg/mL) to the samples. Heat the samples for an additional 5 min at 70°C and again, immediately transfer to ice for 2 min (*see* **Note 12**).
4. RNA markers are treated in the same way as is the negative control (no RNA). The samples, standards and controls are briefly microfuged for 5 s and then loaded onto the gel. Run the gel for approx 2 h at 60 V in 1X MOPS buffer until the bromphenol blue runs 75% of the length of the gel.
5. Visualize and photograph the RNA gel under UV light using a transilluminator.

3.2. In Vitro Translation

3.2.1. Translation Reaction

1. Thaw 1 m*M* amino acid mixture (without methionine), [^{35}S]methionine (*see* **Note 9**) and mRNA in ice. Quickly thaw extract by holding sample in a room temperature water bath. As soon as the extract is thawed, place on ice (*see* **Note 8**). Use capped plastic tubes or covered microwell plates to avoid changes in reaction volume due to evaporation.
2. Heat the template mRNA at 67°C for 10 min and immediately cool on ice (*see* **Note 12**).
3. Assemble components in the following order: nuclease-free H_2O, amino acid mixture, RNasin inhibitor, [^{35}S]methionine, and wheat-germ extract. To avoid pipetting small volumes, prepare a mastermix with the following concentrations per 25-µL sample: 0.5 µg of the purified rAT_{1a}-receptor mRNA; 2 µL of 1 m*M* amino acid mixture without methionine; 0.5 µL RNasin inhibitor;

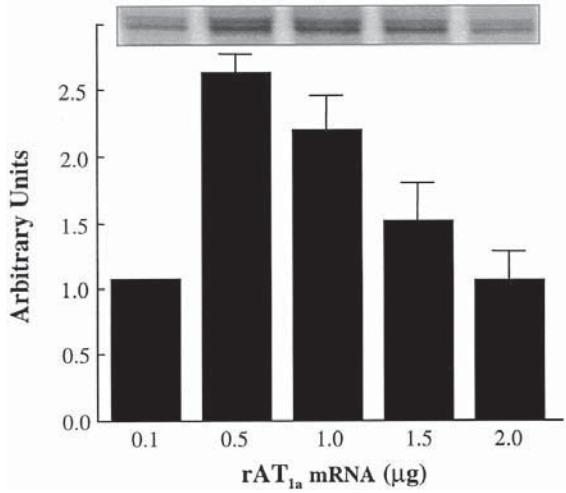

Fig. 2. Dose-response curve. AT_{1a} receptor mRNA is translated in wheat-germ extracts for 1 h as a function of mRNA concentration (0.1–2 μg). The translated protein is analyzed by SDS gel electrophoresis. The size of the rAT_{1a}-receptor translated protein is determined by low-range prestained SDS-PAGE markers and is 41–43 kDa. Autoradiograms of SDS gels are quantified by phosphorimaging and expressed in arbitrary units. The data are the mean ± S.E.M. from three to four experiments.

1.25 μL [^{35}S]methionine; and 12.5 μL wheat-germ lysate in a total volume of 25 μL (**Figs. 2–6**).

4. Prepare the Bovine Mosaic Virus (BMV) control RNA in a similar manner (*see* **Note 16**); add 0.5 μg BMV RNA (@0.5 μg/μL) to the 25 μL reaction.
5. Incubate samples and controls in a water bath at 25°C for 1.5 h.
6. To terminate the translation reaction, add 15 μL SDS-β-mercaptoethanol solution to 5 μL of the translation reaction on ice (*see* **Note 19**). The remaining sample is frozen until further use.

3.2.2. Assessment of [^{35}S]methionine Incorporation

1. Quantify the percent ^{35}S-methionine incorporation. Remove 1 μL from the 25-μL completed translation reactions including the sample, as well as the positive and negative controls and add to Eppendorf tubes containing 98 μL of 1 *M* NaOH/2% H_2O_2.
2. Vortex and incubate at 37°C for 10 min (*see* **Note 17**).
3. Terminate the reaction by adding 900 μL ice-cold 25% TCA/2% casamino acids (*see* **Note 17**).
4. Wet a Whitman GF/C glass fiber filter with ice-cold 5% TCA. Collect the precipitated translation product from 250 μL of the TCA reaction mixture by vacuum filtration. Rinse the filter with 3 mL of ice-cold 5% TCA. Repeat this rinsing step

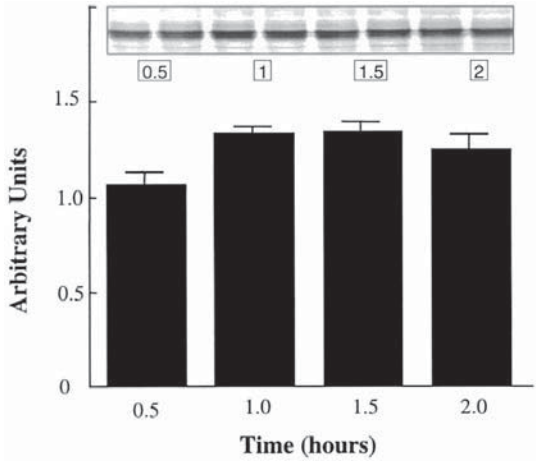

Fig. 3. Time-course. AT_{1a}-receptor mRNA (1 μg) is translated in wheat-germ extracts as a function of time (0.5–2 h). Autoradiograms of SDS gels are quantified by phosphorimaging and expressed in arbitrary units. The data are the mean ± S.E.M. from three to four experiments.

two additional times. Last, rinse with 3 mL acetone (*see* **Note 17**). Allow the filter to dry for 10 min. Count the ^{35}S-incorporation in a liquid scintillation counter using 3 mL of scintillation fluid per filter. After adding scintillation cocktail, mix well and let sit at least 30 min before counting (*see* **Note 17**).

5. To determine total counts present in the reaction, spot a 5-μL sample of the TCA reaction directly onto a filter. Dry the filter for 10 min and count as above. The measured counts per minute (cpm) are the cpm of the unwashed filter.
6. Perform the following calculations to determine percent incorporation and fold stimulation (*see* **Note 17**):

$$\frac{\text{cpm of washed filter}}{\text{cpm of unwashed filter} \times 50} \times 100 = \text{percent incorporation}$$

$$\frac{\text{cpm of washed filter}}{\text{cpm of negative control washed filter}} = \text{fold stimulation}$$

3.2.3. SDS-Polyacrylamide Gel Preparation

1. Clean glass plates with detergent, rinse with D&D water, then with ethanol/acetone mixture (1:1). Allow to air-dry. Touch plates only with gloved hands.
2. Assemble the vertical mini gel apparatus according to the manufacture's instructions. A relatively thin (0.5–1-mm) gel is required for optimal conditions.
3. A 15% resolving gel is prepared in a Buchner flask by mixing 2.3 mL D&D water, 5.0 mL 30% acrylamide, 2.5 mL 1 *M* Tris-HCl (pH 8.8) and 100 μL 10% SDS. The solution is degassed for 15 min by stirring under vacuum.

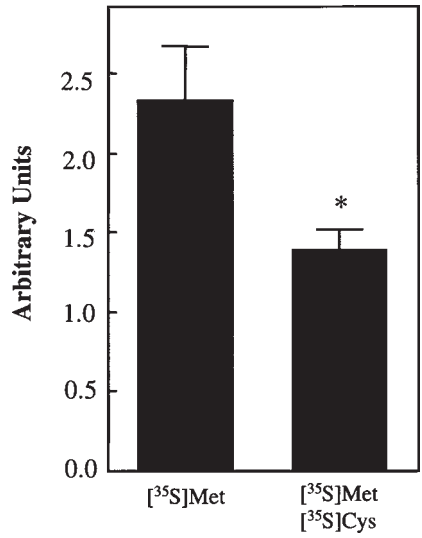

Fig. 4. Effect of single vs double radiolabeling. AT_{1a} receptor mRNA (1 μg) is translated in wheat-germ extracts for 1 h in the presence of [^{35}S]methionine and in the presence of both [^{35}S]methionine and [^{35}S]cysteine. Autoradiograms of SDS gels are quantified by phosphorimaging and expressed in arbitrary units. The data are the mean ± S.E.M. from three to four experiments.

4. 100 μL of 10% ammonium persulfate and 4 μL TEMED are added to the gel mixture (*see* **Note 11**). The resolving mixture is then gently mixed and slowly poured between the glass plates, with care taken to avoid introducing air bubbles. Sufficient space (2–3 cm) is left for pouring the 5% stacking gel. D&D water (1–2 mL) is overlaid onto the 15% gel.
5. After 30 min, the overlay water is poured off and the remaining liquid is removed by blotting onto filter paper. Do not touch the gel.
6. The stacking gel is prepared by mixing 1.4 mL D&D water, 330 μL 30% acrylamide, 250 μL 1.5 *M* Tris-HCl (pH 6.8), 20 μL 10% ammonium persulfate, 20 μL 10% SDS, and 2 μL TEMED in a 50-mL sterile tube. The contents of the tube are gently swirled to avoid air bubbles from forming (*see* **Note 11**).
7. The stacking gel is then poured onto the polymerized resolving gel. The teflon combs are carefully inserted into the stacking gel. Bubbles are avoided while inserting the combs. More stacking gel is added to completely fill the spaces of the comb. Allow stacking gel to polymerize (approx 30 min).
8. The gel is placed in the vertical mini gel electrophoresis apparatus. The bottom and top reservoirs of the mini gel apparatus are filled with the 1X Tris-glycine buffer. After gently removing the combs from the gel, each well is washed several times with 1X Tris-glycine buffer using a 25-gage needle and a 1-mL syringe (*see* **Note 18**). Avoid prerunning the gel before loading the samples because this will destroy the discontinuity of the buffer system.

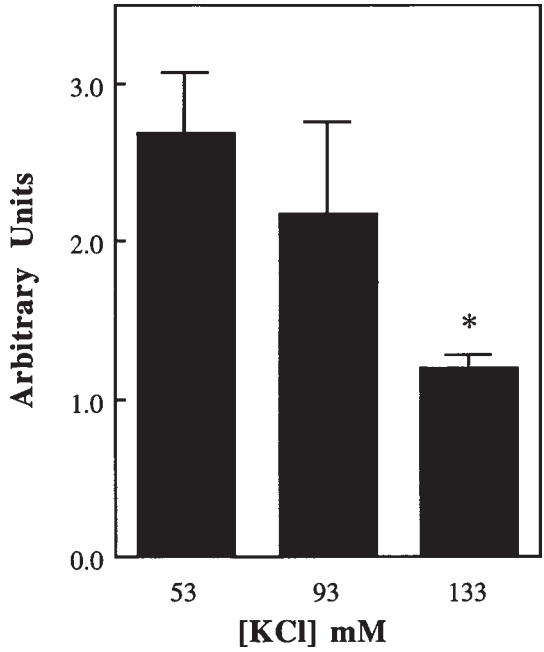

Fig. 5. Effect of KCl concentration. AT_{1a} receptor mRNA (1 μg) is translated in wheat-germ extracts for 1 h as a function of KCl concentration (53–133 m*M*). Autoradiograms of SDS gels are quantified by phosphorimaging and expressed in arbitrary units. The data are the mean ± S.E.M. from three to four experiments.

3.2.4. Electrophoresis

1. Translated reaction products are heated at 100°C for 2 min and then left at room temperature until loading onto the gel (*see* **Note 20**).
2. On a denaturing 15% SDS polyacrylamide gel, 20 μL of sample is loaded per lane (*see* **Note 21**). The samples are electrophoresed for 2 h at a constant current of 15 mA in the stacking gel (approx 30 min) and 30 mA in the separating gel (approx 1.5 h) ***(26)***. Run until the bromphenol dye front is about to enter the bottom buffer tank (*see* **Note 21**).
3. After the gel finishes running, the top glass plate is carefully removed (*see* **Note 22**).
4. The gel is blotted onto a piece of Whatman filter paper that is approx 20% larger than the gel. After blotting the filter paper on three paper towels (*see* **Note 22**), the gel is wrapped with Saran Wrap and dried on a gel dryer at 80°C for 1 h.
5. The dried gel is exposed for 1 h to a phosphorimager screen for phosphor autoradiography (*see* **Note 23**) followed by quantitation of the bands ([^{35}S]methionine labeled rAT_{1a}-receptor protein) using ImageQuant (Macintosh version 1.2) software (*see* **Note 24**).

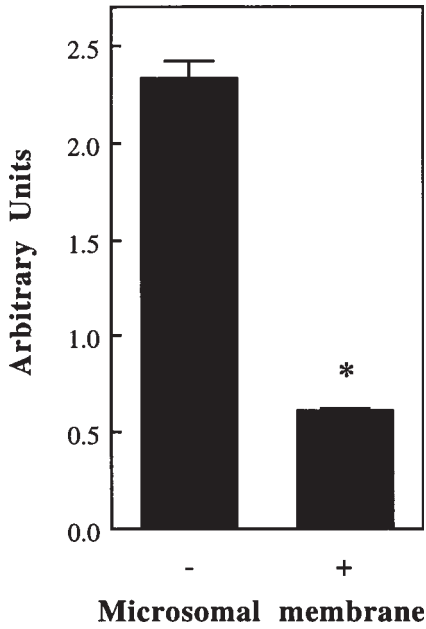

Fig. 6. Effect of canine microsomal membranes. AT_{1a}-receptor mRNA (1 μg) is translated in wheat-germ extracts for 1 h in the absence (–) and presence (+) of canine microsomal membranes (1.5 μL/25 μL reaction volume). Autoradiograms of SDS gels are quantified by phosphorimaging and expressed in arbitrary units. The data are the mean ± S.E.M. from three to four experiments.

4. Notes

1. No detectable translation of the rAT_{1a}-receptor mRNA is observed using rabbit reticulocyte lysates under a variety of experimental conditions that include rAT_{1a} mRNA from 0.1–2 μg, 25 and 37°C, 0.5–2 h, 53–133 m*M* KCl, 0.5–2 m*M* Mg acetate. and in the absence and presence of dog microsomal membranes (1.5 μL/25 μL reaction volume).
2. DEPC, acrylamides, and formaldehyde are suspected carcinogens and thus are only used in the fume hood. When weighing out acrylamides, a charcoal face mask is worn for protection.
3. To obtain best results, RNase contamination must be avoided. RNases liberated during cell lysis are inhibited by inclusion of RNase inhibitors such as RNasin. Introduction of trace amounts of RNase from other sources in the laboratory must be prevented. RNases on laboratory glassware and metal are destroyed by heat inactivation; heat glassware and metal instruments such as forceps, spatulas, and razor blades at 180°C for 12 h before use. Sterile disposable plasticware (e.g., pipet tips and microfuge tubes) is essentially free of RNase contamination and is freshly autoclaved whenever possible. Rolls of aluminum foil and Saran Wrap

are dedicated for RNA work only. These rolls are handled with fresh gloves and inner layers are taken for use in order to minimize possible RNase contamination. Likewise, bags of weigh boats are dedicated for RNA use only. All solutions are prepared using RNase-free glassware, DEPC-treated D&D water, and chemicals reserved exclusively for RNA work. Reagents are aliquoted whenever possible to minimize crossover contamination should a stock solution become contaminated with trace amounts of RNase. Electrophoresis tanks are treated with a solution of 3% H_2O_2 for 20 min at room temperature followed by thoroughly rinsing with DEPC-treated D&D water. Other cautions include using disposable sterile pipets and changing gloves frequently when working with RNA.

4. Autoclaving the DEPC water removes trace DEPC. This step is necessary because DEPC is capable of modifying purine residues in RNA by carboxymethylation. Carboxymethylated RNA is translated at far slower rates than unmethylated RNA.
5. DNA templates are subcloned into appropriate plasmids containing bacteriophage promoters (e.g., CMV) and RNA polymerases (e.g., T7) upstream from the template DNA (e.g., rAT_{1a} receptor) (**Fig. 1**). Before in vitro transcription, plasmids are linearized with restriction enzymes (e.g., *Xho*I) that cut the plasmid 3' to the template DNA coding for the 5'LS RNA; however, if SP6 is used, the plasmid is left supercoiled since SP6-mediated transcription is more efficient using supercoiled DNA. A run-off transcript is generated by in vitro transcription, which terminates downstream of the cloned sequence.
6. Enzymes are stored in a non-frost-free freezer. The temperature cycles in frost-free freezers. This temperature cycling denatures labile proteins such as enzymes and thus is avoided. Likewise, solutions containing labile proteins are never vortexed because vortexing introduces air bubbles that denature proteins and thereby inhibit their activity. Instead, solutions containing labile proteins are gently mixed by stirring with a pipet tip. Similarly, avoid repeated freeze thawing of reagents to minimize damage to the structure of molecules such as proteins and nucleic acids.
7. Most eukaryotic mRNAs contain a $m^7G(5')ppp(5')G$ cap at the 5' end, which is important for the binding of translation initiation factors and contributes to mRNA stability *(27)*.
8. Wheat-germ lysates are handled gently. Vortexing the lysates is avoided because foaming caused by vortexing can denature the translation initiation factors critical for translation. The lysates are gently pipeted up and down (or the tube can be gently flicked with a finger). The lysates are thawed on ice. Lysates once thawed are NOT refrozen and reused. There is inherent variability in translation activity between preparations. Therefore, test various preparations and store sufficient amounts of the most effective lysates. If commercial preparations are used, purchase large amounts of effective lot numbers.
9. Fresh [^{35}S]methionine (translational grade) is used for the translation experiments. The yield of translated mRNAs is best if the [^{35}S]methionine is used within 3 wk from the date it is synthesized. Older [^{35}S]methionine dissociates from

amino acids and labels other proteins in the lysate leading to higher backgrounds and sample smearing. There are reports of a 42-kDa band with some grades of [^{35}S]methionine ***(22,28)***. This has not been a problem using Amersham International Redivue L-[^{35}S]methionine, AG1094. Nonradioactive methods are available ("Transcend nonradioactive translation detection system") in which biotinylated lysine residues are incorporated into nascent proteins during translation. However, wheat-germ extracts contain endogenous biotinylated proteins that may be difficult to distinguish from biotinylated translation products.

10. The purity of the acrylamide will be indicated by the pH. Anything above pH 7.0 is not of sufficient purity for use in gel electrophoresis. Acrylamide is light sensitive and oxidizes if exposed to light.
11. Ammonium persulfate must be prepared fresh. When TEMED and ammonium persulfate are added together, the gel is poured within a few minutes (<5 min) to avoid polymerization outside the glass plates. Minimize bubble formation by degassing before addition of ammonium persulfate and TEMED.
12. When DNA and RNA are finally resuspended in DEPC-treated D&D water after an ethanol precipitation step, care is taken to make sure no residual salts or ethanol are left in the sample since these contaminants inhibit enzymes such as polymerases and translation initiation factors. Place nucleic acid samples under vacuum for the minimum time necessary to remove trace ethanol (usually 5–10 min). Overdrying makes it difficult to resuspend the nucleic acids. Dissolve the nucleic acid-ethanol precipitates in DEPC-treated D&D water. For RNA, denature at 75–80°C for 2 min and then place quickly on ice. This treatment breaks up aggregates and disrupts local regions of secondary structure, which significantly improves translation efficiency, especially for GC-rich mRNA ***(29)***. RNA used for in vitro translation experiments is not frozen and thawed more than once (*see* **Note 6**). RNA samples are stored at –80°C.
13. The tubes containing the PicoGreen and RiboGreen reagents are stored wrapped in aluminum foil and are diluted in the dark in order to minimize photodegradation caused by light exposure. Furthermore, the PicoGreen and RiboGreen reagents are prepared in plastic vessels because these reagents absorb to glass. The diluted lambda DNA and 16S ribosomal RNA standards used for the standard curves are not stored and are diluted just before use. Approx, 2 mL of the 1:200 diluted PicoGreen or RiboGreen reagents are required per standard curve; 1 mL is required per sample.
14. Do not assemble the components of the transcription reaction on ice; assemble at room temperature in order to avoid precipitating the spermidine and consequently, the template DNA. Spermidine is used to stabilize RNA polymerases ***(20)***. The RNA samples, however, are thawed on ice. Use a cabinet incubator to avoid condensation that occurs in heat blocks.
15. The Ribomax large-scale system is used to produce large amounts of RNA (2–6 mg/mL) per mL reaction volume; this yield is approx 10–20-fold higher than produced in standard transcription reactions.
16. The control RNA is an in vitro synthesized capped RNA that codes for BMV RNA. In the translation of BMV, four viral proteins are synthesized. These are 109 kDa,

94 kDa, 35 kDa, and the 20 kDa coat protein. A fifth protein, 15 kDa, may also be observed; this is a translation product related to the coat protein. The negative control measures the background level of ^{35}S-incorporation and reveals any contaminating translated product, whereas the positive control assures that the system is working.

17. The $NaOH/H_2O_2$ mixture deacylates charged tRNA and facilitates the precipitation of radiolabeled proteins by the 25% TCA/2% casamino acid mixture. Acetone bleaches out the red color in reticulocyte lysates, which can cause quenching during scintillation counting. The range of percent incorporation is typically between 1% for poorly translated genes and up to 20% for highly expressed genes. The fold stimulation of the translation over the negative control ranges from 10 to 50-fold, depending on gene expression. In the case of the rAT_{1a} receptor, we typically generate 10% incorporation and 100-fold stimulation of translation over the negative control (no RNA).
18. The wells are washed extensively to remove unpolymerized acrylamide, which will interfere with the sample entering the gel.
19. A 3:1 ratio of SDS-βME solution to sample is added to the sample before loading on the gel. The volume of the sample loaded onto the gel is critical; 5 μL is sufficient to load onto a minigel and 12.5 μL is the maximum volume. Its worth noting that increasing the sample volume does not necessarily result in increasing the signal visualized on the gel. In fact, increasing the volume of sample can result in streaking patterns throughout the gel caused by too much protein, which ultimately increases the background. Other causes of smearing are the presence of ethanol in the sample (*see* **Note 12**). Care is taken when altering the ratio of the sample to the sample buffer because the final concentration of reducing agents available to denature the samples may be insufficient.
20. High-molecular-weight complexes are formed upon heating the sample, which interferes with electrophoresis and increases background radioactivity in the gel. Therefore, it is important not to heat the samples for more than 2 min at 100°C.
21. Loading higher amounts of sample can cause smearing caused by unincorporated [^{35}S]methionine. This smearing phenomenon can be reduced by washing the gel in water for 15–30 min. If higher amounts of sample are used, the SDS concentration may have to be increased in order to ensure that all the proteins are bound to the SDS. If background under these conditions becomes a problem, pretreatment with 1/10 vol of 1 mg/mL RNase A or an RNase cocktail (Ambion, cat. no. 2286) for 5 min at room temperature will digest the amino acyl tRNAs, which sometimes produce background bands.
22. To easily remove the glass plates, a squirt bottle of buffer can be used to gently ease the gel off the top plate. Care is taken in lifting the top plate in order to avoid stretching the gel. Destaining the gel for 15–30 min is not necessary if prestained SDS-PAGE standards are used. Washing the gel is also not necessary if no more than 5 μL of sample is loaded per lane. Drying the gel on sufficient filter paper (two sheets) is important because ridges can develop on the autoradiogram from the gel dryer, which can interfere with visualizing the radioactive bands. Note

that free amino acids migrate with the dye front. Therefore, the lower buffer chamber will be contaminated with ^{35}S if the dye front runs off the gel.

23. Alternatively to phosphorimaging, X-ray autoradiography combined with fluorography can be performed. Fluorography enhances the sensitivity of the ^{35}S detection. Follow the manufacturer's directions for fluorography [e.g., Amersham's Amplify fluorographic reagents (cat. no. NAMP100) or New England Nuclear's Enhance™ (cat. no. NEF-992)] ***(30)***. The advantage of phosphorimaging compared to X-ray autoradiography is that phosphorimaging is 10–250X more sensitive and 10X faster. Furthermore, phosphorimaging has a linear dynamic range of five orders of magnitude compared to less than 2 for X-ray film and, phosphorimaging can easily quantify the radioactivity in the individual bands.
24. The optimum conditions for the translation reaction were determined empirically. The optimum dose was determined from a mRNA dose response curve (**Fig. 2**) and is 0.5 μg. Above 2 μg RNA, the reaction is inhibited. mRNA saturates the lysate for translation at a concentration of approx 0.5–1.0 μg/25 μL reaction volume. A time-course revealed that the degree of translated protein increases up to 1 h at which point there is no significant further product formation (**Fig. 3**). The system is labile at temperatures above 30°C. Optimal activation is observed between 25–30°C. Double labeling of the rAT_{1a} mRNA with [^{35}S]methionine/[^{35}S]cysteine (Pro-Mix [^{35}S], 1200 Ci/mmol; 2.5 mCi/175 μL; Amersham; cat. no. AGQ 0080) did not improve the signal/noise ratio compared to labeling the rAT_{1a} with [^{35}S]methionine alone (**Fig. 4**). Wheat germ is particularly sensitive to variations in potassium concentrations. The optimum potassium concentration depends upon the mRNA. At [KCl] lower than 70 m*M*, small mRNAs are preferentially translated while above 70 m*M*, larger mRNAs are translated more efficiently ***(20,31)***. In the case of the rAT_{1a} receptor, the optimum concentration lies between 50 and 90 m*M*; at higher concentrations of potassium (≥250 m*M*), there is a 54% decrease in the rate of translation of the rAT_{1a} receptor (**Fig. 5**). (Note that the wheat germ provided by Promega contributes 53 m*M* potassium to the final reaction.) Although the major product of rAT_{1a}-receptor translation is a broad major band between 41–43 kDa in size, smaller minor bands of 34 and 26 kDa were also observed. Using an antibody to the rAT_{1a} receptor ***(32)*** we found that these smaller bands were also recognized by the antibody. Because the antibody is targeted towards the carboxyl tail (amino acids 350–359) of the receptor, these smaller bands are likely caused from initiation at inappropriate internal sites with termination at the correct site. This phenomenon arises from "leaky scanning," which results from translation initiation at internal downstream methionines ***(33)***. Addition of canine microsomal membranes increases polypeptide translocation into vesicles but reduces the amount of polypeptides synthesized and therefore, its not surprising that the yield was less in the presence of microsomal membranes (**Fig. 6**).
25. If no translation is observed under the conditions outlined, determine if inhibitors are present in the mRNA preparation: mix the mRNA with the control RNA and

examine if the BMV translation is inhibited relative to translation of the BMV in the absence of AT_1-receptor mRNA. The most likely inhibitors are trace amounts of salt and ethanol in the transcribed RNA (*see* **Note 12**).

References

1. McDowell, M. J., Joklik, W. K., Villa-Komaroff, L., and Lodish, H. F. (1972) Translation of reovirus messenger RNAs synthesized in vitro into reovirus polypeptides by several mammalian cell-free extracts. *Proc. Natl. Acad. Sci. USA* **69,** 2649–2653.
2. Shiroki, K. and Nomoto, A. (1999) In vitro translation extracts from tissue culture cells. *Methods Mol. Biol.* **118,** 449–458.
3. Pelham, H. R. and Jackson, R. J. (1976) An efficient mRNA-dependent translation system from reticulocyte lysates. *Eur. J. Biochem.* **67,** 247–256.
4. Jackson, R. J. and Hunt, T. (1983) Preparation and use of nuclease-treated rabbit reticulocyte lysates for the translation of eukaryotic messenger RNA. *Methods Enzymol.* **96,** 50–74.
5. Matthews, G. M. and Colman, A. (1995) The *Xenopus* egg extract translation system, in *Methods in Molecular Biology: In Vitro Transcriptions and Translation Protocols*, vol. 37 (Tymms, M. J., ed.), Humana Press, Totowa, NJ, pp. 199–213.
6. Carlier, A. R. and Peumans, W. J. (1976) The rye embryo system as an alternative to the wheat system for protein synthesis in vitro. *Biochim. Biophys. Acta* **447,** 436–444.
7. Roberts, B. E. (1973) Tobacco mosaic virus RNA directs the synthesis of a coat protein peptide in a cell-free system from wheat. *J. Mol. Biol.* **80,** 733–742.
8. Erickson, A. H. and Blobel, G. (1983) Cell-free translation of messenger RNA in a wheat germ system. *Methods Enzymol.* **96,** 38–50.
9. Mori, Y., Matsubara, H., Murasawa, S., Kijima, K., Maruyama, K., Tsukaguchi, H., et al. (1996) Translational regulation of angiotensin II type 1A receptor. Role of upstream AUG triplets. *Hypertension* **28,** 810–817.
10. Elton, T. S., Zhao, X., and Martin, M. M. (1999) Translational regulation of the human angiotensin II type 1 receptor. *FASEB J.* **13,** A1471.
11. Thompson, D. and Van Oosbree, T. (1992) TNT™ lysate coupled transcription/translation: comparison of the T3, T7 and SP6 systems. *Promega Notes* **38,** 13,14.
12. Pelham, H. R., Sykes, J. M., and Hunt, T. (1978) Characteristics of a coupled cell-free transcription and translation system directed by vaccinia cores. *Eur. J. Biochem.* **82,** 199–209.
13. Craig, D., Howell, M. T., Gibbs, C. L., Hunt, T., and Jackson, R. J. (1992) Plasmid cDNA-directed protein synthesis in a coupled eukaryotic in vitro transcription-translation system. *Nucleic Acids Res.* **20,** 4987–4995.
14. Curnow, K. M., Pascoe, L., Davies, E., White, P. C., Corvol, P., and Clauser, E. (1995) Alternatively spliced human type 1 angiotensin II receptor mRNAs are translated at different efficiencies and encode two receptor isoforms. *Mol. Endocrinol.* **9,** 1250–1262.

15. Krishnamurthi, K., Verbalis, J. G., Zheng, W., Wu, Z., Clerch, L. B., and Sandberg, K. (1999) Estrogen regulates angiotensin AT_1 receptor expression via cytosolic proteins that bind to the 5' leader sequence of the receptor mRNA. *Endocrinology* **140,** 5435–5438.
16. Kim, N. S., Yamaguchi, T., Sekine, S., Saeki, M., Iwamuro, S., and Kato, S. (1998) Cloning of human polyubiquitin cDNAs and a ubiquitin-binding assay involving its in vitro translation product. *J. Biochem. (Tokyo)* **124,** 35–39.
17. Boado, R. J. and Pardridge, W. M. (1997) The 5'-untranslated region of GLUT1 glucose transporter mRNA causes differential regulation of the translational rate in plant and animal systems. *Comp. Biochem. Physiol. B. Biochem. Mol. Biol.* **118,** 309–312.
18. Blagosklonny, M. V., Toretsky, J., Bohen, S., and Neckers, L. (1996) Mutant conformation of p53 translated in vitro or in vivo requires functional HSP90. *Proc. Natl. Acad. Sci. USA* **93,** 8379–8383.
19. Speirs, J. (1993) *In vitro Translation of Plant Messenger RNA*, vol. 10, Academic, London, pp. 33–56.
20. Davies, J. W., Aalbers, A. M., Stuik, E. J., and Van Kammen, A. (1977) Translation of cowpea mosaic virus RNA in a cell-free extract from wheat germ. *FEBS Lett.* **77,** 265–269.
21. Jagus, R. (1987) Translation in cell-free systems. *Methods Enzymol.* **152,** 267–276.
22. Walter, P. and Blobel, G. (1983) Signal recognition particle: a ribonucleoprotein required for cotranslational translocation of proteins, isolation and properties. *Methods Enzymol.* **96,** 682–691.
23. Van Herwynen, J. F. and Beckler, G. S. (1995) Translation using a wheat-germ extract, in *Methods in Molecular Biology: In Vitro Transcriptions and Translation Protocols*, vol. 37 (Tymms, M. J., ed.), Humana Press, Totowa, NJ, pp. 245–251.
24. Pe'ery, T. and Mathews, M. B. (1997) Synthesis and purification of single-stranded RNA for use in experiments with PKR and in cell-free translation systems. *Methods* **11,** 371–381.
25. Krishnamurthi, K., Zheng, W., Verbalis, A. D., and Sandberg, K. (1998) Regulation of cytosolic proteins binding *cis* elements in the 5' leader sequence of the angiotensin AT_1 receptor mRNA. *Biochem. Biophys. Res. Commun.* **245,** 865–870.
26. Sambrook, J., Fritsch, E. F., and Maniatis, T. (1989) *Molecular Cloning, A Laboratory Manual.* Cold Spring Harbor Laboratory Press, Cold Spring Harbor, NY.
27. Krieg, P. A. and Melton, D. A. (1984) Functional messenger RNAs are produced by SP6 in vitro transcription of cloned cDNAs. *Nucleic Acids Res.* **12,** 7057–7070.
28. Jackson, R. J. (1991) Potassium salts influence the fidelity of mRNA translation initiation in rabbit reticulocyte lysates: unique features of encephalomyocarditis virus RNA translation. *Biochim. Biophys. Acta.* **1088,** 345–358.
29. Karr, S. R., Rich, C. B., Foster, J. A., and Przybyla, A. (1981) Optimal conditions for cell-free synthesis of elastin. *Coll. Relat. Res.* **1,** 73–81.
30. Bonner, W. M. and Laskey, R. A. (1974) A film detection method for tritium-labelled proteins and nucleic acids in polyacrylamide gels. *Eur. J. Biochem.* **46,** 83–88.

31. Benveniste, K., Wilczek, J., Ruggieri, A., and Stern, R. (1976) Translation of collagen messenger RNA in a cell-free system derived from wheat germ. *Biochemistry* **15,** 830–835.
32. Giles, M. E., Fernley, R. T., Nakamura, Y., Moeller, I., Aldred, G. P., Ferraro T, et al. (1999) Characterization of a specific antibody to the rat angiotensin II AT1 receptor. *J. Histochem. Cytochem.* **47,** 507–516.
33. Dasso, M. C., Milburn, S. C., Hershey, J. W., and Jackson, R. J. (1990) Selection of the 5'-proximal translation initiation site is influenced by mRNA and eIF-2 concentrations. *Eur. J. Biochem.* **187,** 361–371.

11

Quantitation of Angiotensin II Receptors by Competitive Reverse-Transcription Polymerase Chain Reaction

Wei Wu, Aqing Yao, and Donna H. Wang

1. Introduction

1.1. Competitive RT-PCR Principle

Becker-Andre and Hahlbrock first described competitive RT-PCR ***(1)***. In the competitive RT-PCR, a synthetic RNA/DNA control (competitor), generally called internal standard, is coamplified with the target nucleic acid in the same tube ***(2,3)***. Ideally, both target and internal standard will amplify with equivalent efficiency, and products will be distinguishable after amplification by their sizes. Thus, the internal standards that competitive RT-PCR requires should be very close in composition to the target sequences. Quantification is then performed by comparing the PCR signal of the target amplicon with the PCR signal obtained with known concentrations of the internal standard. Most competitive RT-PCR protocols use serial dilutions of competitor with a constant amount of unknown mRNA in the RT-PCR process ***(4)***. This procedure requires 4–8 reactions for each sample in order to plot the ratio of products against the amount of added competitor to determine the equimolar amount for each unknown sample. Calibration curves, relating the logarithm of the ratio of both PCR products to the logarithm of the initial amount of competitor, are then constructed. If both target and competitor amplify with equivalent efficiency, the amount of initial target mRNA can be obtained from the point on the curve where target and standard values are equal.

1.2. Basic Procedures in Competitive RT-PCR

1.2.1. Extraction of Nucleic Acids

Many protocols are already used for RNA extraction. To ensure proper performance of quantitative competitive RT-PCR, the methods used for preparing the nucleic acids must be optimized. Particularly, before quantitation of mRNA,

From: *Methods in Molecular Medicine, vol. 51: Angiotensin Protocols*
Edited by: D. H. Wang

it is essential to optimize RNA quality by eliminating genomic DNA with RNase-free DNase I. RNA quality can be determined by gel electrophoresis and optical density analysis.

1.2.2. Construction of Internal Standards for Competitive PCR

Before constructing internal standard, suitable primers (forward and reverse primers) corresponding to the target template should be designed. Internal standards are DNA or RNA fragments sharing the primer recognition sequences with target sequences. The simplest way to differentiate target product from standard product is by size difference ***(5)***. This can be achieved by constructing standards harboring the same sequence as the specific target, but containing a deletion or an insertion. Cloning of DNA standards involves enzymatic reactions such as digestion with specific restriction enzymes and ligation. For synthesis of internal standard RNA (cRNA), the competitive DNA is placed in plasmid vectors under the control of an RNA polymerase promoter. After linearization of the vector, large amounts of cRNA are transcribed in vitro. The cRNA is then incubated with RNase-free DNase I to get rid of DNA template. Subsequently, quality and copy number of the cRNA should be determined by gel electrophoresis and spectrophotometer.

1.2.3. Reverse Transcription (RT)

Moloney murine leukemia virus (MMLV) or avian myeloblastosis virus (AMV) are used for RT.

The RT-PCR process can be simplified by the use of *Tth* DNA polymerase possessing both reverse transcriptase and polymerase activity. MMLV or AMV is used to synthesize single-stranded cDNA from total tissue RNA in the presence or absence of a serial of dilutions of the internal standard cRNA.

In addition to target RNA, internal standard cRNA, and reverse transcriptase, RT process requires reverse primer and RT reaction buffer. The procedure contains two steps: first, single-strand cDNA extension by incubation at 42°C for 50 min; and second, single-strand cDNA separation by denaturation from RNA-cDNA hybrid at 90°C for 10–15 min.

1.2.4. PCR

PCR procedure requires single-stranded cDNA template, forward primer and reverse primer, PCR reaction buffer, dNTP, and *Taq* DNA polymerase or *Tth* DNA polymerase. Double-stranded cDNA is synthesized and amplified using PCR thermal cycler following the routine program. First, template is denatured at 94°C for 2 min. Second, PCR proceeds for 30 cycles including denaturation (94°C for 30 s), annealing (temperature varies depending on primer properties, generally 50°C–65°C for 45 s) and extension (72°C for 1–3 min, depending on the size of PCR products). Third, PCR products are elongated at 72°C for 5–10 min. Finally, reaction stops at 4°C.

1.2.5. Detection and Quantitation of PCR Products

PCR products of different sizes are usually separated by conventional gel electrophoresis, capillary gel electrophoresis or high-performance liquid chromatography (HPLC) ***(6)***. Common practice is to use gel electrophoresis for separation of the PCR products and to visualize the DNA bands by ethidium bromide staining or Southern blot ***(7)***. A Phosphor-Imager can be used for quantitation. Alternatively, DNA/RNA real-time quantitative PCR machines (ABI PRISM 7700 and GeneAmp 5700) are available now. Information regarding these products is accessible over the Internet (http://www.pebio.com/ab/about/pcr/sds/).

1.3. Quantitation of Angiotensin II Receptors (AT1A, AT1B) by Competitive RT-PCR

Angiotensin II initiates a variety of cellular responses through activation of its receptors. AT1A and AT1B have been identified to be the two major subtypes of angiotensin II receptors. Llorens-Cortes and our group first quantitated the expression of AT1A and AT1B in rat liver, kidney, lung, aorta, and adrenal gland using competitive RT-PCR technique ***(8,9)***. These studies present a new approach for the specific quantification of AT1A and AT1B receptor mRNAs by RT-PCR in the presence of an AT1 receptor cRNA as internal standard. Absolute quantities of mRNA are then determined by extrapolation using the standard curve generated with the internal standard.

2. Materials

2.1. RNA Preparation

1. Solution D: 4.0 *M* guanidine thiocyanate, 25 m*M* sodium citrate, pH 7.0, 0.5% Sarcosyl, and 0.1 *M* 2-mercaptoethanol (added before use).
2. DEPC (diethyl pyrocarbonate)-treated H_2O.
3. 2.0 *M* sodium acetate, pH 4.0.
4. Phenol (water saturated):chloroform:isoamyl alcohol (25:24:1).
5. 100% isopropanol.
6. 75% ethanol.
7. Rat tissues.
8. Homogenizer.
9. Sorvall SS-34 and Beckman SW-28 rotors.
10. Silanized and autoclaved SW-28 polyallomer tubes.

2.2. Internal Standard (cRNA) Preparation

1. Plasmid pSK-AT1A containing partial regulatory and coding sequences of the rat AT1A receptor gene (from *Kpn*I to *Sac*I site, nucleotide –182 to 1034) (*see* **Note 1**).
2. Restriction endonucleases and reaction buffers (*Eco*RI, *Acc*I, *Sal*I, and corresponding reaction buffers).

3. *T7* RNA polymerase.
4. RNase-free DNaseI.
5. QIAquick Gel Extraction Kit (QIAGEN Inc., Valencia, CA). Components of the kit: QIAquick spin columns, buffers, and collection tubes.
6. DNA Blunting and Ligation Kit (Fermentas, Amherst, NY). Components of the kit: Klenow fragment, 3.0 U/μL, 10X Klenow fragment reaction buffer [100 μL of 0.5 *M* Tris-HCl, pH 8.0 at 25°C, 50 m*M* $MgCl_2$, 10 m*M* dithiothreitol (DTT)], 0.5 m*M* for each dNTP, *T4* DNA ligase, 2.0 U/μL, 10X ligation buffer (100 μL of 400 m*M* Tris-HCl, 100 m*M* $MgCl_2$, 100 m*M* DTT, 5.0 m*M* ATP, pH 7.8 at 25°C), PEG 400 solution, control DNA and ddH_2O.
7. Phenol (water saturated).
8. 20 m*M* for each ATP, CTP, GTP, and UTP.
9. 1.0 *M* DTT.
10. Phenol (water-saturated): chloroform: isoamyl alcohol (25: 24:1).
11. 3.0 *M* sodium acetate pH 5.2.
12. 100% isopropanol.
13. DEPC-treated H_2O.
14. 0.8% agarose gel

2.3. Primers

1. A forward primer: 5'-CACCTATGTAAGATCGCTTC-3'.
2. Position: 295–314 bp of AT1A gene.
3. A reverse primer: 5'-GCACAATCGCCATAATTATCC-3'.
4. Position: 739-719 bp of AT1A gene (*see* **Note 2**).

2.4. RT Reaction

1. MMLV RT (200 U/μL, Gibco-BRL, Gaithersburg, MD).
2. Total RNA and internal standard cRNA.
3. 10 μ*M* reverse primer.
4. 5X RT reaction buffer: 250 m*M* Tris-HCl, pH 8.3, 375 m*M* KCl, 15 m*M* $MgCl_2$, 2.5 m*M* NTP.
5. DEPC-treated H_2O.

2.5. PCR Amplification

1. RT products (including single-stranded cDNA).
2. 10 μ*M* forward primer.
3. 10 μ*M* reverse primer.
4. *Taq* DNA polymerase (5.0 U/μL, Sigma Chemical Company, St. Louis, MO).
5. 10X PCR reaction buffer: 100 m*M* Tris-HCl, pH 8.3, 500 m*M* KCl, 15 m*M* $MgCl_2$, 0.01% gelatin.
6. 2.5 m*M* for each dNTP.
7. 10 μCi/μL [α-^{32}P] dCTP (Amersham Pharmacia Biotech, Piscataway, NJ).
8. ddH_2O.
9. PCR thermal cycler.

2.6. Southern-Blot Analysis

1. 1.5% agarose.
2. 100 bp DNA molecular weight marker.
3. DNA loading buffer: 40% sucrose, 0.1% bromophenol blue, 0.1% xylene cyanol.
4. 10 mg/mL ethidium bromide.
5. 20X SSC: 3.0 *M* NaCl, 0.3 *M* sodium citrate, adjust to pH 7.0 with 1.0 *M* HCl.
6. DNA denaturation solution: 1.5 *M* NaCl, 0.5 *N* NaOH.
7. Neutralization solution: 1.0 *M* Tris-HCl pH 7.4, 1.5 *M* NaCl.
8. cDNA probe fragment (from –178 to + 562 of rat AT1A cDNA).
9. 10 μCi/μL [α-^{32}P] dCTP (Amersham Pharmacia Biotech).
10. Random Primers DNA Labeling System (Gibco-BRL). Components: random primers buffer mixture (0.67 *M* HEPES, 0.17 *M* Tris-HCl, 17 m*M* $MgCl_2$, 33 m*M* 2-mercaptoethanol, 1.33 mg/mL BSA, 18 OD_{260} U/mL oligodeoxyribonucleotide primers, hexamers, pH 6.8.), dNTP (0.5 m*M* dNTP each in 1.0 m*M* Tris-HCl, pH 7.5), Klenow fragment (3.0 U/μL), stop buffer [0.5 *M* ethylenediaminetetraacetic acid (EDTA), pH 8.0], control DNA (5.0 ng/μL pBR322 DNA/*Rsa* I fragments in 10 m*M* Tris-HCl, pH 7.4, 5.0 m*M* NaCl, 0.1 m*M* EDTA), ddH_2O.
11. DNA Mini-Spin column (Worthington Bio. Co., Freehold, NJ).
12. 50X Denhardt's solution (5.0 g Ficoll, type 400, 5.0 g polyvinylpyrrolidine, 5.0 g BSA, fraction V).
13. Prehybridization solution: 6X SSC, 5X Denhardt's solution, 0.5% SDS, 100 μg/mL denatured salmon sperm DNA.
14. Nylon filter.
15. Fluorescence ruler.
16. UV light and photography system.
17. 46 × 57 cm Whatman 3 MM paper and paper towel.
18. Sponge.
19. Glass rod.
20. Hybridization tubes.
21. Hybridization oven.
22. Washing solutions (1X SSC, 0.1% SDS, and 0.25X SSC, 0.1% SDS).
23. Phosphor-Imager (Molecular Dynamics, Sunnyvale, CA).

2.7. Quantitation of RT-PCR Products

1. 15 mL 5% polyacrylamide gel [10X TBE 1.5 mL, 30% polyacrylamide 2.5 mL, H_2O 11 mL, 10% ammonium persulfate 50 μL (APS), N,N,N'N'-tetramethylethyenediamine (TEMED) 15 μL].
2. 100 bp DNA molecular-weight marker.
3. 50 mL ddH_2O.
4. Gel Drying System (Fisher Scientific, Pittsburgh, PA).
5. Phosphor-Imager (Molecular Dynamics, Sunnyvale, CA).

3. Methods

3.1. RNA Preparation

The following procedure is for 0.5 g of tissue.

1. Remove tissues from rats or take tissues out of liquid nitrogen quickly.
2. Cut them into pieces and transfer them to a 25-mL SW-28 tube.
3. Add 10 mL of Solution D.
4. Homogenize tissue with two or three 10-s bursts.
5. Add 1.0 mL of 2.0 *M* sodium acetate (pH 4.0) and mix thoroughly by gentle inversion.
6. Add 10 mL of phenol:chloroform:isoamyl alcohol (25:24:1) and mix by vortexing for 10–15 s, place on ice for 15–20 min.
7. Centrifuge at 12,000*g* for 20 min at 4°C.
8. Carefully transfer the top aqueous phase to a fresh DEPC-treated tube.
9. Add an equal volume of 100% isopropanol and incubate the sample at –20°C for 2 h.
10. Pellet RNA by centrifugation at 12,000*g* for 15 min at 4°C.
11. Discard supernatant and resuspend RNA pellet in 4.0 mL of solution D and vortex until RNA is dissolved.
12. Add equal volume of 100% isopropanol and incubate at –20°C for more than 1 h.
13. Centrifuge at 14,000*g* for 15 min at 4°C.
14. Wash pellet with 5–10 mL of ice-cold 75% ethanol and pellet once more.
15. Discard supernatant and dry RNA pellet at ambient temperature.
16. Resuspend RNA in 200 μL of DEPC-treated H_2O and take 1.0 μL RNA to test OD_{260nm} and store the rest at –70°C (*see* **Note 3**).

3.2. Internal Standard Preparation

3.2.1. Construct of AT1 internal standard

1. Mix 2.0 μL (1.0 μg/μL) of plasmid pSK-AT1A, 1.0 μL (10 U/μL) of *Acc*I, 1.0 μL (10 U/μL) of *Eco*RI, 2.0 μL of 10X buffer, and 14 μL of ddH_2O. Incubate at 37°C for 1 h.
2. Run sample on 0.8% agarose gel, 80 V for 1.5 h.
3. Cut out a 4.0-kb band using a razor blade and recover DNA fragments by QIAquick Gel Extraction Kit.
4. Blunt and ligate purified DNA by DNA blunting and ligation kit.
5. Obtain plasmid pAT1-Int containing a mutant AT1A cDNA with a 51-nucleotide deletion (nucleotide 509–560). Complete AT1A, but not AT1B, has an *Eco*RI site within two primers, which can be used to distinguish PCR products of AT1A from AT1B by *Eco*RI digestion (**Fig. 1**).
6. Prepare large amount of plasmid pAT1-Int.

3.2.2. Preparation of Internal Standard cRNA

1. Mix 10 μL (1 μg/μL) of plasmid pAT1-Int, 5.0 μL (10 U/μL) of *Sal*I, 10 μL of 10X buffer, and 75 μL of ddH_2O. Incubate at 37°C for 1 h.

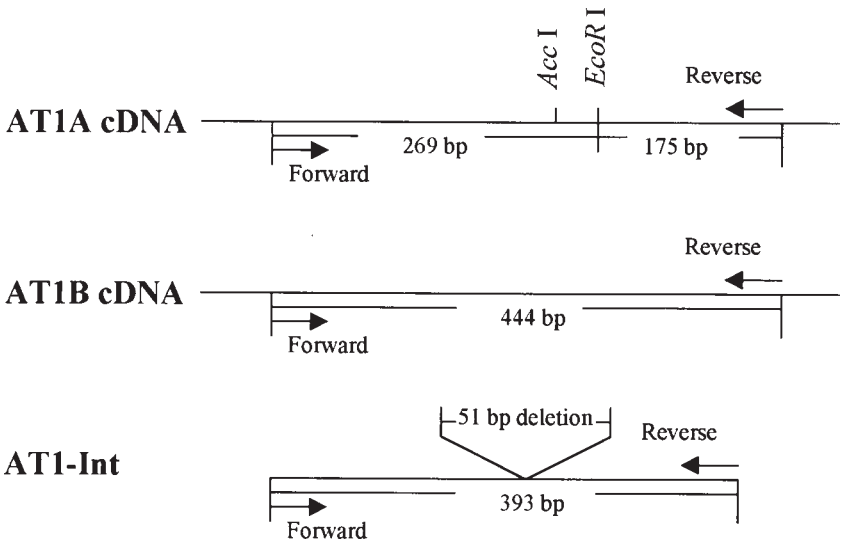

Fig. 1. cDNA structures for rat angiotensin II receptor AT1A, AT1B, and internal standard AT1-Int. Left arrows indicate forward primers and right arrows indicate reverse primers. After *Eco*RI digestion, AT1A cDNA is cleaved into two fragments (269 bp and 175 bp), whereas AT1B cDNA (444 bp) and the internal standard (393 bp) remain the same sizes.

2. Run sample on 0.8% agarose gel and recover linearized DNA using QIAquick Gel Extraction Kit.
3. Mix 5 μg of linearized pAT1-Int, 20 μL of 5X transcription buffer, 2.5 μL of 20 m*M* each NTP, 1.0 μL of 1.0 *M* DTT, 100 U of *T7* RNA polymerase. Add H_2O to make final volume of 100 μL. Incubate at 37°C for 2 h.
4. Add 5.0 U RNase-free DNase I. Incubate at 37°C for 20 min (*see* **Notes 4** and **5**).
5. Add an equal volume of phenol and vortex vigorously for 30 s.
6. Spin at 14,000*g* for 3 min at 4°C.
7. Remove supernatant and add an equal volume of phenol:chloroform:isoamyl alcohol (25:24:1).
8. Vortex for 30 s and spin at 14,000*g* for 3 min at 4°C.
9. Mix supernatant with an equal volume of chloroform in a new tube.
10. Vortex for 30 s and spin at 14,000*g* for 4 min at 4°C.
11. Transfer supernatant to a 1.5-mL Eppendorf tube and add 10 % volumes of 3.0 *M* sodium acetate pH 5.0 and an equal volume of 100% isopropanol.
12. Mix and spin at 14,000*g* for 10 min at 4°C and resuspend pellet in 20 μL of DEPC-treated H_2O.
13. Measure cRNA concentration and ratio of OD_{260nm}/OD_{280nm} by spectrophotometer and check the quality of synthesized cRNA by running a 0.8% agarose formaldehyde gel.

3.3. Reverse Transcription (First Stranded cDNA Synthesis)

1. In 1.5-mL tubes (4–8 tubes), mix 5.0 μg RNA and internal standard cRNA with serial dilutions depending on mRNA abundance.
2. Add DEPC-treated H_2O to 14.5 μL.
3. Add 0.5 μL of 10 m*M* reverse primer. Mix and incubate at 70°C for 10 min.
4. Place the tubes on ice for 5 min.
5. Add 4.0 μL of 5X RT reaction buffer.
6. Add 1.0 μL of MMLV.
7. Mix and incubate at 42°C for 50 min.
8. Incubate at 90°C for 10–15 min and place the tubes at 4°C for PCR.

3.4. PCR

1. Mix 4.0 μL of RT products, 4.0 μL of 10X PCR, 1.6 μL of 2.5 m*M* for each dNTP, 0.5 μL (5.0 U/mL) of *Taq* DNA polymerase, 0.8 μL of 10 μ*M* forward primer, 0.8 μL of 10 μ*M* reverse primer, and 0.1 μL of [α-^{32}P] dCTP. Add ddH_2O to 40 μL and mix gently.
2. Place tubes into a PCR thermal cycler and run program as follows:
   a. 94°C for 2 min.
   b. 94°C for 30 s, 55°C for 45 s, 72°C for 1 min, 30 cycles.
   c. 72°C for 5 min.
   d. 4°C for as long as you desire.

3.5. Digestion of PCR Products of AT1A and AT1B

1. In a tube, add 10 μL of PCR products and 1.0 μL of 10 U/μL *Eco*RI.
2. Mix well and incubate at 37°C for 2 h.

3.6. Southern-Blot Analysis

1. Set up PCR without isotope. Load 10 μL of undigested or digested PCR products on 1.5% agarose gel containing 0.5 ng/mL ethidium bromide and run gel at 3.5 V/cm for 1.5 h.
2. Photograph the gel with a ruler (minimize the time that the gel is exposed to UV). Trim away any unused areas with a razor blade.
3. Soak the gel in 2–3 vol of denaturation solution for 30 min with gentle agitation. Rinse the gel briefly with ddH_2O, and then soak the gel twice in 2–3 vol of neutralization solution for 20 min each.
4. Cut one piece of nylon filter that is 1 mm larger than the gel in both dimensions and wet filter in ddH_2O completely.
5. Add 10X SSC in a tray. Place a large piece of sponge in tray and wet sponge completely, and then make sure the level of liquid is 2–5 mm below the top of sponge. Place two pieces of 3MM wick that are larger than the gel on sponge and get rid of air bubbles between wick and sponge using a glass rod.
6. Drain and invert gel and place it on the top of Whatman 3MM wick. Remove air bubbles between gel and 3MM paper. Cover tray but not the gel with Saran Wrap or Parafilm.

7. Place wet filter on the top of the gel. Make sure there are no bubbles between filter and gel.
8. Wet two pieces of Whatman 3MM papers that are the same size as the gel in 2X SSC and place them on the top of filter. Smooth out any bubbles with a glass rod.
9. Place towels on the top of the 3MM paper. Put a glass plate on the top and a 0.5 kg of weight on glass plate.
10. Allow the transfer to proceed for 12–24 h.
11. Dissemble transfer system and mark filter by cutting upper right-hand corner. Soak filter in 2X SSC for 5 min.
12. Drain filter and place it flat on a piece of 3MM paper. Crosslink it for about 1 min by UV at wavelength of 320 nm.
13. Place filter in hybridization tube and add 5 mL prehybridization solution. Prehybridize for 3 h at 65°C in a hybridization oven.
14. Prepare probe by Random Primers DNA Labeling System. Boil the labeled probe at 100°C for 5 min then place it on ice immediately.
15. Remove prehybridization solution and add new prehybridization solution.
16. Add denatured probe to the hybridization tube. Hybridize for 12–24 h at 65°C. Remove filter and wash as follows: 1X SSC, 0.1% SDS, room temperature (twice, each for 15 min), followed by 0.25X SSC, 0.1% SDS at 65°C (twice, each for 15 min).
17. Cover the filter with Saran Wrap.
18. Place it on Phosphor-Imager Storage Phosphor Screen and close the cassette.
19. Put the cassette into the Phosphor-Imager to quantitate the radioactivity of bands.

3.7. Quantitation of RT-PCR Products

1. Load ¼ volumes of PCR products or digested PCR products on 5% polyacrylamide gel. Run gel at 100 V for 1 h.
2. Dissemble gel-running system and mark the gel by cutting off the upper right-hand corner.
3. Wash the gel with 50 mL of ddH_2O in a tray.
4. Drain the gel, lay it on a piece of 3MM paper and cover it with Saran Wrap.
5. Dry the gel using Gel Drying System at 80°C for 1 h.
6. Place the dried gel on Phosphor-Imager Storage Phosphor Screen and close the cassette.
7. Put the cassette into the Phosphor-Imager to quantitate the radioactivity of bands.

4. Notes

1. The key of successful competitive RT-PCR is to have equal amplification efficiency for the target genes and competitor genes. Thus, first, the optimized fragment size difference between target and internal standard genes should be chosen to ensure the equal amplification efficiency and good visualization. Second, similar base composition is required for target and standard genes. Finally, the difference between the initial amount of target gene and standard gene should not be excessive so that the amount of products of both templates exceed the deletion limit before the end of the exponential phase is reached.

2. If two pairs of primer are used, they should be compatible with similar melting temperature and without primer–primer binding. Furthermore, the sequences for primer binding should be pretty identical for target and standard genes.
3. Initial tissue RNA amount for RT should be optimized depending on AT1 receptor abundance in the tissues. For instance, we used 2.0 μg of total RNA for the kidney tissue and 0.5 μg of total RNA for the aorta tissue ***(10)***.
4. Template RNA should not be contaminated with genomic DNA after DNase I treatment. Run 0.8% agarose formaldehyde gel and measure optical density to determine RNA quality. In addition, it is strongly recommended to use proper pipets for accuracy and aerosol tips to avoid any contamination.
5. Negative control tubes are necessary at both RT and PCR reactions to monitor any contamination.

Acknowledgments

This work was supported in part by National Institute of Health grants HL-52279 and HL-57853. Dr. Wang is an Established Investigator of the American Heart Association.

References

1. Becker-Andre, M. and Hahlbrock, K. (1989) Absolute mRNA quantification using polymerase chain reaction. A novel approach by PCR aided transcript titration assay (PATTY) *Nucleic Acids Res.* **17,** 9437–9446.
2. Hayward-Lester, A., Oefner, P. J., Sabatini, S., and Doris, P. A. (1995) Accurate and absolute quantitative measurement of gene expression by single-tube RT-PCR and HPLC. *Genome Res.* **5,** 494–499.
3. Zimmermann, K. and Mannhalter, J. W. (1996) Technical aspects of quantitative competitive PCR. *Biotechniques* **21,** 268–279.
4. Reischl, U. and Kochanowsk, B. (1995) Quantitative PCR: a survey of the present technology. *Mol. Biotechnol.* **3,** 55–71.
5. Vanden Heuvel, J. P., Tyson, F. L., and Bell, D. A. (1993) Construction of recombinant RNA templates for use as internal standards in quantitative RT-PCR. *Biotechniques* **14,** 395–398.
6. de Kant, E., Rochlitz, C. F., and Herrmann, R. (1994) Gene expression analysis by competitive and differential PCR with anti-sense competitors. *Biotechniques* **17,** 934–942.
7. Apostolakos, M. J., Schuermann, W. H. T., Frampton, M. W., Utell, M. J., and Willey, J. C. (1993) Measurement of gene expression by multiplex competitive polymerase chain reaction. *Anal. Biochem.* **213,** 277–284.
8. Llorens-Cortes, C., Greenberg, B., Huang, H. M., and Corvol, P. (1994) Tissular expression and regulation of type I angiotensin II receptor subtypes by quantitative reverse transcriptase-polymerase chain reaction analysis. *Hypertension* **24,** 538–548.
9. Wang, D. H., Du, Y., Yao, A. Q., and Hu, Z. Y. (1996) Regulation of type I angiotensin II receptor and its subtype gene expression in kidney by sodium loading and angiotensin II infusion. *J. Hypertens.* **14,** 1409–1415.
10. Wang, D. H., Du, Y., and Yao, A. Q. (1996) President's symposium. Regulation of the gene-encoding angiotensin II receptor in vascular tissue. *Microcirculation* **3,** 237–239.

12

Analysis of RNA by Northern-Blot Hybridization

Patricia E. Gallagher and Debra I. Diz

1. Introduction

Northern-blot hybridization, also referred to as Northern blotting, is one of several methods developed to detect the presence, to determine the size, and to quantify specific cellular mRNAs. By this method, total RNA or poly(A)$^+$ mRNA, prepared from the cells or tissue of interest, is fractionated by size on a denaturing agarose gel. The separated RNAs are transferred to a membrane by capillary action or under a vacuum and hybridized to a labeled probe with a base sequence complementary to all or part of the target mRNA. Analysis of hybridization signals determines whether the gene of interest is expressed in the cells or tissue, as well as the size and relative quantity of the target mRNA, if appropriate markers are used.

The following method for Northern-blot hybridization is a modification of several previously published procedures ***(1–5)***.

2. Materials

2.1. Isolation of Total RNA

1. TRIzol Reagent (Gibco-BRL/Life Technologies, Gaithersburg, MD).
2. Sterile glass-Teflon or power homogenizer.
3. Chloroform.
4. Isopropyl alcohol.
5. Deionized water treated with diethylpyrocarbonate (DEPC-treated water): DEPC (1.0 mL) is incubated with 1 L of deionized water overnight and the mixture is sterilized in the autoclave.
6. Cold 70% ethanol in DEPC-treated water

2.2. Isolation of Poly(A$^+$) RNA

1. 5.0 *M* NaOH.
2. DEPC-treated water.

From: *Methods in Molecular Medicine, vol. 51: Angiotensin Protocols*
Edited by: D. H. Wang © Humana Press Inc., Totowa, NJ

3. 0.1 *M* NaOH.
4. 2.0-mL glass column.
5. Oligo(dT) cellulose: 0.5 g suspended in 1.0 mL 0.1 *M* NaOH.
6. Binding buffer: 20 m*M* Tris-HCl, pH 7.5, 1.0 m*M* ethylenediaminetetraacetic acid (EDTA), 0.5 *M* LiCl, 0.2% sodium dodecyl sulfate (SDS).
7. 2X binding buffer: 40 m*M* Tris-HCl, pH 7.5, 2.0 m*M* EDTA, 1.0 *M* LiCl, 0.4% SDS.
8. Wash buffer: 20 m*M* Tris-HCl, pH 7.5, 1.0 m*M* EDTA, 0.15 *M* LiCl, 0.2% SDS.
9. Elution buffer: 20 m*M* Tris-HCl, pH 7.5, 1.0 m*M* EDTA, 0.2% SDS.
10. 5.0 *M* ammonium acetate.
11. Cold absolute ethanol.
12. Cold 70% ethanol.

2.3. Fractionation of RNA by Gel Electrophoresis

1. Molecular biology grade agarose.
2. DEPC-treated water.
3. 10X 3-(N-morpholino)-propanesulfonic acid (MOPS) buffer: 0.4 *M* MOPS, pH 7.0, 0.1 *M* sodium acetate, 10 m*M* EDTA.
4. Formaldehyde.
5. Agarose gel electrophoresis apparatus with gel casting mold and well-forming comb.
6. 12.3 *M* formamide.
7. Gel loading buffer: 1X MOPS, pH 7.0, 0.25% bromophenol blue, 0.25% xylene cyanol, 50% sterile glycerol.
8. 0.25 *M* ammonium acetate.
9. Ethidium bromide (5 μg/mL) in 0.5 ammonium acetate.
10. UV transilluminator.

2.4. Transfer of RNA to Membranes

1. DEPC-water.
2. 20X SSC: 3 *M* NaCl, 0.3 *M* sodium citrate, pH 7.0.
3. A commercial sponge.
4. Glass dish.
5. Whatman 3MM filter paper.
6. Plastic wrap.
7. Nylon or nitrocellulose membrane.
8. Paper towels.
9. Glass plate.
10. 0.2–0.4 kg weight.
11. 2X SSC: 0.3 *M* NaCl, 30 m*M* sodium citrate, pH 7.0.
12. Vacuum oven or UV transilluminator.

2.5. Hybridization of Probe

1. 6X SSC: 0.9 *M* NaCl, 90 m*M* sodium citrate, pH 7.0.
2. Hybridization oven and tubes or heat sealer, heat-sealable bag, and rotating water bath or incubator.
3. 5X SSC: 7.5 *M* NaCl, 75 m*M* sodium citrate, pH 7.0.

4. 50X Denhardt's solution: 5 g bovine serum albumin (BSA), 5 g polyvinylpyrrolidine, 5 g Ficoll 400 on 500-mL DEPC-treated water; filter sterilize.
5. Prehybridization/hybridization buffer: 50 m*M* sodium phosphate, pH 7.0, 5X SSC, 5X Denhardt's solution, 50% (w/v) formamide, 1% (w/v) SDS, 100 μg/mL denatured salmon sperm DNA.
6. Radiolabeled or fluorescent-labeled DNA or RNA probe in prehybridization/hybridization buffer.
7. 2X SSC: 0.3 *M* NaCl, 30 m*M* sodium citrate, pH 7.0.
8. 2X SSC/0.1% SDS (w/v).
9. 0.2X SSC/0.1% SDS (w/v).
10. Plastic wrap.
11. X-ray film, intensifying screen, X-ray cassette.
12. Stripping solution: 40 m*M* Tris-HCl, pH 7.5, 1% SDS, 0.1X SSC.

3. Methods

3.1. Isolation of Total RNA or Poly(A^+) RNA

1. Tissue is homogenized in TRIzol reagent at a concentration of 50–100 mg/mL using a sterile glass-Teflon or power homogenizer. Monolayer cells are lysed directly on the culture dish following the removal of the media by adding 3.0 mL TRIzol reagent per 100-mm dish. Cells grown in suspension are isolated by centrifugation and resuspended in 1.0 mL TRIzol reagent per 5–10 × 10^6 animal, plant, or yeast cells, or 1 × 10^7 bacterial cells (*see* **Notes 1–6**).
2. The samples are placed in a capped test tube and can be frozen for processing later or incubated at 15–30°C for 10–15 min followed by the addition of 0.2 mL chloroform/mL of TRIzol reagent.
3. The mixtures are shaken by hand for 15 s, incubated at 15–30°C for 10-15 min, and the aqueous phase is separated from the red, phenol-chloroform phase by centrifugation at 10,000*g* for 15 min at 4°C.
4. The aqueous phase collected in a new tube is mixed with isopropyl alcohol (one-half the volume of the TRIzol reagent used in the initial homogenization) and incubated at 15–30°C for 10 min.
5. The RNA precipitate is isolated by centrifugation at 10,000*g* for 10 min at 4°C. The precipitate often is not visible or forms a gel-like pellet at the side or bottom of the tube.
6. The RNA pellet is gently rinsed with 70% ethanol in DEPC-treated water. The tubes are inverted and air-dried to remove excess ethanol. Do not allow the pellets to dry completely to avoid difficulties with resuspension.
7. The pellets are resuspended in 15–50 μL DEPC-treated water. The solution can be heated at 55°C for 10 min to aid the resuspension process. Approx 1–10 μg of total RNA is obtained per mg tissue or 5–15 μg per 10^6 mammalian cells.

3.2. Isolation of Poly(A^+) mRNA

In some instances, particularly the detection and quantification of rare mRNAs, it is preferable to use poly(A^+) mRNA instead of total RNA as the source material for the Northern-blot analysis.

1. A glass column is rinsed with 10 mL 5.0 *M* NaOH followed by 20 mL DEPC-treated water.
2. A slurry of oligo(dT) cellulose (0.5 g/1.0 mL 0.1 *M* NaOH) is poured into the column, washed with 10–20 mL DEPC-treated water, and rinsed with 20 mL binding buffer. The size of the column is based on the resin capacity supplied by the manufacturer.
3. Approx 2 mg total RNA in DEPC-treated water is heat denatured at 70°C for 10 min followed by the addition of an equal volume of 2X binding buffer.
4. The denatured RNA is loaded on the column resin at approximately 10 mL/h. The resultant eluate is passed through the resin two more times to ensure complete binding.
5. The resin is rinsed with wash buffer until the optical density at 260 nm is at a minimum.
6. Poly(A^+) mRNA, released from the resin with elution buffer, is collected in 0.5-mL fractions in sterile microfuge tubes.
7. Fractions containing the mRNA are determined by monitoring the optical density at 260 nm.
8. If desired, the poly(A^+) mRNA can be further purified by a second chromatography through a new or reequilibrated oligo(dT) cellulose column (*see* **Note 7**).
9. The pooled fractions are mixed with one-tenth-volume 5.0 *M* ammonium acetate and 2.5 volumes cold absolute ethanol and the sample is incubated overnight at –20°C or for 60 min in an ethanol/dry ice bath.
10. The mRNA precipitate is isolated by centrifugation in a microfuge at 4°C for 20 min.
11. The subsequent pellet is washed twice with 70% ethanol to remove residual SDS, and dissolved in DEPC-treated water. Approx 1% of the starting total RNA is isolated as poly$(A)^+$ RNA.

3.3. Fractionation of RNA by Gel Electrophoresis

The RNA is separated under denaturing conditions to eliminate secondary structures formed in by intramolecular base pairing.

1. Agarose (1.0 g) is dissolved by boiling in 72 mL DEPC-treated water and cooled to 60°C in a water bath followed by the addition of 10 mL 10X MOPS running buffer and 18 mL formaldehyde in a fume hood. This mixture yields a 1% agarose gel, which separates RNA molecules of 0.5–10 kb. The agarose concentration is varied depending on the size range of the RNA molecules to be fractionated. Additionally, the recipe may be increased or decreased depending on the amount of the mixture required to fill the gel apparatus.
2. The mixture is poured into a gel former and allowed to set in a fume hood. The gel should be about 3–6 μm thick with wells of sufficient size to hold 60 μL of sample (*see* **Note 8**).
3. 11 μL RNA (0.5–3.0 μg poly$(A)^+$ RNA or 5–20 μg total RNA) is mixed with 25 μL 12.3 *M* formamide, 9.0 μL formaldehyde, and 5 μL 10X MOPS buffer and heated to 60°C for 15 min to denature the sample.

4. The mixture is cooled, followed by the addition of 10 μL gel loading buffer and duplicate samples are loaded into wells on the opposite side of the gel. One lane will be stained and the other will be transferred to a nylon or nitrocellulose membrane for hybridization.
5. The RNA is fractionated in 1X MOPS buffer at 5–6 V/cm in a fume hood or closed apparatus until the blue dye marker has migrated one-half to two-thirds the length of the gel. The gel running time is usually about 3 h.
6. The gel is removed from the electrophoresis apparatus and the lanes to be stained are cut from the remainder of the gel containing the lanes to be transferred to the membrane.
7. The gel piece to be stained is covered with 0.25 *M* ammonium acetate and incubated for 40 min at room temperature with a change in the soaking solution after half the time has elapsed. This will remove the formaldehyde, which will bind to the ethidium bromide and enhance background staining.
8. The soaking solution is removed and the gel piece is incubated in ethidium bromide (0.5 μg/mL) in 0.25 *M* ammonium acetate for 40 min at room temperature (*see* **Note 9**).
9. The RNA bands are visualized by illumination with UV light and photographed with a ruler to later identify band positions. If the background fluorescence is too intense to see the RNA, the gel can be destained in 0.25 *M* ammonium acetate for 10–40 min at room temperature.
10. If total RNA is fractionated, the rRNA is seen as sharp bands. If poly(A^+) mRNA is fractionated, mixtures of RNA molecules of known size are purchased commercially and loaded into adjacent wells as molecular weight markers.

3.4. Transfer of RNA to Membranes

1. The gel is washed in DEPC-treated water with gentle agitation for 10 min to remove the formaldehyde and equilibrated in 20X SSC (10 gel volumes) for an additional 20 min with agitation.
2. The 20X SSC soaking step is repeated with fresh solution.
3. A sponge, washed with DEPC-treated water, is placed in a glass dish filled about two-thirds with 20X SSC. Three pieces of Whatman 3MM filter paper, the size of the sponge, are layered on the sponge and wetted with 20X SSC.
4. The edges of the gel are covered in plastic wrap about 1 cm, the gel is placed on the filter paper comb-side down, and any air bubbles are removed by rolling a glass pipet over the surface of the gel.
5. Nylon or nitrocellulose membrane (*see* **Notes 10** and **11**), the size of the exposed gel surface, is soaked first in DEPC water for 5 min. Nitrocellulose membranes receive a second soaking in 20X SSC for 10 min.
6. The nylon or nitrocellulose membrane is placed on the gel, air bubbles are removed by rolling a glass pipet over the membrane, and the membrane surface is covered with 20X SSC. The bottom side of the gel should be in contact with the membrane to minimize the distance the RNA must migrate out of the gel to the membrane.

7. Five pieces of Whatman 3MM filter paper, wetted with 20X SSC and cut to the size of the membrane, are placed on the membrane and air bubbles are removed as described.
8. A stack of paper towels (about 4 cm in height), also cut to the size of the membrane, is placed on the filter paper.
9. Finally, a glass plate is placed on the paper towels and a 0.2–0.4 kg weight is added on top. The stack is incubated overnight to allow transfer of the RNA from the gel to the membrane.
10. The recovered membrane is marked with pencil to indicate the proper orientation, rinsed with 2X SSC to remove excess salt and any adhering agarose fragments, and dried on a piece of Whatman 3MM filter paper.
11. The gel is stained with ethidium bromide, as aforementioned, to ensure efficient transfer of the RNA to the membrane.
12. The nitrocellulose or nylon membrane is heated between two pieces of Whatman 3MM filter paper in a vacuum oven at 80°C for 2 h to immobilize the RNA and to remove the formaldehyde. Alternatively, dried nylon membranes can be wrapped in plastic wrap and irradiated RNA-side down on a UV transilluminator or in a Stratagene Stratalinker UV light box (*see* **Note 12**). A covalent binding of the RNA to the membrane is produced by UV light, allowing multiple probe analysis of the membrane.

3.5. Hybridization of Probe

1. The nylon or nitrocellulose membrane is wet with 6X SSC and placed in a hybridization oven tube followed by the addition of 1.5 mL prehybridization/hybridization solution/10 cm^2 of membrane. If a hybridization oven is not available, the wetted membrane can be placed in a heat-sealable polyethylene bag, the prehybridization/hybridization solution is added, and the bag sealed
2. The membrane is rotated in the hybridization oven for 3 h at 50°C for DNA probes or 60°C for RNA probes (*see* **Note 13**). Alternatively, membranes contained in heat-sealed bags can be incubated in a rotating water bath or incubator.
3. The probe (10–15 mL) in prehybridization/hybridization solution is added to the hybridization tube or bag and rotation of the membrane is continued overnight at the indicated temperature. The final concentration of a radiolabeled probe in the hybridization solution should be about 10–15 ng/mL, if the specific activity is in the range of 10^8 dpm/μg or 2–4 ng/mL if the specific activity is 10^9 dpm/mg.
4. The hybridization solution is removed, twice the volume of 2X SSC/0.1% SDS is added, and the membrane is rotated or agitated for 5 min at room temperature. The 2X SSC/0.1% SDS solution is changed and the membrane is incubated for an additional 5 min with rotation or agitation. For convenience, the membrane is removed from heat-sealable bags and placed in a plastic box for these wash procedures.
5. The wash solution is removed and the membrane is incubated twice in an equal volume of 0.2X SSC/0.1% SDS for 5 min at room temperature with rotation or agitation.

6. If an increased stringency wash is desired, the membrane is incubated twice in 0.2X SSC/0.1% SDS (warmed to 45°C) for 15 min at 45°C.
7. For higher stringency washes, two additional incubations in 0.1X SSC/0.1% SDS (warmed to 70°C) for 15 min at 70°C are performed.
8. The last wash solution is removed and the membrane is rinsed with 2X SSC at room temperature, the excess liquid is blotted dry, and the membrane is stored in plastic wrap. The membrane should not dry completely, if subsequent stripping and additional hybridization is desired.
9. Hybridization of the radiolabeled probe to the fractionated RNA is visualized by autoradiography with X-ray film using an intensifying screen (*see* **Note 14**). Band intensity is determined using a densitometer.
10. Generally, membranes are rehybridized with a control probe for subsequent normalization and quantification of the target signals (*see* **Note 15**). Hybridized probes can be stripped from nylon membranes with boiling water to use the blots multiple times. To remove bound probe, the nylon membrane is incubated in 80°C water for 10 min in a hybridization bag containing stripping solution.
11. The stripping solution is removed and the process is repeated three times.
12. The membrane is blotted dry on filter paper and analyzed by autoradiography for a radiolabeled probe or chemiluminescent detection for a fluorescence-labeled probe to ensure complete stripping of the probe occurred (*see* **Notes 16** and **17**).
13. If the hybridization probe remains, repeat the above procedure at 100°C or incubate the membrane at 65°C for 10 min in stripping solution mixed with an equal volume of formamide.

4. Notes

1. Gloves must be worn at all times when handling RNA samples or equipment used in RNA extraction, because of the ribonucleases found on the skin.
2. All glassware should be baked at 150°C in a dry heat oven for at least 2 h to eliminate all RNase activity or sterile, disposable glass or plasticware should be used.
3. Each laboratory personnel should have their own reagents and labware to prevent cross-contamination with RNases.
4. Solutions used for RNA studies should be prepared with DEPC-treated water and sterilized, whenever possible.
5. It is preferable to use equipment specifically designated for RNA experiments. If this is not feasible, all equipment pieces should be soaked in 2–5% SDS for 2–4 h.
6. DEPC is a suspected carcinogen and should be handled accordingly. Formaldehyde is toxic to the skin and the vapors can damage eye and respiratory tissue. All procedures involving formaldehyde should be performed in a fume hood.
7. The oligo(dT) cellulose can be cleaned by washing with 0.3 *M* NaOH and then loading buffer containing 0.02% (w/v) sodium azide until the pH returns to 7.5.
8. The agarose gel should be thick enough to provide an ample sized well for the sample volume, however, it should be noted that the thinner the gel the more efficient the transfer of the RNA to the hybridization membrane.

9. The ethidium bromide concentration should not exceed 10 μg/mL gel solution. Ethidium bromide can be added to the gel prior to electrophoresis, if it is not possible to run a duplicate sample for subsequent analysis by ethidium bromide staining. However, ethidium bromide adversely affects the transfer efficiency of the RNA to the membrane.
10. Nitrocellulose and nylon membranes should be handled with blunt-ended forceps only to avoid contamination by RNases.
11. Nitrocellulose membranes are more fragile and less suitable for reprobing than nylon membranes. In addition, nylon membranes have a higher binding capacity for nucleic acids than nitrocellulose membranes, however nylon membranes are more likely to have a high background. These characteristics should be considered in choosing the appropriate membrane.
12. UV crosslinkers and transilluminators should be properly calibrated as under-irradiation will not provide adequate linking of the RNA to the membrane and over-irradiation will damage the RNA.
13. Double-stranded DNA, antisense single-stranded DNA or antisense RNA can be used as a probe to identify gene-specific RNAs by Northern-blot hybridization. RNA probes have higher sensitivity than DNA probes, but can be less stable because of RNase degradation.
14. Speckled background on the X-ray film often indicates that there are unincorporated nucleotides in the probe preparation. Nonspecific hybridization, caused by insufficient washing of the membrane, produces a "blotchy" background.
15. Preliminary studies should be performed to ensure that the transcription of the positive control mRNA, used for normalization and quantification, is not affected by the experimental procedure. For example, GADPH mRNA, a conventional standard, is up-regulated by Ang II ***(6)***, hence, we use the abundant, housekeeping, transcript EF1α as a positive control mRNA.
16. It is imperative that all of the previously used probe is stripped from the blot before another round of hybridization is attempted, as the signal from the first probe could result in erroneous identification and quantification of the second mRNA analyzed.
17. Generally, nylon membranes can be stripped four or five times before irreversible damage occurs.

Acknowledgment

This study was supported by grants from the National Institutes of Health, HL-51952, and the National Science Foundation, IBN-9631166.

References

1. Zyskind, J. W. and Bernstein, S. I. (1989) Gel blotting, probe preparation, hybridization and hybrid detection, in *Recombinant DNA Laboratory Manual*, Academic, San Diego, CA, pp. 118–134.

2. Sambrook, J., Fritsch, E. F., and Maniatis, T. (1989*) Molecular Cloning: A Laboratory Manual*, 2nd ed. Cold Spring Harbor Laboratory Press, Cold Spring Harbor, New York.
3. Krumlauf, R. (1996) Northern blot analysis, in *Methods in Molecular Biology, Volume 58: Basic DNA and RNA Protocols*, (Harwood, A. J., ed.), Humana, Totowa, NJ, pp. 113–118.
4. Trayhurn, P. (1996) Northern blotting. *Proc. Nutr. Soc.* **55,** 583–589.
5. Greenberg, M. E. and Bender, T. P. (1999) Preparation and analysis of RNA, in *Current Protocols in Molecular Biology* (Ausubel, F. M., Brent, R., Kingston, R. E., Moore, D. D., Seidman, J. G., Smith, J. A., and Struhl, K., eds.), Wiley, New York, pp. 4.0.1–4.10.11.
6. Lassegue, B., Alexander, R. W., Nickenig G., Clark M., Murphy T. J., Griendling K. K. (1995) Angiotensin II down-regulates the vascular smooth muscle AT1 receptor by transcriptional and post-transcriptional mechanism: evidence for homologous and heterologous regulation. *Mol. Pharmacol.* **48,** 601–609.

13

Use of the Ribonuclease Protection Assay for the Analysis and Characterization of Target mRNAs

Scott C. Supowit and Donald J. DiPette

1. Introduction

Some of the most widely used techniques in the area of molecular biology involve the isolation, analysis, and quantification of RNA molecules, specifically mRNA molecules that code for proteins of interest. Indeed, the characterization of any gene entails the analysis of the spatial and temporal distribution of RNA expression. In many types of studies, it is also necessary to quantify alterations in the synthesis of specific mRNA species that occur both under normal physiological conditions and in the pathophysiology of diseases such as hypertension. To date, the three most popular methods to characterize RNA molecules and determine the abundance of a particular mRNA in a total or poly (A) sample are Northern-blot analysis, ribonuclease protection assays (RPAs), and reverse transcription-polymerase chain reaction (RT-PCR). In theory, each of these techniques can be used to quantify either the relative or absolute level of an individual RNA species in a population. However, in practice, each method has inherent technical and practical limitations that may pose significant problems under certain circumstances ***(1,2)***.

In light of the recent explosion in the number of reviews (including a chapter in this volume), articles, and technical bulletins that deal with RT-PCR, we will focus primarily on the RPA particularly as it compares to Northern-blot analysis that is still considered the standard for the detection and quantification of mRNA levels despite the development of more sensitive techniques ***(1,2)***. In this chapter, we will discuss the theoretical aspects of the RPA including what information can be obtained with this assay as well as the advantages and disadvantages of this technique. The details on the methods needed to construct

From: *Methods in Molecular Medicine, vol. 51: Angiotensin Protocols*
Edited by: D. H. Wang

the vectors used to generate the hybridization probes and perform the RPA are readily available in molecular biology laboratory manuals such as Maniatis *(3)*. However, based on our experience with this assay, discussions with other researchers who use the RPA, and an informal search of the recent literature, we strongly recommend that investigators use commercially available RPA kits because of their ease of use, reliability, and reproducibility. We have had excellent results with the products from Ambion, Inc. These include not only the RPA kit itself, but also the in vitro transcription kit and the probes for the internal standards. These kits, which will be discussed in more detail later in the chapter, come with in depth protocols on how to perform the assay as well as troubleshooting information. We have found that following these protocols exactly as described gives superior results. For this reason, it is why we have not included a detailed protocol in this chapter.

2. Northern-Blot Analysis—Advantages and Disadvantages

As stated previously Northern blot analysis remains the standard for analysis and quantification of mRNA. It is also the most commonly used technique for RNA analysis. The reason for the continued popularity of Northern analysis is that it is low tech, easy to use, and provides a considerable amount of information about the mRNA being studied. Northern-blot analysis allows for both relative and absolute quantification of mRNA content. It is the only method that gives the size of the mRNA species, and it is by far the easiest technique to determine the presence of alternatively spliced or multiple mRNAs generated from a single locus *(1,2)*. It should be noted that in order to distinguish between members of multigene families the mRNAs must be of different sizes. In addition, regardless of what the investigator plans to use the RNA for (analysis, cloning, etc.) Northern blot analysis is the superior method for evaluating the integrity of the isolated RNA.

One consideration, particularly if an investigator is just beginning to work with RNA, is the ease of use and the equipment needed to perform Northern-blot analysis. First, this technique only requires the use of agarose-gel electrophoresis equipment that is readily available and relatively inexpensive. Given the availability of commercially supplied RNA isolation kits, it is now a straightforward process for even a novice to consistently isolate high-quality RNA preparations from either cells or tissues. Once the RNA samples are prepared, Northern-blot analysis requires very little manipulation of the RNA. There are no enzymatic treatments or amplification steps required that might compromise the samples *(1–3)*.

Like other methods of mRNA analysis Northern blots can be used for relative or absolute quantitation. Relative quantitation compares mRNA levels across multiple samples on the same blot using an internal control for sample

normalization. This internal control is usually the RNA transcript of a housekeeping or constitutively expressed gene such as ribosomal RNA, actin, cyclophilin, and others ***(1,2)***. This, however, requires that the blot be stripped and rehybridized with the internal control specific probe that is a time-consuming process. This, of course is one disadvantage with Northern-blot analysis. Results are expressed as ratios of the gene-specific signal to the internal control signal. This yields a corrected relative value for the gene specific product in each sample. These values may be compared between samples to give the relative expression of the target RNA in the samples ***(1,2)***. Absolute quantitation of a particular mRNA is done by constructing a standard curve against which the target mRNA signal can be compared. To do this, one uses different concentrations of an exogenous standard (usually an artificial sense target RNA) which is spiked into RNA samples ***(1,2)***.

When compared to the other two techniques used for RNA analysis Northern blotting is the most versatile in regards to the type of probe that can be used in the hybridization reaction. In addition to high-specific activity, DNA probes labeled by random-priming or nick-translation, it is possible to generate antisense RNA probes of even higher specific activity through the use of in vitro transcription vectors ***(1)***. This technique also allows for the use of labeled synthetic oligonucleotide probes and can also tolerate probes with only partial homology such as a cDNA from a different species. A second example is a genomic DNA fragment that contains an exon or part of an exon that encodes a part of the target mRNA ***(1)***.

Even, though Northern-blot analysis is the method of choice in numerous laboratories, there are several disadvantages associated with this technique. The first is that of the three methods, Northern blotting is the most vulnerable to RNA degradation. If RNA samples are only slightly degraded, there is a significant reduction in the quality of the data and the ability to accurately quantify the levels of the target mRNA is also diminished. It has been demonstrated that a single cleavage in 20% of a 4-kb target will decrease the signal by 20% and increase the background of the blot ***(1)***. However, this should not be a problem for most investigators if they use proper RNase-free technique. Second, a more serious limitation is that the Northern-blot assay is the least sensitive of the three techniques. If one is dealing with a low-abundance mRNA (<50,000 copies/cell), it can present a real problem ***(1)***. There are, however, ways to greatly increase the sensitivity of this assay. As stated previously, one can generate very high-specific activity antisense RNA probes via in vitro transcription. It is also possible to get a significant enrichment of the mRNA population present in a total RNA sample by using oligo dT selection to purify the poly (A) mRNA species ***(1–3)***. This latter strategy is particularly useful because the maximum sample size for a typical RNA gel is approx 20 μg. The reasons

for this are physical constraints inherent in gel electrophoresis result in a marked loss of resolution at high RNA concentrations and it is also possible to saturate the transfer membrane when using greater than 20 μg of RNA *(2)*. Third, the Northern-blot assay is usually the most time-consuming of the three techniques, particularly if one is interested in analyzing multiple mRNA species. In addition to the time required for transferring the fractionated RNA to the membrane, it is not usually possible to add the probes for the target RNA and the RNA used for the internal control at the same time. If this is the case, then one must first hybridize with one probe (usually the one specific for the target RNA) and then perform the autoradiography or use a PhosphorImager. The membrane must then be stripped and rehybridized with the second probe. If multiple mRNAs are to be analyzed, then several cycles of hybridization, stripping, and rehybridization are required.

3. Ribonuclease Protection Assay

3.1. Materials

Refer to the protocol provided by the commercial supplier.

3.2. Methods

An extremely useful and sensitive alternative to Northern-blot analysis is the RPA. The basis of RPAs is solution hybridization of an antisense RNA probe (radiolabeled or nonisotopically labeled) with an RNA sample containing the RNA species of interest (**Fig. 1**).

1. To generate the probe a segment of DNA containing all or part of the gene of interest is inserted into a polycloning site immediately downstream from a bacteriophage T7 or SP6 promoter, in an orientation that leads to the production of antisense RNA *(3)*.
2. The recombinant plasmid is digested with a restriction enzyme that cleaves at a site within the gene or at a site in the plasmid downstream from it. The linearized plasmid is then transcribed on the presence of ^{32}-P-labeled rNTPs with the appropriate RNA polymerase to produce an RNA that extends from the initiation site of the promoter to the end of the DNA fragment.
3. An excess of the antisense probe is used in the hybridization reaction so that all complementary sequences are driven into RNA:RNA hybrids.The amount of radiolabled RNA required to drive hybridization to completion is usually determined empirically in preliminary experiments *(3)*.
4. Following the hybridization reaction, which is usually performed overnight, excess single-stranded probe and unhybridized RNA molecules, both target and nontarget, are degraded by RNase treatment. Double-stranded RNA molecules generated by the hybridization of the RNA probe with the target RNA are protected from the action of the ribonucleases.

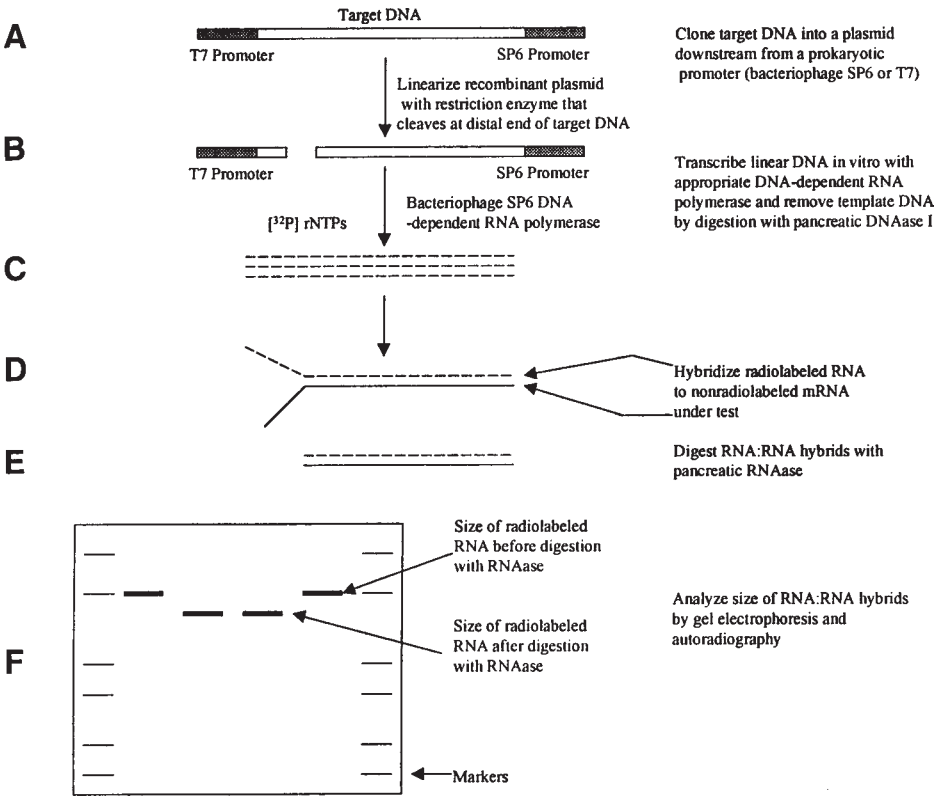

Fig. 1. Outline of the standard ribonuclease protection assay.

5. The protected hybrids can then be fractionated by denaturing polyacrylamide electrophoresis and visualized by autoradiography. Because the RNA:RNA hybrids are visualized directly on the gel no transfer to a membrane is required. Also, the RPA offers at least ten times the sensitivity of Northern blots and allows multiplexing, the use of multiple probes in a single assay. The marked increased in sensitivity and the ability to multiplex are the primary reasons why investigators choose to use the RPA instead of Northern-blot analysis. These advantages as well as the disadvantages of the RPA are discussed in more detail in the following section.

4. Ribonuclease Protection Assay—Advantages and Disadvantages

The key element of the RPA that allows for the significant enhancement of sensitivity is solution hybridization. Solution hybridization is far more efficient than filter based hybridization and can accommodate up to 100 μg total or

poly (A) of sample RNA compared to the 20 μg maximum sample size for Northern blotting. Whereas the detection limit of Northern-blot analysis is approx 50,000 copies of mRNA use of the RPA lowers this limit to approx 4,000 copies of mRNA ***(1–3)***. In practice, this means that even low-abundance mRNAs can be analyzed using this method unless one is limited by a very small sample size. In our laboratory, we have been able to detect (overnight exposure) calcitonin gene-related peptide mRNA, an abundant mRNA species produced in dorsal root ganglia sensory neurons, using only 100 ng of total RNA (unpublished data). The RPA is also much more tolerant of partial RNA degradation compared to Northern analysis. For example, a single cleavage in 20% of a 4-kb mRNA may only cause as little as a 1% loss of signal since cleavage is only detected in the region of overlap with the probe ***(2)***.

The RPA is also an excellent method to quantify either relative or absolute amounts of the RNA of interest. Like Northern-blot analysis, relative quantification compares mRNA levels across multiple samples on the same gel using an internal control for sample normalization. Like Northern-blot analysis, the control probe is targeted to an RNA whose level remains constant. However, unlike Northern-blot analysis, the probes for the target RNA and the internal control are both added to each sample provided that the protected hybrids are of different sizes. Moreover, gel to gel comparisons can be done by calculating the fold changes in each sample. Absolute quantification of an RNA species is also straightforward and, as in Northern-blot analysis, involves generating a concentration curve of synthetic sense strand target to which experimental sample signals can be compared.

The RPA is also the method of choice for multiplex quantification of several RNA species in the same sample. Another advantage of solution hybridization is that individual probe–target interactions are completely independent such that several target RNAs and appropriate controls may be assayed simultaneously ***(1,2)***.The use of multiple probes in a single assay increases the quantity and quality of data that can be obtained compared to separate analysis of individual mRNAs. Experimental variability is greatly reduced by measuring target mRNAs in the same sample. This assay results in a lower level of background than Northerns, because there is no filter and nonspecific binding of probe to results in the formation of short regions of duplex, which are well separated from the true protected hybrids on a denaturing gel. In addition, cross-hybridization of the probe to closely related mRNAs, which can sometimes compromise accurate quantification in the Northern, is not a problem with the RPA because mismatched regions of the RNA duplex are cleaved by the ribonucleases.

The primary limitation of the RPA is that this assay does not provide information about the size of the transcript. Protected fragment size is determined

entirely by the homologous region of probe with the target that is usually only several hundred nucleotides. Another drawback to performing RPAs is that one can only use antisense RNA probes. Genomic DNA fragments, cDNA inserts and oligonucleotides will not work in this assay. The RPA is also somewhat inflexible in terms of probe size. Probes ranging in size from 150 to 600 bases are preferable. Shorter probes provide less signal, whereas longer probes may produce smeary signals caused by probe breakdown products ***(1)***. Regardless of the probe length, it is important that the length of the complementary portion of the probe (the part which binds to the target RNA and is protected in the assay) be resolvable from the full length probe when run on a gel. This is accomplished by setting up the in vitro transcription reaction so that a portion of the plasmid vector (usually part of the polycloning site) is transcribed as part of the antisense probe. This ensures that the protected fragment migrates differently from the full-length probe. Therefore, the resulting signal caused by probe–target hybridization and not to incomplete digestion of the probe alone ***(3)***. Probe specific activities can be varied depending on the needs of the investigator. Probe specific activities between 10^5 and 10^6 cpm/ng are recommended. Higher specific activity can be used for increased sensitivity. These are prepared by reducing the molar ratio of unlabeled to labeled nucleotide in the in vitro transcription reaction. However, these probes are less stable than those with lower specific activity and will degrade significantly after a day or two. Lower specific activity probes, by contrast, are good for approx 1 wk after preparation ***(2)***. Finally, the region of the probe that is complementary to the target sequence must typically be completely homologous. Thus, partially related sequences usually cannot be analyzed ***(1,2)***.

In summary, the RPA is an excellent alternative to the Northern-blot assay. It has the sensitivity to analyze virtually any mRNA species without isolating poly (A) RNA and it is the method of choice for quantifying multiple mRNAs simultaneously. Like the Northern, it is low tech, requiring electrophoresis and other equipment commonly found in many laboratories. In our experience, the RPA is somewhat more difficult to perform compared to the Northern, however, with practice one should be able to become proficient with this assay in a relatively short period of time. As discussed previously commercially supplied kits are available to perform virtually all steps of the RPA. These include in vitro transcription kits for the generation of the antisense RNA probes, the RPA kits, and plasmid vectors that contain the templates for a number of internal control RNAs. In addition to the standard RPA kits which are suitable for most applications, there are also some specialized kits available. For example, lysate RPAs utilize a procedure in which labeled RNA probe is hybridized directly with cellular RNA in a cell or tissue lysate without prior RNA isolation. Another kit employs a high-speed hybridization system, which accelerates

hybridization greater than 100-fold allowing reactions to go to completion in a matter or minutes rather than hours.

References

1. Lader, E. (1996) Strategies for quantitation of mRNA: Northern blotting, RPA, and RT-PCR analysis. *Ambion Tech. Notes* **4,** 1.
2. Flick, P. and Anson, J. (1995) Methods of RNA analysis. *Amersham Life Science* **22,** 1–7.
3. Sambrook, J., Fritsch, E. F., and Maniatis, T. (1989) *Molecular Cloning: A Laboratory Manual,* 2nd ed. Cold Spring Harbor Laboratory Press, Cold Spring Harbor, NY, pp. 7.71–7.78.

14

In Situ Hybridization

Susan Riggs Runge, Zhaoyong Hu, and Marschall S. Runge

1. Introduction

In situ hybridization (ISH) is employed principally to detect mRNA within cells and tissues. ISH begins with the synthesis of a nucleic acid probe complementary in sequence to a cellular target. Through incorporation of a radioactive nucleotide into the probe, a cellular target may be visualized using autoradiography. A nonradioactive variation of this technique utilizing digoxigenin has been championed by some researchers, but our experience has been that radioactive probes produce more reliable and accurate results. Although not a difficult technique, ISH incorporates many steps, which must be performed with care and precision to obtain useful results.

A major advantage of ISH is that it provides a method for studying gene regulation under physiologic circumstances in individual cells or groups of cells within a tissue. This has certainly been the case for studies of the renin–angiotensin system (RAS). Whether in the kidney, adrenal gland, or the blood vessel wall, expression of components of the RAS, such as the angiotensin II (Ang II) receptors, is cell-specific and highly regulated. Indeed, recent studies of Ang II–receptor (AT1 and AT2 subtypes) mRNA expression through ISH have led to a more complete understanding of the role of these genes in development ***(1,2)***, adrenal function ***(3,4)***, arterial hypertrophy ***(5)***, and in other settings.

In this chapter, we describe the methods that we have utilized to study components of the RAS ***(6)***, as well as a number of other genes of interest ***(7,8)***. We have divided the section into four large categories (1) probe preparation, (2) specimen preparation, (3) hybridization, and (4) autoradiography. Because of length considerations, many details are omitted here, and the reader is referred to excellent references on *in situ* hybridization by Hogan ***(9)***, Wilkinson ***(10)***, and Wilcox ***(11)***.

From: *Methods in Molecular Medicine, vol. 51: Angiotensin Protocols*
Edited by: D. H. Wang

2. Materials

2.1. Probe Preparation

1. Plasmid (such as PCRII) containing gene of interest and Sp6 and T7 promoters.
2. Appropriate restriction enzymes.
3. 1% agarose gel in 1X TAE buffer [40 m*M* Tris-acetate, 2 m*M* ethylene diamine tetraacetic acid (EDTA), pH 8.5].
4. 25:24:1 phenol/chloroform/isoamyl alcohol. Chloroform is a carcinogen. Wear gloves and safety glasses and work in a chemical fume hood.
5. 3 *M* sodium acetate, pH 5.2, and 3 *M* sodium acetate, pH 6.0.
6. Ice-cold 100% ethanol.
7. TE buffer (10 μ*M* Tris-HCl, 1 μ*M* EDTA, pH 7.5), 1 *M* dithiothreitol (DTT).
8. ^{35}S-UTP @ 1000 Ci/mmol (Amersham).
9. MAXIscript SP6/T7 kit (Ambion), which includes Sp6,T7 RNA polymerase, 10X transcription buffer with RNase inhibitor, ATP, GTP, CTP, nuclease-free water, and DNase I.
10. Agarose, 37% formaldehyde, 10X MOPS stock solution.

2.2. Specimen Preparation

1. Cells or tissue of interest.
2. Freshly made 4% paraformaldehyde (PFA) in RNase-free PBS at 4°C. Paraformaldehyde is toxic. Wear gloves and a mask and work in a chemical fume hood.
3. Tissueplus Paraffin (Fisher), embedding molds, forceps, xylene, and ethanol dilutions (70%, 95%, and 100%). Xylene should be used in a chemical fume hood. Dispose of according to local safety regulations.
4. Superfrost/Plus slides (Fisher).
5. Tissue flotation bath (Fisher) with DEPC-treated water. DEPC may be a carcinogen. Wear gloves and safety glasses and work in a chemical fume hood.
6. Microtome (we use Zeiss HM 325) capable of cutting 5-μm sections.

2.3. Hybridization

1. Two sets of slide racks, one labeled “For RNase Use Only.”
2. Ten or more staining dishes.
3. Five or more large plastic containers labeled “For RNase Use Only” (for posthybridization washes).
4. Xylene, ethanol dilutions (100%, 95%, 75%), 10X PBS stock solution.
5. Proteinase K solution (0.1 *M* Tris-HCl, 50 m*M* EDTA, pH 8.0 with 1–10 μg proteinase K per mL). Proteinase K may be prepared as a 10 mg/mL stock solution and stored at –20°C in aliquots.
6. Glycine solution (2 mg/mL in PBS).
7. Freshly prepared triethanolamine (TEA) buffer. TEA buffer is prepared by adding 18.57 g triethanolamine-Cl to 900 mL water. Dissolve and adjust pH to 8.0 with NaOH. Adjust final volume to 1 L with water for a 0.1 *M* solution. Add acetic anhydride to TEA buffer for some steps. Acetic anhydride is harmful to skin and mucous membranes. Wear gloves and safety glasses and work in a chemical fume hood.

8. Hybridization Mix A—as described in *Current Protocols in Molecular Biology* ***(12)***: Deionized formamide (50%), 10 m*M* Tris-HCl pH 8.0, 0.3 *M* NaCl, 1 m*M* EDTA, 1X Denhardt's solution, 500 μg/mL yeast tRNA, 100 m*M* DTT, 500 μg/mL poly (A), 10% polyethylene. Store hybridization mix in aliquots at –20°C. Formamide is hazardous. Follow manufacturer's instructions for its use.
9. Moisture chamber with moisture buffer (10 m*M* Tris-HCl, pH 7.4 with 50% formamide, 0.3 *M* NaCl, 1 m*M* EDTA).
10. Water bath at 55°C.
11. SSC 20X stock solution (Sigma).
12. β-mercaptoethanol.
13. RNase A stock solution (10 mg/mL) (Sigma), in RNase buffer (10 m*M* Tris-HCl, pH 8.0, 500 m*M* NaCl, 1 m*M* EDTA).
14. Ethanol 70%/ 0.3 *M* ammonium acetate.
15. Ethanol 95%/0.3 *M* ammonium acetate.
16. Ethanol 100%.

2.4. Autoradiography, Photography, and Analysis

1. Water bath at 45°C.
2. Kodak NTB-2 radiographic emulsion.
3. Slide box with dessicant capsules, light-impermeable bags.
4. Kodak D19 developer.
5. Kodak fixative.
6. Biomax MR-1 X-ray film.
7. Microscope (Nikon E600) with darkfield condenser.
8. Kodak 160NC color negative film for final photographs.

3. Methods

3.1. Probe Preparation

1. Separate transcripts for sense and antisense probes are treated as below. The antisense probe will hybridize specifically to the mRNA of interest, whereas the sense probe will serve as a control for nonspecific hybridization.
2. Linearize plasmid that contains gene of interest using standard methods. The restriction enzymes and conditions used will vary according to the cDNA insert. Confirm linearization and length of insert by agarose gel (1%) electrophoresis in TAE buffer.
3. Purification of linearized DNA. Extract with phenol/chloroform (fivefold excess), vortex, centrifuge at 13,000*g* (Savant SFR13K) for 10 min. Add 10 μL 3 *M* sodium acetate, pH 5.2 (per 100-μL probe), and a 2.5-fold excess of cold ethanol (100%). Vortex and then incubate on ice for 30 min. Centrifuge at 13,000*g* (Savant SFR13K) for 10 min. Remove supernatant by aspiration. Wash the pellet in 70% ethanol. Aspirate excess ethanol and air-dry pellet. Resuspend pellet in nuclease-free water to a final concentration of 1 μg/μL.

   All steps from here forward should be performed using a RNase-free technique. For those not familiar with the RNase-free technique, we strongly

recommend reviewing a standard text (such as ref. *12*). In particular, all glassware, laboratory supplies and chemicals, and racks for washes and RNase treatment should be kept completely separate from glassware, laboratory supplies and chemicals, and racks for routine laboratory use to avoid contamination with RNases.

4. Synthesize radioactive mRNA probe using MAXIscript SPT7 kit following manufacturer's instructions. Remove template cDNA by adding 1 μL DNase 1, incubate for 15 min at 37°C, add 1 μL yeast tRNA, and then add nuclease-free water to a final volume of 100 μL.
5. Probe purification. Extract with phenol/chloroform (100 μL), centrifuge for 10 min at 13,000*g* to remove denatured protein and transfer supernatant to a fresh tube. Precipitate RNA probe by adding 10 μL 3 *M* sodium acetate (pH 6.0) and 250 μL cold ethanol to the supernatant. Vortex and then incubate at –20°C for 30 min. Centrifuge for 10 min at 13,000*g*. Aspirate supernatant and wash pellet with 70% ethanol. Aspirate remaining ethanol and air-dry. Resuspend into 100 μL TE buffer (total volume) with 100 m*M* DTT (final concentration). The probe is now ready for use or can be stored at –70°C for at least 1 wk (some investigators store purified probes for as long as several weeks).
6. Confirm probe size and integrity. Subject 1 μL probe to denaturing gel electrophoresis [agarose (1%)-formaldehyde (3%) in 1X MOPS] for 1 h at 80 V. Dry gel and expose to X-ray film for 30 min. To determine probe activity in cpm, pipet 1 μL of probe directly into 5 mL scintillation fluid and count in a scintillation counter (*see* **Note 1**).

3.2. Specimen Preparation

1. Identify tissue or cell of interest. Rinse tissue in cold phosphate-buffered saline (PBS) (RNase-free). Fix tissue at 4°C using freshly made 4% paraformaldehyde (in RNase-free PBS) for appropriate length of time (2–10 min for cells to 12 h for some tissues), (*see* **Note 2**). During this entire process, the tissue must be kept at 4°C to minimize RNA degradation.
2. If fixed tissue is to be processed at a later time, wash fixed tissue in 70% ethanol for 30 min at room temperature twice. Tissue samples may be stored in 70% ethanol at 4°C in tightly capped vials for several months.
3. Dehydration and embedding. We process tissues (in an embedding casette, Fisher) using an automated procedure (Hypercenter XP, Shandon). The general principle is to pass fixed tissues through a series of increasing concentrations of ethanol and, finally, xylene, followed by embedding in paraffin. As an alternative to the automated procedure, dehydration can be accomplished manually using the following steps. First, pass tissue through graded dilutions of ethanols at room temperature: 30 min in 70% ethanol two times, 30 min in 95% ethanol two times, and 30 min in 100% ethanol two times. Wash tissue in xylene three times for 30 min at room temperature. The final step in manual tissue processing is to pass the tissue through paraffin (60°C) for 30 min, twice.

4. Tissue samples in paraffin are embedded in an appropriately sized mold (the mold is removed after the embedded sections harden, before sectioning). For details, please *see ref.* ***9.***
5. Make 5-μm sections and float onto surface of a flotation bath containing DEPC-treated water (50°C) for 15 min. Float sections onto Superfrost/Plus slides (Fisher). Air-dry slides overnight.

3.3. Hybridization

3.3.1. Prehybridization

1. Dewax sections on slides by passing them through xylene three times for 10 min each and rehydrate through a graded series of ethanol concentrations: 5 min in 100% ethanol twice, 5 min in 95% ethanol, 5 min in 70% ethanol. (Programmable slide processing equipment can be used for these dewaxing and rehydration steps.) Wash slides in 2X SSC, then heat denature in 2X SSC at 70°C for 15 min.
2. Treat samples with proteinase K solution (as described in materials) for 30 min at 37°C (*see* **Note 3**). Stop digestion by washing in 2 mg/mL glycine in PBS for 1 min. Wash samples with PBS (1X) for 2 min.
3. Refix samples in paraformaldehyde (4%) for 5 min, then rinse in 3X PBS for 2 min. Finally, wash samples in PBS (1X).
4. Equilibrate slides in TEA buffer (freshly prepared in DEPC water, pH 8.0) for 2 min.
5. Transfer slides to fresh TEA buffer and add acetic anhydride to a final concentration of 0.25%. Agitate slides for 5 min. Add additional acetic anhydride to a final concentration of 0.5%, and agitate slides for an additional 5 min. This is an important step to decrease background (by blocking reactive groups on tissue sections).
6. At this point, hybridization can be performed or slides can be stored for later use. If hybridization is to be performed immediately, slides are washed with 2X SSC. If hybridization is to be performed at a later date, slides are dehydrated by passage through graded ethanol concentrations (70%, 95%, and 100%), then air-dried completely, wrapped in plastic, and stored at –70°C. If slides have been stored they should be allowed to warm to room temperature (while still wrapped in plastic) for 1 h prior to proceeding with the following steps.
7. Place slides in moisture chamber (*see* **Note 4**). Perform prehybridization by pipeting 200 μL of Hybridization Mix A (without probe) onto each slide. Place moisture chamber in hybridization oven for 2 h at 55°C. Place slides upright in a slide rack (on paper towels) and place slide rack back in hybridization oven for 5 min to drain excess hybridization solution.

3.3.2. Hybridization

1. Remove the frozen aliquots of both sense and antisense probes and heat at 70°C for 10 min. Dilute each probe with Hybridization Mix A to a final concentration

of 1×10^6 cpm/mL. An adequate amount of each probe (at this concentration) should be prepared for the anticipated number of slides.
2. Label slides "sense" or "antisense" or with a blinded code. Although this may seem obvious, it is critical for later interpretation of data. Also, to avoid bias in interpretation, we prefer to use a code to label slides in many experiments.
3. Place slides in moisture chamber and add 100 µL of diluted probe to each slide.
4. Carefully apply coverslips to each slide (*see* **Note 5**).
5. Place moisture chamber in hybridization oven for 16 h at 55–60°C (*see* **Note 6**).

3.3.3. Posthybridization Washes and RNase Digestion

1. Prewarm all washing solutions listed below to 55°C, except RNase solution and an aliquot of 2X SSC used immediately after RNase treatment, which should remain at room temperature. Add β-mercaptoethanol (β-ME) to each solution just before using.
2. Remove cover slips from slides and discard in radioactive waste.
3. Dip each slide, one at a time, in 4X SSC containing 50% formamide and 100 m*M* β-ME at 55°C. Discard this wash solution in radioactive waste.
4. Wash slides in 2X SSC containing 100 m*M* β-ME at 55°C for 30 min with agitation (*see* **Note 7**). Repeat this step.
5. RNase digestion. Immerse slides in RNase (20–40 µg/mL) in RNase buffer (10 m*M* Tris-HCl, pH 8.0 , 500 m*M* NaCl, 1 m*M* EDTA), *without* agitation, at room temperature for 30 min. Wash slides in 2X SSC at room temperature for 10 min with agitation.
6. Wash slides with 2X SSC containing 100 µ*M* β-ME at 55°C for 30 min with agitation. Repeat this step.
7. Wash slides with 1X SSC containing 100 µ*M* β-ME at 55°C for 30 min with agitation.
8. Wash slides with 0.5X SSC containing 100 µ*M* β-ME at 55°C for 30 min with agitation.
9. Final optional high-stringency wash of slides is with 0.1X SSC containing 100 µ*M* β-ME at 55°C or 60°C for 30 min to 2 h (*see* **Note 8**).
10. Dehydration of sections. Transfer slides through washes containing 75% ethanol/0.3 *M* ammonium acetate for 5 min, then 95% ethanol/ 0.3 *M* ammonium acetate for 5 min. Finally, wash slides in 100% ethanol for 5 min and air-dry.

3.4. Autoradiography, Photography, and Analysis

1. Estimating exposure time. Prior to exposing slides at –70°C , we advise estimating the time required for exposure by first exposing slides to X-ray film for 2 to 3 d. A strong signal at 2 d indicates an approximate final development time of 3 wk. This will vary depending upon which probe is used.
2. Warm photographic emulsion in a water bath at 45°C for 30 min.
3. Place all materials to be used in following steps in the darkroom. The following steps are performed in the darkroom under red light.

4. Dip slides, two at a time and back to back, into emulsion and air-dry completely.
5. Place slides in a exposure box containing dessicant capsules. Wrap the exposure box in black light-impermeable bags to protect them from moisture and light and store at –70°C (*see* **Note 9**).
6. After exposure, warm slides to room temperature before developing. Develop slides in the dark in Kodak D-19 for 3 min at room temperature, then rinse in deionized water. Then fix in Kodak fixative for 3 min. Wash slides in flowing tap water for 30 min. It is important to remove excess emulsion from the backs of slides by scraping with a razor blade.
7. Counterstain slides with hematoxylin (or other tissue stains), dehydrate through increasing concentrations of ethanol, and apply cover slip with permanent mounting medium.
8. View slides with both brightfield and darkfield microscopy (*see* **Note 10**).
9. An alternative method for *in situ* hybridization is to use an immunogold technique rather than a radioactive technique (*see* **Note 11**).

4. Application to the Renin-Angiotensin System

Numerous investigators have used ISH to characterize regulation of important components of the RAS under both physiologic and pathophysiologic conditions. Our investigation of angiotensin II gene regulation began with the description of Ang II (AT1) protein expression using specific antibodies ***(13)***. More recently, ISH has been applied toward the study of Ang II (both AT1- and AT2-receptor subtypes) expression in the adrenal gland ***(6)***. In this setting, ISH, using specific probes, made it possible to delineate the differential effects of aldosterone on AT1- and AT2-receptor expression. **Figure 1** illustrates the specificity that can be obtained using ISH.

5. Conclusion

ISH is an extremely sensitive and specific method for examining gene regulation at the mRNA level in tissues and cells. In this chapter, we have described the technique of ISH in detail and the usefulness of its application to the study of the renin-angiotensin system.

6. Notes

1. Optimal probe length for use in paraffin-embedded tissue sections is 300–800 base pairs. Larger probes may have reduced efficiency of hybridization and smaller probes tend to result in high background counts. Before use, a probe should be demonstrated to be pure (a single clear band by gel electrophoresis) and of high activity ($10^6 – 10^8$ cpm/μL).
2. Tissue fixation times are highly variable between tissues. We prefer 4% paraformaldehyde, a crosslinking fixative. Small tissues, like mouse aorta, require only about 4 h fixation, whereas larger tissues may require 12 h. Perfusion of organs is desirable if possible. Overfixation should be avoided.

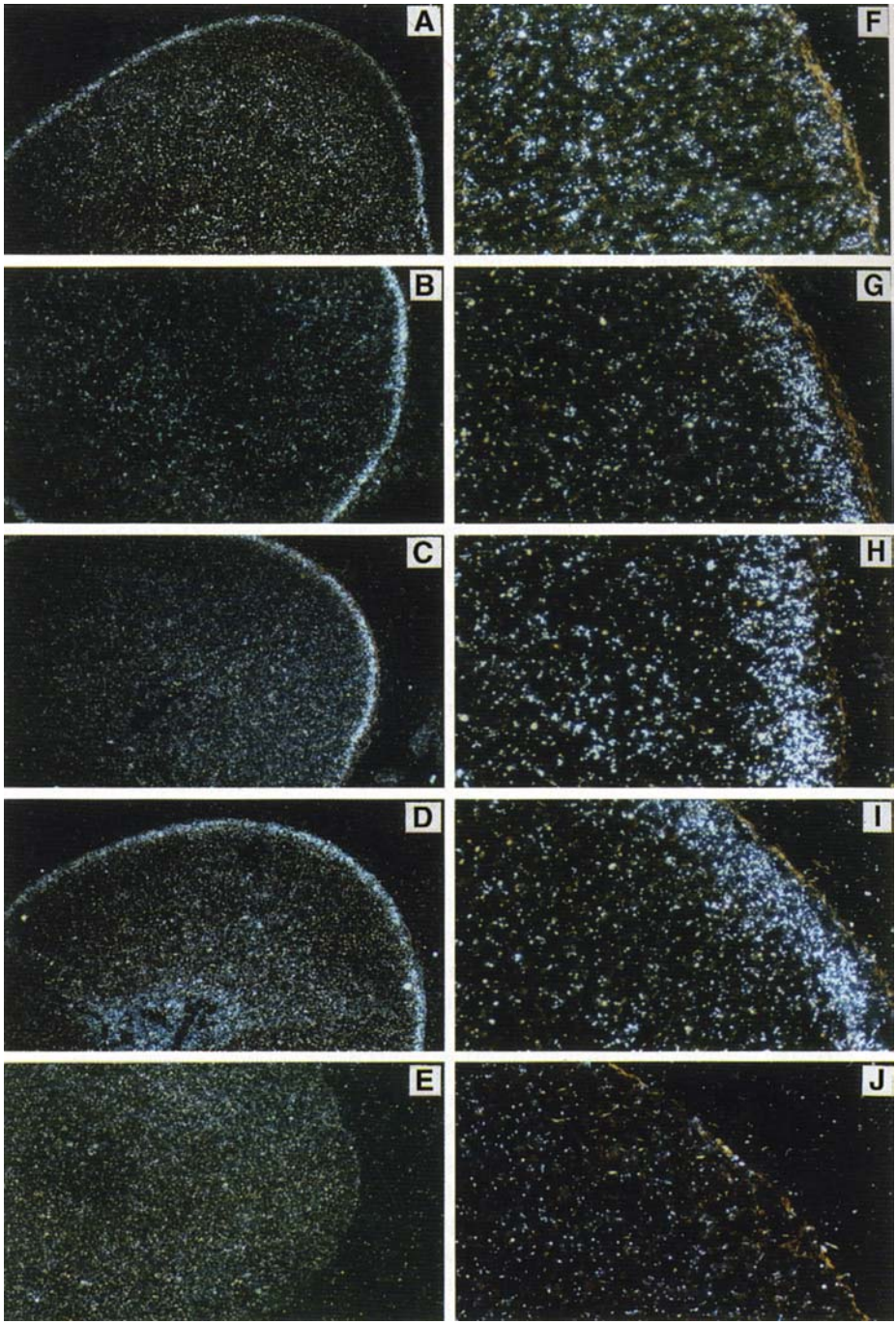
A
F
B
G
C
H
D
I
E
J

3. The optimum concentration of proteinase K must be determined for each tissue using the highest possible concentration. However, overdigestion with proteinase K will result in loss of target mRNA and poor morphology.
4. The moisture chamber is made using a Nunc Bio-Assay covered dish (24 × 24 × 2.5 cm). Filter paper is cut to fit the bottom of this dish and wet with moisture buffer. Pairs of glass rods are used to support slides so that slides do not rest upon the filter paper. Vacuum grease (Hi-temp-vac, VWR) is used to forge an air-tight seal between lid and container.
5. Recently, we have performed hybridizations successfully without coverslips. This requires about 600 μL probe/Hybridization Mix per slide.
6. Hybridization may be performed under more stringent conditions (at higher temperatures) for longer probes to reduce background.
7. We perform this and the following washes in a 600-mL volume of wash solution. The volume of wash solution should be at least 10 mL per slide.
8. If after evaluation of initial results, high background is present, we advise adding one or more high-stringency washes at this step.
9. According to emulsion specifications, exposure can be performed at 4°C, but we have obtained optimal results performing exposures at –70°C. Do not store slides in a place where ^{32}P has been stored or high background will result.
10. Appropriate controls and evaluation of results: As in all scientific systems, the choice of proper controls for ISH is critical to obtaining reliable and meaningful results and for avoiding potential pitfalls. For ISH, the use of sense probes to control for nonspecific hybridization is especially important. One should also always consider the use of positive control probes when developing a new system. It is also useful to employ cell-type-specific probes. For example, when examining expression of a gene of interest in the arterial wall, the use of a probe for von Willebrand's factor (synthesized only in the endothelium) will allow distinction between endothelial cells and nonendothelial-derived cells *(7)*. Thus, in any single experiment, it is often necessary to include at least three controls (the sense control for the probe of interest, a positive control probe, and a cell-specific probe).

Fig. 1. (*Opposite page*) Representative photomicrographs showing the localization of AT_1 (AT_{1A} and AT_{1B}) mRNAs in the adrenal glands of rats fed a normal sodium diet (NS; A, original magnification ×40; F, original magnification X200), NS + Prazosin (NS + PR; B, orignal magnification ×40; G, original magnification X200), low-sodium diet (LS; C, original magnification ×40; H, original magnification X200), and LS+PR (D, original magnification ×40; I, original magnification X 200) by ISH. The changes in AT_1 mRNAs after low-sodium and/or prazosin treatment are primarily for the zona glomerulosa. Photomicrographs hybridized to ^{35}S-labeled sense probes are shown in E (original magnification ×40) and J (original magnification X200). (Reprinted with permission from Wang, D. H. et al. (1997) *Hypertension*; 30 (part I), 345–350.)

11. Labeling with immunogold is an alternative to the use of radioactive probes in ISH: Its signal, like the silver grain in radioactive ISH, is spherical and highly dense and is thus easily distinguished from biological structures. It can be visualized both by bright field and dark field microscopy. Gold labeling has some advantages over radioactive labeling. It is a nonradioactive technique so it is, theoretically, a safer technique. In addition, the entire procedure is shorter, and the results can be determined much more quickly because no long exposure time is necessary as with the radioactive technique. Many steps for this are shared with the protocol described in this chapter for the use of radioactive probes. Additional information necessary to successfully perform ISH using the immunogold technique is available elsewhere (we use Boehringer Mannheim antidigoxigenin gold and silver enhancement reagents).

References

1. Miyazaki, Y., Tsuchida, S., Forgo, A., and Ichikawa, I. (1999) The renal lesions that develop in neonatal mice during angiotensin inhibition mimic obstructive nephropathy. *Kidney Int.* **55,** 1683–1695.
2. Hubert, C., Gasc, J. M., Berger, S., Schutz, G., and Corvol, P. (1999) Effects of mineralocorticoid receptor gene disruption on the components of the renin-angiotensin system in 8 day old mice. *Mol. Endocrinol.* **13,** 297–306.
3. Matsubara, H., Sugaya, T., Murasawa, S., Nozawa, Y., Mori, Y., Masaki, H., et al. (1998) Tissue-specific expression of human angiotensin II AT1 and AT2 receptors and cellular localization of subtype mRNAs in adult human renal cortex using *in situ* hybridization. *Nephron* **80,** 25–34.
4. Naruse, M., Tanabe, A., Sugaya, T., Naruse, K., Yoshimoto, T., Seki, T., et al. (1998) Differential roles of angiotensin receptor subtypes in adrenocortical function in mice. *Life Sci.* **63,** 1593–1598.
5. Parker, S. B., Wade, S. S., and Prewitt, R. L. (1998) Pressure mediates angiotensin II-induced arterial hypertrophy and PDGF-A expression. *Hypertension* **32,** 452–458.
6. Wang D. H., Qiu, J., Hu, Z., and Du, Y. (1997) Regulation of Type 1 Angiotensin II receptor in adrenal gland. *Hypertension* **30,** 345–350.
7. Wilcox, J. N., Rodriguez J., Subramanian, R., Ollerenshaw, J., Zhong, C., Hayzer, D. J., et al. (1994) Characterization of thrombin receptor expression during vascular lesion formation. *Circ. Res.* **75,** 1029–1038.
8. Ruef, J., Hu, Z. Y., Li-Yan, Y., Wu, Y., Hanson, S. R., Kelly, A. B., et al. (1997) Induction of vascular endothelial growth factor in balloon-injured baboon arteries: a novel role for reactive oxygen species in atherosclerosis. *Circ. Res* **81,** 24–33.
9. Hogan, B., Beddington, R., Costantini, F., and Lacy, E. (1994) *Manipulating the Mouse Embryo—A Laboratory Manual.* Cold Spring Harbor Laboratory Press, Cold Spring Harbor, NY.
10. Wilkinson, D. G., ed. (1993) In Situ *Hybridization—A Practical Approach.* Oxford University Press, Oxford, England.

11. Wilcox, J. N. (1993) Fundamental principles of *in situ* hybridization. *J. Histochem. Cytochem.* **41,** 1725–1733.
12. Ausubel, F. M., et al., eds. (1998) *Current Protocols in Molecular Biology.* Greene, Wiley, New York.
13. Paxton, W. G., Runge M., Horaist, C., Cohen, C., Alexander, R. W., and Bernstein, K. E. (1993) Immunohistochemical localization of rat angiotensin II AT_1 receptor. *Am. J. Physiol.* **264(6 Pt 2),** F989–F993.

15

Immunohistochemical Detection of Angiotensin II Receptor

Zhi-Qin Wang and Robert M. Carey

1. Introduction

This chapter deals with immunohistochemical detection of low copy molecules in tissue. We will focus on peptide receptors, but the same principles apply to hormones, autacoid substances, enzymes, and signaling molecules. Several approaches are currently available to characterize receptor distribution in tissue: (1) radioligand binding autoradiography, (2) immunohistochemistry (IHC), and (3) *in situ* hybridization (ISH). Each method yields different types of information. ISH identifies cells that express a specific mRNA and, therefore, are likely to express the protein of interest. However, the site of mRNA transcript expression for a receptor may be different from the site of receptor binding or protein expression. Although radioligand binding autoradiography provides a good measure of functional receptor expression, precise subcellular localization of receptor expression is not possible. Moreover, pharmacological ligands specific for a single-receptor subtype are not always available. IHC is necessary for cell-specific localization of receptor expression within tissue. The resolution and sensitivity achieved with IHC is far greater than that obtained with classic autoradiography techniques although antireceptor antibody cannot discriminate between receptor proteins undergoing synthesis, transport, or degradation. The principle behind the increased resolution is based on the excellent sensitivity and specificity of the antibody–antigen interaction. The antiserum can be raised by polyclonal or monoclonal antibody technology against a variety of antigens ranging from a single amino acid to large cellular glycoproteins. We have successfully localized different receptors such as dopamine D_{1A} and D_3 receptors and the angiotensin II type 2 receptor in kidney,

From: *Methods in Molecular Medicine, vol. 51: Angiotensin Protocols*
Edited by: D. H. Wang

heart, and adrenal gland ***(1–6)***, of which receptor-specific mRNA is expressed in substantially lower quantities.

Both angiotensin II receptor types (i.e., type-1 and type-2) contain seven transmembrane-spanning domains, and are G-protein coupled ***(7)***. Several research groups have successfully applied IHC to localize angiotensin II type-1 and type-2 receptors in the kidney, heart, adrenal gland, and brain ***(5,6,8–11)***. This chapter is not intended to be a comprehensive account of all IHC techniques. Instead, we will briefly review some of general principles for light microscopic immunoenzyme IHC studies, and then give an outline of ABC peroxidase technique in cryostat sliced sections, as routinely used in our laboratory ***(1–6)***. More detailed information is available elsewhere ***(12)***.

1.1. Antibody

IHC analysis requires antibodies with sufficient affinity and specificity to recognize proteins of interest. Commercially available antibodies may serve this purpose. Otherwise, they need to be developed by researchers.

Recent advances in molecular cloning have made design and generation of antireceptor antibody possible without the need for large quantities of purified whole receptor proteins. Instead, specific synthetic oligo-peptides or bacterially expressed fusion proteins against particular receptor epitopes can be used as antigens. When using specific protein sequences as immunogens, the investigator should choose areas of potentially high immunogenicity. These molecular domains should consist of unique amino acid motifs, contain polar and hydroxy amino acids, and these domains should be present in intracellular or extracellular, rather than in the transmembrane, region. Areas that are affected by post-translational modification, such as signal peptides, or sites to be glycosylated or phosphorylated, should be avoided if possible. It is helpful to use a gene database program such as GenBank or Swiss Prot to choose the best unique sequence. Computer-assisted algorithms, i.e., Jameson-Wolf antigenic index ***(13)***, can be used to predict sequence antigenicity (hydrophilicity, surface probability, chain flexibility, and secondary structure). Antipeptide or antifusion protein antibodies can be generated to target a specific receptor. A short peptide (15–25 amino acids) used for production of antipeptide antibody is derived from the primary sequence of the receptor and has relatively fewer epitopes. It is usually conjugated with a different carrier protein, such as keyhole limpet hemocyanin (KHL) or bovine serum albumin (BSA), to generate an adequate immune response. In contrast, a larger sequence, which contains several native epitopes, can be subcloned into an expression vector to produce a fusion protein for animal immunization.

Once antiserum is generated, one can perform affinity purification and/or separate IgGs from the whole serum using commercially available columns.

Rigorous testing is critical using tissues expressing the receptor, and cells that do not express the receptor in their native state, but are transfected with cDNA of the receptor of interest. Western-blotting analysis and immunoprecipitation should be performed to test antibody for its specificity and possible cross-reactivity in these transfected and nontransfected cells.

Immunocytochemistry can directly test the utility of the antibody against the native receptor under nondenaturing conditions. Although antibodies used for Western blotting or immunoprecipitation do not require absolute specificity, those intended for IHC must be specific.

1.2. Tissue Preparation

Proper collection and fixation of tissues is critical for maintaining receptor immunogenicity. Tissue must be fixed to prevent postmortem protein degradation, to protect the tissue from physical damage by hardening, and to preserve cellular architecture. Fixation may be accomplished by immersion or vascular perfusion. Fixation should be performed immediately because delay permits autolysis and drying. Freezing prior to fixation can cause major morphological changes. For animal studies, postmortem autolytic changes often are avoidable as animals can be perfused coincident with death. Human tissue is substantially more difficult to collect and fix reliably. Generally, human tissue blocks should be cut into pieces less than 1-cm thick and fixed by submersion.

The choice of fixative depends on the sensitivity of the antigen to particular reagents. Aldehyde fixatives (paraformaldehyde and formaldehyde), which crosslink primary amines in tissues, are most versatile and practical because they preserve cellular morphology and are mild enough to maintain immunoreactivity of antigenic epitopes. The duration of fixation is also important; the longer the exposure to fixative, the more crosslinkage occurs. This may improve tissue integrity, but may decrease antibody penetration and denature the receptor protein. Precipitating organic solvents such as acetone, methanol, or ethanol can also be used, but cellular morphology is not as well preserved as with crosslinking fixatives.

The use of fixed and permanently embedded tissue (e.g., paraffin blocks) offers the advantage of very good morphological preservation together with convenient handling and storage of the specimens. However, some antigens do not survive unchanged through the infiltration with organic chemicals and the heat necessary to harden the embedding material. Generally speaking, antigens in frozen sections are not damaged or made inaccessible because of the presence of an embedding matrix. If the tissue block is infiltrated with 30% sucrose before it is frozen, relatively good morphology may be obtained. One disadvantage of cryostat-cut sections is the formation of ice-crystal artifacts in the form of holes and enlarged cells, and possible membrane damage. Moreover,

frozen tissue blocks are neither permanent nor easily handled, especially when sections need to be cut from the same specimen on repeated occasions.

1.3. ABC-Peroxide IHC Staining Technique

Indirect strategies are popular IHC detection methods. There are numerous commercially available detection systems based on detection of the primary antibody with a second IgG. The secondary antibody is either directly tagged with an enzyme marker or flurophore, or conjugated with biotin for flexible detection with avidin-enzyme or avidin-flurophore conjugates. Horseradish peroxidase is most commonly used immunohistochemical label with 3,3'-diaminobenzidine (DAB) as chromogenic substrate, which polymerizes upon oxidation with H_2O_2 and produce a brown color that contrasts well with nuclear hematoxylin staining. The sensitivity of peroxidase detection system is superior, and the reaction product is quite stable, and can be viewed repeatedly even after long storage. Immunoflurescence-based detection is excellent for colocalization of two proteins using separate fluorophore labels with distinct emission spectra, but is subject to photobleaching. Endogenous horseradish peroxidase usually present in high concentration in red blood cells can interfere with specific immunostaining. Pretreatment of the tissue sections with methanol-H_2O_2 may help to quench the activity of endogenous horseradish peroxidase. The Avidin-Biotin Complex Method (ABC) uses three reagents: a primary antibody, a secondary antibody that is chemically bound to the vitamin biotin, and a complex of the glycoprotein avidin that is bound to biotin and peroxidase. One molecule of avidin has the ability to bind nonimmunologically four molecules of biotin, which is essentially irreversible because it is at least 10^6 times stronger than most antibody–antigen reactions. The strong affinity gives this method excellent sensitivity. The positive brown reaction product is quite stable. The signal can be observed and photographed under brightfield optics.

2. Materials

1. Phosphate-buffered saline (PBS, pH 7.4): dissolve sodium phosphate dibasic 1.48 g, sodium phosphate monobasic 0.43 g, sodium chloride 7.20 g in 1 L of distilled water.
2. 4% paraformaldehyde in PBS. Mix with stir bar and heat to 60°C in the fume hood. Add 4–5 drops of 1 *N* NaOH to help dissolve. Store at 4°C and use within 24 h.
3. 30% sucrose in PBS.
4. OCT tissue embedding medium (Tissue-tek, Miles Laboratories).
5. Superfrost plus slide (Fisher Scientific).
6. PAP pen slide marker (Research Products International).

7. 3% hydrogen peroxide in methanol: mix 30% hydrogen peroxide solution 3.0 mL and methanol 97.0 mL.
8. Primary antibody: AT_2 receptor-specific polyclonal antibody raised in rabbits against a synthetic peptide sequence derived from the NH-terminal extracellular tail (MKDNFSFAATSRNITSS, amino acids 1–17) of the native rat AT_2 receptor (5, 6, and 11).
9. VECTASTAIN ABC Staining kit (Vector Laboratories): includes blocking serum (normal goat serum), biotinylated affinity-purified secondary antibody, avidin DH solution and biotinylated horseradish peroxidase.
10. DAB Peroxidase Substrate Tablet Set (Sigma): dissolve one tablet of DAB buffered substrate and one tablet of urea hydrogen peroxide in 5 mL of distilled water. Filter through 0.45 mm filter before use. Keep both the DAB and the DAB-hydrogen peroxide out of the light since DAB is light sensitive. DAB also may be a carcinogen. Use a hood and gloves, and save the used DAB solutions in bottles to be picked up by the laboratory safety officer.
11. Saturated lithium carbonate solution: dissolve 1.54 g of lithium carbonate in 100 mL distilled water.
12. Permount histological mounting medium (Fisher Scientific).

3. Methods

1. Perfuse anesthetized rat transcardially with PBS, followed by 4% paraformaldehyde in PBS in a well-ventilated area. The tissue of interest (kidney or heart) is removed and stored in additional fixative solution at 4°C for 2–4 h (*see* **Note 1**).
2. The tissue is rinsed for 30 min in PBS, then immersed in 30% sucrose in PBS overnight (*see* **Note 2**).
3. Freeze the tissue in OCT embedding medium and store in a –70°C freezer. Tissue blocks are stable for 1–2 yr.
4. Cut serial, 5–10-μm sections and collect onto Superfrost gelatin-coated, glass slides, let dry at room temperature for 30 min, and place in a slide box at –70°C. Cut sections are stable for months at –70°C.
5. Take out tissue sections and allow to come to room temperature, remove OCT around the tissue section with tweezers. The slide is placed in a moist chamber, which prevents the section from drying during the staining procedure. Rinse with PBS for 5 min to remove cryoprotectant (sucrose).
6. Preincubate with 3% hydrogen peroxide methanol solution for 30 min to block endogenous peroxidase activity.
7. Rinse in three changes of PBS, 5 min each.
8. Draw a circle around the tissue section on the slide with a PAP pen. Block sections with 3% blocking goat serum (usually need 200–250 μL per slide) in PBS for 60 min (*see* **Notes 3** and **4**).
9. Remove blocking solution by aspiration and add primary antibody in 1.5% blocking serum in PBS (*see* **Note 5**). Incubate sections overnight at 4°C.
10. Rinse for 10 min in PBS, 3X.
11. Incubate for 45 m in inbiotinylated goat antirabbit IgG secondary antibody in PBS.

12. Rinse for 10 min in PBS, 3X.
13. Incubate for 60 min in ABC solution in PBS, which is made up at least 20 min prior to use.
14. Rinse tissue in PBS for 10 min, 3X.
15. Apply freshly made (15–20 min before use) DAB solution, react for 1–3 min (*see* **Note 6**).
16. Rinse tissue for 5 min in distilled H_2O, 3X.
17. Counterstain with hematoxylin for 45–60 s.
18. Wash in tepid tap water.
19. Stain with saturated lithium carbonate solution for 30 s until the section turns blue.
20. Dehydrate through 70%, 90%, and 100% ethyl alcohol for 3 min each, and then clear with xylene for 3 min.
21. Mount cover slip over the section with Permount (*see* **Note 7**).

4. Notes

1. HistoCHOICE fixative (Amresco Inc.) is a new, ready-to-use, noncrosslinking fixative for tissues and cells. It is an odorless solution that can be easily disposed of down the drain and is gentle to tissues. Fixation with this complex mixture of agents will retain not only tissue structure, but also antigenic sites and nucleic acids. We have obtained excellent results using HistoCHOICE fixative as a primary fixative for fresh tissue.
2. Allow the tissue block to sink in the sucrose solution before freezing it. This is a good indicator of satisfactory cryoprotection.
3. Endogenous biotin or biotin receptors in various tissues may make extra blocking procedures necessary. In addition, avidin preparations sometimes bind nonspecifically to certain cellular components, probably because of electrostatic interactions. Commercial avidin-biotin blocking kits (Vector Laboratories, DAKO) can be used for this purpose.
4. If immunohistochemical masking of antigenic epitopes occurs, as often seen in aldehyde-based fixatives, the antigen retrieval method may be considered to unmask epitope. Use of detergents (0.3–2% Triton X-100 or saponin, 0.2% Nonidet P-40) in buffers and antibody diluents is a popular method of permeabilizing the cell membrane and improving antibody penetration, Tissue sections can also be treated with various proteolytic enzymes (0.06% pronase, 0.1% trypsin, or 0.4% pepsin), chemical denaturing reagents, or heated in a microwave oven.
5. Various dilutions of antibody must be tested to identify optimal concentrations that yield the highest specific signal relative to the lowest background. Different laboratory conditions warrant individual determination.
   A key component of establishing the specific immunostaining signal is the use of appropriate controls. For a polyclonal antibody, a preimmune antibody fraction collected from then same animal prior to immunization with the antigen can be employed. Normal (nonimmune) serum pooled from the same animal species may be substituted if the preimmune control is not available. For a monoclonal

antibody, the culture supernatants from control hybridoma cell lines or ascites fluid from animals infected with unrelated hybridomas may serve as control. The antibody should not elicit positive signal in negative control samples such as nontransfected cells under conditions in which the antibody recognizes receptors in positive control samples such as receptor-transfected cells.

A preadsorption control is the most important control in IHC. In the ideal situation, all tissues or cells normally stained by the antibody will not stain following preadsorption of the primary antibody with the cognate antigen. However, preadsorption of the antibody against the conjugated carrier protein (e.g., KLH or BSA) should not alter the staining pattern. This control is not perfect, however, because there is still the potential that antibodies may crossreact with more than one antigen. Thus, the tested antigen may bind to the antibody, but the antibody may be capable of binding to a similar antigen in the tissue. The antiserum can be combined with a fivefold (by weight) excess of synthetic peptide antigen in a small volume of PBS. The mixture is allowed to stand for 12–24 h at 4°C, with mild agitation. The antigen-antibody mixture is spun at 100,000*g* for 20 min. Any precipitating antigen–antibody complexes formed should be in the pellet. The supernatant is pipetted into a clean vial and can be used in place of the primary antibody in the usual IHC protocol.

6. Generally, 1–3 min incubation in DAB solution is required for adequate staining while maintaining clean background in control sections. If the reaction product is very light after 3 min, longer times can be tried as long as the control remains clean. There should be no azide in the tissue and any of the buffers used when horseradish peroxidase reaction product is developed. Azide will effectively inhibit the peroxidase immunodetection.
7. The aforementioed staining can be easily modified for paraffin-embedded tissue sections. Deparaffinize paraffin sections by immersing sections 2 × 10 min in xylene, 1 × 3 min in 100% ethyl alcohol , 1 × 3 min in 95% ethyl alcohol. Then hydrate to PBS for 3 min.

Acknowledgments

The work discussed herein was supported in part by a NIH grant R01-HL-59948 to Dr. Robert M. Carey.

References

1. O'Connell, D. P., Botkin, S. J., Ramos, S. I., Sibley, D. R., Ariano, M. A., Felder, R. A., and Carey, R. M. (1995) Localization of dopamine D_{1A} receptor protein in rat kidneys. *Am. J. Physiol.* **268,** F1185–F1197.
2. Ozono, R., O'Connell, D. P., Wang, Z. Q., Moore, A. F., Sanada, H., Felder, R. A., and Carey, R. M. (1997) Localization of the dopamine D_1 receptor protein in the human heart and kidney. *Hypertension* **30,** 725–729.
3. Aherne, A. M., Vaughan, C. J., Carey, R. M., and O'Connell, D. P. (1997) Localization of dopamine D_{1A} receptor protein and messenger ribonucleic acid in rat adrenal cortex. *Endocrinology* **138,** 1282–1288.

4. O'Connell, D. P., Vaughan, C., Lane, E., Botkin, S. J., Wang, Z. Q., Felder, R. A., and Carey, R. M. (1998) Expression of the dopamine D_3 receptor in the rat kidney. *Hypertension* **32,** 886–895.
5. Ozono, R., Wang, Z. Q., Moore, A. F., Inagami, T., Siragy, H. M., and Carey, R. M. (1997) Expression of the subtype-2 angiotensin (AT_2) receptor protein in rat kidney. *Hypertension* **30,** 1238–1246.
6. Wang, Z. Q., Moore, A. F., Ozono, R., Siragy, H. M., and Carey, R. M. (1998) Immunolocalization of subtype 2 angiotensin II (AT_2) receptor protein in rat heart. *Hypertension* **32,** 78–83.
7. Griendling, K. K., Lassehue, B., and Alexander, R. W. (1996) Angiotensin receptors and their therapeutic implications. *Ann. Rev. Pharmacol. Toxicol.* **36,** 281–306.
8. Paxton, W. G., Runge, M., Horaist, C., Cohen, C., Alexander, R. W., and Bernstein, K. E. (1993) Immunohistochemical localization of rat angiotensin II AT_1 receptor. *Am. J. Physiol.* **264,** F989–F995.
9. Harrison-Bernard, L. M., Navar, L. G., Ho, M. M., Vinson, G. P., and El-Dahr, S. S. (1997) Immunohistochemical localization of ANG II AT_1 receptor in adult rat kidney using a monoclonal antibody. *Am. J. Physiol.* **273,** F170–F177.
10. Phillips, M. I., Shen, L., Richards, E. M., and Raizada, M. K. (1993) Immunohistochemical mapping of angiotensin AT_1 receptors in the brain. *Regul. Pept.* **44,** 95–107.
11. Wang, D. H., Qiu, J., and Hu, Z. (1998) Differential regulation of angiotensin II receptor subtypes in the adrenal gland: role of aldosterone. *Hypertension* **32,** 65–70.
12. Harlow, E. and Lane, D. P. (1988) Antibodies: *A Laboratory Manual.* Cold Spring Harbor Laboratory Press, Cold Spring Harbor, NY.
13. Jameson, B. A. and Wolf, H. (1988) The antigenic index: a novel algorithm for predicting antigenic determinants. *Comput. Appl. Biosci.* **4,** 181–186.

16

Western Blotting

Nageswara R. Madamanchi and Marschall S. Runge

1. Introduction

Western blotting is employed for the detection of proteins and other macromolecules immobilized on nitrocellulose membranes. This rapid and sensitive method enables the identification and quantification of a specific protein from cell lysates or a mixture of proteins. Following the resolution on denaturing sodium dodecyl sulfate (SDS)-polyacrylamide gel electrophoresis (SDS-PAGE), the constituent polypeptides are transferred electrophoretically to a nitrocellulose membrane ***(1)***. The membrane is incubated in a solution containing primary antibody and the resultant antigen–antibody complex is detected by using appropriately labeled ligands. The most common method is based on the enzyme-linked immunodetection of antigen-specific antibodies using anti-IgG secondary antibodies conjugated with either horseradish peroxidase (HRP) or alkaline phosphatase (AP). Visualization of antibody–antigen complex is achieved through the use of an enhanced chemiluminiscent (ECL) method. It is possible to detect as little as 10–50 ng of protein with AP-conjugated secondary antibody and 0.5–1.0 ng of protein with HRP-conjugated secondary antibody using high affinity and high titer primary antibodies.

2. Materials

1. Samples for analysis by Western blotting.
2. Mini-Protean II Electrophoresis cell (Bio-Rad, Hercules, CA) for the resolution of the proteins.
3. 30% acrylamide and 0.8% *bis*-acrylamide solution. Acrylamide monomer is a neurotoxin. Wear gloves and mask when preparing solutions. Filter the solution through a 0.45-μm filter and store at 4°C in a dark place. The solution is stable for at least 1 mo.

From: *Methods in Molecular Medicine, vol. 51: Angiotensin Protocols*
Edited by: D. H. Wang

4. 1.5 *M* Tris-HCl, pH 8.8 (X4). Filter through a 0.45-μm filter and store at room temperature.
5. 0.5 *M* Tris-HCl, pH 6.8 (X4). Filter through a 0.45-μm filter and store at room temperature.
6. 10% (w/v) SDS solution. Store at room temperature.
7. 10% ammonium persulfate. Store at 4°C for up to 1 mo.
8. TEMED.
9. 4X SDS sample buffer: 0.25 *M* Tris-HCl, pH 6.8, 30% glycerol, 4% SDS, 0.05% w/v bromophenol blue, and 5% β-mercaptoethanol (β-ME). Prepare the sample buffer without β-ME. Add 25 μL β-ME to 475 μL 4X sample buffer. Dilute the sample 4:1 with 4X sample buffer, boil at 95°C for 5 min before loading.
10. 5X electrophoresis buffer: 25 m*M* Tris, 192 m*M* glycine, 0.1% SDS, pH 8.3. Because 1X buffer has a pH of 8.3, do not adjust the pH of the stock. Can be stored at room temperature.
11. Preparation of cell lysates: Solubilization of the protein of interest from the cells in an immunoreactive and undegraded form is an important consideration in the preparation of cell extracts. Many cytosolic and nuclear proteins are solubilized in buffers containing nonionic detergents such as Nonidet P-40 (NP40) or Triton X-100. Hence, a typical lysis buffer for Western blotting has either 50 m*M* Tris-HCl, pH 7.5, or 20 m*M* HEPES, pH 7.4, 10 m*M* dithiothreitol (DTT), 1% Triton X-100, 10% glycerol, 20 μg/mL aprotinin, 1 μg/mL leupeptin, 100 μg/mL phenylmethylsulfonylfluoride (PMSF).
12. For the extraction of membrane-bound proteins, the lysis buffer requires a combination of anionic detergent such as sodium deoxycholate and nonanionic detergents. The RIPA buffer containing 50 m*M* Tris-HCl, pH 7.5, 150 m*M* NaCl, 1 m*M* EGTA, 1% NP40, 0.5% sodium deoxycholate, 0.1% SDS, 20 μg/mL aprotinin, 1 μg/mL leupeptin, and 100 μg/mL PMSF is routinely used for the solubilization of membrane-bound proteins.
13. Electrophoretic blotting system such as the mini trans-blot electrophoretic transfer cell (Bio-Rad).
14. Transfer buffer: 25 m*M* Tris, 192 m*M* glycine, 20% v/v methanol, with or without 0.025%–0.1% SDS, pH 8.3. Store at 4°C.
15. Protein molecular-weight standards, prestained (Bio-Rad or Sigma). No reconstitution is necessary. Heat at 95°C for 1 min and load 10 μL for minigel.
16. Nitrocellulose membrane (0.45-μm pore size) such as Hybond ECL (Amersham, UK).
17. Ponceau S protein staining solution.
18. Premium quality HRP-conjugated secondary antibody. Supplied either as an aqueous solution or lyophilized powder containing protein stabilizers. Lyophilized powders can be reconstituted either in 50% glycerol or water. Antibodies reconstituted in water are preferable and stored in small aliquots at –20°C.
19. Plastic box large enough to hold the blot submerged in a small volume of antibody solution.
20. Reciprocal shaker.

21. Wash buffer (TBS-T buffer): 10 m*M* Tris-HCl, pH 8.0, 150 m*M* NaCl, 0.1% Tween-20.
22. Blocking buffer: TBS-T buffer containing 5% blotting-grade nonfat dry milk
23. Flat-tipped forceps, Saran Wrap.
24. Western blotting detection reagents (Amersham, UK).
25. X-ray film cassette, Kodak X-Omat AR or Amersham hyperfilm ECL, Film processing machine.

3. Methods

3.1. Quantification of Protein in Cell Lysates

1. Protein content in cell lysates is routinely measured using a Bio-Rad protein assay based on the method of Bradford ***(2)***. This simple and fast method relies on a shift in the absorbance of an acidic solution of Coomassie Brilliant Blue G-250 dye from 465–595 nm on binding of the protein. This method is relatively free from interference by common reagents (*see* manufacturer's list) with the exception of sodium hydroxide and high concentrations of detergents.
2. The routinely used microassay is ideal for measuring proteins in a 1- to 10–μg range. Pipet 800 μL of standard solution containing 2, 4, 6, 8, and 10 μg BSA or sample solution into 1.5-mL Eppendorf tube. Water or water containing lysis buffer is pipetted into a tube for a reagent blank. Add 200 μL of concentrated dye reagent to each tube and vortex. After 5 min incubation at room temperature, read the absorbance at 595 nm against the reagent blank. For Western blotting, cell lysates containing equal amounts of protein are resolved by SDS-PAGE. Usually 30 μg of total protein is resolved on the gels for blotting purposes. However, 10–15 μg protein is sufficient in the case of abundant proteins, such as stress proteins and structural proteins.

3.2. SDS-PAGE Analysis of Cell Lysates

1. Polyacrylamide gels are formed by the polymerization of acrylamide monomer in the presence of small amounts of crosslinking agent *bis*-acrylamide (N,N'-methylene-*bis*-acrylamide). The polymerization occurs through the action of ammonium persulfate, which generates free radicals, and the formation of free radicals is catalyzed by TEMED (N,N,N',N'-tetramethylethylenediamine). The pore size in polyacrylamide gels decreases with an increase in acrylamide concentration.
2. SDS-PAGE is the method of choice for the qualitative analysis of the protein mixtures. In SDS-PAGE gels, protein samples are mixed with sample buffer that contains β-ME and SDS, and boiled for 5 min at 95°C before loading (*see* **Note 1**). SDS, an anionic detergent, binds the hydrophobic regions of proteins and separates them into component subunits, whereas β-ME reduces the disulfide bonds holding the protein subunits into sulfhydral groups. SDS binding imparts a large negative charge to the denatured polypeptides, masking any charge present in the absence of SDS. The protein–SDS complexes move toward the anode in an

electric field. Because the protein-SDS complexes have the same charge for unit length, the mobility of the complexes depends on their size. Wear gloves and a face mask when weighing out SDS because it is an irritant to mucous membranes.

3. Wipe clean, dry glass plates with 70% ethanol and assemble to form a glass plate sandwich as described by the manufacturer. Clamp the glass plate sandwich to the casting stand. The buffers used in the denaturing SDS-PAGE gel are as described by Laemmli ***(3)***.
4. Mix the following in a 50-mL conical tube for preparing separating gel (*see* **Table 1**) (*see* **Note 2**).
5. Pour the separating gel solution into the glass plate sandwich along an edge of one of the spacers until the height of the solution is 5 cm. Overlay the gel solution with isobutyl alcohol or 50% methanol and allow the gel to polymerize at room temperature for 30 min.
6. Pour off the overlaying layer of methanol and wash the separating gel twice with distilled water. Prepare the stacking gel 30–60 min prior to the running.
7. For the preparation of stacking gel, mix 1.7 mL 30% acrylamide:0.8% *bis*-acrylamide, 2.5 mL 0.5 *M* Tris-HCl, pH 6.8, 5.6 mL distilled water, 0.1 mL 10% (w/v) SDS, 0.1 mL 10% ammonium persulfate, and 0.01 mL TEMED in a 50 mL conical tube. Add the stacking gel solution onto the surface of the separating gel and insert a clean, dry Teflon comb into the solution. Do not introduce any air bubbles in the tooth edges of the comb. Add additional stacking solution to fill the spaces in the comb. Allow the stacking gel solution to polymerize at room temperature for 30 min. Carefully remove the teflon comb from the stacking gel and wash out any unpolymerized acrylamide solution with distilled water using a squirt bottle. Remove the gel sandwiches from the casting stand and snap them to inner cooling core, as described by the manufacturer. Mark the bottom of the wells as this step facilitates loading of the sample. Lower the inner cooling core into the lower buffer chamber of the electrophoresis cell. Fill the upper buffer chamber with the electrophoresis buffer to a level half-way between the short and long plates. Add buffer to the lower buffer chamber to cover the bottom of the gel, and remove air bubbles from the bottom of the gel by swirling with a pipet.
8. Prepare the sample as aforementioned and load the samples just above the bottom of the well using a pipettor with gel loading tips. Add equal volume of 1X sample buffer to any empty wells. Load 10 µL of prestained protein molecular weight standards in one of the wells. Fill the remainder of the lower chamber with electrophoresis buffer. Cover the electrophoresis cell with the lid and connect to a power supply ensuring that electrodes have proper polarity. Run the gels at constant current (30 mA/gel). Under constant current conditions, the voltage will increase to offset the increase in the resistance of the gel during electrophoresis. Some manufacturers recommend running the minigels under constant voltage (200 V) as minielectrophoresis systems are known to dissipate the heat generated by the initial high current. Turn off the power supply when the bromophenol blue in the sample dye reaches the bottom of the gel. Minigels usually run approx 45 min.

Table 1
Recipes for Preparing SDS-PAGE Separating Gels

Stock solution	Final acrylamide concentration in the separating gel (%)			
(mL)	7.5%	10%	12%	15%
30% acrylamide 0.8% *bis*-acrylamide	5.0	6.7	8.0	10
1.5 *M* Tris-HCl, pH 8.8	5.0	5.0	5.0	5.0
Distilled water	9.7	8.0	6.7	4.7
10% (w/v) SDS	0.2	0.2	0.2	0.2
10% ammonium persulfate	0.1	0.1	0.1	0.1
TEMED	0.007	0.007	0.007	0.007

9. Remove the glass plate sandwich from the casting stand and pry open the glass plates using one of the spacers or a plastic wedge. Remove the upper glass plate and discard the stacking gel.

3.3. Western Blotting and Immunodetection of Proteins

1. Equilibrate the gel in transfer buffer for 10 min to remove the electrophoresis buffer salts (*see* **Note 3**). Submerge the fiber pads in transfer buffer for 15 min. Cut two pieces of Whatman 3 MM paper and nitrocellulose membrane to the size of the gel. Use powder-free gloves to handle gel, filter paper, and the membrane as any contaminating grease from hands interferes with the transfer. Soak filter papers in a small volume of transfer buffer. Float the nitrocellulose membrane in deionized water in a tray and ensure that it is wet uniformly.
2. Place the cassette flat on a clean surface with cathode side down. Place one piece of wet filter paper on presoaked fiber pad laid on the cathode side of the cassette. Place the equilibrated gel on the filter paper. Place and align the nitrocellulose membrane on the gel without trapping any air bubbles (*see* **Note 4**). Place the second wet filter paper on top of the nitrocellulose membrane, again, not trapping any air bubbles. Gently roll a glass rod or a small piece of plastic pipet on the filter to remove any bubbles trapped in the gel sandwich. Finally, place another presoaked fiber pad on the filter facing the anode side and clamp the cassette tightly. Place the cassettes in the module, ensuring proper polarity. Place the module in the tank and pour the cold transfer buffer to the top (*see* **Note 5**). Stir the transfer buffer during the transfer to maintain uniform conductivity and temperature.
3. Connect the transfer unit to the power supply, again making sure that the polarity of the electric leads is maintained properly. Run the transfer at 100 V for 1–2 h. Turn off the power supply and remove the nitrocellulose membrane from the gel sandwich. Wash the membrane thoroughly with distilled water to remove any traces of transfer buffer. The transfer efficiency can be checked by either staining the gel with Coomassie blue or staining the membrane with Ponceau S solution [0.1%

(w/v) Ponceau S in 5% (v/v) acetic acid]. Ponceau S binds the proteins reversibly and the membrane can be easily destained by soaking in water for 10 min.

4. Incubate the membrane in freshly prepared blocking buffer (TBS-T solution containing 5% blotting grade nonfat dry milk) in a plastic box for 1 h on a rocker or orbital shaker. If necessary, the membrane can be left in the blocking buffer overnight at 4°C. Place the membrane in the plastic box with protein side facing upwards. The blocking solution blocks the nonspecific protein binding sites on the membrane and prevents the subsequent background problems (*see* **Note 6**). The lids of the pipet tip boxes are ideal for this purpose and the smaller boxes need as little as 10 mL of solution to cover the membrane.
5. Dilute the primary antibody in the blocking solution and incubate the membrane in antibody solution for 1 h on a shaker at room temperature (*see* **Note 7**). The primary antibody dilution should be determined empirically by doing a dot blot of the antigen. Most of the commercially available polyclonal and monoclonal antibodies can be used at 0.1-μg/mL concentration, in combination with luminescence-based detection systems.
6. Pour off the primary antibody and wash the membrane with three changes of 200 mL TBS-T buffer for 5 min each on a shaker at room temperature. Do not skimp on the washes as washing away nonspecifically bound primary antibody is important for avoiding background. The primary antibody can be reused 1–2 times, but storing more than 2 wk at 4°C is not recommended as it may result in bacterial contamination.
7. Incubate the membrane in HRP-conjugated secondary antibody for 30–60 min on a shaker. The dilution of the secondary antibody is empirically determined and made in blocking buffer (TBS-T containing 5% nonfat dry milk). We routinely use goat anti-rabbit IgG (H+L) peroxidase conjugate (Gibco-BRL, cat. no. 13859-012), goat anti-mouse IgG (H+L) peroxidase conjugate (Gibco-BRL, cat. no. 13871-017) at 1:3000 dilution, or donkey anti-goat IgG (H+L) peroxidase conjugate (Jackson Immunoresearch Laboratories, PA) at 1:4000 dilution. When using enzyme-conjugated secondary antibody, make sure that the antibody is against IgG of the species in which the primary antibody is raised.
8. Pour off the secondary antibody and wash the membrane with three changes of 200 mL TBS-T buffer for 5 min each on a shaker.
9. Drain off the excess buffer and incubate the membrane in chemiluminescence blotting detection solution for 1 min at room temperature with gentle rocking. We routinely use enhanced chemiluminescence (ECL) Western-blotting detection reagents (Amersham, UK, Cat. No. RPN 2106) in our laboratory (*see* **Note 8**). This method is based on the emission of light by a cyclic diacylhydrazide, luminol, when it is oxidized in alkaline conditions in a reaction catalyzed by HRP and hydrogen peroxide ***(4)***. Oxidation of luminol in the presence of phenols enhances the luminescence by increasing the light output approx 1000-fold and extending the emission time. The light emission peaks in 5–20 min and has a half-life of approx 60 min. Blue light-sensitive X-ray film such as Hyperfilm ECL has been shown to respond to the light produced from enhanced ECL in a

linear manner and is the film of choice for the direct quantification of proteins using densitometry.

10. Remove the membrane from the detection solution and drain off the excess reagent by holding the edge of the membrane against a tissue paper. Place the membrane on Saran Wrap, fold back wrap to form a liquid-tight seal, and smooth out any air pockets. Place the membrane with protein side up in a film cassette and expose in a darkroom to X-ray films such as X-Omat AR or Hyperfilm ECL. Optimum exposure time varies from 5 s to 5 min and should be determined empirically. The membrane can be stored in refrigerator for reprobing.

3.4. Reprobing the Western-Blotting Membranes

Western-blotting membranes can be reprobed at least twice with antibodies. For reprobing, the membranes are submerged in stripping buffer consisting of 62.5 m*M* Tris-HCl, pH 6.7, 2% SDS, and 100 m*M* β-ME at 50°C for 30 min in a water bath with agitation. Following stripping, the membranes are washed twice in large volumes of TBS-T buffer for 10 min each at room temperature and incubated in blocking buffer for 1 h before proceeding with the immunodetection.

3.5. Immunoprecipitation/Western Blotting

In immunoprecipitation/Western blotting, cell lysates are incubated with specific antibody raised against a target protein and the antibody–antigen complexes are collected by adsorption to protein A or G that has been covalently attached to either agarose or Sepharose beads (*see* **Notes 9** and **10**). Typically, 100–500 μg total cellular protein is incubated with 1–2 μg of primary antibody for 1 h to overnight at 4°C on a shaker with end-over-end rotation. Then, the antibody–antigen complex is incubated with 40 μL (50% slurry) protein A or G agarose for 1 h and the antibody–antigen complex on agarose beads is collected by centrifugation at 2000*g* for 2 min at 4°C. The supernatant is discarded and pellet is washed with the lysis buffer three times. The beads are boiled in sample buffer at 95°C for 5 min and loaded on the gel.

3.6. Western Blotting in the Study of the Renin–Angiotensin System

Development of subtype-specific inhibitors of angiotensin II receptors and molecular cloning techniques have clearly established the presence of at least two major classes of angiotensin II receptors, referred to as AT_1 and AT_2 ***(5)***. Both the receptors are coupled to G proteins and mediate the diverse and complex physiological responses of angiotensin. The binding of angiotensin II to AT_1 or AT_2 receptors leads to the activation of a downstream signaling cascade with a unique spatial and temporal expression and the effects of activated AT_1 and AT_2 receptors are quite often antagonistic in nature. Angiotensin II has

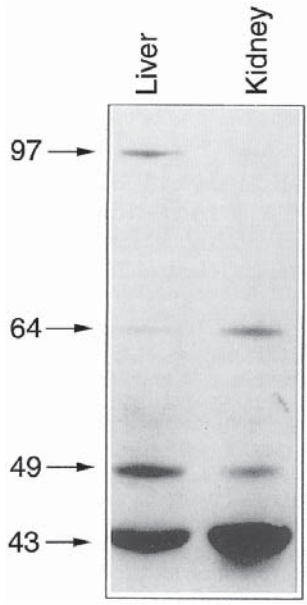

Fig. 1. Western analysis of AT_1 receptor in rat liver and kidney homogenates. Twenty micrograms of protein were resolved on 10% SDS-PAGE gel and transferred to Immobilon-P membrane. The membrane was probed with AT_1 receptor antipeptide antiserum (*see* **Note 8**). The 49-kDa band represents the rat AT_1 receptor and the 64-kDa band may be a glycosylated form of the protein. The 43- and 97-kDa bands are nonspecific bands (reprinted with permission from *ref.* ***5***).

been shown to activate protein phosphorylation pathways such as mitogen-activated protein kinase (MAPK) and Janus kinase and signal transducers and activators of transcription (JAK-STAT) ***(6)***.

Our investigation of angiotensin II gene regulation began with the development of polyclonal rabbit anti-peptide antisera for rat AT_1 ***(5)***. Using antibody raised against the peptide composed of amino acids 15–24 from the NH_2-terminal extracellular domain of the rat AT_{1A} receptor coupled to the COOH-terminal cysteine, we observed four bands in the Western blots of rat liver and kidney homogenates (**Fig. 1**). The 49-kDa band represented the AT_1 receptor, whereas the 64-kDa band may be a glycosylated form of the receptor. Availability of commercial antibodies for both AT_1 and AT_2 receptors (Santa Cruz Biotechnology, Inc., CA) and antibodies for several other proteins activated by angiotensin II has made it possible to use Western blotting to study gene regulation in the renin–angiotensin system.

4. Notes

1. Because the pH of Tris buffers is influenced by temperature, the pH of the working solution should be measured. To avoid the degradation of proteins by proteases, the lysates should be kept on ice prior to and after adding the sample buffer. Samples can be left at room temperature, at the time of gel loading, and after boiling. Partial oxidation of proteins leads to the appearance of double bands on the blots and this can be avoided by increasing the concentration and using fresh β-ME.
2. Determine the percentage of acrylamide in the separating gel by the molecular size of the target protein sought to be analyzed. Typically, 7.5% denaturing SDS-PAGE gels are used for the separation of proteins in the molecular size range of 25–200 kDa; 10% SDS-PAGE gels for 15–70-kDa proteins; and 15% SDS-PAGE gels for 12–45-kDa proteins. The stacking gel used is the same, irrespective of the separating gel used. Resolution of proteins in 5–20-kDa molecular size range is achieved by using Tris-tricine buffer systems ***(7)***.
3. Elution efficiency of proteins from the gel and the binding capacity of the membrane are the two important factors that influence the transfer efficiency in Western blotting. The elution of proteins from the gel is affected by factors such as the thickness and acrylamide concentration of the gel, protein size, the pH of the transfer buffer, and the presence and concentration of SDS and methanol in the transfer buffer. The binding capacity is affected by the type of membrane used and the composition of the transfer buffer. In general, gels with higher acrylamide pecentage and greater thickness transfer less efficiently and need longer transfer times. Methanol decreases the elution from the gels by fixing the proteins in the gel, while it enhances the binding capacity of the membrane by enhancing the hydrophobic interaction of the proteins with the membrane. Removing or lowering the concentration of methanol from the transfer buffer improves the elution of proteins from the gel. SDS at a concentration of 0.1% in the transfer buffer enhances the transfer of all proteins, particularly those larger than 60 kDa in size. However, SDS can interfere with protein binding to the membrane and should not be used in the transfer buffer for the nylon membranes ***(8)***.
4. Nitrocellulose membranes with a pore size of 0.45 μm are routinely used for blotting purposes. However, membranes with 0.2 μm pore size might bind low-molecular-weight proteins more efficiently. Polyvinylidene difluoride (PVDF) membranes are preferred in blots intended for N-terminal protein sequencing and amino acid analysis as they are resistant to acidic or basic conditions and organic solvents. Wet the PVDF membrane in methanol before use.
5. Protein blotting by semidry systems is an effective alternative to tank transfer systems. In the semidry system, the gel and the membrane are held horizontally between two buffer-saturated Whatman 3MM filter papers, which are in direct contact with two plate electrodes that are close together. The advantage of the semidry system lies in its rapidity and requirement for small amounts of buffer. In a semidry system, the filter paper and blotting membrane should be of the same size as the gel and properly aligned to avoid the possibility of a short circuit.

However, a tank transfer system is preferable to a semidry system for the transfer of high-molecular-weight proteins as it enables longer transfer times.

6. High background is one of the common problems encountered during immunodetection. Blocking the nonspecific binding sites of primary and secondary antibodies is important for avoiding high background stain. Quality blocking agents should be used as trace contaminants may interfere with antigen–antibody interaction. We have routinely obtained good blots using blotting-grade nonfat dry milk from Bio-Rad. Gelatin (3% w/v) has been suggested as an alternative to dry milk, particularly, when using antiphosphotyrosine antibodies. However, gelatin is a poor blocking agent in our opinion. A combination of 1% (w/v) nonfat dry milk and 1% bovine serum albumin (fraction V, Sigma) in TBS-T is recommended by some manufacturers for use with antiphosphotyrosine antibodies. Using the primary and secondary antibodies at the highest possible dilutions for positive results, freshly prepared blocking solution, increasing the wash times and volumes of wash buffers, and optimizing the X-ray film exposure times are important for avoiding high background. Incubating the membranes at 4°C also decreases the nonspecifc binding ***(9)***.
7. Some antibodies recognize protein epitopes that are involved in secondary or tertiary structures and do not recognize the proteins denatured in the SDS-PAGE gels. This occurs more frequently with monoclonal than with polyclonal antibodies. In such cases, the proteins are resolved on nondenaturing PAGE gels in discontinuous conditions. For this, the Tris-HCl, pH 6.3, Tris-HCl, pH 8.8, Tris-glycine, pH 8.3 (electrophoresis buffer), and sample buffers are prepared without 0.1% SDS and the samples are not boiled. The separation of proteins in nondenaturing gels depends on a combination of properties such as size, shape, and charge. In some cases, an antibody that recognizes the protein in solution will not recognize the same protein on blotting membrane. Such antibodies are used only for immunoprecipitation.
8. Before the advent of chemiluminescence, the antigen–antibody complex was visualized through the activity of a marker enzyme conjugated with the secondary antibody. In the case of alkaline phosphatase conjugated secondary antibody, the membrane is incubated in alkaline phosphatase substrate solution containing nitroblue tetrazolium and 5-bromo-4-chloro-3-indolyl phosphate until the appearance of a blue–purple product (**Fig. 1**). Alkaline phosphatase hydrolyzes 5-bromo-4-chloro-3-indolyl phosphate into a corresponding indoxyl compound, which upon oxidation and dimerization forms an insoluble blue indigo that is deposited on the filter. Hydrogen ions released during the dimerization process reduce nitroblue tetrazolium to a purple colored insoluble diformazan, which is also deposited on the filter. The reaction is stopped by removing the membrane from the enzyme substrate solution and washing the membrane in PBS containing 2 m*M* EDTA. For HRP conjugated secondary antibody, the membrane is incubated in a horseradish peroxidase substrate solution containing 3,3'-diaminobenzidine and hydrogen peroxide. Oxidation of 3,3'-diaminobenzidine results in the appearance of red–brown insoluble complex on the membrane.

9. Both protein A and G bind to the F_c portion of the constant region of immunoglobulins. However, their binding capacity depends on the immunoglobulin class, subclass, and species type. Although protein A binds antibodies from human, rabbit, and guinea pig most tightly, protein G is better for antibodies from mouse, sheep, cow, and horse ***(10)***. This discrepancy in the specificity ranges of proteins A and G can be circumvented by using various commercially available protein A and G agarose conjugates. The prominent heavy (55-kDa) and light (27-kDa) chain immunoglobulin bands that appear with some primary and secondary antibody combinations can be reduced by using primary antibody agarose conjugate rather than protein A or G agarose.
10. Appearance of many nonspecific bands is another problem often encountered in immunodetection. This problem occurs more often when using crude antibody preparations and can be redressed to a major extent through affinity purification of the primary antibody. In immunoprecipitation experiments, preadsorption of the sample with preimmune serum from the same animal in which the antibody is raised lessens the appearance of nonspecific bands. Peptide neutralization is another procedure for the identification of antibody–specific antigen bands. For neutralization, antibody, at the highest dilution to give positive result, is incubated with fivefold excess of peptide antigen in a small volume of PBS for 2 h at room temperature and the antibody–peptide mixture is used for immunodetection.

References

1. Towbin, H., Staehelin, T., and Gordon, J. (1979) Electrophoretic transfer of proteins from polyacrylamide gels to nitrocellulose sheets: procedure and some application. *Proc. Natl. Acad. Sci. USA* **76,** 4350–4354.
2. Bradford, M. M. (1976) A rapid and sensitive method for the quantitation of microgram quantities of protein utilizing the principle of protein-dye binding. *Anal. Biochem.* **72,** 248–254.
3. Laemmli, U. K. (1970) Cleavage of structural proteins during the assembly of the head of bacteriophage T4. *Nature* **227,** 680–685.
4. Whitehead, T. P., Kricka, L. J., Carter, T. J., and Thorpe, G. H. (1979) Analytical luminescence: its potential in the clinical laboratory. *Clin. Chem.* **25,** 1531–1546.
5. Paxton, W. G., Runge, M., Horaist, C., Cohen, C., Alexander, R. W., and Bernstein, K. E. (1993) Immunohistochemical localization of rat angiotensin II AT_1 receptor. *Am. J. Physiol.* **264,** F989–F995.
6. Marrero, M. B., Schieffer, B., Li, B., Sun, J., Harp, J. B., and Ling, B. N. (1997) Role of Janus kinase/signal transducer and activator of transcription and mitogen-activated protein kinase cascades in angiotensin II- and platelet-derived growth factor-induced vascular smooth muscle cell proliferation. *J. Biol. Chem.* **272,** 24,684–24,690.
7. Schagger, H. and von Jagow, G. (1987) Tricine-sodium dodecyl sulfate-polyacrylamide gel electrophoresis for the separation of proteins in the range from 1 to 100 kDa. *Anal. Biochem.* **166,** 368–379.

8. Peluso, R. W. and Rosenberg, G. H. (1987) Quantitative electrotransfer of proteins from sodium dodecyl sulfate-polyacrylamide gels onto positively charged nylon membranes. *Anal. Biochem.* **162,** 389–398.
9. Thean, E. T. and Toh, B. H. (1989) Western Blotting: temperature dependent reduction in background staining. *Anal. Biochem.* **177,** 256–258.
10. Kruger, N. J. (1996) Detection of polypeptides on blots using secondary antibodies or protein A, in *The Protein Protocols Handbook* (Walker, J. M., ed.) Humana, Totowa, NJ, pp. 313–321.

17

Quantification of Angiotensin-Converting Enzyme (ACE) Activity

Qing Cheng Meng and Kathleen H. Berecek

1. Introduction

Angiotensin-converting enzyme (ACE) is a dipeptidyl carboxypeptidase (EC 3.4.15.1) whose physiologic action is the conversion of AI to AII, and as such, it plays an important role in the regulation of blood pressure and fluid balance. ACE has been localized to endothelial cells throughout the body and epithelial cells in gut and kidney. It exists both as a membrane-bound enzyme and in a freely soluble form in plasma. The importance of the membrane-bound form is underscored by the recently described local renin–angiotensin system (RAS) in various organs, including heart, blood vessels, and kidney ***(1)***. In the heart and vascular smooth muscle, the local RAS is believed to play an important role in hypertrophy and remodeling. Accordingly, accurate and reliable methods for measurement of tissue (i.e., membrane bound) ACE activity are important, as well as soluble ACE activity.

2. Measuring ACE Activity

Several methods for the measurement of ACE activity have been described, with that of Cushman and Cheung ***(2)*** being most commonly utilized. This method uses the ACE–specific substrate hippuryl-his-leu (HHL) coupled with spectrophotometric detection of the product hippuric acid (HA). Other methods for quantitating ACE activity utilize bioassay ***(3)***, radioisotopic ***(4,5)***, fluorometric ***(6)***, and high performance liquid chromathography (HPLC) procedures ***(7,8)*** for measurement of the product. These assays were cumbersome, and have low sensitivity and/or reproducibility because of incomplete inhibition of the enzyme and/or the presence of interfering substances, resulting in high blank values. The availability of purified preparations of ACE and complete analysis of its amino

From: *Methods in Molecular Medicine, vol. 51: Angiotensin Protocols*
Edited by: D. H. Wang

acid sequence has made possible generation of specific antibodies to ACE and development of radioimmunoassays for ACE protein. Using polyclonal antibodies to human lung ACE raised in rabbits, Alhenc-Gelas et al. developed a sensitive, direct radioimmunoassay (RIA) for human ACE ***(9)***. This method has the advantage that ACE inhibitors do not interfere with it, thus permitting enzyme content to be monitored in patients and experimental animals undergoing ACE-inhibitor treatment. Meanwhile, it is impossible to monitor ACE activity instead of enzyme content by RIA method, especially in underdoing ACE-inhibitor treatment in clinic. The expense and difficulty of generating high affinity, high titer antibodies, the difficulty of separating bound from free ligands, and the possible reactivity of anti-ACE antibodies with catalytically inactive metabolites of ACE have limited the application of direct RIAs for ACE. In addition, most methods for ACE activity measure the soluble form of the enzyme. Membrane-bound ACE activity in tissues has been quantitated utilizing trypsin pretreatment to remove the active enzyme from the cell membranes. Trypsin extraction removes the membrane binding sequences from ACE and, thus, produces subtle alterations in the size and charge of the molecule ***(10)***. Whether these effects alter the catalytic activity of the enzyme is uncertain. Standard detergent extraction procedure may result in incomplete extraction of ACE from membranes. In addition, they may cause high blank values in the spectrophotometric ACE assay because of difficulty in removing the detergent, which interferes with the spectrophotometric quantitation of HA.

2.1. Results

We have developed a sensitive method for the accurate and reproducible quantitation of membrane-bound ACE activity in tissue, as well as soluble ACE activity in blood, in which ACE is extracted with detergent and reaction product is isolated from the reaction mixture by HPLC, thus eliminating interference from the detergent and reaction byproducts. This method is a modification of the Cushman and Cheung procedure, which utilizes the artificial substrate HHL and quantitates the product HA by UV detection at 228 nm. The active site-specific ACE inhibitor captopril is used to inhibit the enzyme in blank samples and increase the specificity of the assay.

3. Materials

3.1. Animals

Healthy mongrel dogs of both sexes weighing 18–25 kg ($N = 6$).

3.2. Apparatus

1. Pump, a Type U6K injector equipped with a 1-mL sample loop.
2. Phenyl analytical column (250 mm × 4.6 mm id, 5-μm particle size).

3. UV detector set at 228 nm.
4. One-channel recorder.

3.3. Reagents

1. Hippuryl-his-leu (HHL): substrate for ACE.
2. Hippuric acid (HA): reaction product.
3. Captopril: ACE-specific inhibitor.
4. Triton-100 and ethyl acetate.

3.4. Buffers

1. 0.02 *M* potassium phosphate buffer and 0.1 *M* phosphate buffer (pH 8.3) for tissue homogenization and tissue resuspension, respectively.
2. 0.3 *M* NaCl, 0.01% Triton X-100, 10^{-4} *M* $ZnC1_2$, and 5 m*M* HHL as substrate in 0.1 *M* phosphate buffer (pH 8.3) for reaction mixture.

All solvents used were of HPLC grade and other chemicals used were of analytical grade.

4. Methods

4.1. Animals

1. Dogs ($N = 6$) underwent induction of a deep surgical plane of anesthesia with isoflurane inhalation anesthesia, and then were subjected to thoracotomy.
2. The heart was arrested with a lethal dose of KCl and removed from the chest, rapidly cooled in ice-cold phosphate buffer, and placed on a stainless steel tray on ice.
3. The heart and lung were then dissected, and tissue (right and left atria, right and left ventricles [apex, mid, base], and septum and both lungs *en bloc*) was flash frozen in liquid N_2 and stored at –80°C. Dissection of heart was performed carefully excluding endo- and epicardium from tissue sample.

4.2. Activity Assay with HPLC Separation

1. Tissues were homogenized in 0.02 *M* potassium phosphate buffer (pH 8.3), centrifuged at 40,000*g* for 20 min at 4°C and washed three times with the same buffer. The final tissue pellet was resuspended to a concentration of 0.2 g/mL in 0.1 *M* phosphate buffer; from this 50 μL of homogenized tissue was removed for assay.
2. Tissue extracts (50 μL) were incubated with 500 μL of a reaction mixture containing 0.3 *M* NaCl, 0.01% Triton X-100, 10^{-4} *M* $ZnC1_2$ and 5 m*M* HHL as substrate in 0.1 *M* phosphate buffer, pH 8.3, at 37°C for 30 min.
3. A second 50-μL tissue aliquot was preincubated with 0.1 m*M* captopril for 30 min at room temperature prior to the addition of HHL as a tissue blank in order to define specific ACE activity. The enzymatic reactions were terminated by addition of 500 μL of 1 *N* HC1.

4. The HA formed by the reaction of ACE on HHL (500 μL) was extracted from the acidified solution into 1.5 mL of ethyl acetate by vortex mixing for 15 s. After brief centrifugation, a 1-mL aliquot of each ethyl acetate layer was transferred to a clean tube and dried by heating at 120°C for 30 min.
5. The dried HA samples were redissolved in 0.5 mL of the HPLC mobile phase, which contained 15% acetonitrile (CH_3CN) in 0.1 *M* ammonium phosphate buffer (v/v), pH 6.8, and applied to a reverse phase Alltima 5 μm-phenyl HPLC column.

4.3. HPLC Separation of HHL and HA

1. The HPLC separation of HHL and HA was carried out at 35°C at a flow rate of 1.0 mL/min. The protein content of samples was determined according to Lowry et al. ***(11)***. Values for protein content of samples were tightly correlated with wet weights of the tissues (10 μg protein/mg wet weight of heart tissue). Therefore, all data were expressed as units of HA formed per gram tissue wet weight (1 U = 1 μmol HA formed/min at 37°C).
2. The intraassay and interassay coefficients of variation of a standard sample of dog lung were 3.5% (*N* = 6) and 4.6% (*N* = 6), respectively.
3. Under the isocratic condition aforementioned, a clear separation of HA from HHL was achieved for standard compounds (**Fig. 1**, left panel). A representative chromatogram obtained in an assay of ACE activity in a normal dog left ventricle is shown in the middle panel of **Fig. 1.** Note that the HA peak is easily quantifiable and that a large HHL peak is present. In the absence of HPLC separation, as in the standard Cushman and Cheung assay, this can create interference of greater magnitude than the value for the HA generated in the reaction, yielding negative values for ACE activity. The right panel of **Fig. 1** depicts the results of adding captopril to the reaction mixture: generation of HA was clearly reduced with a corresponding increase in the HHL peak. In addition, spiking samples with standard HA (0.1 ng) resulted in increased amplitude of the HA peak, confirming the identity of the compound. Standard curves were used to quantitate the amount of HA formed and were linear over the concentration range studied (**Fig. 2**).

4.4. ACE Activity Assay without HPLC Separation (Standard Cushman and Chung Method)

1. A method similar to ACE assay with HPLC separation, but the final washed pellet was retained and dissolved in 5 m*M* CHAPS overnight at 4°C instead of Triton X-100. This extraction procedure has been shown to be as efficient as Triton X-100 extraction for tissue ACE because a prolonged period is allowed for CHAPS to extract the enzyme from the membrane ***(10)***.
2. The dried HA samples were redissolved in distilled H_2O and read in a Shimadzu UV recording spectrophotometer at 228 nm.
3. Data were calculated using the method of Cushman and Cheung ***(2)***. In the standard methodology, CHAPS was used to extract membranes because nondialyzable Triton X-100 interferes with the spectrophotometric assay.

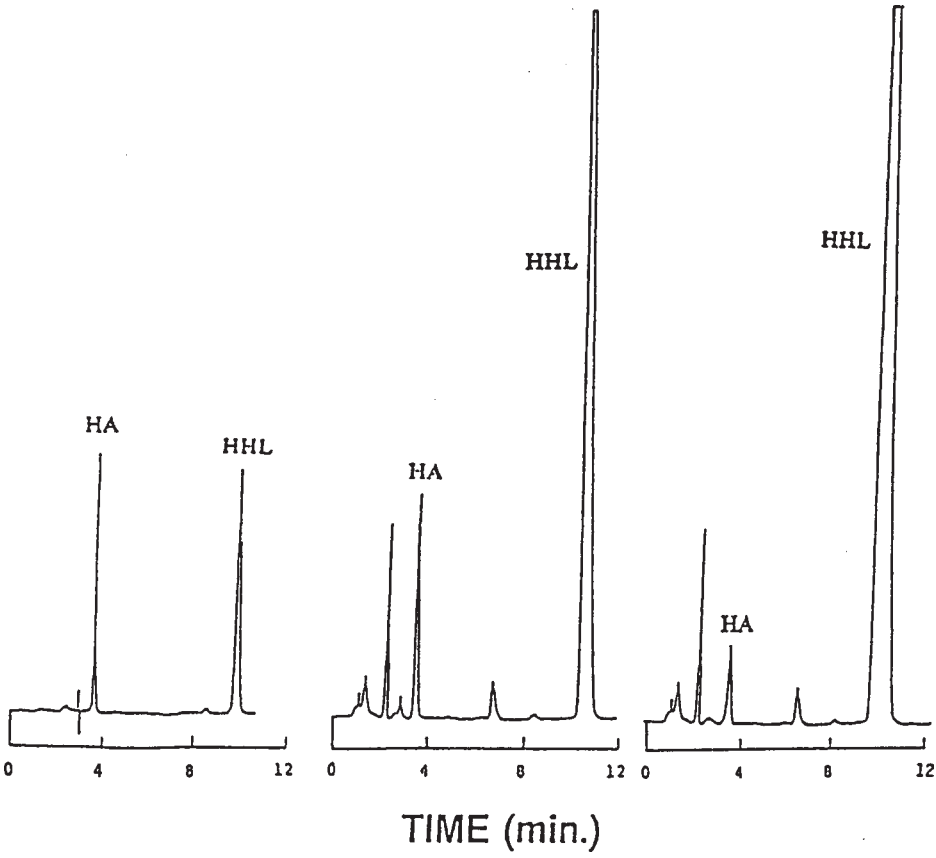

Fig. 1. HPLC chromatograms. Left panel: chromatography for 0.01 μg hippuric acid (HA) and hippuryl histidyl-leucine (HHL) standards. Middle panel: Chromatogram from dog left ventricle assay (1 mg of midwall) showing HA peak and persistent substrate (HHL) peak following a 40-μL HPLC injection from the final reaction product after extraction. Right panel: Chromatogram from dog left ventricle assay in the presence of 0.1 m*M* captpril following a 90-μL HPLC injection from the final reaction product after extraction.

4.5. The Comparison Between HPLC ACE Assay and Standard ACE Assay

1. ACE activity assay was performed by the standard Cushman and Cheung method and our HPLC-based method on aliquots of the left ventricle of the same dog. **Figure. 3** shows the comparison between the Cushman and Cheung (standard) and HPLC-based (new) assays in dog left ventricle (midwall).

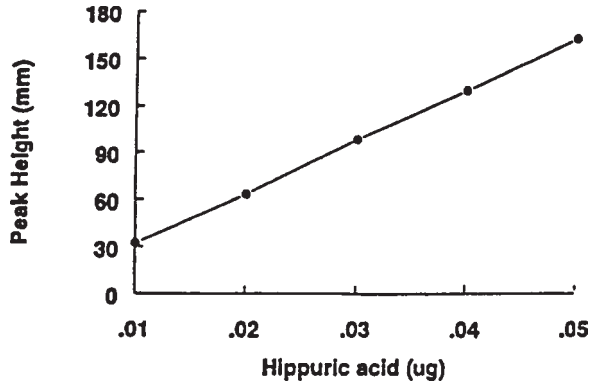

Fig. 2. Standard curve for hippuric acid from HPLC chromatograms.

2. ACE activity measured with the HPLC-based assay was 1.24 ± 0.18 mU/g ($N = 6$), four-fold the values obtained with the standard Cushman and Cheung assay (0.31 ± 0.09 mU/g, $N = 6$).
3. ACE activity measurement in right ventricle and midwall of left ventricle of six normal dogs by both HPLC and standard methods are summarized in **Fig. 4**.
4. The HPLC–based analysis revealed a significant difference (right > left) in ACE activity between the ventricles; this regional difference in ACE expression was not evident when ACE activity was measured by the unmodified Cushman and Cheung technique. Our observation of two-fold increase in ACE activity in the right ventricle compared with the left confirms the previous report of Urata ***(12)*** in normal and failing human hearts.
5. Furthermore, ACE activity when measured by the HPLC assay was greater (four- and ten-fold, respectively) in both left and right ventricles than when measured by the Cushman and Cheung assay.

4.6. Recovery Experiment

1. Recovery of HA from the ethyl acetate liquid extraction procedure was determined from known molar quantities of standard HA solution subjected to the same conditions as the tissue assay.
2. Briefly, a 5-m*M* solution of HA was prepared in 0.01% Triton X-100, 0.02 *M* phosphate buffer (pH 8.3); 500 µL was transferred into a dry test tube and combined with 500 µL of 1 *N* HCl.
3. The mixture was agitated on a vortex-mixer for 30 s and centrifuged at 3000*g* for 20 min; then, 500 µL of the solution was transferred to a tube containing 1.5 mL of ethyl acetate and vortexed.
4. After centrifugation, 1 mL of the upper organic layer was transferred to a tube and dried by heating at 120°C for 30 min.
5. The extracted samples were injected into the HPLC under the conditions aforementioned, and recovery of HA was calculated from the ratio of measured HA to the amount injected.

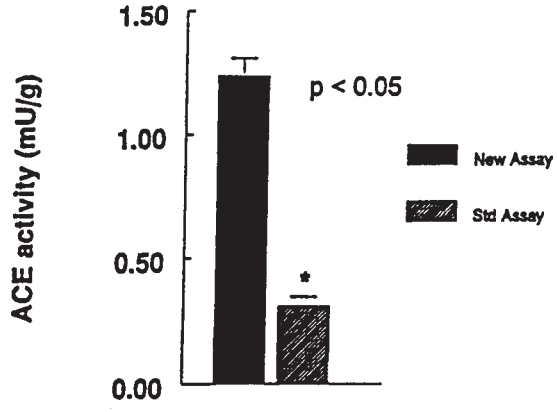

Fig. 3. Comparison of HPLC-based assay (new) with standard Cushman and Cheung assay on tissue from dog left ventricle (midwall). Results are mean ± SEM. $N = 6$ for each new group. Asterisk (*) indicates a significant difference between the new and the standard assays ($P < 0.05$).

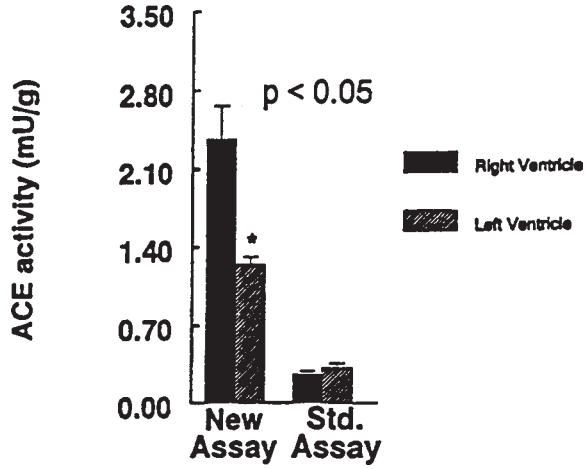

Fig. 4. Tissue ACE activity heterogeneity in normal canine hearts (left ventricle and right ventricle); comparison between HPLC-based assay (left bars) with standard Cushman and Cheung assay (right bars). Results are mean ± SEM. $N = 6$ for each group. Asterisk (*) indicates a significant difference between values for right and left ventricle by the HPLC assay ($P < 0.05$).

6. Recovery of HA from detergent extracted samples was 97% with the HPLC separation/detection method compared with 91% reported in the literature for the standard procedure of Cushman and Cheung ***(2)***.

4.7. Kinetic Studies

1. Dog lung tissue was used for kinetic studies of tissue ACE activity utilizing the HPLC assay protocol.
2. Tissue was prepared and ACE activity determined as aforementioned utilizing the ACE-specific substrate HHL and the active site-directed ACE inhibitor captopril.
3. K_m and V_{max} were determined according to the method of Eisenthal and Cornish-Bowden ***(13)***. Briefly, initial velocities (V_o) at various initial substrate concentrations (S_o) were determined from the initial slopes of their corresponding time-dependent studies. Direct linear plots of V_o against S_o were then generated, defining a family of lines. K_m and V_{max} were determined from median values between the points of intersection (of these lines) projecting onto the abscissa and ordinate, respectively.
4. Values for K_m (1.34 ± 0.08 m*M*) and V_{max} (36.8 ± 11.5 × 10^{-10} *M*/min) showed that the assay characteristics are in agreement with published results obtained using purified of ACE (**Fig. 5**) ***(10)***. Utilizing our HPLC method, the time dependence of tissue ACE activity was linear out to 30 min (**Fig. 6**).

4.8. Data Analysis

1. Peaks for HA and HHL were identified by comparison with the retention time of standard compounds. Standard solutions of HA were prepared daily. A solution of 10 μg/mL HA was prepared in the HPLC mobile phase and diluted serially to provide calibration standards.
2. Values are expressed as means ± SEM. Student's unpaired *t*-test was used for comparisons between groups. Differences were considered to be statistically significant at the $P < 0.05$ level.

5. Notes

1. The new HPLC-based assay was able to increase the sensitivity of the assay, permitting accurate quantitation of ACE activity in 4–5-mg samples of normal dog heart. ACE activity measured with the HPLC-based assay was 1.24 ± 0.18 mU/g ($n = 6$), four-fold the values obtained with the standard Cushman and Cheung assay (0.31 ± 0.09 mU/g, $n = 6$).
2. Values for K_m (1.34 ± 0.08 m*M*) and V_{max} (36.8 ± 11.5 × 10^{-10} *M*/min) of ACE showed that the assay characteristics are in agreement with published results obtained using purified preparations of ACE. Moreover, by utilizing the ACE-specific inhibitor, captopril, specificity was improved without interfering with the HPLC detection of HA and HHL.
3. This method will be useful in studies of the role of the tissue RAS in the pathogenesis of cardiovascular disease in animal models and humans, as well as in documenting the effects of ACE inhibitor and angiotensin II antagonist therapy on these processes.

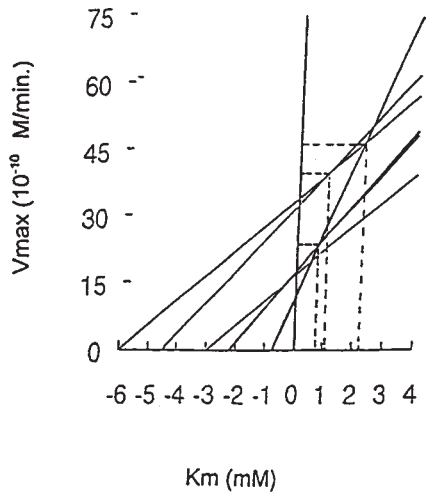

Fig. 5. Direct linear plot for canine lung ACE activity as determined by the HPLC assay. K_m and V_{max} were determined by averaging the corresponding values from the points of intersection between the dashed lines and the abscissa and ordinate, respectively.

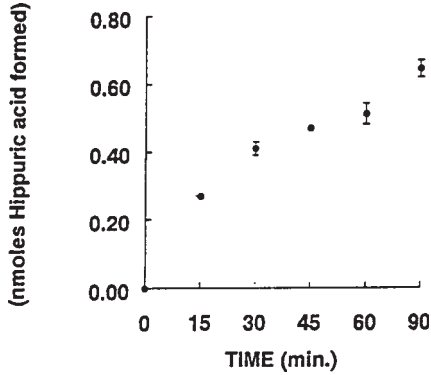

Fig. 6. Time dependene of HPLC-based assay in canine lung in the presence of 1.5 m*M* HHL. Each point is the mean ± SEM of three determinations.

References

1. Oparil, S., Meng, Q. C., Sun, S. D., Chen, Y. F., and Dell'Italia, L. (1996) Tissue angiotensin converting enzyme, in *Vascular Endothelium: Responses to Injury.* Catravas J. D., et al. (eds), Plenum, New York, pp 205–239.
2. Cushman, D. W. and Cheung, H. S. (1971) Spectrophotometric assay and properties of the angiotensin-converting enzyme of rabbit lung. *Biochem. Pharmacol.* **20,** 1637–1648.

3. Andersen, J. B. (1967) Converting enzyme activity in liver damage. *Acta Pathol. Microbiol. Scand.* **71,** 1–7.
4. Rohrbach, M. S. and Deremee, R. A. (1979) Serum angiotensin converting enzyme activity in sarcoidosis as measured by a simple radiochemical assay. *Am. Rev. Respir. Dis.* **119,** 761–767.
5. Ryan, J. W., Chung, A., Ammons, C., and Carlton, M. L. (1977) A simple radioassay for angiotensin-converting enzyme. *Biochem. J.* **167,** 501–504.
6. Friedland, J. and Silverstein, E. (1976) A sensitive fluorometric assay for serum angiotensin converting enzyme. *Am. J. Clin. Pathol.* **66,** 416–424.
7. Nagamatsu, A., Soeda, S., and Inokuchi, J. L. (1978) Rapid estimation of angiotensin I-converting enzyme activity by high-speed liquid chromatography. *Yakugaku Zasshi* **98,** 1296–1299.
8. Chiknas, S. G. (1979) A liquid chromatography-assisted assay for angiotensin-converting enzyme (peptidyl dipeptidase) in serum. *Clin. Chem.* **25,** 1259–1261.
9. Alhenc-Gelas, F., Weare, J. A., Johnson, R. L., Jr., and Erdös, E. G. (1983) Measurement of human converting enzyme levels by direct radioimmunoassay. *J. Lab. Clin. Med.* **101,** 83–96.
10. Lanzillo, J. J., Stevens, J., Dasarathy, Y., Yotsumoto, H., and Fanburg, B. L. (1985) Angiotensin-converting enzyme from human tissues. Physicochemical, catalytic, and immunological properties. *L. Biol. Chem.* **260,** 14,938–14,944.
11. Lowry, O. H., Rosebrough, N. J., Farr, A. L., and Randall, R. J. (1951) Protein measurement with the Folin phenol reagent. *J. Biol. Chem.* **193,** 265–275.
12. Urata, H. (1990) Identification of a highly specific chymase as the major angiotensin II forming enzyme in the human heart. *J. Biol. Chem.* **265,** 22,348–22,357.
13. Eisenthal, R. and Cornish-Bowden, A. (1974) The direct linear plot. A new graphical procedure for estimating enzyme kinetic parameters. *Biochem. J.* **139,** 715–720.

18

Quantification of Angiotensin Peptides

Qing Cheng Meng and Kathleen H. Berecek

1. Introduction

There is an endogenous renin–angiotensin system in the kidney, and angiotensin (Ang) II generated within the kidney may play an important role in the regulation of renal hemodynamics and sodium excretion ***(1–6)***. Assessment of the functional significance of the intrarenal renin–angiotensin system requires accurate and sensitive measurement of the Ang peptides in renal tissue. These measurements have been problematic because of methodologic difficulties, and very variable Ang peptide levels have been reported in extracts of rat kidney ***(7–13)***. Radioimmunoassay (RIA) procedures carried out on crude tissue extracts have produced inaccurate results because of interference and/or crossreactivity with biologically inactive metabolites of the Ang peptides that are present in high concentrations in tissues. Additional problems include the instability of the Ang peptides during extraction from tissue, in part because of the cleavage of peptide bonds by tissue peptidases; incomplete extraction from tissue stores; variable recoveries from solid-phase extraction on octadecylsilica gel (C_{18}) cartridges, which are commonly used for the preliminary clean-up of samples before high-performance liquid chromatography (HPLC), and the difficulties inherent in gradient elution techniques for HPLC ***(13)***. We have recently developed a simplified method for extracting Ang peptides from brain tissue ***(14)***.

In this chapter, we adapted our novel method for the extraction, separation, identification, and quantitation of Ang like immunoactivity from tissue to examine the effects of dietary NaCl intake on intrarenal Ang I, II, and III levels in salt-sensitive spontaneously hypertensive rats (SHR-S) and salt-resistant Wistar-Kyoto (WKY) and Sprague-Dawley (SD) rats.

From: *Methods in Molecular Medicine, vol. 51: Angiotensin Protocols*
Edited by: D. H. Wang

2. Materials

Animals: Male SHR-S and WKY rats were obtained at 7 wk of age from Taconic Farms (IBU-3 colony; Germantown, NY); male SD rats were obtained at the same age from Charles River Breeding Laboratories (Wilmington, MA).

Apparatus: The HPLC system consisted of two Model 501 pumps, a Type U6K injection valve equipped with a 1-mL sample loop, a uBondapak phenyl precolumn, an analytical uBondapak phenyl column (300 × 3.9 mm i.d., 10-μm particle size), a tunable Model 484 UV detector (all from Waters Associates, Milford, MA) set at 200 nm, a one-channel recorder (Kipp and Zonen BD 40; Alltech Associates, Inc., Deerfield, IL), and a Model 2110 fraction collector (Bio-Rad Laboratories).

Reagents: The ^{125}I-(Ile^5) Ang I and II (specific activity 2000 Ci/mmol) used for RIA and recovery studies were purchased from Amersham (Arlington Heights, IL) . Synthetic standard peptides, including Ang I, II, and III and the ***(3–8)*** peptides, were purchased from Bachem Fine Chemicals (Torrance, CA). Ang ***(1–7)*** was kindly provided by Dr. Mahesh Khosla of the Cleveland Clinic Foundation (Cleveland, OH). All chemicals used were purchased from Sigma (St. Louis, MO) and of analytical grade.

3. Methods

Frozen tissue was extracted in 2-*M* acetic acid and then subjected to solid phase extraction with the cation exchange resin AG 50W × 4. Angiotensin peptides were separated by reversed-phase HPLC on a phenyl silica gel column with an eluent consisting of 20% acetonitrile in 0.1 *M* ammonium phosphate buffer, pH 4.9, and quantitated by radioimmunoassay. The elution of standard peptides under isocratic conditions revealed clear resolution of Ang I, II, III, and the ***(1–7)*** and ***(3–8)*** peptides. Recoveries of both labeled and unlabeled Ang peptide standards from the extraction step were >90%.

3.1. Animals

Three days after arrival, half of the rats, in each group (SHR-S, WKY rats and SD rats) were placed on an 8% NaCl diet (ICN Biochemicals Purina Chow with 8% NaCl, Irvine, CA), while the other half remained on the basal 1% NaCl diet. After three weeks on the diets, rats were decapitated without prior anesthesia and the kidneys were rapidly removed, immediately frozen in liquid nitrogen, and stored at –80°C.

3.2. Extraction

The frozen kidney tissue was placed into 2 *M* acetic acid (1:10 wt/vol) and then homogenized immediately in a Polytron homogenizer. Each tissue sample

was boiled for 30 min in 2 *M* acetic acid, and then an additional 2 *M* acetic acid was added (1:10 wt/vol). The homogenate was centrifuged (30,000*g* at 4°C for 60 min), and the supernatant was collected and lyophilized overnight to dryness. The residue was taken up in 5 mL of distilled water and again centrifuged as above. The supernatant was then subjected to solid-phase extraction with the hydrogen form of the analytical grade cation exchange resin AG 50W × 4 (200–400 mesh). The resin was prewashed with water; its pH was adjusted to 6.0 with NaOH, and aliquots of approx 3 g were placed into glass column (6-mm inside diameter). Samples of kidney extract were loaded onto the columns and washed with 15 mL of distilled water. The columns were eluted with 10 mL of 3 *M* ammonia; the eluate was lyophilized overnight to dryness and then reconstituted in 500 μL of the mobile phase of the HPLC system. A 350-μL aliquot of each sample was injected into the HPLC for separation of the Ang peptides.

3.3. HPLC Separation of Ang Peptides

All HPLC separations were carried out at ambient temperature at a flow rate of 1.0 mL/min. The mobile phase consisted of 20% acetonitrile in 0.1 *M* ammonium phosphate buffer (vol/vol), pH 4.9. Eluate fractions (400 μL) were collected in plastic polypropylene tubes. Fractions with retention times corresponding to those of synthetic Ang, II, and III standards were subjected to RIA immediately after elution from the column.

Clear separation of unlabeled synthetic standard Ang I, Ang II, Ang III, Ang ***(1–7)***, and Ang ***(3–8)*** peptides was achieved with our HPLC conditions (**Fig. 1**). Mixtures of 5–10 ng of each peptide were applied to the column. **Figure 2** shows a typical HPLC elution pattern of renal extracts from four individual SHR-S on the 8% NaCl diet. The HPLC eluates were assayed by use of the Ang I and II RIA. Three distinct peaks of immunoreactive material eluted with retention times identical with those of synthetic Ang I, II, and III. Each vertical bar represents the amount of immunoreactive material in a single 400-μL fraction of HPLC column eluate.

3.4. Recoveries

The recovery of Ang I and II from the extraction step was estimated by two independent methods. In the first, [^{125}I]Ang I (range of 3.1×10^7 to 6.0×10^5 cpm; 200 pg to 10 ng) and [^{125}I]Ang II (range of 2.9×10^7 to 6.2×10^5 cpm; 200 pg to 10 ng) were added to kidney tissue samples before homogenization, and ^{125}I-labeled material was measured in the HPLC fraction. In the second, 0.2×10^{-6} to 10×10^{-6} μmol of unlabeled Ang I and II dissolved in 200 μL of 1 m*M* HCl was added to tissue samples before homogenization, and Ang I and II were measured by RIA in the HPLC fractions. Values for Ang I and II in

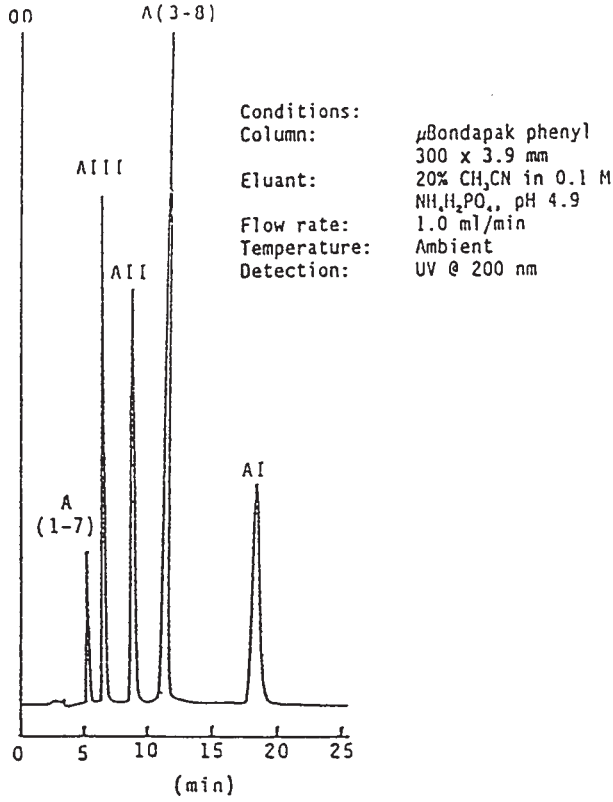

Fig. 1. HPLC separation of synthetic Ang peptides on a μBondapak Phenyl column (300 × 3.9-mm inside diameter, 10-μm particle size) under the isocxratic conditions described in the Test (pH 4.9). UV detection at 200 nm. Samples: A (1–7), Ang (1–7); AIII, Ang III; AII, Ang II; A (3–8), Ang (3–8); AI, Ang I. A total of 5–10 μg of each peptide were applied to the column.

untreated kidney tissue were subtracted from the values obtained for kidney tissue, with exogenous Ang I and II added in order to assess recovery.

The recoveries of [^{125}I]Ang I and [^{125}I]Ang II added to tissue samples through all of the acetic acid extraction, purification, and separation procedures were 93 ± 2 and 91 ± 2%, respectively, over the entire 50-fold dose range examined ($N = 6$). The^{125}I-labeled Ang were eluted from the HPLC column as single peaks, suggesting that they were not degraded during sample handling. The recoveries of unlabeled synthetic Ang I and II added to tissue samples through all of the extraction, purification, and separation procedures were 91 ± 9 and 90 ± 1%, respectively, ($N = 6$). Dried residues of eluates from the AG-50W-X4 columns did not interfere with the RIA.

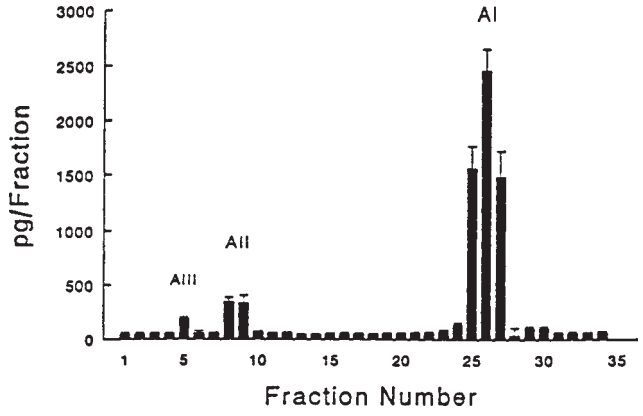

Fig. 2. RIA measurement of Ang-like immunoactivity in samples eluted from HPLC derived from four individual kidneys (N = 4). Ang-like immunoactive peptides extracted from kidneys were separated by HPLC and identified by RIA. Each HPLC fraction volume was 400 μL. AI, AII, and AIII, Ang I-, Ang II-, and Ang-like immunoactivity. Values are means ± SE.

3.5. Radioimmunoassay

Antibodies to Ang I and II were raised in our laboratory in New Zealand white rabbits immunized against the peptides conjugated to poly-L-lysine, as previously described ***(14,15)***. The crossreactivity of anti-Ang I antiserum with Ang II and of anti-Ang II antiserum with I was <0.5%; the crossreactivity of anti-Ang II antiserum with Ang III was 100%. The sensitivity of the RIA for Ang I was 4 pg/mL; for Ang II, it was 2 pg/mL. Aliquots (100 μL) of each relevant fraction of column effluent were subjected to RIA immediately after collection. RIA for Ang I was carried out in polystyrene tubes; for Ang II, it was carried out in polypropylene tubes. To correct for possible nonspecific interference with RIA, the extraction procedure was performed without the application of a kidney sample. Dried residues of column eluates were used as blanks in the RIA.

Figure 3 shows the Ang I, II, and III contents of kidney from SHR-S and WKY and SD rats maintained on either 1% or 8% NaCl diets for three weeks. These data show that renal Ang II levels are significantly higher in SHR-S than in WKY or SD rats on either diet and that dietary NaCl supplementation suppresses Ang II in the normotensive, NaCl-resistant WKY and SD strains, but not in SHR-S. These findings are consistent with an enhanced (compared with the normotensive, NaCl-resistant WKY, and SD strains) role for Ang II in the kidney of SHR-S, particularly under conditions of dietary NaCl supplementation.

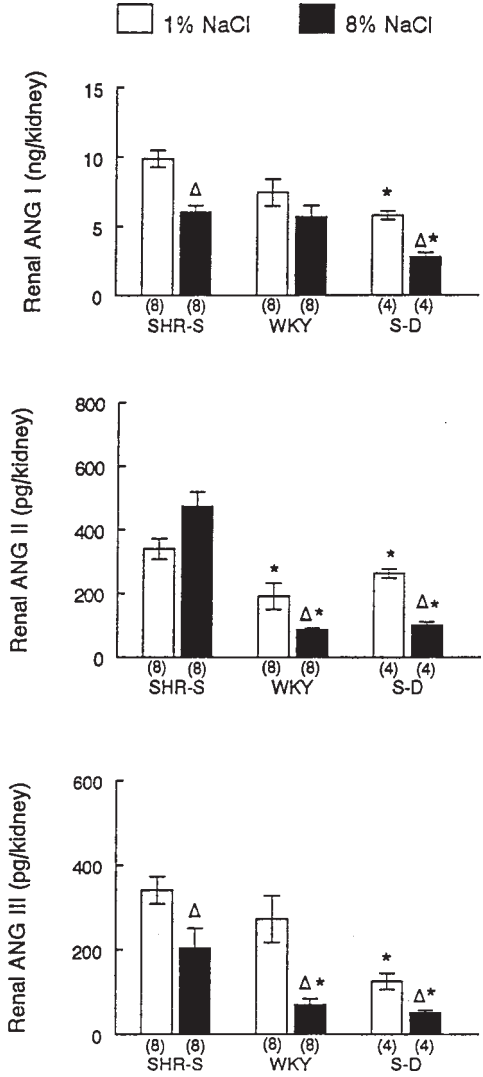

Fig. 3. Effects of basal sodium (1% NaCl) and high-sodium (8% NaCl) diets for 3 wk on rat renal Ang I and II levels in SHR-S and WKY rats. Values are means ± SE. $\Delta P < 0.05$, compared with respective values of SHR-S. $*P < 0.05$, compared with respective values of SHR-S.

References

1. Abe, Y., Okahara, T., Kishimoto, T., and Yamamoto, K. (1979) Intrarenal role of renin-angiotensin system in the regulation of renal hemodynamics. *Jpn. J. Pharmacol.* **29,** 325–333.

2. Mendelsohn, F. A. O. (1982) Angiotensin II: evidence for its role as an intrarenal hormone. *Kidney Int.* **22,** S78–S81.
3. Campbell, D. J. (1987) Tissue renin-angiotensin system: sites of angiotensin formation. *J. Cardiovasc. Pharmacol.* **10,** S1–S8.
4. Phillips, M. I., Speakman, E. A., and Kimura, B. (1993) Levels of angiotensin and molecular biology of the tissue renin angiotensin system. *Regul. Pept.* 43: 1–20.
5. Rosivall, L., Narkates, A. J., Oparil, S., and Navar, L. G. (1987) De novo intrarenal formation of angiotensin II during control and enhanced renin secretion. *Am. J. Physiol. (Renal Fluid Electrolyte Physiol.)* **21,** F1118–F1123.
6. Cogan, M. G. (1990) Angiotensin II: a powerful controller of sodium transport in the early proximal tubule. *Hypertension* **15,** 451–458.
7. Mendelsohn, F. A. O. (1976) A method for measurement of angiotensin II in tissues and its application to rat kidney. *Clin. Sci. Mol. Med.* **51,** 111–125.
8. Mendelsohn, F. A. O. (1979) Evidence for the local occurrence of angiotensin II in rats kidney and modulation by dietary sodium intake and converting enzyme blockade. *Clin. Sci.* **57,** 173–179.
9. De Silva, P. E., Husain, A., Smeby, R. R., and Khairallah, P. A. (1988) Mrasurement of immunoreactive angiotensin peptides in rat tissues: some pitfalls in angiotensin II analysis. *Anal. Biochem.* **174,** 80–87.
10. Campbell, D. J., Lawrence, A. C., Tawrie, A., Kladis, A., and Valentijn, A. J. (1991) Differential regulation of angiotensin peptides levels in plasma and kidney of the rat. *Hypertension* **18,** 763–773.
11. Fox, J., Guan, S., Hymel, A. A., and Navar, L. G. (1992) Dietary Na and ACE inhibition effects on renal tissue angiotensin I and II and ACE actibity in rats. *Am. J. Physiol.* **262,** F902–F909.
12. Guan, S., Fox, J., Mitchell, K. D., and Navar, L. G. (1992) Angiotensin and angiotensin converting enzyme tissue levels in two-kidney, one clip hypertensive rats. *Hypertension* **20,** 763–767.
13. Matsushima, Y., Kawamura, M., Akabane, S., et al. (1988) Increases in renal angiotensin II content and tubular angiotensin II receptors in prehypertensive spontaneously hypertensive rats. *J. Hypertens.* **6,** 791–796.
14. Haber, E., Koerner, T., Page, L. B., Kliman, B., and Purnode, A. (1969) Application of a radioimmunoassay for angiotensin I to the physiologic measurement of plasma renin activity in normal human subjects. *J. Clin. Endocrinol. Metab.* **29,** 1349–1355.
15. Page, L. B., Haber, E., Kimura, A. Y., and Purnode, A. (1969) Studies with the radioimmunoassay for angiotensin II, and its application to measurement of renin activity. *J. Clin. Endocrinol. Metab.* **29,** 200–206.

19

Radiolabeling of Angiotensin Peptides

Robert C. Speth and Joseph W. Harding

1. Introduction

1.1. Overview

The use of radioiodinated angiotensins has contributed greatly to our knowledge of the renin–angiotensin system (RAS). This chapter provides brief descriptions of the application of radioiodinated angiotensins and other radioiodinated compounds to study the RAS and the issues that must be considered when using radioiodinated angiotensins. In addition, this chapter provides a detailed description of a method for the preparation and purification of both iodine^{125} (^{125}I) and iodine^{127} (^{127}I)-labeled angiotensin-related ligands.

1.2. Contributions of Radioiodinated Angiotensins and Related Compounds to Our Understanding of the Renin–Angiotensin System

Radiolabeled angiotensins have been used for more than 30 yr since Dietrich ***(1)*** radiolabeled angiotensin II (Ang II) with iodine^{131} (^{131}I) to study Ang II antibodies. The measurement of angiotensin peptides is now done exclusively by radioimmunoassay employing radioiodinated angiotensins (cf., preceding chapter by Berecek and Meng). The formation of Ang I by renin is commonly assayed by radioimmunoassay with ^{125}I- labeled Ang I. The initial characterization of Ang II receptors ***(2)*** and subsequent subtyping of Ang II into AT_1 and AT_2 subtypes has been highly dependent of the use of ^{125}I-labeled AT_2 selective ligands, such as CGP 42112 ***(3)*** and ^{125}I-labeled angiotensins ***(4)*** (cf., Chapter 21 by Thibault and Schiffrin). In addition, characterization of angiotensin-converting enzyme (ACE) and its tissue distribution has been accomplished in part using ^{125}I-labeled ACE inhibitors such as 351A ***(5,6)***. More recently, the identification of angiotensin IV (Ang IV) receptors has been

From: *Methods in Molecular Medicine, vol. 51: Angiotensin Protocols*
Edited by: D. H. Wang

based on radioligand binding studies using ^{125}I-labeled ligands specific to Ang IV receptors ***(7,8)***.

Identification of angiotensin receptors during biochemical purification procedures has been dependent on labeling of the receptors with radioiodinated angiotensins that can be crosslinked to the receptors, e.g., by photoaffinity labeling ***(9,10)***.

Localization of angiotensin II and angiotensin IV receptors with the use of receptor autoradiographic techniques (cf., Chapter 22) has also been exclusively dependent on ^{125}I-labeled angiotensins.

1.3. Perspectives on the Radioiodination of Angiotensin-Related Ligands

Since the seminal observation of Hunter and Greenwood ***(11)*** describing the ability of chloramine T to oxidize iodide, allowing it to react with tyrosine residues on proteins, there has been a steady stream of radioiodinated proteins and peptides that have been generated with this procedure. The chloramine T reaction is by far the most commonly used procedure for radioiodination of angiotensins and related peptides. The reason for the popularity of the chloramine T procedure for radioiodination of angiotensin-related ligands is because all of these ligands have a single tyrosine or phenolic moiety with which the ^{125}I molecule reacts to form a covalent bond.

The monoradioiodinated peptide can be easily resolved from the uniodinated and multiply iodinated peptide by a one-step high-performance liquid chromatography (HPLC) purification step; thus, the specific activity can be calculated based on the specific activity of ^{125}I, which is 17.4 Ci/mg. Multiplied by 125 mg/mmol, the molar specific activity of ^{125}I is 2175 Ci/mmol. Because only the single tyrosine moiety is labeled, the radioiodinated product is extremely reproducible from batch to batch.

1.3.1. ^{125}I-Labeled Ligands versus ^{131}I- and ^{3}H-Labeled Ligands

It is fortuitous that the ^{125}iodine addition to angiotensin related ligands has benign effects on the ability of ligands to interact with angiotensin receptors, ACE, or angiotensin antibodies. Whereas early studies suggested that iodination of angiotensins diminished their ability to bind to Ang II receptors [*see* review by Lin et al. ***(12)***], it is now well established that it is the diiodinated angiotensins that are unable to bind with high affinity to Ang II receptors. Also, monoiodinated angiotensins are efficacious and bind with high affinity to Ang II receptors ***(2,12,13)***.

However, the benign nature of the addition of the iodine molecule should not be taken for granted. Monoiodoangiotensin II is not Ang II, and it can have

subtle differences in affinity for Ang II receptors. Moreover, there has been no systematic characterization and comparisons across species of the affinity of iodoangiotensins relative to noniodinated angiotensins, or for the various AT_1- and AT_2- receptor subtypes. Thus, studies attempting to determine maximal binding capacity (B_{MAX}) and the dissociation constant (K_D) of Ang II receptors should use only monoiodinated Angiotensin-receptor ligands. The use of a monoradioiodinated Angiotensin ligand at a single concentration, generally less than the K_D concentration, together with the corresponding noniodinated ligand to determine B_{MAX} and K_D, is fraught with complications and can easily generate inaccurate values.

Although Hunter and Greenwood used ^{131}I to radiolabel proteins, the use of ^{131}I to radiolabel proteins and peptides is rarely used at this time. This is because the half-life of ^{131}I is so short (8 d) it limits the useful life of a batch of ^{131}I-labeled radioligand to no more than a few days. In addition, the specific activity (16,250 Ci/mmol) tends to be higher than that needed to assay most components of the RAS. If ^{131}I-labeled ligands were used, more radioactivity would be used to attain a similar receptor occupancy as is obtained with a ^{125}I-labeled ligand. This would be of advantage only if there were extremely low levels of the component of the RAS or if only a small amount of tissue were available for sampling. In addition, the higher specific activity of ^{131}I, hence the higher amount of radioactivity needed to examine receptor binding at concentrations equivalent to ^{125}I-labeled ligands, makes it a greater safety hazard than ^{125}I (*see* **Subheading 1.4.1.**).

Despite the fact the tritium (^3H) labeling of angiotensin-related ligands offers the benefit of not causing a significant structural modification of the radioligand, ^3H-labeled angiotensin-related ligands are rarely used to study the RAS. This is caused in part by the low specific activity of ^3H-labeled compounds relative to ^{125}I-labeled compounds. The specific radioactivity of ^3H is 29 Ci/mmol, which is 1.3% that of ^{125}I. Even if 3 to 4 ^3H molecules are attached to the radioligand, the specific activity is still only about 5% of that of the mono^{125}I-labeled radioligand (2175 Ci/mmol).

Another drawback to using ^3H vs ^{125}I is the low energy of the particles emitted from ^3H. To do receptor autoradiography with ^3H requires a special film that has no protective coating over the emulsion layer of the film, e.g., Ultrofilm or Hyperfilm ^3H, because the beta particles emitted by ^3H cannot penetrate through the protective coating. Such film is both costly and difficult to work with because of its increased susceptibility to scratching. The energy of the particles emitted by ^{125}I is sufficiently high as to be able to penetrate the protective coating of most standard autoradiography films.

1.4. Radioiodination of Angiotensins and Related Compounds

1.4.1. Safety Issues

Prior to beginning any work with radioactive iodine, one should review the safety precautions needed to use radioactive iodine without endangering human health. Many of these precautions are common sense and standard good laboratory practices, however, there are some special concerns associated with the use of ^{125}I. The major health concern associated with the use of ^{125}I is thyroid toxicity. The thyroid gland avidly takes up iodine, which it uses to make thyroid hormones. Thus, if an individual takes in ^{125}I, either by ingestion or inhalation, the ^{125}I will concentrate in the thyroid gland with potential toxic effects via free-radical generation. In the process of radioiodination, and to some extent via normal oxidative events, iodide forms volatile iodine (I_2), which can be inhaled. Thus, all procedures involving the use of ^{125}iodide should be carried out in a fume hood that prevents any volatile I_2 from escaping into the laboratory. Users of ^{125}I should routinely have thyroid scans to be certain that the procedures in use are preventing ^{125}I intake.

The other primary concern associated with the use of radioiodine is surface contamination that can be transmitted outside of the laboratory leading to inadvertant intake. It is critically important to wear protective gloves and change them often when working with radioiodine. Some experts recommend double-gloving to minimize accidental skin contamination, which may occur if a glove tears or is defective. This can adversely affect dexterity, however, and increase the likelihood of a spill. If using a single pair of gloves, an individual's hands should be monitored for surface ^{125}I contamination with a survey meter at frequent intervals. If skin contamination is detected, hands should immediately be washed with soap and a hand brush to remove the surface contamination. It is also important to wear protective apparel (e.g., a lab coat and eye protection) to protect from exposure to ^{125}I that could splash from a dropped container. NEN Life Science Products (Boston, MA), from whom we routinely obtain ^{125}I, recommends the use of disposable lab coats to preclude having to wash contaminated lab coats and possibly contaminating laundry facilities.

Most commercial suppliers of ^{125}I provide instructions on the safe use of ^{125}I, which should be reviewed prior to handling this material. In addition, institutions that work with radioioisotopes have radiation safety coordinators who are available to assist users in devising safe-handling practices for ^{125}I.

One additional reminder is that all containers used to store ^{125}I should be labeled with marking tape that bears the radioactive materials symbol, states that the material is radioactive, and has a place to indicate the identity and amount of the radioisotope and a reference date.

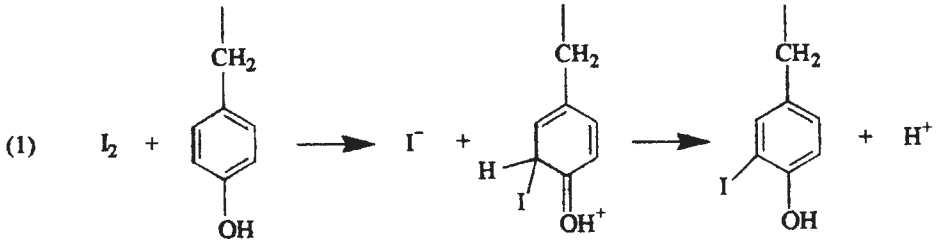

1.4.2. Procedures for Preparation of Radioiodinated Angiotensins and Related Compounds

1.4.2.1. Radioiodination Reaction Chemistry

A variety of methods could theoretically be used to iodinate standard angiotensin peptides. The common thread that connects the various methods is that they oxidize I^- to I_2, which is then available to participate in the electrophilic attack of the phenolic ring of tyrosine. This attack is directed at the aromatic ring carbons ortho to the phenolic OH of the tyrosine ring. The directionality of the reaction is derived from the ability of the oxygen electrons of the OH to participate in resonance stabilization of the tetrahedral intermediate that is formed following I addition (*see* **Eq. 1**).

1.4.2.2. Reagents Commonly Used for Radioiodinations

The major determinant in choosing the most effective oxidizing agent for the generation of I_2 is the sensitivity of the protein or peptide to be labeled to oxidation. Sensitivity reflects the protein or peptide's content of functionally critical oxidizable amino acids like cysteine, methionine, and tryptophan. A related concern is the protein or peptide's sensitivity to reducing agents. This is of particular concern when the parent compound contains disulfide linkages and the iodination method involves the addition of a reducing agent as a means of terminating the iodination reaction. Because standard angiotensins contain neither readily oxidizable nor reduceable amino acids, these considerations do not typically play a role in the choice of iodination protocols. The iodination of modified angiotensins containing any of the sensitive amino acids, however, requires the careful selection of iodination procedure.

Of the many potential iodination methods that could be used for radiolabeling angiotensins, only four will be discussed below. These include methods that utilize chemical oxidizing agents—chloramine T (described in detail in **Subheading 3.**), IODO-BEADS® (immobilized chloramine T), IODO-GEN®, and an enzymatic method employing lactoperoxidase. The most simple methods employ chloramine T (N-chloro-p-toluenesulfonamide), which is a water-

soluble oxidizing agent that relies upon the acidity of sulfur to extract electrons from 2 I^- yielding I_2. The advantages of this method are that it is simple and inexpensive. The major disadvantage is that the chloramine T, which is a strong oxidizing agent, comes into intimate contact with the parent protein or peptide in solution, often resulting in oxidation of amino acids that are critical for biological function. Again, standard angiotensins contain no such sensitive amino acids and, as such, the use of chloramine T is appropriate. IODO-BEADS®, manufactured by Pierce (Rockford, IL), are simply chloramine T immobilized on polystyrene beads. Because the chloramine T is not in solution, oxidation only occurs at the surface of the beads. Because of the smaller size and, thus, faster diffusion rate of $^{125}I^-$ compared to the parent compound, the I^- has more points of contact with the oxidizing surface and is, therefore, preferentially oxidized, sparing the critical amino acids in the target compound. Thus, this method is theoretically gentler and is better at preserving biological activity than is chloramine T in solution. IODO-GEN®, also made by Pierce, combines this surface oxidation feature with a weaker oxidizing agent, 1,3,4,6-tetrachloro-3α,6-α-diphenylglycouril. This product has often been used to iodinate proteins and peptides that contain oxidizable amino acids. A final major difference between the use of chloramine T in solution and IODO-BEADS® or IODO-GEN® is that the chloramine T in solution method requires the use of a reducing agent (typically, $Na_2S_2O_5$) to stop the oxidation reaction, resulting in the destruction of disulfide links; methods that employ IODO-BEADS® or IODO-GEN® simply require the physical separation, e.g., centrifugation of the solution containing the radioiodinated compound from the bead-immobilized oxidizing agent. Although these methods have distinct advantages over chloramine T in terms of the preserving oxidizable or reducible amino acids, such advantages are not required for the successful iodination of standard angiotensins.

A final approach to preserving critical amino acids is to use an enzyme, such as lactoperoxidase, to oxidize I^- to I_2. Lactoperoxidase employs hydrogen peroxide (H_2O_2) as the oxidizing agent. This oxidation reaction is slower and preferentially results in the oxidation of the more easily oxidizable I^-. The enzyme is typically immobilized, again exploiting the differences in the diffusion rates of I^- and the larger peptides or proteins. Finally, some methods do not involve the direct addition of H_2O_2, but include a second enzyme, such as glucose oxidase, that generates H_2O_2 from β-D-glucose, in order to maintain a low, but constant concentration of H_2O_2. This low level of oxidation and the immobilized enzymes serve to facilitate the selective oxidation of I^- as compared to amino acids in the target. Again, the use of a reducing agent is unnecessary because the bead-immobilized enzyme(s) can be removed by simple centrifugation. Although the lactoperoxidase/glucose oxidase method is very effective

for iodinating angiotensins, the advantages and accompanying expense of the method are not necessary to achieve successful iodination of angiotensins.

1.4.3. Procedures for Purification of Radioiodinated Angiotensins and Related Compounds

Several procedures are available for purification of monoradioiodinated angiotensin-related ligands. As reviewed by Speth and Husain ***(14)***, initial procedures included ion-exchange chromatography or preparative electrophoresis. With the advent of reverse phase HPLC, however, the purification of monoradioiodinated angiotensin-related ligands became a simple and rapid one-step procedure. The drawback, however, is that the HPLC system and the detector systems can be costly to set up. And, unless considerable time and effort is expended to remove ^{125}I contamination from the HPLC system, it needs to be dedicated exclusively to the preparation of radioiodinated ligands. In our laboratory, the HPLC system and the fume hood in which it is located is dedicated to purification of radioiodinated ligands. To maintain such a dedicated system, this laboratory serves as is a centralized service center (Peptide Radioiodination Service Center), providing radioiodinated ligands to users on a cost-recovery basis.

2. Materials

2.1. Equipment Needed for Preparation and Purification of Radioiodinated Angiotensin-Related Ligands

1. Fume hood.
2. 12 × 75 mm glass culture tubes.
3. Siliconized or low-protein retaining 0.4 or 1.5 mL microcentrifuge tubes cat. no. 02-681-320, Fisher Scientific, Pittsburgh, PA) for radioligand storage.
4. Radioactive labeling tape.
5. Laboratory mixer, e.g., Vortex® mixer.
6. Pipettors, e.g., Finnpipet®, Eppendorf®, 0.5–10, 10–200, and 100–1000-μL volumes.
7. Siliconized or low-protein retaining pipet tips; 0-200-μL volume for addition of reagents (cat. no. 05-541-14, Fisher Scientific), ultramicro (0–10 μL) for determining the concentration of ^{125}I-labeled ligands (cat. no. T-141LR, United Scientific Products, San Leandro, CA) and 100–1000 μL (cat. no. 21-381-8B, Fisher Scientific) for transfer of radioligands to storage tubes.
8. HPLC system. A low-cost single-pump isocratic system is sufficient to provide purified monoradioiodinated ligands.
9. HPLC injector with a loading reservoir and injection syringe of 500 μL is recommended for large-scale radioiodinations.
10. C18 reverse-phase HPLC column (Microsorb-MV 100 Å, 300 mm, R0086200C5, Varian, Walnut Creek, CA, or equivalent).

11. Flow-through ultraviolet (UV) detector capable of monitoring peptide bonds at 210 nm. This is not essential, but is strongly recommended for monitoring the elution of the uniodinated and moniodinated ligand, and chloramine T.
12. Flowthrough radioiodine detector (Model 170 Beckman Instruments, Fullerton, CA, or equivalent). This is also not essential, but is strongly recommended to allow only the desired peak of radioactive material to be saved.
13. Fraction collector. If it is not possible to monitor the column effluent with a UV and radioiodine detector, one can save fractions eluting from the column and monitor them for UV absorption using a standard UV spectrophotometer and for radioiodine using a gamma counter.
14. Gamma counter. This is essential to monitor the yield of the radioiodination reaction and determine the concentration of radioiodinated ligand. A sodium iodide crystal counter is best, but it is also possible to use a liquid scintillation spectrometer for measurement of ^{125}I, although this requires the extra step of adding liquid-scintillation cocktail to quantitate the amount of ^{125}I.

2.2. Solvents and Stabilizer

1. Phosphoric acid (reagent grade, P6560, Sigma Chemical Co., St. Louis, MO, or equivalent). Acetic acid can be substituted for phosphoric acid. The advantage of using acetic acid is that the free-acetate ion can be removed by evaporation. However, the disadvantage of using acetic acid is that it absorbs at 210 nm more than phosphoric acid, making it more difficult to accurately monitor the ligand peaks eluting from the HPLC column.
2. Triethylamine (T0886, Sigma or equivalent).
3. HPLC water (HPLC Grade, W5-4, Fisher Scientific, Fairlawn, NJ or equivalent).
4. Acetonitrile (HPLC Grade, A995-4, Fisher Scientific or equivalent).
5. Bovine albumin (certified peptidase-free, A3059 Sigma or equivalent). Large stocks of 100 mg/mL of bovine albumin can be made and aliquotted into microcentrifuge tubes for freezer storage.

2.3. Reagents

1. 500-m*M* sodium phosphate buffer, pH 7.5 (S0751, monosodium phosphate and S0876 disodium phosphate, Sigma or equivalents).
2. Ligand to be radioiodinated, usually at 1 m*M* concentration in distilled water.
3. Carrier-free sodium ^{125}iodide (NEZ-033H, New England Nuclear, Boston, MA or equivalent) (*see* **Note 5** for further information.)
4. Chloramine T (C9887, Sigma or equivalent) 4 mg/mL in distilled water, made fresh on day of radioiodination.
5. Sodium metabisulfite $Na_2S_2O_5$ (S1516, Sigma or equivalent). 5 mg/mL in distilled water, made fresh on day of radioiodination.
6. Potassium iodide (P2963, Sigma, or equivalent) 20 mg/mL in distilled water.

3. Methods

The procedure for radioiodination of angiotensins is derived from the procedures of Hunter and Greenwood ***(11)*** and ***(12)***.

3.1. Radioiodination Step

As aforementioned, the radioiodination step should be carried out in a fume hood that has been certified for the use of sodium ^{125}iodide.

1. Add 200 μL of the 500 m*M* sodium phosphate buffer to the 12 × 75-mm culture tube.
2. Add ligand to be radioiodinated.
   a. In our laboratory, peptides and other ligands are routinely stored frozen at 0.5–4 m*M* concentrations in water and are thawed immediately prior to use.
   b. Because millicurie amounts of radioiodinated ligands are routinely produced in this laboratory, 5–25 μL of the ligand stock is added to the culture tube.
   c. The amount of ligand can be scaled down as needed to prepare microcurie lots of radioiodinated ligands.
3. Add sodium ^{125}iodide.
   a. Different concentrations of ^{125}iodine can be obtained commercially. We use a concentrated stock of ^{125}iodine (NEZ-033H, NEN Life Science Products, Boston, MA), which is approx 360 mCi/mL.
   b. At a concentration of 360 mCi/mL, the molar concentration of ^{125}iodine is 166 μ*M*, or 166 pmol/mL.
   c. For routine radioiodinations, 5 to 25 μL of this sodium ^{125}iodide (830–4075 pmol, or 1.8–9 mCi) is added to the glass culture tube. For preparation of microcurie amounts of radioiodinated ligands, the amount of ^{125}iodine can be scaled down as needed.
   d. It is critical to the success of the radioiodination to make sure that the molar ratio of ligand to ^{125}iodine is at least 10:1. This minimizes the possibility of forming diiodinated radioligand at the expense of the desired monoiodinated radioligand. However, the ratio of ligand to radioiodine should not exceed 50:1 or there is an increased risk that the uniodinated ligand (which elutes from the reverse-phase HPLC column first) will not be completely resolved from the monoiodinated ligand. Such contamination of the iodinated ligand will lower the specific activity of the preparation and compromise the utility of the iodinated ligand.
   e. The preparation of millicurie amounts of radioligand decreases the likelihood that trace contaminants, e.g., iodide or background ^{125}I bleed from the HPLC column will significantly affect the purity of the mono^{125}I-labeled ligand.
4. Add 20 μL of the freshly prepared chloramine T to the culture tube and mix on a laboratory shaker for 15–20 s. Do not allow the reaction to continue for longer than 20 s as it will lead to an increased amount of diiodination of the ligand and may damage the ligand.
5. Add 30 μL of the freshly prepared sodium metabisulfite solution no more than 20 s after the addition of chloramine T to stop the reaction. Continue mixing for an additional 15–20 s.
6. Add 10 μL of potassium iodide as a carrier for the ^{125}iodide. This will minimize the amount of ^{125}iodine that is initially retained on the HPLC, which, over time, would contribute to a high background bleed of ^{125}I from the HPLC column.

7. The reaction mixture is aspirated into the HPLC injector-loading syringe for application to the HPLC column.
   a. To increase the transfer of radiolabeled material from the reaction tube to the HPLC column, the culture tube in which the radioiodination is carried out is rinsed with 150 µL of mobile phase by mixing on a laboratory mixer. This rinse is also aspirated in the injector-loading syringe, and the complete volume is injected onto the column.

3.2. Purification of Monoradioiodinated Angiotensin-Related Ligands

Once the radioiodinated ligand has been prepared, it is immediately purified by HPLC. It is recommended that the HPLC also be located in the fume hood because there is a residual amount of unreacted ^{125}I in the reaction mixture.

1. Preparation of triethylamine phosphate (TEAP) mobile phase.
   a. 5.6 mL of phosphoric acid is added to 1 L of HPLC water. Triethylamine is added dropwise until the pH is 3.0.
   b. The desired proportion of acetonitrile (based on information presented in **Table 1**) is added to a flask containing TEAP. The mixture is degassed for 1–2 min under vacuum with stirring.
2. The C18 reverse-phase HPLC column is equilibrated with the triethylamine phosphate: acetonitrile mobile phase.
3. The reaction mixture is applied to the HPLC column and eluted in the mobile phase.
4. Because retention times can vary considerably with small changes in the proportion of acetonitrile, it is recommended that a sample of unlabeled material be applied to the column to determine its retention time.
   a. If the retention time varies considerably from the expected retention time indicated in **Table 1**, it is possible that the mono^{125}I-labeled material may elute at the same time as the chloramine T, or may elute too soon to be fully resolved from the peak of the uniodinated material. In such cases, the proportion of acetonitrile should be adjusted up or down as needed to shorten or prolong, respectively, the retention time of the unlabeled material to assure that the mono^{125}I-labeled material does not contain any contaminants from the reactants (*see* **Note 8** for further information).

3.3. Collection of Monoradioiodinated Material

If one has access to a flowthrough ^{125}I monitor, one can save the major mono-^{125}I-labeled ligand-containing fraction as it elutes from the HPLC column (examples shown in **Figs. 1** and **2**) at the approximate times shown in **Table 1**. If a flowthrough ^{125}I monitor is not available, it is necessary to use a fraction collector to collect the eluent from the HPLC column. Because the retention times are relatively short, the fraction collector should be set to collect no more than 15-s fractions.

Table 1
Resolution of Radioiodinated Angiotensin-Related Ligands

Ligand	Acetonitrile (%)	Rf Values (min)		
		Uniodinated	Monoiodinated	Diiodinated
Ang I	24	4.5	8.3	14.5
Ang II	20	4.3	9.8	19.7
Dogfish Ang II	20	4.1	9.9	18.0
Ang III	19	4.6	9.6	18.6
Ang IV	22	3.4	6.8	11.7
BPK Ang IV	24	4.8	9.1	15.0
Ang (1–7)	14	3.0	8.1	18.6
Sar^1 Ang II	19	5.5	13.0	23.9
Sar^1, Ile^8 Ang II	18	3.2	6.3	12.0
Sar^1, Val^5, BPA^8 Ang II	22.5	4.3	6.9	11.2
CGP 42112	24	3.6	6.4	12.8
351A	15	3.7	8.0	14.3

Approximate retention times for uniodinated, monoiodinated and diiodinated angiotensin related ligands on a reverse phase C_{18}, 100-micron particle size, HPLC column (Microsorb-MV #R0086200C5, Rainin LC and Supplies, Walnut Creek, CA) at the specified mobile phase acetonitrile percentage at a flow rate of approx 1.8 mL/min. The target range for *Rf* for the uniodinated ligand was 3 to 5 min. Variations in *Rf* values for the uniodinated ligand shown in the table are largely caused by the need to resolve the monoiodinated ligand from the chloramine T peak. Retention times may vary considerably if the percentage of acetonitrile differs from the desired concentration. The aqueous component of the isocratic mobile phase is 83 m*M* phosphate (from phosphoric acid) adjusted to pH 3.0 with triethlyamine. Flow rates for these mobile phases greater than 1.8 mL/min exceed the limiting pressure of 3500 psi for this column. Numbers in superscripts denote amino acid substitutions at residues corresponding to the numbering of the residues in Ang I. Sar is sarcosine, BPA is benzoylphenylalanine, a photosensitive amino acid that has been used to crosslink ligand to receptors ***(18)***, CGP 42112 is an AT_2-selective ligand ***(3)***. BPK Ang IV is $benzoylphenylalanine^8$, His^9, Leu^{10}, Lys^{11} Ang IV.

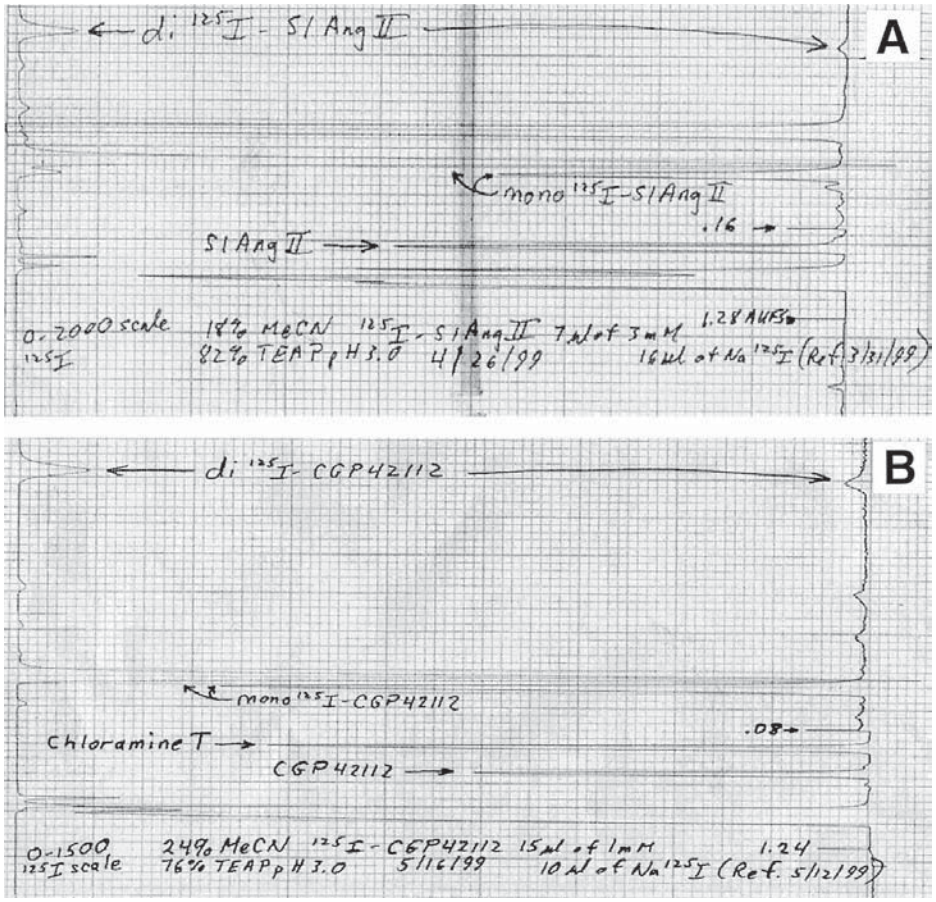

Fig. 1. Chromatograms of radioiodinations of angiotensin-related peptides. (**A**) Chromatogram of a radioiodination mixture of Sar[1], Ile[8] Ang II, sodium ^{125}iodide chloramine T, sodium metabisulfite, potassium iodide, and sodium phosphate buffer was injected onto a C_{18} reverse-phase HPLC column. The reactants were eluted isocratically with 18% acetonitrile and 82% triethylamine phosphate, pH 3.0. The pen on the right-hand side traces the UV 210 nanometer absorbing material eluting from the column and also contains the event marker. The first tick on the lower-right side of the panel indicates the time of injection of the mixture onto the column. The initial sensitivity of the chart recorder pen was 2.56 absorbance units full scale (AUFS). The light lines on the chart paper indicate 24-s intervals, the intermediate lines denote 2 min intervals, and the darkest lines indicate 4-min intervals. At approx 4 min after injection of the mixture onto the column, the sensitivity of the right-hand pen was changed to 0.16 AUFS and is indicated by a tick mark. The pen on the left-hand side indicates ^{125}iodine elution from the HPLC column and is offset by one light chart paper line from the tracing by the right-hand pen. Unreacted Sar[1], Ile[8] Ang II eluted at

3.4. Quantitation of Monoradioiodinated Material

The concentration of mono^{125}iodinated ligand is generally quite high and necessitates the use of small aliquots for gamma counting. Triplicate 2-μL aliquots are placed in 12 × 75-mm glass culture tubes for gamma counting. (The accuracy of measurement of the 2-μL samples is greatly improved by the use of ultramicro pipet tips.) The amount of ^{125}I in the tubes is determined with a sodium iodide crystal detector-containing gamma counter. The cpm value obtained is then corrected for efficiency (the efficiency of our gamma counter is 67% for samples in 12 × 75-mm culture tubes. The dpm value is divided by 4828.5 dpm/fmol and divided by 2 μL to obtain a value of fmol/μL or nanomoles/liter (n*M*). Using the procedures aforementioned, concentrations of mono^{125}I-labeled ligand in excess of 200 n*M* can be obtained.

For counting fractions collected with a fraction collector, 2 μL should also provide a reliable estimate of the ^{125}I concentration of each fraction. Based on the profile of the ^{125}I elution, the fraction containing the mono^{125}I-labeled

---

approx 3.1 min in this chromatogram, whereas mono ^{125}I- Sar^{1}, Ile^{8} Ang II eluted at approx 6.3 min. Di ^{125}I- Sar^{1}, Ile^{8} Ang II eluted at approx 11.8 min. Chloramine T absorbs at UV 210 and its elution at approx 8.1 min is indicated by the greater than full-scale peak on the chromatogram. Unreacted ^{125}I elutes in the void volume of the HPLC column at approx 2 min as shown by the left-hand pen tracing. There is a minor peak that precedes the primary ^{125}I- Sar^{1}, Ile^{8} Ang II peak that may be a minor ^{125}I- Sar^{1}, Ile^{8} Ang II stereoisomer. The peak that is saved as ^{125}I- Sar^{1}, Ile^{8} Ang II is the major peak encompassing more than 90% of the arbitrarily determined scale of the chart recorder. Di ^{125}I- Sar^{1}, Ile^{8} Ang II can be seen to elute much later than the mono ^{125}I- Sar^{1}, Ile^{8} Ang II peak. Other ^{125}I peaks are unidentified. The yield of this reaction, which constitutes the major peak of the left-hand pen was 2.7 mCi, which accounts for approx 65% of the ^{125}I added. **(B)** Chromatogram of a radioiodination mixture of CGP 42112, sodium iodide chloramine T, sodium metabisulfite, potassium iodide, and sodium phosphate buffer was injected onto a C_{18} reverse-phase HPLC column. The reactants were eluted isocratically with 24% acetonitrile and 76% triethylamine phosphate, pH 3.0. The initial sensitivity of the chart recorder pen was 1.28 AUFS. At approx 4.5 min after injection of the mixture onto the column the sensitivity of the right-hand pen was changed to 0.08 AUFS and is indicated by a tic mark. Unreacted CGP 42112 eluted at approx 3.8 min in this chromatogram, whereas mono ^{125}I- CGP 42112 eluted at approx 8.4 min. Di ^{125}I-CGP 42112 eluted at approx 19 min. Chloramine T eluted at approx 5.3 min as indicated on the chromatogram. The peak that is saved as ^{125}I- CGP 42112 is the major peak shown to encompass greater than 95% of the arbitrarily determined scale of the chart recorder. Other ^{125}I peaks are unidentified. The yield of this reaction, which constitutes the major peak of the right-hand pen was 2.5 mCi, which accounts for approx 72% of the ^{125}I added.

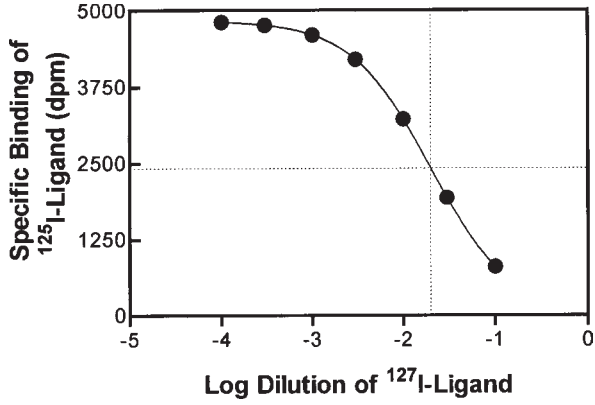

Fig. 2. Theoretical plot of competition by ^{127}I-labeled ligand against ^{125}I-labeled ligand. For this example, the K_D value for the ^{125}I-labeled ligand has been empirically defined to be 1 n*M*, the concentration of the ^{125}iodine-labeled ligand is also 1 n*M*, and the amount of receptor in the assay is 2 fmol. The assay volume is 100 µL, so the total ligand added is 100 fmol. The highest amount of specifically bound radioligand (4828 dpm) is only 1% of the total amount of radioligand added, so it is not necessary to correct for the change in radioligand concentration at the end of the incubation from the initial concentration of radioligand. The curve shown in the figure was generated by the computer program PRISM (Graphpad Software, San Diego, CA) using the "One site competition" subroutine using the equation described in the text. The value obtained by the program for log IC_{50} for the ^{127}I-labeled ligand, shown with dashed lines on the *X*- and *Y*-axes, is –1.699, or 0.02. This IC_{50} value is then subjected to the Cheng-Prusoff equation ***(16)*** described in the text, to yield a value of 0.01. Because the K_I for the ^{127}I-ligand is theoretically identical to that of the ^{125}I-labeled ligand, then the concentration of ^{127}I-ligand is 1 n*M* at a dilution of 0.01. The concentration of the undiluted ^{127}I-ligand (1 n*M*/0.01) is then calculated to be 100 n*M*.

ligand should be easily identified. If the peak is contained in more than one fraction, the fractions should be combined.

To verify the specific activity of the mono^{125}I-labeled ligand, a self-displacement assay can be run using a known quantity of nonradioiodinated ligand (*see* **Note 3** for further information).

3.5. Preservation and Storage of Radioiodinated Ligands

Radioautolysis is a significant problem for radioiodinated ligands. To decrease the extent to which the decomposition of individual radioligand molecules destroys adjacent radioligand molecules, bovine albumin is added to each batch of radioligand at a final concentration of 2 mg/mL (20 µL of 100 mg/mL freezer stock per 1 mL of radioligand solution). The bovine albu-

min molecules act as a sink for absorption of the impact of the free radicals generated by the decomposition of the ^{125}I atoms. Because the amount of bovine albumin exceeds that of the radioligand by more than 1000-fold, this greatly decreases the probability for a free radical to cause destruction of a radioligand molecule.

Often, the concentration of mono^{125}I-labeled peptide in the saved fraction is in excess of 500 n*M*. In such cases, the fraction is diluted with water, which is thoroughly mixed in, to keep the concentration of radioligand to less than 500 n*M*. The bovine albumin is generally added after this dilution is made, to ensure that there is always 2 mg/mL in the solution.

Each batch of radioligand is aliquotted and stored in siliconized or low-retention microcentrifuge tubes. The tubes are stored in a non-frost-free, –20°C freezer in lead containers to minimize environmental exposure to the gamma and X-rays that eminate from ^{125}I. The use of a non-frost-free freezer avoids the temperature fluctuations that occur within a frost-free freezer that can adversely affect the radioligand stability.

The size of the aliquot of radioligand is enough to provide sufficient radioligand for an individual experiment and to minimize the number of freeze-thaw cycles to which the radioligand is subjected. Some investigators prefer not to refreeze aliquots of radioligand, in which case the size of the aliquots should be smaller. If necessary, more than one aliquot should be combined to provide sufficient radioligand for an experiment.

4. Notes

1. Situations requiring nonradioisotopic dilution of the radioligand. On occasion, it may be necessary to use a lower specific-activity radioiodinated angiotensin-related ligand than the pure monoradioiodinated species, e.g., for receptor autoradiography where one wants to use a near-saturating concentration of radioligand, but the receptor density is extremely high ***(15)***. It may not be possible to obtain ^{125}I- containing calibration standards that have as high a density as the radiolabeled samples. In such cases, it is not readily possible to calibrate the optometric density of the film for the amounts of ^{125}I present in the tissue samples (*see* **Note 4**).

   Another example is if one does a saturation-binding assay in which the concentrations of radioligand are more than 20 n*M*. Such a situation might arise if the K_D of the receptor for the radioligand is 5–10 n*M*, and one wants to be sure to have radioligand concentrations considerably above the K_D concentration. The large amount of ^{125}I might be considered a safety hazard; it might cause a higher level of contamination of laboratory equipment, e.g., a cell harvester, and there may be some concern for HPLC-solvent effects on the tissue unless the radioligand preparation has been desalted by gel chromatography or a volatile mobile phase has been evaporated.

Another use for nonradioisotopic ligands, as noted below, is to determine the specific activity of preparations of ^{125}I-labeled ligands suspected of having isotopic dilution with ^{127}I.

To meet these challenges, nonradioisotopic sodium ^{127}iodide can be used to radioiodinate angiotensin-related ligands. The procedure is similar to that used to prepare radioiodinated angiotensin-related ligands; however, larger amounts of peptide and ^{127}I must be used to generate micromolar concentrations of non-radioactive monoiodinated angiotensin-related ligands ***(14,15)***.

2. HPLC purification of nonradioisotopically iodine (^{127}I)-labeled angiotensin ligands. It is necessary to have the HPLC column and mobile-phase conditions set up to mimic those for the corresponding ^{125}I-angiotensin related ligand, since there will not be any ^{125}iodine peak sensed by the radioiodine detector. Alternatively, the ^{127}I can be spiked with a trace amount of ^{125}I sufficient for monitoring of the peak by the radioiodine detector. This has the advantage of providing a good estimate of the concentration of the ^{127}I-labeled ligand in the column eluate.
3. Quantitation of ^{127}I-labeled ligands. There are several methods to determine the concentration of the ^{127}I-angiotensin-related ligand that is collected ***(14)***. The easiest method is to add ^{125}I to the ^{127}I in a precise ratio, e.g., 1:1000. As aforementioned, this can help to identify the peak of ^{127}I-labeled ligand as it elutes from the column. The concentration of the nonradioactively monoiodinated angiotensin-related ligand is determined by measuring the concentration of ^{125}I in a gamma counter and multiplying by 1000. The small proportion (0.1%) of monoradioiodinated ligand should not significantly affect the concentration of monoiodinated ligand, which should remain virtually constant.

   A second way to determine the concentration of ^{127}I-labeled angiotensin-related ligand is to quantitate its concentration of iodotyrosine spectrophotometrically at 275 nm. Most of the absorption at 275 nm by iodinated angiotensin-related ligands is caused by iodotyrosine ***(14)***.

   Another way to determine the concentration of nonradioactively monoiodinated angiotensin-related ligand is by self-displacement assay, as represented in **Fig. 2.** For this procedure, it is necessary to have the same ^{125}I-labeled angiotensin-related ligand and a tissue source rich in Ang II receptors or the component of the RAS of interest.

   The procedure we use to determine the concentration is to derive a maximal binding (B_{MAX}) and dissociation constant (K_D) value for specific ^{125}I-labeled radioligand binding (binding that is inhibited by a saturating concentration of natural ligand for the Ang II receptor, or other component of the RAS). The equation for this is:

$$B = B_{MAX} * H/(K_D + H)$$

   where B = specifically bound radioligand at a given concentration of radioligand and H = the concentration of radioligand.

   At the same time, an approx K_D concentration of ^{125}I-labeled ligand is incubated with the tissue in the presence of undiluted and sequential dilutions of ^{127}I-labeled ligand, usually at half-log intervals, to determine specific binding

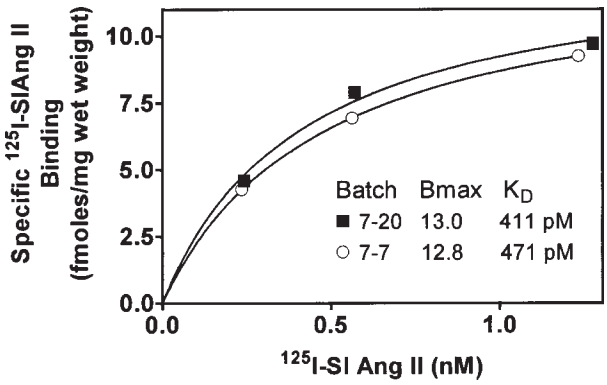

Fig. 3. Example of comparison of two different batches of ^{125}I-SI Ang II. In response to concern over the quality of batch 7–20, it was assayed in a binding assay in comparison with the previous batch, 7–7. The tissue used to compare the two batches was frozen rat liver membranes. The liver membranes were prepared and assayed for ^{125}I-SI Ang II binding essentially as described previously ***(19)***, except that the assay medium contained 150 m*M* NaCl, 1 m*M* Na_2EDTA, 0.1 m*M* Bacitracin, and 50 m*M* $NaPO_4$, pH 7.2. The assay was run 14 and 27 d after preparation of these radioligands, respectively. The lines drawn in the figure represent the best fit to the equation: $B = B_{MAX} * H / (H + K_D)$, as described in the text. If there was significant contamination of batch 7-20 with ^{127}I-labeled ligand, the B_{MAX} would be lower than that for batch 7-7 and the K_D would also be less. As can be seen, there is little difference in the B_{MAX} and K_D values between these two batches of ^{125}I-SI Ang II.

in the presence of varying concentrations of the ^{127}I-labeled ligand. An IC_{50} is then derived from this data using the equation:

$$B = B_O - (B_O * I/(IC_{50} + I)$$

where B = specifically bound radioligand at a given concentration of ^{127}I-labeled ligand (in units of dilution), B_O = specifically bound radioligand in the absence of ^{127}I-labeled ligand, I = the concentration of ^{127}I-labeled ligand in the assay tube (expressed as units of dilution), and IC_{50} is the dilution of the ^{127}I-labeled ligand that causes a 50% reduction in specific binding of the ^{125}I-labeled radioligand.
An alternative equation to derive the IC_{50} by the computer program PRISM is:
B = nonspecific binding + (specific binding/$(1 + 10^{(I - \log IC50)})$.
The dilution that is determined to be the IC_{50} is then converted to a K_I value (in units of dilution) using the Cheng-Prusoff ***(16)*** equation:

$$K_I = IC_{50} / (1 + H/K_D)$$

Because the K_I of the ^{127}I-labeled ligand should be identical to the K_D of the ^{125}I-labeled ligand, the dilution determined to be the K_I is multiplied by the K_D of the ^{125}I-labeled ligand to determine the concentration of the ^{127}I-labeled ligand

preparation. The example shown in **Fig. 2** more fully describes the determination of the ^{127}I-labeled ligand concentration.
Ideally, two or more of the procedures should be used to obtain quantitatively similar results to verify the accuracy of the estimates of the concentration of the ligand.

4. Compensating for excessive ^{125}I-labeling of tissues in autoradiography studies. If it is not possible to prepare ^{127}I-labeled ligand, or an autoradiography has already been done in which the concentration of tissue-bound ^{125}I-labeled ligand exceeds that of the ^{125}I-labeled calibration standards, one can wait until a new set of ^{125}I-labeled calibration standards becomes available (Amersham-Pharmacia has a fresh lot of ^{125}I-labeled calibration standards every 4 mo). The tissue samples can then be apposed to film with the new standards that will contain approx 4 times as much radioactivity as the previously produced ^{125}I-calibration standards. It will be necessary to calculate the amount of ^{125}I that the calibration standards represent at the time the receptor autoradiography was done by increasing the value of the standards based on the first order rate constant for ^{125}I decay:
dpm = dpm on reference date * $e^{(\text{days before reference date} * \ln 2/60\ \text{d})}$.

   For example, if one did the autoradiography 30 d before the calibration date of the new calibration standards, the value that the standards represent 30 d prior to their calibration date = dpm on reference date * $2.718^{(30 * 0.693/60)}$ = 1.414 times the value on the reference date.
5. Carrier-free ^{125}I. Although not absolutely essential, it is important to use carrier-free ^{125}I for preparation of monoradioiodinated ligand. This is because mono^{125}iodinated ligands maintain a constant specific activity, as shown by Catt and Baukal ***(17)***. This concept is known as the Decay-Catastrophe Hypothesis. It posits that when the ^{125}I molecule decomposes, the event is sufficiently catastrophic as to cause destruction of the molecule to which it is attached. So, there is no nonradioactive angiotensin-related compound formed following the decomposition of the ^{125}I. Thus, there is no change in the specific activity of a pure mono-^{125}I-labeled preparation of radioligand. There is, however, a first-order logarithmic decline in the concentration of the mono-^{125}I-labeled preparation of radioligand that has the same half-life as that of ^{125}I. If there is significant contamination of the ^{125}I with nonradioactive ^{127}I, this will produce a stable iodinated ligand that will not decay. Thus, as the radioligand preparation ages, the concentration of radioligand decreases, but the concentration of the ^{127}I-labeled ligand remains constant. As a result, the specific activity of such a preparation will change over time in a manner that depends on the initial purity of the ^{125}I. If the exact proportion of nonradioactive impurity is known, it is possible to calculate the change in specific activity on a daily basis, e.g., if the radioligand is 80% ^{125}I and 20% ^{127}I at the time of iodination, the specific activity will be 1740 Ci/mmol at the time of the iodination. Thirty days after the time of iodination, the specific activity will be 1607 Ci/mmol. Making such daily corrections can be cumbersome and is a potential source of error that can be avoided by using carrier-free ^{125}I.
6. Prevention of contamination with iodine^{127}. It is critically important to avoid contamination of reagents, plasticware, and glassware with iodide molecules prior

to radioiodination of the radioligand. If there is any iodide salt contamination, the specific activity of the radioiodinated ligand will be lowered. To avoid such contamination only the highest quality reagents and solvents should be used. It is important to be meticulous in making sure that clean, disposable, glassware and plasticware is always used.

7. Correction of specific activity for contamination with iodine^{127}. If there is concern that there is contamination of the mono^{125}I-labeled material with ^{127}I, one can compare a previous batch of mono^{125}I-labeled material with the suspect batch, as shown in **Fig. 3**, or make a new batch and compare it to the suspect batch. When making a new batch, be sure to make up all fresh solutions and use freshly opened disposable labware.

   Another way to precisely determine the specific activity of the suspect radioligand is to run a self-displacement assay, as shown in **Fig. 2**, with a known amount of ^{127}I-labeled ligand. If the K_D of the ^{125}I-labeled ligand is identical to the K_D of the ^{127}I-labeled ligand, then there is no contamination of the ^{125}I-labeled ligand with ^{127}I. If the K_D of the ^{125}I-labeled ligand is less than the K_I of the ^{127}I-labeled ligand, than the ^{125}I-labeled ligand is contaminated with ^{127}I. If it is necessary to use the ^{127}I contaminated radioligand, the specific activity can be determined by dividing the theoretical specific activity of ^{125}I (2175 Ci/mmol) by the ratio of the K_I for the ^{127}I-labeled ligand to the K_D of the contaminated ^{125}I-labeled ligand. For example, if the K_I of the ^{127}I-labeled ligand is 1 n*M* and the K_D of the contaminated ^{125}I-labeled ligand is 0.6 n*M*, the specific activity of the contaminated ^{127}I-labeled ligand is 2175 Ci/mmol / (1 n*M*/0.6 n*M*) = 1305 Ci/mmol.
8. Resolution of problems in HPLC purification of ^{125}I-angiotensin-related ligands. On occasion, the resolution of mono^{125}I-labeled ligand from the HPLC may be less than desirable, e.g., the chloramine T may elute too close to the mono ^{125}I-labeled ligand peak. In such cases, it is possible to rechromatograph the ^{125}I-labeled ligand to improve its purity. This should be done prior to adding bovine serum albumin (BSA) as a preservative, because the BSA will tend to stick to the HPLC column and can alter its performance. To minimize the reduction in the concentration of the ^{125}I-labeled ligand that invariably occurs upon repurification, the makeup of the mobile phase should be adjusted to shorten the retention time of the ^{125}I-labeled ligand. Generally, a 1% increase in the proportion of acetonitrile is sufficient to shorten the retention time of the ^{125}I-labeled ligand by 2–3 min. This would also have the effect of increasing the separation of the ^{125}I-labeled ligand peak from the chloramine T peak. Another way to assure that the repurified ^{125}I-labeled ligand peak will be as concentrated as possible is to use the maximum injector loop capacity to readminister the material to the HPLC column.

Acknowledgments

This work was supported in part by the Peptide Radioiodination Service Center, Washington State University. The authors thank Jeanne Jensen for editorial assistance.

References

1. Dietrich, F. M. (1967) Immunochemical analysis of rabbit antibodies against angiotensin II. *Immunochemistry* **4,** 65–76.
2. Lin, S.-Y. and Goodfriend, T. L. (1970) Angiotensin receptors, *Am. J. Physiol.* **213,** 1319–1328.
3. Whitebread, S., Mele, M., Kamber, B., and de Gasparo, M. (1989) Preliminary biochemical characterization of two angiotensin II receptor subtypes. *Biochem. Biophys. Res. Commun.* **163,** 284–291.
4. Chiu, A. T., Herblin, W. F., McCall, D. E., Ardecky, R. J., Carini, D. J., Duncia, J. V., et al. (1989) Identification of angiotensin II receptor subtypes. *Biochem. Biophys. Res. Commun.* **165,** 196–203.
5. Mendelsohn, F. A. O., Chai, S. Y., and Dunbar, M. (1984) In vitro autoradiographic localization of angiotensin-converting enzyme in rat brain using ^{125}I-labelled MK351A, *J. Hypertens.* **2,** 41–44.
6. Speth, R. C. and Husain, A. (1988) Distribution of angiotensin converting enzyme and angiotensin II receptor binding sites in the rat ovary. *Biol. Reprod.* **38,** 695–702.
7. Harding, J. W., Wright, J. W., Swanson, G. N., Hanesworth, J. M., and Krebs, L. T. (1994) AT4 receptors: specificity and distribution. *Kidney Int.* **46,** 1510–1512.
8. Miller-Wing, A. V., Hanesworth, J. M., Sardinia, M. F., Hall, K. L., Wright, J. W., Speth, R. C., et al. (1993) Central angiotensin IV binding sites: distribution and specificity in guinea pig brain. *J. Pharmacol. Exp. Ther.* **266,** 1718–1726.
9. Laporte, S. A., Boucard, A. A., Servant, G., Guillemette, G., Leduc, R. and Escher, E. (1999) Determination of peptide contact points in the human angiotensin II type I receptor (AT1) with photosensitive analogs of angiotensin II. *Mol. Endocrinol.* **13,** 578–586.
10. Bosse, R., Servant, G., Zhou, L. M., Boulay, G., Guillemette, G. and Escher, E. (1993) Sar1-p-benzoylphenylalanine-angiotensin, a new photoaffinity probe for selective labeling of the type 2 angiotensin receptor. *Regul. Pept.* **44,** 215–223.
11. Hunter, W. M. and Greenwood, F. C. (1962) Preparation of iodine-131 labeled human growth hormone of high specific activity. *Nature* **194,** 495–496.
12. Lin, S.-Y., Ellis, H., Weisblum, B., and Goodfriend, T. L. (1970) Preparation and properties of iodinated angiotensins. *Biochem. Pharmacol.* **19,** 651–662.
13. Husain, A., Pajka, S. F., Taylor, S. M., and Speth, R. C. (1986) Monoiodinated angiotensin II is a potent, full agonist analog of angiotensin II. *J. Pharmacol. Exp. Ther.* **239,** 71–77.
14. Speth, R. C. and Husain, A. (1984) Preparation and one-step purification of mono-^{125}I-angiotensin II for radioligand binding assays. *J. Pharmacol. Methods* **11,** 137–150.
15. Lu, X.-Y., Grove, K. L., Zhang, W., and Speth, R. C. (1995) Pharmacological characterization of angiotensin II AT2 receptor subtype heterogeneity in the rat adrenal cortex and medulla. *Endocrine* **3,** 255–261.
16. Cheng, Y.-C. and Prusoff, W. H. (1973) Relationship between the inhibition constant (K_I) and the concentration of inhibitor which causes 50 per cent inhibition (I_{50}) of an enzymatic reaction. *Biochem. Pharmacol.* **22,** 3099–3108.

17. Catt, K. J. and Baukal, A. (1973) Prolonged retention of high specific activity by ^{125}I-labeled angiotensin II-a consequence of "decay catastrophe". *Biochim. Biophys. Acta* **313,** 221–225.
18. Kauer, J. C., Erickson-Viitanen, S., Wolfe, H. R., Jr., and DeGrado, W. F. (1986) p-Benzoyl-L-phenylalanine, a new photoreactive amino acid. Photolabeling of calmodulin with a synthetic calmodulin-binding peptide. *J. Biol. Chem.* **261,** 10,695–10,700.
19. Grove, K. L. and Speth, R. C. (1993) ^{3}H-Losartan binds to a non-angiotensin II binding site in the rat liver. *Biochem. Pharmacol.* **46,** 1653–1660.

20

Assays for Radiolabel-Photoaffinity Labeling of Angiotensin Receptors

Jacqueline Pérodin, Antony A. Boucard, Richard Leduc, Emanuel Escher, and Gaétan Guillemette

1. Introduction

Photoaffinity labeling is a useful method to covalently bind two interacting moieties whether they be substrate and enzyme or ligand and receptor. Irreversibly labeling any particular molecule is a practical way of detecting the latter throughout the course of a characterization or a purification procedure.

Different types of photolabels have been synthesized throughout the years and have proven their efficacy ***(1–3)***. These compounds have been used on many different types of enzymes such as chymotrypsin ***(4)***, calmoduline ***(5,6)***, protein kinases ***(7)***, and receptors like cholecystokinin ***(8)***, vasopressin ***(9)***, nicotinic acetylcholine ***(10)***, and angiotensin II (AngII) receptors ***(11,12)***. In this chapter, our procedure for photoaffinity labeling of the AT_1 and AT_2 receptors with an AngII analog synthesized in our laboratory, [Sarcosine^1, Valine^5, *p*-Benzoyl-L-phenylalanine^8]AngII, will be described.

1.1. Principles of Photoreaction

The nonnatural amino acid *p*-benzoylphenylalanine (Bpa) incorporated in our analog is the photoreactive entity. In the presence of UV light (approx 350–360 nm), Bpa absorbs a photon that results in the promotion of one electron from a nonbonding *sp2*-like *n*-orbital on the oxygen to an antibonding π-orbital of the carbonyl group, *i.e.* the oxygen becomes a highly reactive free radical (O•) (*see* **Fig.1**). This radical readily reacts with any weak C-H bond in its immediate environment (within a radius of 3.1 Å around the ketone oxygen) to form a new covalent bond, thus irreversibly binding the Bpa to its adjacent protein ***(2,12)***.

From: *Methods in Molecular Medicine, vol. 51: Angiotensin Protocols*
Edited by: D. H. Wang © Humana Press Inc., Totowa, NJ

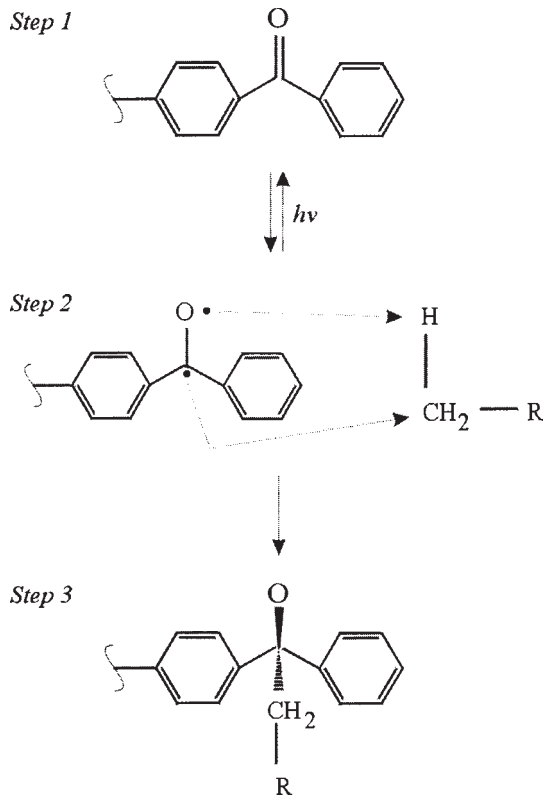

Fig. 1. Mechanism of covalent modification following photoactivation.

In order to trace and detect the photolabel-receptor complex, radiolabeling the photolabeling ligand, [Sar^1, Val^5, L-Bpa^8]Ang II, with ^{125}Iodine prior to use is required. The resulting peptide, [Sar^1,^{125}I-Tyr^4,Val^5, L-Bpa^8]Ang II, will simply be referred to as [Bpa^8]Ang II (*see* chapter on "Radiolabeling of angiotensin peptides").

1.2. Nitrene Analogs vs Benzophenone Analogs

Nitrene compounds, such as the much-used aryl azides (i.e., *p*-azidophenylalanine), diazirines and diazo esters, have been widely used in the past as photolabeling agents. Although they are stable in the dark in solution, care needs to be applied while manipulating them in ambient light. More recently, benzophenone compounds have demonstrated significant advantages. Benzophenones are chemically more stable than nitrene derivatives. They can be handled in ambient lighting because they will only become activated in presence of UV light. Benzophenones preferably react with weak C–H bonds, whereas nitrenes

preferably bind O–H bonds. Finally, the greatest advantage of benzophenone derivatives is the fact that they are reactivatable. Indeed, once it is in its activated form, it can either react with the adjacent protein or return to its initial inactivated state where it is ready to be reactivated by a new photon.

The efficacy of a photosensitive ligand is very much linked to its affinity for its cognate receptor. A good example is the photolabeling efficacy of [Bpa^1]Ang II on the AT_1 receptor that is much decreased compared to the photolabeling efficacy on the AT_2 receptor. This decrease seems primarily caused by a lower affinity of [Bpa^1]Ang II for AT_1 (K_D of 17 n*M*) than for the AT_2 receptor (K_D of 1 n*M*). We have evaluated a photolabeling efficacy of 40% for [Bpa^8]Ang II on the AT_1 receptor and of 60% on the AT_2 receptor (for evaluation of photolabeling efficacy, *see* **Note 9**).

2. Materials

General note: Photolabeling of either AT_1 or AT_2 receptors are essentially done under the same conditions (*see* **Note 1**). In the following protocol, COS-7 cells transfected with an eukaryotic expression vector encoding the human AT_1 receptor are used.

2.1. Reversible Binding Step

1. Confluent COS-7 cells expressing the AT_1 receptor (10 cm Petri dish).
2. –80°C refrigerator.
3. Water bath at 37°C.
4. Rubber policeman.
5. 10 mL glass pipets.
6. Conical 15 mL polypropylene tubes.
7. Refrigerated centrifuge (4°C).
8. Vortex mixer.
9. Ice-cold washing buffer: 25 m*M* Tris-HCl (pH 7.4), 100 m*M* NaCl, and 5 m*M* $MgCl_2$.
10. Room temperature incubation buffer: 25 m*M* Tris-HCl (pH 7.4), 100 m*M* NaCl, 5 m*M* $MgCl_2$, and 0.1% [w/v] bovine serum albumin (BSA).
11. ^{125}I-[Sar^1, Val^5, L-Bpa^8]Ang II (1000 Ci/mmol) stored at –20°C.

2.2. UV Light Irradiation

1. Ice-cold washing and photolabeling buffer: 25 m*M* Tris-HCl (pH 7.4), 100 m*M* NaCl, and 5 m*M* $MgCl_2$.
2. UV lamp (365 nm) (Mercury vapor lamp serial number JC-Par38 from Westinghouse and Raymaster black light filters number 5873 from Gates and Co. Inc., Long Island, NY).
3. Plastic four-well plate.
4. Ice bucket.

2.3. Solubilization of the Covalent Complex

1. Refrigerated centrifuge (4°C).
2. m-RIPA buffer: 50 m*M* Tris (pH 8.0), 150 m*M* NaCl, 0.5% deoxycholate, 0.1% SDS, and 1% Nonidet P-40 (NP40).
3. 1.5 mL microcentrifuge tubes.
4. Water bath at 37°C.

3. Methods

3.1. Reversible Binding Step

1. Gently discard the culture medium from the COS-7/AT_1 transfected cells.
2. Wash once with 10 mL of ice-cold washing buffer. Discard the buffer.
3. Freeze cells for 20 min or more at –80°C (*see* **Note 2**).
4. Thaw cells in a water bath at 37°C for 1–2 min.
5. Add 10 mL of ice-cold washing buffer.
6. With a policeman, gently scrape the broken cells off the bottom of the dish.
7. Collect suspension after brief mechanical dispersion using the pipet.
8. Transfer into a 15-mL conical polypropylene tube (keep on ice until next step).
9. Centrifuge at 500*g* for 10 min at 4°C. Discard the supernatant.
10. Resuspend the pellet in 1 mL of room temperature incubation buffer (containing 0.1% BSA).
11. Add ^{125}I-[Bpa^{8}]Ang II (1000 Ci/mmol) to a final concentration of 3 n*M* (*see* **Notes 3** and **4**).
12. Incubate at room temperature for 90 min in the dark.

3.2. UV Light Irradiation

1. After incubation, centrifuge at 2500*g* for 10 min at 4°C. Discard the supernatant (*see* **Note 5**).
2. Without disturbing the pellet, wash once with 1 mL of ice-cold washing buffer (*see* **Note 6**).
3. Quickly resuspend the pellet in 400 µL of ice-cold washing buffer (*see* **Note 7**) and transfer the suspension each into one well of the cold four-well plate.
4. Place back the cover on the four-well plate and put it on ice.
5. Place the four-well plate (on ice) under the UV lamp for 1 h (*see* **Note 8**). The UV lamp should be 6–8 cm above the plate. Keep an aliquot (25–50 µg) on ice for evaluation of photolabeling efficacy (*see* **Note 9**).

3.3. Solubilization of the Covalent Complex

1. After photolabeling, mechanically disperse and recollect into a 1.5-mL microcentrifuge tube.
2. Centrifuge at 2500*g* for 10 min at 4°C. Discard the supernatant.
3. Add 100 µL of m-RIPA buffer and incubate at 0°C for 45 min.
4. Centrifuge at 13,000*g* for 15 min at 4°C.
5. Transfer the supernatant into a new microcentrifuge tube. Discard the pellet.
6. Store at –20°C until needed (*see* **Note 10**).

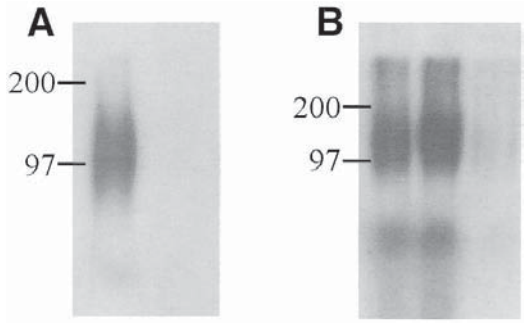

Fig. 2. Autoradiography of photolabeled AT_1 and AT_2 receptors. After photolabeling with [Sar^1,Val^5,L-Bpa^8]Ang II, cellular proteins were solubilized, denatured, and submitted to SDS-PAGE 7.5% acrylamide separating gel followed by autoradiography. **(A)** *Lane 1* shows photolabeled AT_1 receptor with an apparent molecular weight of 109 kDa (glycoprotein); *Lane 2* shows displacement of the photolabel from AT_1 by 10^{-6} *M* of L-158,809 prior to photolysis. **(B)** *Lane 1* shows photolabeled AT_2 receptor with an apparent molecular weight of 140 kDa (glycoprotein); *Lane 2* shows that photolabeling of AT_2 is unaffected by the presence of 10^{-6} *M* of L-158,809; *Lane 3*, shows displacement of the photolabel from AT_2 by 10^{-6} *M* of PD123319 prior to photolysis.

4. Notes

1. As aforementioned, photolabeling of either AT_1 or AT_2 receptors are done under the same experimental conditions. In the case where both receptor types would be present in a tissue, it is possible to selectively label a receptor type by using a selective antagonist for one of the receptor types. Ideally, transfection of the AT_1 or AT_2 receptor into cell lines that do not express any of the two receptor types, such as COS-7 cells, is a good approach. For those who do not have access to any transfection system, adrenal glomerulosa cells are a rich source of AT_1 receptor ***(13)***, and PC-12 cells or human myometrium cells are a rich source of AT_2 receptor ***(12,14)***.
2. The freeze-thaw cycle breaks the cells. Consequently, the experiment is done with broken cell membranes.
3. To reduce nonspecific binding, we use a concentration of radioligand corresponding to its K_D value so that about 50% of the total population of receptors will be occupied at equilibrium.
4. To verify the specificity of the labeling at this point, add a selective antagonist (i.e., L-158,809 for AT_1 or PD123319 for AT_2) at a concentration corresponding to about 100 times its K_D.
5. During the centrifugation, turn on the UV lamps to be ready for the following steps.
6. This step is done mainly to get rid of excess radioactive photolabel on the walls of the tube. The washing solution should be ice cold to prevent dissociation of the bound ligand from its receptor.

7. It is important to be in absence of BSA at this step to avoid photolabeling of BSA.
8. UV lamps produce heat. Make sure that the sample is maintained at a low temperature.
9. The yield of covalent incorporation is evaluated by assessing the ratio of acid-resistant binding after photolysis over total binding (before photolysis).
10. At this point, the solubilized photolabeled receptor can be used for different purposes. **Fig. 2** *(see previous page)* shows an autoradiography of photolabeled AT_1 and AT_2 receptors after analysis by sodium dodecyl sulfate-polyacrylamide gel electrophoresis (SDS-PAGE). Note that the AT_1 and AT_2 receptors migrate as large diffuse bands because of their glycosylated nature.

References

1. Bayley, H. and Knowles, J. (1977) Photoaffinity labeling. *Methods Enzymol.* **46,** 69–114.
2. Dormán G. and Prestwich, G. D. (1994) Benzophenone photophores in biochemistry. *Biochemistry* **33,** 5661–5673.
3. Dohlman, H. G., Thorner, J., Caron, M. G., and Lefkowitz, R. J. (1991) Model systems for the study of seven-transmembrane-segment receptors. *Annu. Rev. Biochem.* **60,** 653–688.
4. Escher, E. and Schwyzer, R. (1975) Photoaffinity labelling of chymotrypsin. Synthesis of photorecognizable ligands. *Helv. Chim. Acta* **58,** 1465–1471.
5. Kauer, J. C., Erickson, V. S., Wolfe, H. J., and Degrado, W. F. (1986) p-Benzoyl-L-phenylalanine, a new photoreactive amino acid. Photolabeling of calmodulin with a synthetic calmodulin-binding peptide. *J. Biol. Chem.* **261,** 10,695–10,700.
6. O'Neil, K. T. and DeGrado, W. F. (1989) The interaction of calmodulin with fluorescent and photoreactive model peptides, evidence for a short interdomain separation. *Proteins* **6,** 284–293.
7. Pomerantz, A. H., Rudolph, S. A., Haley, B. E., and Greengard, P. (1975) Photoaffinity labeling of a protein kinase from bovine brain with 8-azidoadenosine 3',5'-monophosphate. *Biochemistry* **14,** 3858–3862.
8. Ji, Z., Hadac, E. M., Henne, R. M., Patel, S. A., Lybrand, T. P., and Miller, L. J. (1996) Direct identification of a distinct site of interaction between the carboxyl-terminal residue of cholecystokinin and the type A cholecystokinin receptor using photoaffinity labeling. *J. Biol. Chem.* **272,** 24,393–24,401.
9. Phalipou, S., Cotte, N., Carnazzi, E., Seyer, R., Mahe, E., Jard, et al. (1997) Mapping peptide-binding domains of the human V1a vasopressin receptor with a photoactivatable linear peptide antagonist. *J. Biol. Chem.* **272,** 26,536–26,544.
10. Corbin, J., Wang, H. H., and Blanton, M. P. (1998) Identifying the cholesterol binding domain in the nicotinic acetylcholine receptor with [125I]azido-cholesterol. *Biochim. Biophys. Acta* **1414,** 65–74.
11. Laporte, S. A., Boucard¸ A. A., Servant, G., Escher, E., Guillemette, G., and Leduc, R. (1999) Determination of peptide contact points in the human angiotensin II type 1 (AT1) receptor with photosensitive analogs of angiotensin II. *Mol. Endocrinol*. **13,** 578–586.

12. Servant, G., Laporte, S. A., Leduc, R., Escher, E., and Guillemette, G. (1997) Identification of Angiotensin II-binding domains in the rat AT_2 receptor with photolabile angiotensin analogs. *J. Biol. Chem.* **272,** 8653–8659.
13. Boulay, G., Servant, G., Luong, T. T., Escher, E., and Guillemette, G. (1992) Modulation of Angiotensin II binding affinity by allosteric interaction of Polyvinyl Sulfate with an intracellular domain of the DuP-753-sensitive angiotensin II receptor of bovine adrenal glomerulosa. *Mol. Pharmacol.* **41,** 809–815.
14. Servant, G., Boulay, G., Bossé, R., Escher, E., and Guillemette, G. (1993) Photoaffinity labeling of subtype 2 Angiotensin receptor of human myometrium. *Mol. Pharmacol.* **43,** 677–683.

21

Radioligand Binding Assay

Gaétan Thibault and Ernesto L. Schiffrin

1. Introduction

Characterization and cloning of the AT_1 and AT_2 receptors would not have been possible without an assay that could detect and measure the density and affinity of these receptors. The most frequently used, if not the only, methodological approach used to investigate these receptors is the radioligand binding assay performed either in a test tube with tissue-membrane preparations or cultured cells, or on tissue sections (the latter revealed by autoradiography). This chapter will only deal with the test-tube radioligand binding assay. In this assay, a radiolabeled ligand (labeled with ^{125}I or ^{3}H, for example) is incubated with a membrane preparation or cells in presence of receptor subtype-specific antagonist or agonist. After reaching equilibrium, the receptor-bound tracer is separated from the free tracer by rapid filtration through glass fiber filters or by centrifugation. The amount (cpm) of bound tracer is then used to calculate the density and affinity of each receptor subtype. Alternatively, other experiments can be designed to derive kinetics of association and dissociation or saturation.

In the method we use and describe in this chapter, ^{125}I-[Sar^1,Ile^8] Ang II is used as the radioligand to detect total AT receptors. Specific antagonists of the AT_1- and AT_2-receptor subtypes are added to the incubation mixture to generate competition curves and discriminate between the receptor subtypes.

2. Materials

1. Ang II, as well as other angiotensin peptides (Ang IV, [Sar^1,Ile^8] Ang II, [Sar^1] Ang II), can be bought from any good peptide supplier like Peninsula Laboratories (Belmont, CA), Peptides International (Louisville, KY), Bachem California (Torrance, CA), or Calbiochem-Novabiochem Corporation (San Diego, CA). Losartan (AT_1-receptor antagonist) was obtained from Dupont Merck Pharma-

From: *Methods in Molecular Medicine, vol. 51: Angiotensin Protocols*
Edited by: D. H. Wang

ceutical Company (Wilmington, DE), whereas PD 123319 (AT_2-receptor antagonist) can only be bought from Research Biochemical International (Natick, MA). These compounds are dissolved in distilled water to prepare a stock solution at a concentration of 10^{-3} *M*. Small aliquots (approx 50 μL) are then kept at –20°C.

2. Binding buffer: 0.05 *M* Tris-HCl, pH 7.4, 5 m*M* $MgCl_2$, 1 μ*M* aprotinin, 0.1% Bacitracin, 0.5 m*M* phenyl methyl sulfonyl fluoride (PMSF), 0.4 μ*M* phosphoramidon, and 0.5% bovine serum albumin (BSA). Because of the instability of PMSF in water, PMSF is added at the last moment from a 0.25-*M* stock solution prepared in methanol or isopropanol (*see* **Note 5**). When studying cultured cells (in 24-well plate) or isolated cardiomycytes, culture medium containing 25 m*M* HEPES, and 0.1% BSA, is used, such as Dulbecco's modified essential medium (DMEM) or medium 199 (M199), respectively, adjusted to pH 7.4.
3. $Na^{125}I$ (approx 17 mCi/μg, in NaOH solution) can be bought from Amersham Pharmacia Biotech (Baie d'Urfé, Province of Québec, Canada).
4. Bovine milk lactoperoxidase (L 8257), available from Sigma (St. Louis, MO), is dissolved at 1 mg/mL in 0.05-*M* phosphate buffer, pH 7.4, and kept frozen in small aliquots.

2. Methods

The nonselective antagonist [Sar^1,Ile^8] Ang II ***(1)*** is our preferred radioligand, rather than Ang II, because it is more resistant to aminopeptidase degradation during the course of binding experiments with membranes or cells (*see* **Note 6**), and it has a better affinity for AT_1 and AT_2 receptors than Ang II ***(2)***. ^{125}Iodine labeling is performed by the lactoperoxidase method on the Tyr 4 of the peptide ***(3)***. Subsequent purification of the monoiodinated peptide from unlabeled and diiodinated peptide and labeling reagents is made by reverse-phase high-pressure liquid chromatography (HPLC) ***(4)***.

Five micrograms of [Sar^1,Ile^8] Ang II (dissolved in water) are added to 40 μL phosphate buffer, pH 7.4, in a polyethylene microcentrifuge tube. Ten microliters of $Na^{125}I$ (1 mCi) is then added followed by 10 μL (10 μg) lactoperoxidase. The reaction is started by three successive additions of freshly diluted 0.002% H_2O_2 (diluted from a 30% solution) at 5 min intervals. After each addition of H_2O_2, the reaction volume is gently mixed by pipeting or by flicking the tube. Immediately after the 15-min incubation, the reaction mixture is injected on a reverse-phase HPLC column (either a C_4- or C_{18}-bonded phase can be used) (*see* **Note 7**). The HPLC gradient consists of a CH_3CN gradient of 10–50% in 0.1% trifluoroacetic acid at a flow rate of 1 mL/min and a gradient slope of 0.5%/min. One-milliliter fractions are collected in 12 × 75-mm polystyrene tubes containing 100 μL of 1% BSA. Free ^{125}I elutes in the flowthrough fractions whereas monoiodinated [Sar^1,Ile^8] Ang II elutes at fractions 40–45. The diiodinated peptide elutes two to three fractions latter. The binding activity of the radioactive fractions can be tested by radioligand binding assay. The

active fractions are then pooled and stored at –20°C. In order to avoid repetitive freezing and thawing, the labeled material is kept in small aliquots of 3 – 5 × 10^6 cpm/tube. We usually collect between 4 – 8 × 10^8 cpm, with a specific activity of approx 1500 Ci/mmol (*see* **Note 1**). The specific activity can be measured according to Morris ***(5)***. The iodinated peptide can be kept at –20°C for a maximum of 2 mo.

Binding assay can be performed either on cultured or isolated cells, or on membrane preparations. Indeed, we have observed that it is often simpler to work on cultured cells than on membrane preparation coming from these same cells. Preparation of cellular membranes often resulted in the destruction and loss of receptors. In the cases of tissues and organs, there is no choice, and membranes must be partially purified from homogenates.

2.1. Membrane Preparation

Hearts (or other tissues), collected in cold phosphate-buffered saline (PBS), are blotted on paper towels to remove blood, added (20 mL/g of wet weight) to 0.05 *M* $NaHCO_3$, pH 8.2, containing 1 m*M* PMSF, and homogenized in ice with a Polytron at a setting of six for three periods of 15–20 s. The homogenate is centrifuged at 1000*g* for 10 min and the supernatant kept apart. The pellet is rehomogenized by the same procedure in the same buffer (10 mL/g). Both supernatants are pooled and centrifuged at 40,000*g* for 20 min. The final pellet, consisting of a crude membrane preparation, is dispersed in 0.05 *M* Tris-HCl, pH 7.4, 1 m*M* PMSF in order to obtain a concentration of 3–5 mg of protein per milliliter. The binding assay is preferentially performed on fresh membrane preparations, because AT receptors do not appear to be very stable when frozen. However, under some circumstances, such as when working with renal vascular tissue and renal glomeruli, we have found that samples can be snap-frozen in liquid nitrogen without too much loss of binding density.

2.2. Isolated Cells

Freshly isolated cells can be used for determination of Ang II binding properties ***(6)***. This is especially the case with adult cardiac myocytes (*see* **Note 9**). Adult cardiac myocytes are very sensitive to external conditions, and are hard to keep in culture without destruction or dedifferentiation. Accordingly, we prefer to do the binding experiments immediately after isolation. Cardiac myocytes obtained by collagenase digestion in a Langherdoff system ***(7)***, are suspended in M199 with 0.1% BSA. It is advisable to verify whether or not protease that was used to isolate the cells may have altered the receptors. Alternatively, cardiac myocytes can be seeded on laminin-coated (1.5 μg/cm^2) 24-well culture plates and used the day after for binding as for cultured cells.

2.3. Cultured Cells

Very often, cells need to be submitted to external agents or stimuli to examine receptor regulation. It is then more appropriate to analyze Ang II binding directly on the cells rather than preparing a membrane fraction. In this case, as with cardiac fibroblasts or neonatal cardiomyocytes *(6,8)*, binding is performed directly in 24-well culture plates.

3. Radioligand Binding Assay

3.1. Saturation Assay

In saturation assays, increasing amounts of radioligand are incubated with sufficient quantity of biological material to saturate the AT receptors. Usually, the quantity of protein or cells is chosen in order to get a reasonable radioactive signal (approx 3000 to 5000 cpm) with a concentration of 120 p*M* of ^{125}I-[Sar^1,Ile^8] Ang II (approx 60,000 cpm). The same quantity of material is then used to generate a saturation curve by increasing the radioligand from 0 to 1–2 n*M*. Nonspecific binding for each radioligand concentration is determined in presence of 10^{-6} *M* [Sar^1,Ile^8] Ang II.

3.2. Competition Assay

In competition assays, the quantity of biological material that generates a signal of 3000–5000 cpm is incubated with increasing concentrations of specific agonists or antagonists. Competition with increasing concentrations of [Sar^1,Ile^8] Ang II, [Sar^1] Ang II, or Ang II that present similar affinities for AT_1 and AT_2 receptors will result in progressive and eventually complete displacement of the tracer. Competition with losartan (AT_1 antagonist) and with PD 123319 (AT_2 antagonist) will reveal the different proportions of receptor subtypes in the tissue of interest (*see* **Notes 2–4**).

The experimental conditions are the following. In a total volume of 250 µL, membranes (50 µL) are incubated in duplicate in presence of 120 p*M* ^{125}I-[Sar^1,Ile^8] Ang II (100 µL) and increasing concentrations of drug (usually from 10^{-13} to 10^{-6} *M*) (100 µL) in binding buffer. We found that 13 concentrations are enough to generate a nice and smooth curve that will allow detailed analysis. The diluted drugs are prepared by making 10-fold serial dilutions and, from each order of magnitude dilution, a threefold dilution. In this way, the final concentrations of drug will be: 1×10^{-6} *M*, 3.33×10^{-7} *M*, 1×10^{-7} *M*, 3.33×10^{-8} *M*, down to 1×10^{-13} *M*. The experimenter must not forget that the initial concentration of drug must be 2.5-fold higher because the dilution factor in the test tube. After reaching equilibrium (90 min at room temperature), the reaction volume is aspirated onto No. 34 glass fiber filters (Schleicher & Schuell, Keene, NH) (*see* **Note 8**) and washed twice with 4 mL 0.05 *M* Tris-HCl, NaCl

0.15 *M*, pH 7.2, with a 30-well cell harvester (Brandel, Gaithersburg, MD). To reduce nonspecific binding, glass fiber filters are presoaked in washing buffer for 30 to 45 min prior to filtration. Filters are then collected and counted in a γ-counter. With a 30-well cell harvester, it is possible to do a complete displacement set with sufficient data points to generate a smooth curve. With isolated cells, such as adult cardiomyocytes, a similar protocol is used except that the binding buffer is replaced by a medium like M199, that will support living cells.

On cultured cells grown in 24-well plates, incubation is performed directly in the plate with a total incubation volume of 500 µL/well in DMEM containing 0.1% BSA. Following incubation, the medium is aspirated with a vacuum pump and cells are washed twice with DMEM-BSA. Cells are then solubilized with 0.5 mL of 1 *N* NaOH and counted.

3.3. Analysis of the Data

Conveniently, mathematical softwares exist that can analyze saturation and competition curves, determine whether there is one or several binding sites, and obtain the density of sites and affinity of the sites detected. KELL is the EBDA-LIGAND software originally designed by McPherson ***(9)*** that can be bought from Biosoft (Ferguson, MO). Allfit is a shareware made available through the Web by Dr. A. DeLéan ***(10)*** at the following address: http://www.pharmco.umontreal.ca/Delean.htm#Haut.

In those softwares, the affinity of the radioligand must be known: it is often assumed that it has the same affinity as the parent compound. This may not be true, as we have demonstrated with iodinated ANP ***(4)***. The affinity of the radioligand must always be verified by saturation analysis since the presence of a molecule of iodine can greatly affect its binding properties. In our hands when assessed by saturation experiments and Scatchard analysis, ^{125}I-[Sar^{1},Ile^{8}] Ang II presented an affinity of 0.4 n*M* on cardiac fibroblasts ***(7)*** whereas the unlabeled peptide displayed a 0.2 n*M* affinity by competition experiments (**Table 1**).

4. Notes

1. Over the years, we have observed that the major problem in iodination of peptides is the low yield of the radiolabeling process. This is mainly caused by bad reagents because of their age or repetitive freezing and thawing of the peptide. Dissolved peptides must always be kept in small aliquots of 50 µL in well-closed microcentrifuge tubes to avoid dessication by repetitive thawing and freezing. Any solution of lactoperoxidase older than 1 yr should be discarded. Thirty percent H_2O_2 is preferably bought in small quantity (100 mL) and discarded after 1 yr.
2. Losartan, the AT_1 antagonist, cannot discriminate between AT_{1A}- and AT_{1B}-receptor subtypes. There is only 5% difference in the amino acid sequence of these two receptors and, presently, there are no ligands that can recognize

Table 1
Binding Properties of Ang II Receptors on Cardiac Cells

Tissue	Affinity (K_d)	Density (B_{max})	Receptor subtype
Adult cardiac fibroblasts	approx 0.2 n*M*	approx 70,000 sites/cell	> 95 % AT_1
Adult cardiomyocytes	approx 0.2 n*M*	< 15 fmol/mg or approx 200–300 cpm /50,000 cells	> 90% AT_1

Data from **refs.** ***(6,7,14,15)***.

one or the other subtype ***(11)***. RT-PCR is the only appropriate method to detect these isoforms.

3. Several AT_1 antagonists are currently available and can be used instead of losartan in competition experiments, including valsartan, irbesartan, candesartan, eprosartan, telmisartan. All have very high affinity towards AT_1 receptors. Concerning the AT_2 receptor, PD 123177 can substitute for PD 123319.
4. Up to now AT_{1A}, AT_{1B}, and AT_2 receptors are the only angiotensin receptors cloned. Although existence of other pharmacologically distinct receptors has been proposed, their sequences is not available yet ***(12)***. We have explored the presence of an AT_4 receptor in the rabbit heart. We used primary cultures of rabbit cardiac fibroblasts, as well as isolated adult myocytes in an attempt to reveal the presence of these receptors. Essentially, the same methodology (radiolabeling of Ang IV and radioligand binding assay) as aforementioned was used except that equilibrium was reached in 2 h at 37°C. As illustrated in **Fig. 1** and **Table 2**, rabbit cardiac cells exhibit a high level of ^{125}I-Ang IV binding, with binding affinity in the nanomolar range. Interestingly, binding is only partially displaceable with classical AT_1 and AT_2 ligands (Ang II, [Sar^1,Ile^8] Ang II, losartan, and PD 123319). In this system, Ang II is at least 100 times less potent than Ang IV. These data indicate that either the classical AT_1 and AT_2 receptors behave atypically in the rabbit heart or distinct AT_4 receptors do exist and are the predominant AT receptor in the rabbit heart. This may suggest that Ang II in the rabbit may not be the mature peptide. Whether or not this rabbit AT_4 receptor has similar intracellular coupling as AT_1 or AT_2 receptors remains to be elucidated.
5. Degradation of the radiolabeled peptide is usually minimal under the conditions suggested here. In some cases, such as after longer incubation times or use of large quantity of membranes, protease-mediated degradation of the radiolabeled peptide may occur. In this case, the extent of degradation must be verified by HPLC using the same methodology as for purification of the radiolabeled ligand. If more than 30% of degradation is found, additional protease inhibitors may have to be used.
6. ^{125}I Ang II can be substituted by ^{125}I-[Sar^1,Ile^8] Ang II without any problem, unless protease degradation is an important event.

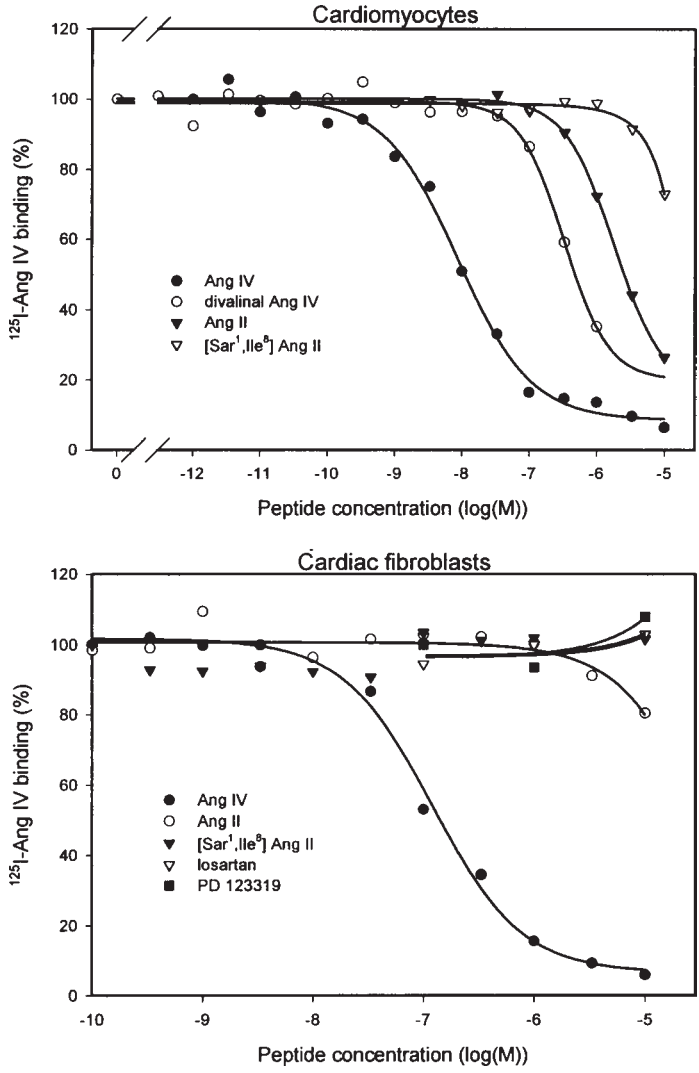

Fig. 1. Competition curves of ^{125}I-Ang IV on isolated rabbit cardiomyocytes and 24-well plate cultured rabbit cardiac fibroblasts.

Table 2
Binding Properties of Ang IV on Rabbit Cardiac Cells

Cells	Affinity (K_d)	Density (sites/cell)
Adult cardiomyocytes	13.3 n*M*	Approx 45,000
Adult cardiac fibroblasts	100 n*M*	Approx 15,000

7. Purification of radiolabeled peptide as described here requires the availability of an HPLC system that is exclusively devoted to this purpose. It is also possible to purify radiolabeled peptide by relatively simple procedures. Purification can be assessed by extraction either with C_{18} Sep-Pak cartridges or glass beads. In the case of C_{18} Sep-Pak (Millipore Corp., Milford, MA) the radiolabeled peptide is retained by hydrophobic adsorption and then eluted with an organic solvent. The cartridge is first activated with 10 mL of acetonitrile and washed with 10 mL of 0.1% TFA. The radiolabeling reaction mixture is deposited on the cartridge, which is then washed extensively with 20 to 40 mL of 0.1% TFA to remove any free ^{125}I. The radioactivity in the eluant should be monitored until it remains stable. Iodinated peptide is then eluted with 60% acetonitrile in 0.1% TFA.
   Glass has intrinsic hydrophobic and polar group allowing retention of peptides. Vycor glass powder (No. 7930, Corning, Corning, NY) can be used to extract peptides. The radiolabeling reaction mixture is added directly to heat-activated, dehydrated glass beads (35 mg) ***(13)***. After vortexing and mixing for 10 min, the sample is centrifuged and the supernatant discarded. The beads are then washed twice with 5 mL distilled water. Elution is made with 2 mL of 40% acetone in 0.25 *N* HCl. After 10 min of shaking and centrifugation, the supernatant is recovered.
   The main advantage of these methods is their rapidity. However, it is important to mention that these procedures will only remove free iodine, and most reagents will not separate the intact peptide from the mono- and diiodinated forms. Consequently, the quality of the final labeled ligand, that may be sufficient for radioimmunoassay, may not be good enough to assess binding parameters.
   If a small quantity of tracer is used only occasionally, it may then be advisable to buy the iodinated peptide. ^{125}I-Ang II and ^{125}I-[Sar^{1},Ile^{8}] Ang II can be bought from Amersham Pharmacia Biotech (Baie d'Urfé, PQ), ICN Biomedical (Costa Mesa, CA), or NEN Life Science Products (Boston, MA). ^{125}I-Ang IV is sold by NEN Life Science Products only.
8. We currently use No. 34 glass fiber paper from Schleicher and Schuell. This can be replaced by Whatman GF/C (Whatman Inc., Clifton, NJ) or by Gelman Type A/E (Pall Gelman Laboratory, Ann Arbor, MI) papers. Other paper types can also be used, but they must be tested to verify nonspecific binding, particulate retention, and speed of filtration.
9. It appears that adult cardiac myocytes express very low density of AT receptors ***(6)*** (**Table 1**). The radioligand binding assay may then not be sensitive enough to quantitate them adequately. In the case of the rat heart, we successfully obtained about approx 3×10^6 cells per heart. because it would requires about 5×10^5 cells to get a radioactive signal of 2000 to 3000 cpm/tube, it then becomes almost impossible to generate a complete displacement curve from a single heart. Assuming that the dissociation constant remains similar between different experimental groups, the density of sites may then be estimated by comparing the cpm bound for a fixed number of cells.

Acknowledgments

This work was supported by grants from the Medical Research Council of Canada and by Merck Frosst Canada

References

1. Chang, R. S., Lotti, V. J., Chen, T. B., and Fawell, S. E. (1990) Two angiotensin II binding sites in rat brain revealed using [^{125}I]Sar^{1},Ile^{8}-angiotensin II and selective nonpeptide antagonists. *Biochem. Biophys. Res. Commun.* **171,** 813–817.
2. Chen, T. B., Lotti, V. J., and Chang, R. S. (1992) Characterization of the binding of [^{3}H]L-158,809: a new potent and selective nonpeptide angiotensin II receptor (AT1) antagonist radioligand. *Mol. Pharmacol.* **42,** 1077–1082.
3. Morrison, M. and Bayse, G. S. (1970) Catalysis of iodination by lactoperoxidase. *Biochemistry* **9,** 2995–3000.
4. Murthy, K. K., Thibault, G., Schiffrin, E. L., Garcia, R., Chartier, L., Gutkowska, J., et al. (1986) Disappearance of atrial natriuretic factor from circulation in the rat. *Peptides* **7,** 241–246.
5. Morris, B. J. (1976) Specific radioactivity of radioimmunoassay tracer determined by self-displacement: a reevaluation. *Clin. Chim. Acta* **73,** 213–216.
6. Fareh, J., Touyz, R. M., Schiffrin, E. L., and Thibault, G. (1997) Cardiac type-1 angiotensin II receptor status in deoxycorticosterone acetate-salt hypertension in rats. *Hypertension* **30,** 1253–1259.
7. Fareh, J., Touyz, R. M., Schiffrin, E. L., and Thibault, G. (1996) Endothelin-1 and angiotensin II receptors in cells from rat hypertrophied heart. Receptor regulation and intracellular Ca^{2+} modulation. *Circ. Res.* **78,** 302–311.
8. Touyz, R. M., Fareh, J., Thibault, G., Larivière, R., and Schiffrin, E. L. (1996) Modulation of Ca^{2+} transients in neonatal and adult rat cardiomyocytes by angiotensin II and endothelin-1. *Am. J. Physiol.* **270,** H857–H868.
9. McPherson, G. A. (1985) Analysis of radioligand binding experiments: a collection of computer programs for the IBM PC. *J. Pharmacol. Methods* **14,** 213–228.
10. DeLéan, A. P. J., Munson, P. J., and Rodbard, D. (1978) Simultaneous analysis of families of sigmoïdal curves: application to bioassay, radioligand assay, and physiological dose-response curves. *Am. J. Physiol.* **235,** E97–E102.
11. Inagami, T. (1999) Molecular biology and signaling of angiotensin receptors. *J. Am. Soc. Nephrol.* **11,** S2–S7.
12. Smith, R. D. (1996) Atypical (non-AT_1, non-AT_2) angiotensin receptors, in *Recent Advances in Cellular and Molecular Aspects of Angiotensin Receptors* (Raizada, M. K., Phillips, M. I., and Sumners, C., eds.). Plenum, New York, pp. 237–245.
13. Gutkowska, J., Genest, J., Thibault, G., Garcia, R., Larochelle, P., Cusson, J. R., et al. (1987) Circulating forms and radioimmunoassay of atrial natriuretic factor. *Endocrinol. Metab. Clin. North Am.* **16,** 183–198.

14. Touyz, R. M., Fareh, J., Thibault, G., and Schiffrin, E. L. (1996) Intracellular Ca^{2+} modulation by angiotensin II and endothelin-1 in cardiomyocytes and fibroblasts from hypertrophied hearts of spontaneously hypertensive rats. *Hypertension* **28,** 797–805.
15. Meggs, L. G. H., Huang, H., Cheng, W., Li, P., Capasso, J. M., Anversa, P., and Lorell, B. H. (1993) Regulation of angiotensin II receptors on ventricular myocytes after myocardial infarction. *Circ. Res.* **72,** 1149–1162.

22

Autoradiographic Localization and Quantification of Components of the Renin–Angiotensin System in Tissues

Siew Yeen Chai, Andrew M. Allen, Jialong Zhuo, Ingrid Moeller, and Frederick A. O. Mendelsohn

1. Introduction

In situ radioligand binding with autoradiography allows localization and quantification of bound radiolabeled ligands in tissues. This is a very sensitive technique that enables the characterization of binding kinetics and ligand specificity and the quantification of the amount of radioligand bound in different structures within the tissue. This technique is complementary to the higher resolution of immunohistochemical localization of proteins or binding sites on fixed tissue sections and *in situ* hybridization histochemical localization of mRNA.

We have successfully used this technique to map the distribution of the different components of the renin–angiotensin system (RAS), particularly in the brain where we have provided extensive maps of angiotensin receptors and angiotensin converting enzyme (ACE). We found high levels of angiotensin AT_1 receptors in many brain regions that were important for blood pressure regulation, fluid homeostasis, and pituitary hormone release. We also found that the distribution of receptors in these regions was highly conserved in different species. These findings further support the important role angiotensin II plays in these physiological processes. The distribution of ACE correlated well with the presence of angiotensin AT_1 receptors in many brain regions, suggesting that angiotensin II is generated close to its sites of action in the central nervous system.

From: *Methods in Molecular Medicine, vol. 51: Angiotensin Protocols*
Edited by: D. H. Wang © Humana Press Inc., Totowa, NJ

2. Materials

2.1. Angiotensin AT_1 and AT_2 Receptors

In our initial autoradiographic studies, we used the radiolabeled, high-affinity agonist, Sarcosine[1] angiotensin II to map the distribution of angiotensin receptors *(1–3)*. We subsequently changed to the peptide antagonist, Sarcosine[1], Isoleucine[8] angiotensin II (Sar[1], Ile[8] Ang II) (Peninsula Laboratories, Belmont, CA) because this ligand produces the best image with the lowest non-specific binding and binds with a 10-fold higher affinity to the receptor than angiotensin II *(4–8)* (**Fig. 1**). Upon the discovery of the angiotensin AT_1 and AT_2 receptors, the technique was further modified by the addition of unlabeled, subtype selective, antagonists to our incubation buffer to discriminate between the receptor subtypes *(9,10)* (**Fig. 2**). To visualize the AT_1 receptors, 10 μ*M* PD123319 (Parke Davis, Pharmaceutical Research Division, Ann Arbor, MI) was added to the incubation. Conversely, AT_2 receptors were visualized by the addition of 10 μ*M* losartan (Dupont Merck, Research and Development, Wilmington, DE) to the incubation. Although AT_1- and AT_2-receptor subtype-specific antagonists are available, they are not ideal for use as radiolabeled ligands for in vitro autoradiographic studies as these compounds, when radioiodinated, produce high levels of nonspecific binding.

2.2. Angiotensin Converting Enzyme (ACE)

The availability of potent, tight-binding, and specific inhibitors of ACE has provided excellent ligands with which to map the distribution of and quantify the levels of the enzyme on tissue sections in vitro. We have developed a highly sensitive in vitro technique to quantify ACE using a derivative of the ACE inhibitor lisinopril (N-[(s)-1-carboxy-3-phenylpropyl]-L-lysyl-L-proline). The compound, known as "351A" (Dupont Merck), contains a tyrosine residue on the lysine side-chain of lisinopril that enables the incorporation of ^{125}I to the molecule without interfering with its binding to the catalytic site of ACE *(11–17)*.

2.3. Renin

In contrast to ACE, where potent, high-affinity inhibitors are available for use as radiolabeled ligands to map and quantify the distribution of the enzyme, renin inhibitors are not very specific and their affinities for the enzyme are highly dependent on the species the enzyme is found in. Many of the earlier renin inhibitors were developed from the peptide substrate of the enzyme that differs in amino acid sequence in the different species. We have developed an in vitro autoradiographic method to map the distribution of renin in

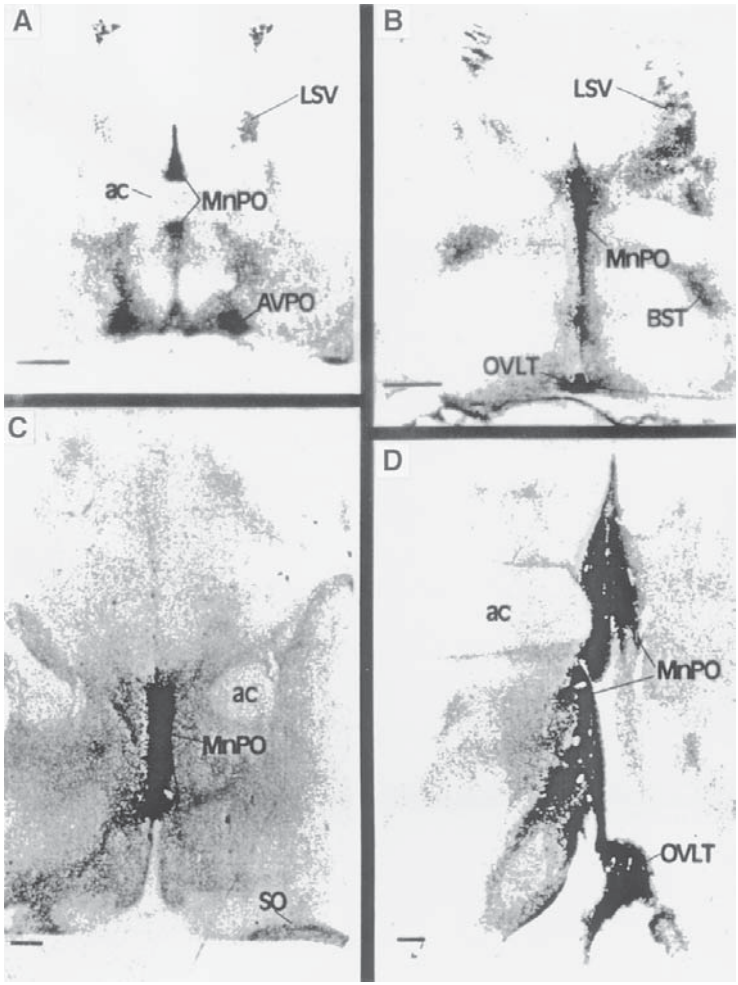

Fig. 1. Photomicrographs of ^{125}I-[Sar^{1}, Ile^{8}] angiotensin II binding in coronal sections of the rostral hypothalamus from **(A)** rat, **(B)** rabbit, **(C)** sheep, and **(D)** human demonstrating high levels of binding in the median preoptic nucleus (MnPO) and the organum vasculosum of the lamina terminalis (OVLT). The other abbreviations used are: ac—anterior commissure, AVPO—anteroventral preoptic nucleus, BST—bed nucleus of the stria terminalis, LSV—lateral septal nucleus, ventral part, and SO—supraoptic nucleus. Black represents high densities of binding and white background.

canine tissues using one of these renin inhibitors, H77 (H-dHis-Pro-Phe-His-Leu-Leu-Val-Tyr-OH), that exhibits a relatively high affinity for the dog enzyme ***(18,19)***.

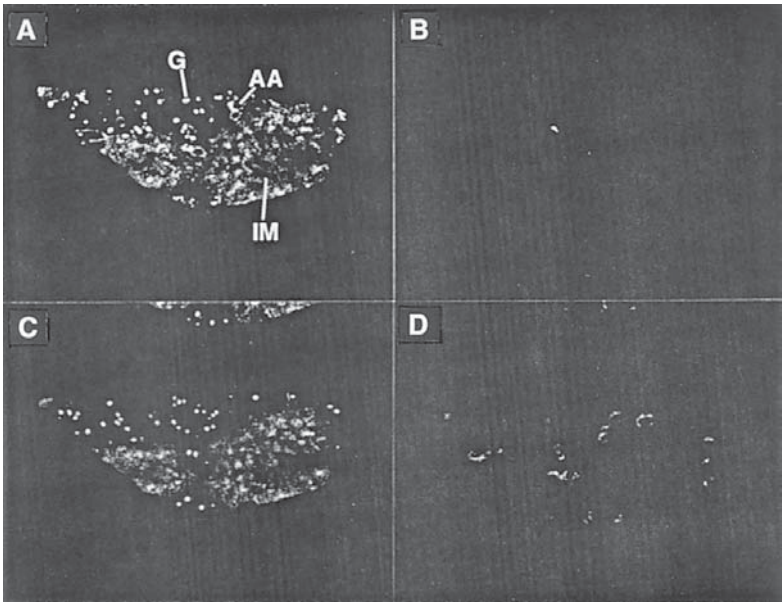

Fig. 2. Photomicrographs of ^{125}I-[Sar^{1}, Ile^{8}] angiotensin II binding in adjacent sections through a human kidney. Panel A represents total binding, panel B—nonspecific binding in the presence of 1 μ*M* unlabeled angiotensin II amide, panel C—AT_1 receptors (binding in the presence of 10 μ*M* PD 123319), and panel D—AT_2 receptor (binding in the presence of 10 μ*M* losartan). The abbreviations used are AA—afferent arteriole, G—glomerulus, and IM—inner medulla. White represents high densities of binding and black background.

2.4. Angiotensin AT_4 Receptors

The 3–8 fragment of angiotensin II was initially thought to be an inactive degradative product of angiotensin II because this hexapeptide exhibited a very weak affinity for the angiotensin II-receptor subtypes. However, angiotensin II (3–8), also known as angiotensin IV, was later shown to elicit distinctive physiological effects by binding to a pharmacologically distinct site. A committee set up in 1994 to determine the nomenclature of the angiotensin-receptor subtypes named this binding site the AT_4 receptor. The AT_4 receptor is pharmacologically characterized as the binding site that exhibit highest affinity for angiotensin IV, followed by angiotensin III and angiotensin II. We have subsequently shown that the AT_4 receptor in the sheep brain also binds LVVYPWTQRF, a decapeptide that we purified from sheep cerebral cortex ***(20)***.

The most commonly used radiolabeled ligand for this receptor is ^{125}I-angiotensin IV ***(21,22)***. Angiotensin IV used in our experiments was obtained from Peninsula Laboratories (Belmont, CA).

3. Methods

3.1. In Vitro Localization and Quantification of Angiotensin AT_1 and AT_2 Receptors on Frozen Tissue Sections

3.1.1. Preparation of Radiolabeled Ligand

[Sar^1, Ile^8] Ang II is radiolabeled using a protocol provided by Prof. J. W. Harding, Department of Veterinary and Comparative Anatomy, Washington State University, Pullman.

1. 200 μg of [Sar^1, Ile^8] Ang II dissolved in 10 μL of 0.05 *M* acetic acid, is reacted with 2 mCi of $Na^{125}I$ using immobilized lactoperoxidase (100 μg in 100 μL distilled water) and glucose (50 μL of 1% solution in 100 m*M* $NaPO_4$ buffer, pH 7.4) for 2 h at room temperature.
2. Following the 2 h reaction, unreacted $Na^{125}I$ is removed by passing the reaction mixture through a Sep Pak C_{18} cartridge with 0.05% trifluoroacetic acid.
3. The radioiodinated peptide is then eluted from the cartridge with 5 mL of 75% acetronitrile in 0.05% trifluoroacetic acid.
4. The reaction product is reduced to a third of its volume by evaporation in a fume cupboard and ^{125}I-[Sar^1, Ile8] Ang II isolated by high-pressure liquid chromatography (HPLC) on a C_{18} column using 14% acetronitrile in triethylamine phosphate to elute the radioligand.
5. Aliquots of the radiolabeled ligand are then stored at –20°C until use for a maximum of 6–8 wk.

3.1.2. Preparation of Tissue Sections

1. The animals are killed by an overdose of barbiturate anesthetic or by decapitation and the tissues removed as quickly as possible and snap frozen in isopentane maintained at –40°C on a bed of dry ice.
2. Large tissues, in particular, the brains of larger species of animals, are blocked into 3 × 2-cm blocks before freezing for ease of cutting.
3. Frozen sections of 10–20-μm thickness are then cut in a cryostat at –20°C and thaw-mounted onto gelatine-coated microscope slides.
4. The sections are then dehydrated under reduced pressure at 4°C for at least 2 h and then stored with desiccant at –70°C until use.

3.1.3. Binding with Radiolabeled Ligand

1. Once at room temperature, the sections are initially preincubated for 15 min at room temperature in 10 m*M* sodium phosphate buffer (pH 7.4) containing 150 m*M* sodium chloride and 5 m*M* sodium ethylenediamine tetraacetic acid (EDTA) to remove endogenously bound ligand.
2. The sections are then transferred into a fresh volume of buffer to which has been added 0.4 m*M* Bacitracin, 0.2% bovine serum albumin (BSA) and 130 p*M* ^{125}I-[Sar^1, Ile^8] Ang II (approx 500,000 cpm/mL) for 1 h at room temperature. Nonspecific binding is determined on adjacent sections by including 1 m*M* of unlabeled [Sar^1, Ile^8] Ang II or Ang II amide in the incubation buffer.

3. For the determination of AT_1 or AT_2 receptor subtypes, adjacent sections are incubated in the presence of 10 μ*M* PD 123177 to visualize the AT_1 receptors or 10 μ*M* losartan to visualize the AT_2 receptors.
4. Following the incubation, the sections are washed in ice-cold phosphate-buffered saline (PBS) pH7.4, to remove nonspecifically bound radiolabeled ligand and then dried under a stream of cool air.

3.1.4. Detection of AT_1 and AT_2 Receptors on Tissue Sections

1. Dry film : the sections are loaded into X-ray cassettes together with a set of radioactivity standards (as in **Subheading 3.1.5.**), and exposed to Agfa-Scopix CR3B or Kodak Ektascan EB1 X-ray film for 1 to 4 wk. The films are then developed in a Kodak RP O-mat automatic developer.
2. Liquid emulsion: the sections are fixed in paraformaldehyde vapor for 2 h at 80°C, dehydrated through increasing concentrations of ethanol, defatted in xylene and dipped in Amersham LM-1 nuclear emulsion. After exposure for 1 to 4 wk, the sections are developed in Kodak D19 developer for 3 min at 20°C, washed in distilled water and fixed in Ilford Hypam Rapid Fixer (40 parts) and Ilford Hardener (1 part).

3.1.5. Preparation of Radioactivity Standards

1. Twenty micrometers sections are cut from a 5-mm diameter cylindrical core of either brain or kidney that has been frozen.
2. The circular sections are then thaw mounted onto gelatin-coated slides and air-dried.
3. A range of known ^{125}I-radioactivity, prepared by serial dilution of the radiolabeled ligand, is then applied onto the tissue disks in a volume of 5 mL and dried.
4. Mean protein content of adjacent disks is measured after digestion of the tissue in 1.0 *M* sodium hydroxide.
5. The area of the tissue disk is determined and the value of mean protein content per unit area is calculated.
6. The radioactivity standards are corrected for radioactive decay using the equation $Nt = No \times e^{-kt}$ where Nt is the corrected radioactivity level at time t, No is the original level of radioactivity, t is the time elapsed from the preparation of the standards to the middle of the exposure period, and k is the decay constant based on the half-life of the isotope (the k value of ^{125}I is 0.0116 day^{-1}).

3.1.6. Quantification of X-Ray Film

The autoradiographs generated on the X-ray films are then quantified by computerized densitometry using an microcomputer imaging device (MCID) system (Imaging Research Inc., Ontario, Canada). The radioactivity standards that have been included in each film exposure enable the conversion of optical density on the films to radiolabeled ligand bound per unit area (dpm/mm^2). We are, therefore, able to accurately quantify the density of angio-

tensin receptors on tissue sections and have extended our studies to investigate the regulation of angiotensin receptors under different physiological and pathological conditions ***(23–26)***.

3.1.7. High-Resolution Localization of the AT_1 and AT_2 Receptors on Tissue Slices

Because in vitro receptor autoradiographic localization of the AT_1 and AT_2 receptors on frozen sections may not provide adequate cellular resolution, we have modified the autoradiographic technique to localize the receptors on fresh tissue slices both at light and electron microscopic levels ***(27)***.

1. The animal is killed by a lethal dose of sodium pentobarbitone, the tissue removed quickly, and sliced into 1-mm-thick slices that are further cut into 1 × 1-mm blocks.
2. The blocks are then preincubated in carbogen-saturated (95% O_2, 5% CO_2) Krebs buffer (124 m*M* NaCl, 26 m*M* $NaHCO_3$, 3 m*M* KCl, 1.4 m*M* KH_2PO_4, 2.4 m*M* $CaCl_2$, and 4 m*M* glucose), pH 7.2, for 30 min at 22°C.
3. The tissue slices are then incubated for 1 h at room temperature in Krebs buffer containing 5 m*M* EGTA, 0.2% BSA, and 260 p*M* ^{125}I-[Sar^1, Ile^8] Ang II for 1 h at 22°C.
4. Nonspecific binding is determined in parallel incubations in the presence of 1 μ*M* unlabeled Ang II amide.
5. Following the incubation, the tissue slices are washed four times in ice-cold Krebs buffer for 5 min each.
6. The tissue slices are then fixed in 2.5% glutaldehyde in 0.01 *M* phosphate buffer, pH 7.3, for 1 h at 22°C and washed twice for 5 min each in 0.1 *M* phosphate buffer containing 5% sucrose.
7. The tissue slices are postfixed in 2.5% aqueous osmium tetroxide, dehydrated through graded acetone and embedded in Araldite-Epon.
8. For higher-resolution light microscopic autoradiography, 0.7-μm sections are cut, positioned onto chrom-alum coated microscope slides, and exposed to Kodak NTB2 liquid emulsion for up to 60 d at 4°C. The slides are then developed in Kodak D19, and lightly counterstained with 1% methylene blue.
9. For electron microscopic autoradiography, 60–90-nm sections are cut with a diamond knife and positioned onto celloidin-coated microscope slides, and exposed to Ilford K5 liquid emulsion for 60 d at 4°C. The slides are then developed in Kodak D19 and the sections floated onto water, picked up onto mesh grids, and stained with uranyl acetate and lead citrate.

3.1.8. Detection of Angiotensin Receptors After In Vivo Infusion of ^{125}I-[Sar^1, Ile^8] Ang II

The advantage of using an in vivo delivery system to localize the AT_1 and AT_2 receptors is the ligand can be crosslinked onto the receptor by paraformaldehyde and/or glutaldehyde thereby providing good preservation of tissue

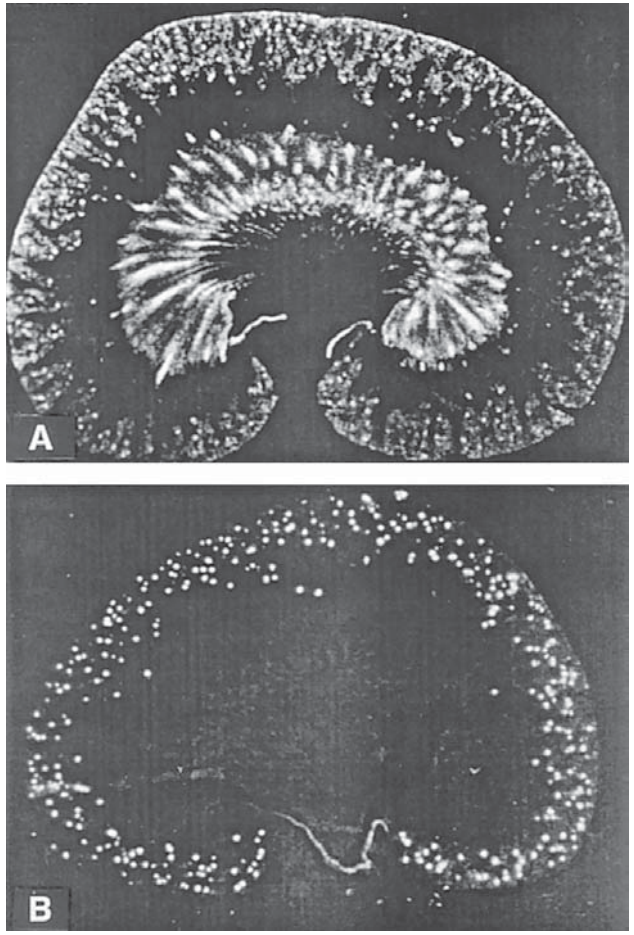

Fig. 3. Photomicrographs. **(A)** Coronal section through a rat kidney illustrating the specific binding of ^{125}I-[Sar^{1}, Ile^{8}] angiotensin II in vitro. **(B)** Coronal section through a rat kidney after in vivo infusion of ^{125}I-angiotensin II. We believe that the difference in distribution of the two radiolabeled ligands is because of the in vivo occupancy of the receptor sites by endogenous intrarenal angiotensin II.

morphology. The disadvantage is the restricted access of the systemically administered radiolabeled ligand to receptor sites on the cell surface (**Fig. 3**). Radioiodinated angiotensin II is used as the radiolabeled ligand for the in vivo infusion to ensure maximum crosslinking of the radiolabeled ligand to the receptor by glutaldehyde. We have developed this technique to determine the cellular distribution of angiotensin AT_1 and AT_2 receptors in the rat kidney *(28–29)* (**Fig. 4**).

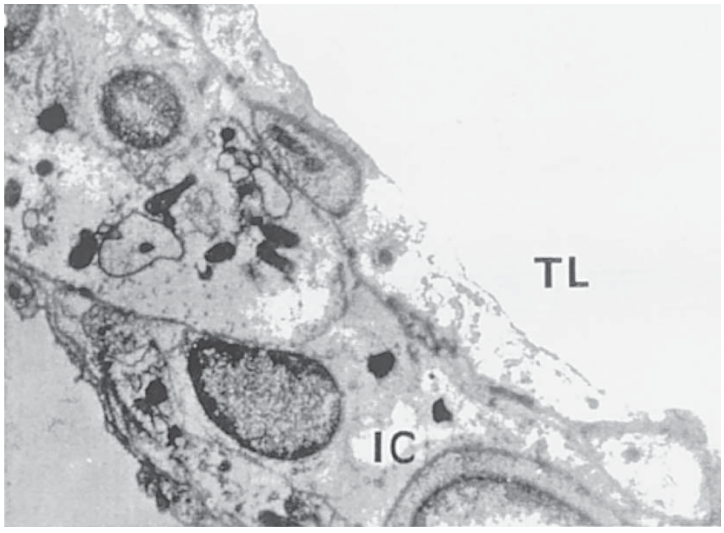

Fig. 4. Electron microscopic autoradiograph showing in vivo labeling of the angiotensin AT_1 receptor in the interstitial cells (IC) in the inner stripe of the outer medulla of the rat kidney. The silver grains are seen as black spots over the interstitial cells. The other abbreviation used is TL – thin limb of the loop of Henle. (stain:uranyl acetate, lead citrate, magnification: ×6750).

1. Male Sprague-Dawley rats are anesthetized, their left jugular vein cannulated, and the descending aorta and renal arteries exposed for perfusion-fixation.
2. The rats are then infused with either 80 μCi of ^{125}I-Ang II in 300 μL of PBS or, to determine nonspecific binding, 20 nmol of [Sar^1, Ile^8] Ang II in 300 mL of PBS followed by 80 μCi of ^{125}I-Ang II after 10 min.
3. 10 min after infusion of the radiolabeled ligand, the kidneys are perfused with cold PBS to flush out the blood followed by 150 mL of 2.5% glutaldehyde in phosphate buffer.
4. The kidneys are then removed and bisected. One half of the kidney is processed for dry film autoradiography as aforementioned. Blocks of kidney 1 × 1 mm are taken from the outer cortex and inner medulla of the other half of the kidney.
5. The blocks are fixed further in 2.5% glutaldehyde at room temperature for 2 h, followed by three washes in 0.1 *M* phosphate buffer containing 5% sucrose.
6. The blocks are then postfixed in 2.5% aqueous osmium tetroxide, dehydrated through graded acetone, and embedded in Araldite-Epon.
7. Sixty to 90-nm sections are cut from the tissue blocks positioned onto celloidin-coated microscope slides, dipped in Ilford K5 liquid emulsion and exposed for up to 80 d at 4°C.
8. The sections are then developed and processed as described in **Subheading 3.1.7.**

3.2. Localization and Quantification of ACE on Frozen Tissue Sections

3.2.1. Preparation of the Radiolabeled Ligand

1. 250 ng of 351A is dissolved in 10 μL of distilled water and reacted for 60 s with 1 mCi $Na^{125}I$ and 10 μg chloramine T in 60 μL 0.25 *M* sodium potassium phosphate buffer.
2. The reaction is then terminated with 10 μL 5 mg/mL sodium metabisulphite and the reaction mixture loaded onto a Sephadex C25 column that has been equilibrated with 0.01 *M* ammonium acetate pH 3.0. The column is then washed with 20 mL of 0.01 *M* ammonium acetate.
3. Iodinated 351A is eluted with 0.1 *M* ammonium acetate buffer pH 3.5.
4. Aliquots of ^{125}I-351A are then stored at –20°C and used within 8 wk.

3.2.2. Preparation of Tissue Sections

For the binding of ^{125}I-351A, we use tissues that are lightly fixed with 1% paraformaldehyde. We found that this process provides slight improvement in tissue morphology without affecting the binding of the radiolabeled ligand.

1. For rat tissues, the animal is anesthetized with sodium pentobarbitone, and perfused via an intracardiac cannula with 200 mL of phosphate buffered saline, pH 7.4 at 4°C, followed by 200 mL of 1% paraformaldehyde.
2. The tissues are then dissected out and snap frozen. Tissues are sectioned and stored as described in **Subheading 3.1.2.**

3.2.3. Binding with ^{125}I-351A

1. The sections are subjected to a 15-min preincubation in a buffer containing 10 m*M* sodium phosphate, 150 m*M* sodium chloride, and 0.2% BSA, pH 7.4 at 20°C.
2. This is followed by a 1-h incubation in fresh buffer to which has been added 130 p*M* ^{125}I-351A (approx 500,000 cpm/mL). A set of enzyme standards is included in each incubation procedure to enable calibration of optical densities on the X-ray film in terms of enzyme activity. Preparation of the enzyme standards is described in **Subheading 3.2.4.**
3. Nonspecific binding is determined on adjacent sections by including either 1 μ*M* lisinopril (the ACE inhibitor) or 1 m*M* EDTA in the incubation buffer.
4. After incubation, the sections are washed four times for 1 min each in ice-cold PBS and then dried under a stream of cold air.
5. The sections are then exposed to X-ray film together with either the enzyme standards that have been subjected to the incubation procedure or a set of radioactivity standards as described for quantifying ^{125}I-[Sar^1, Ile^8] Ang II binding. An example of ACE distribution in human brain as detected by ^{125}I-3251A binding is depicted in **Fig. 5**.

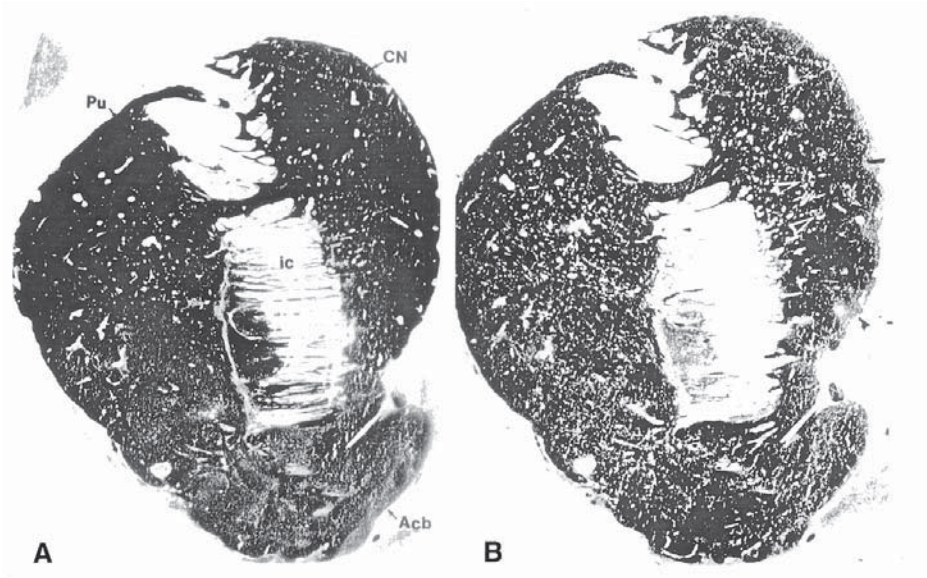

Fig. 5. Adjacent sections of the human striatum cut in the coronal plane illustrating **(A)** ^{125}I-351A binding and **(B)** acetylcholinesterase staining. A higher density of ^{125}I-351A binding is observed in the striosomes—the acetylcholinesterase-poor regions of the striatum (arrowheads). The abbreviations used are Acb—nucleus accumbens, CN—caudate nucleus, ic—internal capsule, and Pu—putamen.

3.2.4. Preparation of Enzyme Standards

We devised a system to calibrate the gray levels of the images captured on X-ray film to concentrations of ACE activity on the tissues ***(12)***.

1. The standards are prepared by serial dilutions of caudate putamen membranes in 1% gelatin dissolved in PBS.
2. Five-milliliter aliquots are then applied onto gelatin-coated slides, dried at 4°C in a desiccator, and then carried through the same incubation procedure as for the tissue sections.
3. The standards are exposed simultaneously with the incubated sections to X-ray film.
4. Samples of the membrane suspension are also assayed for ACE activity using the synthetic peptide substrate *Hip-His-Leu* and fluorimetric detection of the liberated product *His-Leu*.

3.2.5. Quantification of In Vivo Tissue Occupancy of ACE Inhibitors

The unique property of many ACE inhibitors to bind tightly to the catalytic site of the enzyme with high affinity has enabled us to develop a tech-

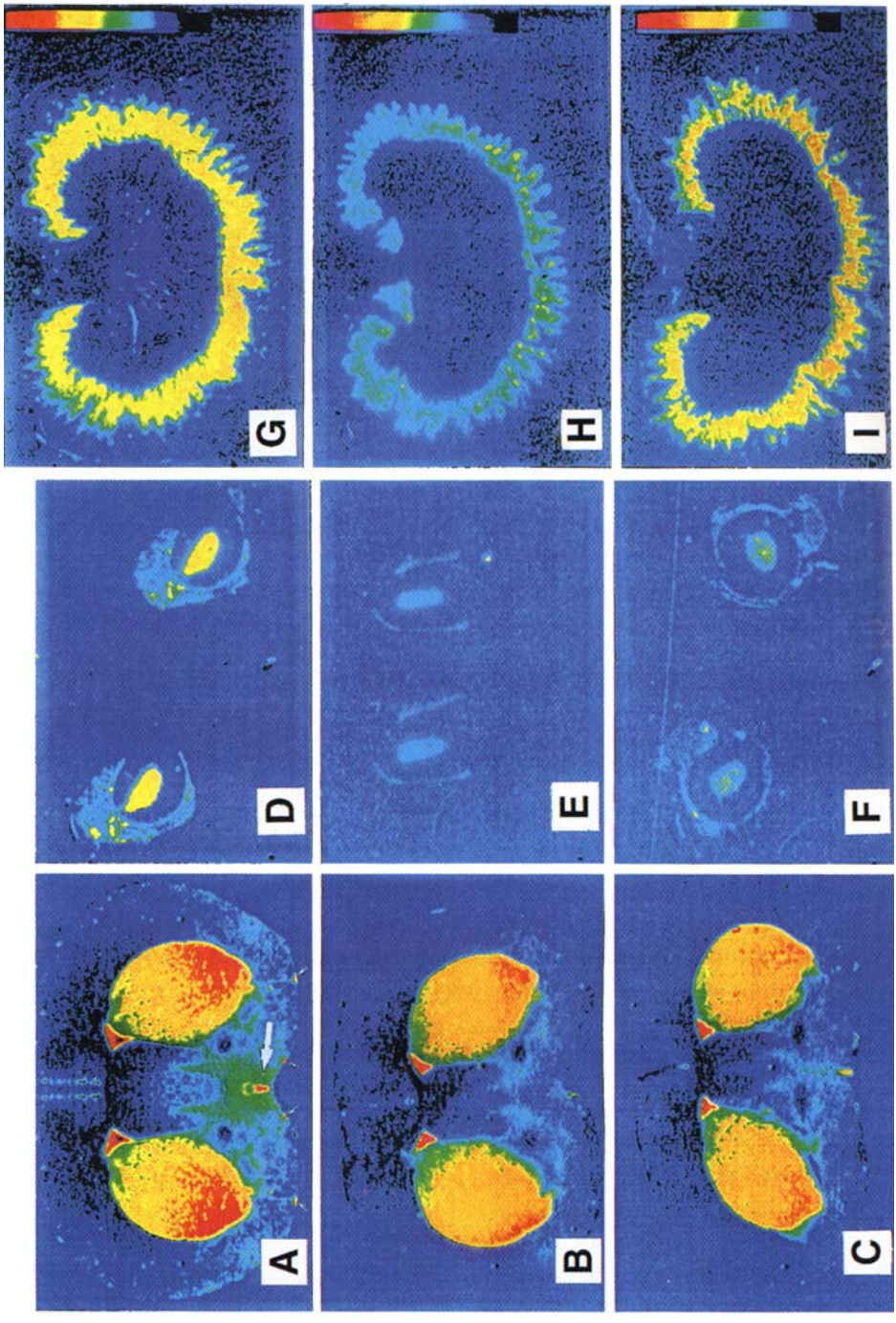
A
B
C
D
E
F
G
H
I

nique to assess in vivo occupancy of these inhibitors on tissue ACE. We have been able to quantify the degree of inhibition of ACE in different tissues in rats and humans following acute or chronic administration of the enzyme inhibitors ***(30–34)*** **(Fig. 6)**.

1. The rats that have either received an acute dose of an ACE inhibitor or have been chronically administered an ACE inhibitor in the drinking water are given a lethal dose of sodium pentobarbitone, the tissues dissected out and frozen as described in **Subheading 3.1.2.**
2. 20-μm frozen sections are then cut, thaw-mounted onto gelatine-coated slides and dehydrated for at least 2 h.
3. The sections are then subjected to a 1 h incubation in PBS containing 0.2% BSA to which has been added 130 p*M* ^{125}I-351A (approx 500,000 cpm/mL). A set of enzyme standards is included in each incubation procedure to enable calibration of optical densities on the X-ray film in terms of enzyme activity.
4. After incubation, the sections are put through a series of washes and exposed to X-ray film as described in **Subheading 3.2.3.**

3.2.6. Determination of Total ACE Activity Compared to the Free Enzyme on Tissue Sections

Chronic treatment with ACE inhibitors leads to an induction of serum ACE in a number of species of animals including human. This complicates the interpretation of enzymatic activity of ACE as an index of the effectiveness of its inhibitors. ACE is a metallopeptidase that is susceptible to chelating agents such as EDTA to dissociate Zn^{2+} from the active site to yield the inactive apoenzyme. The effect is reversible because removal of EDTA and the addition of Zn^{2+} will completely restore enzymatic activity. We have utilized this characteristic property of enzyme to quantify the amount of total compared to free ACE in tissue sections after ACE inhibition ***(35)***.

1. Rats are given an ACE inhibitor (e.g., lisinopril, 10 mg/kg/d) in the drinking water for 2 wk. Control rats are given tap water to drink.

Fig. 6. *(facing page)* Computer-generated, pseudocolor images of ^{125}I-351A binding in rat brain **(A–C)**, rat adrenal **(D–F)**, and rat kidney **(G–I)**. Sections **A, D, G** are obtained from a control rat, sections **B, E, H** are obtained from a rat 4h after receiving a single oral dose of 1 mg/kg of perindopril and sections **C, F, I** are obtained from a rat 24-h after receiving a single oral dose of 1 mg/kg perindopril. The color code is as follows: red represents high levels of binding, yellow and green—moderate, and blue—low levels of binding. The large arrow marks the position of the organum vasculosum of the lamina terminalis, a circumventricular organ that has a deficient blood brain barrier. The smaller arrows mark the positions of cerebral blood vessels. The high levels of ACE in these structures are markedly inhibited by the single dose of perindopril.

2. The animals are then given a lethal dose of sodium pentobarbitone, the tissues removed rapidly, and snap-frozen as aforementioned.
3. To determine the levels of free ACE in the tissues, 20-μm frozen sections are cut and processed for autoradiography as described in **Subheading 3.2.3.** with the preincubation step omitted.
4. In order to determine the total amount of ACE, alternate sections are initially incubated in PBS containing 1 m*M* EDTA for 1 h at 20°C to dissociate the ACE inhibitor that is occupying the active site of the enzyme.
5. The sections are then washed four times in PBS without EDTA at 4°C and then incubated in PBS containing 50 μ*M* $ZnCl_2$, 0.2% BSA and 0.3 μCi/mL ^{125}I-351A at 20°C for 1 h.
6. After the incubation step, the sections are washed in ice-cold PBS as described above and exposed to X-ray film.

3.3. Localization of Renin on Tissue Sections

3.3.1. Preparation of the Radioligand ^{125}I-H77

1. 200 nmoles of H77 dissolved in 100 μL of 0.01 *M* hydrochloric acid, is reacted with 2 mCi of $Na^{125}I$, 100 mg of lactoperoxidase, and 500 μg of glucose for 2 h at room temperature, similar to the procedure described for iodination of [Sar^1, Ile^8] Ang II.
2. The reaction mixture is then passed through a Sep Pak C_{18} column to remove the unreacted sodium iodide, which is eluted with 0.05% trifluoroacetic acid followed by the elution of the ^{125}I-H77 with 75% acetonitrile in 0.05% trifluoroacetic acid.
3. The eluate containing ^{125}I-H77 is then injected into an HPLC column and eluted with 24% acetonitrile in triethylamine phosphate pH 3.0.
4. The radiolabeled ligand is then stored in aliquots at –20°C for a maximum of 8 wk.

3.3.2. Preparation of Tissue Sections

1. The dogs are killed by an overdose of sodium pentobarbitone, the kidneys removed and perfused with ice-cold saline solution, followed by 1% paraformaldehyde in PBS, pH 7.4 via the renal artery.
2. The kidneys are then cut into 2 × 2 × 1-cm blocks, and soaked in 4% paraformaldehyde in PBS, pH 7.4, containing 10% sucrose overnight at 4°C.
3. The kidneys are then frozen in isopentane chilled to –40°C on dry ice.
4. Ten- or 20-μm sections are cut on a cryostat and dehydrated as described for ^{125}I-[Sar^1, Ile^8] Ang II binding.

3.3.3. Incubation with Radiolabeled Ligand

1. The sections are preincubated in 10 m*M* sodium phosphate, pH 7.4, containing 150 m*M* sodium chloride, 0.2% BSA for 15 min at room temperature.
2. This is followed by a 60-min incubation in a fresh volume of buffer containing 330 p*M* ^{125}I-H77 (0.5 μCi/mL), 1 μ*M* N-acetyl-pepstatin, and 0.1% Triton X-100.
3. Nonspecific binding is determined on adjacent sections in a parallel incubation in the presence of 1 μ*M* unlabeled H77.

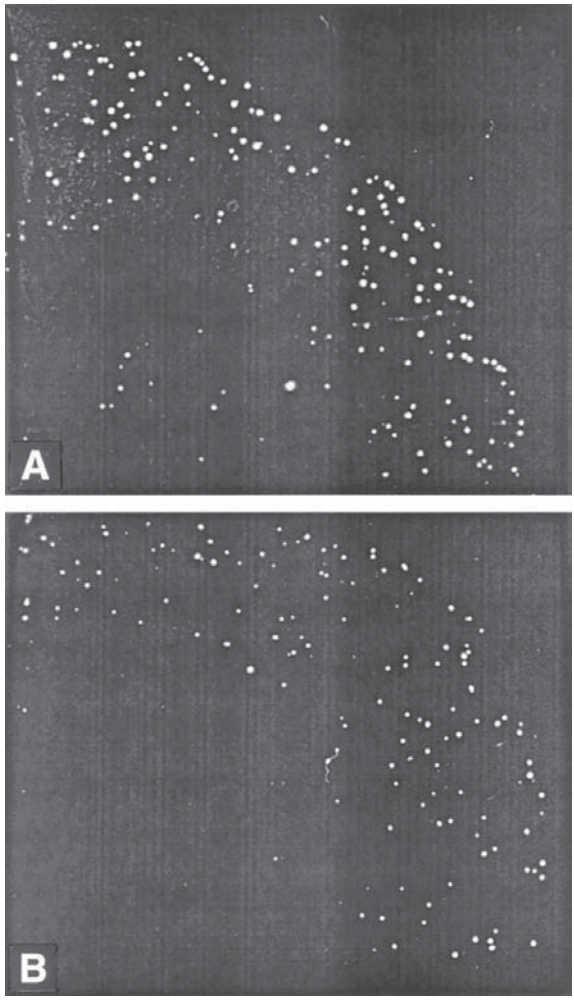

Fig. 7. Photomicrographs of ^{125}I-H77 binding in dog kidney **(A)** in the absence of 1 μ*M* N-acetyl-pepstatin in the incubation buffer and **(B)** in the presence of 1 μ*M* N-acetyl-pepstatin in the incubation buffer. The silver grains indicated by bright spots on a dark background represent renin found in the juxtaglomerular apparatus.

4. After the incubation, the sections are subjected to four successive 1-min washes in ice-cold PBS and dried under stream of cold air.
5. The 20-μm sections are then loaded onto X-ray cassettes and exposed to X-ray film as described for the previous radiolabeled ligands. An example of renin distribution in dog kidney as detected by ^{125}I-H77 binding is seen in **Fig. 7**.
6. The 10-μm sections are fixed by immersion in 5% glutaraldehyde, 2% paraformaldehyde made up in PBS pH 7.4 for 60 min at 4°C.

7. The sections are then dehydrated through graded alcohol, defatted in xylene, rehydrated, and air-dried.
8. After defatting, the sections are dipped in liquid nuclear emulsion LM-1, and exposed for 14 d in a light-tight box with silica gel.
9. The sections are then developed with Kodak D19 developer for 4 min at 17°C, rinsed with water, and fixed with Ilford Rapidfix/Ilford Hardener (in a ratio of 40:1) and counterstained with hematoxylin and eosin.

3.4. Localization and Quantification of Angiotensin AT_4 Receptors

3.4.1. Preparation of the Radiolabeled Ligand

1. Five hundred nanograms of angiotensin IV is reacted with 1 mCi of $Na^{125}I$ and 10 μg of chloramine T in a buffer containing 0.25 *M* sodium potassium phosphate, pH 7.4 at 22°C for 60 s.
2. The reaction is stopped by the addition of 10 μL of 5 mg/mL sodium metabisulphite.
3. The mixture is then loaded onto a Sep Pak C_{18} cartridge and the radioiodinated peptide eluted with a methanol gradient from 20% and 80% in 0.1% trifluoroacetic acid.

3.4.2. Preparation of Tissue Sections

Fixation of the tissue sections with an aldehyde attenuates the binding of the radiolabeled ligand. Therefore, fresh frozen tissue sections are used, the preparation of which is identical to that of ^{125}I-[Sar^1, Ile^8] Ang II binding.

3.4.3. Incubation of the Radioligand

1. Sections are preincubated in an isotonic buffer, 50 m*M* Tris-HCl buffer, pH 7.4, 150 m*M* NaCl, and 5 m*M* EDTA for 30 min at 22°C.
2. The sections are then incubated in 50 m*M* Tris-HCl, pH 7.4, 150 m*M* NaCl, 5 m*M* EDTA, 100 μ*M* phenylmethylsulfonyl fluoride, 20 μ*M* bestatin, and 0.1% BSA, containing approx 200 p*M* ^{125}I-angiotensin IV, for 2 h at 22°C. **Figure 8** demonstrates ^{125}I-angiotensin IV binding in guinea pig brain.
3. Nonspecific binding is determined in parallel incubations on adjacent sections in the presence of 1 μ*M* angiotensin IV.
4. Following the incubation, the sections are given 3 × 2 min washes in the isotonic buffer, at 4°C and then air-dried.
5. The sections are then exposed to X-ray film for 1–5 wk, together with a set of radioactive standards or dipped in liquid emulsion for cellular localization of the AT_4 receptor (**Fig. 9**).
6. After exposure, the sections are counterstained with hematoxylin and eosin for histological examination.

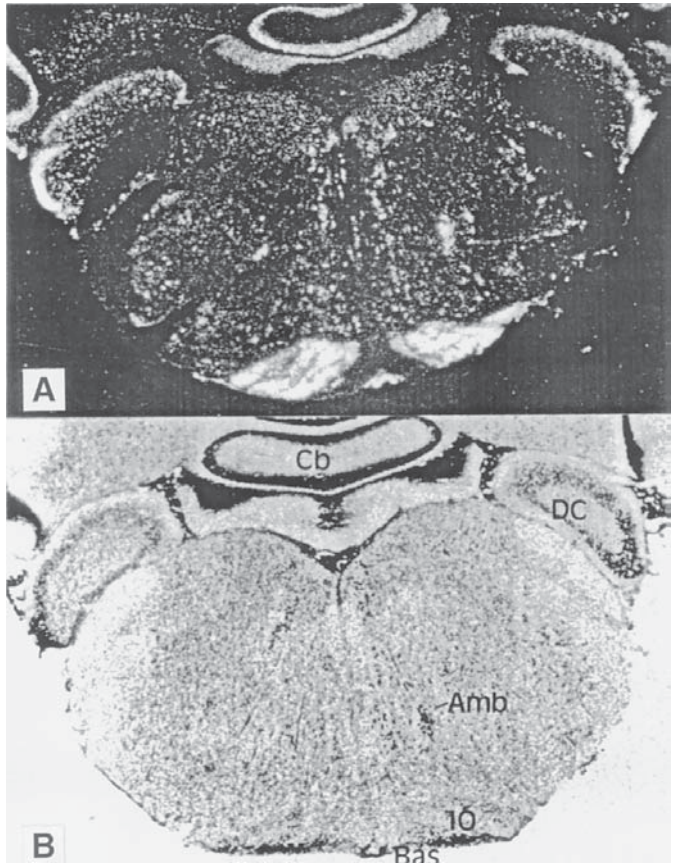

Fig. 8. Photomicrograph of ^{125}I-angiotensin IV binding in a coronal section through the guinea pig medulla oblongata **(A)** and the adjacent Nissl-stained section **(B)**, illustrating high densities of binding in the inferior olivary nucleus (IO), dorsal cochlear nucleus (DC), and the granular layer of the cerebellum (Cb). Other abbreviations used are: Amb—nucleus ambiguus and Bas—basilar artery.

4. Notes

1. *Determining the Integrity of the Radiolabeled Peptide:* The integrity of the radiolabeled peptide ligand before and during the incubation procedure can be assessed by HPLC with detection of the radioactivity peaks. This is essential if the radiolabeled ligand used is a peptide susceptible to degradation. For the case of ^{125}I-[Sar^1, Ile^8] Ang II:
   a. 2 mL of the incubation buffer before and after incubation with tissue sections are collected, partially concentrated by passing the solutions through a Sep Pak C_{18} cartridge to remove proteins.

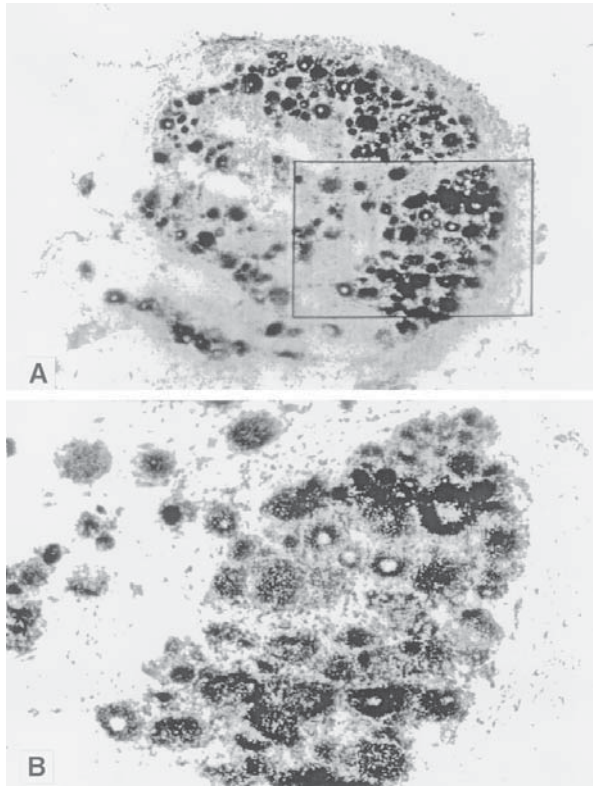

Fig. 9. Photograph of a liquid emulsion-dipped section through the dorsal root ganglia of the sheep at lower **(A)** and higher **(B)** magnification illustrating the binding of ^{125}I-angiotensin IV throughout the cytoplasm of cell bodies of sensory neurones.

b. The radioiodinated peptide is eluted with 75% acetonitrile in 0.05% trifluoroacetic acid.
c. The eluted peptide is then concentrated by evaporation under stream of air and 100 μL (approx 20,000 cpm) is injected into the HPLC column and eluted with 14% acetonitrile in triethylamine phosphate, pH 3.0.
d. Half-mL samples are collected and counted.
e. The elution profile of the radiolabeled ligand that has been subjected to incubation with tissue sections is compared to the elution profile of the nonincubated radioligand to determine the extent of degradation.

2. *Preparation of Tissues for In Vitro Receptor Autoradiography:* In vitro receptor-autoradiographic detection of the angiotensin II-receptor subtypes is carried out on fresh frozen tissues as fixation with aldehydes disrupts the binding of the radiolabeled ligand to the receptor. Smaller tissue blocks are frozen for 10 s; tissue turns white when ready; whereas larger blocks are frozen for longer. How-

ever, freezing for too long at temperatures that are too cold may cause tissues to crack.

3. *Preparation of Microscope Slides:* Slides may be coated with gelatine or silane to improve the adherence of tissues. In addition, the cleanliness of slides is important for tissue adherence and in reducing nonspecific binding. A common procedure for gelatine coating slides is as follows:
   a. Commercially available precleaned slides are soaked in 70% ethanol overnight.
   b. The slides are then loaded onto slide racks, and rinsed twice in distilled water before being dipped in 0.5% gelatine solution containing 0.05% chromium potassium sulphate.
   c. The slides are then air-dried and stored in clean slide boxes until used.
4. *Preparation of Cryostat Sections:* Sections are slowly thaw-mounted onto slides to improve adherence and also prevent formation of air bubbles. The dehydration of sections before storage at –70°C is important in preventing formation of ice crystals and in ensuring stability of the receptors during storage.
5. *Detection of Image on X-Ray Film:* Image formation on the X-ray film results from the conversion of silver ions on the emulsion of the film to silver atoms by the radioactivity emitted from the tissue sections. The optical density on the film is dependent on both the amount of radioactivity present on tissue sections and the time of exposure. With increased radioactivity present or increased time of exposure, the optical density response on the film plateaus. Therefore, in order to measure regions of high and low densities within the same tissue section, the exposure period of the sections to the film is altered to encompass the detection range within the linear portion of the dose response curve. An image processor that transforms the monochromatic gray scales on the X-ray film to a pseudocolor image can be used to facilitate discrimination of different gray levels on the X-ray film.
6. *Sensitivity of the Technique for the Detection of ACE:* A conservative estimate of the sensitivity of this technique to quantify the binding of ^{125}I-351A is based on the following :
   a. The lowest standard of 10 dpm/mm^2, which is readily detectable after a 7-d exposure.
   b. The smallest area of approx 0.2 mm^2 in which we can repeatedly measure our sample.
   c. The assumption that one molecule of ^{125}I-351A binds to one molecule of ACE. This yields the remarkable sensitivity of approx 15 molecules of ACE per μm^2.
7. *Determination of Nonspecific Binding for ^{125}I-351A:* There is a whole range of specific ACE inhibitors that exhibit nanomolar affinity for the enzyme, including fosinoprilat, ramiprilat, and perindoprilat, which can be used to determine the nonspecific binding of ^{125}I-351A. However, a more simple method to determine nonspecific binding involves the use of EDTA. ACE is a metalloproteinase that is dependent on Zn^{2+} for its catalytic activity. The binding of ^{125}I-351A to the active site of ACE can be dissociated by the addition of chelating agents such as 1 m*M* EDTA.

8. *Determination of the In Vivo Occupancy of ACE:* Because most of the ACE inhibitors exhibit a high affinity for the active site of the enzyme, we utilized this property of the compounds to assess in vitro the occupancy of the enzyme after oral administration of the ACE inhibitor. In order to ensure that the ACE inhibitor that has been administered in vivo still occupies the catalytic site of the enzyme in the tissue sections during the incubation procedure, the preincubation step is omitted. The method described in **Subheading 3.2.5.** will determine the levels of free ACE (the amount of ACE unoccupied by inhibitor) in tissue sections which can then be compared to total ACE determined in **Subheading 3.2.6.**
9. *Use of a Substrate Analogue Inhibitor of Renin to Visualise the Enzyme in Tissue Sections:* The nonspecific aspartyl protease inhibitor, N-acetyl-pepstatin is added to the incubation buffer to inhibit binding of ^{125}I-H77 to other aspartyl proteases. N-acetyl-pepstatin is a potent inhibitor of cathepsin D with an IC_{50} value of 9.3 n*M*. but is a weak renin inhibitor with an IC_{50} of 2.5 μ*M*. We found that in the dog kidney, the binding of ^{125}I-H77 to juxtaglomerular region was specific for renin whereas binding to the intervening cortex and outer medulla was not specific (**Fig. 7**). One other disadvantage of this radioligand is its limited use in a few animal species because this renin inhibitor exhibit the highest potency in inhibiting dog renin with a 100-fold lower potency for rat renin.

Conclusions

We have developed a series of angiotensin-receptor antagonists and enzyme inhibitors for use as radiolabeled ligands to map and quantify the different components of the renin–angiotensin system in tissue sections. Some of these radiolabeled ligands proved highly successful. For example, the use of ^{125}I-[Sar^1, Ile^8] Ang II to map the distribution of AT_1 and AT_2 receptors in the human brain where we detected the AT_1 receptors in sites not found in rodents ***(9,25)***. We have also successfully used ^{125}I-351A to map and quantify tissue ACE ***(11–17)***, and have subsequently adapted the technique to investigate tissue ACE regulation and determination of in vivo drug occupancy ***(30–34)***. Other radiolabeled ligands, such as the substrate analogue inhibitor of renin, ^{125}I-H77, have restricted usage in only a few species and have to be used in combination with N-acetyl-pepstatin to inhibit binding to other aspartyl proteases ***(18,19)***.

Nevertheless, the use of in vitro autoradiography to investigate the tissue distribution of components of the RAS has revealed many previously unsuspected sites in which to study the actions of the effector peptides, angiotensin II, and angiotensin IV.

Acknowledgments

This work was supported by grants from the National Health and Medical Research Council of Australia (including the NHMRC Block Grant Reg Key

Number 983001), the National Heart Foundation of Australia, and the G. Harold and Leila Y. Mathers Charitable Foundation.

References

1. Mendelsohn, F. A. O., Quirion, R., Saavedra, J. M., Aguilera, G., and Catt, K. J. (1984) Autoradiographic localization of angiotensin II receptors in rat brain. *Proc. Nat. Acad. Sci. USA* **81,** 1575–1579.
2. Mendelsohn, F. A. O., Dunbar, M. S., Allen, A. M., Chou, S. T., Millan, M. A., Aguilera, G., and Catt, K. J. (1986) Angiotensin II receptors in the kidney. *Fed. Proc.* **45,** 1420–1425.
3. Mendelsohn, F. A. O., Millan, M. A., Quirion, R., Aguilera, G., Chou, S. T., and Catt, K. J. (1987) Localization of angiotensin II receptors in rat and monkey kidney by in vitro autoradiography. *Kidney Int.* **31,** s40–s44.
4. McKinley, M. J., Allen, A. M., Clevers, J., Paxinos, G., and Mendelsohn, F. A. O. (1987) Angiotensin receptor binding in human hypothalamus: autoradiographic localization. *Brain Res.* 420, 375–379.
5. McKinley, M. J., Allen A. M., Clevers J., Denton D. A., and Mendelsohn F. A. O. (1986) Autoradiographic localization of angiotensin receptors in the sheep brain. *Brain Res.* **375,** 373–376.
6. Allen, A. M., Chai, S. Y., Clevers, J., McKinley, M. J., Paxinos, G., and Mendelsohn, F. A. O. (1988) Localization and characterization of angiotensin II receptor binding and angiotensin converting enzyme in the human medulla oblongata. *J. Comp. Neurol.* **269,** 249–264.
7. Mendelsohn, F. A. O., McKinley, M. J., Allen, A. M., Clevers, J., Denton, D. A., and Tarjan, E. (1988) Localization of angiotensin II receptor binding in rabbit brain by in vitro autoradiography. *J. Comp. Neurol.* **270,** 372–384.
8. Marley, P. D., Bunn, S. J., Wan, D. C. C., Allen, A. M., and Mendelsohn, F. A. O. (1989) Localization of angiotensin II binding sites in the bovine adrenal medulla using a labeled specific antagonist. *Neuroscience* **28,** 777–787.
9. MacGregor, D. P., Murone, C., Song, K., Allen, A. M., Paxinos, G., and Mendelsohn, F. A. O. (1994) Angiotensin II receptor subtypes in the human central nervous system. *Brain Res.* **675,** 231–240.
10. Song, K., Allen, A. M., Paxinos, G., and Mendelsohn, F. A. O. (1992) Mapping of angiotensin-II receptor subtype heterogeneity in rat brain. *J. Comp. Neurol.* **316,** 467–484.
11. Mendelsohn, F. A. O., Chai, S. Y., and Dunbar, M. (1984) In vitro autoradiographic localization of angiotensin converting enzyme in rat brain using 125I-labeled MK351A. *J. Hypertens.* **2,** 41–44.
12. Chai, S. Y., Paxinos, G., and Mendelsohn, F. A. O. (1987) Angiotensin converting enzyme in rat brain visualized by in vitro autoradiography. *Neuroscience* **20,** 615–627.
13. Chai, S. Y., Christie, M. J., Beart, P. M., and Mendelsohn, F. A. O. (1987) Effects of nigral dopaminergic lesions and striatal excitotoxin lesions on brain converting enzyme. *Neurochem. Int.* **10,** 101–107.

14. Chai, S. Y., McKenzie, J. S., McKinley, M. J., and Mendelsohn, F. A. O. (1990) Angiotensin converting enzyme in human forebrain and midbrain visualized by in vitro autoradiography. *J. Comp. Neurol.* **219,** 179–194.
15. Chai, S. Y., McKinley, M. J., Paxinos, G., and Mendelsohn, F. A. O. (1991) Angiotensin converting enzyme in the monkey (macaca fascicularis) brain visualized by in vitro autoradiography. *Neuroscience* **42,** 483–495.
16. Yamada, H., Fabris, B., Allen, A. M., Jackson, B., Johnston, C. I., and Mendelsohn, F. A. O. (1991) Localization of angiotensin converting enzyme in rat heart. *Circ. Res.* **68,** 141–149.
17. Rogerson, F. M., Schlawe, I., Paxinos, G., Chai, S. Y., McKinley, M. J., and Mendelsohn, F. A. O. (1995) Localization of angiotensin converting enzyme by in vitro autoradiography in the rabbit brain. *J. Chem. Neuroanat.* **8,** 227–243.
18. Song, K., Zhuo, J., Chai, S. Y., and Mendelsohn, F. A. O. (1992) A new method to localize active renin in tissues by autoradiography: application to dog kidney. *Kidney Int.* **42,** 639–646.
19. Zhuo, J., Anderson, W. P., Song, K., and Mendelsohn, F. A. O. (1996) Autoradiographic localization of active renin in the juxtaglomerular apparatus of the dog kidney: effects of sodium intake. *Clin. Exp. Pharmacol. Physiol.* **23,** 291–298.
20. Moeller, I., Lew, R. A., Mendelsohn, F. A. O., Smith, A. I., Brennan, M. E., Tetaz, T. J., and Chai, S. Y. (1997) The globin fragment, LVV-haemorphin-7, is an endogenous ligand for the AT_4 receptor in the brain. *J. Neurochem.* **68,** 2530–2537.
21. Moeller, I., Chai, S. Y., Oldfield, B. J., McKinley, M. J., Casley, D., and Mendelsohn, F. A. O. (1995) Localization of angiotensin IV binding sites to motor and sensory neurones in the sheep spinal cord and hindbrain. *Brain Res.* **701,** 301–306.
22. Moeller, I., Paxinos, G., Mendelsohn, F. A. O., Aldred, G. P., Casley, D., and Chai, S. Y. (1996) Distribution of AT_4 receptors in the macaca fascicularis brain. *Brain Res.* **712,** 307–324.
23. Mendelsohn, F. A. O., Allen, A. M., and Figdor, R. (1986) A cortical gradient in glomerular angiotensin II receptors and their regulation during altered dietary NaCl intake. *Kidney Int.* **30,** 628.
24. Yamada, H. and Mendelsohn, F. A. O. (1989) Angiotensin II receptor binding in the rat hypothalamus and circumventricular organs during dietary sodium deprivation. *Neuroendocrinology* **50,** 469–475.
25. Allen, A. M., MacGregor, D. P., Chai, S. Y., Donnan, G. A., Kaczmarczyk, S., Richardson, et al. (1992) Angiotensin II receptor binding associated with nigrostriatal dopaminergic neurons in human basal ganglia. *Ann. Neurol.* **32,** 339–344.
26. Jenkins, T. A., Chai, S. Y., and Mendelsohn, F. A. O. (1997) Upregulation of angiotensin II AT_1 receptors in the mouse nucleus accumbens by chronic haloperidol treatment. *Brain Res.* **748,** 137–142.
27. Zhuo, J., Alcorn, D., Allen, A. M., and Mendelsohn, F. A. O. (1992) High resolution localization of angiotensin II receptors in rat renal medulla. *Kidney Int.* **42,** 1372–1380.

28. Zhuo, J. L., Alcorn, D., and Mendelsohn, F. A. O. (1993) Intrarenal Ang II modulates AT1 Ang II receptor binding to type I interstitial cells in rat renal medulla in vivo. *Hypertension* **22,** 409.
29. Zhuo, J., Alcorn, D., McClausland, J., Casley, D. J., and Mendelsohn, F. A. O. (1994) In vivo occupancy of angiotensin II subtype 1 receptors in rat renal medullary interstitial cells. *Hypertension* **23,** 838–843.
30. Sakaguchi, K., Chai, S. Y., Jackson, B., Johnston, C. I., and Mendelsohn, F. A. O. (1988) Inhibition of tissue angiotensin converting enzyme : quantitation by autoradiography. *Hypertension* **II(3),** 230–238.
31. Sakaguchi, K., Jackson, B., Chai, S. Y., Mendelsohn, F. A. O., and Johnston, C. I. (1988) Effects of perindopril on tissue angiotensin converting enzyme activity demonstrated by quantitative in vitro autoradiography. *J. Cardiovasc. Pharmacol.* **12,** 710–718.
32. Sakaguchi, K., Chai, S. Y., Jackson, B., Johnston, C. I., and Mendelsohn, F. A. O. (1988) Differential angiotensin converting enzyme inhibition in brain after oral administration of perindopril demonstrated by quantitative inn vitro autoradiography. *Neuroendocrinology* **48,** 223–228.
33. Fabris, B., Yamada, H., Cubela, R. B., Jackson, B., Mendelsohn, F. A. O., and Johnston, C. I. (1990) Characterization of cardiac angiotensin converting enzyme (ACE) and in vivo inhibition following oral quinapril to rats. *Brit. J. Pharmacol.* **100,** 651–653.
34. Zhuo, J., Froomes, P., Casley, D., Liu, J. J., Murone, C., Chai, S. Y., Buxton, B., and Mendelsohn, F. A. O. (1997) Perindopril chronically inhibits angiotensin converting enzyme in both the endothelium and adventitia of the internal mammary artery in patients with ischemic heart disease. *Circulation* **96,** 174–182.
35. Kohzuki, M., Johnston, C. I., Chai, S. Y., Jackson, B., Perich, R., Paxton, D., and Mendelsohn, F. A. O. (1991) Measurement of angiotensin converting enzyme induction and inhibition using quantitative *in vitro* autoradiography:tissue selective induction after chronic lisinopril treatment. *J. Hypertens.* **9,** 579–587.

23

Measurement of Intracellular Free Calcium Ion Concentration in Vascular Smooth Muscle Cells

Fluorescence Imaging of Cytosolic Calcium

Rhian M. Touyz and Ernesto L. Schiffrin

1. Introduction

Changes in intracellular free calcium ion concentration ($[Ca^{2+}]_i$) play a major role in vascular smooth muscle cell function ***(1,2)***. Elevation of $[Ca^{2+}]_i$ is an important regulator of multiple downstream signaling pathways and it is a major determinant of vascular smooth muscle contraction ***(1–3)***. Agonists, such as angiotensin II (Ang II), endothelin-1, and vasopressin, that mediate effects through G protein-coupled receptors, increase $[Ca^{2+}]_i$ by inducing Ca^{2+} mobilization from intracellular sarcoplasmic/endoplasmic reticular stores, and by stimulating transplasmalemmal Ca^{2+} influx ***(4–6)***. One of the earliest measurable events resulting from Ang II stimulation of vascular smooth muscle cells, is a rapid, phospholipase C (PLC)-mediated hydrolysis of phosphatidylinositol 4,5-bisphosphate, to produce two second messengers, 1,2 diacylglycerol and inositol 1,4,5-trisphosphate (IP_3) ***(7,8)***. The water-soluble messenger IP_3, binds to specific IP_3 receptors to release Ca^{2+} from nonmitochondrial intracellular stores.

The early methods used to measure $[Ca^{2+}]_i$ included microinjection of calcium-sensitive proteins such as aequorin, use of microelectrodes, and the Null Point technique ***(9,10)***. A major advance in $[Ca^{2+}]_i$ determination was made in the 1980s when fluorescent calcium indicators became available ***(11,12)***. The most widely used fluorescent Ca^{2+} indicators are derivatives of the Ca^{2+}-chelator, BAPTA, itself a double-aromatic analog of the common Ca^{2+}-chelator, ethyleneglycol *bis*(β-aminoethyl ether)-N,N,N',N'-tetraacetic acid (EGTA). The four carboxyl groups of BAPTA provide the Ca^{2+} binding site of the

From: *Methods in Molecular Medicine, vol. 51: Angiotensin Protocols*
Edited by: D. H. Wang © Humana Press Inc., Totowa, NJ

probes, and occupation of this site by Ca^{2+} alters the fluorescent properties of the indicator ***(13,14)***. The particular characteristics of the probes are determined by the fluorophores added to the basic BAPTA backbone. One of the most useful advances in this field was the development of these indicators that could be introduced to cells noninvasively. This has been facilitated by the incorporation of an acetoxymethyl ester group that allows membrane permeability and once inside the cell is cleaved by nonspecific esterases, trapping the dye in the cytoplasm ***(13,14)***. Many fluorescent indicators are available, the individual specifications of which relate to the concentration and type of ion that is to be measured, the cell type, and importantly, the instrumentation available for measurement. Currently, the most widely used Ca^{2+} indicators are indo-1 and fura-2, both of which bind Ca^{2+} in a 1:1 stoichiometry. Our indicator of choice for the measurement of $[Ca^{2+}]_i$ in cultured vascular smooth muscle cells, is the acetoxymethyl ester of fura-2 (fura-2AM).

1.1. Basic Principles

Figure 1 demonstrates the major steps involved in fluorescence imaging of intracellular free calcium. The first stages involve tissue preparation, fluorophore loading, and selection and setting up of the microscope and the second stage involves data acquisition, data storage, and calcium calibration ***(15)***. Many types of tissue preparations can be used for imaging studies such as freshly isolated cells, cultured cells, tissue segments, and intact organs. Confocal microscopy can be used with all of these tissue preparations. Conventional, wide-field fluorescence microscopy is most commonly used with cells. The majority of our investigations have been performed on cultured cells grown on round glass coverslips, and descriptions in the present chapter will be based on this type of preparation.

1.1.1. Fluorescent Calcium Dyes

A wide variety of fluorescent Ca^{2+} indicators for detecting changes in $[Ca^{2+}]_i$ over the range of <50 n*M* to >50 μ*M* is currently available. There are three major groups of Ca^{2+}-sensitive fluorophores based on the type of spectral response to Ca^{2+} binding. The first group of dyes exhibit large decreases in the wavelengths required for peak absorbance (excitation) with Ca^{2+} binding, simultaneously with a change in fluorescence quantum yield, and includes fura-2, fura-red, and quin-2. The second group of dyes exhibits a change in the quantum yield or fluorescence efficiency (change in brightness) with Ca^{2+} binding, and includes fluo-3, calcium green, rhod-2, calcium orange, and calcium crimson. The third group of dyes exhibits shifts in both the absorption and emission characteristics and includes indo-1. Each probe has a unique excitation and/or emission spectrum for a given concentration of free Ca^{2+}, and the

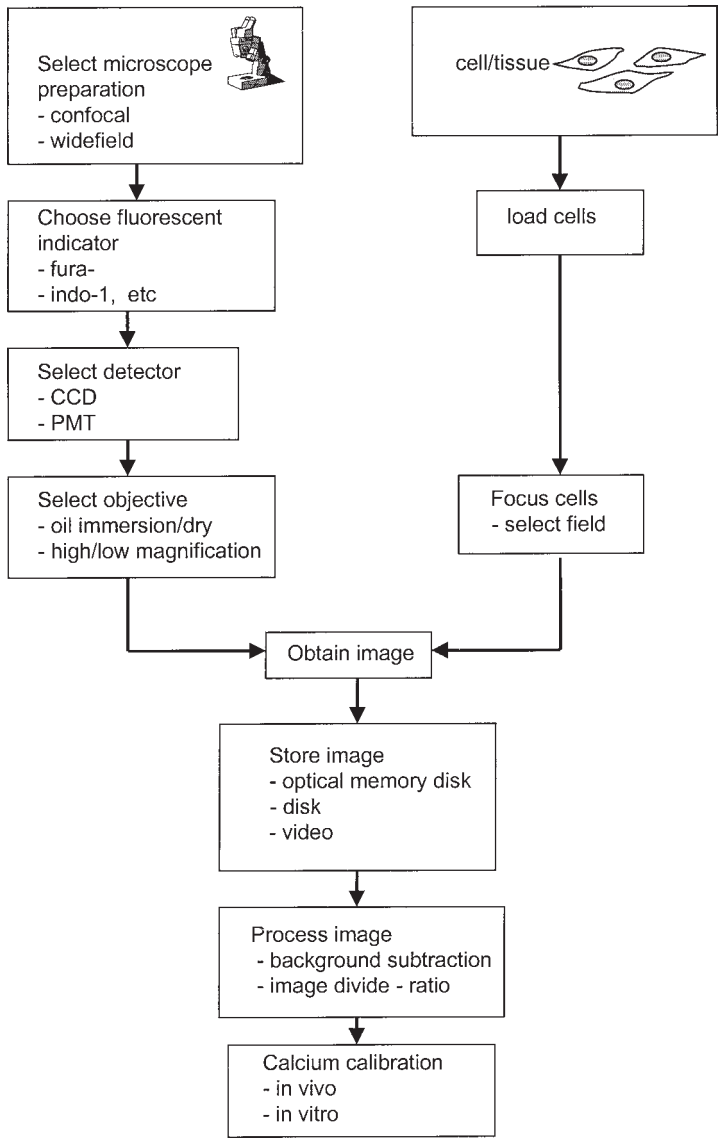

Fig. 1. Schematic diagram demonstrating the major steps in fluorescence imaging of cytosolic calcium.

presence of these spectrally distinct forms results in a distinct isosbestic point in the spectra (point where fluorescence is independent of ion concentration). These spectra can be mathematically described by the ratio of two points on any spectral curve, providing calibration curves relating $[Ca^{2+}]_i$ to the fluorescence ratio.

The fluorescent dye selected must have a dissociation constant (K_d) that must be compatible with the $[Ca^{2+}]_i$ range of interest. Indicators have a detectable response in the concentration range from approx 0.1 × K_d to 10 × K_d. Although these constants are detailed in the catalogs of the major suppliers of commercially available fluorophores, each investigator using these probes should establish the K_d with their own experimental setup and tissue preparations, as factors such as pH, temperature, ionic strength, viscosity, protein binding, and the presence of other ions may influence the K_d. Molecular Probes (Eugene, OR) quotes the K_d of the Ca^{2+}:fura-2 complex as 224 n*M*.

Fura-2 has become the dye of choice for ratio-imaging microscopy and is the indicator that we routinely use to study $[Ca^{2+}]_i$ in vascular smooth muscle cells. Fura-2 is a ratiometric Ca^{2+} indicator, that is UV-excitable. Upon binding Ca^{2+}, fura-2 exhibits an absorption shift that is observed by scanning the excitation spectrum between 300 and 400 nm, while monitoring the emission (**Fig. 2**). The unbound form of fura-2 exhibits peak fluorescence following excitation at 380 nm, with an emission wavelength of approx 510 nm. Following Ca^{2+} binding, there is a shift in the excitation spectrum to a peak of 340 nm with no apparent change in the emission spectrum ***(11–14)***. This shift is associated with significant changes in fluorescence intensity of both forms of the dye (an increase in fluorescence at 340 nm and a decrease in fluorescence at 380 nm). The fluorescence intensities at both wavelengths can be used to produce a fluorescence ratio (340/380) that is representative of $[Ca^{2+}]_i$. The dual excitation, single-emission properties of fura-2 have advantages in that measurement of $[Ca^{2+}]_i$ is independent of dye concentration, cell thickness, excitation light intensity, and camera sensitivity. Furthermore, the signal-to-noise ratio is much larger, thereby increasing the sensitivity of the indicator ***(13,14)***.

1.1.2. Cell Loading

The loading of cells with fluorescent Ca^{2+}-sensitive indicators is based on exposing the tissue to esterified derivatives of the selected fluorophore, and after a time period, removing nonsequestered dye. Many cell loading methods have been developed including acetoxymethyl (AM) ester loading, cationic liposome delivery, electroporation, hypoosmotic shock, scrape loading, microinjection, and patch clamp pipet perfusion. The most commonly used procedure for loading fluorescent ion indicators is the AM technique, which is noninvasive and technically straightforward. The carboxylate groups of indicators for Ca^{2+} and other cations and the phenolic hydroxyl groups of pH indicators are derivatives of acetoxymethyl or acetate esters, respectively, rendering the indicator permeant to membranes and insensitive to ions. This enables the modified dyes to cross the plasma membrane into the cytoplasm where nonspecific cellular esterases cleave the acetoxymethyl ester moiety

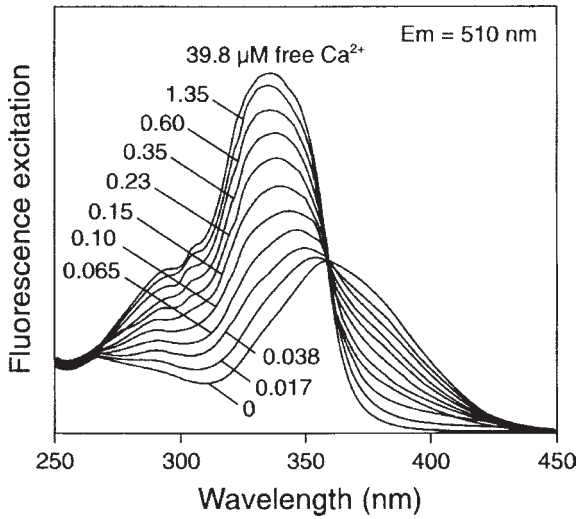

Fig. 2. Fluorescence excitation spectra of fura-2 in solutions containing zero to 39.8 μ*M* free Ca^{2+}. Reproduced with permission from Molecular Probes.

from the molecule, trapping the free acid form in the cytoplasm. Only the free-acid form and not the esterified counterparts act as calcium indicators. This principle enables significant accumulation of the dyes inside cells. The amount that accumulates depends on various factors and varies from cell type to cell type. Factors such as the concentration of esterified dye, the length of the incubation period, the level of intracellular esterases and the relative permeability of the plasma membrane to the free-acid form can influence uptake and retention of the dye. The solubility of dyes can be increased using dispersing agents such as Pluronic F-127, serum, or bovine serum albumin.

1.1.3. Measurement of Fluorescent Light

Fluorescence measurements from single cells under a microscope can be performed using an imaging device, such as silicon-intensified target and charge-coupled device cameras, or a nonimaging photometric transducer, such as a photomultiplier tube (PMT) ***(16)***. Cameras have the advantage of providing a complete image of the fluorescence within a dye-loaded cell and, therefore, the intracellular distribution of Ca^{2+}. PMTs provide a signal proportional to the amount of light falling on their light-sensitive surface and thus provide a measure of total fluorescence being emitted from the cell, rather than an image. The choice of camera or PMT depends on the requirements and specific needs of the experiment. If rapid measurements (1000–5000 data points/s) are required, a PMT is recommended, whereas if spatial

information is important, then an imaging device is needed. In our studies, we use a CCD camera that allows us to investigate the spatial distribution of Ca^{2+} within cells, as well as to examine the differential responses of a group of cells within a wider visual field.

1.1.4. Calibration

Calibration for free-ion concentrations can be performed by two methods, either imaging free-acid solutions of the probe with various known ion concentrations (in vitro method) or imaging the cells of interest loaded with the ester derivative of the probe under permeabilized conditions (in vivo method).

In vitro calibration of the probe is performed by adding small, identical aliquots of dye to Ca^{2+}-buffered solutions ***(15)***. The simplest method for initial calibration is to prepare two solutions of medium, one containing 5 m*M* $CaCl_2$, which will saturate the dye with free Ca^{2+} and result in the maximum ratio obtainable. The second medium should have the $CaCl_2$ substituted by 1–10 m*M* (EGTA), which will chelate all free Ca^{2+} to result in the minimum ratio obtainable. Both must contain the free-acid form of the indicator at a concentration of approx 75 μ*M*, which is the approximate concentration found in cells loaded with the ester derivative. Fluorescence images are collected for all solutions, including a blank (dye-free solution), at the wavelength combinations to be used in experiments. Individual images should be background subtracted (subtract the average intensity of the blank solution or subtract images on a pixel-by-pixel basis), before calculation of a ratio image (pixel-by-pixel image division). After background correction, individual values at each wavelength and ratio values are determined in high and low Ca^{2+} concentrations to obtain values that can be used in Eq. 1 ***(17)***:

$$[Ca^{2+}]_i = [(R - R_{min})/(R_{max} - R)]K_d \times \beta \quad (1)$$

This procedure provides estimates of R_{min} and R_{max}, which are used in the mathematical formula to calculate $[Ca^{2+}]_i$. R is the measured ratio of the sample, R_{min} is the ratio when there is no Ca^{2+} present, R_{max} is the ratio when the probe is saturated. The raw 380-nm value at minimum Ca^{2+} concentration (R_{min}) is divided by the raw 380-nm value at maximum concentration (R_{max}), to give the β value. K_d is the dissociation constant of the probe.

In vivo calibration is a more difficult process, but it is preferable because it reveals the intracellular relationship between the indicator and Ca^{2+} ***(18,19)***. The cells are loaded with the AM ester derivative of the dye and the cell membrane is permeabilized to ions with a specific ionophore. We use ionomycin (10 μ*M*), but other investigators have used Br-A23187, Triton-X, saponin, and digitonin. The R_{max} measurements should be made in elevated extracellular $[Ca^{2+}]$ to saturate the probe within the cell. Addition of ionomycin causes a

rapid, sustained increase in intracellular $[Ca^{2+}]_i$ that reaches maximum within 10–15 s. This event should be recorded and captured. The R_{min} value is determined on the same field of cells by washing the cells two or three times with Ca^{2+}-free buffer containing 1–10 m*M* EGTA. Transplasmalemmal transport, resulting in binding of free Ca^{2+} may take a few min. Using the obtained values for R, R_{max}, R_{min}, and β, the $[Ca^{2+}]_i$ can be calculated using **Eq. 1**. The use of the equation in calculating $[Ca^{2+}]_i$ depends on the assumptions that the intracellular dye is fully esterified, that the only source of fluorescence within the cell comes from the fura-2, and that the spectral properties of the dye are the same inside and outside the cell.

2. Materials

1. Fura-2AM (Molecular Probes): 1 m*M* stock solution in dimethyl sulfoxide (DMSO).
2. Pluronic F-127 (20% in DMSO).
3. Modified Hank's buffer (in m*M*): 137 NaCl, 4.2 $NaHCO_3$, 3 Na_2HPO_4, 5.4 KCl, 0.4 KH_2PO_4, 1.3 $CaCl_2$, 0.5 $MgCl_2$, 10 glucose, 5 HEPES, pH 7.4.
4. EGTA stock solution: 30 m*M* in modified Hank's buffer containing nominal $CaCl_2$ (0.15 m*M*).
5. Ionomycin from *Streptomyces conglobatus:* free acid (Molecular Probes) prepared as a 1 m*M* stock solution in DMSO.
6. Ca^{2+}-rich buffer: modified Hank's buffer containing 20 m*M* $CaCl_2$.
7. Round glass coverslips (25 mm diameter), washed, dried, and sterilized.
8. Glass rings, 3–4 mm diameter.
9. High vacuum silicone grease (Dow Corning Co., Midland, MI).
10. Fine forceps.
11. Coverslip holder (Attofluor cell chamber that holds 25 mm diameter round coverslips and mounts in a standard 35 mm diameter stage holder (Molecular Probes), or Leiden chamber (Medical Systems Corp., Greenville, NY).
12. Image analysis hardware and software.

2.1. Hardware Components

The equipment that we use for single-cell calcium imaging is the Attofluor Ratio Vision system (Atto Instruments Inc., Rockville, MD).

1. Light source: Excitation wavelengths of 340 and 380 nm are required for the ratiometric measurements of $[Ca^{2+}]_i$ using fura-2. The equipment utilizes a 100-W mercury lamp that emits an even spectrum of illumination over the UV range.
2. Filters: The filter chamber houses a filter changer insert plate that has four moving arms to which the excitation filters are attached. There are two arms on each side of the plate. The standard filters are 10 nm bandpass 334 nm, 460 nm, 380 nm, and 488 nm. The 334 nm and 380 nm filters are used for fura-2 (*see* **Note 1**).
3. Microscope: Inverted microscope equipped for epifluorescence with a ×40 oil immersion objective (Zeiss, Oberkochen, Germany) is used for the visualization

of fura-2-loaded cells. The longer wavelength of emitted fluorescence is separated from the excitation wavelengths by passing through a dichroic mirror and then a 510-nm barrier filter. Emitted light then passes into the eyepiece or the CCD camera.

4. Camera: We use a CCD image-intensifying camera. Light emitted from the specimen through the microscope is focused on a high-gain hybrid image intensifier. The output from this is then passed via a fiber-optic taper to a CCD image sensor and then into the video unit box. The camera control unit houses the camera power supply and intensifier, and gain controls.
5. Control processor: The control processor is the controlling computer within the Attofluor RatioVision system. The processor communicates with the filter changer plate, video unit, printers, monitors, keyboards, and image-processing units.
6. Monitors: We use two-color monitors in our image analysis system, one for text where commands are given and one for displaying the images obtained directly from the image-intensifying camera.

3. Methods—Measurement of $[Ca^{2+}]_i$ Using Cell Monolayers

3.1. Preparation of Fura-2AM

1. Prepare a 1 m*M* stock solution of fura-2AM in anhydrous DMSO. Divide into aliquots (30–50 μL) and store dessicated at –20°C. This procedure prevents the spontaneous ester hydrolysis that may occur in moist environments.
2. Before loading, the DMSO stock solution should be diluted at least 1:200 in serum-free culture medium or modified Hank's buffer to a final concentration of 1–10 μ*M*.
3. The nonionic and nondenaturing detergent Pluronic F-127 may be added to help disperse the fluorescent probe in the loading medium. Final concentration should be 0.02%.

3.2. Loading Cells with Fura-2AM

1. Fura-2AM is light-sensitive and all preparations should be performed in a dark room.
2. Vascular smooth muscle cells grown on round glass coverslips in six-well multiwell plates (approx 90% confluency) are washed with DMEM and incubated for 24–30 h in serum-free DMEM.
3. The quiescent cells are washed with prewarmed modified Hanks buffer two to three times.
4. Add 2 mL warmed modified Hank's buffer containing 4 μ*M* fura-2AM, prepared as aforementioned, to the well (*see* **Note 2**).
5. Cover the plate with aluminium foil and incubate at room temperature for 30 min (*see* **Note 3**).
6. Remove the loading buffer and wash the loaded cells three times with fresh warmed modified Hank's buffer (2 mL/wash) to remove excess dye.
7. Allow cells to stand at room temperature for 15 min to ensure complete deesterification of the fura-2AM molecule.

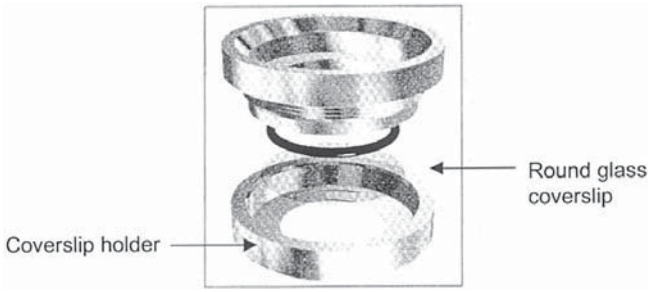

Fig. 3. Attofluor cell chamber. This is a durable and practical coverslip holder designed for viewing live cell specimens on upright or inverted microscopes. It accepts 25-mm-diameter round coverslips and mounts in a standard 35-mm-diameter stage holder. Reproduced with permission from Atto Instruments.

3.3. $[Ca^{2+}]_i$ Measurements

1. All measurements should be performed in a dark room. We carry out experiments at room temperature to minimize subcellular compartmentalization of the intracellular dye (*see* **Note 3**).
2. Using fine forceps, carefully remove the glass coverslip containing cells from the well and place into a coverslip holder (**Fig. 3**).
3. Evenly apply vacuum grease to the lower surface of four small glass rings.
4. Carefully place the small glass rings onto the glass coverslip, making sure that a tight seal forms between the glass ring and the coverslip (**Fig. 4**) (*see* **Note 4**). This procedure enables four separate experiments to be performed on one coverslip. If glass rings are not available, the coverslip can be used for a single experiment.
5. Add 50 μL of warmed (37°C) modified Hanks buffer to each ring. If rings are not used, add 900 μL buffer to the coverslip chamber.
6. The coverslip holder is placed on the stage of an inverted microscope and a field of cells focused using light microscopy.
7. By running through the software program, and using fluorescence microscopy, cells are then illuminated in order to visualize and select an appropriate field of cells and specific regions of interest.
8. The intensifier gain of the CCD camera is then set to a level, such that the image in view displays the widest possible range of the 255 gray levels available. In practice, the pixels representing the highest light intensity at 380 nm should be set at a gray level of 255.
9. The field of view is then moved to an area that is devoid of any cells for the purpose of measuring background fluorescence.
10. An averaged image of each of the 343- and 380-nm images is captured and stored (*see* **Note 5**).
11. The image sequence is subjected to background subtraction, which is performed by the image analysis software on command. The 343-nm background is sub-

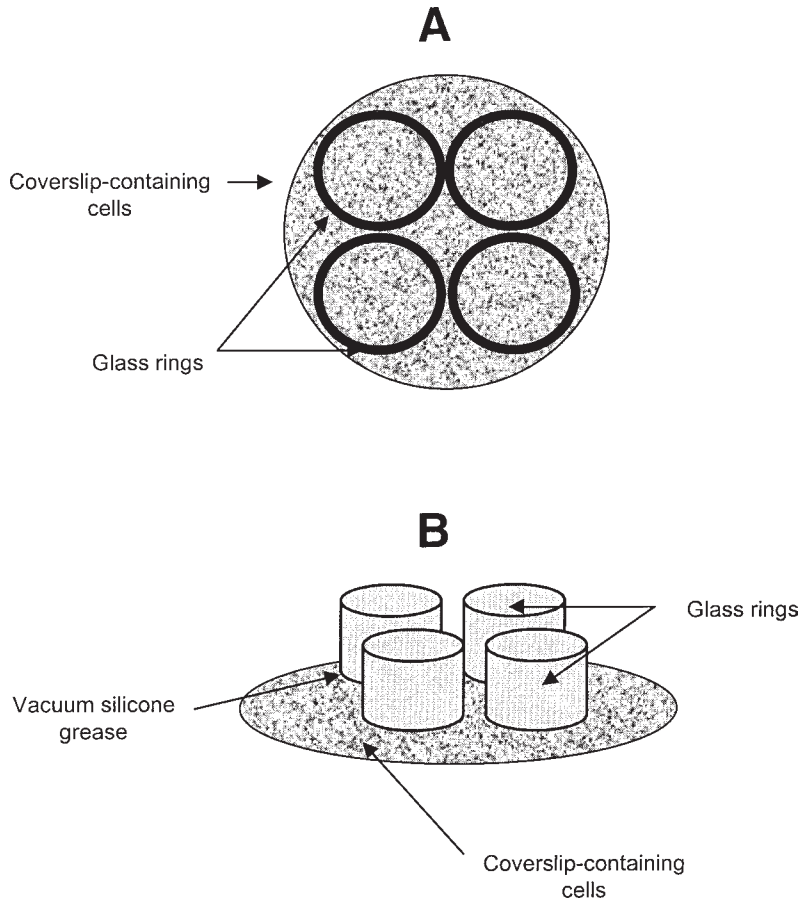

Fig. 4. A coverslip chamber containing a glass coverslip with four glass rings mounted and sealed on top of the coverslip. The glass rings physically isolate four separate regions on the coverslip-containing cells, enabling four separate experiments per coverslip. **(A)** is a top view of the preparation and **(B)** is a side view.

tracted from each of the 343-nm images on a pixel-by-pixel basis, and similar processing is performed with the 380-nm background and images.

12. The methods described for image processing here are for experiments performed using the Attofluor RatioVision system. The procedure for image capture, data acquisition, calibration, and data analysis may have to be adapted for individual use, depending on the system used and the software available (*see* **Note 6**).
13. Agonists, such as Ang II, are added directly onto the cells. In preparations in which glass rings have been used, a volume of 50 μL should be added. In prepa-

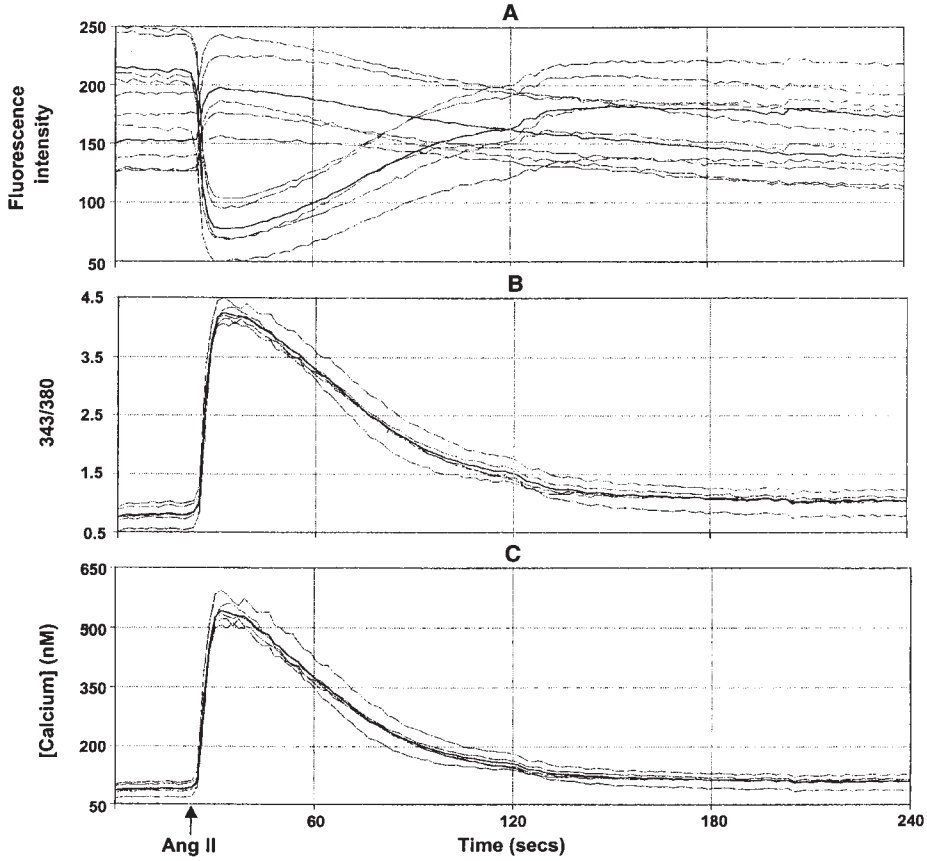

Fig. 5. Vascular smooth muscle cells loaded with fura-2 and stimulated with angiotensin II (Ang II) (10^{-7} *M*). **(A)** is the individual 343- and 380-nm fluorescence values, **(B)** is the 343/380 ratio, and **(C)** is the final $[Ca^{2+}]_i$ calibrated trace. Tracings represent responses in five cells. The bold tracing is the mean of the five cells. The arrow indicates time of Ang II addition.

rations without glass rings, a volume of 100 µL should be added (*see* **Note 7**). The increase in fluorescence ratio varies between cell types. For example, in astrocytes, Ang II doubles the 343/380 ratio, whereas in vascular smooth-muscle cells, the ratio increases three- to fourfold (**Fig. 5**).

14. Graphical analysis of $[Ca^{2+}]_i$ in single cells in cell populations can be obtained following delineation of the cells of interest using the "region of interest" command. A graphical representation of the changes in $[Ca^{2+}]_i$ is constructed using the RatioVision software (*see* **Note 8**).

3.4. Calibration

1. $[Ca^{2+}]_i$ can be calculated from the ratio of the 343/380 nm fluorescent values using the equation of Grynkiewicz et al. ***(17)*** as in **Subheading 1.1.4.**).
2. To determine R_{max} (this can be done at the end of an experimental run or on a separate coverslip), increase extracellular $[Ca^{2+}]$ to 10 n*M* by adding the Ca^{2+}-rich buffer and then add the Ca^{2+} ionophore, ionomycin (10 μ*M*). Following the addition of ionomycin, there is a large increase in the 343/380 ratio.
3. R_{min} is determined by adding EGTA (3 m*M*). Following the addition of EGTA, there is a decrease in the 343/380 ratio.
4. Before applying the R, R_{min}, and R_{max} values to the equation, they need to be corrected for autofluorescence. Autofluorescence is determined by measuring the fluorescence produced by coverslips that have not been loaded with fura-2, Values for R, R_{max}, and R_{min} are subsequently corrected by subtracting the 343- and 380-nm autofluorescence values.
5. In our preparations, corrected values for R_{max} and R_{min} in vascular smooth muscle cells are 6–10 and 0.2–0.6, respectively (*see* **Note 9**).
6. $[Ca^{2+}]_i$ can now be automatically calculated using the computer software.

4. Notes

1. The system that we use to measure fura-2 fluorescence has a filter combination of 343 and 380 nm. Other systems use different filter combinations such as 340/380 and 345/385.
2. We use fura-2 at a concentration of 4 μ*M*. This concentration may be too low or too high in some cell types. Too much dye can be toxic to the cells and too little dye can result in a weak signal-to-noise ratio. Load wells one at a time. If multiple wells are loaded with fura-2 simultaneously, the prolonged time period of cell loading in the second and subsequent wells will result in subcellular compartmentalization of fura-2.
3. Some investigators load cells at 37°C for longer time periods. We have found that vascular smooth muscle cell loading for 30 min at room temperature results in homogeneous and stable dye distribution. Although the principles governing the distribution of dye within cells have not yet been fully defined it has been demonstrated that longer loading times enhance the appearance of dye within subcellular organelles and that a lower loading temperature favors a uniform cytoplasmic distribution, as well as a lower rate of extrusion of dye from cells ***(20)***. Organic anion transport inhibitors, such as probenecid, can prevent the accumulation of fluorescent dyes by organelles ***(20)***.
4. Do not use too much grease as this will reduce the area of the coverslip available for viewing and may result in blurring of the fluorescent image.
5. The signal that emerges from the image-intensifying CCD camera is an analog signal that is a voltage varying continuously with time. Therefore, the signal must undergo an analog-to-digital conversion. This is achieved by sampling the analog voltage at regular time periods along each scan line, which divides each line

into small picture elements (pixels). The voltage at each pixel is then read as an 8-bit number that is assigned a gray level, corresponding to the light intensity of that particular pixel, in the range of 0–255. The final image is then subject to a pseudocoloring of each pixel, where each gray level is assigned a different color.

6. The number of images that can be captured in one sequence depends on the size of the image being captured and on the size of the image memory available.
7. Addition of agonists should be applied very carefully to the cell chamber, as too much pressure and force can result in detachment of the cells under investigation.
8. Several other methods of data presentation and analysis of results are available depending on the system used and the software available. These include 3-D histogram analysis, sequential images, and video display of real-time images.
9. Calibration of the signals can be difficult and should be performed carefully. If data are expressed as the absolute $[Ca^{2+}]_i$, rather than the change in fluorescence, R_{max}, R_{min}, and autofluorescence must be measured every day. When comparing responses between preparations, calibration factors (R_{max}, R_{min}, and β) should be consistent between preparations.

Acknowledgments

This work was supported by grants from the Medical Research Council of Canada, the Heart and Stroke Foundation of Canada, and the Fonds de la recherche en sante du Québec.

References

1. Claphan, D. E. (1995) Calcium signaling. *Cell* **80,** 259–268.
2. Berridge, M. J. and Dupont, G. (1994) Spatial and temporal signaling by calcium. *Curr. Opin. Cell Biol.* **6,** 267–274.
3. Karaki, H., Ozaki, H., Hori, M., Mitsui-Saito, M., Amano, K., Harada, K., et al. (1997) Calcium movements, distribution and functions in smooth muscle. *Pharmacol. Rev.* **49,** 157–230.
4. Touyz, R. M. and Schiffrin, E. L. (1997) Role of calcium influx and intracellular calcium stores in angiotensin II-mediated calcium hyperresponsiveness in smooth muscle from spontaneously hypertensive rats. *J. Hypertens.* **15,** 1431–1439.
5. Touyz, R. M., Deng, L-Y., Li, J-S., and Schiffrin, E. L. (1996) Differential effects of vasopressin and endothelin-1 on vascular contractile and calcium responses in pressurized small arteries from spontaneously hypertensive rats. *J. Hypertens.* **14,** 983–991.
6. Douglas, S. A. and Ohlstein, E. H. (1997) Signal transduction mechanisms mediating the vascular actions of endothelin. *J. Vasc. Res.* **34,** 152–164
7. Berridge, M. J. (1993) Inositol trisphosphate and calcium signaling. *Nature* **361,** 315–325.
8. Griendling, K. K., Ushio-Fukai, M., Lassègue, B., and Alexander, R. W. (1997) Angiotensin II signaling in vascular smooth muscle. New concepts. *Hypertension* **29,** 366–373.
9. Ridgway, E. B. and Ashley, C. C. (1967) Calcium transients in single muscle fibres. *Biochem. Biophys. Res. Commun.* **29,** 229–234.

10. Murphey, E., Coll, K., Rich, T. L., and Williamson, J. R. (1980) Hormonal effects on calcium homeostasis in isolated hepatocytes. *J. Biol. Chem.* **255,** 6600–6608.
11. Tsien, R. W. (1981) A non-disruptive technique for loading buffers and indicators into cells. *Nature* **290,** 527–528.
12. Tsien, R. Y., Pozzan, T., and Rink, T. J.(1982) Calcium homeostasis in intact lymphocytes: cytoplasmic free calcium monitored with a new, intracellularly trapped fluorescent indicator. *J. Cell Biol.* **94,** 325–334.
13. Roe, M. W., Lemasters, J. J., and Herman, B. (1990) Assessment of fura-2 for measurements of cytosolic free calcium. *Cell Calcium* **11,** 63–73.
14. Tsien, R. Y., Rink, T. J., and Poenie, M. (1985) Measurement of cytosolic free Ca^{2+} in individual cells using fluorescence microscopy with dual excitation wavelengths. *Cell Calcium* **6,** 145–157.
15. Williams, D. A. (1995) Fluorescence imaging of cytosolic calcium, in *Measurement and Manipulation of Intracellular Ions*, vol. 27 (Kraicer, J. and Dixon, S. J., eds.), Academic, New York, pp. 69–81.
16. Goldman, W. F., Bova, S., and Blaustein, M. P. (1990) Measurement of intracellular Ca^{2+} in cultured arterial smooth muscle cells using fura-2 and digital imaging microscopy. *Cell Calcium* **11,** 221–231.
17. Grynkiewicz, G., Poenie, M., and Tsien, R. Y. (1985) A new generation of Ca^{2+} indicators with greatly improved fluorescence properties. *J. Biochem. Sci.* **260,** 3440–3450.
18. Williams, D. A. and Fay, F. S. (1990) Intracellular calibration of the fluorescent calcium indicator fura-2. *Cell Calcium* **11,** 75–63.
19. Iredale, P. A. and Dickenson, J. M. (1995) Measurement of intracellular free calcium ion concentration in cell populations using fura-2, in *Signal Transduction Protocols,* vol. 41 (Kendall, D. A. and Hill, S. J., eds.), Humana, Totowa, NJ, pp. 203–213.
20. Moore, E. D. W., Becker, P. L., Fogarty, K. E., Williams, D. A., and Fay, F. S. (1990) Ca^{2+} imaging in single living cells: theoretical and practical issues. *Cell Calcium* **11,** 157–179.

24

Measurement of Phospholipase D Activation in Vascular Smooth Muscle Cells

Rhian M. Touyz and Ernesto L. Schiffrin

1. Introduction

Phospholipase D (PLD), which hydrolyzes phospholipids (primarily phosphatidylcholine) to generate phosphatidic acid, is an essential component in cellular signal transduction ***(1,2)***. Phosphatidic acid and its dephosphorylated product 1,2 diacylglycerol, are important intracellular second messengers that play critical roles in various cell types including vascular smooth muscle cells ***(3,4)***. The human PLD gene 1 has been cloned and expressed. The expressed mammalian PLD has a molecular weight of approx 120 and has both catalytic and transphosphatidylation activities with phosphatidyl choline as substrate ***(5)***. PLD activation can be initiated by various agonists that fall into two main categories: (1) agents that signal through tyrosine kinase-dependent pathways, e.g., growth factors, and (2) agents that signal through seven transmembrane receptors, acting through trimeric membrane G proteins, e.g., angiotensin II and endothelin-1 ***(6–9)***. The molecular mechanisms by which Ang II receptors couple to PLD have recently been identified. The $G\beta\gamma$ subunits as well as their associated $G\alpha_{12}$ subunits, mediate Ang II-induced PLD activation via Src-dependent mechanisms in vascular smooth muscle cells. Small molecular-weight G protein RhoA is also involved in these signaling cascades ***(10)***.

Two main methods are used to determine PLD activity: (1) measurement of the generation of the intracellular products (choline and phosphatidic acid), and (2) the transphosphatidylation method, which is based on the ability of PLD to stimulate a transphosphatidylation reaction in the presence of a primary alcohol ***(11,12)***. Normally, PLD-induced formation of a phosphatidyl

From: *Methods in Molecular Medicine, vol. 51: Angiotensin Protocols*
Edited by: D. H. Wang © Humana Press Inc., Totowa, NJ

intermediate utilizes water as a nucleophilic acceptor to generate phosphatidic acid. In the presence of a short-chain primary aliphatic alcohol such as methanol, ethanol, propanol, or butanol, phosphatidic acid generated by PLD is transferred to the primary alcohol forming the corresponding phosphatidylethanol without any other metabolite ***(12,13)***. Because phosphatidylalcohol is a poor substrate for phosphatidate phosphohydrolase, it accumulates within the cells. This property is used as an "index" or marker for measuring activation of PLD in response to external stimuli in intact cells and cell-free preparations. This chapter focuses on the method for determining PLD activity in cultured vascular smooth-muscle cells, using the transphosphatidylation assay ***(12–14)***. The method for measuring choline and choline phosphate generation will also be briefly described.

2. Materials

1. [^{3}H] myristate.
2. Buffer A: 137 m*M* sodium chloride, 4.2 m*M* sodium hydrogen carbonate, 0.35 m*M* sodium dihydrogen phosphate, 0.5 m*M* magnesium chloride, 0.4 m*M* magnesium sulphate, 1.26 m*M* calcium chloride, 5.37 m*M* potassium chloride, 10 m*M* HEPES, pH 7.4, 1% (w/v) bovine serum albumin (BSA), 10 m*M* glucose.
3. Ethanol.
4. Angiotensin II (Ang II), or other specific agonists.
5. Methanol.
6. Chloroform.
7. Thin-layer chromatography (TLC) plates (silica gel 60A LK6D sheets: Whatman Inc.).
8. 2,2,4 Trimethylpentane (isooctane).
9. Ethylacetate.
10. Acetic acid.
11. Iodine.
12. Scintillation fluid.
13. [^{3}H]choline chloride.
14. Buffer B: Dulbecco's modified Eagle's medium (DMEM) containing 10 m*M* glucose, 20 m*M* HEPES, pH 7.4, and 1% BSA (w/v), (prepared in buffer A).
15. Dowex-50-H$^+$.

3. Methods

3.1. Measurement of PLD by the Transphosphatidylation Assay

The transphosphatidylation method has been used on a variety of cell types, both in cell suspensions and in monolayers. The methodology described here has been developed for vascular smooth muscle cells grown in monolayer culture. It may be necessary to adapt this protocol for other cell types.

3.1.1. Labeling of Phospholipids

1. Vascular smooth muscle cells are grown in six-well multiwell plates until 70–80% confluent. The culture medium is then changed to quiescent medium containing 2 μCi/mL [^{3}H] myristate (*see* **Notes 1** and **2**). The cells are cultured for another 24–30 h in a humidified incubator (95% air; 5% CO_2).
2. The medium is removed and the cells are washed three times, 10 min per wash, in prewarmed buffer A (0.5 mL) to remove excess label. Appropriate care should be taken when discarding radiolabeled material.
3. The washed cells are then incubated in buffer A containing 1% ethanol (1.5 mL/well) at 37°C. Allow cells to equilibrate for approx 10 min (*see* **Note 3**).
4. The stimulation is initiated by adding Ang II (or other agonists) at required concentrations. Ensure that a control sample containing only ethanol and no agonist is also prepared. After the required time, the incubation is terminated by placing the multiwell dishes on ice, aspirating the buffer, and adding 0.5 mL ice-cold methanol (CH_3OH).
5. The multiwell dishes are kept on ice until the cells are scraped.
6. The cells in the CH_3OH are then scraped with a cell scraper into a glass vial (screw top with good seal). Each well is carefully washed with an additional 0.5 mL CH_3OH, which is then added to the appropriate glass vial (total volume, 1 mL).
7. Add 1 mL chloroform ($CHCL_3$) to each vial. Cap vials and vortex for 1 min.
8. The vials are left to stand at room temperature for 1 h or at 4°C overnight.
9. Add 800 mL distilled water to give a final $CHCL_3$:CH_3OH:H_2O ratio of 1:1:0.8. Vortex again for 1 min.
10. The samples are then centrifuged to separate the phases (1200g for 5 min at 4°C).
11. Three phases should be present: the top aqueous phase, a middle (insoluble material) phase, and a lower chloroform (organic) phase. Using a glass Pasteur pipet, the upper and middle phases are carefully removed, leaving the lower organic phase, which contains the labeled phospholipids, including [^{3}H] phosphatidylethanol (PEt) (*see* **Note 4**).
12. Transfer 800 μL of the organic phase to a clean glass tube.
13. The organic phase is evaporated under nitrogen, and stored at –80°C for use at a later stage, or redissolved in 20 μL of $CHCL_3$ for immediate assay.

3.1.2. Thin Layer Chromatography

1. The thin-layer chromatography (TLC) plates (silica gel 60A LK6D sheets: Whatman Inc.) are heat-activated for 30 min at 100°C. Allow plates to cool at room temperature and then mark the cooled plates with a horizontal line approx 2 cm from the bottom.
2. Resuspend the frozen sample in 25 μL $CHCL_3$: CH_3OH (19:1 [v/v]) together with 5 μL unlabeled PEt. Add another 25 μL $CHCL_3$: CH_3OH (19:1 [v/v]) to each sample.
3. The sample is carefully applied at the center of each lane below the 2-cm pencil mark (**Fig. 1**). A stream of hot air (a hair dryer can be used) is applied to evaporate the $CHCL_3$.

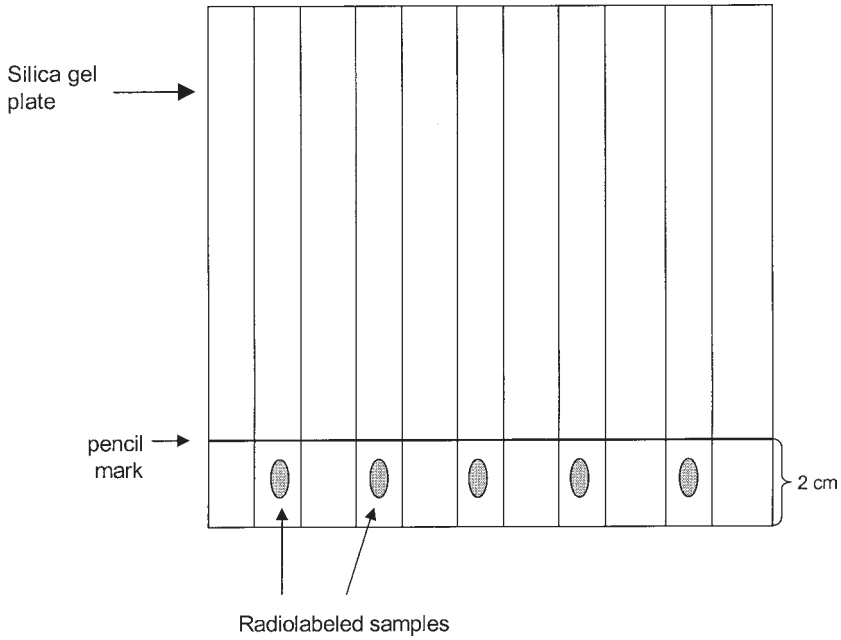

Fig. 1. Silica gel plate with multiple lanes for individual samples. The plate is marked approx 2 cm from the bottom with a pencil. The samples are spotted in the center of each lane below the pencil mark.

4. Once prepared, the TLC plates can be run (two at a time) in appropriate TLC gel tanks using a solvent phase of 2,2,4-trimethylpentane(isooctane):ethylacetate:-acetic acid:water (50:110:20:100). The solvent is prepared in a separating funnel ensuring good mixing: the aqueous phase should be completely removed. The solvent should be made and used on the day of the experiment. The plate is developed under nonequilibrium conditions as the TLC tank is used unlined. This allows for the PEt to run farther up the plate giving better resolution.
5. Normal solvent migration takes approx 90 min to reach 1 cm from the top of the plate. Once resolved, the plates are air-dried (in a chemical hood) and then placed in a TLC tank containing a beaker of iodine. The iodine vapor binds the unlabeled tracer (placed in a control/sample-free lane) to indicate the position of the [^{3}H]PEt, and this region is outlined with a pencil. The region containing the metabolite of interest is then scraped from the plate into scintillation vials, containing 10 mL scintillation fluid. The radioactivity is determined by scintillation counting 12 h later. This allows for the samples to completely leach from the silica gel into the scintillant. Results can be expressed as the percentage increase in PEt compared to control conditions (**Fig. 2**), or as cpm/well.

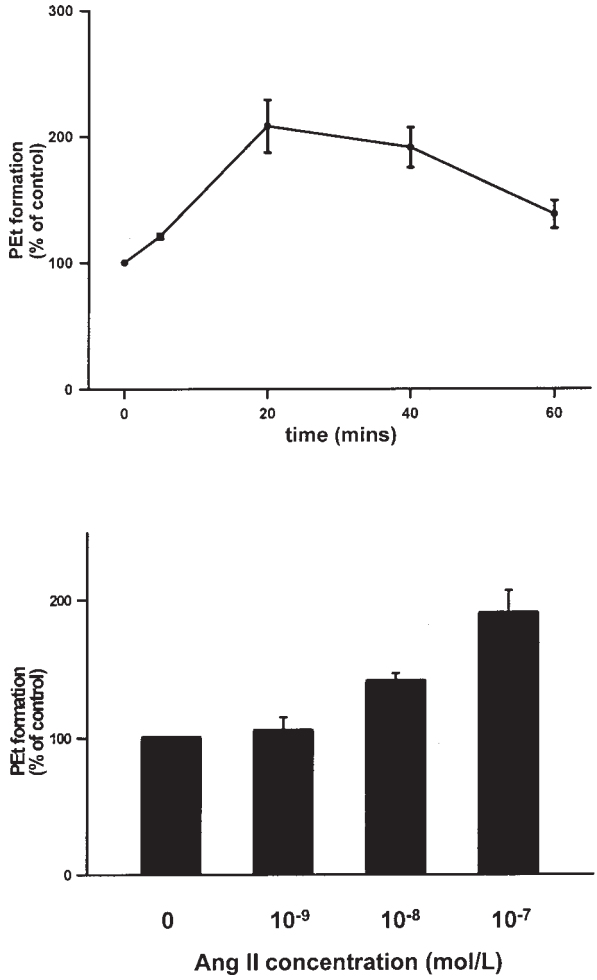

Fig. 2. *Upper panel:* Line graph demonstrates the time course of angiotensin II (Ang II) (10^{-7} mol/L) effects on PEt formation in cultured vascular smooth muscle cells derived from small arteries from gluteal biopsies of human subjects. *Lower panel:* Bar graphs demonstrate effects of increasing concentrations of Ang II on PEt formation in cultured vascular smooth-muscle cells from human small arteries. Cells were stimulated with Ang II for 20 min.

3.2. Determination of Choline and Choline Phosphate Generation by Ion Exchange Separation

Choline metabolites can be separated by various methods including TLC and ion-exchange separation ***(9,15)***. Ion-exchange separation is simple and rapid ***(15,16)***.

1. Vascular smooth muscle cells (80–90% confluency), cultured in 24-well multiwell plates, are labeled for approx 24–36 h with [^{3}H] choline chloride (1–2 μCi/mL) in DMEM containing 2% fetal calf serum. The radiolabel concentration and length of labeling may vary depending on different cell types.
2. The radiolabeled medium is replaced with 0.5 mL serum-free DMEM and cells incubated for 2 h at 37°C prior to commencement of the experiment.
3. The cells are then washed in buffer B containing DMEM, 10 m*M* glucose, 20 m*M* HEPES, pH 7.4, and 1% (w/v) BSA (prepared in buffer A) for 5, 10, and 30 min.
4. The wash buffer is aspirated and the cells stimulated with 150 μL agonists, diluted in buffer B, for the required time periods.
5. The incubations are terminated by placing the plates on ice and adding 0.5 mL ice-cold methanol to each well. This allows for the determination of choline metabolites associated with the cell and those released into the medium. To determine only cell-associated metabolites, the medium is aspirated prior to methanol addition and fresh buffer added to maintain the methanol:water ratio (1:2).
6. The cells are scraped into glass vials and the well washed with an additional 0.2 mL of methanol.
7. Add 310 μL $CHCL_3$ to each tube. The tubes are then vortexed for 1 min and allowed to stand at room temperature for 20 min (or overnight at 4°C).
8. An additional 390 μL $CHCL_3$ and 480 μL H_2O are added to the tubes. The tubes are mixed and then centrifuged at 1200*g* for 5 min to separate the phases.
9. The upper aqueous phase is aspirated (800 μL) and made up to 5 mL with H_2O. This is loaded onto a 1-mL Dowex-50 H^+ column. The runthrough is collected with a water wash of approx 6 mL as the glycerophosphocholine fraction. An aliquot (2 mL) of this fraction is transferred to a scintillation vial. Scintillant is added and the radioactivity determined.
10. Add another volume of water to the column (approx 15 mL for a 1-mL column). The runthrough is collected as the choline phosphate fraction. An aliquot (2 mL) of this fraction is transferred to a scintillation vial. Scintillant is added and the radioactivity determined.
11. The choline fraction is then eluted with approx 6 mL of 1 *M* KCl. Scintillation fluid is added to the whole sample and the radioactivity determined.

4. Notes

1. Cells do not necessarily have to be maintained in quiescent medium unless one is examining phosphorylation interactions with PLD.
2. [^{3}H]olate, [^{3}H]palmitate, or [^{3}H]myristate can be used to radiolabel the phospholipids. The concentrations may have to be adjusted for different cell types, but generally concentrations of 2–5 μCi/mL are used.
3. Various short-chain aliphatic alcohols can be utilized in the transphosphatidylation assay, for example: methanol, propanol, ethanol, and butanol. Ethanol and butanol are commonly used because they are effective at low concentrations and have minimal toxic effects.

4. Glass Pasteur pipets should be used to remove the organic phase. Two methods can be applied. First, one can remove the upper phase, then rotate the tube to partition the insoluble "disk" onto the side of the tube before aspirating the chloroform phase. Second, one can place the Pasteur pipet directly through the two upper phases and into the chloroform phase. Both methods are difficult and extreme care should be taken to avoid aspiration of the insoluble or aqueous phases along with the chloroform.
5. Using the basic transphosphatidylation assay and selective pharmacological inhibitors, one can investigate the roll of various intracellular factors that may play a role in PLD activation. Inhibition of Rho proteins can be affected using C3 exoenzyme of *Clostridium botulinum*, protein kinase C (PKC) inhibitors, and tyrosine kinase inhibitors can be used to determine the role of PKC and tyrosine kinases, respectively, in PLD activation and dihydro-D-erythro-sphingosine (sphinganine) can be used to inhibit PLD activity. Cell-permeant maniupulators should be added to cells at least 20 min prior to the agonist stimulation. The cell-impermeant agents must be introduced either by electroporation or cell permeabilization.

Acknowledgments

This work was supported by grants from the Medical Research Council of Canada.

References

1. Gomez-Cambronero, J. and Keire, P. (1998) Phospholipase D: a novel major player in signal transduction. *Cell. Signal.* **1096,** 387–397.
2. Billah, M. M. (1993) Phospholipase D and cell signaling. *Curr. Opin. Immunol.* 114–123.
3. Dhalla, N. S., Xu, Y-J., Sheu, S-S., Tappia, P. S., and Panagia, V. (1997) Phosphatidic acid: a potential signal transducer fro cardiac hypertrophy. *J. Mol. Cell Cardiol.* **29,** 2865–2871.
4. Moolenaar, W. H. (1995) Lysophosphatidic acid, a multifunctional phospholipid messenger. *J. Biol. Chem.* **270,** 12,949–12,952.
5. Hammond, S. M., Altshuller, Y. M., Sung Tsung-C., Rudge, S. A., Rose, K., Engelbrecht, JoA., et al. (1995) Human ADP-ribosylation factor-activated phosphatidylcholine-specific phospholipase D defines a new and highly conserved gene family. *J. Biol. Chem.* **270,** 29,640–29,648.
6. Natarajan, V., Scribner, W. M., and Vepa, S. (1996) Regulation of phospholipase D by tyrosine kinases. *Chem. Phys. Lipids* **80,** 103–116.
7. Wright, H. M. and Malik, K. U. (1996) Prostacyclin formation elicited by endothelin-1 in rat aorta is mediated via phospholipase D activation and not phospholipase C or A2. *Circ Res.* **79,** 271–276.
8. Touyz, R. M. and Schiffrin, E. L. (1999) Ang II-stimulated generation of reactive oxygen species in human vascular smooth muscle cells is mediated via PLD-dependent pathways. *Hypertension* **34,** 976–982.

9. Lassègue, B., Alexander, R. W., Clark, M., Akers, M., and Griendling, K. (1993) Phosphatidylcholine is a major source of phosphatidic acid and diacylglycerol in angiotensin II-stimulated vascular smooth muscle cells. *Biochem. J.* **292,** 509–517.
10. Ushio-Fukai, M., Alexander, R. W., Akers, M., Lyons, P. R., Lassègue, B., and Griendling, K. K. (1999) Angiotensin II receptor coupling to phospholipase D is mediated by the βγ subunits of heterotrimeric G proteins in vascular smooth muscle cells. *Mol. Pharmacol.* **55,** 142–149.
11. Yang, S. F., Freer, S., and Benson, A. A. (1967) Transphosphatidylation of phospholipase D. *J. Biol. Chem.* **242,** 477.
12. Kobayashi, M. and Kanfer, J. N. (1987) Phosphatidylethanol formation via transphosphatidylation by rat brain synaptosomal phospholipase D. *J. Neurochem.* **48,** 1597–1603.
13. Gustavsson, L. and Alling, C. (1987) Formation of phosphatidylethanol in rat brain by phospholipase D. *Biochem. Biophys. Res. Commun.* **142,** 958–963.
14. Bacon, K. B. (1997) Analysis of signal transduction following lymphocyte activation by chemokines, in *Methods in Enzymology* (Horuk, R., ed.), Academic, New York, pp. 340–362.
15. Cook, S. J. and Wakelam, M. J. O. (1989) Analysis of the water soluble products of phosphatidylcholine breakdown by ion exchange chromatography: bombesin and c-kinase stimulated choline generation in Swiss 3T3 cells. *Biochem. J.* **263,** 581–587.
16. Wakelam, M. J. O., Hodgkin, M., and Martin, A. (1995) The measurement of phospholipase D-linked signaling in cells, in *Methods in Molecular Biology: Signal Transduction Protocols*, vol. 41 (Kendall, D. A. and Hill, S. J., eds.), Humana Press, Totowa, NJ, pp. 271–279.

25

Measurement of Cyclic AMP and Cyclic GMP in *Xenopus* Oocytes Stimulated with Angiotensin II and Atrial Natriuretic Factor

Hong Ji

1. Introduction

Angiotensin type-1 receptors (AT_1 receptors) mediate various physiological actions of angiotensin (Ang II) via multiple-signal transduction pathways ***(1)***. In addition to the phospholipase C pathway and dihydropyridine-sensitive voltage-dependent calcium channels, AT_1 receptors can couple to inhibition of adenylate cyclase via the guanine nucleotide binding protein G_i. Beside acting directly through G_i, AT_1 receptors can modulate levels of cyclic AMP (cAMP) indirectly through receptor crosstalk. cAMP is a major second messenger of many G protein coupled receptors. One group of receptors (e.g., β-adrenoreceptors, A_2 adenosine, D_1 dopamine, H_2 histamine, and some prostanoid receptors) elevate cAMP by activating adenylate cyclase through G_s, whereas a second group (α_2 adrenoreceptors, A_1 adenosine, D_2 dopamine, $5HT_1$, metabotropic glutamate, and μ opioid receptors) reduce cAMP levels by inhibiting adenylate cyclase via G_i. Accumulating evidence indicates that signaling crosstalk can occur between AT receptors and receptors for atrial natriuretic factor (ANF) ***(2)***, bradykinin ***(3)***, catecholamines ***(4)***, adrenocorticotropin releasing hormone ***(5)***, vasopressin ***(6)***, and dopamine ***(7)***. Ang II is also found to indirectly modulate cyclic GMP (cGMP) levels via nitric oxide ***(8,9)***.

Xenopus laevis oocytes have been used extensively in biomedical research because of their large size and unique unicellular features. With the development of microinjection techniques, *Xenopus* oocytes have provided one of the most successful systems for studying secretion, transcription, and translation of injected molecules including DNA, RNA, and proteins ***(10,11)***. We have used *Xenopus* oocytes to investigate Ang II-induced cell–cell communication

From: *Methods in Molecular Medicine, vol. 51: Angiotensin Protocols*
Edited by: D. H. Wang © Humana Press Inc., Totowa, NJ

via gap junctions ***(12)***, to compare AT-receptor pharmacologies and signal-transduction pathways between mammalian and amphibian species ***(13,14)***, to clone mammalian AT receptors ***(15,16)***, and to study the role of endogenous AT receptors in oocyte maturation ***(14,17)***. The technical aspects of using microinjected *Xenopus* oocytes for expression studies have been comprehensively reviewed ***(18)***. In this chapter, we describe a simple, accurate, and sensitive method for measuring the physiologically important cyclic nucleotide second messengers, cAMP and cGMP in the *Xenopus* oocyte. Data are also presented on Ang II and ANF modulation of intraoocyte and extracellular cAMP and cGMP levels.

2. Materials

2.1. Preparation of Xenopus laevis *Oocytes*

2.1.1. Reagents and Solutions Required for Xenopus *Oocyte Preparation*

1. Deionized and distilled water (D&D water).
2. Charcoal filtered tap water.
3. *Xenopus laevis* female adult frogs (Xenopus I, Ann Arbor, MI).
4. 0.001% potassium permanganate (Sigma; cat. no. P 9810) bath: Dissolve 100 mg of potassium permanganate in 10 L filtered tap water. For convenience, the permanganate bath is made just before use.
5. Frog brittle (Nasco, cat. no. SA05960).
6. 0.2% m-aminobenzoate (Sigma; cat. no. A 5040): Dissolve 2 g of 3-aminobenzoic acid ethyl ester per liter of filtered tap water. Prepare fresh at time of anesthesia.
7. Modified Barth's solution (MBS) [82.5 m*M* NaCl, 2.5 m*M* KCl, 1 m*M* $MgCl_2$, 1 m*M* $CaCl_2$, 5 m*M* HEPES (pH 8.0), 1 m*M* NaH_2PO_4 (pH 7.8), supplemented with penicillin (10 IU/mL), streptomycin (10 μg/mL), and gentamycin (100 μg/mL)]: Prepare stock solutions of 4.125*M* NaCl (241.07 g/L, Sigma, cat. no. S 7653), 2.5*M* KCl (306.3 g/L, Sigma, cat. no. P 1338), 1 *M* $MgCl_2$ (203.3 g/L, Sigma, cat. no. M 0250), 1 *M* $CaCl_2$ (147 g/L, Sigma, cat. no. C 7902), 1 *M* HEPES (238.3 g/L, Sigma, cat. no. H 3375), 1 *M* NaH_2PO_4 (120 g/L, Sigma, cat. no. S 0751). Combine 200 mL of 4.125 *M* NaCl, 10 mL of 2.5 *M* KCl, 10 mL of 1 *M* $MgCl_2$, 10 mL of 1 *M* $CaCl_2$, 50 mL of 1 *M* HEPES, 10 mL of 1 *M* NaH_2PO_4 plus 8 L of D&D water. Add 10 mL of penicillin/streptomycin (10,000 U/10 mg, Gibco-BRL, cat. no. 15140-122) and 20 mL of gentamicin (50 mg/mL, Gibco-BRL, cat. no. 15750-029). Titrate pH to 7.8 with 1 *N* HCl and adjust final volume to 10 L. Filter through a 0.2-μm millipore filter. Store in 1 L aliquots in sterile glass bottles at 4°C (*see* **Note 1**).
8. 6% Trichloroacetic acid (TCA) (Sigma; cat. no. T 9159): First prepare a 100% (w/v) TCA stock solution by dissolving 500 g of TCA in 227 mL D&D water; next, add 1 mL of 100% TCA to 15.67 mL D&D water to prepare 6% TCA.
9. Dry ice/acetone bath: Add acetone (Sigma, cat. no. A 4206) to the top of the dry-ice level in an ice bucket to form a slushy mixture (*see* **Note 2**).

2.1.2. Equipment Required for Xenopus Oocyte Preparation

1. Refrigerator for maintaining oocytes at 18°C (Fisher Scientific, cat. no. 13-255-7) (*see* **Note 3**).
2. Forty-gallon fish tank for housing frogs (commercial pet store).
3. Charcoal filtering system (Hydro, Rockville, MD).
4. Surgical tools: scissors (Roboz, cat. no. RS 6702), dissecting forceps for skin ***(19)*** (Roboz, cat. no. RS 5310), dissecting forceps for muscle and ovary (Roboz, cat. no. RS 4976), silk sutures (4/0) with half-circle triangular surgical needle (Roboz, cat. no. Sut-1066-31), and suture needle holder (Roboz, cat. no. RS 7822).
5. Oocyte isolation tools: forceps (Roboz, cat. no. RS 4905).
6. Stereomaster zoom microscope (Fisher Scientific, cat. no. 12-562-10).
7. 100-mm sterile plastic Petri dishes (Fisher Scientific, cat. no. 08-757-12).
8. Oocyte transfer pipet: Break the tip of a Pasteur pipet (Fisher Scientific, cat. no. 22-378-893) to an approx 1.5-mm diameter; polish the tip edge by flaming.

2.2. Cyclic-AMP/Cyclic-GMP Radioimmunoassay

2.2.1. Reagents and Solutions Required for cAMP and cGMP Radioimmunoassays

1. 3-Isobutyl-1-methylxanthine (IBMX)—broad spectrum phosphodiesterase (PDE) inhibitor (Calbiochem, cat. no. 410957).
2. Angiotensin II (Ang II) (human) (Peninsula, cat. no. 7002).
3. Atrial natriuretic factor (ANF) (rat) (Peninsula, cat. no. 9103).
4. Phosphate-buffered saline (PBS) [137 m*M* NaCl, 1.6 m*M* KCl, 10 m*M* Na_2HPO_4, 2 m*M* KH_2PO_4, pH 7.4]: Dissolve 8 g NaCl, 0.2 g KCl, 1.44 g Na_2HPO_4 (Sigma, cat. no. S 0876), and 0.24 g KH_2PO_4 in 800 mL D&D water. Titrate to pH 7.4 (*see* **Note 4**) before adjusting final volume to 1 L. Filter through a 0.2-μm millipore filter and store in 100 mL aliquots in sterile glassware at 4°C.
5. 1 μ*M* cAMP stock prepared in PBS. To ensure accurate standard curves, check the concentration by spectrophotometric measurement at 258 nm; the extinction coefficient is 14, 650 L/mol/cm. Store in 1-mL aliquots at –20°C.
6. 1 μ*M* cGMP stock prepared in PBS. To ensure accurate standard curves, check the concentration by spectrophotometric measurement at 254 nm; the extinction coefficient is 12, 950 L/mol/cm. Store in 1-mL aliquots at –20°C.
7. Acetylation mixture: Prepare a 1:2 ratio of acetic anhydride (Sigma; cat. no. A 6404) and triethylamine (Sigma; cat. no. T 0886). Mix 1 mL acetic anhydride with 2 mL of triethylamine immediately before use. Store acetic anhydride and triethylamine individually at room temperature.
8. 2.5% normal rabbit serum in PBS (NRS/PBS): Add 2.5 mL NRS (Hazleton Laboratories) (*see* **Note 5**) to 97.5 mL PBS. Make fresh before each experiment. Store antiserum at –20°C in 5-mL aliquots.
9. 1:400 dilution of antiserum in PBS (AS/PBS): Add 25 μL antiserum (Hazleton Laboratories) (*see* **Note 5**) to 10 mL PBS. Store antiserum at –20°C in 0.1-mL aliquots.

10. 7.5% Polyethylene glycol in PBS (PEG/PBS): Dissolve 7.5 g of PEG (mol wt 8000) (Sigma, cat. no. P2139) in 100 mL PBS (*see* **Note 6**). Store at 4°C.
11. Adenosine 3',5'-cyclic phosphoric acid 2'-*O*-succinyl, [^{125}I]-iodotyrosine methyl ester (^{125}I-succinyltyrosine-cAMP) (Hazleton Laboratories) (*see* **Note 5**): Dilute isotope to 20,000 cpm/100 µL PBS immediately before use. Store at 4°C.
12. Guanosine 3',5'-cyclic phosphoric acid 2'-*O*-succinyl, [^{125}I]-iodotyrosine methyl ester (^{125}I-succinyltyrosine-cGMP) (Hazleton Laboratories) (*see* **Note 5**): Dilute isotope to 20,000 cpm/100 mL PBS immediately before use. Store at 4°C.
13. Goat anti-cAMP IgG (second antibody) (Hazleton Laboratories) (*see* **Note 5**). Store at –20°C in 0.2-mL aliquots.

2.2.2. Equipment Required for cAMP and cGMP Radioimmunoassays

1. High-speed centrifuge (Beckman Instruments Co., model no. GS-6R).
2. Vortex Mixer (Fisher Scientific, cat. no. 37615).
3. Glass stirring rod (Fisher Scientific, cat. no. 11-380B).
4. 4°C incubator (cold room or refrigerator).
5. SpeedVac concentrator and refrigerated condensation trap (Savant Instrument Inc., model no. SVC100H).
6. Gamma counter (Packard Instrument Co., Model COBRA Auto Gamma).

3. Methods

3.1. Preparation of Xenopus laevis Oocytes

1. Immediately upon receiving transported frogs, treat animals with 0.001% potassium permanganate solution for 20–30 min (*see* **Note 7**). Rinse frogs under tap water before returning to a fish tank containing charcoal filtered tap water (*see* **Note 8**). Animal husbandry conditions require 3–4 L of water per frog at 18–22°C and 20–30 cm deep. The frogs should be kept on a year-round 12-h light/dark cycle. Feed frogs twice weekly with frog brittle**.** Exchange tank water several hours after feeding with charcoal filtered water (*see* **Note 8**).
2. Anesthesia: Before each surgery, immerse frog in a 0.2% m-aminobenzoate bath until animal movement has stopped (*see* **Note 9**). Transfer animal, abdominal-side up, onto a tray filled with ice. Double check that the frog is deeply anesthetized by touching the abdominal skin with forceps and making sure there is no response. Proceed with the surgery.
3. Swab with alcohol and make an approx 10-mm dorsal incision on the lower abdomen (**Fig. 1**) with sterile scissors and forceps. Remove several ovarian lobes as necessary for the experiment and transfer to Petri dishes containing MBS. Usually oocytes from 1/4–1/2 of an ovary is plenty, unless large quantities of oocytes are needed.
4. After removal of the ovary, sew back the muscle with three individual silk sutures. Then, sew the skin layers together with three individual silk sutures. Before returning to the fish tank, allow the frog to recover in a separate container filled with cool filtered tap water (*see* **Note 7**) until fully awake from anesthesia. Recovery typically takes 30 min (*see* **Note 10**).

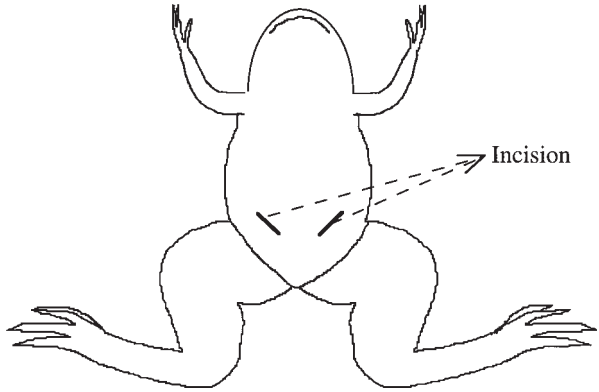

Fig. 1. Diagram of incision for ovary surgery on *Xenopus* frog. The incision should be made on lower abdominal side at an approx 45° angle and the cut should be about 1-cm long.

5. Put ovary in a Petri dish containing MBS. Rinse through serial Petri dishes containing MBS. Cut the lobes of the ovary into small pieces so that the oocytes are exposed to the medium. Place 4–8 lobes per Petri dish containing MBS. Store at 18°C until use.
6. Transfer one lobe to a fresh Petri dish containing MBS. Dissect individual oocytes manually with sterile forceps (*see* **Note 11**). Stage the oocytes under the microscope using the criterion described in **Table 1**. Separate atretric damaged oocytes (**Fig. 2A**) from viable (**Fig. 2B**) stage V–VI oocytes (*see* **Note 12**) ***(20,21)*** by transferring good quality oocytes to a clean Petri dish with MBS, and maintain in an 18°C incubator. The viable oocytes are transferred to fresh petri dishes containing MBS daily (*see* **Note 11**).

3.2. Cyclic-AMP/Cyclic-GMP Radioimmunoassay

3.2.1. Assay Design

1. Transfer oocytes (5 oocytes/tube, which is equivalent to approx 1.3 mg cell protein) into 12 × 75 mm glass tubes containing 210 µL MBS. To start experiment, add 60 µL of 2.5 µ*M* Ang II and/or 5 µ*M* ANF supplemented with 5 µ*M* IBMX (*see* **Note 13**). Incubate at 18°C for the duration of the experiment.
2. To determine the extracellular cyclic nucleotide accumulation of cAMP and/or cGMP, an aliquot of the supernatant (100 µL) is directly assayed by radioimmunoassay.
3. To determine the intracellular cyclic nucleotide accumulation of cAMP and/or cGMP, oocytes are washed by serially transferring oocytes to three glass tubes containing 5 mL of MBS supplemented with 1 µ*M* IBMX. Cyclic nucleotides are then extracted from the oocytes using TCA to denature the cellular protein. Oocytes are transferred to glass tubes containing 300 µL of ice-cold 6% TCA. The tubes are immediately frozen in a dry ice/acetone bath (*see* **Note 2**). After

Table 1
Stages of Oocyte Development

Stage	Size (μm)	Shape	Color
I	50–300	Oval	Translucent
II	300–450	Oval	White opaque
III	450–600	Round	Light brown
IV	600–1000	Round	Uneven light brown
V	1000–1200	Round	White and brown poles
VI	1200	Round	White and brown poles separated by a white belt

thawing, the oocytes are homogenized by vortexing samples in the presence of a glass stirring rod and the homogenate is centrifuged for 20 min at 12,000*g*. The supernatant is transferred to a fresh tube and lyophilized for subsequent radioimmunoassay of cAMP and/or cGMP.

3.2.2. Radioimmunoassay

The standard curves are set up in duplicate plus duplicate tubes for each unknown sample (*see* **Tables 2** and **3** for details). Typically, 12 × 75 mm glass tubes are used. Be sure to use tubes that fit into the gamma counter because the precipitate is counted.

1. Make cAMP or cGMP standards as follows: Mark a set of tubes A–I. In tube I, dilute 1:100 from 1 μ*M* stocks to a final concentration of 10 n*M*. Then, make serial 1:1 dilutions with PBS into tubes H, G, F, E, D, C, B, A. Aliquot 100 μL of each standard into the standard curve tubes, as in **Table 2**. The final concentrations of cAMP or cGMP are also shown in **Table 3**.
2. Resuspend the lyophilized sample(s) from **Subheading 3.2.1.3.** in 250 μL PBS. Aliquot 100 μL in duplicate into the unknown sample tubes.
3. Acetylation: Using a repeat pipettor, pipet 10 μL of acetylation mixture into all tubes while concurrently vortexing samples (*see* **Note 14**). Incubate 15 min at room temperature.
4. Add 100 μL NRS/PBS to the TC and NSp tubes only.
5. Add 100 μL AS/PBS to all tubes except the TC and NSp tubes.
6. Add 100 μL ^{125}I-succinyltyrosine ester-cAMP or ^{125}I-succinyltyrosine ester-cGMP (20,000 cpm/100 μL) to all tubes.
7. Mix by vigorously shaking the racks of tubes. Incubate at 4°C overnight.
8. Add 100 μL second antibody (*see* **Note 15**), plus 1 mL 7.5% PEG in PBS to all tubes except the TC tubes; vortex.
9. Incubate at 4°C for 30 min.
10. Centrifuge all tubes except the TC tubes, for 20 min at 2,000*g***.**
11. Remove supernatant from all tubes except the TC tubes by slowing and gently pouring supernatant off. Count tubes in a γ-counter.

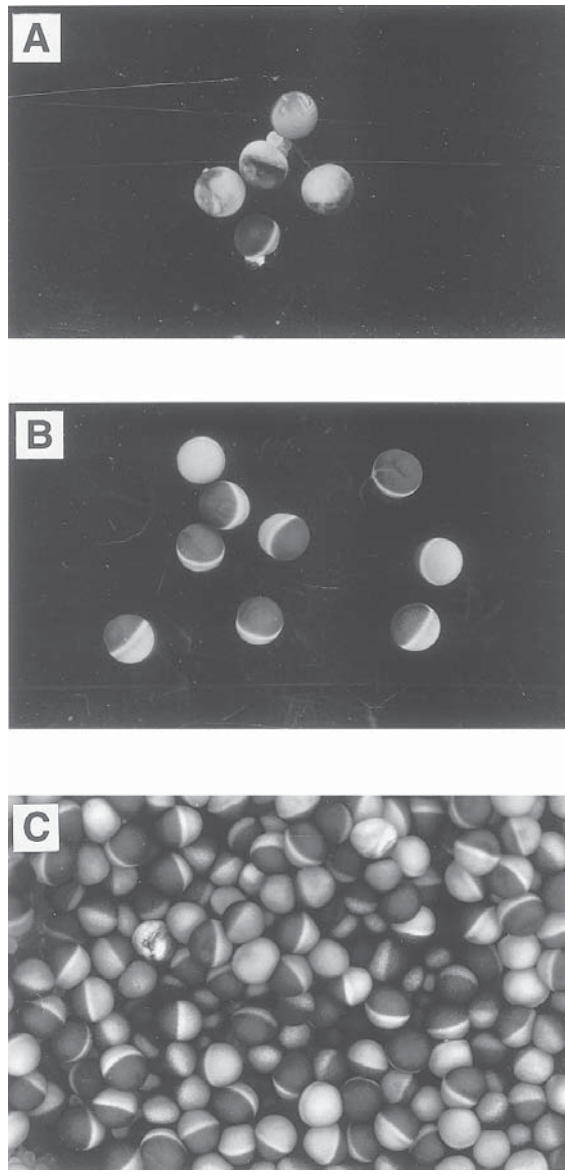

Fig. 2. *Xenopus* oocytes. **(A)** Atretic or damaged oocytes. **(B)** Viable good quality oocytes. **(C)** Good-quality ovary.

3.2.3. Data Analysis

After counting the samples, plot the standard curve as the fractional amount of radioactivity bound vs the log of the nucleotide (cAMP or cGMP) concen-

Table 2
^{125}I-cAMP or ^{125}I-cGMP Radioimmunoassay

Tube	TC	NSp	Bo	Standard curve (A–I)	Unknown samples
PBS (μL)	100	100	100		
Standard cAMP or cGMP (μL)				100	
Unknown sample (μL)					100
Acetylation (μL)	10	10	10	10	10
NSR/PBS (μL)	100	100			
AS/PBS (μL)			100	100	100
^{125}I-succinyl-cAMP (μL) or ^{125}I-succinyl-cGMP	100	100	100	100	100

Note the following abbreviations: TC, total counts; NSp, nonspecific binding; and Bo, total radiolabel bound.

Table 3
cAMP and cGMP Standard Curve

Tube	A	B	C	D	E	F	G	H	I
(μL)	100	100	100	100	100	100	100	100	100
(pmol/mL)	0.03	0.07	0.15	0.3	0.6	1.2	2.5	5	10
(fmol/tube)	3	7	15	30	60	120	250	500	1,000

tration (abscissa). Computer programs are available for analyzing radioimmunoassays. For example, GraphPad (GraphPad, San Diego, CA) can be used to generate estimates for slopes and EC_{50} values. Such programs also allow calculation of unknown cyclic nucleotide levels using the equation:

$$\text{pmol} = (\text{total volume/aliquot}) \times EC_{50} \times F^{H}$$

where F is the inverse of the fractional displacement:

$$F = (\text{maximum-minimum})/(\text{sample dpm-minimum})$$

where ^{H} is the negative inverse of the slope.

The final data shown are typically expressed as pmol/mg protein for cAMP and fmol/mg protein for cGMP (*see* **Note 16**) (**Figs. 3** and **4**). The threshold for the radioreceptor assay is 3 fmol/tube. The basal levels of intracellular cAMP are 13.3 pmol/mg protein; extracellular levels are below the detection limit of the radioimmunoassay. Basal levels of intracellular and extracellular cGMP in the oocyte are 20 fmol/mg protein and 10 fmol/mg protein, respectively. It is

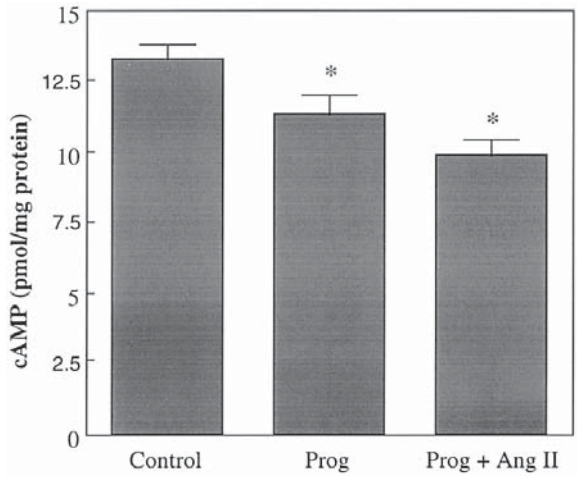

Fig. 3. Effects of progesterone and angiotensin II on intraoocyte cAMP production. Oocytes (5 /tube) were treated with 3 μ*M* progesterone for 2 min in the presence and absence of Ang II at room temperature before intracellular cAMP was measured by radioimmunoassay. The results are expressed as the mean ± SEM of three observations. *$p < 0.03$, $n = 9$ with Student's *t*-test.

possible to further increase the signal of the assay by increasing the number of oocytes from 5 to 25, increasing the volume of sample used from 300 μL to 1.5 mL and assaying 500 μL. Simultaneous measurement of other factors is also possible. For example, both extracellular cAMP and cGMP levels and inositol 1,4,5-trisphosphate ***(14)*** can be simultaneously measured.

4. Notes

1. MBS should be sterile. Oocytes are very sensitive to degradation by bacteria in the media and the incubation temperature of 18°C does not significantly inhibit bacterial growth.
2. Most marking-pen labels rub off in dry-ice/acetone baths. Be careful to prevent this by keeping the top part of the tubes above the dry-ice line or label with ballpoint ink on labeling tape.
3. If an 18°C refrigerator is not available, a heated water bath placed in the cold room can work just as well.
4. The pH of the PBS must be 7.4 for optimal results. Lower pH levels will lead to insensitive radioimmunoassays.
5. Other sources of reagents are listed: cAMP (Calbiochem, cat. no. 116801); cGMP (Calbiochem, cat. no. 370656); rabbit anti-cAMP IgG (Calbiochem, cat. no. 116820); rabbit anti-cGMP IgG (Calbiochem, cat. no. 370659); normal rabbit serum (Calbiochem, cat. no. 566475); ^{125}I-succinyltyrosine cAMP (New England

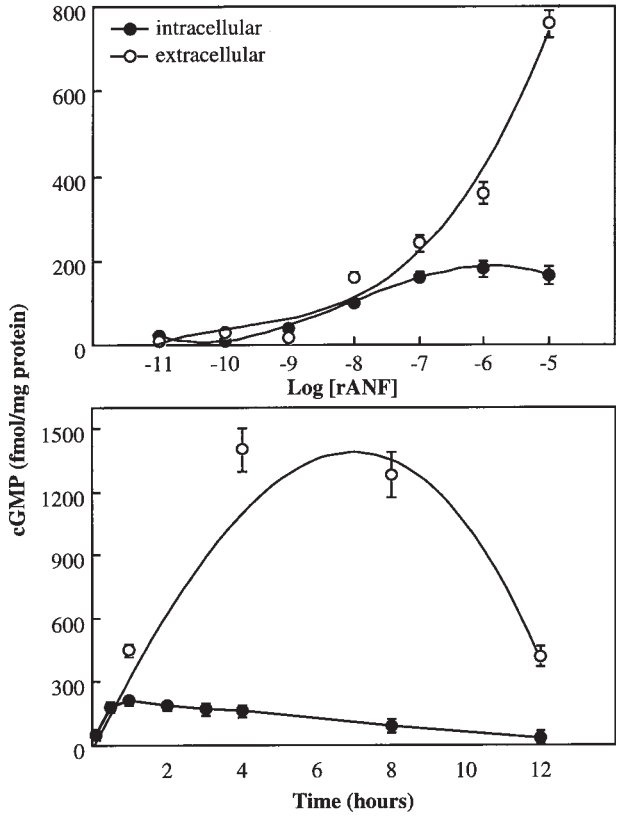

Fig. 4. Dose- and time-dependent stimulation of intracellular and extracellular cGMP production by ANF. **(A)** Dose response. Oocytes (5 /tube) were incubated in the presence of increasing amounts of ANF for 2 h at room temperature. **(B)** Time course. Oocytes (5/ tube) were incubated in the presence of 1 μ*M* ANF, and the intracellular (filled circle) and extracellular (open circle) cGMP were determined over 12 h. The results are expressed as the mean ± SEM of three observations.

Nuclear, cat. no. NEX-130); and ^{125}I-succinyltyrosine cGMP (New England Nuclear, cat. no. NEX-131). Alternatively, anti-cAMP IgG, anti-cGMP IgG, and second antibodies can be generated ***(22)*** and ^{125}I-succinyltyrosine cAMP and ^{125}I-succinyltyrosine cGMP can be iodinated using free sodium ^{125}I ***(23)***.

6. Polyethylene glycol (PEG) is available in various molecular weights (e.g., 200–10,000). Avoid lower molecular weight PEGs (< 8000) because they will not be as effective at precipitating the antibody complex.
7. The permanganate bath will cause the frogs to turn yellow and to slough their skin, which helps the frogs ward off initial infections. The next day the water should be changed to remove the dead skin. It is important to keep frogs

under close observation for the first week after shipment because they are particularly susceptible to infection caused by the stress of shipping. If possible, wait 3 wk before performing any surgery. It is also crucial to avoid exposing frogs to warm water (>25°C) at any time. High-temperature exposure will lower their immune resistance to bacterial infections and will result in an increased incidence of "red foot" syndrome (bacterial septicemia) in the frog colony ***(24)***. The symptoms of red foot include hemorrhaging around the belly, thighs, and webbing of the feet and edemic swelling of the body. Unless treated immediately, red foot is fatal. This is a highly contagious disease and will rapidly spread through the colony. However, injecting 50 mg/kg body weight of chloramphenicol intramuscularly for five consecutive days can cure these frogs. [Each frog weighs approx 30 g; thus, approx 1.5 mg of chloramphenicol is injected per frog.] Wait at least 1 mo before using these cured frogs because their oocytes are generally of poor quality and also because the stress of surgery makes them more susceptible to red foot recurrence. Other relatively common problems are nematode infections. Frogs suffering from nematode infections present with discolored gray skin, which is accompanied by sloughing of the skin and marked weight loss. Treat these frogs by adding 100 μg/mL thiabendazole (Sigma; T8904) to the frog water 24 h before exchanging to fresh water.

8. It is important to only expose frogs to charcoal filtered water because the chlorine commonly found in tap water is toxic. Alternatively, before adding frogs, incubate tap water several days to allow chlorine to evaporate. Minimize aeration of the water to avoid promoting the growth of aerobic bacteria. Regarding this, it is important to keep the frog tanks clean by frequent water changes, especially after feeding. Avoid exposing frogs to D&D water because these animals require the salts be removed by preparing D&D water.
9. Alternatively, place the frog in an ice bath; however it takes longer to anesthetize the frog using ice (about 45 min). The combination of these two methods is the best procedure.
10. After a 3-wk recovery, the frogs can be reoperated on the opposite side of the abdomen. After a 2-mo recovery period, the frogs can then be operated for a second cycle on the left and right sides. The recovery period is necessary to ensure high-quality oocytes. The oocytes can be surgically removed several times before the population of oocytes are depleted. If oocytes are consistently bad (**Fig. 2A**), inject 800-1000 IU human chorionic gonadotropin (Sigma, Cat. No. C5297) into the dorsal lymph sac to induce ovulation. Wait 3 mo for the next cycle ***(18)***. The average life span of a frog is 5 yr.
11. There are two methods generally used to isolate oocytes. The method of choice is the manual dissection, which we describe in this protocol. The second technique involves treating oocytes with collagenase ***(21)***. Whole sections of ovaries are gently rotated at room temperature for 2 h in 25 mL calcium-deficient MBS containing 0.2% type II collagenase (Calbiochem, cat. no. 234155). Oocytes are then washed extensively in calcium deficient MBS before transferring to regular MBS. The collagenase method makes separating oocytes and removing the follicular

cells easier and thus minimizes the loss of viable oocytes caused by mechanical damage. On the other hand, collagenase itself can damage the oocyte membrane leading to poor viability ***(25,26)***. In some cases, collagenase treatment is unavoidable. For example, removing the follicular layer is necessary for electrophysiological studies. The material released by degenerating oocytes can provide a substrate for bacterial and fungal growth. Furthermore, as oocytes degrade, proteases are released into the medium, which can attack healthy oocyte membranes. Thus, it is critical to change the MBS frequently while sorting oocytes, especially as the MBS becomes turbid. Sometimes the oocytes look healthy, but are extremely turgid because of a loss in osmotic regulation; such oocytes are extremely bouncy. It is important to recognize and remove bad oocytes before they release large amounts of cytosolic components into the medium. Typically, we use 1 L of MBS per isolation of 500 oocytes. For these same reasons, it is also absolutely necessary to daily transfer the viable oocytes to Petri dishes containing fresh MBS. The presence of more than 50% nonviable oocytes after sorting generally means that the oocyte quality is poor and not advisable for use in experimentation; similarly, it is recommended to incubate oocytes for a few hours prior to running an experiment in order to discover and remove these atretic oocytes.

12. Oogenesis encompasses six stages (I–VI) of development (**Table 1**) over a 3-mo period ***(20)***. All six stages are generally present in the ovary (**Fig. 2C**). In general, stage V–VI oocytes (approx 1.1 mm in diameter) are the most appropriate for experimental purposes because of their large size. Stage V–VI oocytes are considered good quality when the oocyte animal pole is clearly distinguished and not mottled in appearance (**Fig. 2B**). Splotchy appearances or extruding cytoplasm (**Fig. 2A**) predict rapid degradation. If using albino oocytes ***(15)***, size and resilience of the membrane is used to determine quality, because color is absent. If the ovary has many good-quality stage V–VI oocytes (**Fig. 2C**), it is advised to keep the frog alive for future experiments because frogs that possess good oocytes often continue to do so (*see* **Note 10**).
13. Either general or specific phosphodiesterases (PDE) can be used. For example, Rolipram (Calbiochem, cat. no. 557330) selectively inhibits type-IV cAMP-specific PDE, whereas Zaprinast (Calbiochem, cat. no. 684500) is specific for the type V cGMP-dependent PDE.
14. Acetylation markedly increases the detection limit of the cyclic nucleotide radioimmunoassays by 10-fold. Substitution at the 2'-*O* position increases the sensitivity of cAMP because the acetylated cAMP has a higher affinity for the antibody and competes with labeled cyclic nucleotide derivatives far better than the unsubstituted cyclic nucleotides. Acetylation must be done one tube at a time using glass tubes. The simplest method is to hold the tube in your left hand over the vortex and hold the repipeter (e.g., Brinkman, cat. no. 2226000-6) in your right hand. Add the acetylation mixture and immediately vortex.
15. Alternative methods for separating the free-iodinated cyclic nucleotide from antibody-bound radiolabeled cyclic nucleotide involves precipitation with ammonium sulfate ($(NH_4)_2SO_4$) ***(27)*** or charcoal ***(28)***. Solid-phase radioimmunoassays

are now available ***(29)***, as well as microradioimmunoassays using a phosphor imager ***(30)***.

16. The endogenous amphibian AT receptor is coupled to inhibition of adenylate cyclase. In oocytes, treat with 3 μ*M* progesterone for 2 min, cAMP levels were reduced by 15% as compared to the control; in the presence of 500 n*M* Ang II, cAMP levels were significantly reduced by 26% (**Fig. 3**). These findings are consistent with the inhibitory effects of Ang II on adenylate cyclase in liver ***(31)***, adrenal glomerulosa cells ***(32,33)***, and cardiac myocytes and fibroblasts ***(34)***. *Xenopus* oocytes also possess endogenous ANF receptors that respond to ANF by increasing intracellular and extracellular cGMP in a dose (**Fig. 4A**) and time (**Fig. 4B**) dependent manner. Maximal dose and time effects for intracellular cGMP accumulation were observed at 1 μ*M* ANF and 1 h respectively. In contrast, extracellular cGMP continued to increase up to 5 μ*M* ANF and peaked between 6–8 h. Ang II (500 n*M*) did not have any effect on a 1 μ*M* ANF-induced 60-min increase in cGMP (ANF, 250 ± 13; ANF + Ang II, 248 ± 15; $n = 6$ each), which is consistent with previous reports demonstrating that Ang II did not inhibit ANF-induced cGMP production in adrenal glomerulosa cells ***(35)***.

In conclusion, this optimized radioimmunoassay in *Xenopus* oocytes is rapid, efficient, and adaptable to high-throughput screening. Furthermore, the *Xenopus* oocyte system is an excellent model for evaluating the role of the adenylate cyclase and guanylate cyclase signal-transduction pathways in AT- and ANF-receptor action and in receptor-crosstalk mechanisms. In addition, this model system can be used to investigate structure-function analysis of AT- and ANF-receptor signaling components ***(36,37)***, as well as transcriptional and post-transcriptional mechanisms of gene regulation ***(38)***.

References

1. Ohnishi, J., Ishido, M., Shibata, T., Inagami, T., Murakami, K., and Miyazaki, H. (1992) The rat angiotensin II AT_{1A} receptor couples with three different signal transduction pathways. *Biochem. Biophys. Res. Commun.* **186,** 1094–1101.
2. Palaparti, A. and Anand-Srivastava, M. B. (1998) Angiotensin II modulates ANP-R2/ANP-C receptor-mediated inhibition of adenylyl cyclase in vascular smooth muscle cells: role of protein kinase C. *J. Mol. Cell. Cardiol.* **30,** 1471–1482.
3. Siragy, H. M. and Carey, R. M. (1999) Protective role of the angiotensin AT_2 receptor in a renal wrap hypertension model. *Hypertension* **33,** 1237–1242.
4. Inoue, T., Mi, Z., Gillespie, D. G., Dubey, R. K., and Jackson, E. K. (1999) Angiotensin receptor subtype 1 mediates angiotensin II enhancement of isoproterenol-induced cyclic AMP production in preglomerular microvascular smooth muscle cells. *J. Pharmacol. Exp. Ther.* **288,** 1229–1234.
5. Richard, D. E., Laporte, S. A., Bernier, S. G., Leduc, R., and Guillemette, G. (1997) Desensitization of AT_1 receptor-mediated cellular responses requires long term receptor down-regulation in bovine adrenal glomerulosa cells. *Endocrinology* **138,** 3828–3835.

6. Klingler, C., Ancellin, N., Barrault, M. B., Morel, A., Buhler, J. M., Elalouf, J. M., et al. (1998) Angiotensin II potentiates vasopressin-dependent cAMP accumulation in CHO transfected cells. Mechanisms of cross-talk between AT_{1A} and V_2 receptors. *Cell. Signal.* **10,** 65–74.
7. Hussain, T., Abdul-Wahab, R., Kotak, D. K., and Lokhandwala, M. F. (1998) Bromocriptine regulates angiotensin II response on sodium pump in proximal tubules. *Hypertension* **32,** 1054–1059.
8. Pollman, M. J., Yamada, T., Horiuchi, M., and Gibbons, G. H. (1996) Vasoactive substances regulate vascular smooth muscle cell apoptosis. Countervailing influences of nitric oxide and angiotensin II. *Circ. Res.* **79,** 748–756.
9. Matsubara, H. (1998) Pathophysiological role of angiotensin II type 2 receptor in cardiovascular and renal diseases. *Circ. Res.* **83,** 1182–1191.
10. Hopwood, N. D. and Gurdon, J. B. (1990) Activation of muscle genes without myogenesis by ectopic expression of MyoD in frog embryo cells. *Nature* **347,** 197–200.
11. Seidman, S., Aziz-Aloya, R. B., Timberg, R., Loewenstein, Y., Velan, B., Shafferman, A., et al. (1994) Overexpressed monomeric human acetylcholinesterase induces subtle ultrastructural modifications in developing neuromuscular junctions of *Xenopus laevis* embryos. *J. Neurochem.* **62,** 1670–1681.
12. Sandberg, K., Bor, M., Ji, H., Markwick, A. J., Millan, M. A., and Catt, K. J. (1990) Angiotensin II-induced calcium mobilization in oocytes by signal transfer through gap junctions. *Science* **249,** 298–301.
13. Ji, H., Sandberg, K., and Catt, K. J. (1991) Novel angiotensin II antagonists distinguish amphibian from mammalian angiotensin II receptors expressed in *Xenopus laevis* oocytes. *Mol. Pharmacol.* **39,** 120–123.
14. Ji, H., Sandberg, K., Bonner, T. I., Catt, K. J. (1993) Differential activation of inositol 1,4,5–trisphosphate-sensitive calcium pools by muscarinic receptors in *Xenopus laevis* oocytes. *Cell Calcium* **14,** 663–676.
15. Sandberg, K., Markwick, A. J., Trinh, D. P., and Catt, K. J. (1988) Calcium mobilization by angiotensin II and neurotransmitter receptors expressed in *Xenopus laevis* oocytes. *FEBS Lett.* **241,** 177–180.
16. Sandberg, K., Ji, H., Clark, A. J., Shapira, H., and Catt, K. (1992) Cloning and expression of a novel rat angiotensin II receptor subtype. *J. Biol. Chem.* **267,** 9455–9458.
17. Sandberg, K., Bor, M., Ji, H., Carvallo, P. M., and Catt, K. J. (1993) Atrial natriuretic factor activates cyclic adenosine 3',5'-monophosphate phosphodiesterase in *Xenopus laevis* oocytes and potentiates progesterone-induced maturation via cyclic guanosine 5'-monophosphate accumulation. *Biol. Reprod.* **49,** 1074–1082.
18. Seidman, S. and Soreq, H. (1997) *Transgenic* Xenopus. Humana, Totowa, NJ, p. 28.
19. Cheng, H. S., So, S. C., Law, S. H., and Chan, H. C. (1999) Angiotensin II-mediated signal transduction events in cystic fibrosis pancreatic duct cells. *Biochim. Biophys. Acta* **1449,** 254–260.
20. Dumont, J. N. (1972) Oogenesis in *Xenopus laevis* (Daudin). I stages of oocytes development in laboratory maintained animals. *J. Morphol.* **136,** 153–180.
21. Miller, J. L. (1983) Use of microinjection techniques to study protein kinase and protein phosphorylation in amphibian oocytes. *Methods Enzymol.* **99,** 219–226.

22. Horton, J. K. and Baxendale, P. M. (1995) Mass measurements of cyclic AMP formation by radioimmunoassay, enzyme immunoassay, and scintillation proximity assay. *Methods Mol. Biol.* **41,** 91–105.
23. Patel, A. and Linden, J. (1988) Purification of ^{125}I-labeled succinyl cyclic nucleotide tyrosine methyl esters by high-performance liquid chromatography. *Anal. Biochem.* **168,** 417–420.
24. Wu, M. and Gerhart, J. (1991) Raising *Xenopus* in the laboratory. *Methods Cell Biol.* **36,** 3–18.
25. Dascal, N. (1987) The use of *Xenopus* oocytes for the study of ion channels. *CRC Crit. Rev. Biochem.* **22,** 317–387.
26. Smith, L. D., Xu, W. L., and Varnold, R. L. (1991) Oogenesis and oocyte isolation. *Methods Cell Biol.* **36,** 45–60.
27. Steiner, A. L., Parker, C. W., and Pipnis, D. M. (1972) Radioimmunoasay for cyclic nucleotides. *J. Biol. Chem.* **247,** 1106–1113.
28. Harper, J. F. and Brooker, G. (1975) Femtomole sensitive radioimmunoassay for cyclic AMP and cyclic GMP after 2'0 acetylation by acetic anhydride in aqueous solution. *J. Cyclic Nucleotide Res.* **1,** 207–218.
29. Daniels, C. K., Zhang, L., Musser, B., and Vestal, R. E. (1994) A solid-phase radioimmunoassay for cyclic AMP. *J. Pharmacol. Toxicol. Methods* **31,** 41–46.
30. Berg, W. and Hornbeck, P. V. (1993) A micro-radioimmunoassay for the measurement of intracellular cAMP. *Biotechniques* **15,** 56–59.
31. Bauer, P. H., Chiu, A. T., and Garrison, J. C. (1991) DuP 753 can antagonize the effects of angiotensin II in rat liver. *Mol. Pharmacol.* **39,** 579–585.
32. Woodcock, E. A. and Johnston, C. I. (1984) Inhibition of adenylate cyclase in rat adrenal glomerulosa cells by angiotensin II. *Endocrinology* **115,** 337–341.
33. Marie, J. and Jard, S. (1983) Angiotensin II inhibits adenylate cyclase from adrenal cortex glomerulosa zone. *FEBS Lett.* **159,** 97–101.
34. Everett, A. D., Heller, F., and Fisher, A. (1996) AT_1 receptor gene regulation in cardiac myocytes and fibroblasts. *J. Mol. Cell. Cardiol.* **28,** 1727–1736.
35. Ganguly, A., Chiou, S., West, L. A., and Davis, J. S. (1989) Atrial natriuretic factor inhibits angiotensin-induced aldosterone secretion: not through cGMP or interference with phospholipase C. *Biochem. Biophys. Res. Commun.* **159,** 148–154.
36. Thekkumkara, T. J., Thomas, W. G., Motel, T. J., and Baker, K. M. (1998) Functional role for the angiotensin II receptor (AT_{1A}) 3'-untranslated region in determining cellular responses to agonist: evidence for recognition by RNA binding proteins. *Biochem. J.* **329,** 255–264.
37. Conchon, S., Barrault, M. B., Miserey, S., Corvol, P., and Clauser, E. (1997) The C-terminal third intracellular loop of the rat AT_{1A} angiotensin receptor plays a key role in G protein coupling specificity and transduction of the mitogenic signal. *J. Biol. Chem.* **272,** 25,566–25,572.
38. Wang, X., Nickenig, G., and Murphy, T. J. (1997) The vascular smooth muscle type I angiotensin II receptor mRNA is destabilized by cyclic AMP-elevating agents. *Mol. Pharmacol.* **52,** 781–787.

26

Measurement of Nitric Oxide Formation

Christian Thorup and Leon C. Moore

1. Introduction

Nitric oxide (NO) is a simple gaseous monoxide that is involved in a variety of biological mechanisms in the mammalian body ***(1)***. NO is produced by a group of enzymes, nitric oxide synthases. One of the more important functions of NO is to regulate the tone of blood vessels ***(2)***. As one of the most potent vasodilators known, NO modulates the vasoconstrictive action of humoral factors, including angiotensin II (Ang II). Therefore, a well-controlled balance between Ang II and NO is required for normal hemodynamic function in all blood vessels ***(3–6)***.

Several recent studies have demonstrated that an increased level of Ang II stimulates the release of NO from the endothelium ***(7–13)***. Ang II might stimulate NO release in at least two different ways. The first is via a direct stimulation of Ang II receptors. Administration of Ang II to intact blood vessels, as well as cultured endothelial cells, has been shown stimulate NO release ***(7–12)***. Inhibition of AT_1-receptors clearly blunts this effect, but is not sufficient to fully inhibit Ang II-stimulated NO released ***(12)***. Therefore, it is likely that the AT_2-receptor is also involved in this response ***(13)***. Second, Ang II-induced vasoconstriction alters the shear stress exerted on the vascular wall, and this can stimulate NO production ***(14)***. In investigating the vascular effects of Ang II, it is important to recognize that, although the dominant effect of Ang II is to constrict arterial vessels, the net response also reflects Ang II-induced production of substances like NO that moderate the constriction.

In this chapter, we describe a technique for direct measurements of NO formation from isolated perfused vessels. We have performed these measurements on renal resistance artery segments, but the technique could be used to study arterial vessels from other organs. The technique employs a NO-sensi-

From: *Methods in Molecular Medicine, vol. 51: Angiotensin Protocols*
Edited by: D. H. Wang © Humana Press Inc., Totowa, NJ

tive microelectrode, similar to that described by Malinski ***(15)***, combined with a system for perfusion of small blood vessels in vitro. The electrode system is highly sensitive and can detect NO concentrations in the nanomolar range.

Detection of NO is performed using a three-electrode system, where NO is oxidized to nitrate (NO_3^-) the final product of electrochemical oxidation of NO. The oxidation takes place on a porphyrin-electroplated carbon-fiber electrode that is coated with Nafion. Measurements of NO oxidation at the elctrode surface are made using differential-pulse amperometry using a computer-based, commercially available electrochemical system (EMS-100, Bio-Logic Science Instruments, Grenoble, France).

2. Materials

2.1. Electrode System

1. Porphyrin and Nafion solutions were obtained from Bio-Logic Science Instruments; fused-silica capillary (outer diameter [od 430 μm, id 320 μm), carbon fiber (30 μm), and platinum wire (0.25 mm) obtained from World Precision Instruments, Sarasota, FL; thin-wall capillary glass (od 1 mm, id 0.75 mm) and silver wire (0.2–0.25 mm) obtained from Warner Instruments, Hamden, CT; conductive silver paint (Silver Print) obtained from Allied Electronics, Fort Worth, TX; common 5 min epoxy resin.
2. EMS-100 Electrochemical System obtained from Bio-Logic Science Instruments; PC-compatible Pentium computer.

2.2. Perfusion System

1. Capillary glass (od 2 mm), double-lumen theta glass capillary tubing (od 2 mm), and plexiglass flowthrough electrode holder (model PESW-N20P/10) obtained from Warner Instruments.
2. Plastic perfusion chamber (volume approx 1 mL) with servo-controlled heating system (model TC-1) obtained from Cell Micro Controls, Virginia Beach, VA; compressed air source with low-flow range regulator; output pressure gage (0–300 mmHg) obtained from Fisher Scientific, Pittsburgh, PA; electronic pressure transducer and monitor suitable for blood pressure measurement (0–300 mmHg); stereo microscope (X6–40) on a large swivel stand; silicone rubber tubing (od 3/32" id 1/32") and fiberoptic illuminator with flexible light guide and 1.0-mm rigid light probe obtained from Cole-Palmer Instrument Co., Vernon Hills, IL; 2 micropipet holders and 2 Prior micromanipulators obtained from Stoelting, Inc., Wood Dale IL; 20–40 mL glass vials with teflon-lined septum lids, small pinch clamps for occluding silicone rubber tubing, and 1-cm lengths of 18-gage stainless-steel tubing (made from hypodermic needles) used for connecting silicone rubber tubing, 25-gage hypodermic needles.
3. Krebs Ringer solution containing L-arginine (0.1 m*M*).

2.3. Calibration Setup

1. Tank of NO gas with a low-flow regulator, Krebs-Ringer solution.
2. Battery-powered magnetic stirrer (Cole-Parmer), glass beaker (10 mL), gas-tight syringe (1–10 μmL), small DC beaker heater, 5-mL glass vials with septum lid.

3. Methods

3.1. Electrode System

3.1.1. NO-Electrode

Electrodes can be purchased from Bio-Logic Science Instruments. However, NO-electrodes do not have a long shelf-life and should be used within a few weeks after production. However, preparation of electrodes is not difficult with the EMS-100 system. For maximum sensitivity, we recommend that electrodes are prepared within a few days of the experiment.

Figure 1 shows the NO-electrode that we used. It measures the NO concentration of the effluent from a perfused vessel segment, and the NO sensitive electrode and the reference electrode is located within the micropipet used to cannulate the vessel. Assembly is facilitated with a stereomicroscope.

1. Cut the carbon fiber (approx 10 cm) and silver wire (approx 20 cm). Clean the silver wire with fine steel wool or other abrasive to remove any oxidation, and clean thoroughly with methanol to remove any oils.
2. Cut the fused silica capillary tubing (approx 7 cm) and the 1-mm od glass capillary tubing (approx 8 cm).
3. Insert the carbon fiber into the silica capillary so that it protrudes from both ends.
4. Insert the silver wire into the glass capillary (od 1 mm) so that it protrudes from both ends.
5. Attach the carbon fiber and the silver wire with conductive silver paint.
6. Slide the fused-silica capillary into the glass capillary, keeping the silver wire-carbon fiber connection intact.
7. Glue the connection between the silica and glass capillaries, and seal both ends with a two-component 5-min epoxy resin. Take care to minimize the amount of epoxy on the carbon fiber. After the epoxy has set, cut the carbon fiber to a length of 0.5–1 mm.

The electrode is then treated following the instructions in the EMS-100 user manual. The following steps are involved, and are automated by the EMS-100 system.

1. The electrode is electrochemically pretreated in phosphate buffer solution (pH 7.4) by applying a series of potential patterns to the carbon fiber. The reference and auxiliary electrodes are also placed in the buffer. The first pattern is a 50-Hz square wave (0–2.9 V) for 20 s. The second is a DC signal (0.8 V) for 5 s. The third is 1.5 V for 5 s.

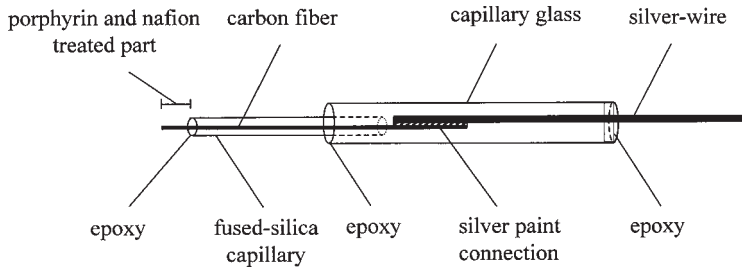

Fig. 1. Illustration of NO sensitive electrode. The drawing is not to scale, and the pieces are attached with epoxy resin where indicated.

2. The carbon-fiber electrode, along with the reference and auxiliary electrodes, is then placed in a 0.5-m*M* solution of tetrakis 3-hydroxy-4-methoxy phenyl nickel porphyrin (NiTHMPP) solution in 0.1 *M* NaOH (*see* **Note 1**). The carbon fiber electrode is polarized to 1.2 V for 10 min. This step coats the carbon fiber with nickel porphyrin, which enhances the sensitivity to NO. When completed, rinse the electrode well, and let dry in air.
3. The final step is to apply a hydrophobic layer to the electrode to increase the selectivity of the electrode to aqueous electroactive compounds. This is done by dipping the electrode in a nondiluted Nafion solution for 5 s, and allowing the tip to dry in air with the tip upward for 2–3 min. This step is then repeated.
4. Store the electrodes in the dark, as the porphyrin compound is light sensitive.

3.1.2. Reference Electrode, Ag:AgCl

1. Cut silver wire (approx 15 cm), remove any oxidation and oils with methanol.
2. Immerse the end of the silver wire and a platinum wire into a small beaker containing 1 *M* HCl.
3. Attach the wires to a power supply, and apply 2.5 V. When the voltage is applied, small bubbles of hydrogen will be formed on the silver wire, and it develops a light gray color.
4. After approx 30 s, turn off the power, remove the silver electrode, and rinse well.

3.1.3. Auxiliary Electrode

1. Cut silver wire (approx 15 cm) and clean. Platinum wire can also be used.

3.2. Perfusion System

The perfusion system consists of two glass cannulae placed in a temperature-controlled Plexiglas chamber (1 mL). A schematic drawing of the set up is shown in **Fig 2**.

1. The proximal cannula is pulled from a 2-mm od theta glass (two barrels) that was bent (approx 45°) and fire-polished to obtain a tip diameter of approx 200 μm.

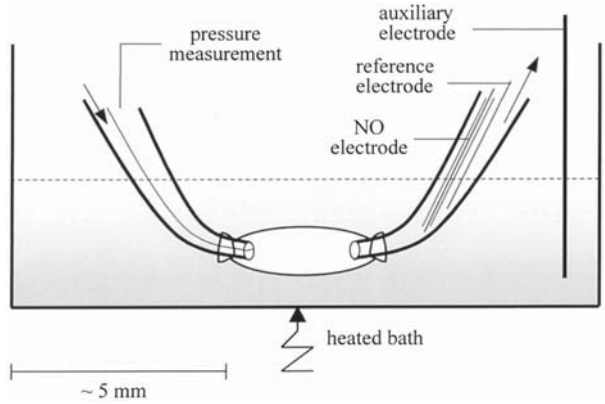

Fig. 2. Illustration of the vessel perfusion setup. The NO and reference electrodes are placed within the distal perfusate collection cannula and are exposed to the fluid leaving the vessel segment. These electrodes are mounted into the cannula with a flowthrough electrode holder (**Fig. 3**). The auxiliary electrode is placed in the bath.

One barrel of the theta glass is used for perfusion and the other for continuous luminal pressure measurements. Using a stereomicroscope, the vessel segment is tied to the two cannulae and slightly stretched (*see* **Note 5**).

2. The distal cannula is pulled out of a normal 2-mm od glass, bent, and fire-polished as above. This cannula drains into a length of small silicone rubber tubing. Before attaching the vessel segment, the entire system is filled with perfusate solution, and the tip of the cannulae is kept below the level of the fluid in the bath.
3. The vessel segment is then perfused with Krebs Ringer solution at a constant pressure (normally 80 mmHg) and at a constant low flow rate (*see* **Note 6**). To maintain high luminal pressure at low perfusate flow, we use an adjustable flow resistor on the outflow from the system, consisting of a fine screw clamp that compresses the silicone rubber tubing. Alternatively, a long section of silicone rubber tubing can be placed on the outflow port of the flowthrough electrode holder and elevated to a height appropriate to hold luminal pressure at a high level while maintaining a low flow.
4. To apply drugs to the lumen of the vessel, we use a simple system of pressurized glass vials (approx 40 mL). The vials are fitted with septum tops penetrated by two hypodermic needles. One is a short needle connected to a pressure manifold, the second is a long needle to deliver the perfusate. We switch between perfusates by moving small pinch clamps (small surgical bulldog clamps work well) that occlude the small silicone rubber tubing. We connect the rubber tubing with small plastic T-junctions and short lengths of 18-gage stainless steel tubing made from hypodermic needles. However, any system that allows switching of perfusion solutions at constant pressure could also be used.

5. The bath is warmed to 37°C with a servo-controlled heating system. Measurements can be made with continuous flow through the bath, or with no flow. In the latter case, only relatively short measurements, should be made (approx 15 min), as fluid evaporation from the shallow bath will slowly alter the bathing fluid composition. Drugs can be added to the bath, but the added volume should be much less that 1 mL and should be prewarmed. Indeed, the NO electrode is very temperature sensitive, and reliable measurements can only be made under constant temperature conditions. We illuminate the vessel with a small, rigid fiber-optic light pipe that is placed below the fluid surface in the bath to minimize reflections. Although not essential, we use a CCD camera and video display to visualize the vessel during measurements.

3.2.1. Constructing the Perfusion Cannulae

1. Pull the glass capillaries (plain od 2 mm and theta glass od 2 mm) to a tip diameter of approx 200 μm using an electrode puller or small flame. Fire-polish the tips and bend to approx 45° as close to the tip as possible.
2. The proximal (theta) glass cannula consists of two barrels.
3. Bend two small hypodermic needles (25 gage) about 30°.
4. Insert one needle a few millimeters into one of the channels at the rear of the cannula, and glue in place with epoxy resin.
5. Let dry, and then second needle into the second channel. Make sure that the glue fills the lumen of the channel, but does not cover the tip of the needle.
6. Connect appropriate silicone rubber tubing for the perfusion line, and polyethylene tubing for the pressure channel using standard Luer fittings.
7. Mount the dual-channel cannula on a micromanipulator using appropriate electrode holders. Attach the pressure monitoring line to a pressure transducer to measure pressure within the vessel lumen.
8. Place the distal cannula in the plexiglass flowthrough electrode holder and insert the NO-electrode, as well as the Ag:AgCl-reference electrode as shown in **Fig. 3**. Adjust the position of the NO electrode so that it is as close as possible to the tip of the cannula.
9. Attach the distal cannula assembly to micromanipulator with a standard microelectrode holder. To preserve the integrity of the electrode, care must be taken to avoid flexing or touching anything with the exposed length of carbon fiber.
10. Put a silicone rubber tube on the outflow port of the holder compressed by an adjustable fine-screw clamp. In this way, it becomes possible to adjust the flow through the system.

3.3. Calibration of Electrode

Calibration of the electrode is performed before each experiment. Use freshly prepared differential dilutions of a NO-saturated (approx 1.5 m*M*) Krebs bicarbonate-Ringer solution. It is important to perform calibrations under constant stirring and constant temperature conditions.

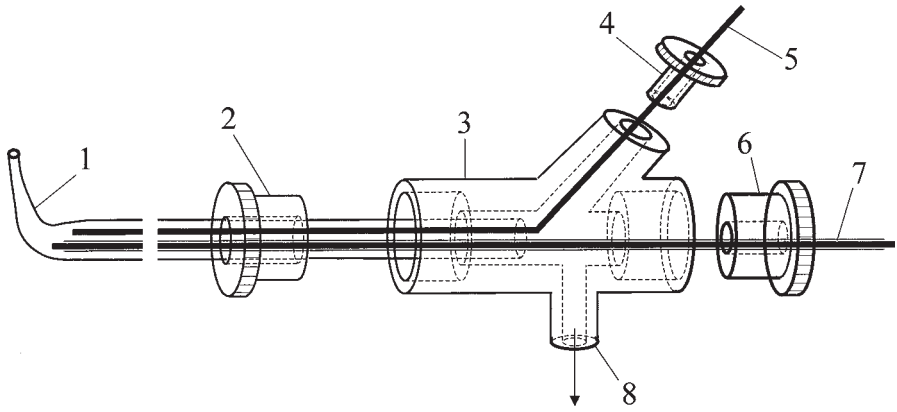

Fig. 3. Illustration of the flowthrough electrode holder ***(3)***. The drawing is not to scale. Part 1 is the collection glass cannula (2-mm od glass) into which the NO electrode ***(7)*** and the reference electrode ***(5)*** are inserted. Parts 2, 4, and 6 are treaded, and the electrodes are sealed with rubber gaskets (not shown). Fluid flows into the system at the tip and leaves via the drain port ***(8)***.

1. In a fume hood, bubble a 5–10 mL volume of Krebs bicarbonate-Ringer solution in a glass vial with a gas-tight teflon-lined septum lid fitted with a vent for about 30 min.
2. Using gas tight syringes make differential dilutions of the NO-saturated Krebs-Ringer solution in vials with gas-tight teflon septum lids.
3. Place the NO-electrode together with a Ag:AgCl reference electrode and the Ag auxillary electrode in a beaker with a known volume of Krebs-Ringer solution. Start the constant stirring and warm the solution to 37°C. Warming can be accomplished with small DC jacket heater placed around the beaker.
4. Begin to measure NO concentration while slowly aspirating the solution into the cannula at a rate equal to that used in the perfusion experiments.
5. Add volumes of pre-warmed NO saturated Krebs-Ringer solution with a gas-tight syringe to get the desired concentrations. An example of a calibration curve is shown in **Fig 4**. Note that NO is relatively stable and has a long half-life at low concentrations ***(16)***.

3.4. Measurements of NO

Measurements of NO-oxidation at the electrode surface are made using differential-pulse amperometry using a computer-based electrochemical system (EMS-100, Bio-Logic Science Instruments). The NO and Ag:AgCl reference electrodes are in the distal perfusion cannula, whereas the silver auxiliary electrode is placed in the bath. The NO electrode is polarized to holding voltage of 0.67 V and a 0.1-V pulse of 20 ms duration is applied every 100 ms. The electrode oxidation current, which varies linearly with ambient NO concentration,

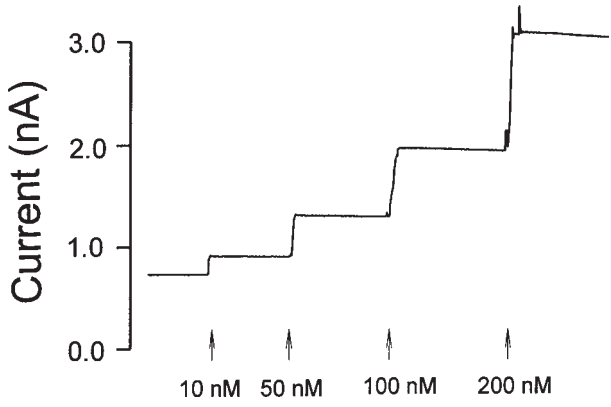

Fig. 4. Typical NO calibration curve made in a stirred beaker at constant temperature.

is sampled twice, 1 ms before the rise and fall of the applied pulse (**Fig. 5**). The differential current evoked in response to the pulse is averaged over 20 periods, and the resulting 2-s mean values are recorded for analysis.

3.5. Dissection of Vessels

In our studies, we measured NO formation in large renal resistance arteries harvested from anaesthetized Sprague-Dawley rats. We have also performed measurements on renal artery and aortic segments from mice. The only criteria, given the dimensions of our perfusion cannulae, are that the vessel segment is 2–3 mm long, 250–400 mm in diameter, and have no more than a few small branches. We obtain appropriate renal vessel segments by using the preparative methods developed for the in vitro juxtamedullary nephron preparation *(17,18)*.

1. A male Sprague-Dawley rat (weighing approx 250 g) is anesthetized by an injection of Inactin (110 mg/kg, Research Biochemicals Inc., Natick, MA).
2. The rat is heparinized and the left kidney is exposed via an abdominal incision.
3. The kidney is catheterized via the aorta, cleared of blood with a gassed Krebs-Ringer-bicarbonate solution containing 4% albumin, and the kidneys are removed under perfusion.
4. The kidney is dissected while perfused to expose the perihilar cortex, and major arteries supplying the rest of the kidney are ligated.
5. Segments of renal arteries (tertiary branches of the renal artery or primary arcuate arteries) are carefully dissected free of connective tissue, and all small branches are ligated in situ.
6. The segments (250–400 μm in diameter and 2–3 mm long) are then excised and transferred to the temperature-controlled chamber.
7. The segment is mounted on the perfusion system and tied to the cannulae.

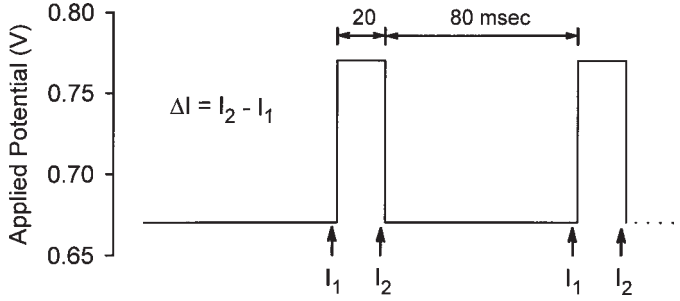

Fig. 5. Potential waveform applied to the NO selective electrode during differential-pulse amperometry. Electrode current is sampled at the time points indicated by the arrows, and the difference is recorded.

4. Notes

1. Although we obtained the porphyrin and Nafion solutions from Bio-Logic Instruments, these substances can also be obtained from other sources. The NiTHMPP must then be solubilized in 0.1 *M* NaOH, and kept cold and dark. The solution lasts for about a week.
2. It is worth reiterating that the NO-electrodes we use are highly sensitive to flow rate and temperature. These variables must be held constant during measurements. In addition, the NO electrode is easily damaged, as the selectivity of the electrode is highly dependent on the integrity of the Nafion coating. Proper control measurements must be made to avoid artifacts and to verify that the measured electrode currents do, in fact, arise from the oxidation of NO. Further, the NO standard solutions are unstable and must be made fresh and used promptly.
3. Measurements of NO using the present system do not provide an absolute measure of NO formation by the vessel segment. The electrode is placed outside the vessel and the distance between the site of production and detection is not insignificant at low perfusion rates. However, under constant flow conditions, the NO concentration of the vessel effluent will change in parallel with segment NO production.
4. The endothelial layer of the isolated vessel is easily damaged during dissection and mounting on the perfusion setup. Therefore, the viability of the vessel segments should be tested before an experiment. This can be done by initiating each experiment by increasing the concentration of L-Arg or by administration of carbachol or some other stimulator of NO release.
5. In our measurements, we chose not to fully stretch the vessel segment to its *in situ* length to prevent changes in vessel tone. This was done to avoid any change in shear stress on the vascular endothelium.
6. Perfusion at a constant flow rate is important, as the reaction at the electrode surface is diffusion-limited, and the electrode current is strongly influenced by advective transport of NO to the electrode. We use a low rate of perfusion because

the NO concentration measured at the electrode is determined by the ratio of rate of NO production over the perfusion rate. Hence, the rate of perfusion should be set at a level low enough to obtain a measurable signal, while being high enough to have a reasonable response time.

7. The EMS-100 system makes use of differential-pulse amperometry. The major advantages of differential-pulse amperometry are that it greatly reduces the effects of baseline drift, and it increases the selectivity of the electrode. Baseline drift is reduced because both current measurements will drift in parallel, while the difference remains stable. The selectivity of the measurement is enhanced because this method reduces the effects of interfering substances that are oxidized at lower potentials. In perfused vessels, such substances might include ascorbate, norepinephrine, and other endogenous amines. As these substances react essentially equally at both of the potentials applied during differential-pulse amperometry, the effect on the differential current is minimized. To our knowledge, all other commercially available NO measuring systems use constant-voltage (approx 0.7 V) amperometry. Although this approach offers somewhat greater sensitivity than the differential-pulse method, great care must be taken to determine to what extent the measured currents can be attributed to the oxidation of NO. This requires repeating key measurements at reduced potentials (approx 0.4 V) where NO does not react, and subsequent correction of the responses obtained at 0.7 V. Indeed, it must always be kept in mind that the selectivity of these electrodes is mainly dependent on the integrity of the gas-permeable hydrophobic Nafion coating on the electrode. If this barrier is damaged, the selectivity of the electrode is greatly compromised.

References

1. Moncada, S., Palmer, R. M., and Higgs, E. A. (1991) Nitric oxide: physiology, pathophysiology, and pharmacology. *Pharmacol. Rev.* **43,** 109–142.
2. Navar, L. G., Inscho, E. W., Majid, D. S. A., Imig, J. D., Harrison-Bernard, L. M., and Mitchell, K. D. (1996) Paracrine regulation of the renal microcirculation. *Physiol. Rev.* **76,** 425–536.
3. Ohishi, K., Carmines, P. K., Inscho, E. W., and Navar, L. G. (1992) EDRF-angiotensin II interactions in rat juxtamedullary afferent and efferent arterioles. *Am. J. Physiol.* **263,** F900–F906.
4. Sigmon, D. H., Carretero, O. A., and Beierwaltes, W. H. (1992) Angiotensin dependence of endothelium-mediated renal hemodynamics. *Hypertension* **20,** 643–650.
5. Takenaka, T., Mitchell, K. D., and Navar, L. G. (1993) Contribution of angiotensin II to renal hemodynamic and excretory responses to nitric oxide synthesis inhibition in the rat. *J. Am. Soc. Nephrol.* **4,** 1046–1053.
6. Ikenaga, H., Fallet, R. W., and Carmines, P. K. (1996) Basal nitric oxide production curtails arteriolar vasoconstrictor responses to ANG II in rat kidney. *Am. J. Physiol.* **2712,** F365–F373.

7. Boulanger, C. M., Caputo, L., and Levy, B. I. (1995) Endothelial AT1-mediated release of nitric oxide decreases angiotensin II contractions in rat carotid artery. *Hypertension* **26,** 752–757.
8. Hennington, B. S., Zhang, H., Miller, M. T., Granger, J. P., and Reckelhoff, J. F. (1998) Angiotensin II stimulates synthesis of endothelial nitric oxide synthase. *Hypertension* **31,** 283–288
9. Zou, A. P., Wu, F., and Cowley, A. W., Jr. (1998) Protective effect of angiotensin II-induced increase in nitric oxide in the renal medullary circulation. *Hypertension* **31,** 271–276.
10. Pueyo, M. E., Arnal, J. F., Rami, J., and Michel, J. B. (1998) Angiotensin II stimulates the production of NO and peroxynitrite in endothelial cells. *Am. J. Physiol.* **274,** C214–C220.
11. Thorup, C., Kornfeld, M., Winaver, J. M., Goligorsky, M. S., and Moore, L. C. (1998) Angiotensin II stimulates nitric oxide release in isolated perfused renal resistance arteries. *Pflugers Arch.* **435,** 432–434.
12. Thorup, C., Kornfeld, M., Goligorsky, M. S., and Moore, L. C. (1999) AT-1 receptor inhibition blunts angiotensin II-stimulated nitric oxide release in renal arteries. *J. Am. Soc. Nephrol.* **10,** S220–S224.
13. Gohlke, P., Pees, C., and Unger, T. (1998) AT2 receptor stimulation increases aortic cyclic GMP in SHRSP by a kinin-dependent mechansim. *Hypertension* **31,** 349–355.
14. Juncos, L. A., Ren, Y. L., Arima, S. J., Garvin, J., Carretero, O. A., and Ito, S. (1996) Angiotensin II action in isolated microperfused rabbit afferent arterioles is modulated by flow. *Kidney Int.* **49,** 374–381.
15. Malinski, T., Mesaros, S., and Tomboulian, P. (1996) Nitric oxide measurements using electrochemical methods. *Methods Enzymol.* **268,** 58–69.
16. Schmidt, K., Desch, W., Klatt, Kukovetz, W. R., and Mayer, B. (1997) Release of nitric oxide from donors with known half-life: a mathematical model for calculating nitric oxide concentrations i aerobic solutions. *Naunyn-Schmiedeberg´s Arch. Pharmacol.* **355,** 457–462.
17. Casellas, D. and Moore, L. C. (1990) Autoregulation and tubuloglomerular feedback in juxtamedullary glomerular arterioles. *Am. J. Physiol.* **258,** F660–F669.
18. Casellas, D. and Navar, L. G. (1984) In vitro perfusion of juxtamedullary nephrons in rats. *Am. J. Physiol.* **246,** F349–F358.

27

Measuring Renin Secretion from Juxtaglomerular Cells

Armin Kurtz and Frank Schweda

1. Introduction

The development of specific receptor inhibitors of angiotensin II and the generation of genetic knockout models of the different components of the renin–angiotensin–aldosterone (RAAS) cascade has confirmed previous and has created new evidence for elementary functions of the RAAS for the body.

The RAAS cascade is initiated by the proteolytic cleavage of angiotensin I (ANG-I) from angiotensinogen. To our knowledge, this is the most relevant physiological regulatory step in controlling the activity of the RAAS cascade. Several proteases or protease activities have been suggested to catalyze the generation of ANG-I from angiotensinogen (ANG-O), but up to now there is only common agreement on renin to specifically cleave ANG-I from ANG-O. Renin has been originally found in the kidney and it has subsequently been localized to the terminal parts of the afferent arterioles, to the so-called juxtaglomerular granular (JGG) cells. Meanwhile, it is known that physiologically active renin is also synthesized outside of JGG cells such as in proximal tubules of the kidneys, vascular smooth-muscle cells in different organs, and in the placenta. Whereas renin produced at those sites may be relevant for so-called local renin angiotensin systems, there is no doubt that the bulk of renin in the body is produced and secreted by the JGG cells, which in turn, determine the activity of the systemic RAAS, but probably also of the intrarenal RAAS. This view is supported by the observations that only renin synthesis and renin secretion in JGG is controlled by systemic negative-feedback loops involving angiotensin II, the blood pressure, or the sodium bal-

From: *Methods in Molecular Medicine, vol. 51: Angiotensin Protocols*
Edited by: D. H. Wang © Humana Press Inc., Totowa, NJ

ance of the organism. In view of such a key role of renin originating from JGG cells for the control of the systemic and intrarenal RAAS, the function of JGG cells, in particular the mechanisms regulating renin gene expression and renin secretion, have attracted major interest. For the study of renin secretion, therefore, a variety of models has been developed that will be described in the following. Those models include in vivo approaches and several in vitro approaches such as kidney slice incubation, isolated perfused juxtaglomerular apparatus, isolated perfused kidneys, and isolated JGG cell preparations, of which the latter two models will be described in detail.

1.1. In Vivo Models

For the assessment of renin secretion from JGG cells, in vivo measurement of renin in the plasma is considered as a reliable parameter. Renin in the plasma can be measured by immunological methods when appropriate antibodies and tracers are available such as for human renin ***(1,2)***. If immunological methods are not available the so-called "plasma renin concentration" (PRC) is the best parameter. PRC reflects the intrinsic proteolytic property of the plasma to generate ANG-I from angiotensinogen (ANG-O) with exogenous ANG-O being added in excess. If endogenous ANG-O is present in sufficient amounts in the plasma so that its availability is not essentially rate limiting for the proteolytic activity of renin to generate ANG-I, then simple determination of plasma renin activity (PRA) is the most easiest way to obtain information about renin secretion from JGG cells in vivo. It should be noted that PRA values are always lower than PRC values indicating a certain limitation of the renin activity by the available endogenous substrate.

To obtain more direct information about renin secretion from the kidneys in vivo, catheter techniques have been developed that allow to take blood samples from the renal artery and the renal vein. In conjunction with the flow rate through the kidney, renin secretion rates from individual kidneys can thus be calculated from the difference of plasma renin activity or plasma renin concentration between renal venous blood and renal arterial blood. This method is best established for dogs ***(3)***.

Although the direct information about cellular mechanisms that control renin release is limited in those in vivo experiments, such measurements provide valuable information about the secretory activity of JGG cells in vivo and, moreover, allow to test the physiological relevance of concepts that are deduced from in vitro experiments as mentioned later. Moreover, essential information about the mechanisms by which renal nerve activity or the salt balance of the organism influence renin secretion can only be gained with in vivo experiments.

1.2. In Vitro Models

1.2.1. The Isolated Perfused Kidney

The isolated perfused kidney model has been established for rat, rabbit, and dog kidneys ***(4,5)***. By that, renin secretion from JGG cells is assessed by measuring renin activity in the arterial influate and the venous effluate. Renin secretion rates are then calculated as the product of the difference between venous and arterial renin activity and the perfusion flow rate. Isolated kidneys are driven either in the single-path mode, in which the perfusate goes through the kidney a single time or in the recirculation mode in which the perfusate circuits through the isolated kidney. The advantage of the single-path mode is the requirement of a less-sophisticated experimental setup and the fact that the perfusate entering the kidney via the arterial limb can be kept renin free, so that renin activity appearing in the venous effluate directly reflects secreted renin. The recirculating mode to run isolated kidneys on the other hand allows a more physiological composition of the perfusate what indeed can be relevant for the functional behavior of JGG cells. The perfusate in recirculating system, therefore, contains albumin at physiological concentrations to establish a normal oncotic pressure of the perfusate, as well as red blood cells to maintain sufficient oxygen supply to the kidneys.

Both albumin and red blood cells are normally not used in the single-path mode because of cost reasons. A comparison of both methods reveals that more complex regulations of renin secretion from JGG cells such as the regulation by the perfusion pressure or by the macula densa are better preserved in kidneys perfused with albumin and red blood cells than in those perfused without these constituents.

The isolated perfused kidney model is suitable to study receptor-mediated modulation of renin secretion, regulation of renin secretion by the perfusion pressure, or by the macula densa, as well as the interaction between endothelial cells and JGG cells. The isolated perfused kidney model, however, is still a complex model that provides more indirect conclusions rather than direct information about regulatory events in JGG cells.

1.2.2. Isolated Juxtaglomerular Cells

The most direct approach to study renin secretion at the cellular level is the use of isolated juxtaglomerular granular cells. Methods to isolate JGG cells from mouse and rat kidney have been developed, and basically, these methods comprise a combination of mechanical and enzymatical separation techniques followed by density separation. Those methods allow a significant enrichment of JGG cells in a single-cell preparation, but nonetheless, it must be mentioned

that they always end up with mixed-cell populations containing a variable portion of JGG cells. Those primary isolates can then be used for superfusion experiments, in which freshly isolated JGG cells are packed into superfusion columns ***(6)***. More frequently, however, isolated JGG cells are used for primary culture in which the culture conditions are chosen for maintenance of the cells rather for proliferation ***(7,8)***. Those primary cultured JGG cells can be used to study receptor regulated renin secretion, but also to determine signaling cascades involved in the regulation of renin secretion. As with cell cultures in general, it has to be kept in mind that signaling pathways may get altered in vitro by a change of the expression of key enzymes relevant for the particular signaling pathways. Moreover, JGG cells in primary culture release to the bulk of stored renin within the first days of culture ***(7)***. Renin synthesis as reflected by renin mRNA levels also ceases after a few days and it is assumed that JGG cells transform to vascular smooth muscle cells with ongoing culture. This process of transformation is accelerated under culture conditions that promote cell proliferation, such as a higher content of serum in the culture medium. Therefore, it is reasonable to use primary cultures of JGG cells within the first days after isolation, when they allow to follow renin secretion and also renin synthesis over hours where it is not possible with other in vitro models.

Further attempts have been made to assay renin secretion also from single cultured JGG cells. So far, two approaches have been reported to be successful, namely the hemolytic plaque assay and membrane capacitance measurements of single JGG cells. Whereas the normal procedure to measure renin secretion from cultured JGG cells utilized the measurement of the renin activity in the cell culture supernatant and thus reflects overall renin secretion from all JG cells in a culture dish, allows the hemolytic plaque assay to determine simultaneously renin secretion from several individual JGG cells of a culture dish. To this end, primary cultures of JG cells are incubated with sheep erythrocytes coated with antigamma-globulin. In addition, renin-antibodies are added to the culture medium. In the vicinity of renin-secreting cells, halos of renin antibodies form, which then react with the erythrocytes to lyse them. Consequently, an erythrocyte-free zone develops around each renin-secreting cell the size of the halo being dependent on the amount of renin secreted ***(9,10)***. This method, however, is rather sophisticated and it is, therefore, not frequently used to study renin secretion from single JGG cells.

Another rather new approach to study renin secretion from single JGG cells is the measurement of single-cell capacitance, which has been established to assay exocytosis from a variety of cells, but primarily from individual mast cells or adrenal chromaffin cells. It was shown recently that this methodological approach is also successful to study secretory events in single JG cells ***(11)***. It should be noted, however, that JG cells cannot be identified by changes of

membrane capacitance and that, therefore, additional efforts are required to assure that a certain cell under investigation is, in fact, a renin-secreting cell. Such a conformation could be achieved, for example, by a single-cell RT-PCR for renin mRNA at the end of the experiments.

In view of the difficult direct accessibility of native renal JG cells, it has also been attempted to generate stable JG cell lines. These attempts were successful as far as a juxtaglomerular cell line from in vivo SV-40 T-antigen transfected mice could be obtained (As 4.1. cell line) ***(13)***. The advantage of this cell line is that it continuously produces renin at a high level and that the cells proliferate well ***(14)***. A major disadvantage of this cell line, however, is that it does not secrete active renin in a regulated fashion and that also the regulation of renin synthesis appears to be different from that seen in native JG cells ***(15,16)***.

2. Materials

2.1. In Vivo Models

1. For determination of plasma-renin activity commercially available assay.
2. Angiotensinogen for determination of plasma-renin concentration.

2.2. In Vitro Models

2.2.1. The Isolated Perfused Kidney

1. Technical equipment for isolated perfused kidneys as illustrated in **Fig. 1** (*see* **Notes 3** and **5**).
2. Animals: rats 250–300 g body weight.
3. Dialysate: Na^+ 140 m*M*, K^+ 5 m*M*, Ca^{2+} 2.5 m*M*, Mg^{2+} 1.2 m*M*, Cl^- 104 m*M*, HCO_3^- 25 m*M*, HPO_4^{2-} 0.72 m*M*, urea 6 m*M*, glucose 8.3 m*M*, polyfructosan 1 g/L, oxalacetate 1 m*M*, pyruvate 2 m*M*, L-lactate 2 m*M*, glutamate 2 m*M*, methionine 0.5 m*M*, alanine 2 m*M*, serine 2 m*M*, glycine 2 m*M*, arginine 1 m*M*, proline 2 m*M*, isoleucine 1 m*M*, aspartic acid 3 m*M*, Antidiuretic hormone 10 mU/mL. Ampicillin 30 mg/L and floxacillin 30 mg/L are added to inhibit possible bacterial growth in the medium.
4. Perfusion medium: Dialysate supplemented with 60 g/L bovine serum albumin (BSA) and freshly washed human erthroycytes at a final hematocrit of 5–10% (*see* **Note 4**).

2.2.2. Isolated Juxtaglomerular Cells

1. Animals: C57BL6 mice 4–6 wk old.
2. Buffer solution 1: 130 m*M* NaCl, 5 m*M* KCl, 2 m*M* $CaCl_2$, 10 m*M* glucose, 20 m*M* sucrose, 10 m*M* tris(hydroxymethyl)aminomethane hydrochloride, pH 7.4.
3. Collagenase, trypsin.
4. Percoll (prepare 30% isosmotic solution with buffer 1).
5. Cell culture medium: RPMI-1640 medium containing 0.66 U/mL insulin, 100 U/mL penicillin, 100 μg/mL streptomycin, and 2% fetal calf serum (FCS).

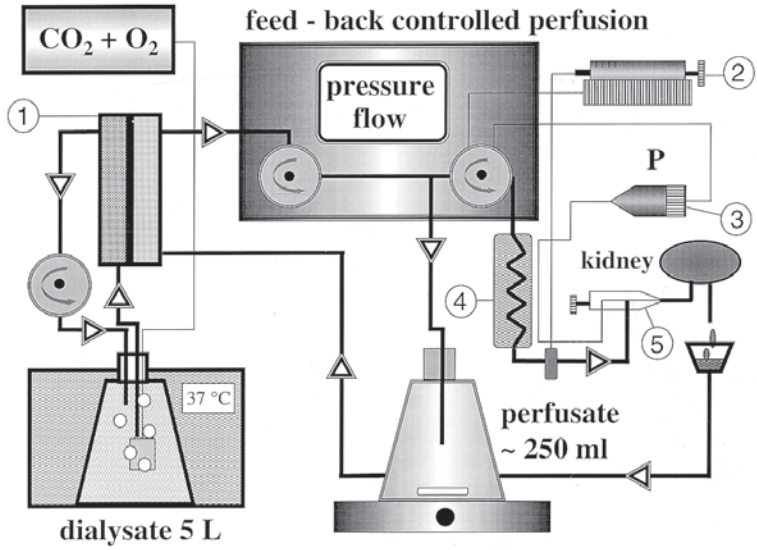

Fig. 1. Experimental setup for perfusing an isolated rat kidney in a recirculating system. Abbreviations: 1. Hemodialyzer. 2. Feedback-regulated perfusor pump for administration of drugs to the perfusion medium. 3. Statham-pressure transducer. 4. Water jacket 37°C. 5. Double-barreled cannula.

6. Plasma of bilaterally nephrectomized rats.
7. Buffer 2: 0.2 mol/L maleate buffer (pH 6.0), 5 mmol/L phenyl methyl sulfonyl fluoride (PMSF), 10 mmol/L ethylenediamine tetraacetic acid (EDTA), and 0.1% gentamycin.

3. Methods

3.1. In Vivo Models

3.1.1. Determination of Plasma–Renin Activity with Commercially Available Assays

In the following section, determination of the plasma–renin activity using an angiotensin I radioimmunoassay (RIA) is described. In principle, in a first step, angiotensin I is generated during an incubation period at 37°C, the amount of angiotensin I being dependent on the amount of active renin in the sample. In a second step, the angiotensin I RIA is performed, which is based on the competition of the angiotensin I in the samples and a radioactive labeled angiotensin I to be assayed for a limited number of angiotensin I antibody-binding sites, which are fixed on the surface of special tubes. After the RIA incubation, the amount of labeled angiotensin I bound to the antibodies is inversely related to the amount of angiotensin I in the sample.

1. Collect blood samples in prechilled tubes with EDTA as an anticoagulant (*see* **Note 1**).
2. Keep samples at 4°C and centrifuge them at 2000*g* to recover the plasma. If the assay is not performed immediately, samples should be stored at –20°C in aliqouts of 500 µL.
3. Put generation tubes containing aliquots of 500 µL of the sample in an ice bath and add 10 µL PMSF; (enzymatic inhibitor, inhibits the degradation of angiotensin I in the sample) and 50 µL generation buffer (EDTA-potassium-phosphate-buffer, adjusts pH to 6.0 for a higher sensitivity for low-renin-activity samples [*see* **Note 2**]). After mixing, two aliquots of 200 µL each are transferred into generation tubes.
4. One of these tubes is incubated at 37°C while the other one remains in the ice bath (sample blanks). After 90 min, the incubated tube is immediately placed in the ice bath as well.
5. Transfer 50 µL of each sample and also of each blank in an angiotensin I antibody-coated tube and add 500 µL of ^{125}J-labeled angiotensin I. After mixing, an incubation period at room temerature ranging from 3 to 24 h follows.
6. After the incubation period, the content of the tubes is aspirated and the radioactivity of the tubes is measured.
7. As standards with fixed concentrations of angiotensin I are supplied with the kit, a calibration curve can be obtained. Using this curve, the plasma–renin activity can be determined by interpolation.

3.2. In Vitro Models

3.2.1. The Isolated Perfused Kidney (according to Schurek and Alt [4]); Fig. 1

1. Rats are anesthetized with 150 mg/kg of 5-ethyl-(1'-methyl-propyl)-2-thiobarbituric acid (Inactin) and a catheter is inserted into the jugular vein. Volume loss during the following surgical preparation is substituted by intermittent injections of physiological saline via this catheter.
2. The abdominal cavity is opened by a midline incision and the right kidney is exposed and placed in a thermoregulated metal chamber.
3. The right ureter is cannulated with a small polypropylene tube (PP-10), which is connected to a larger polyethylene catheter (PE-50).
4. After intravenous injection of heparin (2 U/g) via the jugular vein catheter, the aorta is clamped distal to the right renal artery and the large vessels branching off the abdominal aorta are ligated. A double-barreled cannula (for perfusion and for pressure measurement) is inserted into the abdominal aorta distally of the clamp and is placed close to the origin of the right renal artery. After ligation of the aorta proximal to the right renal artery, the aortic clamp is quickly removed and perfusion is started *in situ* with perfusate (without red blood cells) with an initial flow rate of 8 mL/min.
5. The right kidney is then excised and perfusion at constant pressure (100 mmHg) is established. For this purpose, the renal-artery pressure is monitored through

the inner part of the perfusion cannula (Statham Transducer P 10 EZ) and the pressure signal is used for feedback control of a peristaltic pump.

6. The perfusion circuit is closed by draining the venous effluent via a metal cannula back into a reservoir (200–220 mL). To this reservoir, freshly washed human blood cells are added to yield a hematocrit of 5–10% (*see* **Note 4**). To improve the functional preservation of the preparation, the perfusate is continuously dialyzed against a 25-fold volume of the same composition as the perfusion medium, but lacking erythrocytes and albumin (*see* **Note 3**). For oxygenation of the perfusion medium the dialysate is gassed with a 95% oxygen, 5% carbon dioxide mixture. Under these conditions, both glomerular filtration and filtration fraction remain stable for at least 90 min at values of about 1 mL/min × g and 7%, respectively.
7. Perfusate flow rates are obtained from the revolutions of the peristaltic pump, which is calibrated before and after each experiment. Renal flow rate and perfusion pressure are continuously monitored by a potentiometric recorder. After establishing the reperfusion loop, perfusate flow rates and renin-secretion rates usually stabilize within 15 min.

Drugs to be tested in their effects on renin secretion can either be added to the dialysate, which requires higher amounts of the substances or can be infused into the arterial limb of the perfusion circuit directly before the kidneys at 3–6% of the rate of perfusate flow with a feed-back triggered perfusor.

For determination of perfusate, renin-activity aliquots (about 0.1 mL) are simulatenously drawn from the arterial limb of the circulation and from the renal venous effluent, respectively. The samples are centrifuged at 1500*g* for 15 min to remove red cells and the supernatants are stored at –20°C until assayed for renin activity. Renin-secretion rates can be calculated from the arterio-venous differences of renin activity and the perfusate flow rate. **Figure 2** shows a representative tracing of renin secretion from an isolated perfused rat kidney, which was stimulated by isoproterenol 30 min after start of the perfusion.

3.2.2. Isolated Juxtaglomerular Cells (according to Della Bruna et al., 1991) ***(Fig. 3)***

Preparation of primary cultures starting with one mouse yielding 20–30 well of a 96-well plate.

1. The mouse (C57BL) is killed by cerival dislocation and the kidneys are aseptically removed.
2. The kidneys are drowned in chilled sterile buffer 1 solution and they should be processed within the next 10 min.
3. The two kidneys are then decapsulated and the papilla is removed. Each kidney is cut into longitudinal halves and the halves are then minced with a scalpel blade to obtain tissue pieces of about about 1-mm^3 size. This should be done under a laminar or horizontal laminar flow bench, and the mincing procedure should not take longer than 5 min.

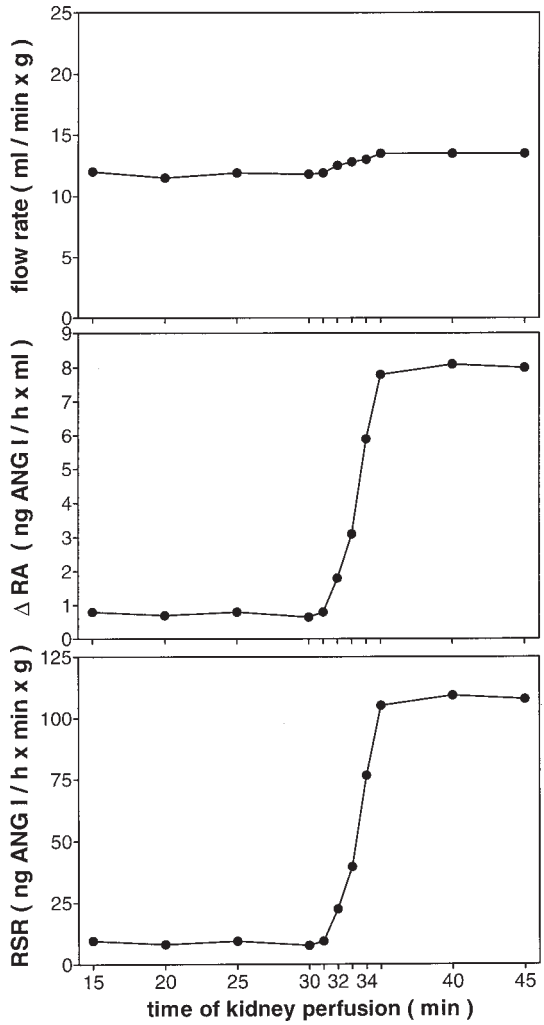

Fig. 2. Representative tracings of perfusate flow rate (at constant pressure of 100 mmHg) (upper panel), difference of renin activity of perfusate between venous effluate and arterial limb (middle panel), and renin secretion rates (lower panel) in an isolated perfused rat kidney. Thirty minutes after start of perfusion, isoproterenol at a final concentration of 10 nmol/L was infused into the perfusion medium at the arterial limb until end of the experiment.

4. The minced tissue of two kidneys is then suspended in a flask containing 30 mL of prewarmed buffer 1, supplemented with 0.25% trypsin and 0.1% collagenase (0.5 U/mg). The flask is kept in a water bath at 37°C and the suspension is gently stirred with a magnetic bar.

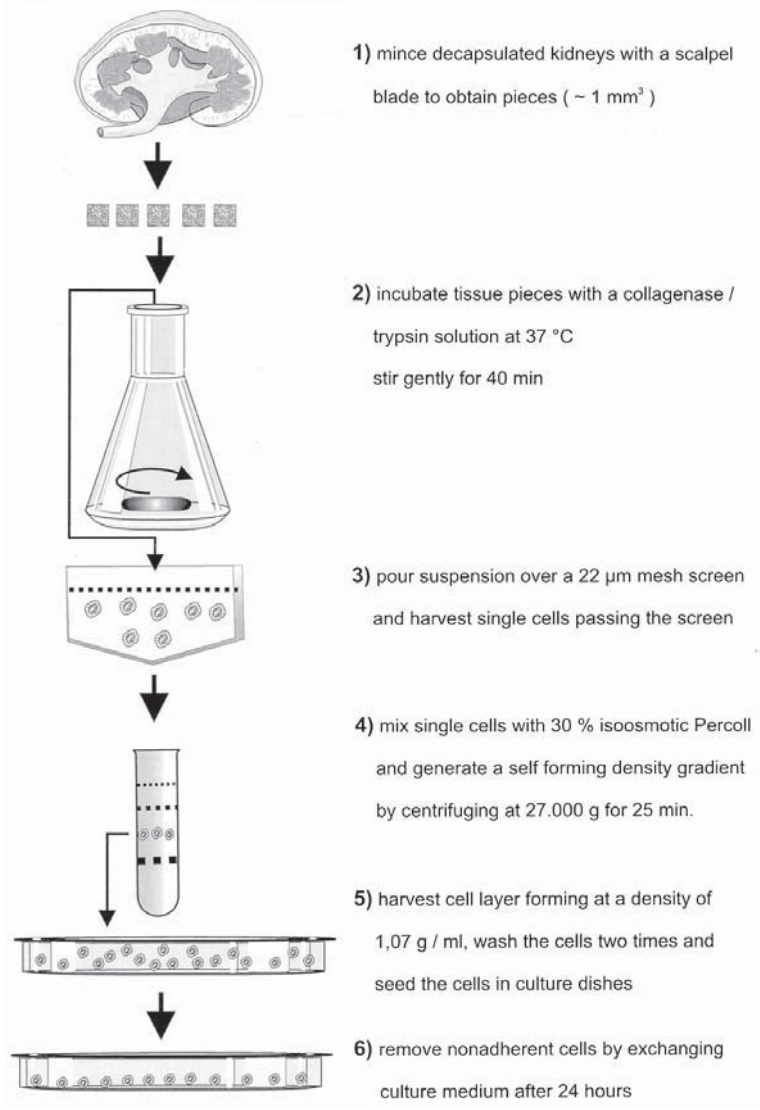

Fig. 3. Scheme summarizing the sequence of essential steps to generate primary cultures of mouse juxtaglomerular granular cells. For more details, see text.

5. After 40 min of incubation the suspension is poured over a 22-µm mesh-nylon screen and single cells passing the screen are collected, washed twice, and resuspended in 4 mL of buffer 1.
6. This volume is then mixed with 56 mL of cold (4°C) 30% isoosmotic Percoll in buffer 1.

7. The Percoll cell suspension is then distributed to two tubes each containing 30 mL and centrifuged at 27,000*g* for 25 min at 4°C.
8. Typically 4 bands with accumulated cells develop in the gradient and the third band from top with a density of 1.07 g/mL is then harvested by aspiration (*see* **Note 6**).
9. These cells are then freed from Percoll by washing in buffer 1.
10. After washing, the cells are resuspended in 3 mL RPMI-1640 medium containing 0.66 U/mL insulin, 100 U/mL penicillin, 100 μg/mL streptomycin, and 2% FCS.
11. This suspension is then distributed in 100-μL aliquots into 96-well plates. The cultures are incubated at 37°C in humidified atmosphere containing 5% CO_2 in air.
12. After 24 h of primary culture, the culture medium is throughly removed, and the cultures are carefully washed once with 100 μL RPMI-1640 medium containing 2% FCS to remove all nonadherent cells (*see* **Note 7**).
13. Then, the cultures are ready for experiments on renin secretion. The experiments are started by adding 100 μL of fresh and prewarmed culture medium together with the chemicals of interest.
14. At the end of the experiments, the cell-conditioned supernatants are collected and centrifuged at 1000*g* at room temperature to remove detached cells. The supernatants are then stored at –20°C until assayed for renin activity.
15. The sediment is resuspended in 100 μL phosphate-buffered saline (PBS) containing 0.1% of Triton X-100, which then are added to the respective culture well to lyse the cells. The culture plates are gently shaken for 45 min at room temperature. The lysed cell material is then stored at –20°C until further processing.

Renin release is estimated from the appearance of renin activity in the cell-conditioned medium. To normalize renin secretion to the amount of cells, the protein concentration in the lysed cell fraction should be determined. An even more robust method to normalize secreted renin to the amount of cells is the calculation of the fractional release of renin. For this purpose, renin activity is not only determined in the cell supernatant, but also in the lysed cell fraction. Renin secretion is then related to the total amount of renin activity in each culture well and is given, therefore, as the fraction of *renin activity released/(renin activity released + renin activity remaining in the cells*). This parameter has turned out as a highly reproducible measure that minimizes differences among different culture wells of the same preparation or between different cell culture preparations ***(12)***. Basal renin release within 20 h should amount to about 15% of the total renin activity.

Renin activity of cell supernatant and cell lysate is assayed by the generation of Ang I from excess substrate (Ang 0). Aliquots of cell supernatant and cell lysate are incubated for 90 min at 37°C with aliquots of diluted plasma of bilaterally nephrectomized rats for 90 min. If predilution of samples is required, they are diluted with the reaction buffer, which consists of 0.2 mol/L maleate buffer (pH 6.0), 5 mmol/L PMSF, 10 mmol/L EDTA, and 0.1% gentamycin.

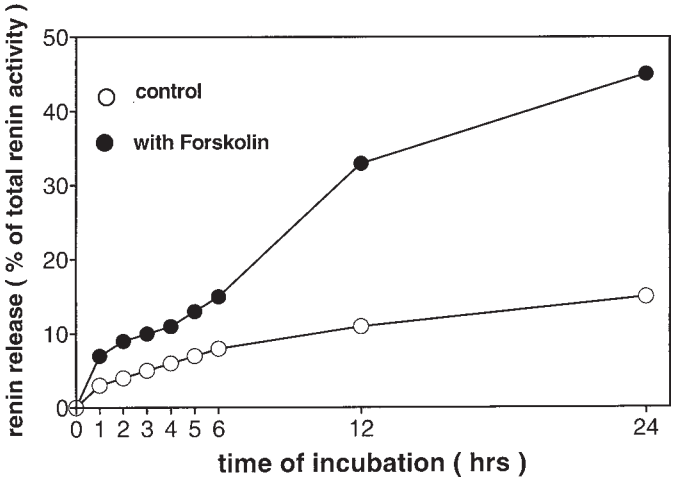

Fig. 4. Representative tracings of renin secretion from primary cultures of mouse juxtaglomerular granular cells. Renin-secretion rates are given as fractional release of renin, as described in the text. Renin-secretion rates are shown for cells under control conditions or under incubation with 10 μmol/L forskolin, an established adenylate-cyclase activator.

After 90 min the reaction is stopped by placing the test tubes in an ice bath. The generated ANGI is determined by a commercially available RIA.

Figure 4 shows representative tracings of renin secretion from cultured mouse JGG cells under basal conditions and under stimulation with the adenylate-cyclase activator forskolin.

4. Notes

4.1. In Vivo Models

1. Do not use heparin as an anticoagulant, as it interferes with angiotensin I generation.
2. Consider that the proteolytic renin activity is pH dependent and that the pH optimum of renin is species specific. It may be necessary, therefore, to modify the pH of the incubation solution provided with the kits for plasma renin activity, which are optimized for human plasma-renin activity.

4.2. In Vitro Models

4.2.1. The Isolated Perfused Kidney

3. To optimize the functional behaviour of the isolated kidneys, it is recommended to use a new hemodialyzer for each kidney.
4. The human erythrocytes should be washed again briefly prior to addition to the perfusion medium.
5. All glassware and tubings coming in contact with dialysate or perfusion medium must be sterilized prior to use.

4.2.2. Isolated Juxtaglomerular Cells

6. Because of clumping of cells in the Percoll gradient, it may be difficult at the beginning to clearly sparate cell layers 2 and 3. It is recommended for the beginner, therefore, to harvest cells of layer 2 also together with the cells of layer 3. With ongoing practice, it will be easier to selecetively harvest cell layer 3 from the gradient.
7. Before the start of the experiments on renin release (i.e., after attachment of the cells for 24 h) it is important to carefully, but nonetheless thoroughly, wash the cultures to remove not only cell debris and nonattached cells, but also to remove renin that has been relased into the medium during the attachment period. Because this released renin activity is rather high, even smaller amounts of remaining cell-culture medium can produce a marked "background" renin activity for the studies on regulated renin release.

References

1. Derkx, F. H., Steunkel, C., Schalekamp, M. P., Visser, W., Huisveld, I. H., and Schalekamp, M. A. (1986) Immunoreactive renin, prorenin, and enzymatically active renin in plasma during pregnancy and in women taking oral contraceptives. *J. Clin. Endocrinol. Metab.* **63,** 1008–1015.
2. Simon, D., Badouaille, G., Pau, B., and Guyene, T. T., Corvol, P., Menard, J. (1987) Measurement of active renin by the 4G1 anti-human renin monoclonal antibody. *Clin. Exp. Hypertens. A* **9,** 1333–1340.
3. Gross, R., Hackenberg, H. M., Hackenthal, E., and Kirchheim, H. (1981) Interaction between perfusion pressure and sympathetic nerves in renin release by carotid baroreflex in conscious dogs. *J. Physiol.* **313,** 237–250.
4. Schurek, H. J. and Alt, J. M. (1981) Effect of albumin on the function of perfused rat kidney. *Am. J. Physiol.* **240,** F569–F576.
5. Scholz, H., Kaissling, B., Inagami, T., and Kurtz, A. (1991) Differential response of renin secretion to vasoconstrictors in the isolated perfused rat kidney. *J. Physiol.* **441,** 453–468.
6. Albinus, M., Finkbeiner, E., Sosath, B., and Osswald, H. (1998) Isolated superfused juxtaglomerular cells from rat kidney: a model for study of renin secretion. *Am. J. Physiol.* **275,** F991–F997.
7. Della Bruna, R., Pinet, F., Corvol, P., and Kurtz, A. (1991) Regulation of renin secretion and renin synthesis by second messenger in isolated mouse juxtaglomerular cells. *Cell Physiol. Biochem.* **1,** 98–110.
8. Della Bruna, R., Pinet, F., Corvol, P., and Kurtz, A. (1995) Opposite regulation of renin gene expression by cyclic AMP and calcium in isolated mouse juxtaglomerular cells. *Kidney Int.* **47,** 1266–1273.
9. Carey, R. M., Geary, K. M., Hunt, M. K., Ramos, S. P., Forbes, M. S., Inagami, T., et al. (1990) Identification of individual renocortical cells that secrete renin. *Am. J. Physiol.* **258,** F649–F659.
10. Everett, A. D., Carey, R. M., Chevalier, R. L., Peach, M. J., and Gomez, R. A. (1990) Renin release and gene expression in intact rat kidney microvessels and single cells. *J. Clin. Invest.* **86,** 169–175.

11. Friis, U. G., Jensen, B. L., Aas, J. K., and Skott, O. (1999) Direct demonstration of exocytosis and endocytosis in single mouse juxtaglomerular cells. *Circ. Res.* **84,** 929–936.
12. Kurtz, A., Kaissling, B., Busse, R., and Baier, W. (1991) Endothelial cells modulate renin secretion from isolated juxtaglomerular cells. *J. Clin. Invest.* **88,** 1147–1154.
13. Sigmund, C. D., Okuyama K., Ingelfinger, J., Jones, C. A., Mullins, J. J., Kane, C., et al. (1990) Isolation and characterization of renin expressing cell lines from transgenic mice containing a renin promoter viral oncogene fusion construct. *J. Biol. Chem.* **265,** 19,916–19,922.
14. Jones, C. A., Petrovic, N., Novak, E. K., Swank, R. T., Sigmund, C. D., and Gross, K. W. (1997) Biosynthesis of renin in mouse kidney tumor As4.1 cells. *Eur. J. Biochem.* **243,** 181–190.
15. Petrovic, N., Kane, C. M., Sigmund, C. D., and Gross, K. W. (1997) Downregulation of renin gene expression by interleukin-1. *Hypertension* **30,** 230–235.
16. Jensen, B. L., Lehle, U., Müller, M., Wagner, C., and Kurtz, A. (1998) Interleukin-1 inhibits renin gene expression in As4.1 cells but not in native juxtaglomerular cells. *Eur. J. Physiol.* **436,** 673–678.

28

Measurement of Regional Blood Flow in the Kidney Using Laser–Doppler Flowmetry

Richard J. Roman, David L. Mattson, and Allen W. Cowley, Jr.

1. Introduction

The study of regional blood flow in the kidney has been fraught with difficulties. Quantitation of perfusion of the inner cortex and medulla of the kidney has been especially challenging to measure because there is no way to directly visualize the large or small blood vessels in these areas. Furthermore, there has been a lack of reliable techniques to measure tissue blood flow in the kidney. In order to appreciate fully the technical demands of measuring changes in regional blood flow within the kidney, it is necessary to first understand the complex structure of the renal microcirculation.

1.1. The Renal Circulation

There are several unique features of the renal circulation that make the determination of regional blood flow a challenge. First, perfusion of the kidney is highly heterogeneous. Tissue blood flows range from 700 mL × min^{-1} × 100 g^{-1} in the renal cortex to around 50 mL × min^{-1} × 100 g^{-1} in the renal papilla ***(1–5)***. Structural differences exist in the microvasculature with each region containing specialized vascular structures that serve the excretory function of the kidney ***(6,7)***. Thus, the renal vasculature not only supplies the metabolic needs of the tissue, but also serves for the ultrafiltration of solutes and water in the glomerulus, uptake of the tubular reabsorbate into the peritubular capillary network, and the preservation of the osmotic gradient in the renal medulla. The renal microcirculation also regulates tubular function by influencing the composition of, and the hydrostatic pressure within, the renal interstitium. The double capillary circulation of the kidney is unique and consists of a high-pressure glomerular capillary bed for filtration arranged in series with a low-

From: *Methods in Molecular Medicine, vol. 51: Angiotensin Protocols*
Edited by: D. H. Wang © Humana Press Inc., Totowa, NJ

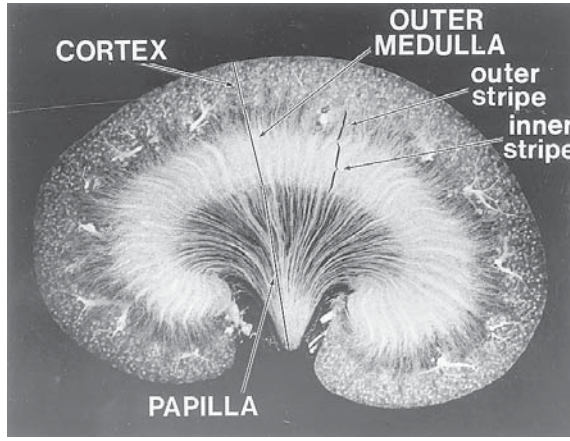

Fig. 1. Silicone rubber (Microfil) cast of the renal vasculature of the rat.

pressure peritubular capillary bed that supplies nutrients and reabsorbs fluid taken up by the renal tubules. All other organs of the body are homogeneously perfused by arteries and veins interconnected by a single capillary bed that supplies the metabolic needs of the tissue.

A latex cast of the renal vasculature of a rat is presented in **Fig. 1.** The perfusion of the kidney can be divided into four zones, i.e., the cortex, the outer stripe of the outer medulla, the inner stripe of the outer medulla, and the papilla (or inner medulla). In the renal cortex, the blood entering the kidney is distributed via the arcuate and interlobular arteries to afferent arterioles and glomerular capillary tufts. The blood leaving glomeruli via efferent arterioles enters a dense peritubular capillary network that supplies the metabolic needs of the cortical tubules. Approx 90% of the renal blood flow remains in the renal cortex and perfuses these dual capillary beds ***(3,6,7)***. However, glomeruli are not homogeneously distributed within the renal cortex and the number of glomeruli per unit volume of tissue decreases from the superficial to the deeper layers of the renal cortex ***(1)***. As a result, cortical blood flow falls from around 700 mL × min^{-1} × 100 g^{-1} of tissue in the most superficial layers of the renal cortex to around 300 mL × min^{-1} × 100 g^{-1} of tissue near the junction of the cortex and the outer medulla ***(1–3)***.

The efferent arteriole of some of the juxtamedullary glomeruli gives rise to the descending vasa recta that supply blood to the outer medulla and the papilla or inner medulla. The vasa recta circulation, which traverses the outer stripe of the outer medulla in vascular bundles, receives less than 10% of the blood flow to the kidney ***(6,7)***. The outer stripe of the outer medulla does not contain many secondary capillary networks, which accounts for the relative avascular appear-

ance of this zone. In the inner stripe of the outer medulla, many of the vasa recta branch and perfuse a dense capillary network that supplies the metabolic needs of the medullary thick ascending loops of Henle. This network, termed the *frizzled zone*, accounts for the pronounced filling of capillaries in the interbundle region in the inner stripe of the outer medulla. Blood flow in this region averages about 200 mL × min^{-1} × g^{-1} of tissue ***(1)***. A fraction of descending vasa recta capillaries continue on and enter the inner medulla. Throughout this region, the descending vasa recta regularly branch and give rise to ascending vasa recta. Only about 10% of the descending vasa recta entering the inner medulla eventually reach the tip of the papilla. As a result, blood flow at the tip of the renal papilla is less than 1% of renal blood flow, averaging between 50–100 mL × min^{-1} × 100 g^{-1} of tissue ***(1,3)***.

Given the diverse nature of the renal circulation and the profound influence that changes in renal hemodynamics may have on the excretion of water and electrolytes, there has been a tremendous amount of interest in defining the influence of angiotensin and other paracrine factors on the intrarenal distribution of blood flow. Many techniques have been applied toward this end including the extraction of indicators secreted by renal tubules, indicator-dilution curves of diffusible substances (H_2, ^{85}Kr, ^{133}Xe, heat), and the accumulation of ^{125}I-albumin, ^{51}Cr-red blood cells, and radiolabeled microspheres in the renal medulla. Blood flow in the vasa recta capillaries at the tip of the papilla has also been studied using videomicroscopy. Each of these methods has been thoroughly reviewed and each is subject to criticisms because of the assumptions required for their use, and the invasive nature of some methods. Furthermore, none of the methods could provide continuous measurements of medullary flow or could be adapted for long-term continuous measurements of blood flow in conscious animals. For this reason, during the late 1970s and early 1980s, work in this area virtually came to a halt because of the limitations in the available techniques for the study of this circulation ***(5,8,9)***. The recent development of laser–Doppler flowmetry has reenergized this field and now provides investigators with a reliable method to quantify changes in regional flow of red blood cells. However, as discussed in this chapter, laser–Doppler flowmetry can only provide valid measurements when used with an appropriate understanding of the underlying principles and limitations of this technology. In the remainder of this chapter, we will outline the principles of laser–Doppler flowmetry, describe protocols for the measurement of regional blood flow in the kidney of anesthetized and conscious rats, and review some of the pitfalls and problems associated with this technique.

1.2. Principle of Laser–Doppler Flowmetry

Laser–Doppler flowmeters operate based on the principle of the Doppler shift of laser light. Coherent laser light emitted at a single wavelength is directed at a

tissue through a fiberoptic source; the reflected light is collected by another fiber and directed at a photodetector. Most of the reflected light is simply scattered and reflected by the tissue and is detected as a DC signal on the output of the photodetector. Only a small fraction of the incident light that interacts with moving red blood cells (RBCs) or other particles in the tissue is shifted in frequency. The magnitude of the frequency shift is proportional to the velocity of the RBCs. Theoretically, this value should be 1 kHz/mm/s and the number of photons shifted in frequency is proportional to the fraction of moving RBC in the illuminated volume of tissue (volume fraction of capillaries in tissue × intravascular hematocrit). The shifted light forms interference bands and can be visualized as a speckle pattern appearing in the tissue. This fluctuating light produces an AC "noise signal" when directed via the fiberoptic probe onto the face of a photodetector. This signal is then analyzed via an analog circuit or digitally as a power spectrum and the total power of the AC signal in the range of frequencies from 0.03 to 20 kHz is taken as the flux of RBCs in the tissue ***(10)***. *See* **Notes 1–3** for discussion of limitations for this technique.

2. Materials

For implanted fibers, see the following.

1. Flowmeter-Perimed model Pf3d (Stockholm, Sweden).
2. Optical fiber Edmund Scientific model F2532 (Barrington, NJ).
3. Optical coupling connectors—Perimed model PF318:2.
4. Silica immersion solution and silica liquid #50350 Cargille Laboratories (Cedar Grove, NJ).
5. Latex epoxy adhesive-FibreGlast Developments (Dayton, OH).

3. Methods

3.1. Method 1—Acute Measurements of Renal Papillary Blood Flow with an Exposed Renal Papilla

It is possible to measure blood flow flux using an optical probe externally directed at the tip of a surgically exposed renal papilla in anesthetized rats. The Munich Wistar rat strain, before the age of 10 wk, possesses a long papilla whose tip extends down into the ureter that can be exposed through a surgical incision of the surrounding ureter. Alternately, the tip of the papilla can be surgically exposed in other rat strains by creating a papillary window. In this technique, a small portion of the overlying cortical tissue is surgically removed about one week before the study so the tissue has time to heal prior to the acute experimental manipulation and measurement of papillary blood flow ***(11)***.

1. For acute studies in our laboratory, rats are anesthetized with ketamine (30 mg/kg, im) and Inactin (50 mg/kg, ip). This combination provides a long-lasting stable

level of anesthesia and does not lower arterial pressure. The rats are then placed on a heated surgical table to maintain body temperature at 36.5°C.

2. Cannulas are placed into the jugular vein for infusions, in the femoral artery for the measurement of arterial pressure, and in the ureter for collection of urine. The rats receive an intravenous infusion of 1% bovine serum albumin (BSA) in a 0.9% sodium chloride solution at a rate of 15 μL/min/100 g throughout the experiment.
3. The left kidney is placed dorsal side up in a holder that is positioned above the abdominal aorta. Making a longitudinal incision in the ureter from the tip to the base of the papilla exposes the papilla.
4. The flux of RBCs in the papilla is measured using a dual channel, Pf3d laser–Doppler flowmeter (Perimed) by shining a large 2.5-mm diameter external fiberoptic laser light probe (Pf 316 or 347) 1 mm from the tip of the papilla. The flux of RBCs in the superficial renal cortex is measured by shining the same probe and instrument combination 1 mm from the surface of the cortex. Typically, the laser–Doppler flow signal is expressed as a percentage change from control taken as the signal measured immediately before an experimental maneuver.

It is very convenient to use Munich Wistar rats for studies in which an external optical fiber is to be used since surgical removal of the overlying cortical portion of the kidney is not required. However, other strains can be used if one creates a papillary window as we have previously described ***(11)***. The amount of renal cortical tissue removed by the surgical window approach is very small and results in no measurable changes of total renal blood flow or glomerular filtration rate ***(11)***. Both approaches enable the use of a large external integrating probe that records from such a large area that the reading is almost positionally independent in both the renal cortex and the papilla. It should also be recognized that this is the only method that allows one to compare the absolute values of flow signals between different groups of rats. Moreover, we have reported that these values are highly correlated to levels of cortical and medullary blood flow measured using an electromagnetic flowmeter and the accumulation of radiolabeled RBCs in the papilla, respectively. A comparison of blood flow measured by laser–Doppler flowmetry (LDF) and RBC flow measured by the accumulation of ^{51}Cr-labeled RBCs in the papilla of young and old rats showed a strong correlation reported between these two independent methods. This demonstrated that LDF provides a useful method to measure blood flow in the kidney. This approach has been successfully used to measure differences in the blood flow in the renal cortex and papilla between different groups of animals. The major limitation to this approach is that blood flow cannot be measured in the inaccessible regions of the deep renal cortex and outer medulla. Furthermore, the use of large optical probes precludes the fine mapping of discrete ischemic areas.

3.2. Renal Cortical and Medullary Blood Flow Measurements with Acutely Implanted Optical Fibers in Anesthetized Rats

1. To measure blood flow in inaccessible regions of the kidney (the deep cortex and outer medulla) by LDF, small diameter optical fibers were implanted into these, and other regions of the kidney in anesthetized rats as reported in several studies from our laboratory ***(12–16)***.
2. The implanted fibers consisted of 500-μm diameter fiberoptic strands (Mitsubishi Cable American, NY) interfaced with a Perimed model 318A external probe designed for this application. The loss of light at the connection between the implanted optical fiber and the external probe is minimized by introducing fused silica matching liquid into the connection (no. 50350; Cargille Laboratories).
3. The optical fibers are implanted to the proper depth in the kidney by passing the fiber through a small hole in the renal capsule made with a 25-gage needle. A small amount of cyanoacrylic glue is then used to hold the fiber and seal it onto the renal capsule. Though the depth of insertion of the optical fiber into the renal tissue is variable depending on the size of the animal, fibers are typically implanted 1 mm deep to measure superficial cortical blood flow, 3 mm to measure deep cortical flow, 5 mm to measure changes of outer medullary blood flow (the so-called red medulla), and 7 mm beneath the surface to measure changes in inner medullary flow (the white medullary region).
4. It is important that the fibers are inserted perpendicular to the flow in the renal papilla in order to avoid the obstruction of flow in vasa recta capillaries that moves along the long axis of the papilla.
5. Alternatively, a number of investigators have used needle probes 0.3–0.5 mm in diameter to measure flow in different regions of the kidney. Our experience with these probes has not been favorable in that the tissue tends to continue to bleed and these probes tend to be very positional-dependent. We find that there is minimal bleeding following the insertion of plastic fiberoptic probes. Because the region from which tissue blood flow is measured is the undisturbed tissue beyond the tip of the fiber, it appears that the implantation of the fiber does not significantly alter the regional renal blood flow and the minimal tissue damage along the fiber track produces no measurable change in total renal blood flow or glomerular filtration rate.
6. At the end of each experiment, the location of the implanted fibers is confirmed and the extent of any injury is assessed by dissecting the kidney and examining the regions surrounding the fiber. Once this technique is mastered, it is unusual that experiments have to be excluded based on incorrect positioning of the fiber or because of tissue damage or occlusion of blood flow in the recorded area or excessive bleeding.

The advantage of the implanted optical fiber approach is that it is relatively simple and provides reliable measures of changes in flow to regions of the kidney that are otherwise inaccessible. The probes are small enough so that

this technique has been successfully applied for studies in the mouse kidney *(17)*. However, it should also be recognized that because the implanted fibers measure flow in only a small and discrete location, it is necessary to design studies in which paired measurements are made (control and experimental) in the same animal. It is not possible to compare the absolute flow signal measured by these probes between groups of animals (*see* **Note 1**).

Examples of renal inner medullary blood flow measurements obtained with implanted optical fibers for LDF and vasa recta capillary RBC velocity measurements in different groups of anesthetized rats are illustrated in **Fig. 2**. These data were obtained from separate groups in which blood flow and RBC velocity were measured during two control periods, two experimental periods, and two post-control periods in rats infused with AVP (2 ng/kg/min) or the vasopressin V1 receptor agonist [Phe^2, Ile^3, Orn^8]AVP (2 ng/kg/min). These data clearly demonstrate that the relative changes in blood flow measured with implanted optical fibers for LDF in the renal inner medulla are consistent with the changes measured in separate groups of rats using videomicroscopy techniques *(13)*. Further examples of the utility of the implanted optical fiber technique are presented in **Fig. 3** in which the relationship between renal perfusion pressure and the relative changes in superficial cortical blood flow, deep cortical blood flow, outer medullary blood flow, and inner medullary blood flow are depicted *(12)*. Through the use of the implanted optical fibers, changes in the differential regulation of blood flow in previously inaccessible regions of the kidney can be easily measured during different experimental maneuvers**.**

3.3. Chronic Measurements of Regional Renal Blood Flow in Conscious Rats with Implanted Optical Fibers for LDF

The data described above demonstrate the utility of the implanted fibers for measurements in anesthetized animals. We have recently adapted this technique for use in conscious rats for periods of days to weeks following fiber implantation *(18–20)*.

1. Rats were anesthetized with a mixture of acepromazine (5 mg/kg; im) and ketamine (50 mg/kg; im). The femoral artery and vein were cannulated for measurement of arterial pressure and for delivery of intravenous solutions, respectively.
2. A left flank incision was used to expose the kidney and optical fibers were inserted in the caudal pole of the kidney. The tip of the superficial cortical fiber is implanted to a depth of 2 mm in the renal cortex whereas the medullary fiber is inserted to a depth of 5 mm into the medulla. As shown in **Fig. 4** the medullary fiber is placed nearly perpendicular to the direction of vasa recta capillary flow to ensure that the flow is measured in a region of the papilla in which inflow and outflow of blood in the vasa recta capillaries is undisturbed.

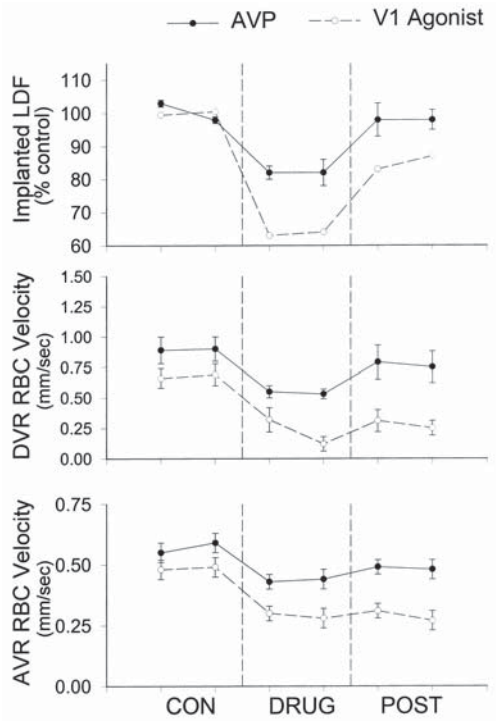

Fig. 2. The top panel of this figure compares the flow response of the renal inner medulla (top panel) as measured by laser–Doppler flowmetry (implanted LDF) to an iv dose of arginine vasopressin (AVP; 2 ng/kg/min) and a vasopressin V1 receptor agonist (V1 Agonist; 2 ng/kg/min) in the rat. Note that the changes in the laser–Doppler signal correspond to the RBC velocity in the descending vasa recta (DVR; middle panel) and the ascending vasa recta (AVR; bottom panel). Data regraphed from **ref. *13***.

3. Both fibers are secured at the point of entry on the surface of the kidney with cyanoacrylate glue around the edge of a latex washer that encircles the fibers at a predetermined distance from the tip of the fibers. The fibers were then anchored to the surrounding back muscles and subsequently tunneled to the neck where they were secured as they were exteriorized at the back of the neck.
4. The fibers and the catheters were then passed through a spring that was brought out the top of the home cage and attached to a swivel device to provide the rat with unrestricted movement. Animals are given 6–10 d to recover from surgery before a study.
5. The optical fibers are constructed from a single model plastic optical fiber (model F2532) purchased from Edmund Scientific.
   a. The fibers were cut with a sharp razor blade to a length of 25 cm. It was determined by microscopic inspection that special polishing of the cut fiber is not necessary in these types of experiments.

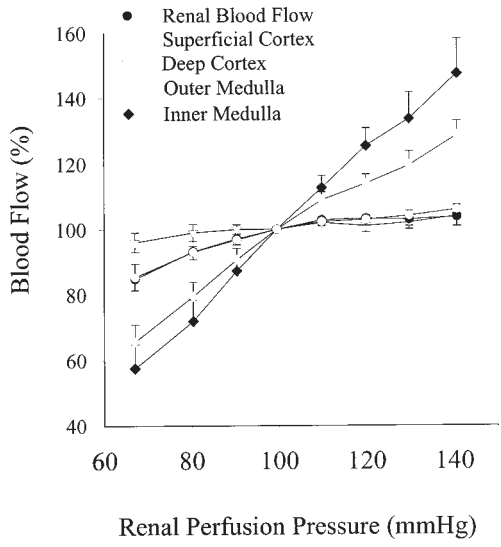

Fig. 3. The relationship between renal perfusion pressure blood flow is depicted for the whole kidney (renal blood flow) and four regions of the kidney in the volume expanded rat. Measurements in the superficial cortex were made using an external laser–Doppler flow probe while measurements in the deep cortex, outer medulla, and inner medulla were made using implanted fibers for laser–Doppler flowmetry. Measurements were made in groups of rats with 5–7 rats/group. (Reprinted with permission from **ref. *12***.)

b. One end of the fiber was shaped over heat to have a 180° curve with a radius of 1 cm using a heat gun. A low level of heat is applied to create the required bend, but not to destroy the external fiber cladding that is required to maintain the internal reflective integrity of the fiber. This configuration of the fiber stabilizes the fiber as the rats move and prevents it from being pulled out of the kidney.
c. Both fiber tips are pushed through a small circular piece of latex (5-mm diameter; latex surgical glove material) leaving one tip protruding 2 mm and the other protruding 5 mm.
d. The fibers are secured to the latex with epoxy adhesive (FibreGlast Developments). The external portions of the fibers not implanted into the kidney are sheathed with silastic tubing (0.03 in id and 0.065 in od; Dow Corning, Midland, MI). This minimizes damage to the external cladding of the fiber from abrasions especially as the fiber runs through the spring and swivel assembly that protects the fiber from the animal.
e. Before implantation of any fiber, the flow signals from the laser–Doppler flowmeters and their external master probes are normalized by placing the probes into a motility standard solution consisting of a 1% suspension of 10-μm latex beads and adjusting the outputs to read a flux value of 2.5 V and a red cell

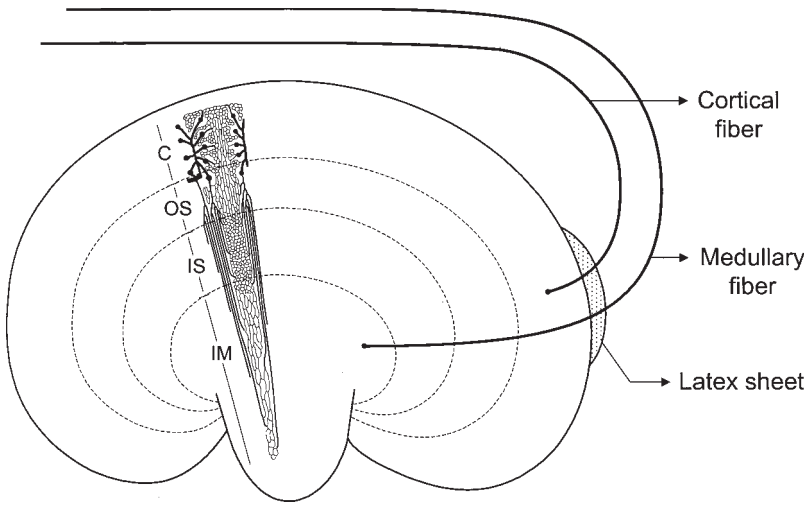

Fig. 4. Diagram showing the orientation of the implanted fibers used for the chronic measurement of CBF and MBF in the conscious rat.

fraction output of 7.5 V. The optical fibers are then connected to the master probes with the outputs from the total-coupled probe system (optical fiber connected to the master probe) checked in the same motility standard solution.

f. Only fibers in which the output signal remains above 2.3 and 7.3 V are suitable for an experiment. Anything less indicates loss of light or optical coupling and the fiber should be discarded. This approach ensures that the optical coupling to the probe and outputs of the flowmeters are standarized so that differences in the output between should reflect differences in tissue perfusion rather than differences in optical properties of the instruments and probes. It should also be recognized that the current digital design of commercially available laser-Doppler flowmeters do not allow for any type of adjustable calibration of the output signals from the flowmeters that was possible with the the last of the analog instruments (model PF3, Perimed).

6. Following recovery from surgery, the instrumented rats need to be trained for about 1 wk to rest quietly in a tubular Plexiglas restrainer. Although movement artifacts are detected, measurement of regional blood flow with the rats restrained in these tubes, minimizes these low-frequency flow spikes sufficiently enough that it is relatively easy to measure small changes in tissue blood flow. Movement artifacts are also easy to recognize in a record as large, low-frequency spikes in the records that can easily be removed by manual examination of the record or with simple computer algorithms that filter the data.
7. We typically measure cortical and medullary blood flow signals simultaneously in a given animal by connecting the exteriorized ends of the implanted fibers to the master probes using optical coupling connectors (model PF 318:2, Perimed).

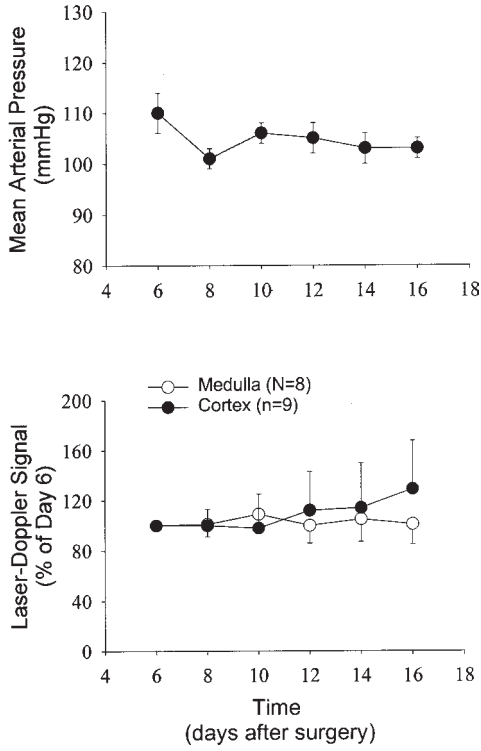

Fig. 5. The stability of the daily recordings of cortical and medullary blood flow obtained from the implanted fibers in conscious rats is shown in the lower panel. The laser–Doppler blood flow signal is presented as a percent of the control flow signal measured on day 6 following surgery. Each point represents the mean and standard error from 8–9 rats. The top panel shows the stability of blood pressure. (Reprinted with permission from **ref. *18***.)

A drop of a silicon immersion fluid (Cargille Laboratories) is used at the interface of the connection for complete optical matching.

The reproducibility of the flow signals was originally evaluated in nine rats. Average flow signals were obtained on alternative days from the implanted cortical and medullary fibers and it found the coefficient of variation of the flow signals recorded on six different days was 6% for the cortical fibers and 8.5% for the medullary measurements. No significant difference among any of the days of recording were found in the baseline flow signals recorded with either the cortical or medullary fibers between days 6 and 16 (**Fig. 5**; ***18***). The minimal detectable changes calculated with data obtained from 14 rats were 1% and 8% for cortical and medullary measurements, respectively. To further

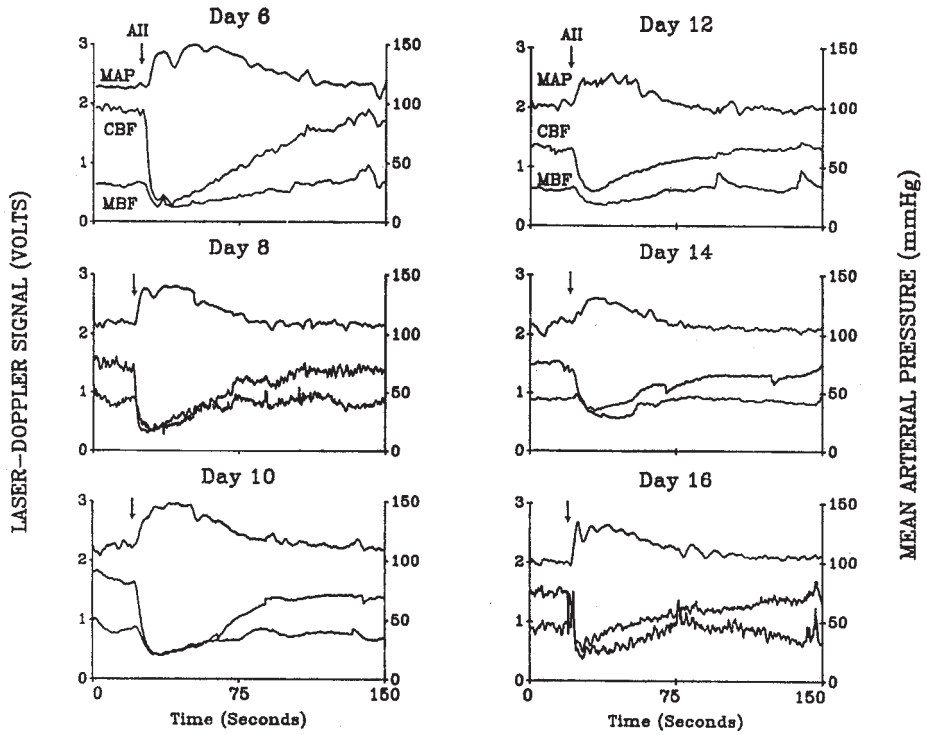

Fig. 6. The reproducibility of the changes in CBF, MBF, and mean arterial pressure (MAP) to a daily bolus iv injection of angiotensin II (AII; 12.5 ng) in a conscious rat is shown. (Reprinted with permission from **ref.** ***18***.)

validate the ability of the implanted fiber technique to quantiate changes in blood flow, the daily blood flow response to a fixed stimulus was examined in the rats. The response in mean arterial pressure (MAP), cortical blood flow (CBF), and medullary blood flow (MBF) following an intravenous bolus of angiotensin II (Ang II; 15 ng) in a single rat on days 6, 8, 10, 12, 14, and 16 following surgery is depicted in **Fig. 6** ***(18)***. This response was similar in all rats with no significant difference detected in the average response on any of the days. It should be recognized that measurements obtained during the first 6 days after surgery are quite variable so that experimental control data cannot be collected for at least 1 wk following surgery (a convenient period for training of the rats).

Having had more than 10 yr of experience with this system, it now appears that the average instrumented rat can be expected to provide functional data for a period of about 1 mo. Thereafter, mechanical stresses upon the fibers together with breakdown of the arterial and venous indwelling catheters results in an increasing unreliable experimental environment. Nevertheless, the use of

implanted optical fibers coupled with LDF provides, at this time, the only method of reproducibly determining sequential changes in regional blood flow in unanesthetized rats. It is a challenging technique (*see* **Notes 1–3**), but it has been successfully utilized for various protocols by eight different investigators in our laboratory ***(19–26)***.

3.4. Applications of LDF in Studying Angiotensin Actions on Regional Blood Flow in the Rat Kidney

1. LDF has been used to determine observed increases in medullary flow acutely with changes in renal perfusion pressure ***(12,27,28)*** and volume expansion ***(29)***.
2. Similarly, we have characterized the responses to various hormone and paracrine factors. In general, acetylcholine, bradykinin, nitric oxide, atrial natriuretic peptide, adenosine, calcium channel blockers, and converting enzyme inhibitors have been reported to increase MBF, whereas Ang II, catecholamines, vasopressin, sympathetic nerve stimulation and inhibitors of nitric oxide synthase, and cyclooxygenase reduce MBF ***(30)***.
3. A number of studies have also examined the changes in renal cortical and MBF seen in spontaneously hypertensive rats (SHR) following treatment with a converting enzyme inhibitor or a calcium antagonist ***(19,31)***. Similarly, blood flow responses to changes in daily sodium intake or L-arginine administration have been studied in Dahl salt-sensitive rats ***(21)***.
4. Previous studies in the dog using microspheres and accumulation of labeled RBCs and albumin have indicated that Ang II has a selective effect to constrict the renal medullary circulation. This lowers renal interstitial pressure, sodium excretion, and blunts the pressure natriuresis relationship. Long-term administration of low doses of Ang II induces sodium-sensitive hypertension in the dog. Moreover, papillary blood flow is reduced in sodium retaining states associated with activation of the renin angiotensin system such as following sodium depletion, heart failure, and AV shunt.
5. With the advent of LDF, many studies were done to determine the role of the renin–angiotensin system in the control of the intrarenal distribution of blood flow in the rat. These studies have shown that the rat responds very differently to Ang II compared to dogs. Converting enzyme inhibitors markedly increase MBF (**Fig. 7**), sodium excretion, and the pressure natriuresis relationship in the rat. However, these effects appear to be mediated by increases in intrarenal levels of kinins rather than Ang II because they can be blocked by kinin B2 receptor antagonists ***(32)***. Moreover, relatively large doses of Ang II are needed to lower MBF, blunt the pressure natriuresis relationship, and promote the development of hypertension in the rat. Thus, the rat seems to be resistant to the renal medullary vasoconstrictor actions of Ang II.
6. The observation that Ang II does not alter blood flow in the renal medulla has been explored in a number of studies. Interestingly, administration of Ang II leads to a decrease in diameter of isolated perfused outer medullary descending vasa recta (OMDVR) ***(33)***. However, administration of Ang II in the isolated, blood-perfused juxtamedullary nephron preparation fails to alter vasa recta diameter ***(34)***. Intravenous infusion of nonpressor amounts of Ang II to anesthe-

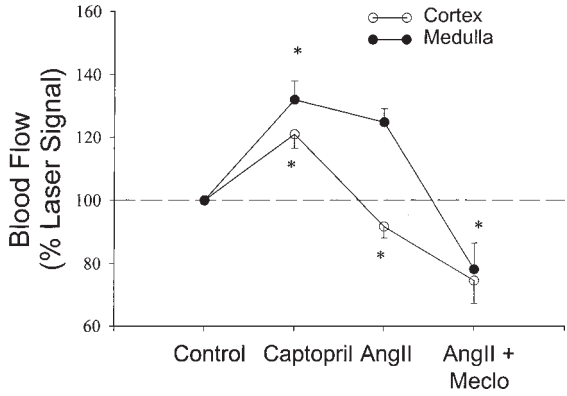

Fig. 7. This figure summarizes the effects of an iv infusion of captopril (2 mg/kg), an infusion of angiotensin II (Ang II; 20 ng/kg/min) and meclofenamate (meclo; 2 mg/kg) on cortical and medullary blood flow in anesthetized rats. The data are expressed as a percent of the control cortical and papillary laser–Doppler blood flow signals. *Indicates significant difference from the value in the preceding period. (Reprinted with permission from **ref. *32***.)

tized rats does not alter renal MBF as measured by LDF (**Fig. 8**, ***15,32***). Ang II decreases renal medullary blood flow if administered concurrently with an inhibitor of prostaglandin synthesis (**Fig. 7**, ***32***) or nitric oxide synthase (**Fig. 8**, ***15,34***). Indeed, coadministration of prostaglandin E_2 blocked the Ang II-induced vasoconstriction in the isolated OMDVR studies. It is possible that vasodilatory agents such as nitric oxide and prostaglandins produced by tubular epithelial or interstitial cells, counteract the vasoconstrictor effects of Ang II in the renal medullary circulation under normal conditions. This may be a protective effect to ensure adequate nutritive flow to the structures of the inner and outer medulla during conditions when Ang II and other vasoconstrictor mechanisms would be activated.

Recently, experiments have been performed to evaluate the potential interaction of Ang II and nitric oxide (NO) in the long-term control of renal CBF and MBF and mean arterial blood pressure in conscious, chronically instrumented rats ***(26)***. Intravenous infusion of a low dose of Ang II (3 ng/kg/min) did not alter renal CBF, renal MBF, or mean arterial pressure under basal conditions. Moreover, a threshold dose of the NO synthase inhibitor L-NAME (75 μg/kg/min) was determined that did not alter renal hemodynamics or blood pressure when infused directly into the renal medullary interstitial space during short- or long-term studies in conscious rats. The coadministration of intravenous Ang II (3 ng/kg/min) with renal medullary interstitial L-NAME (75 μg/kg/min), however, led to a significant decrease in MBF after 20 min of infusion that was sustained during a 5-d infusion protocol (**Fig. 9**). The 30% decrease in renal

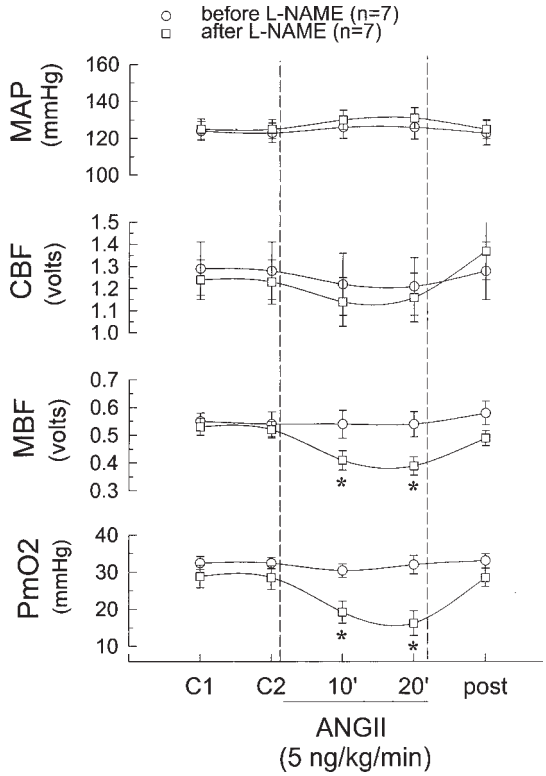

Fig. 8. The response of mean arterial pressure, CBF and MBF (measured by LDF), and medullary tissue oxygen to an iv infusion of angiotensin II (Ang II) in the presence of L-NAME (closed circles) and absence of L-NAME (closed circles) in anesthetized rats. C1 and C2 are control periods and post is the postcontrol period. *Indicates significant difference from control. (Reprinted with permission from **ref. *15***.)

MBF occurred despite no detectable change in renal CBF and was accompanied by a 20-mmHg increase in mean arterial blood pressure. These data in conscious rats indicate that NO synthase provides a potent buffering system in the renal medulla to oppose the vasoconstrictor actions of Ang II that would normally result in hypertension.

4. Notes

1. The advantage of LDF for measuring regional blood flow in the kidney is that it provides a continuous measurement of blood flow in discrete areas of tissue (approx 1 mm^3) and it is relatively noninvasive. As discussed below, the technique can be used to measure tissue blood flow in both acute and chronic studies. It can respond to very small changes in regional capillary RBC density, velocity,

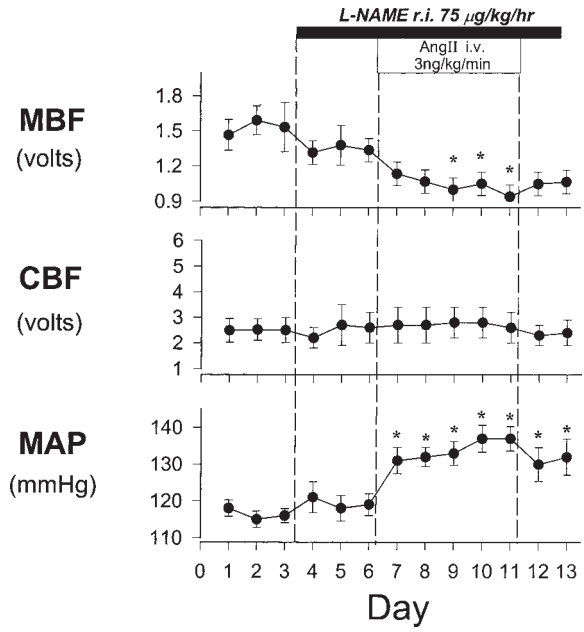

Fig. 9. Average daily responses to chronic iv infusion of angiotensin II (Ang II; 3 ng/kg/min) for medullary flood flow (MBF) and cortical blood flow (CBF) measured by LDF in conscious rats. L-Name was given into the renal interstitium (r.i.) before and during the Ang II infusion. *Indicates significant differences from L-NAME control period. (Reprinted with permission from **ref. *26***.)

and flux ***(29,35)***. The major limitation of this technique is that it has not been possible to calibrate the Doppler flow signal to obtain an absolute measure of blood flow in different tissues ***(8,9)***. This is in part because of the fact that there is no gold standard method for measuring tissue blood flow in the kidney that can be used to calibrate the laser–Doppler flowmeter signal. This has limited the use of these instruments to making paired measurements of changes in blood flow at fixed locations in different regions of the kidney.

2. Another technical problem is that the blood flow signal is highly dependent on probe geometry. With smaller probes, the orientation of the probe to the tissue must be considered. In general, larger probes record from a larger volume of tissue and detect a higher total flow signal. Some manufacturers, notably analog instruments from Perimed Corporation have recognized this and provided a simple in vitro flow standard and an adjustable gain so the flow signal from different probes can be normalized. This allows for some consistency in readings between instruments and probes. However, most of the newer digital-based instruments do not have adjustable gains and provide outputs that are probe and instrument dependent. This problem needs to be addressed in the design of future

instruments and seriously limits the usefulness of these instruments. For example, investigators often measure CBF with a larger probe and MBF using a needle electrode and try to compare the relative signals in both circulations or even the percentage change in flow in both regions. However, if the large diameter and small diameter probes are placed in the same standard solution or directed at the same location on the renal cortex of a rat, the larger probe would record from a larger area and would also record a much higher flow. Obviously, the flux per unit volume of illuminated tissue or standard is not different and the readings from the two instruments cannot be compared. Moreover, there is no assurance that the linear range of the two instruments or even the percentage change in flux signal is recorded by the two probes is linearly related to one other. This becomes a practical problem when, as is typically done, one compares the percentage change in flow in different regions of the kidney to instruments and probes that have not been normalized. For this reason, most of our work has been done with the older PF3d Perimed laser–Doppler flowmeters that have been modified to provide an adjustable output gain that allows for normalization and standarization of the flow signal between instruments and probes.

3. Another major limitation of this technology that is not widely recognized is the potential complication of multiple scattering. Laser–Doppler flowmeters are based on the assumption that the bandwidth of the backscattered laser light broadens in proportion to the mean velocity of RBCs and that the amplitude of the signal is proportional to the number of moving blood cells in the tissue ***(10,35)***. These assumptions are correct if the fraction of RBCs in tissue is small in proportion to the total volume of tissue. However, in the renal circulation, the volume fraction of RBCs in tissue ranges from 2% to 5%, which exceeds the range of volume fractions in which these instruments are linear. At these higher RBC fractions, there is a high likelihood that the incident photons will interact with more than one moving RBC before being reflected back to the photodetector. Under these conditions, changes in the Doppler flow signal underestimate RBC flux because of multiple scattering. This is analogous to the nonlinearity introduced in absorbance measurements at high solute concentrations. Practically, this means that every instrument and probe combination has a different linear range over which the instruments act as a tissue flowmeter. Outside of this linear range, the instruments will produce a signal proportional to changes in mean RBC velocity, but they will be unable to detect increases in RBC number and underestimate changes in tissue red cell flux. This can lead to serious errors in the interpretation of experimental results. It is imperative that each investigator provide some evidence that the particular instrument and probe combination responds to RBC flux over the range of tissue hematocrits expected in a given experimental preparation.
4. A final problem is that there are now four different manufacturers of these instruments, which differ in design and principle with no accepted standards by which to compare readings from one instrument to another. Most investigators try to overcome this problem by presenting the results as percent change from control with the probe localized in a fixed location. However, this limits comparisons

between studies and may lead to false conclusions when comparing relative changes in blood flow in the renal cortex and medulla in which the tissue hematocrit and optical properties of the tissue differ greatly. Moreover, the frequency response and linear ranges of the instruments differ greatly. In some instruments using small fibers, the flow signals are very positional and probe dependent. Most of the newer digital instruments offer no way to standardize the output between probes and do they not provide the same reading when recording from the same location on a relatively homogenously perfused organ such as the renal cortex. These problems and misuse of the instruments by various investigators have reduced the use of these powerful instruments to paired measurements on a single spot before and after an experimental maneuver. It should be recognized, however, that if there was a universal acceptance of an appropriate flow standard for probes and instruments this technique would be able to provide output signals that are highly reproducible between laboratories and proportional to the absolute level of blood flow in different regions of the kidney between animals.

In summary, the recent development of the LDF has provided a unique tool for the study of regional blood flow in the kidney. Despite the theoretical problems associated with measuring blood flow in highly perfused tissue, several studies have indicated that the laser–Doppler flow signals obtained from the cortex and papilla reflect changes in tissue blood flow measured with other techniques. The advantages of the LDF are (1) it provides a continuous index of tissue perfusion; (2) it is noninvasive; (3) cortical and papillary blood flow can be measured in the same animal; and (4) it allows for intra-animal comparisons of blood flow in different regions of the kidney. The limitations of the technique are that it may underestimate changes in blood flow when hematocrit or the number of perfused vessels changes in the region of interest, because the LDF apparently responds primarily to changes in the velocity of RBC's in highly perfused tissues. Moreover, it has not been possible to obtain an absolute blood flow calibration of the laser–Doppler signal because there are no accepted techniques for measuring regional blood flow in the kidney in tissue volumes comparable to those sampled by the LDF.

References

1. Brenner, B. M., Zatz, R., and Ichikawa, I. (1986) The renal circulation, in *The Kidney* (Brenner, B. M. and Rector, F. C., eds.), W. B. Saunders, Philadelphia, PA, pp. 93–123.
2. Mimran, A. (1987) Regulation of renal blood flow. *J. Cardiovasc. Pharmacol.* **10,** 51–59.
3. Cupples, W. A. (1986) Renal medullary blood flow: its measurement and physiology. *Can. J. Physiol. Pharmacol.* **64,** 873–880.
4. Knox, F. G., Ritman, E. L., and Romero, J. C. (1984) Intrarenal distribution of blood flow: evolution of a new approach to measurement. *Kidney Int.* **25,** 473–479.

5. Aukland, K. (1980) Methods for measuring renal blood flow: total flow and regional distribution. *Ann. Rev. Physiol.* **42,** 543–555.
6. Zimmerhackl, B. L., Robertson, C. R., and Jamison, R. L. (1987) The medullary microcirculation. *Kidney Int.* **31,** 641–647.
7. Kriz, W. (1981) Structural organization of the renal medulla: comparative and functional aspects. *Am. J. Physiol.* **241,** R3–R16.
8. Pallone, T. L., Robertson, C. R., and Jamison, R. L. (1990) Renal medullary microciruclation. *Physiol. Rev.* 70, 885–920.
9. Roman, R. J., Carmines, P. K., Loutzenheser, R., and Conger, J. D. (1991) Direct studies on the control of the renal microcirculation. *J. Am. Soc. Nephrol.* **2,** 136–149.
10. Bonner, R. F. and Nossal, R. (1990) Laser Doppler Flowmetry (Shepard, A. P. and Oberg, P. A., eds.), Kluwer Academic, Boston, MA, pp. 17–45.
11. Roman, R. J. and Smits, C. (1985) Laser-Doppler determination of papillary blood flow in young and adult rats. *Am. J. Physiol.* **25,** F115–F124.
12. Mattson, D. L., Lu, S., Roman, R. J., and Cowley, A. W., Jr. (1993) Relationship between renal perfusion pressure and blood flow in different regions of the kidney. *Am. J. Physiol.* **264,** R578–R583.
13. Nakanishi, K., Mattson, D. L., Gross, V., Roman, R. J., and Cowley, A. W., Jr. (1995) Control of renal medullary blood flow by vasopressin V1 and V2 receptors. *Am. J. Physiol.* **269,** R193–R200.
14. Franchini, K. G. and Cowley, A. W., Jr. (1996) Sensitivity of the renal medullary circulation to plasma vasopressin. *Am. J. Physiol.* **271,** R647–R653.
15. Zou, A-P., Wu, F., and Cowley, A. W., Jr. (1997). Protective effect of angiotensin II-induced increase in nitric oxide in the renal medullary circulation. *Hypertension* **31,** 271–276.
16. Park, F., Zou, A-P., Maeda, C., Szentivanyi, M., Jr., and Cowley, A. W., Jr. (1998) Arginine vasopressin-mediated stimulation of nitric oxide within the rat renal medulla. *Hypertension* **32,** 896–901.
17. Gross, V., Lippoldt, A., Bohlender, J., Bader, M., Hansson, A., and Luft, F. C. (1998) Cortical and medullary hemodynamics in deoxycorticosterone acetate-salt hypertensive mice. *J. Am. Soc. Nephrol.* **9,** 346–354.
18. Lu, S., Mattson, D. L., Roman, R. J., Becker, C. G., and Cowley, A. W., Jr. (1993) Assessment of changes in intrarenal blood flow in conscious rat using laser-Doppler flowmetry. *Am. J. Physiol.* **264,** R578–R583.
19. Lu, S., Mattson, D. L., and Cowley, A. W., Jr. (1994) Renal medullary captopril delivery lowers blood pressure in spontaneously hypertensive rats. *Hypertension* **23,** 337–345.
20 Mattson, D. L., Lu, S., Nakanishi, K., Papanek, P. E., and Cowley, A. W., Jr. (1994) Effect of chronic renal medullary nitric oxide inhibition on blood pressure. *Am. J. Physiol.* **266,** H1918–H1926.
21. Miyata, N. and Cowley, A. W., Jr. (1999) Renal intramedullary infusion of L-arginine prevents reduction of medullary blood flow in Dahl salt-sensitive rats. *Hypertension* **33,** 445–450.

22. Franchini, K. G. and Cowley, A. W., Jr. (1996) Renal cortical and medullary blood flow responses during water restriction: role of vasopressin. *Am. J. Physiol.* **270,** R1257–R1264.
23. Cowley, A. W., Jr., Skelton, M. M., and Kurth, T. M. (1998) Effects of long-term vasopressin receptor stimulation on medullary blood flow and arterial pressure. *Am. J. Physiol.* **275,** R1667–R1673.
24. Gross, V., Kurth, T. M., Skelton, M. M., Mattson, D. L., and Cowley, A. W., Jr. (1998) Effects of daily sodium intake and angiotensin II upon cortical and medullary renal blood flow in conscious rats. *Am. J. Physiol.* **274,** R1317–R1323.
25. Nakanishi, K., Mattson, D. L., and Cowley ,A. W., Jr. (1995) Role of renal medullary blood flow in the development of L-NAME hypertension in rats. *Am. J. Physiol.* **268,** R317–R323.
26. Szentizvanyi, M., Jr., Maeda, C. Y., and Cowley, A. W., Jr. (1999) Local renal medullary L-NAME infusion enhances the effect of long-term angiotensin II treatment. *Hypertension* **33,** 440–445.
27. Roman, R. J., Lombard, J. H., Cowley, A. W., Jr., and Garcia-Estan, J. (1988) Pressure-diuresis in volume-expanded rats: cortical and medullary hemodynamics. *Hypertension* **12,** 168–176.
28. Cowley, A. W., Jr., Mattson, D. L., Lu, S., and Roman, R. J. (1995). The renal medulla and hypertension. *Hypertension* **25,** 663–673.
29. Fenoy, F. J. and Roman, R. J. (1991) Effect of volume expansion on papillary blood flow and sodium excretion. *Am. J. Physiol.* **260,** F813–F822.
30. Roman, R. J. and Zou, A-P. (1993) Influence of the renal medullary circulation on the control of sodium excretion. *Am. J. Physiol.* **265,** R963–R973.
31. Fenoy, F. J., Kauker, M. L., Milicic, I., and Roman, R. J. (1992) Normalization of pressure-natriuresis by nisoldipine in spontaneously hypertensive rats. *Hypertension* **19,** 49–55.
32. Mattson, D. L. and Roman, R. J. (1991) Role of kinins and AII in the renal hemodynamic response to captopril. *Am. J. Physiol.* **260,** F670–F679.
33. Pallone, T. L. (1994) Vasoconstriction of outer medullary vasa recta by angiotensin II is modulated by prostaglandin E_2. *Am. J. Physiol.* **266,** F850–F857.
34. Harrison-Bernard, L. M., Albert, D. F., and Cook, A. K. (1999) Nitric oxide modulation of outer medullary descending vasa recta diameter. *FASEB J.* **13,** A720 (abstract).
35. Nilsson, G. E., Tenland, T., and Oberg, P. A. (1980) Evaluation of a laser Doppler flowmeter for measurement of tissue blood flow. *IEEE Trans. Biomed. Eng.* **27,** 597–604.

29

Measurement of Renal Tubular Angiotensin II

John D. Imig and L. Gabriel Navar

1. Introduction

The proximal tubules play a critical role in providing the kidneys with their ability to regulate body fluid volume and electrolyte composition. One major function is the reabsorption of sodium and other electrolytes which is caused, in part, by angiotensin II (Ang II), a peptide that is made up of eight amino acids. By activating Ang II receptors on both the basolateral and luminal membranes, Ang II serves a major function in determining how the kidney processes sodium. Intrarenally formed Ang II is a paracrine modulator of both renal hemodynamic and tubular transport function ***(1,2)***. Ang II generated in the proximal tubule is uniquely positioned to serve as a selective regulator of tubular transport function ***(2,3)***. Increases in proximal tubule Ang II concentrations stimulate sodium reabsorption and tubular acidification ***(2)***. Intratubular Ang II levels can be regulated independently of the circulating renin–angiotensin system ***(3–5)***. In addition to Ang II, its precursors, angiotensin I and angiotensinogen, are also found in high concentrations in proximal tubular fluid ***(2–4)***. Thus, measurement of proximal tubular Ang II concentrations is requisite for understanding the role of this peptide in the maintenance of fluid and electrolyte balance.

The successful measurement of proximal tubular angiotensin peptides requires lengthy micropuncture protocols and a highly sensitive radioimmunoassay. Although Ang II concentrations in the proximal tubular fluid are in the nanomolar range and much greater than plasma concentrations, proximal tubular sample collections yield only 0.8–1.0 μL per rat. These samples contain only a few femtomoles of total Ang II content and, thus, an assay with the ability to measure these small quantities is required. The Ang II

From: *Methods in Molecular Medicine, vol. 51: Angiotensin Protocols*
Edited by: D. H. Wang © Humana Press Inc., Totowa, NJ

radioimmunoassay is a competitive substrate binding assay. A known amount of radiolabeled Ang II competes with an unknown quantity of the unlabeled sample Ang II for binding sites on an antibody. A specific antibody generated against Ang II and reliable radiolabeled Ang II gives consistent and accurate measurements.

2. Materials

2.1. Pipets and Solutions

1. Glass capillary tubes 0.8 mm × 0.49 mm (type N-51-A) ordered from Drummond Scientific.
2. Chromerge ordered from Fisher Scientific.
3. Siliconizing solution contains 90% Sigmacote SL2 (Sigma Chemical) and 10% ethanol.
4. Artificial tubular fluid contains (in mmol/L) 135 NaCl, 5 KCl, 10 $NaHCO_3$, 1 $MgSO_4$, 1 $CaCl_2$, 1 Na_2HPO_4/NaH_2PO_4 and 4 urea (pH 7.40).

2.2. Antibody and Radioactive Label

Rabbit antiangiotensin II (human) antisera obtained from Phoenix Pharmaceuticals (*see* **Note 1**). Reconstitute lyophilized serum with 50 μL of distilled water for undiluted antiserum. Dilute 1:500 with assay buffer and store at –70°C. The working stock is made by diluting 1 mL of the 1:500 dilution with 9 mL of assay buffer for a 1:5000 antibody dilution. Aliquot 100 μL of the 1:5000 dilution in polypropylene microcentrifuge tubes and store in –20°C freezer.

Monoiodinated ^{125}I-labeled Ang II obtained from Amersham Pharmacia Biotech stored at –20°C (*see* **Note 2**).

2.3. Radioimmunoassay

1. Assay diluent: 50 m*M* sodium phosphate buffer (6.9 g/L NaH_2PO_4~H_2O), 1 m*M* Na_4 ethylenediaminetetraacetic acid (EDTA), 0.25 m*M* thimerosal, and 0.25% heat-inactivated bovine serum albumin (BSA) in ultraprure water. Adjust the pH to 7.4, stir solution and heat at 57°C for 1 h before bringing up solution to final volume.
2. The 10X assay diluent for the charcoal solution is made by dissolving 69 g/L NaH_2PO_4~H2O, 10 m*M* EDTA, and 2.5 m*M* thimerosal in ultraprure water. Adjust the pH to 7.4, stir solution, and heat at 57°C for 1 h before bringing up solution to final volume.
3. Charcoal solution: dissolve 0.01 g/mL dextran and 0.1 g/mL charcoal in 900 μL ultrapure water, 97 μL 10X assay diluent, and 3 μL 30% human albumin solution.
4. Ang II is made as a 2 n*M* (200 fmol/100 mL) solution with assay diluent and frozen at –20°C (*see* **Note 3**).

3. Methods

3.1. Preparing Glass Capillary Tubes

1. Glass capillary tubes are soaked overnight in a beaker containing chromerge.
2. The chromerge is dumped out the next morning and distilled water is continuously run through the beaker for 4 h to rinse the tubes.
3. The glass capillary tubes are placed in a conical tube with a sponge on the bottom. The conical tube is centrifuged for 1–2 min to force all the water in the capillary tubes to the sponge.
4. The glass capillary tubes are then soaked in Sigmacote SL2 siliconizing solution for 1 h.
5. Glass capillary tubes are placed in a plastic vacuum dessicator with a vacuum applied overnight. The glass capillary tubes are now siliconized and ready to be pulled for micropuncture.
6. Glass capillary tubes are pulled by a micropipet puller to a tip diameter of 10–15 μm for a collecting micropipet or 5–6 μm for an injection micropipet and placed in a micropipet storage jar (World Precision Instruments, Sarasota, FL) until the day of the experiment.

3.2. Collection of Tubular Fluid Sample

3.2.1. Animal Preparation

1. Rats are anesthetized with pentobarbital (50 mg/kg *intraperitoneally*) and placed on a thermostatically controlled table to maintain body temperature at 37°C.
2. A tracheotomy is performed and the animals allowed to breath air enriched with oxygen by placing the exterior end of the tracheal cannula inside a small plastic chamber into which humidified 95% O_2 and 5% CO_2 is continuously passed.
3. The left femoral artery is cannulated to allow monitoring of arterial blood pressure with a Statham pressure transducer. The left jugular vein is cannulated to allow for infusion of additional anesthetic and solutions.
4. Isotonic saline (0.9%) containing 6 g/dL bovine albumin is infused intravenously at a rate of 1.2 mL/h during surgery and is switched to an isotonic saline solution containing 1 g/dL albumin for the duration of the experiment.

3.2.2. Proximal Tubular Fluid Collection

1. The left kidney is exposed via a flank incision, freed from surrounding connective tissue, and placed in a plastic cup. An agar wall is built around the kidney to form a saline well.
2. Using a stereomicroscope, a 4–6 μm tip-diameter micropipet containing artificial tubular fluid with fast green stain is lowered to the surface of the kidney with a micromanipulator. The stain is injected into a tubular segment with a microperfusion pump system. A proximal tubule with several surface segments is identified.
3. A collecting micropipet is back-filled with Sudan black-stained castor oil with a blunt 30 gauge needle. The micropipet is inserted into a mid to late proximal tubule segment and a free flow-fluid sample is collected for 10 to 30 minutes.

4. Immediately after collection, the tubular fluid sample is transferred to a constant-bore glass capillary tube and the volume determined with a slide comparator (Gaertner, Chicago, IL).
5. The sample is then quickly transferred into an ice-chilled 1.5–2 mL polypropylene microcentrifuge tube containing 1 mL of 100% high-pressure liquid chromatoghraphy (HPLC)-grade methanol. Three to four proximal tubular fluid samples are obtained from each animal and the samples pooled to yield a total volume of about 1 μL for analysis of Ang II concentrations.

3.3. Processing of Tubular Fluid Sample

Proximal tubular samples are stored at –20°C in methanol until assayed (*see* **Note 4**). The samples are dried overnight in a vacuum centrifuge (Savant, Hicksville, NY) before the start of the assay. The dried residue is reconstituted in 150–300 μL of assay diluent.

3.4. Radioimmunoassay: Checking the Radioactive Label and Antibody

The condition of the radioactive label and antibody should be checked 2 d prior to assaying samples.

1. The radioactive label is prepared in a vial by diluting 35–50 μL I^{125}-Ang II in 2–4 mL of assay diluent.
2. Pipet 100 μL of the radioactive label in a tube and count radioactivity for 3 min with a gamma counter. Radioactivity of 5000 cpm/100 μL of labeled Ang II is optimal for the assay.
3. The working dilution of the antibody (1:5000) is diluted further between 1:50 and 1:300 with assay buffer (*see* **Note 5**).
4. In labeled borosilicate glass tubes (12 × 75 mm) add the amounts of assay buffer, antibody and label indicated in **Table 1** for initial, nonspecific binding and Bo. Vortex tubes and refrigerate at 4°C for 24 h.
5. After the 24-h incubation period, prepare the charcoal solution and take tubes out of the refrigerator.
6. Add 1 mL of assay buffer to the initial tubes and 1 mL of the charcoal solution to the remaining tubes.
7. Centrifuge the borosilicate glass tubes at 2000*g* for 15 min, transfer the supernatant to matching labeled polystyrene plastic tubes, and count radioactivity for 3 min with a gamma counter.
8. Calculate the specific binding for various dilutions of the working antibody stock. The antibody dilution, which yields a 24-h specific binding of 28–33% is used when assaying samples.

3.5. Measuring Tubular Fluid Sample Ang II Concentrations

1. Number and label borosilicate glass tubes (12 × 75 mm). All tubes should be done in triplicate with the exception of one tube per tubular fluid sample.

Table 1
Tube Setup for Ang II Radioimmunoassy

	Assay buffer (μL)	Ang II antiserum (μL)	I^{125}-Ang II label (μL)
Initial	100	50	50
NSB	150	—	50
Bo	100	50	50
Ang II standards	100	50	50
Samples	100	50	50
IRS	100	50	50

2. Serially dilute 0.5 mL of the 2 n*M* (200 fmol/100 μL)Ang II in assay buffer to obtain standards containing 100, 50, 25, 12.5, 6.25, 3.125, 1.56, 0.78, and 0.39 fmol/100 μL.
3. An internal reference standard containing 10 fmol Ang II/100 μL is made up from lyophilized Ang II.
4. In labeled borosilicate glass tubes (12 × 75 mm), add the amounts of assay buffer, antibody and label indicated in **Table 1** for each tube. Vortex and refrigerate tubes at 4°C for 48 h.
5. After the 48-h incubation period, prepare the charcoal solution and take tubes out of the refrigerator.
6. Add 1 mL of assay buffer to the initial tubes and 1 mL of the charcoal solution to the remaining tubes.
7. Centrifuge the borosilicate glass tubes at 2000*g* for 15 min, transfer the supernatant to matching labeled polystyrene plastic tubes, and count radioactivity for 3 min with a gamma counter.

3.6. Analysis of Standard Curve and Samples

1. The ratio of binding to maximum binding (B/Bo) of each standard and sample is corrected for nonspecific binding and expressed as a percentage of maximum binding, and subjected to a log-logit transform (**Table 2**).
2. The Ang II standard values are graphed to produce a standard curve (**Fig. 1**). The detection limit is 0.5 ± 0.1 fmol and is assessed by calculating the maximum binding minus twice the standard deviation. For the Ang II assay, the specific binding averages 35–40% with a nonspecific binding of 1–2%.
3. A regression line through the Ang II standards can be generated by one of several computer programs. Many of these programs can give values for samples or the equation for the regression line can be used to calculate the sample values. Ideally, samples should fall between 15 and 80% of maximum binding (Bo). Proximal tubule samples generally contain 2–16 fmol Ang II depending on the amount of tubular fluid collected.

Table 2
Ang II Radioimmunoassay Standard Curve Results

Ang II fmol	CPM	%B/Bo	LOGIT
0	807	100	
0.39	718	89.0	2.09
0.78	631	78.2	1.28
1.56	561	69.6	0.83
3.125	431	53.4	0.13
6.25	345	42.7	–0.29
12.5	222	27.5	–0.97
25	145	18.0	–1.52
50	84	10.4	–2.16
100	57	7.0	–2.58
200	25	3.1	–3.44
IRS (10 fmol)	282	31.0	–0.80

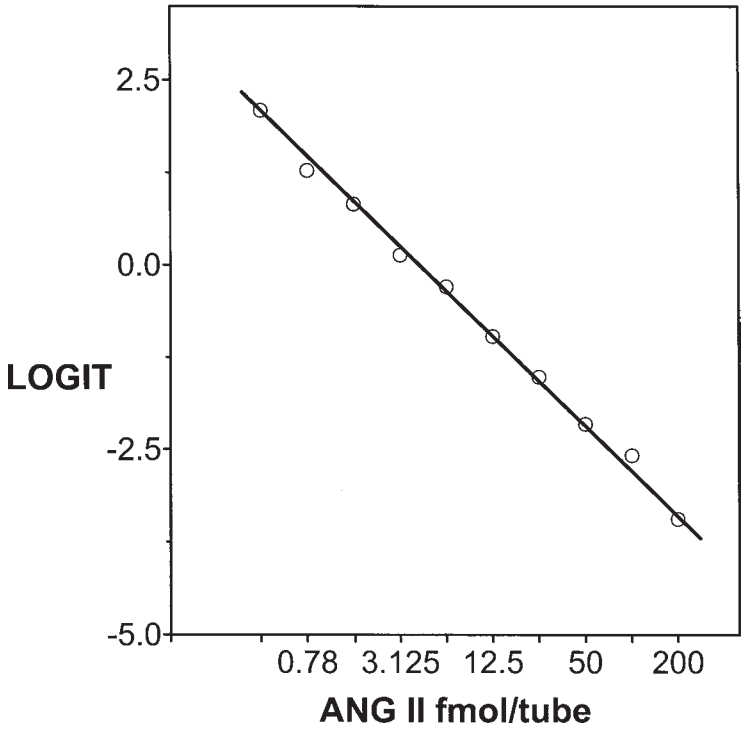

Fig. 1. Example of a standard curve for Ang II assay.

4. Notes

1. Antibody: We tested many commercially available Ang II antisera and chose the Phoenix Pharmaceuticals product. Antisera lots from the same company can vary widely in their ability to measure Ang II and thus, each lot of antisera must be tested separately. The antibody is aliquoted out to minimize the deleterious effects of freeze thawing on antibody activity. We also check the crossreactivity of the antisera to Ang I and other angiotensin fragments every 6 mo (*see* **Note 6**).
2. Storage of the ^{125}I-Labeled Ang II: ^{125}I-Labeled Ang II is obtained the first week that it is produced and checked out immediately. The half-life of ^{125}I is 2 mo and the radiolabeled Ang II is generally good for 6 wk from the production date. The production dates are listed in company catalogs or a calendar can be obtained from the company. As the radioactivity decays the nonspecific binding will increase. We have found that it is very important to check 4-wk and older radiolabeled Ang II prior to assaying samples even if it was working fine the week before. Samples with lower values, such as proximal tubule samples, are scheduled for the first 3 wk following the labeling of Ang II.
3. Angiotensin Standard: We obtain Ang II for the standards from Phoenix Pharmaceuticals, Inc., Belmont, CA, because of its purity. This Ang II yields a single peak when subjected to HPLC separation in our laboratory.
4. Storage of Proximal Tubule Samples: Proximal tubule samples should be stored in methanol at –20°C for a maximum of 1 wk before being assayed for Ang II content. It is very important to make sure the radiolabeled Ang II and antibody are checked out before the assay because there is only enough sample for one measurement. Ang II peptide analysis by HPLC separation requires 4–8 μL and, thus, proximal tubule samples from five to six rats are pooled. The angiotensin peptide content measured following HPLC separation demonstrates that most of the immunoreactive Ang II in the proximal tubule fluid is Ang II (1–8) with similar amounts of angiotensin-(2–8). Ang II measurements following HPLC separation are the same as those of proximal tubule samples assayed directly ***(4)***. Intrasample coefficient of variation for Ang II content measurements averages 7%.
5. Antibody dilution and radiolabeled Ang II: The radiolabeled Ang II is checked with the antibody immediately upon arrival. We have found that if a 1:250 to 1:300 antibody dilution of the working stock gives a specific binding between 30–35%, then the radiolabel is very good and will give reliable data for 5 to 6 wk. Radiolabeled Ang II, which requires 1:50 to 1:150 of the working stock, will generally be okay for 2–3 wk from the date received.
6. Checking Crossreactivity: The antibody we use for Ang II measurements has been extensively characterized by our laboratory. We check the crossreactivity of the Ang II antibody twice a year. The Ang II antisera exhibits similar potencies for Ang II (1–8) and Ang-(2–8). Ang-(3–8) and Ang-(1–7) are detected by the Ang II antisera only at concentrations above 1 million fmol/tube and the displacement of ^{125}I-Ang II is not parallel to that elicited by Ang II. Ang-(1–10), Ang-(2–10), and short COOH-terminal fragments of Ang II are only detected at concentrations more than 100-fold higher that those for Ang II ***(6,7)***.

Acknowledgment

The authors' research is supported by grants from the National Heart Lung and Blood Institute (HL26371 and HL59699).

References

1. Navar, L. G., Harrison-Bernard, L. M., and Imig, J. D. (1998) Compartmentalization of intrarenal angiotensin II, in *Renin-Angiotensin* (Ulfendahl, H. R. and Aurell, M., eds.), Portland, London, pp. 193–208.
2. Navar, L. G., Imig, J. D., Zou, L., and Wang, C. T. (1997) Intrarenal production of angiotensin II. *Semin. Nephrol.* **17,** 412–422.
3. Braam, B., Mitchell, K. D., Fox, J., and Navar, L. G. (1993) Proximal tubular secretion of angiotensin II in rats. *Am. J. Physiol.* **264,** F891–F898.
4. Navar, L. G., Lewis, L., Hymel, A., Braam, B., and Mitchell, K. D. (1994) Tubular fluid concentrations and kidney contents of angiotensins I and II in anesthetized rats. *J. Am. Soc. Nephrol.* **5,** 1153–1158.
5. Seikaly, M. G., Arant Jr., B. S., and Seney Jr., F. D. (1990) Endogenous angiotensin concentrations in specific intrarenal fluid compartments of the rat. *J. Clin. Invest.* **86,** 1352–1357.
6. Fox, J., Guan, S., Hymel, A. A., and Navar, L. G. (1992) Dietary Na and ACE inhibition effects on renal tissue angiotensin I and II and ACE activity in rats. *Am. J. Physiol.* **262,** F902–F909.
7. Zou, L. X., Hymel, L. X., Imig, J. D., and Navar, L. G. (1996) Renal accumulation of circulating angiotensin II in angiotensin II-infused rats. *Hypertension* **27,** 658–662.

30

The In Vitro Blood-Perfused Juxtamedullary Nephron Technique

Edward W. Inscho

1. Introduction

1.1. Study of the Renal Microcirculation

Understanding the endocrine, paracrine, and autocrine mechanisms involved in the regulation of renal hemodynamics has proven an elusive quest ***(1)***. What has emerged, however, is a greater appreciation for the elegance and complexity of the renal microcirculation, which provides exquisite control of renal vascular resistance.

In an effort to better understand the regulation of renal microvascular function, investigators have developed and applied a variety of techniques. Early in vitro approaches involved the grafting of neonatal renal tissue into the hamster cheek pouch. Formation of a successful allograft resulted in a perfused nephrovascular unit composed of an afferent and efferent arteriole with an intact glomerular tuft, but it lacked a fully functional tubular anatomy, thus, eliminating the contributions of tubular paracrine factors that influence renal vascular function ***(2–6)***. In another model, Steinhausen and co-workers induced hydronephrosis to atrophy the tubular structures while retaining a relatively intact microcirculatory anatomy ***(2,7–9)***. This approach was later modified to an in vitro setting ***(10,11)***. Others have examined microvascular function using isolated microvascular segments in perfused, pressurized, or static conditions ***(2,10,12–14)***. All of these techniques provide direct assessment of renal microvascular responses to vasoactive agents and stimuli but all lack the paracrine influences exerted by the renal tubules and the vasomodulatory agents they release.

In 1983, Casellas and co-workers took advantage of the unique characteristics of the rat renal cortex to gain direct access to the juxtamedullary nephrons

From: *Methods in Molecular Medicine, vol. 51: Angiotensin Protocols*
Edited by: D. H. Wang © Humana Press Inc., Totowa, NJ

and microvasculature ***(15)***. Initial experiments focused on micropuncture assessment of renal microvascular and glomerular luminal pressures and responses to vasoactive stimuli. This technique was later modified to allow direct visual access to the microvasculature using a variety of videomicroscopic approaches ***(16–20)***. Direct determination of pre- and postglomerular microvascular responsiveness could be assessed in blood-perfused microvascular segments, which retain their anatomical association with functioning renal tubules. This chapter will detail the preparation of the rat kidney for application of the in vitro blood-perfused juxtamedullary nephron technique as it is currently applied. It will also attempt to point out any little tricks or special considerations that improve the likelihood for success using this technique.

1.2. Overview of the Relevant Renal Anatomy

Daniel Casellas recognized that the inner cortical surface of the rat kidney offered a unique opportunity to study the physiological regulation of a unique population of nephrons ***(15)***. The nephrons that make up the inner cortical surface are the juxtamedullary nephrons, which give rise to long loops of Henle, which penetrate deep into the renal medulla. These nephrons are perfused by long afferent arterioles that fuse with glomeruli located on the inner cortical surface. The efferent arterioles exiting the glomerulus, branch to form the descending vasa recta. The afferent arterioles are longer than usually found in the superficial midcortical region and arise from interlobular arteries or directly from arcuate arteries. All segments of the descending microvascular network are located directly on the inner cortical surface.

Various tubular structures are also visible. Bowmans capsule is readily accessible, as well as portions of the proximal and distal tubules. Occasionally, distal tubular segments can be seen that include the macula densa ***(15)***. Previous studies have shown that proper preparation of the rat kidney for the in vitro study of juxtamedullary microvascular function will result in a preparation with intact microvascular perfusion, maintenance of normal glomerular function, retention of the myogenic and tubuloglomerular feedback components of renal autoregulatory behavior, and appropriate responsiveness to vasoactive stimuli.

2. Materials

2.1. Solutions

1. Tyrodes buffer: 136.9 m*M* NaCl, 0.42 m*M* NaH_2PO_4, 11.9 m*M* $NaHCO_3$, 2.2 m*M* $MgCl_2$, 2.7 m*M* KCl, 1.8 m*M* $CaCl_2$, 5.6 m*M* D-glucose, pH is adjusted to 7.6. Premixed Tyrodes salts (cat. no. T2145) and sodium bicarbonate (S-8761) solutions are available from Sigma Chemical Company; St. Louis, MO (*see* **Note 1**).
2. Kidney perfusate: Tyrodes Buffer containing 5.2g% bovine serum albumin (BSA) (98–99% pure) and the following L-amino acids: 2.0 m*M* alanine, 1.8 m*M* argin-

ine, 0.5 m*M* asparagine, 0.5 m*M* aspartic acid, 0.5 m*M* cysteine, 0.5 m*M* glutamic acid, 1.0 m*M* glutamine, 2.0 m*M* glycine, 0.68 m*M* histidine, 1.0 m*M* isoleucine, 1.0 m*M* leucine, 1.24 m*M* lysine, 0.26 m*M* methionine, 0.5 m*M* phenylalanine, 0.5 m*M* proline, 1.0 m*M* serine, 1.0 m*M* threonine, 0.12 m*M* tryptophan, 0.5 m*M* tyrosine, and 1.0 m*M* valine; pH 7.4. Premixed MEM nonessential amino acid solution (100X) can be obtained from Sigma (cat. no. 7145). Premixed MEM amino acid solution (50X) can be obtained from Gibco-BRL (cat. no. 11130-051). L-Glutamine (200 m*M*) can be obtained from Sigma (cat. no. G7513) (*see* **Note 1**).

3. Kidney superfusate: Tyrodes buffer containing 1.0g% BSA (98–99% pure).
4. Anesthetic: sodium pentobarbital.
5. Angiotensin-converting enzyme (ACE) inhibitors: Captopril or enalaprilat.
6. Heparin: 1000 U/mL.
7. BSA: Fraction V, low heavy metals (<20 ppm), 98–99% purity. (Calbiochem, cat. no. 12659).

2.2. Perfusion Equipment

1. Glass cannula: Approx o.d. 1.27 mm, id 0.9 mm. (*see* **Fig. 1** and **Note 5**).
2. Perfusion chamber: Custom-made, water-jacketed Plexiglas chamber with heat exchanger for superfusate. *See* **Fig. 2** for an illustration and description.
3. Silicone elastomer: For preparing a silicone pedestal to support the kidney. (Sylgard; 184 silicone elastomer kit; Dow Corning Corp.).
4. Perfusion line: Venoset, microdrip primary iv set, vented 70 in.
5. Polyethylene tubing: (PE 50, 90, 205, and 260).
6. Three-way stopcocks.
7. Scintillation vials: Used as the blood reservoir (*see* **Fig. 3**).
8. Vacuum line connected to a vacuum reservoir for collection of spent buffer and perfusate from the perfusion chamber.
9. Water bath: Heated circulating water bath (such as HAAKE).
10. Two pressure transducers: One for the perfusion cannula and one for the perfusate reservoir (*see* **Fig. 3**).
11. Compressed gas: 95% O_2, 5% CO_2.

2.3. Dissection and Blood Collection Materials

1. Waterproof tape.
2. Large surgical forceps and scissors.
3. Dumont # 5 microdissection forceps.
4. Curved microdissection forceps.
5. Angled fine sharp point microdissection forceps.
6. McPherson-Vannas microdissection scissors.
7. Castrovirjo angular microdissection scissors.
8. Dieffenbach, serrafine-curved bulldog microclip.
9. Stainless-steel pins: size 000 insect pins.
10. 10–0 suture, needles attached: Sharpoint AK-0100.

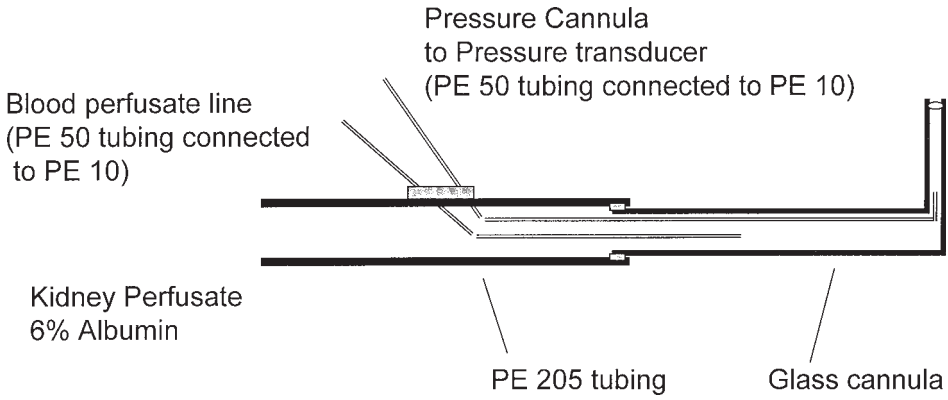

Fig. 1. Diagram depicting the perfusion cannula. The main glass cannula is attached to a piece of PE 205 polyethylene tubing. The PE 205 tubing is connected to a larger perfusion line (Venoset microdrip iv tubing) via a stopcock assembly. This stopcock is open to allow perfusate to flow to the kidney during isolation and microdissection and is closed when the kidney perfusate is switched to reconstituted blood. The 6% albumin kidney perfusion solution passes through this tubing to enter the cannula and the kidney. A second, smaller cannula (PE10) passes through the wall of the PE 205 tubing and extends into the glass barrel. The PE10 tubing is fused to PE 50, which extends back to the blood reservoir. This cannula delivers the blood perfusate to the perfusion cannula when the perfusate is changed from the 6% albumin solution to the reconstituted blood. A second smaller (PE 10) cannula also enters the PE 205 tubing and approaches the tip of the glass perfusion cannula. This PE10 tubing is also fused to a length of PE 50 tubing, which is connected directly to the pressure transducer for measurement of perfusion pressure at the cannula tip. The perforations made by the PE 10 tubing are sealed with silicone glue to prevent loss of pressure or perfusate leakage.

11. 5–0 or 4–0 silk-braided suture.
12. Syringes: 1.0, 3.0, and 12 cm^3.
13. Hemostats.
14. Dissection stereomicroscope.
15. Fiber optic lamp: Used to illuminate the kidney surface during microdissection.
16. 5-μm nylon mesh: Used to filter the reconstituted blood.
17. Filters:
    a. Glass fiber 5-, 0.8-, and 0.2-μm exclusion: Filters perfusate and superfusate solutions.
    b. Sterile syringe filters: Filters plasma, 25-mm cellulose acetate membrane (0.2-μm exclusion; Nalgene #192-2520).
18. Pasteur capillary pipets: 9 in. long, borosilicate: Used to make glass cannulas.
19. Magnetic stirrer and small (2–3 mm) stirring bar: For stirring blood in blood reservoir.

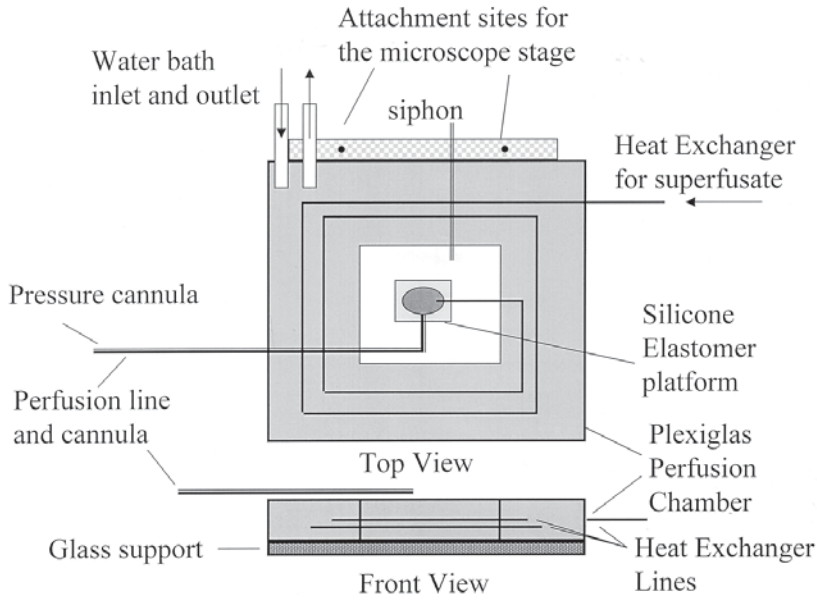

Fig. 2. Diagram of the custom-made perfusion chamber used for studies using the blood-perfused juxtamedullary nephron technique. The chamber consists of a piece of half-inch Plexiglas with a channel milled into it to provide the water jacket. A length of PE 90 tubing is connected to the stainless-steel tubing carrying the warmed superfusate where it exits the chamber. This tubing is positioned on the surface of the kidney with the aid of a curved stainless-steel pin to direct superfusate across the kidney surface. Water pumped from a circulating water bath enters and exits the chamber through the stainless-steel inlet and outlet ports at the rear of the chamber. The middle of the plexiglass block is also cut out to leave a rectangular hole. A stainless-steel heat exchanger, which carries the superfusion solution to the kidney, is wound through water channel. The heated water warms the superfusion solution prior to arrival at the kidney surface. The chamber, containing the heat exchanger, is attached to a piece of plate glass (1/4-in. thick) and tightly sealed with silicone glue. The center of the chamber extends directly to the glass support to which is fixed (silicone glue) a pedestal made of polymerized silicone elastomer. This pedestal is used to mount the prepared kidney for microdissection and study. A stainless-steel siphon port is positioned at the rear of the chamber. This port is attached to a vacuum bottle and is used to aspirate the waste perfusate and superfusate solutions from the chamber bottom throughout the experiment. The perfusion cannula is attached to the chamber surface with waterproof tape.

2.4. Videomicroscopy Equipment

1. Fixed-stage microscope fitted with standard 10×, 20×, and 32× dry objectives and a 40× water immersion objective (*see* **Fig. 4**).

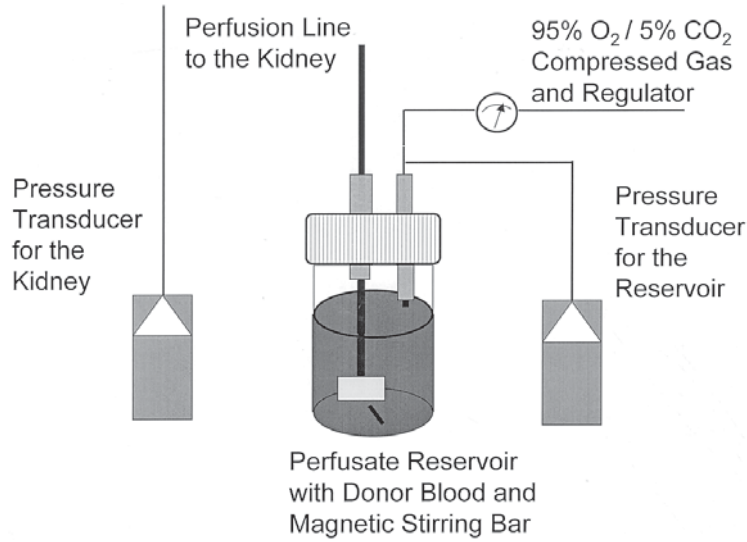

Fig. 3. Illustration of the blood reservoir. Blood is contained in a standard plastic scintillation vial with a modified cap. The cap is modified to allow passage of two stainless-steel lines sheathed in silicone tubing. The silicone sheath provides a tight seal between the tubing and the vial cap to prevent pressure leakage. The vial is pressurized from a compressed gas source containing 95% O_2/5% CO_2. Two pressure transducers are used to monitor reservoir pressure and renal perfusion pressure at the cannula tip. The scintillation vial is positioned on a magnetic stirrer and blood is stirred continuously with the aid of a small stirring bar. The stirring rate is set at the slowest position needed to keep the erythrocytes on suspension.

2. Transillumination light source (epillumination is also suitable).
3. High-resolution video camera for attachment to the microscope.
4. High-resolution video monitor.
5. Time–date generator.
6. Video-image enhancer.
7. VCR for recording video record of the experiment.
8. Video caliper or an image shearing device for measuring changes in vascular diameter.
9. Stage micrometer for calibrating the video caliper or image shearing device.
10. Grass polygraph for recording perfusion pressure.

3. Methods

3.1. Kidney Isolation and Blood Collection

1. Two male Sprague Dawley rats (*see* **Note 2**) weighing between 350–400 g are required for each experiment (a kidney donor and an identically treated blood donor).

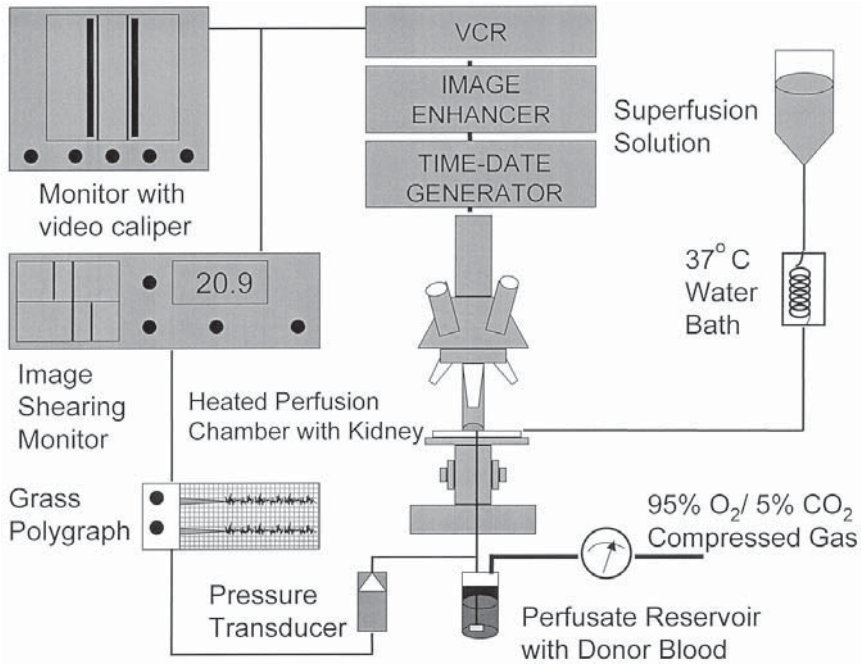

Fig. 4. The videomicroscopy apparatus. The perfusion chamber is affixed to the stage of the light microscope equipped with a high-resolution video camera. The video signal is transmitted through a time–date generator, an image enhancer, and a video cassette recorder (VCR) before being displayed on the video monitor. Vessel diameter is measured using either a calibrated video caliper displayed on the video monitor or an image shearing monitor. The kidney surface is bathed continuously with the superfusion solution. The superfusion solution is preheated to 37°C by the water bath built into the perfusion chamber (shown separately in the illustration). The kidney is perfused with reconstituted blood contained in a perfusion reservoir pressurized with 95% O_2 and 5% CO_2. Perfusion pressure is continuously monitored and recorded by a pressure transducer connected to a polygraph.

2. Rats are anesthetized with sodium pentobarbital (50 mg/kg body weight) and a tracheostomy (PE 260 tubing) is performed to maintain a patent airway.
3. Catheters (PE 50) are placed in a jugular vein for administration of drugs and additional anesthetic, as necessary, and in a carotid artery for blood collection (*see* **Notes 3** and **4**).
4. Animals serving as blood donors undergo a bilateral nephrectomy via two retroperitoneal incisions. Tight ligatures (4.0 or 5.0 silk suture) are placed around the renal artery and vein of each kidney and the blood vessels are ligated.
5. Rats are usually pretreated with ACE inhibitor (captopril or enalaprilat 2 mg/kg) in order to reduce Ang II generation as the kidney and blood are being prepared.

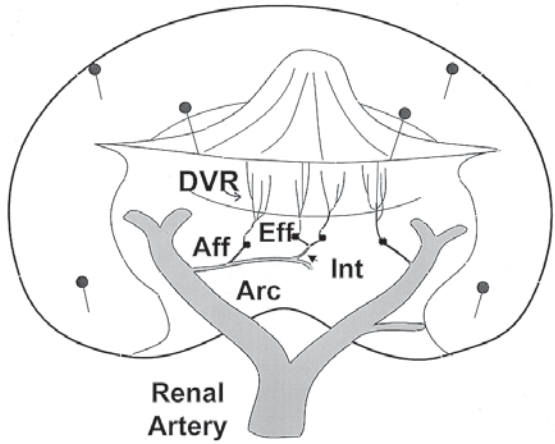

Fig. 5. Illustration depicting the prepared kidney with the inner cortical surface exposed. The kidney is pinned to the silicone elastomer pedestal depicted in **Fig. 2**. The renal artery enters the kidney at the renal hilus and divides into two to three major branches. These branches and the smaller arteries and arterioles they spawn are visible when the renal papilla is lifted and the underlying connective tissue removed. Arcuate (Arc) and interlobular (Int) arteries, afferent (Aff), and efferent (Eff) arterioles and descending vasa recta (DVR) are visible for study. This figure reproduced with permission of the author, Dr. Pamela K. Carmines.

Previous studies have shown that such treatment effectively suppressed plasma ACE activity by 87% for the duration of the experiment. This step can be omitted if treatment with ACE inhibitors will interfere with the experiment.

6. A laparotomy is performed to prepare for isolation of the right kidney (*see* **Note 6**).
7. A tight ligature (4.0 or 5.0 silk suture) is placed around the left renal artery and vein and the left ureter and a loose ligature (4.0 or 5.0 silk suture) is placed around the right renal artery.
8. The mesenteric artery is exposed by shifting the abdominal contents to the right and cleaning the connective tissue away from the visible vascular segment.
9. A tight ligature is placed around the most distal aspect of the exposed segment of the mesenteric artery and a loose ligature is applied near the midpoint of the exposed arterial segment.
10. The small bulldog clip is placed on the most proximal segment of the mesenteric artery immediately adjacent to the abdominal aorta. This clip will occlude arterial blood flow until the glass renal perfusion cannula can be installed.
11. The glass perfusion cannula (*see* **Fig. 1** and **Note 5** for illustration and description) is connected to a perfusion reservoir filled with 150–250 mL of kidney perfusate, maintained at room temperature, and suspended approx 175 cm above the work surface. This elevation generates a perfusion pressure of approx 80 mmHg at the cannula tip.

12. A small incision is made in the mesenteric artery near the distal ligature for insertion of the glass renal-perfusion cannula.
13. The cannula, with free-flowing perfusate, is inserted into the mesenteric artery via the incision and is advanced toward the aorta.
14. The loose ligature placed around the midpoint of the mesenteric artery is gently tightened around the cannula to allow the cannula to slide, but tight enough to prevent hemorrhage between the cannula and the arterial wall when the bulldog clip is withdrawn.
15. The bulldog clip is removed and the cannula is advanced across the abdominal aorta and into the right renal artery.
16. The cannula is tied in place by tightening the ligature on the superior mesenteric artery and by tightening the ligature on the right renal artery around the cannula.
17. The renal vein is ligated near the inferior vena cava and an incision is quickly made in the renal vein, upstream of ligature, to allow venting of the renal venous effluent and to prevent mixing of the perfusate with the blood in the systemic circulation.
18. After the kidney is cannulated and perfused, the blood from the kidney donor is collected to supplement the blood collected from the blood donor.
19. Blood from the kidney donor is collected into a heparinized (500 U) 12-cm^3 syringe via the carotid cannula.
20. Renal perfusion is maintained throughout all ensuing dissection procedures.

3.2. Kidney Microdissection

1. **Figure 5** illustrates the appearance of the prepared kidney (*see* **Notes 6–8**).
2. Following exanguination of the kidney donor, the perfused kidney is removed from the animal and prepared for microdissection.
3. The perfused kidney is decapsulated and cleared of adherent connective and adipose tissue.
4. A longitudinal slice is removed from the lateral aspect of the kidney to expose the renal pelvis. If properly performed, the papilla will remain intact on the remaining two-thirds of the kidney and the main branches of the renal artery will be undamaged.
5. The perfused kidney is gently placed on the silicone elastomer platform in the center of the perfusion chamber and affixed to the platform with stainless-steel pins.
6. The perfusion cannula is carefully anchored to the perfusion chamber with waterproof tape. Care should be taken to maintain a patent renal artery to ensure stable perfusion throughout the dissection procedures and subsequent observation (*see* **Figs. 2** and **5**).
7. The perfusion chamber containing the kidney is placed on the stage of a dissecting microscope.
8. The kidney surface is illuminated with the aid of a fiberoptic lamp.
9. The exposed papilla is gently reflected back to expose the underlying renal pelvic mucosa, adipose and connective tissue that overlays the inner cortical surface of the kidney.

10. The reflected papilla is held in place with stainless-steel pins placed in the lateral aspects of the papilla. This ensures that the long loops of Henle arising from the juxtamedullary nephrons remain patent and, thus, permits tubuloglomerular influences on renal microvascular function to be retained.
11. The pelvic mucosa, connective tissue, and renal veins covering the inner cortex are carefully removed to reveal the renal tubules, glomeruli and superficial microvasculature of juxtamedullary nephrons (*see* **Notes 6–8**).
12. The terminal portions of the arterial vasculature feeding the inner cortex are ligated with tight sutures (10–0 nylon suture).
13. Similar ties are placed around any leaking blood vessel in order to restore renal perfusion pressure and to ensure adequate perfusion of the microvascular segments lying on the inner cortical surface which supply the juxtamedullary nephrons (*see* **Note 8**).

3.3. Preparation of Perfusate Blood

1. After the dissection procedures have been completed and the kidney is positioned on the microscope stage, the kidney perfusate is changed to the reconstituted blood (*see* **Fig. 4** and **Note 4**).
2. The blood collected from kidney and blood donors is pooled and prepared for kidney perfusion as follows.
3. The pooled blood is centrifuged at 2500*g* for 10 min at 4°C.
4. The plasma and packed erythrocytes are collected separately, while the white blood cell fraction is removed and discarded.
5. The erythrocytes are resuspended with saline, centrifuged at 350*g* for 15 min and the supernatant is discarded.
6. Finally, the erythrocytes are resuspended and centrifuged again at 2700*g* for 10 min and the supernatant discarded. These centrifugation steps remove the leukocytes and platelets from the reconstituted blood and wash the erythrocytes before reintroducing them into the prepared kidney.
7. The collected plasma fraction is passed through 5.0- and 0.22-μm glass fiber filters.
8. Erythrocytes are mixed with the filtered plasma to achieve a hematocrit of approx 33%.
9. The reconstituted blood is filtered through a 5-μm nylon mesh to remove any clots or aggregates that might lodge in glomerular capillaries and prevent glomerular perfusion.
10. Thereafter, the blood is continuously stirred in a closed reservoir that is pressurized with a 95% O_2:5% CO_2 gas mixture obtained from a compressed gas source.
11. **Figure 3** illustrates the blood-reservoir configuration. The blood reservoir consists of a standard plastic scintillation vial with a modified cap.
12. Two holes are drilled into the top of the cap and pass through the inner cap seal.
13. A short length of stainless-steel tubing, tightly sheathed in silicone tubing, is inserted into one hole to provide an input port for the compressed gas to pressurize the chamber.

14. A similar, but longer, length of silicone-sheathed stainless-steel tubing is inserted into the second hole. This tubing extends close to the bottom of the vial and serves as the exit port for the perfusate blood to pass to the kidney.
15. One pressure transducer is connected to the gas line to monitor chamber pressure.
16. The second transducer is connected to the cannula (*see* **Fig. 1**) to monitor kidney perfusion pressure.

3.4. Preparation of the Kidney for Videomicroscopy

1. **Figure 4** illustrates the videomicroscopy apparatus. The perfusion chamber containing the prepared kidney is attached to the fixed stage of a light microscope (Nikon Optiphot-2UD) equipped with long working distance achromatic dry (10, 20, and ×32) and water immersion (×40) objectives.
2. Perfusion pressure is monitored continuously using Statham P23D6 pressure transducers connected to a Grass polygraph. Renal perfusion pressure can be varied manually by adjusting the pressure in the perfusate reservoir.
3. The inner cortical surface is bathed with the Tyrodes buffer superfusion solution (1% albumin), which has been warmed to 37°C by passing through the heat exchanger contained within the water-jacketed perfusion chamber **(Fig. 2)**.
4. The kidney is warmed to 37°C and after a 15-min equilibration period, tissue function may be studied using videometric techniques.
5. Drugs, peptides, agonists, and antagonists are administered to the kidney by addition to the superfusate solution, the blood perfusate or both.

3.5. Videomicroscopy

1. Videometric techniques are utilized to measure lumen diameter in selected arteries and arterioles.
2. Determination of microvascular diameter is accomplished using transillumination videomicroscopy ***(17)***.
3. The tissue is transilluminated and the focused image converted to a video signal by a high-resolution Newvicon camera mounted on the trinocular head of a compound microscope.
4. This video signal is electronically enhanced and recorded on videotape for later analysis.
5. A time–date generator is placed in line with the video signal to stamp a time and date on the recorded image for archiving purposes.
6. Vascular inside diameters are measured at a single site either in real time or from videotape, using either a digital image shearing monitor or a video caliper.
7. These measurement devices are calibrated using a stage micrometer with the smallest divisions around 2–10 μm to ensure precision and accuracy. This system typically results in diameter measurements which are reproducible to within 1 μm.
8. Microvascular diameters are measured at the midplane of the focused image. This represents the widest possible diameter that can be obtained at the selected site.
9. Diameter measurements are made by determining the distance between the two internal edges of the microvascular segment being studied. Care must be taken to

make all measurements for a given experiment at exactly the same site because microvascular lumenal diameter varies substantially along the length of the vessel and the magnitude of vasoconstrictor and vasodilator responses is not necessarily uniform from one site to the next.

10. The data obtained from the videometric measurements are used for all subsequent analysis.
11. Vessels should be selected for study on the basis of clear visibility of both vessel walls and the maintenance of a brisk, steady blood flow. If the passage of single red blood cells can be easily discerned, or if flow stops inexplicably during the course of the experiment, the vessel should be discarded.
12. Afferent and efferent arterioles must make a definite connection to a glomerulus.

4. Notes

1. Perfusate composition: As with any biological system, it is important to use carefully prepared solutions. In this preparation, the kidney must be sustained during the isolation and dissection procedures. Previous studies using this technique have demonstrated that if properly performed, the kidney continues to exhibit normal tubular and glomerular function, autoregulatory behavior, and microvascular responsiveness to a wide range of vasoconstrictor and vasodilator substances. Therefore, the conditions and solutions described herein are suitable for the reliable use of this preparation. Inaccurate preparation of perfusate or superfusate solutions usually results in failed experiments or compromised kidney function. Particular attention needs to be paid to the filtration steps, that are intended to remove any particulate materials large enough to occlude glomerular capillaries and upstream microvascular segments. Cessation of blood flow in the selected microvessel disqualifies that blood vessel for inclusion in a data set.
2. Gender differences: Most of the work performed using this technique has been done using kidneys from male rats. The reader is advised that gender-based differences in renal microvascular function may be encountered if kidneys from female rats are used ***(21,22)***.
3. Blood donor rats: Careful preparation of the blood donor rats is important. These rats should receive any treatment regimens or program that the kidney donors are subjected to ensure that the physiological conditions are as close as possible and that vasoactive or vasomodulatory agents in the circulation are similar. The unilateral and bilateral nephrectomy that is performed on the kidney donor and blood donor, respectively, is to minimize further activation of the renin–angiotensin system during surgery and blood collection. Exanguination quickly reduces arterial blood pressure and stimulates enhanced renin secretion from the kidney. Increasing plasma renin activity will markedly increase the circulating angiotensin II concentration and could alter renal microvascular function. Ligation of the renal artery and vein prevent renal renin from entering the circulation during tissue preparation and blood collection.
4. Erythrocytes: Incorporation of erythrocytes in the perfusate achieves two major objectives. First, they provide a physiological system for the delivery of oxygen

to the kidney. Second, they provide a visible marker for adequate perfusion of the microvasculature. Without some indicator of perfusion, it is not possible to determine if the lumenal perfusate is flowing or if it is stagnant. Free-flowing erythrocytes exhibit laminar-flow characteristics in the renal microvasculature and render the appearance of the microvascular lumen as an opaque blur or smear. A clear plasma layer is usually visible in the interior of the microvascular lumen, immediately adjacent to the vessel wall. If blood flow slows or stops, individual erythrocytes can be clearly discerned and represent indicators of inadequate vascular perfusion.

5. Perfusion cannula: The perfusion cannula can be fashioned from any suitable piece of borosilicate glass. The outside diameter must be small enough to allow insertion into the renal artery. The inner diameter must be large enough to permit positioning two PE10 cannulas within the cannula barrel while still allowing unrestricted flow of kidney perfusate. The long end of a 9-in Pasteur pipet works well for this purpose. Cut the end of the pipette to retain as much of the tapered length as possible. Form a 90° turn in the end of the cannula and fire polish both ends. The large end of the glass tubing will fit snugly within the PE 205 tubing and form a good seal.
6. Dissection time: One of the keys to the successful preparation of rats kidneys for studies using this technique is the length of time spent in preparing the kidney. Highly proficient individuals should be able to complete the entire process from cannulation to blood vessel selection in less than 45 min. If such a time is achieved, the likelihood of a successful experiment increases dramatically from approx 50–60% to 80–90%. Kidney isolation and dissection must proceed swiftly and carefully to ensure good perfusion, a clear visual field, and stable microvascular function. The longer the period between opening the abdominal cavity to gain access to the kidney and the beginning of the microvascular study, the poorer the preparation becomes and the likelihood that reliable data will be collected declines.
7. Connective tissue: Microvascular studies using this technique rely heavily on the clarity of the visual field. Extremely careful removal of the connective tissue adjacent to the inner cortical surface is essential to obtaining a usable kidney for study. Leaving too much connective tissue behind will make visualization of the underlying microvascular structures more difficult. This could impair the ability to accurately identify the apposing edges of the microvascular segment being studied and will reduce or eliminate the ability to accurately measure microvascular luminal diameter. Excessive removal of surface connective tissue can result in laceration of the renal cortex and cause excessive hemorrhage from the kidney surface. Such bleeding can markedly reduce or obliterate the clarity of the visual field and impair the ability to identify essential vascular structures.
8. Ligation of leaking or severed vascular elements: For the reasons already discussed, the clarity of the visual field is critical for the success of this technique. During the preparation of the kidney for study, microdissection steps often cut small and large arterial blood vessels on inner cortical surface, on adjacent seg-

ments of the inner cortex, and on the main branches of the renal arteries. These segments must be located and ligated before experiments can be initiated. Failure to do so will impair the ability to perfuse the kidney at physiological pressures because of pressure loss and hemorrhage through severed arteries and arterial branches. Uncontrolled hemorrhage will obliterate the visual field and exhaust the supply of blood perfusate before any meaningful data can be collected. Small microvascular segments on the kidney surface can also be cut during the microdissection. Tying these segments is difficult and sometimes it is more expedient to ligate the nearest accessible feeder artery. This will prevent hemorrhage onto the kidney surface, but will also reduce the total area of perfused kidney available for study.

References

1. Navar, L. G., Inscho, E. W., Majid, D. S. A., Imig, J. D., Harrison-Bernard, L. M., and Mitchell, K. D. (1996) Paracrine regulation of the renal microcirculation. *Physiolog. Rev.* **76,** 425–536.
2. Navar, L. G., Gilmore, J. P., Joyner, W. L., Steinhausen, M., Edwards, R. M., Casellas, D., et al. (1986) Direct assessment of renal microcirculatory dynamics. *Fed. Proc.* **45,** 2851–2861.
3. Greenblatt, M., Choudari, K. V. R., Sanders, A. G., and Joyner, W. L. (1969) Mammalian microcirculation in the living animal, methodological considerations. *Microvasc. Res.* **1,** 420–423.
4. Click, R. L., Joyner, W. L., and Gilmore, J. P. (1979) Reactivity of glomerular afferent and efferent arterioles in renal hypertension. *Kidney Int.* **15,** 109–115.
5. Oestermeyer, C. F. and Bloch, E. H. (1977) In vivo microscopy of hamster renal allografts. *Microvasc. Res.* **13,** 153–180.
6. Sandison, J. C. (1921) the transparent chamber of the rabbit's ear, giving a complete description of improved technic of construction and introduction, and general account of growth and behavior of living cells and tissues as seen with the microscope. *Am. J. Anat.* **17,** 178–208.
7. Steinhausen, M., Kucherer, H., Parekh, N., Weis, S., Wiegman, D. L., and Wilhelm, H. R. (1986) Angiotensin II control of the renal microcirculation: effect of blockade by saralasin. *Kidney Int.* **30,** 56–61.
8. Steinhausen, M., Snoei, H., Parekh, N., Baker, R., and Johnson, P. C. (1983) Hydronephrosis: a new method to visualize vas afferens, efferens, and glomerular network. *Kidney Int.* **23,** 794–806.
9. Steinhausen, M., Sterzel, R. B., Fleming, J. T., Kuhn, R., and Weis, S. (1987) Acute and chronic effects of angiotensin II on the vessels of the split hydronephrotic kidney. *Kidney Int.* **20(Suppl.),** S64–S73.
10. Carmines, P. K. and Fleming, J. T. (1990) Control of the renal microvasculature by vasoactive peptides. *FASEB J.* **4,** 3300–3309.
11. Loutzenhiser, R. and Epstein, M. (1987) Modification of the renal hemodynamic response to vasoconstrictors by calcium antagonists. *Am. J. Nephrol.* **7,** 7–16.

12. Edwards, R. M. (1983) Segmental effects of norepinephrine and angiotensin II on isolated renal microvessels. *Am. J. Physiol.* **244,** F526–F534.
13. Yuan, B. H., Robinette, J. B., and Conger, J. D. (1990) Effect of angiotensin II and norepinephrine on isolated afferent and efferent arterioles. *Am. J. Physiol.* **258,** F741–F750.
14. Conger, J. D., Falk, S. A., and Robinette, J. B. (1993) Angiotensin II-induced changes in smooth muscle calcium in rat renal arterioles. *J. Am. Soc. Nephrol.* **3,** 1792–1803.
15. Casellas, D. and Navar, L. G. (1984) *In vitro* perfusion of juxtamedullary nephrons in rats. *Am. J. Physiol.* **246,** F349–F358.
16. Carmines, P. K., Morrison, T. K., and Navar, L. G. (1986) Angiotensin II effects on microvascular diameters of *in vitro* blood-perfused juxtamedullary nephrons. *Am. J. Physiol.* **251,** F610–F618.
17. Carmines, P. K. and Navar, L. G. (1989) Disparate effects of Ca channel blockade on afferent and efferent arteriolar responses to ANG II. *Am. J. Physiol.* **256,** F1015–F1020.
18. Sanchez-Ferrer, C. F., Roman, R. J., and Harder, D. R. (1989) Pressure-dependent contraction of rat juxtamedullary afferent arterioles. *Circ. Res.* **64,** 790–798.
19. Casellas, D. and Moore, L. C. (1990) Autoregulation and tubuloglomerular feedback in juxtamedullary glomerular arterioles. *Am. J. Physiol.* **258,** F660–F669.
20. Casellas, D. and Carmines, P. K. (1996) Control of the renal microcirculation: Cellular and integrative perspectives. *Curr. Opin. Nephrol. Hypertens.* **5,** 57–63.
21. Steinhausen, M., Ballantyne, D., Fretschner, M., and Parekh, N. (1990) Sex differences in autoregulation of juxtamedullary glomerular blood flow in hydronephrotic rats. *Am. J. Physiol.* **258,** F863–F869.
22. Parekh, N., Zou, A. P., Jungling, I., Endlich, K., Sadowski, J., and Steinhausen, M. (1993) Sex differences in control of renal outer medullary circulation in rats: role of prostaglandins. *Am. J. Physiol.* **264,** F629–F636.

31

In Vitro Proximal Tubule Perfusion Preparation

Jeffrey L. Garvin and Peter J. Harris

1. Introduction

Isolation and perfusion of single nephron segments was first described by Burg et al. ***(1)*** in 1966. This technique has allowed us to study both transepithelial and transmembrane transport in individual nephron segments, including the proximal tubule, under carefully controlled circumstances. This has obvious advantages for experiments that require the epithelium and its junctional complexes to remain intact, but removed from the influences of endogenous neural or humoral mediators, including angiotensins. In addition, control of bath and luminal perfusate compositions and flow rates allows peptides to be added independently to each side of the epithelium. This has particular relevance in the case of angiotensin, which binds to luminal and basolateral receptors and initiates intracellular signal transduction pathways that may differ between the two sites ***(2)***.

The technology to perfuse individual nephron segments arose out of in vitro micropuncture experiments. Nephron segments from rabbits were studied first; later, nephron segments from other animals were examined in order to take advantage of species differences in renal function. For instance, the development of techniques that permit isolation and perfusion of rat proximal nephron segments has greatly aided our understanding of the kidney ***(3)***. This is primarily because of two facts: (1) there is a vast literature on in vivo renal function in the rat, but not in the rabbit, and (2) the physiology of murine kidneys resembles the human kidney more closely than does the rabbit kidney regarding some aspects, such as acid-base handling.

Procedures are presented for: (1) dissection of proximal nephron segments; (2) pipet construction and assembly; (3) proximal tubule perfusion; (4) chemi-

From: *Methods in Molecular Medicine, vol. 51: Angiotensin Protocols*
Edited by: D. H. Wang © Humana Press Inc., Totowa, NJ

cal determinations of solute and solvent fluxes; and (5) preparation of fluorescent-labeled angiotensin suitable for localization of binding in conjunction with measurements of changes in intracellular ionic concentrations. The first three procedures are necessary for tissue preparation; whereas the most fundamental is the fourth, measurements of water and solute fluxes. More sophisticated experiments involve measurement of receptors and their trafficking, as well as intracellular ion concentrations using fluorescent labels. These compounds are well suited to studies of live cells, can be used at concentrations that have tolerable impact on cellular function and transporter kinetics, and can provide appropriate temporal resolution. The kinetics of the uptake of label by cells during internalization of the receptor/angiotensin complex can be studied together with subsequent release of label that may represent recycling of either it or the peptide.

2. Materials

2.1. Pipet Construction and Assembly

1. Rotary puller (Stoelting 51511 micropipet puller, Stoelting, Chicago, IL).
2. Microforge (Stoelting).
3. Borisilicate glass capillary tubing made from R6 glass (Drummond Scientific Co., Broomall, PA) with outside and inside diameters of 0.084–0.064, 0.047–0.040, 0.047–0.027, 0.018–0.012, and 0.187–0.150 in. Drummond usually sells their glass in English rather than metric units, and the Lucite perfusion parts were originally machined to accept the diameters listed above.
4. Weights (0.5, 1.1, and 8 g).
5. Syringe filters.
6. Gas-tight glass syringes.
7. Silicone adhesive.
8. Sylgard elastic polymer.
9. Lucite perfusion pieces and V-tracks.
10. Wooden blocks to hold V-tracks.

2.2. Proximal Tubule Dissection

1. Physiological saline. NaCl 114 m*M*, $NaHCO_3$ 25 m*M*, KCl 4 m*M*, NaH_2PO_4 2.5 m*M*, $MgSO_4$ 1.2 m*M*, Ca lactate$_2$ 2.0 m*M*, Na_3 citrate 1.0 m*M*, alanine 6 m*M*, glucose 5.5 m*M*, gassed with 95% O_2/5% CO_2. Whereas the precise composition of this solution is not critical, proximal tubules are gluconeogenic, and therefore do not utilize glucose as a substrate. Lactate, pyruvate, amino acids, and short-chain fatty acids are preferred substrates.
2. Dumont #5 forceps. At least three pairs, sharpened with jeweler's paper so that their tips exactly match at X100 magnification and are shovel-shaped; plus two blunt pairs, unsharpened, but with their tips matched at low magnification.
3. Jeweler's paper (0.3, 3, 12, and 30 μm grit).

4. Transmitted-light dissecting microscope equipped with a transparent cooling block to maintain 10–12°C.
5. Tissue-slicing blade.
6. Lucite block (1 × 10 × 10 cm)

2.3. Proximal Tubule Perfusion

1. Inverted microscope (Nikon Diaphot).
2. Micromanipulators and brackets for micromanipulators to allow 3-dimensional control of V-tracks.
3. Temperature-regulated chamber designed for solution flow, with a microscope cover glass for a bottom.
4. Transfer pipet (syringe with a screw plunger and a glass capillary attached to the tip).
5. Junk pipet.
6. Timer.
7. 10-cm Petri dish with modeling clay ridge.

2.4. Chemical Determination

1. Raffinose kit (Boehringer-Mannheim cat. no. 428 167).
2. Raffinose (final concentration 5 m*M* in perfusion solution).
3. NanoFlo Microfluorimeter (World Precision Instruments). *See* **Note 4.4.4.**
4. Glucose kit (Sigma cat. no. 16-10).
5. Total CO_2 kit (Sigma cat. no. 132-UV).
6. Ascarite (with holder).

2.5. Preparation of Texas Red-Labeled Angiotensin II (Ang II-TR)

1. Angiotensin II (Ang II) made up in 50-µL aliquots containing 250 nmol peptide in 50 m*M* acetic acid.
2. 200 m*M* $NaHCO_3$ (pH 9.0), made up fresh each time.
3. Texas Red sulfonyl chloride (1 mg in special packaging, Molecular Probes, Eugene, OR, cat. no. T-1905).
4. Anhydrous dimethylformamide (DMF).
5. 1.5 *M* hydroxylamine, pH 8.0–8.5. Dissolve 2.1 g hydroxylamine HCl in 10 mL distilled water and adjust to pH 8.0–8.5 with 5 *M* NaOH. Add distilled water to bring volume to 20 mL.
6. Methanol.
7. Phosphate-buffered saline (PBS).
8. C18 SEP PAK.
9. Sephadex G25 column.

2.6. Loading of Proximal Tubule Cells with Calcium-Selective Dye

1. Fluo-3 AM (acetoxymethyl ester), 1 mg (Molecular Probes, cat. no. F-1241).
2. 20% Pluronic F-127 (Molecular Probes, cat. no. P-3000)

2.7. Imaging of Fluorescein-Based Dye and Ang II-TR

There are many variations in the design of microscope-based systems for multiwavelength imaging ***(4)***, and one particular approach will be described here. Essential issues to consider in specifying a detection system are the time resolution (determined by the nature of the biological events to be monitored), the required light sensitivity of the detection system (determined by the density of binding sites, the photon yield of the fluorophore and the transfer function of the optical system), and the sensitivity of the labeled cells to photon-induced damage.

1. Inverted microscope (Zeiss IM or equivalent) adapted for dual-band fluorescence microscopy by addition of a dual-bandpass dichromatic beam splitter and dual-bandpass emission filter (Chroma Technology Co., Brattleboro, VT). This system allows electronically controled shuttering of excitation light at two wavelengths, 495 ± 10 nm for fluorescein and 575 ± 12 nm for Texas Red. The emission filter has pass bands at 510–550 nm for fluorescein and 610–680 nm for Texas Red.
2. Epi-illumination light source (Oriel, Stratford, CT). A xenon arc lamp provides sufficiently uniform output intensity across the range of wavelengths required. The lamp is fitted in a dual-port housing with each port collimated, shuttered, and filtered (bandpass and infrared) to allow switching between the two excitation wavelengths. After shuttering, excitation beams are recombined using a low-pass dichromatic beam splitter (505-nm cutoff), then directed into the microscope.
3. Image detector. A variety of cameras may be used, including cooled CCD and image-intensified cameras ***(4)***. A suitable system for relatively low time resolution uses a SenSys Peltier-cooled CCD camera (Photometrics, Tucson, AZ). Our system provides image read-out at approx 1-s intervals, but shorter times can be achieved with higher transfer-rate electronics.
4. Computer-based control, image acquisition, and analysis system. Many variations are possible, and options are changing rapidly. We have used "V for Windows" software (Digital Optics, Auckland, New Zealand), but this requires additional image processing and analysis software, such as Image ProPlus (Media Cybernetics, Silver Spring, MD). A more comprehensive solution is available with Axon Imaging Workbench (Axon Instruments Inc., Foster City, CA).

3. Methods

3.1. Pipet Construction

3.1.1. Constriction Pipet

1. Melt a small glass bead onto the end of the microforge filament. (This is necessary for construction of all pipets, but will only be mentioned here.)
2. Mount a piece of 0.018–0.012 glass in the microforge. Make a hook at the end by touching the glass to the filament, heating it to melt a small amount and then moving the pipet down and away from the filament.

3. Relocate the pipet inside the filament. Center the glass between the two sides of the filament and far enough from the tip so there is no differential heating of the glass. Place a 0.5-g weight on the hook and begin heating the glass. The glass will bend, centering the weight. Continue heating until the glass begins to pull (i.e., the glass begins to thin). This is the only way to make sure the weight is centered. Pull the tip of the pipet by heating the glass and allowing the weight to pull it to a diameter of approx 30 μm.
4. Move the glass down so that the filament is about 600 μm from the tip. Remove the 0.5-g weight and replace it with a small wire weight. Heat the glass again, forming a constriction. Stop heating when the inside diameter of the constriction is 15 μm. Melting the glass with little or no weight allows surface tension to constrict the liquid glass. As a result, the outside diameter does not change, but the inside diameter is reduced as the wall thickens, forming the constriction.
5. Remove the wire weight and rotate the pipet 90°. Position the filament at the point where the tip will be cut. Heat the filament just enough to cause the bead to adhere to the pipet. Now move the filament so that the bead touches and adheres to the pipet. As the filament cools, it will break the pipet where the glass bead adheres to it. Heat-polish the tip of the pipet by moving it away from the filament slightly and heating the filament until the glass just begins to melt. The pipet must be in the same plane as the filament or it will bend at this point.
6. Cut the pipet to 13.5 cm and mount it in a 10-cm piece of 0.047–0.027 glass with wax.
7. Calibrate using tritiated inulin or other radioactive compound.

3.1.2. Double-Constriction Pipet

1. Fabricate a single-constriction pipet as above (to **step 5**).
2. Move pipet down and form another constriction so that the volume of the upper chamber is 5 to 10 times the volume of the lower chamber.
3. Create and cut tip as for single-constriction pipet.

3.1.3. Perfusion Pipet

1. Mount a piece of 0.047–0.040 glass in the rotary puller so that most of the pipet is out of the chuck. Place a 1.1-g weight at the end, and pull the glass using approx 22 A and a filament coil with three turns, each 1 cm in diameter. Allow the lower part of the glass to fall at least 10 cm (longer is all right). Remove glass from rotary puller and break at thinnest point. Discard the shorter upper piece and mount the longer bottom piece in the microforge. The bottom piece must be at least 13 cm (*see* **Note 4.1.1.**).
2. Fabricate a hook at the end of the capillary and center it as described before using a 0.5-g weight.
3. Move capillary so that the filament is positioned where the outside diameter of the capillary is 480 μm. Using the 0.5-g weight, pull capillary so that it reaches a diameter of 16 μm.

4. Move capillary up so that the filament is at a point where the pipet is approx 40 μm, and heat so that this region pulls to 16 μm. Continue until a parallel section about 2000 μm long with an outside diameter of 16 μm is formed. (A smaller diameter is acceptable but will increase resistance to perfusion; a diameter below 12 μm is unacceptable.)
5. Once the parallel section has been formed, pull the end of it slightly narrower. This will form a weak area where the glass can be easily broken. Gently grasp weight with fingers and pull. The tip will break at the thinned region with some practice.
6. Rotate pipet 90° and heat-polish end as above.
7. Remove pipet and cut to 12 cm. Heat-polish back end.

3.1.4. Perfusion Holding Pipet

1. Place a piece of 0.084–0.064 capillary in rotary puller with a short length extending past the filament. The filament should have three coils approx 0.7 cm in diameter. Place an 8.4-g weight on glass and pull using 24 A until the weight falls at least 5 cm (*see* **Note 4.1.1.**).
2. Remove glass, break at thinnest section, discard bottom piece, and mount top piece in microforge. The top piece must be at least 12 cm.
3. Make a hook and center as above using the 0.5-g weight.
4. Adjust capillary so that the filament is located where the outside diameter is 640 μm. Pull to 64 μm and make a parallel section 64 μm in diameter and approx 1500 μm long.
5. Remove 0.5-g weight and replace with wire weight.
6. Make a constriction with an inside diameter of 16–20 μm (depending on the size of the perfusion pipet) in the parallel section approx 700–1000 μm from where the capillary was pulled from an outside diameter of 640 μm.
7. Replace 0.5-g weight, and pull off hook and excess glass well below the constriction. This will prevent the tip from bending when it is cut off.
8. Cut and heat-polish tip as above. Then remove pipet and cut it to a length of 9 cm. Heat-polish the end.

3.1.5. Collection Holding Pipet

1. Construct a pipet like the perfusion holding pipet, but without a constriction.
2. Cut to 10, rather than 9 cm.

3.1.6. Exchange Pipet

1. Place a piece of 0.018–0.012 capillary in rotary puller with most of it extending below the filament. Using a 1.1-g weight, pull glass using 22 A and filament with three turns, each 1 cm in diameter. Remove capillary; break and discard top piece. Place bottom piece in microforge (*see* **Note 4.1.1.**).
2. Cut tip at a point where outside diameter is approx 120 μm.
3. Heat-polish tip. Remove pipet from microforge and cut to 13.5 cm.

3.1.7. Sylgard Pipet

1. Mount a four-turn/1-cm filament in the rotary puller. Mount a 0.167–0.150 glass capillary in the rotary puller and place an 8.4-g weight on the end. Begin to pull glass. Once it starts to pull, move filament up slightly. After pulling, the shoulder of the pulled area should be approx 30°. If the angle is shallower, the holding pipet will not reach out the tip (*see* **Note 4.1.1.**).
2. Mount pulled capillary in microforge and make a hook as above. Relocate filament at approx 600 μm. Pull tip to 100–200 μm, break off excess glass, and heat-polish tip as above.
3. Mix a small volume of Sylgard elastic polymer on a piece of foil. Using a needle, a small piece of glass, or other implement, place a small droplet of Sylgard in the tip of the capillary from the outside. Using a can of compressed air, blow Sylgard up and out, coating the inside of the capillary tip. With the heat on the microforge set on low, gently heat the Sylgard to polymerize it. If the heat is too high, the Sylgard will burn. Remove pipet from microforge, cut it to 4.5 cm and heat-polish the back (*see* **Note 4.1.2.**).

3.2. Pipet Assembly

3.2.1. Collection End

1. Place a small amount of silicone oil (viscosity approx 100 cp) in the Sylgard pipet, insert the pipet into the Lucite Sylgard holder, and place on V-track.
2. Using a 15-cm 20-gage needle and 1-mL syringe, add water-equilibrated mineral oil to holding pipet so that the oil extends approx 1 cm past the shoulder.
3. Insert collection holding pipet into its Lucite holder, back first to protect the tip.
4. Mount collection holding pipet assembly on V-track behind the Sylgard assembly.
5. Under a stereomicroscope, move the collection holding pipet assembly forward so that the collection holding pipet enters the Sylgard assembly from the rear. Guide the holding pipet with forceps if necessary to assure that the tip of the collection pipet does not hit the Sylgard pipet assembly. Stop advancing the holding pipet when its tip is at the shoulder of the Sylgard pipet.
6. Insert pin so that the holding pipet assembly can be advanced using the worm drives of the V-track.
7. Advance the holding pipet slowly, adjusting alignment of the Sylgard pipet assembly so that the holding pipet can be advanced out of the Sylgard pipet. The Sylgard pipet should be positioned at the extreme end of the V-track. Connect a piece of tubing to the V-track and the rear end of the holding pipet. Connect a piece of tubing from the V-track to a gas-tight syringe.

3.2.2. Perfusion End

1. Mount V-track on wood block.
2. Backfill perfusion pipet with degassed 150 m*M* NaCl using a 15-cm 20 gage needle mounted on a 0.45-μm syringe filter and 10-mL syringe.
3. Mount perfusion pipet on perfusion-side V-track approx one-third of the distance from the upper end.
4. Attach 30 cm of polyethylene tubing to exhaust port of perfusion assembly.

5. Mount exchange pipet in its holder using dental wax. Adjust length so that the tip of the exchange pipet occupies one-half to two-thirds of the tip of the perfusion pipet (*see* **Note 4.1.3.**).
6. Insert exchange pipet into perfusion pipet assembly from the rear and tighten compression fitting to hold it in place.
7. Backfill perfusion holding pipet with degassed 150 m*M* NaCl using a 15-cm 20 gage needle mounted on a 0.45-μm syringe filter and 10-mL syringe.
8. Mount perfusion holding pipet assembly on perfusion-side V-track from the bottom end, close enough to the bottom so as to avoid breaking the perfusion pipet. Insert holding pipet into its assembly back first.
9. Under a stereomicroscope, advance perfusion pipet forward toward rear-entry hole of holding-pipet assembly. Use forceps to guide perfusion pipet into the rear of the holding-pipet assembly so that its tip does not break.
10. Once the perfusion pipet is safely inside the holding pipet, move holding-pipet assembly up the V-track so that the perfusion pipet is approx 1 cm from the shoulder of the holding pipet. Observe tip of perfusion pipet at all times so you do not run pipets together and break them.
11. Sequentially move perfusion-pipet and holding-pipet assemblies up the V-track to make room for the Sylgard pipet holder.
12. Place about 200 μL of raw Sylgard (without catalyst) into Sylgard pipet and mount it in the holder.
13. Mount Sylgard assembly on V-track from bottom.
14. While observing rear of Sylgard assembly under stereomicroscope, move holding pipet assembly down V-track so that holding pipet enters rear of Sylgard assembly. Be sure perfusion pipet does not exit holding assembly during this process or it will break.
15. Once holding pipet is inside Sylgard assembly, move holding pipet until it is at the shoulder of the Sylgard pipet.
16. Move perfusion pipet forward until it is at the shoulder of the holding pipet.
17. Adjust alignment of the holding pipet, first in the horizontal plane and then in the vertical plane, so that the perfusion pipet will pass out of the holding pipet. As alignment improves, it is necessary to move the perfusion pipet forward. Do not pass the perfusion pipet out of the holding pipet while the tip of the holding pipet is in the Sylgard, which will irreversibly clog the perfusion pipet.
18. Repeat this procedure for the holding pipet and Sylgard. Because this adjustment moves the Sylgard pipet, alignment of the perfusion pipet will not be affected.
19. Pass the tip of the holding pipet out of the Sylgard pipet as soon as possible.
20. Then complete alignment of perfusion pipet. Check alignment by passing perfusion pipet out of holding pipet.
21. Connect exchange pipet to perfusion reservoir, which is a 10-mL syringe mounted on a flex frame so that its height can be adjusted. Place a stopper with a needle passed through it in the perfusion reservoir. Using polyethylene tubing, connect the needle to a gas-tight syringe, connect perfusion exhaust to stopcock and then to a waste bottle, and connect perfusion holding pipet exhaust port to a gas-tight syringe.

3.3. Proximal Tubule Dissection

3.3.1. Rabbit Proximal Convoluted Tubule

1. Anesthetize the rabbit as appropriate. Generally, young rabbits weighing 0.7–1.8 kg are used. Rabbits weighing more than 1.8 kg are difficult to dissect because of increasing amounts of interstitial fibrosis. Pathogen-free animals are generally not necessary (*see* **Note 4.2.1.**).
2. Make a midline incision in the abdomen, exposing the viscera. Move the viscera, exposing the left kidney; then pull it out.
3. Place kidney in physiological saline at 4°C for 1–2 min.
4. Remove kidney from beaker and remove interstitial fat and capsule with forceps.
5. Place kidney on Lucite block with enough cold physiological saline to keep slices wet. Using a tissue-slicer blade, remove 40% of the kidney with a sagittal cut and discard. Proceed to cut sagittal slices as thin as possible, with the tissue slicer blade cutting only the region of the kidney that includes the inner medulla. After five or six slices have been cut, discard remaining kidney. Trim slices by first making a cut to remove the medulla, leaving a hemicircle of cortex. Next, cut hemicircular cortical slice in half, producing two quarter circles from each original slice (*see* **Note 4.2.2.**).
6. Place slices in Petri dish containing physiological saline at 4°C and store on ice.
7. Place Petri dish on cooling stage of dissecting microscope; fill it with physiological saline and place one slice (or a piece of a slice) in the dish (*see* **Note 4.2.3.**).
8. At low magnification, gently pull at cortex with one pair of sharpened Dumont #5 forceps while the other forceps hold the slice in place. Stop when a length of a single proximal convoluted tubule is apparent in a gap as the tissue is pulled apart. Isolate the tissue on both sides of the gap containing the ends of the proximal tubule. Gently tease away surrounding tubules until original tubule is isolated. Once one end of a tubule is free, carefully dissect the other. It is not necessary to dissect until the lower portion is absolutely clean of all debris and other tubules; in fact, leaving small lengths of one or two additional tubules at the lower end is sometimes advantageous (*see* **Notes 4.2.4.** and **4.2.5.**).
9. Once the tubule has been isolated, one end can be cut by breaking the basement membrane using the sharpened needle and then gently pulling on the tubule (*see* **Notes 4.2.6.**).

3.3.2. Rabbit Proximal Straight Tubule

1. Same as in **Subheading 3.3.1.** (to **step 8**).
2. Using blunt Dumont #5 forceps, pull medullary rays from slices. This is accomplished by holding the slice down with one pair of forceps at the bottom of the slice (toward the medulla), grasping a small piece of the slice at the cortical-medullary boundary with the other forceps and pulling toward the cortex. Generally, the slice will tear along a medullary ray. The properties of the proximal nephron change quantitatively with increasing distance from the glomerulus, most notably in the proximal straight tubule. To reduce variability in measured parameters, it is necessary to obtain all tubules from the same level within the cortex.

3. Place Petri dish on cooling stage of dissecting microscope and fill with cold physiological saline.
4. Once five or six rays have been dissected, place them in the Petri dish. With a sharp Dumont #5 forceps, further divide medullary rays under low power until an individual proximal straight tubule is apparent by holding the ray at the bottom with one pair of forceps and tearing upward with the other from the bottom of the ray. Usually, the upper portion of the tubule comes free. Once the upper region of a tubule is free, carefully dissect the lower portion. It is not necessary to dissect until the lower portion is absolutely clean of all debris and other tubules; indeed it is sometimes helpful to leave small lengths of one or two additional tubules at the lower end (*see* **Note 4.2.**, **item 5**).
5. If necessary, you can continue pulling rays apart until only two tubules are attached to each other and then dissect part of one away to obtain a clean free end (*see* **Note 4.2.**, **item 6**).

3.3.3. Rat Proximal Straight Tubule

1. Anesthetize the rat (50–180 g).
2. Make a midline incision in the abdomen and move viscera to the right side of the abdominal cavity, exposing the left kidney. Slowly pour 4°C 150 m*M* NaCl on left kidney while it is still perfused with blood. Use abdominal cavity as holding vessel for cold saline (approx 80 mL over 1 min). This procedure reduces the metabolic activity of the proximal tubules while they still have an adequate supply of oxygen and nutrients. It is virtually impossible to remove a rat kidney quickly enough to prevent ischemic damage without this procedure ***(3)***. This technique is not usually used when dissecting rabbit proximal tubules, but it may prove beneficial.
3. Remove left kidney with forceps and scissors. Place in physiological saline on ice and then proceed as indicated for rabbit proximal straight tubules (**steps 1–5**) (*see* **Note 4.2.**, **item 6.**).

3.4. Tubule Perfusion

1. Load bath reservoir (a 20-mL syringe) with physiological saline.
2. Load perfusion reservoir (a 5-mL syringe) with physiological saline using a syringe with a 0.45-μm filter.
3. After the solution in the perfusion reservoir has warmed to room temperature, exchange fluid in the perfusion pipet by applying pressure on the reservoir via a gas-tight syringe, opening the stopcock at the bottom of the reservoir, as well as the one on the perfusion pipet exhaust. Once 3–4 mL of solution has passed through the perfusion pipet, close the exhaust stopcock.
4. Align pipets on both perfusion and collection sides in both horizontal and vertical planes.
5. Dissect a proximal tubule at least 0.7 mm in length as described before.
6. Place chamber on stage of inverted microscope and fill with cold physiological saline.

7. Transfer tubule to chamber with transfer pipet. The tubule should rest on the bottom of the chamber.
8. Position perfusion pipet at constriction of perfusion holding pipet.
9. Position perfusion holding pipet at one end of the tubule and draw it in by applying suction with a syringe. The tubule should stop at the constriction.
10. While advancing perfusion pipet, apply pressure on the perfusion reservoir so that solution is flowing out of the perfusion pipet. If the pipets are aligned and of the correct size, the perfusion pipet will enter the lumen of the tubule and the lumen will open as solution perfuses it.
11. Raise perfusion end pipets off the bottom of the chamber and open stopcocks on perfusion pipet and perfusion end holding pipet so that any pressure gradients can be eliminated. Move Sylgard pipet forward so that the meniscus of oil extends beyond the end of the perfusion holding pipet.
12. Position the collection holding pipet beyond the end of the Sylgard pipet.
13. Move the collection holding pipet as close to the nonperfused end of the tubule as possible.
14. Using a syringe to create suction at the back of the holding pipet, gently draw the tubule into the collection end holding pipet.
15. Raise the holding end pipets to the same vertical plane as the perfused end.
16. Advance the Sylgard pipet so that silicone oil covers the point at which the tubule enters the collection pipet.
17. Start the bath flowing and turn on the temperature regulator.
18. Adjust the height of the reservoir to achieve a perfusion rate of 5–10 nL/mm/min.
19. Set perfusion rate so that the collection rate is between 5–10 nL/mm/min.
20. Remove tubing from back of collection holding pipet and V-track. Connect tubing to V-track that will hold constriction and junk pipets. Place back end of junk pipet into tubing and drive it into collection holding pipet using rack and pinion. Observe using microscope and advance junk pipet so that the tip is at the shoulder of the collection holding pipet. Using the collection-end syringe, draw solution out of holding pipet until it is below the shoulder. Start the timer and simultaneously remove junk pipet. Replace junk pipet with a constriction pipet that has been filled with mineral oil a small distance past the constriction.
21. Place tip of constriction pipet exactly where the tip of the junk pipet was and begin drawing fluid into the constriction pipet. Maintain the meniscus of the fluid in the same location as when the timer started.
22. When the constriction pipet is filled, stop the timer, remove constriction pipet, and replace with junk pipet. Place constriction pipet on Petri dish with tip up and shaft pressed gently into the clay to hold the constriction pipet while setting up junk pipet.
23. Repeat for each successive collection (*see* **Note 4.3.**).

3.5. Measurements of Solute and Water Fluxes Using Chemical Methods

Chemical methods used to measure fluid and solute fluxes have several advantages over radioactive isotopes. Modern chemical methods are as sensi-

tive as their radioactive counterparts and also permit "real time" measurement of flux. Net fluxes are measured in a single experiment, and chemical methods do not require as many safety precautions as radioactive material ***(5)***. All of the following methods assume that the tubule has been perfused successfully and the perfusion rate adjusted appropriately. The following provide net rather than unidirectional fluxes (*see* **Note 4.4., items 1–3**).

3.5.1. Raffinose

Using raffinose as a volume marker requires that raffinose be added to the physiological saline. Usually, it is added to both perfusion solution and bath at a concentration of 5 m*M*.

1. In a small vial that will hold 400 µL, add NAD 2 mg/mL, alpha galactosidase 8 U/mL and citrate buffer (pH 4.5), forming reagent I.
2. In a test tube, add 3 mL of phosphate buffer (pH 8.6) and enough beta galactose dehydrogenase to achieve a final concentration of 2 U/mL, forming reagent II.
3. De-gas reagent II and load into reservoir of microfluorimeter.
4. Using a double-constriction pipet, collect a sample while drawing solution into the first constriction.
5. Fill pipet to second constriction with reagent II. Wait 3 min, then inject the entire volume of the pipet into the microfluorimeter.

3.5.2. Bicarbonate

1. De-gas 50 mL of distilled water by boiling, then placing on vacuum. It is essential that the water be thoroughly degassed and as little CO_2 as possible be allowed to enter it from the room air.
2. Dilute reagent A containing NADH, Mg, and phosphoenol pyruvate with 26 mL of degassed H_2O so that the final concentrations are 0.123, 3.84, and 0.85 m*M*, respectively. The pH of this solution will be approx 8.0. Gently swirl bottle to dissolve NADH. Place the solution on vacuum immediately.
3. Dilute reagent B containing Mg, phosphoenolpyruvate carboxylase (PEPC), and malate dehydrogenase (MDH) with 0.75 mL of degassed H_2O so that the final concentrations are 26 m*M*, 7332 U/L, and 41066 U/L, respectively. The pH of this solution will be approx 6.5. Place under vacuum.
4. Mix 1.0 mL of reagent A with 0.35 mL of reagent B. Place on ice under vacuum.
5. Load the microfluorimeter reservoir as full as possible. Fill Ascarite holder and place on back of reservoir so that any CO_2 that enters the system is absorbed by the Ascarite.
6. Collect a sample and inject it into the microfluorimeter.

3.5.3. Glucose

1. Dilute reagent to 7.5 rather than 10 mL so that the final concentrations of the ingredients are: ATP 1.3 m*M*, hexose kinase 1333 U/L, NAD 2.0 m*M*, glucose 6 phosphate dehydrogenase 1333 U/L, magnesium 2.8 m*M*, pH 7.5.

2. De-gas under vacuum while warming to approx 35°C.
3. Load glucose reagent into reservoir of microfluorimeter.
4. Collect a sample and inject it into the microfluorimeter.

3.6. Preparation of Ang II-TR

Ang II can be labeled with fluorescein, and such derivatives are commercially available (e.g., Molecular Probes, Inc., Eugene, OR). However, the absorption and emission spectra of fluorescein are similar to the pattern of cell autofluorescence, and the relative intensities of receptor-angiotensin signal and background fluorescence must be considered. An estimate of angiotensin receptor density on proximal tubule cells can be obtained from autoradiographic studies ***(6)*** that indicate approx 1000–5000 sites per cell. Calculations based on the photon yield of the fluorophore show that even if 5000 sites were present and all were occupied, the intensity of the receptor-specific signal would be similar to background. In this situation, it is more effective to use an angiotensin label such as Texas Red with excitation and emission wavelengths distinct from those associated with autofluorescence. It is also possible to use fluorescein-based dyes for simultaneous detection of receptor binding of Texas Red-labeled angiotensin and intracellular ionic composition using dyes selective for calcium, sodium, or pH.

1. Place both columns in a cool room (4°C), and set up a retort stand holding a small glass test tube covered in foil and containing a small magnetic stir bar.
2. Add 1–2 mL of 200 m*M* $NaHCO_3$ to a 50-µL aliquot of Ang II.
3. Add 100 µL of DMF to one vial (1 mg) of Texas Red sulfonyl chloride (*see* **Note 4.5.**, **items 1** and **2.**).
4. Transfer the Ang II solution (from **step 2**) into the glass tube in the cool room and slowly add 50 µL of the Texas Red solution. Stir in the dark in cool room for approx 2 h.
5. Stop the reaction by adding 1.5 m*M* hydroxylamine to a final concentration of 0.15 *M* and stir for approx 1 h.
6. Activate a C18 SEP PAK column with 2 mL of methanol, then 2 mL distilled water (*see* **Note 4.5.**, **item 3**). Discard the effluent.
7. Pass the reaction mixture (from **step 5**) through the SEP PAK column to remove unlabeled Ang II (this should take about 30 s). Then wash with 2 mL distilled water followed by 2 mL each of 10%, 20%, progressively up to 100% methanol. Collect the eluates in polypropylene tubes.
8. Prepare the Sephadex G25 column by flushing with fresh PBS (pH 7.2). This column will remove low-molecular-weight Texas Red byproducts.
9. Examine the eluates from **step 7** and select those that are dark red in color (usually the 20 and/or 30% methanol fractions). Pass these eluates through the Sephadex column and elute with PBS. Collect 1-mL fractions, dilute 1:20 or 1:100 with PBS, and measure fluorescence using a spectrofluorimeter with excitation at 575 nm and

emission 615–620 nm. Usually, there will be major and minor peaks. Pool the fractions representing the major peak; these contain the product.

10. Calculate the concentration of the product by measuring absorbance over the range 200–700 nm (*see* **Note 4.5.**, **item 4**).
11. It is advisable to make sure the labeled Ang II-TR retains biological activity. This can be done with a variety of assays, including measurement of pressor activity following intravenous injection into an anesthetized rat. By comparison with equivalent doses of nonlabeled Ang II, we have found 95% retention of activity.

3.7. Loading of Proximal Tubule Cells with Ion-Selective Dyes

We describe a method for simultaneous imaging of binding of Ang II to tubular receptors and intracellular ionic events associated with binding and internalization *(7)*. Ang II is known to increase intracellular concentrations of sodium *(8)* and calcium *(9)* and, under certain conditions, can affect intracellular pH by activation of luminal sodium/hydrogen exchange and basolateral sodium-bicarbonate cotransport. Selective fluorescent dyes are available for all three ions (e.g., Molecular Probes) and can be introduced into proximal tubules as their acetoxymethyl ester derivatives, which are membrane-permeant.

Rigorous quantitative imaging of these ions requires ratiometric measurements. The ratios of intensities of emission signals for two excitation wavelengths (or one excitation and two emission wavelengths) are used to determine the fluorescence output of the dye independent of changes in its cellular distribution or concentration during the experimental period. The system described here is specific for a receptor ligand plus a single nonratiometric ionic dye for which excitation at a single visible excitation wavelength is used and a single-emission wavelength detected. More complex systems can be constructed to enable the use of ratiometric dyes such as Fura-2 for calcium or SBFI for sodium. These require UV excitation and entail modification of the microscope optics to allow UV transmission. In addition, switching between the two excitation wavelengths (e.g., using a rotating filter wheel or acousto-optical tunable filter) must be incorporated together with an appropriate triple-bandpass emission filter and image collection protocols.

Useful information can be obtained by combining imaging of labeled Ang II binding and Fluo-3, a nonratiometric dye, recording changes in intracellular calcium concentration.

1. Prepare fresh Fluo-3 AM each day by dissolving contents of 1-mg pack in DMSO to obtain stock solution (1 mg/mL or approx 1 m*M*).
2. Dissect and perfuse proximal tubule as described in **Subheadings 3.3.** and **3.4.** using control solutions. Do not allow temperature of bath to rise above room temperature (*see* **Note 4.6.**, **item 1**).
3. Stop bath perfusion and add Pluronic detergent to give final proportion of 20% in bath (*see* **Note 4.6.**, **item 2**).

4. Add Fluo-3 AM (from **step 1**) to give final bath concentration of 20 *M*.
5. Incubate for 15–30 min; then commence bath perfusion to remove excess dye and Pluronic (*see* **Note 4.6.**, **item 3**).

4. Notes

Although the description of techniques in this chapter is detailed, it can by no means be considered complete. Several laboratories have modified the original technique of isolation and perfusion of renal tubules, and new technologies are being applied to this preparation as they develop. Given the very technical nature of isolation and perfusion of renal tubules, these techniques are best learned directly from someone who is already an expert. Initiation of experiments requiring isolated, perfused proximal tubules by the novice can be a trying and frustrating experience, wasting both time and resources.

4.1. Pipet Construction and Assembly

1. The initial pull of a capillary on the rotary puller has a large influence on both the final shape and the ease with which one can alter the shape of the glass on the microforge. If pulls on the rotary puller are not adequate, it will be difficult to make the secondary pulls on the microforge. An indication of this will be long times required for pulling (>30 s) and blackening of the glass caused by Pt leaving the filament and plating the glass. In general, when long tapers are required, the bottom piece of glass is used after pulling on the rotary puller, and both high currents and small weights are needed. If a sharp taper is required, larger weights, lower current, and the top piece are used.
2. When fabricating the Sylgard pipet, one has to be extremely careful to be sure to blow Sylgard out the tip of the Sylgard pipet before heating it; otherwise the Sylgard will polymerize in the tip and the pipet must be discarded. Additionally, if the primary pull of the Sylgard does not create a steep enough shoulder, the holding pipet will not extend past the tip of the Sylgard pipet.
3. If the exchange pipet is too far from the tip of the perfusion pipet, the fluid in the perfusion pipet will not exchange properly.
4. At present, there is only one commercially available source for perfusion equipment, Luigs and Neumann (Ratingen, Germany). The authors have not used this equipment and it may not use capillary tubing of the same dimensions as the original perfusion setups manufactured by White. The only other option available is for an investigator to obtain an original set and have a competent machinist duplicate it because the original maker of perfusion V-tracks and Lucite pieces has passed away.

4.2. Tubule Dissection

1. Rabbits have a tendency to vocalize even when under general anesthesia. Use of local anesthesia at the point of incision may be necessary.

2. Attempts at using mechanical devices to aid in slicing the kidney have generally proved unsatisfactory. With a little practice, one can develop sufficient skill to obtain very thin slices (<1 mm) of uniform thickness.
3. The cooling stage for the dissecting microscope can be low tech (a Petri dish in which water has been frozen) or high tech (Peltier cooling devices). Whereas the latter has certain advantages, such as precise control of temperature and ease of use, the former is simple, inexpensive, and requires little effort.
4. Coating the forceps with albumin prior to use will help prevent sticking. One merely needs to make approx 10% albumin solution, dip the forceps in this solution, and allow them to dry before use. During dissection, the process can be repeated without allowing the forceps to dry with some beneficial effect. Similar coating of the transfer pipet will also prevent tubules from sticking to it.
5. The material from which the forceps are made is not critical. Steel sharpens easily and is not brittle, whereas titanium stays sharp longer, but can be brittle.
6. One of the key factors in successful dissection of proximal tubules is to do everything as quickly as possible, as the tissue is extremely sensitive to anoxic damage. Once one begins fine dissection under the stereomicroscope, it is easy to determine if the tissue is in good shape up to this point. Dissected tubules should be removed from the slices relatively intact, that is, in long pieces that are easily identified as tubules. If the tubules disintegrate when dissected and the tissue seems to "explode" on contact, it is no longer viable and there is no point in continuing. Equally important, and the primary method to decrease dissection time, is to partially dissect a large amount of tissue looking for a tubule that can be isolated easily. This is much faster and yields better results than simply selecting a tubule and dissecting it free. Also, it is possible to dissect tubules from both smaller and larger animals than the range listed above. However, the success rate with large animals drops dramatically, and one must interpret data from younger animals with caution because developmental changes in the kidney may not be complete. This is especially true for murine kidneys, which continue nephrogenesis for approx 14 d after birth. Finally, one has to take great care not to crush the ends of the tubules when dissecting and/or cutting. If this occurs, it becomes extremely difficult to perfuse the tubule.

4.3. Tubule Perfusion

There are several factors that can make perfusion of a tubule difficult. If the pipets are not aligned, the end of the tubule has been damaged, or the pipets are too large, the tubule will not perfuse easily. If the tip of the perfusion pipet is too short or the diameter too large, it will be difficult to set the perfusion rate because small changes in the height of the reservoir will result in large changes in flow. If there is too little or too much oil in either the collection holding pipet or the Sylgard pipet, it will be difficult to maintain perfusion without contamination of the bath. Consequently, a great deal of attention must be paid to numerous details to be successful. Because of this, it is best to set up the perfusion microscope in

an isolated area where one will not be interrupted during the experiment. It also helps to have a very detailed checklist of duties that must be performed each day. Even investigators with more than 20 yr of experience still use such lists.

Much has been made of the effect of albumin in the bath when perfusing individual proximal tubules. Careful study indicates that inclusion of 6% albumin in the bath does not significantly increase fluid absorption or affect tubule viability. Consequently, adding albumin to the bath appears to be an unnecessary complication in isolated, perfused proximal tubule experiments. The implications of this for tubuloglomerular balance in vivo are beyond the scope of this chapter. Additionally, adding albumin to the bath may introduce peptidases that break down Ang II. This explanation is usually given in early reports which showed no effect of angiotensin on proximal nephron transport.

As with all other aspects of tubule perfusion, there are a number of parameters that must be attended to if one is to be successful. If the perfusion/collection rate is too fast, there will appear to be no flux. It is also all but impossible to make a collection in less than 45 s. If the rate is too slow, flux may be underestimated because of the development of a massive gradient across the epithelium. In extreme cases, lumen-to-bath flux can equal bath-to-lumen flux and there will be no apparent net flux. Additionally, if the collection holding pipet is dirty, a meniscus will not form and it will be difficult to determine how much fluid has entered the holding pipet. Frequently it is easier to make a new collection pipet than to clean the old one.

The characteristics of the Sylgard pipet will also affect the ability to make collections. Sylgard pipet tips with smaller diameters are easier to use than larger ones. Also, as described before, the amount and viscosity of the oil in the Sylgard pipet will affect the ability to make collections.

As with so much of tubule perfusion, one learns a standard method, then modifies it to suit his or her personality. This is also true of cleaning the pipets. Some investigators take apart the complete setup every day for cleaning; others use NaOH and HCl every day, but only dismantle the setup once a week. Finally, some very successful investigators clean with NaOH and HCl until the pipets cannot be used any longer because of a plug by organic or inorganic material. The middle ground is recommended until an investigator has gained some experience.

4.4. Chemical Determination

1. Fluorimetric assays are relatively straightforward, but in order to be most effective, one must have a thorough understanding of the fluorimeter, as well as potential sources of noise and interference, and must be able to address problems in a systematic manner. The latter will eventually lead to the ability to analyze a problem with the fluorimeter based on the chart recorder records.

2. To improve accuracy, one should measure samples of the perfusion solution many times so that this value is precisely known. Additionally, when possible, samples of perfusion solution should be measured immediately before and after samples of collected fluid. Standard curves for the compound of interest should be generated at the end of each experiment.
3. Several other compounds have been measured using fluorimetric assays, and the assays described here are only those associated with fluxes actually reported to have been altered by Ang II ***(10,11)***. Certainly these are not the only methods available to measure fluid, bicarbonate and glucose flux. For instance, bicarbonate can also be measured using a picapnotherm ***(12)***. Alternatively, one can use radioactive tracers to determine fluid and solute absorption. Traditionally, methoxyinulin has been used as a volume marker to measure fluid absorption ***(13)***. Measurements of isotopic glucose, amino acid, and inorganic phosphate flux yield unidirectional lumen-to-bath fluxes. The procedure for measuring each of these fluxes is essentially the same. Because glucose, amino acids, and inorganic phosphate can be metabolized into other compounds, flux is measured by loss of material from the lumen, which is assumed to be the unidirectional transepithelial flux. The alternative is to record the appearance of radioactive material in the bath and separate out the various radioactive species using chromatography or other methods, then determine how much of the total radioactivity is actually the compound of interest. This technique is mentioned here so that the reader is aware of this possibility, but it is not routinely performed ***(14,15)***.
4. A microfluorimeter is commercially available from World Precision Instruments (Sarasota, FL) at the time of this writing. The authors have no first-hand experience with this instrument. A microfluorimeter similar in design, but using mostly commercially available components and a minimum amount of machining, can be made for one-third to one-half the price of the commercially available fluorimeter ***(16)***.

4.5. Receptor Binding

1. DMF, rather than DMSO, should be used, as DMSO reacts with sulfonyl chlorides.
2. If the Texas Red does not dissolve, add 900 μL of 200 m*M* $NaHCO_3$ to the vial and mix. Then, in **step 4** take 500 μL of Texas Red solution instead of 50 μL.
3. Solutions should be sucked through the column with a 2-mL syringe, rather than allowed to flow with gravity.
4. Concentration is derived from absorbance using the Beer-Lambert law: Abs = $E \times C \times L$, where E is the absorbance coefficient of the dye (85,000 for Texas Red), C is concentration, and L is the length of the light path in the spectrophotometer.

4.6. Intracellular Signaling Studies

1. The use of room temperature is a compromise between the preferred temperature for maximizing viability of the tubules, which should be around 4°C, and higher temperatures that will facilitate de-esterification of the dye within the cells.

2. Pluronic is used as a dispersing agent for the AM form of the dye, which has low aqueous solubility.
3. The incubation time is an approximation and will need to be pinpointed by trial and error. Shorter incubation periods will result in healthier tubules and permit longer experiments. Conversely, prolonging incubation will result in more extensive dye loading, increased fluorescence output and improved signal-to-noise ratio—but with tubules in poorer condition. A two-phase loading protocol can also be advantageous, with an initial period at low temperature (allowing permeation of the dye) and the remainder at the working experimental temperature (when de-esterification is accelerated).

Acknowledgments

The methods described for fluorescent labeling and imaging were developed in collaboration with Dr. Malea Kneen and Ms. Kathryn Aldred.

References

1. Burg, M. B., Grantham, J. J., Abramov, M., and Orloff, J. (1966) Preparation and study of fragments of single rabbit nephrons. *Am. J. Physiol.* **210,** 1293–1298.
2. Harris, P. J., Hiranyachattada, S., Antoine, A. M., Walker, L., Reilly, A. M., and Eitle, E. (1996) Regulation of renal tubular sodium transport by angiotensin II and atrial natriuretic factor. *Clin. Exp. Pharmacol. Physiol.* **Suppl. 3,** S112–S118.
3. Garvin, J. L. and Knepper, M. A. (1987) Bicarbonate and ammonia transport by isolated, perfused rat proximal straight tubules. *Am. J. Physiol.* **253,** F277–F281.
4. Inoue, S. and Spring, K. R. (1997) *Video Microscopy: The Fundamentals.* Plenum, New York.
5. Garvin, J. L., Burg, M. B., and Knepper, M. A. (1985) Ammonium replaces potassium in supporting sodium transport by the Na-K-ATPase of renal proximal straight tubules. *Am. J. Physiol.* **249,** F785–F788.
6. Zhuo, J., Alcorn, D., Harris, P. J., McCausland, J., Aldred, P., and Mendelsohn, F. A. O. (1995) Angiotensin I receptor subtypes in the kidney: distribution and function. *Nephrology* **1,** 511–525.
7. Kneen, M. M. and Harris, P. J. (1996) Direct visualisation of angiotensin II binding in proximal tubules by fluorescence imaging. *Proc. Aust. Physiol. Pharmacol. Soc.* **27,** 54P.
8. Reilly, A. M., Harris, P. J., and Williams, D. A. (1995) Biphasic effect of angiotensin II on intracellular sodium concentration in rat proximal tubules. *Am. J. Physiol.* **269,** F374–F380.
9. Antoine, A. M., Reilly, A. M., Harris, P. J., and Williams, D. A. (1997) Effect of angiotensin II on intracellular calcium levels in isolated rat proximal tubules. *Proc. Aust. Physiol. Pharmacol. Soc.* **28,** 103P.
10. Garvin, J. L. (1991) Angiotensin stimulates bicarbonate transport and Na^+/K^+ ATPase activity in the proximal nephron. *J. Am. Soc. Nephrol.* **1,** 1146–1152.
11. Garvin, J. L. (1990) Angiotensin stimulates glucose and fluid absorption by rat proximal straight tubules. *J. Am. Soc. Nephrol.* **1,** 272–277.

12. Vurek, G. G., Warnock, D. G., and Corsey, R. (1975) Measurement of picomole amounts of carbon dioxide by calorimetry. *Anal. Chem.* **47,** 765–767.
13. Schafer, J. A., Troutman, S. L., and Andreoli, T. E. (1974) Volume reabsorption, transepithelial potential differences, and ionic permeability properties in mammalian superficial proximal straight tubules. *J. Gen. Physiol.* **64,** 582–607.
14. Barfuss D. W. and Schafer J. A. (1981) Differences in active and passive glucose transport along the proximal tubule. *Am. J. Physiol.* **240,** F322–F332.
15. Barfuss, D. W. and Schafer, J. A. (1979) Active amino acid absorption by proximal convoluted and straight tubules. *Am. J. Physiol.* **236,** F149–F162.
16. Garcia, N. H., Plato, C. F., and Garvin, J. L. (1999) Fluorescent determination of chloride in picoliter samples. *Kidney Int.* **55,** 321–325.

32

Isolated Resistance Artery Preparation

Jos P. M. Wesselman, Paul H. Ratz, and Russell L. Prewitt

1. Introduction

The blood vessels that contribute most to precapillary resistance are known as resistance arteries, consisting of arterioles and small arteries with diameters of less than 500 μm *(1)*. These vessels regulate the vascular resistance, and thus the blood supply, through the adjustment of their lumen diameter, which is accomplished by modulation of the level of tone in the vascular smooth muscle cells. The smooth muscle and endothelial cells in the blood vessel wall are sensitive to a great diversity of stimuli including distending pressure, shear stress, neurohumoral factors, and metabolites. All of these different signals are sensed, integrated, and eventually lead to a response.

In vivo and in vitro methods have been used in attempt to gain more insight into the signal transduction mechanisms by which stimulation results in a particular response in resistance arteries. These two approaches have specific advantages and disadvantages, and the method selected depends strongly on the aim of the study. In vitro systems provide a methodology by which resistance arteries can be studied under carefully controlled conditions. Thus, transduction pathways that may be simultaneously active in vivo, can be separated and individually studied. For resistance arteries, the most frequently utilized in vitro methods are the wire myograph and the pressure myograph.

The wire myograph was developed in 1972 by Bevan and Osher *(2)*, and it was the first method that allowed the determination of mechanical properties of small blood vessels in vitro. In this method, vessel segments are mounted on two fine wires that are clamped at each end to keep the vessel isometric. A displacement device is used to adjust the distance between the two wires, and the force generated by the vessel is measured by a force transducer. In 1981,

From: *Methods in Molecular Medicine, vol. 51: Angiotensin Protocols*
Edited by: D. H. Wang

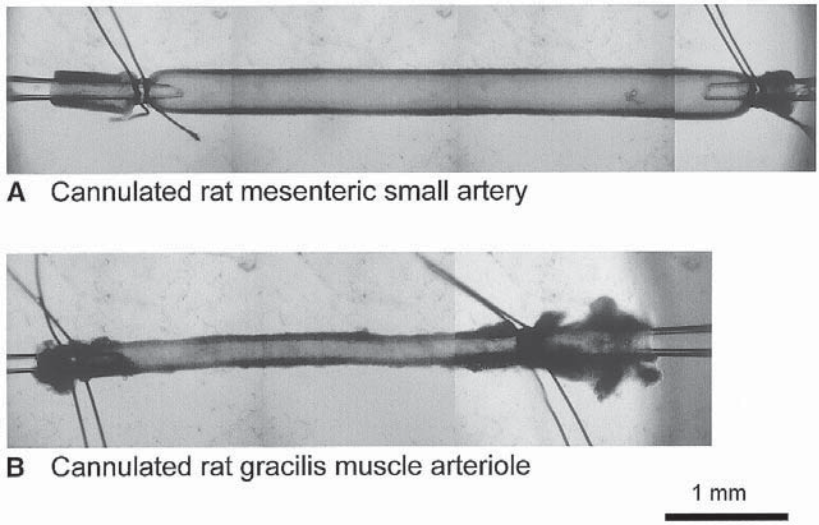

Fig. 1. Photographs of transilluminated cannulated rat first-generation mesenteric **(A)** and first-order gracilis muscle **(B)** resistance arteries. Two 10–0 Ethilon nylon sutures are used on both sides to tie the vessels onto the glass cannulas. See text for a detailed description of the isolation and cannulation procedure.

Duling et al. introduced the pressure myograph ***(3)***, a method where the vessels are mounted on glass cannulas at both ends. Originally, the vessels were held at each end between two concentric pipets, but this technique has been simplified over the years to a procedure where the vessel is tied onto the cannulas with a thin ligature (*see* **Fig. 1**). The intraluminal pressure and flow can be controlled, and the vessel size can be monitored. The pressure myograph is, in many ways, superior to the wire myograph. First, it is less traumatic to the arteries. At those positions where the wires make contact with the luminal side of the vessel, the endothelium is severely damaged. Second, the pressure myograph allows smaller vessels to be examined, down to a diameter of 12 μm. Third, because the pressure myograph allows perfusion and maintenance of the original geometry of the vessels, it is a more physiological model of the in vivo situation ***(1,4)***.

Therefore, this chapter focuses on the cannulated resistance artery preparation, including the components of a pressure myograph system, the construction of glass cannulas and the physiological saline solutions. This is followed by a detailed description of the isolation and cannulation procedure, a survey of possible applications of this technique, and finally, notes on alternative approaches and tips to overcome potential problems.

2. Materials

2.1. Pressure Myograph Systems

Pressure myograph systems consist of the myograph itself, a pressure tower or pump, an upright or inverted microscope with video camera, and a PC with data acquisition and analysis software. These systems are commercially available (Living Systems Instrumentation, Burlington, VT, and JP Trading, Aarhus, Denmark). The myographs are made of inert material (to avoid possible toxicity effects), and contain a vessel bath (volume ranges between 2 and 10 mL), cannula holders (that are adjustable for precise alignment of the vessel), and ports for superfusion, rapid draining and filling, and gas supply (*see* **Note 1**).

Intravascular pressure can be generated by means of a pressure tower or a peristaltic pump. A pressure tower includes one or two fluid reservoirs that are connected to the cannula(s). Adjusting the height of the reservoirs generates the desired hydrostatic pressure, but the maximum is limited by the height of the laboratory ceiling to approx 200 mmHg. Higher pressures can be obtained with a peristaltic pump and the pulsations can be reduced by a windkessel if desired. Pressure transducers are used to continuously register the intravascular pressure. Commercially available pressure servo-control systems can be used to control not only pressure, but intraluminal flow as well. The perfusion rate is determined by the tubing, and ranges between 2.5 μL/min and 2.5 mL/min. These systems allow the maintenance of pressure during flow changes and intraluminal delivery of vasoactive agents.

The myographs are mounted on the stage of an upright or inverted microscope, and the cannulated vessel is transilluminated. The vessel image is recorded with a video camera, and displayed on a TV monitor. The image quality is crucial for an accurate measurement of the vessel dimensions, and using a long working distance objective and a condenser, a resolution of circa 1 μm can be accomplished ***(4)***. The internal and external diameter of the cannulated vessel can be continuously measured by on-line or off-line processing of the video signal. This can be done manually using a video caliper (Texas A&M, College Station, TX) or automatically by an electronic dimension analyzer (Living Systems Instrumentation). For a detailed description of the latter device, see Halpern et al. ***(4)*** and Osol and Halpern ***(5)*** (*see* **Note 2**).

2.2. Construction of Cannulas

Cannulas to which the blood vessels are attached are usually constructed from borosilicate glass capillaries (*see* **Note 3**). Commercially available glass capillary tubing differs in length, internal and external diameter, and thickness which can be chosen depending on the experimental setup and size of blood vessel one wishes to study. For small arteries (diameter: 100–500 μm) we

recommend the use of relatively thick-walled capillaries (external diameter: 1.20 mm and internal diameter: 0.68 mm, World Precision Instruments [WPI], Sarasota, FL), whereas thinner-walled, but more fragile, tubing is appropriate for arterioles (diameter < 100 μm). To make cannulas from these capillaries, a relatively simple micropipet puller can be used (PUL-1, WPI). By optimizing the adjustable parameters, such as heat, delay, or force, the desired shape can be produced. Care should be taken to make a tip with very little taper (*see* **Fig. 1**), to prevent the vessel from sliding off when the pressure is raised. After pulling the cannulas, the tip is broken at the preferred diameter, depending upon the size of the vessel. Subsequently, the tip has to be polished, to prevent damage of the vessel when it is slipped on the cannulas, for example by means of a microforge (MF-9, Narishige, Greenvale, NY). The latter apparatus can also be used to further fine-tune the shape of the cannula (*see* **Note 4**).

The ligature used to tie the vessels onto the cannulas has to meet certain criteria. It has to be thin, roughly between 15 and 30 μm, depending on the size of the vessels. It also has to be supple, as well as strong. In the literature, usually silk or nylon suture is used to secure the vessels to the cannulas. Examples are 10-0 monofilament silk suture (Alcon Laboratories, Fort Worth, TX), or 10-0 Ethilon nylon suture (Ethicon, Somerville, NJ) (*see* **Note 5**).

2.3. Physiological Saline Solution

In order to keep the cannulated resistance artery alive for at least several hours, it has to be kept in a physiological saline solution (PSS), at a pH of 7.4 and a temperature of usually 37°C. An exception is the cremaster muscle arteriole, where a temperature of 33–34°C is used ***(6)***. An excellent control of temperature and pH is of pivotal importance, because certain physiological characteristics of resistance arteries have been shown to depend on these parameters. As an example, temperature was found to affect the calcium sensitivity of the contractile filaments in the vascular smooth-muscle cells of cannulated rat cerebral arteries ***(7)***. Furthermore, Ishizaka et al. demonstrated that a moderate reduction of the pH of the PSS from 7.4 to 7.3 significantly reduced basal smooth muscle tone of cannulated porcine coronary arterioles ***(8)***.

The PSS should be similar in saline composition and osmolality to the blood plasma and interstitial fluid that surrounds the resistance arteries. In published studies on cannulated resistance arteries, the composition of the PSS shows some variation. This can be because of differences in the experimental setup, or in the design of the experiments. Here, we give one example: PSS, composition (in m*M*): NaCl (119), KCl (4.7), KH_2PO_4 (1.18), $MgSO_4$ (1.17), $CaCl_2$ (1.6), $NaHCO_3$ (25), HEPES (10), ethylenediamine tetraacetic acid (EDTA) (0.026), glucose (5.5). The pH is set at 7.4 using 1 *N* NaOH and 1 *N* HCl, and gently bubbling with a 5% CO_2 and 95% air mixture keeps the pH constant

(9,10). This PSS can be used for both superfusion and perfusion of the cannulated vessels (*see* **Note 6**). Ideally, the PSS should be made freshly on the day of the experiment (*see* **Note 7**). Usually, in the pressure myograph setup, the cannulated artery is superfused with a PSS that is pumped from a reservoir where its temperature and pH are controlled.

For the isolation of the resistance arteries, a cold (0–4°C) dissection PSS is used, which may differ from the PSS that is used for superfusion and perfusion *(11,12)*. Usually, the composition (m*M*) of the dissection PSS is based on the modified Ringer solution described by Duling et al.: bovine serum albumin (1%), NaCl (145), KCl (4.7), $CaCl_2$ (2.0), $MgSO_4$ (1.2), glucose (5.0), pyruvate (2.0), MOPS (2.0), EDTA (0.02), NaH_2PO_4 (1.2), at pH 7.4 *(3)*.

In order to study the cannulated resistance artery in the passive state, without any smooth muscle tone, a Ca^{2+}-free PSS is often used. Ca^{2+}-free PSS is usually made by omitting $CaCl_2$ from normal PSS, and including 1 or 2 m*M* EGTA *(13)*. Ca^{2+}-free PSS can be used to determine passive pressure-diameter relations of cannulated resistance arteries *(11,12)*, or to test the involvement of calcium in signal transduction mechanisms *(13)*.

3. Methods

3.1. Isolation and Cannulation of Resistance Arteries

3.1.1. Types of Resistance Arteries

Since Duling et al. introduced the pressure myograph in 1981 *(3)*, many types of resistance arteries of have been studied using that technique. By far, most studies involve resistance arteries from various tissues of the rat. These include mesenteric *(11)*, gracilis muscle *(12)*, cremaster muscle *(6)*, posterior cerebral *(5)*, middle cerebral *(14)*, renal afferent *(15)*, tail *(16)*, uterine *(17)*, and coronary *(18)* arterioles or small arteries. Other resistance artery types that have been studied using the pressure myograph are rabbit mesenteric *(19)*, coronary *(20)*, cerebral *(21)* and pial *(22)*, cat cerebral *(23)*, dog renal *(24)* and ileum *(25)*, pig coronary *(26)* and pulmonary *(27)*, sheep gracilis muscle *(28)*, and hamster cheek pouch, testis, and mesenteric *(3)* arteries. In recent years, an increasing number of studies have been conducted on different types of human cannulated resistance arteries, these include subcutaneous small arteries *(29,30)*, cerebral resistance arteries *(31)*, coronary arterioles *(32)*, fetoplacental small arteries *(33)*, and basilar and middle cerebral small arteries of human infants *(34)*. Note that the references in this section should be considered as representative examples; they are not complete inventories of all the studies on a certain vessel type. Especially, rat mesenteric and gracilis muscle arteries (**Fig. 1**) are used in numerous studies. Therefore, we will describe the method of isolation and cannulation of these vessel types in more detail.

3.1.2. Methods of Isolation and Cannulation

The rats are anesthetized with pentobarbital (50 or 60 mg/kg body weight, intraperitoneally) ***(9)***. For isolation of mesenteric small arteries, a laparotomy is performed and part of the intestine and mesentery are removed and pinned out in a silicone-lined chamber filled with a cold dissection PSS ***(11)***. In the mesenteric circulation, arteries and veins are paired and surrounded with adipose and connective tissue. The anatomy of the arteriolar network is such that the superior mesenteric artery branches off into various generations of resistance arteries. The first-generation arteries can be quite long, >10 mm ***(35)***, and their relaxed internal diameters at the physiological pressure, which is circa 100 mmHg ***(36)***, ranges from 300 to 500 μm ***(11,37)***. As is illustrated by Sun et al. ***(11)*** and McGuffee et al. ***(35)***, vessel length and diameter decrease with the order of generation. The arteries and veins must be carefully isolated from the surrounding tissue, for example by using a stereo microscope (Nikon SMZ-2T, Nikon, Melville, NY), and microinstruments, such as a no. 5 straight forceps (Moria 9980, Fine Science Tools, Foster City, CA), and microdissecting scissors (Roboz RS-5604, Roboz Surgical Instrument Company, Rockville, MD). After the arteries and veins are completely isolated, they can be easily distinguished by their difference in diameter and wall thickness. The artery is excised and transferred to the vessel bath of the myograph.

The gracilis muscle arteriole, known as the muscular branch from the femoral artery, feeds the gracilis muscle, as illustrated by Sun et al. ***(12)***. Because of a large number of branches, cannulated segments of first-order gracilis muscle arterioles are not very long, 3–5 mm ***(38)*** and their relaxed diameter is approx 200 μm ***(12)***. The gracilis muscle is excised and placed in dissection PSS for isolation of the feeding arteriole and/or its second- and third-order branches. Surrounding muscle and connective tissue, as well as the vein that runs alongside, are carefully removed, using the aforementioned dissection microscope and surgical tools. Then, the arteriole is isolated and cannulated.

The cannulation procedure is basically the same for all arteries. While observing through the dissecting microscope, one end of the isolated artery is slipped on the proximal cannula, which is filled with perfusion PSS, and is carefully tied with 10–0 ligature. Subsequently, the perfusion pressure is slightly raised, to circa 20 mmHg, to flush and clear the vessel of blood (*see* **Note 8**), and the other end is tied on the distal cannula. Next, the vessel has to be checked for leaks through small branches or defects. This can be accomplished by pressurizing the vessel, then closing the valves to the pressure reservoir, and verifying that the intraluminal pressure and diameter remain constant. If the vessel is leaking, any branches can be tied off ***(26)***, or the vessel can be recannulated beyond the branch. Note that pressure elevation will not only change the vessel diameter, but also the axial length, which must be adjusted to

prevent any buckling. The cannulation is usually followed by an equilibration period of 30–60 min, during which the temperature is slowly raised to 37°C at a chosen intraluminal pressure (*see* **Notes 9** and **10**).

3.2. Parameters That Can Be Studied

3.2.1. Structural and Mechanical Parameters

By measuring the internal diameter (ID) and external diameter (ED) at different intraluminal pressures, the image of the transilluminated resistance artery can be used to obtain other structural and mechanical vessel parameters. These include the following.

1. Wall thickness: WT = (ED-ID)/2) (μm).
2. Wall cross-sectional area (wall CSA): external CSA – luminal CSA, wall CSA = $\pi(ED^2\text{-}ID^2)/4$) (μm^2).
3. Wall tension: T = pressure (P) × radius (ID/2) (dyn/cm), where 1 mmHg = 1334 dyn/cm^2).
4. Circumferential wall stress: $\sigma = T/WT$ (dyn/cm^2).
5. Incremental distensibility: D_i, which represents the change in ID per mmHg change in P, $D_i = [(1/ID)(DID/DP) \times 100]$ (% / mmHg) ***(39)***.
6. Circumferential strain: $\varepsilon = (ID–ID_o)/ID_o$ (%), where IDo is the original ID at 1 mmHg.
7. Wall-to-lumen ratio (%), which is the ratio between WT and ID.

In addition to the structural and mechanical analysis aforementioned, more detailed information about the resistance artery structure can be obtained by fixing the artery in the chamber and using histology ***(40)*** or electron microscopy ***(30)***. **Figure 2** shows an example of the histological approach.

3.2.2. Intracellular Calcium Concentration

The intracellular calcium concentration, $[Ca^{2+}]i$, of smooth muscle and endothelial cells in cannulated resistance arteries can be measured with various fluorescent Ca^{2+} indicators, such as fura-2 (Molecular Probes, Eugene, OR). This method has been applied on cannulated resistance arteries from rat mesentery ***(10)***, gracilis muscle ***(41)***, cremaster muscle ***(6,42)***, rabbit heart ***(20)***, and hamster cheek pouch ***(43)*** (*see* **Note 11**). **Figure 3** shows an example of the effect of pressure in cannulated rat mesenteric small arteries on luminal CSA and smooth muscle $[Ca^{2+}]i$.

3.2.3. Smooth-Muscle Membrane Potential

In 1984, Harder was the first to report the measurement of smooth muscle membrane potential (Em) in intact cannulated resistance arteries using microelectrodes ***(23)***. This method has been applied in cannulated rat mesenteric ***(44,45)***, rat cerebral ***(46)***, rabbit cerebral ***(21)***, cat cerebral ***(23)***, and dog ileum

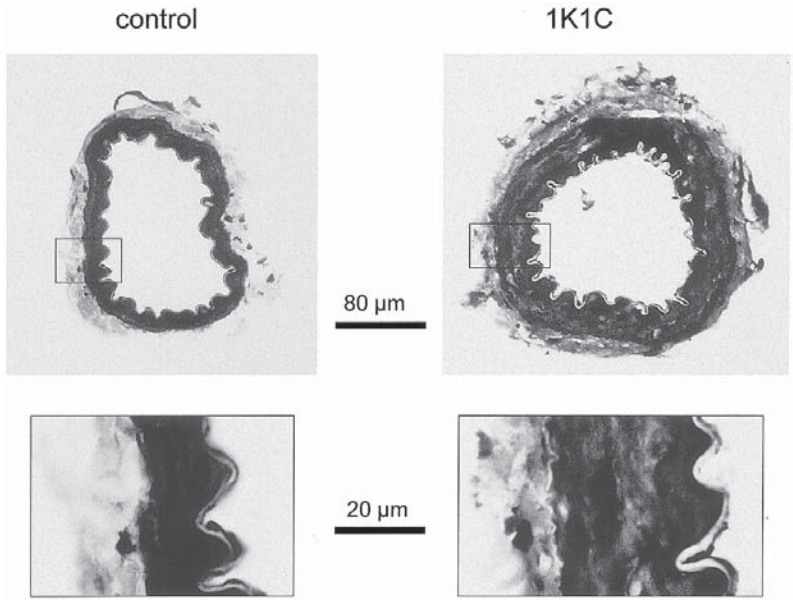

Fig. 2. Histological cross-sections of rat mesenteric arteries of control and one-kidney one-clip (1K1C) hypertensive rats. First-generation rat mesenteric small arteries from control (blood pressure 110 mmHg) and 1K1C hypertensive rats (220 mmHg) were cannulated and pressurized at 90 mmHg. The relaxed internal diameters were 308 and 276 μm, the wall thicknesses 19 and 38 μm, wall areas 18947 and 37150 μm^2, and wall-to-lumen ratios 0.06 and 0.14 for the normotensive and hypertensive arteries, respectively. Subsequently, the arteries were removed from the cannulas, fixed in 10% buffered formalin, dehydrated in graded alcohol, and embedded in paraffin. Sections (5-μm thick) were stained with toluidine blue ***(37)***. Using video-based image analysis, the different layers (intima, media, and adventitia) were measured by means of JAVA software (Jandel Scientific, Corte Madera, CA). By this method, the thicknesses and CSAs of the media alone were 16 and 27 μm, and 9704 and 18869 μm^2 for the normotensive and hypertensive arteries, respectively.

(25), and renal ***(24)*** small arteries (*see* **Note 12**). An example of an Em-measurement in cannulated rat mesenteric small arteries during norepinephrine-induced vasomotion at different pressures is depicted in **Fig. 4**.

3.2.4. Protein Phosphorylation

Traditionally, protein phosphorylation measurements in the vasculature are performed on smooth muscle tissue derived from isometrically clamped strips of large arteries. Nevertheless, several recent studies demonstrate that measurement of phosphorylation of the myosin light chain (MLC) in resistance

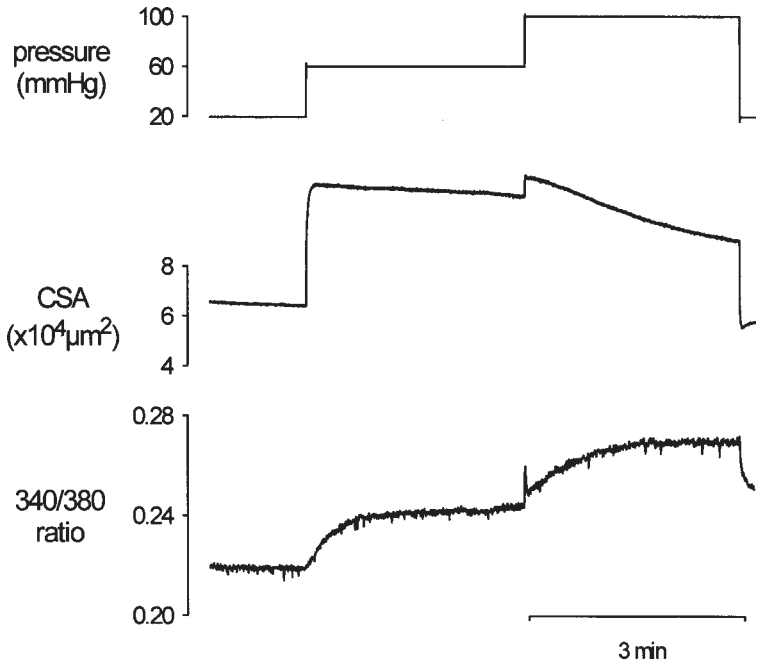

Fig. 3. Effect of pressure on luminal cross-sectional area (CSA) and smooth muscle intracellular calcium concentration, $[Ca^{2+}]i$, of cannulated rat mesenteric small arteries. Luminal CSA was measured using the volumetric fluorescence method described by VanBavel et al. ***(58)*** (*see* **Note 2**). A CSA of 100,000 μm^2 equalizes a diameter of approx 357 μm. The $[Ca^{2+}]i$ was determined using the calcium-sensitive fluorescent dye fura-2, and expressed as 340/380 ratio. This example shows that pressure-induced constrictions (i.e., myogenic responses) are accompanied by an increase in $[Ca^{2+}]i$.

arteries is quite feasible ***(6,47,48)***. Beside MLC, also phosphorylation levels of other proteins can be determined. As an example, we found that angiotensin II stimulates phosphorylation of extracellular signal-regulated kinase 1/2 in rat mesenteric small arteries (**Fig. 5**).

3.2.5. Gene Expression

In recent years, two methods for the measurement of gene expression in cannulated small arteries have been practiced in our laboratory. They are *in situ* hybridization ***(13,37,49)*** and semi-quantitative RT-PCR ***(50)***. These techniques are used to determine the expression of proto-oncogenes, such as c-*fos* and c-*myc*, which are expressed within 1–3 h after stimulation. **Figure 6** shows a typical example of the effect of pressure on c-*fos* expression in rat mesenteric small arteries, determined by means of RT-PCR.

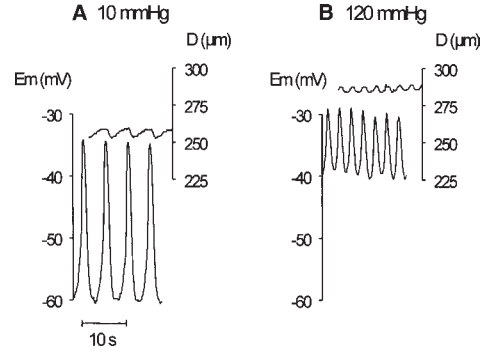

Fig. 4. Effect of pressure on norepinephrine-induced oscillations of diameter and membrane potential, in cannulated rat mesenteric small arteries. Smooth muscle membrane potential (Em) was measured with glass microelectrodes. Oscillations of diameter (D) and Em were induced by 10 μ*M* norepinephrine (NE). These traces show that NE-induced vasomotion is associated with oscillations in Em. Pressure elevation increased the frequency of oscillations in both D and Em. Minima of the Em-oscillations depolarized more with pressure than the maxima. Thus, despite motion of the vessel wall (amplitude D-oscillation approx 10 μm) it is possible to measure Em using microelectrodes.

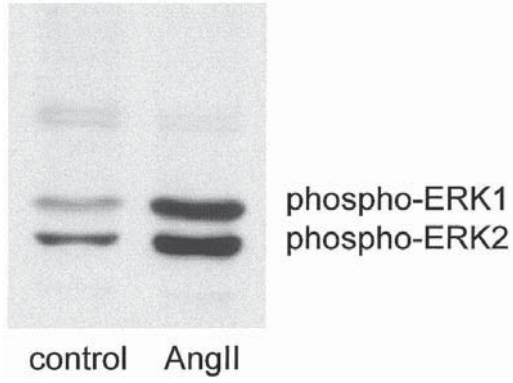

Fig. 5. Angiotensin II stimulates phosphorylation of extracellular signal regulated kinase 1/2 (ERK1/2) in rat mesenteric small arteries. This Western blot shows levels of ERK1 and ERK2 phosphorylation in a rat mesenteric first-generation artery under control conditions and after 5 min exposure to 100 n*M* angiotensin II. In this pilot experiment, the arteries were not cannulated, but were transferred to PSS-filled tubes in a 37°C water bath. The example shows that angiotensin II clearly increased phosphorylation of both ERK1 and ERK2. Each lane of the polyacrylamide gel was loaded with 12 μg of protein, and the transfer blot was reacted with an antibody for dually phosphorylated ERK1/2.

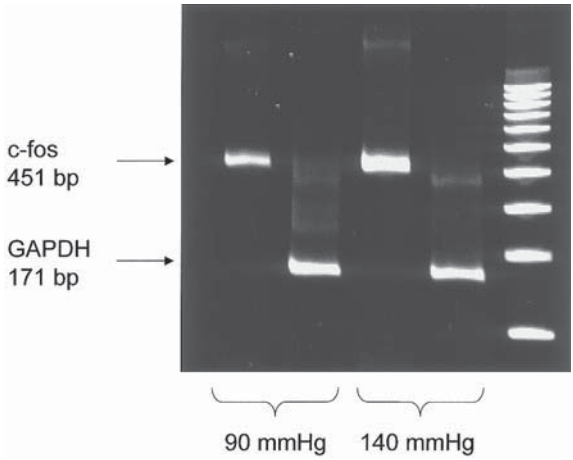

Fig. 6. Pressure stimulates c-*fos* expression in rat mesenteric small arteries. This polyacrylamide gel shows the RT-PCR products of c-*fos* and GAPDH mRNA from cannulated arteries exposed to normal (90 mmHg) and high pressure (140 mmHg) for 1 h. GAPDH was used as a housekeeping gene. The expression of c-*fos*, quantified as c-*fos*/GAPDH ratio, clearly increased with pressure.

3.3. Types of Studies

3.3.1. (Patho) Physiological Studies

The cannulated resistance artery preparation makes an excellent model to study physiological phenomena, because the vessels are close to their in vivo situation and can be investigated under carefully controlled and standardized conditions. The myogenic response (pressure-induced changes of smooth muscle tone) and flow-dependent dilation are perfect examples of such characteristic properties of resistance arteries, and numerous studies have been conducted aiming to reveal their signal transduction mechanisms ***(6,9,10,24,42,51)***. Furthermore, both the myogenic properties ***(14,52)*** and flow-dependent dilation ***(53,54)*** have been shown to be altered in experimental hypertension and diabetes in rats.

3.3.2. Pharmacological Studies

Although pharmacological studies are traditionally conducted on wire-mounted arteries, cannulated resistance arteries are used as well. For example, the interaction of α-adrenoceptor activation and the myogenic response was examined in cannulated resistance arteries ***(38)***. Another example is the investigation of differences in agonist sensitivity of a certain vessel type, when studied either as a wire-mounted or cannulated preparation ***(19,44,55)***.

3.3.3. Vessel Mechanics and Structure

Another application of cannulated resistance arteries is the examination of artery mechanics and structure, and how they change during disease. It is, for example, well known that hypertension changes the structural and mechanical properties of resistance arteries ***(14,29,30,39)***.

3.3.4. Molecular Biological Studies

In our laboratory, the cannulated small artery preparation has been used to study the early mechanisms of arterial remodeling during hypertension. By means of *in situ* hybridization, Allen et al. showed that exposure of cannulated rat mesenteric small arteries to high intraluminal pressure augmented the expression of proto-oncogenes, indicative of the initiation of a growth or remodeling response ***(37,49)***. In recent studies, in which we also used RT-PCR, we focused on the transduction mechanisms by which pressure induces proto-oncogene expression ***(13,50)***.

3.3.5. Organ Culture

An exciting new application of cannulated resistance arteries is organ culture. Several studies by the group of Tedgui showed that cannulated rabbit aorta can be maintained in organ culture for as long as 8 d ***(56)***. Moreover, Bakker et al. recently demonstrated that cannulated rat cremaster muscle arterioles can be cultured in a pressure myograph as well ***(57)***. This new development will open the way to numerous possible experiments, directed, for instance, toward the in vitro demonstration of pressure- or flow-induced arteriolar remodeling.

4. Notes

1. Myographs are obtainable in many specific configurations to allow study of cannulated resistance arteries by different techniques or protocols. For example, models in which the cannulated vessel can be positioned extremely close to the bottom cover slip allow fluorescence measurements (e.g., pH or Ca^{2+}) by means of a fluor objective that has a short working distance. Dual vessel chambers allow investigation of two cannulated vessels simultaneously. To test effects of expensive drugs, there are models with a small bath volume and a heating element in the base (model CH/2/M, Living Systems Instrumentation Inc.). When this is used without superfusion [and a bicarbonate-free PSS, composition (m*M*): NaCl (141.8), KCl (4.69), KH_2PO_4 (1.18), $MgSO_4$ (1.59), EDTA (0.513), $CaCl_2$ (2.79), HEPES (10.0), glucose (5.0), set at pH = 7.4 with 1 *N* NaOH and 1 *N* HCl, at 37°C, no bubbling required], the drug quantity, and thus the experimental costs, can be greatly reduced.
2. An alternative approach for the measurement of the inside diameter of the cannulated artery has been published by VanBavel et al. ***(9,10,58)***. Here, a fluorescent dye, for example, FITC-dextran (40 mg/L, Sigma Chemicals, St. Louis, MO) or

Texas-Red-dextran (250 mg/L, Molecular Probes, Eugene, OR) is added to the perfusate. The dyes are excited by a halogen light source, and the emission light is measured by a photomultiplier tube. Constriction of the vessel pushes the dye back into the cannulas and out of the excitation field, and thereby decreases the fluorescence. Because the concentration of the dye and the length of the excited part of the vessel are kept constant, the photomultiplier signal reflects the cross-sectional area of the vessel lumen. Manual diameter measurements are used to calibrate the photomultiplier signal.

3. Some investigators use polyethylene microtubes for the cannulation of resistance arteries ***(38,41)***.
4. In experiments where the cannulated arteries are subjected to intraluminal flow, the resistances of the cannulas need to be equivalent ***(20,26)***, and one has to make sure that the direction of flow is the same as in vivo ***(54)***.
5. Besides ligature, other methods can be used to attach the vessels to the cannulas, such as a glue (Superbonder 495, Jensen Tools, Phoenix, AZ) ***(29)***.
6. Bovine serum albumin (0.6%, Sigma) can be added to the intraluminal PSS, because Hoogerwerf et al. found that this protects endothelial function ***(59)***.
7. If several experiments are planned in a short time span, for instance 1 wk, it is advised to use three different stock solutions to make the PSS solution. Stock A (10X, in m*M*): NaCl (1190), KCl (47), KH_2PO_4 (11.8), $MgSO_4$ (11.7), EDTA (0.26), HEPES (100). Stock B (20X, in m*M*): $NaHCO_3$ (500), Stock C (20X, in m*M*): $CaCl_2$ (32). On the day of the experiment, 2 L of PSS (same PSS as in **Subheading 2.3.**) can be made by adding 200 mL stock A and 100 mL of stock B and C, and 2 g glucose, to 1.6 L of deionized water. At 37°C, after equilibration with 5% CO_2 and 95% air, the pH is set to 7.4 using 1 *N* NaOH and 1 *N* HCl.
8. If a large pressure is needed to flush out the blood after the first cannula is inserted, one may consider iv injection of heparin to prevent clotting of the blood.
9. To exclude effects from the nerve ending that are present in the preparation, a chemical denervation procedure can be performed, using 6 hydroxydopamine (Sigma). Here, the artery is superfused for 10 min with 300 mg/mL 6-hydroxydopamine, dissolved in PSS without $NaHCO_3$ at pH 4 and 20°C, followed by a 25-min recovery period ***(9,10)***. An alternative approach is a pharmacological blockade of α-adrenoceptors with phentolamine.
10. For removal of the endothelium, different methods have been reported. They include collagenase treatment, injection of air bubbles, and gentle mechanical rubbing. Liu et al. concluded that gentle rubbing is preferred, because it removes the endothelium without damaging the smooth muscle cells ***(60)***.
11. For the measurement of intracellular calcium in cannulated arteries, confocal microscopy is another, more advanced method. The advantage is that fluorescence signals from single cells in their natural environment can be monitored. Furthermore, smooth muscle cells and endothelial cells can be distinguished by their orientation. Limitations are that because of movement of the vessel wall, and the relatively slow image acquisition rate, the analysis of a dynamic $[Ca^{2+}]i$ responses is rather difficult ***(15)***.

12. Voltage-sensitive fluorescent dyes, such as di-8-ANEPPS (Molecular Probes) can be used to measure membrane potential. A possible advantage, compared to the microelectrode technique, is that the fluorescence ratio is insensitive to movement of the vessel wall, which provides the means to measure dynamic membrane potential responses ***(61)***.

References

1. Mulvany, M. J. and Aalkjær, C. (1990) Structure and function of small arteries. *Physiol. Rev.* **70,** 921–961.
2. Bevan, J. A. and Osher, J. V. (1972) A direct method for recording tension changes in the wall of small blood vessels in vitro. *Agents Actions* **2,** 257–260.
3. Duling, B. R., Gore, R. W., Dacey, R. G., Jr., and Damon, D. N. (1981) Methods for isolation, cannulation, and in vitro study of single microvessels. *Am. J. Physiol.* **241,** H108–H116.
4. Halpern, W., Osol, G., and Coy, G. S. (1984) Mechanical behavior of pressurized in vitro prearteriolar vessels determined with a video system. *Ann. Biomed. Eng.* **12,** 463–479.
5. Osol, G. and Halpern, W. (1985) Myogenic properties of cerebral blood vessels from normotensive and hypertensive rats. *Am. J. Physiol.* **249,** H914–H921.
6. Zou, H., Ratz, P. H., and Hill, M. A. (1995) Role of myosin phosphorylation and $[Ca^{2+}]_i$ in myogenic reactivity and arteriolar tone. *Am. J. Physiol.* **269,** H1590–H1596.
7. Gokina, N. I. and Osol, G. (1998) Temperature and protein kinase C modulate myofilament Ca^{2+} sensitivity in pressurized rat cerebral arteries. *Am. J. Physiol.* **274,** H1920–H1927.
8. Ishizaka, H., Gudi, S. R., Frangos, J. A., and Kuo, L. (1999) Coronary arteriolar dilation to acidosis. Role of ATP-sensitive potassium channels and pertussis toxin-sensitive G proteins. *Circulation* **99,** 558–563.
9. Wesselman, J. P. M., VanBavel, E., Pfaffendorf, M., and Spaan J. A. E. (1996) Voltage-operated calcium channels are essential for the myogenic responsiveness of cannulated rat mesenteric small arteries. *J. Vasc. Res.* **33,** 32–41.
10. VanBavel, E., Wesselman, J. P. M., and Spaan, J. A. E. (1998) Myogenic activation and calcium sensitivity of cannulated rat mesenteric small arteries. *Circ. Res.* **82,** 210–220.
11. Sun, D., Messina, E. J., Kaley, G., and Koller, A. (1992) Characteristics and origin of myogenic response in isolated mesenteric arterioles. *Am. J. Physiol.* **263,** H1486–H1491.
12. Sun, D., Kaley, G., and Koller, A. (1994) Characteristics and origin of myogenic response in isolated gracilis muscle arterioles. *Am. J. Physiol.* **266,** H1177–H1183.
13. Miriel, V. A., Allen, S. P., Wade, S. S., and Prewitt, R. L. (1999) Genistein inhibits pressure-induced expression of c-fos in isolated mesenteric arteries. *Hypertension* **34,** 132–137.
14. Dunn, W. R., Wallis, S. J., and Gardiner, S. M. (1998) Remodeling and enhanced myogenic tone in cerebral resistance arteries isolated from genetically hypertensive Brattleboro rats. *J. Vasc. Res.* **35,** 18–26.

15. Yip, K. P. and Marsh, D. J. (1996) $[Ca^{2+}]_i$ in rat afferent arteriole during constriction measured with confocal fluorescence microscopy. *Am. J. Physiol.* **271,** F1004–F1011.
16. Ting, K. N., Dunn, W. R., Davies, D. J., Sugden, D., Delagrange, P., Guardiola-Lemaître, B., et al. (1997) Studies on the vasoconstrictor action of melatonin and putative melatonin receptor ligands in the tail artery of juvenile Wistar rats. *Br. J. Pharmacol.* **122,** 1299–1306.
17. Osol, G. and Cipolla, M. (1993) Interaction of myogenic and adrenergic mechanisms in isolated, pressurized uterine radial arteries from late-pregnant and non-pregnant rats. *Am. J. Obstet. Gynecol.* **168,** 697–705.
18. Park, K. W., Dai, H. B., Lowenstein, E., and Selke, F. W. (1996) Steady-state myogenic response of rat coronary microvessels is preserved by isoflurane but not by halothane. *Anesth. Analg.* **82,** 969–974.
19. Dunn, W. R., Wellman, G. C., and Bevan, J. A. (1994) Enhanced resistance artery sensitivity to agonists under isobaric compared with isometric conditions. *Am. J. Physiol.* **266,** H147–H155.
20. Muller, J. M., Davis, M. J., Kuo, L., and Chilian, W. M. (1999) Changes in coronary endothelial cell Ca^{2+} concentration during shear stress- and agonist-induced vasodilation. *Am. J. Physiol.* **276** H1706–H1714.
21. Knot, H. J. and Nelson, M. T. (1995) Regulation of membrane potential and diameter by voltage-dependent K^+ channels in rabbit myogenic cerebral arteries. *Am. J. Physiol.* **269,** H348–H355.
22. Garcia-Roldan, J. and Bevan, J. A. (1990) Flow-induced constriction and dilation of cerebral resistance arteries. *Circ. Res.* **66,** 1445–1448.
23. Harder, D. R. (1984) Pressure-dependent membrane depolarization in cat middle cerebral artery. *Circ. Res.* **55,** 197–202.
24. Harder, D. R., Gilbert, R., and Lombard, J. H. (1987) Vascular muscle cell depolarization and activation in renal arteries on elevation of transmural pressure. *Am. J. Physiol.* **253,** F778–F781.
25. Smeda, J. S. and Daniel, E. E. (1988) Elevations in arterial pressure induce the formation of spontaneous action potentials and alter neurotransmission in canine ileum arteries. *Circ. Res.* **62,** 1104–1110.
26. Kuo, L., Davis, M. J., and Chilian, W. M. (1990) Endothelium-dependent, flow-induced dilation of isolated coronary arterioles. *Am. J. Physiol.* **259,** H1063–H1070.
27. Liu, Q., Wiener, C. M., and Flavahan, N. A. (1998) Superoxide and endothelium-dependent constriction to flow in porcine small pulmonary arteries. *Br. J. Pharmacol.* **124,** 331–336.
28. Wang, S. Y., Stamler, A., Li, J., Johnson, R. G., and Selke, F. W. (1997) Decreased myogenic reactivity in skeletal muscle arterioles after hypothermic cardiopulmonary bypass. *J. Surg. Res.* **69,** 40–44.
29. Falloon, B. J. and Heagerty, A. M. (1994) In vitro perfusion studies of human resistance artery function in essential hypertension. *Hypertension* **24,** 16–23.
30. Intengan, H. D., Deng, L. Y., Li, J. S., and Schiffrin, E. L. (1999) Mechanics and composition of human subcutaneous resistance arteries in essential hypertension. *Hypertension* **33,** 569–574.

31. Wallis, S. J., Firth, J., and Dunn, W. R. (1996) Pressure-induced myogenic responses in human isolated cerebral resistance arteries. *Stroke* **27,** 2287–2291.
32. Miller, F. J., Jr., Dellsperger, K. C., and Gutterman, D. D. (1997) Myogenic constriction of human coronary arterioles. *Am. J. Physiol.* **273,** H257–H264.
33. Learmont, J. G. and Poston, L. (1996) Nitric oxide is involved in flow-induced dilation of isolated human small fetoplacental arteries. *Am. J. Obstet. Gynecol.* **174,** 583–588.
34. Bevan, R. D., Vijayakumaran, E., Gentry, A., Wellman, T., and Bevan, J. A. (1998) Intrinsic tone of cerebral artery segments of human infants between 23 weeks of gestation and term. *Pediatr. Res.* **43,** 20–27.
35. McGuffee, L. J. and Little, S. A. (1996) Tunica media remodeling in mesenteric arteries of hypertensive rats. *Anat. Rec.* **246,** 279–292.
36. Fenger-Gron, J., Mulvany, M. J., and Christensen, K. L. (1995) Mesenteric blood pressure profile of conscious, freely moving rats. *J. Physiol.* **488,** 753–760.
37. Allen, S. P., Liang, H. M., Hill, M. A., and Prewitt, R. L. (1996) Elevated pressure stimulates protooncogene expression in isolated mesenteric arteries. *Am. J. Physiol.* **271,** H1517–H1523.
38. Watanabe, J., Keitoku, M., Hangai, K., Karibe, A., and Takishima, T. (1993) α-Adrenergic augmentation of myogenic response in rat arterioles: role of protein kinase C. *Am. J. Physiol.* **264,** H547–H552.
39. Laurant, P., Touyz, R., and Schiffrin, E. L. (1997) Effect of pressurization on mechanical properties of mesenteric small arteries from spontaneously hypertensive rats. *J. Vasc. Res.* **34,** 117–125.
40. Pourageaud, F. and De Mey, J. G. (1997) Structural properties of rat mesenteric small arteries after 4–wk exposure to elevated or reduced blood flow. *Am. J. Physiol.* **273,** H1699–H1706.
41. Karibe, A., Watanabe, J., Horiguchi, S., Takeuchi, M., Suzuki, S., Funakoshi, M., Katoh, H., et al. (1997) Role of cytosolic Ca^{2+} and protein kinase C in developing myogenic contraction in isolated rat small arteries. *Am. J. Physiol.* **272,** H1165–H1172.
42. Falcone, J. C., Kuo, L., and Meininger, G. A. (1993) Endothelial cell calcium increases during flow-induced dilation in isolated arterioles. *Am. J. Physiol.* **264,** H653–H659.
43. D'Angelo, G., Davis, M. J., and Meininger, G.A. (1997) Calcium and mechanotransduction of the myogenic response. *Am. J. Physiol.* **273,** H175–H182.
44. Schubert, R., Wesselman, J. P. M., Nilsson, H., and Mulvany, M. J. (1996) Noradrenaline-induced depolarization is smaller in isobaric compared to isometric preparations of rat mesenteric small arteries. *Pflügers Arch.* **431,** 794–796.
45. Wesselman, J. P. M., Schubert, R., VanBavel, E., Nilsson, H., and Mulvany, M. J. (1997) K_{Ca}-channel blockade prevents sustained pressure-induced depolarization in rat mesenteric small arteries. *Am. J. Physiol.* **272,** H2241–H2249.
46. Peng, H., Ivarsen, A., Nilsson, H., and Aalkjær, C. (1998) On the cellular mechanism for the effect of acidosis on vascular tone. *Acta Physiol. Scand.* **164,** 517–525.

47. Hill, M. A., Davis, M. J., Song, J., and Zou, H. (1996) Calcium dependence of indolactam-mediated contractions in resistance vessels. *J. Pharm. Exp. Ther.* **276,** 867–874.
48. Buus, C. L., Aalkjær, C., Nilsson, H., Juul, B., Moller, J. V., and Mulvany, M. J. (1998) Mechanisms of Ca^{2+} sensitization of force production by noradrenaline in rat mesenteric small arteries. *J. Physiol.* **510,** 577–590.
49. Allen, S. P., Wade, S. S., and Prewitt, R. L. (1997) Myogenic tone attenuates pressure-induced gene expression in isolated small arteries. *Hypertension* **30,** 203–208.
50. Wesselman, J. P. M., Wade, S. S., and Prewitt, R. L. (1999) Mechanisms of pressure-induced c-fos expression in cannulated rat small arteries. *FASEB J.* **13,** A45, abstract.
51. Koller, A., Sun, D., Huang, A., and Kaley, G. (1994) Corelease of nitric oxide and prostaglandins mediates flow-dependent dilation of rat gracilis muscle arterioles. *Am. J. Physiol.* **267,** H326–H332.
52. Hill, M. A. and Ege, E. A. (1994) Active and passive mechanical properties of isolated arterioles from STZ-induced diabetic rats. Effect of aminoguanidine treatment. *Diabetes* **43,** 1450–1456.
53. Koller, A. and Huang, A. (1994) Impaired nitric oxide-mediated flow-induced dilation in arterioles of spontaneously hypertensive rats. *Circ. Res.* **74,** 416–421.
54. Tribe, R. M., Thomas, C. R., and Poston, L. (1998) Flow-induced dilatation in isolated resistance arteries from control and streptozotocin-diabetic rats. *Diabetologica* **41,** 34–39.
55. Buus, N. H., VanBavel, E., and Mulvany, M. J. (1994) Differences in sensitivity of rat mesenteric small arteries to agonists when studied as ring preparations or as cannulated preparations. *Br. J. Pharmacol.* **112,** 579–587.
56. Bardy, N., Karillon, G. J., Merval, R., Samuel, J., and Tedgui, A. (1995) Differential effects of pressure and flow on DNA and protein synthesis and on fibronectin expression by arteries in a novel organ culture system. *Circ. Res.* **77,** 684–694.
57. Bakker, E. N. T. P., VanBavel, E., van der Meulen, E. T., and Spaan, J. A. E. (1999) Structural and functional changes of resistance arteries in organ culture. *FASEB J.* **13,** A7, abstract.
58. VanBavel, E., Mooij, T., Giezeman, M. J. M. M., and Spaan, J. A. E. (1990) Cannulation and continuous cross-sectional area measurement of small blood vessels. *J. Pharm. Methods* **24,** 219–227.
59. Hoogerwerf, N., Zijlstra, E. J., Van der Linden, P. J. W., Westerhof, N., and Sipkema, P. (1992) Endothelium function is protected by albumin and flow-induced constriction is independent of endothelium and tone in isolated rabbit femoral artery. *J. Vasc. Res.* **29,** 367–375.
60. Liu, Y., Harder, D. R., and Lombard, J. H. (1994) Myogenic activation of canine small renal arteries after nonchemical removal of the endothelium. *Am. J. Physiol.* **267,** 302–307.
61. Beach, J. M., McGahren, E. D., Xia, J., and Duling, B. R. (1996) Ratiometric measurement of endothelial depolarization in arterioles with a potential-sensitive dye. *Am. J. Physiol.* **270,** H2216–H2227.

33

Measurement of Vascular Density

Andrew S. Greene and Mark J. Rieder

1. Introduction

Determination of the number of microvessels in tissue is of great importance in the assessment of studies of vascular development, angiogenesis, and rarefaction ***(1)***. Numerous techniques, such as immunohistochemical staining, fluorescence injection, and India ink or microfil perfusion have been developed for microvascular visualization. In this section, we describe a microvascular visualization technique ***(2)***, which utilizes rhodamine-labeled *Griffonia simplicifolia* (GS-I) lectin to define both perfused and unperfused microvessels ranging from small arteries (20 μm) to normal capillaries (3–6 μm) to venous capillaries (6–9 μm), combined with a computerized image processing technique that rapidly and automatically determines vascular density in tissue sections ***(3)***.

Though complete descriptions of the microvascular structure require a complex description of vessel diameters, lengths, and branching patterns ***(4)***, other simpler methods exist for quantifying vessel density. One method, as described by Underwood ***(5)***, has been utilized by our laboratory ***(6)*** and others ***(7,8)*** and employs a stereologically based, nondimensional index of vascular density by counting intersections between a microvascular network image and a square-grid overlay. Described here is a fluorescent-staining technique coupled with a novel computerized method to quickly analyze and process a digital vascular image and to automatically count vessel–grid intersections in each tissue-section area. This method dramatically reduces the time spent analyzing each tissue section.

From: *Methods in Molecular Medicine, vol. 51: Angiotensin Protocols*
Edited by: D. H. Wang © Humana Press Inc., Totowa, NJ

2. Materials

2.1. Tissue Sectioning and Preparation

1. Hand-held microtome for sectioning of thick tissues.
2. Sectioning blades (12 cm × 2 cm) available from Thomas Scientific.
3. Microcentrifuge tubes (1.5 mL polypropylene).
4. Rhodamine-labeled *Griffonia simplicifolia* I (GS-I) lectin S (Sigma Chemical Corp., St. Louis, MO).
5. Saline (0.9% sodium chloride).
6. Mounting medium consisting of toluene and acrylic resin (SP ACCU-MOUNT 280, Baxter Scientific, McGaw Park, IL).
7. Glass slides (25 × 75 mm).
8. Glass coverslips (Corning, 22-mm square).
9. Platform rocker (Reliable Scientific).

2.2. Tissue Visualization and Quantitation

1. Video fluorescent microscope system (Olympus ULWD CD Plan, ×20 objective, 1.6 cm working distance and 0.4 numerical aperture) with epi-illumination.
2. Single stage intensified newvicon camera (Cohu, 5000 Series Television Camera).
3. Video imaging system (Data Translation DT2801, Marlboro, MA).
4. All image-processing techniques are implemented using the Image-1 image-processing software package (Universal Imaging Corporation, West Chester, PA).

3. Methods

3.1. Preparing Lectin-TRITC Stock Solution

Dilute Lectin-Tetramethyl-Rhodamine Isothiocyanate (Lectin-TRITC) with saline to a concentration of 1 mg/mL. Once diluted, store in refrigerator. Before use, dilute stock to a final concentration of 30 μL/mL in saline. Protect from light.

3.2. Sectioning and Preparing Tissue Samples

The method described has been used extensively in skeletal muscle, but is also appropriate for other tissue with minor modifications (*see* **Note 1**). Remove the tissue from the animal and rinse in saline. Immediately section muscles by placing on the microtome cutting surface, securing the tendons, and slicing longitudinally, parallel to the orientation of the muscle fibers. We have found that very thick sections (50–100 μm) provide the best images and the most consistent results.

3.3. Staining Tissue Samples

Place tissues into microcentrifuge tubes and cover with saline. Before staining, remove all saline from tissues with a pipet. Add 1 mL of 30 μg/mL lectin solution. Allow tissue to soak in lectin solution for 45 min at room tempera-

ture. Lectin is photosensitive, so keep covered while staining. Rinse tissue with cold saline four times: rinse immediately, rinse and let stand on rocker table approx 10 min, rinse and let stand on rocker 30 min, and then rinse and let stand on rocker table overnight. All rinsing should be done at 4°C.

3.4. Mounting Tissue Samples

Tissue is removed from saline and blotted dry. Any excess connective tissue is removed before mounting. Put tissue on a dry slide and cover with mounting medium. Top with a cover slip and press down slightly. Let slides dry overnight in refrigerator.

3.5. Imaging Tissue Samples

Study samples using a video fluorescent microscope system. Our system consists of an Olympus ULWD CD Plan, ×20 objective, 1.6-cm working distance, and 0.4 numerical aperture with epi-illumination. Each section is examined at ×300 to find representative fields of view. Images are formed using a single-stage intensified newvicon camera (e.g., Cohu, 5000 Series Television Camera). Fields should be chosen based on uniformity of vessel density, staining intensity and structural integrity within the area.

Each image is digitized (Data Translation DT2801) and stored as an 8-bit/pixel image file with a resolution of 512 pixels × 512 pixels. We find that approx 10–20 representative fields from each muscle, counted and averaged through approx 10 sections, provides an excellent assessment of the mean vessel density per sample.

3.6. Automated Vessel Counting

All image-processing techniques described here are implemented using the Image-1 image-processing software package (Universal Imaging Corporation, West Chester, PA) on a personal computer (Gateway 2000 486/33C, North Sioux City, SD) equipped with additional image-processing hardware (Matrox, Dorval, Québec, Canada). The general procedure used to process each image requires loading the digitized image from computer storage and performing a series of digital image processing techniques. From this, a resultant line image of the network is created, and intersections with a computer generated square grid overlay are automatically identified. Vessel–grid intersections are automatically counted and provided a quantitative estimate of vessel density. A detailed description of each step in the procedure is outlined in the following sections.

3.6.1. Processing of the Gray-Level Image

Figure 1A shows an original gray-level image prior to any processing, which displays background shading typical of fluorescence microscopy images ***(9)***. In order to correct this shading, which can compromise differentiation between

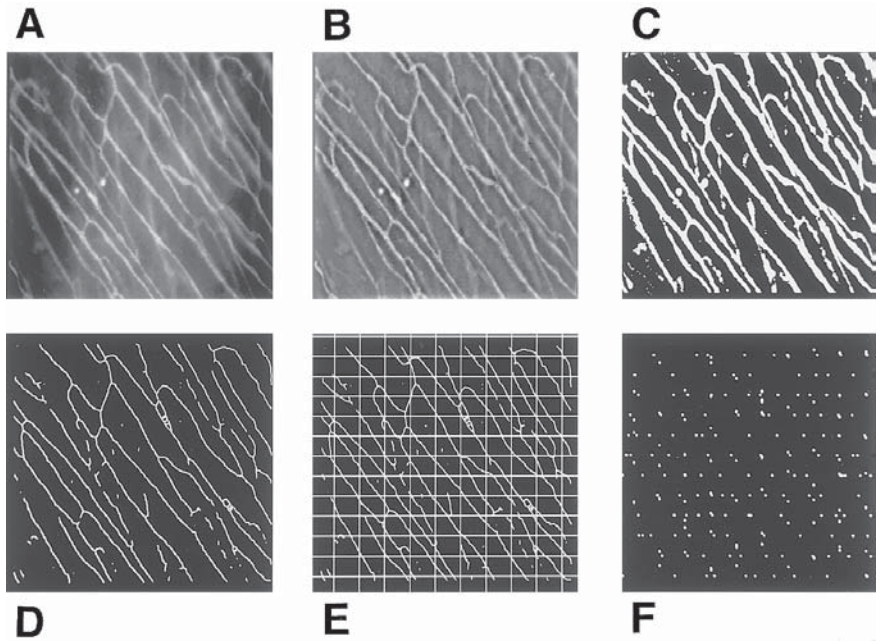

Fig. 1. Processing steps for a typical microvascular digital image. **(A)** Original image; **(B)** original image after low-pass filtering and shading correction; **(C)** binary image showing vessels (white) and background (black); **(D)** binary image after thinning (skeletonizing); **(E)** skeletonized image with grid overlay; **(F)** intersection points of skeleton image and grid which were counted.

vessels and background, a series of six low-pass filtering convolutions are performed ***(10)***. Six successive kernels having a horizontal × vertical neighborhood of 17 × 1, 1 × 17, 1 × 17, 17 × 1, 17 × 1, and 1 × 17 are used. The result of this shading correction is shown in Fig. 1B. Following filtering, the resultant image is normalized by histogram stretching over the new gray-level range.

3.6.2. Evaluation and Image Statistics

In order to determine the appropriate value for subsequent binary thresholding each image is analyzed by computing an intensity histogram. Assuming a Gaussian distribution of intensities, histogram statistics, mean, and standard deviation are determined for each image. The binary threshold *(T)* for the subsequent step is computed from the histogram as

$$T = I[x \cdot n(\mu)] \tag{1}$$

such that $T > \mu$, where I is the gray-level intensity, n is the number of pixels at a given intensity, μ is the mean of the Gaussian distribution, and x is the test

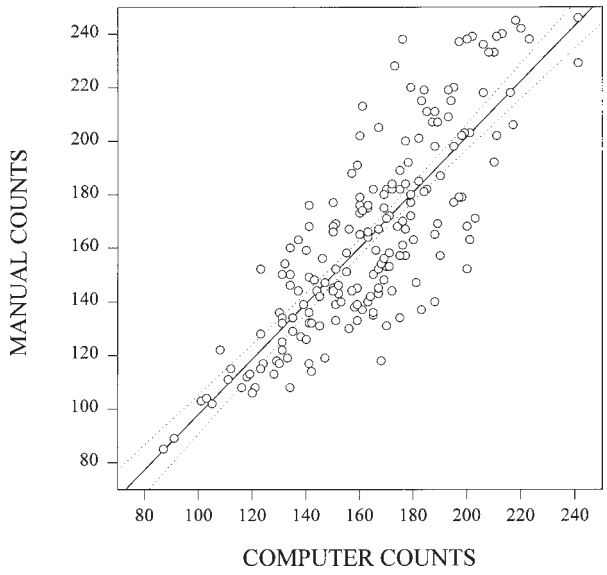

Fig. 2. Comparison of manual counting method to computer automated method showing the regression line and 95% confidence intervals (dashed).

percentage. A binary threshold level *(x)* of 93% has been found to be the optimal gray-level threshold for binary conversion for our system by inspection of the binary images and comparison of computer vs manual counts (*see* **Fig. 2**).

3.6.3. Thresholding of the Gray-Level Image

Thresholding of a gray level image produces a two-color (black and white) image in which all pixels having a gray level less than or equal to the threshold value are set to black (I = 0) and all pixels having a gray level greater than the threshold are set to white (I = 255). The threshold value for each image is determined automatically as aforementioned, using **Eq. 1** with $x = 0.93$. As shown in **Fig. 1C**, thresholding creates an idealized binary image in which the unlabeled tissue background appears black and the putative rhodamine-labeled vessels are white.

3.6.4. Processing of Binary Image

Because of the binary thresholding step, small spotlike areas may appear in the image background. These areas are discontinuous unlike a characteristic vessel. Elimination of these spots is performed by using a digital erosion algorithm, which performs a one pixel contraction around all vessels in the image without causing breaks between consecutive pixels ***(10)***. With this process, any extraneous background pixels inappropriately highlighted as vessels are

effectively eliminated. Processing artifacts, such as vessel discontinuities introduced by the erosion, are corrected by performing a binary dilation algorithm which places an eight pixel white neighborhood around each existing white pixel ***(10)***. Two iterations of this algorithm effectively closes any vessel discontinuities introduced by processing.

3.6.5. Binary Image Thinning (Skeletonizing)

Manual counting of vessel-grid intersection does not take into account vessel thickness, only intersections. Skeletonization reduces the digital image of the vascular network to a series of single pixel width lines. The binary image is skeletonized by eroding the edges of any image objects until only thin lines remained. The algorithm used to achieve this can be stated precisely as follows:

Let P be a point inside of object O.
So is the set of all points on the boundary of object O.
Points $O1$ and $O2 \in So$.
P is a member of the resulting set of points ($S1$) if

1. the distance between P and $O1$ is equal to the distance between P and $O2$ and
2. this distance is the minimum distance between P and any member So.

This set of points ($S1$) for a characteristic vessel lie along its midline, resulting in the reduction of any vessel to a single pixel width line, as shown in **Fig. 1D**.

3.6.6. Counting of Vessel-Grid Intersections

Automated vessel counting is done by counting vessel-grid intersections. After overlaying a computer generated grid on the vessel image, grid intersections are determined by performing a logical AND function between the binary grid overlay and the binary skeletonized vessel image. The resultant image, shown in **Fig. 1F**, consists of white pixels at grid-vessel intersection points and black at all other points. Using the image processing software, each of these pixels is recognized as a single intersection point. These white pixels are automatically counted and correspond to the vessel-grid intersections, providing a quantitative estimate of vessel density. This estimate of vessel density has been carefully correlated with manual counting for verification of this automated technique.

4. Notes

1. Tissues can be fixed in 0.25% formalin for 1–5 d and then stained with lectin. The 0.25% formalin produces a lightly fixed tissue that will degrade with time, but allows up to 5 d before sectioning and staining harvested tissues. To fix tissues, separate different muscle types and put each whole muscle in a separate microcentrifuge tube. If this fixing is done, one must stain for a longer period of time. We have also found that a lower concentration of lectin can be used. The lower lectin

concentration can cause an increased amount of variation in overall staining quality, so it is particularly important to stain on the rocker table. For example, if using 20 μg/mL TRITC-lectin modify the procedure to: Stain for 2 h. Rinse as usual immediately, 10 min, 30 min, and overnight. Mount tissues the next day.

The performance of this computerized vessel counting algorithm was tested against traditional manual counting methods and shown to be highly correlated **(Fig. 2)**. Regression analysis gave a line which was very similar to the line of identity (slope = 1.02, *y*-intercept = –2.5), to be used as the "calibration" for comparing computer counts to manual counts. A comparison of the two methods showed that whereas the computer method was 100% reproducible, human counting may vary based on subjective determination of vessel-grid intersections by the operator. In our laboratory, comparison of three different experienced operators yielded a coefficient of variation of 10%, whereas four other inexperienced operators had a larger coefficient of variation approaching 16%. Because of the same processing of every image, the computer applies the same criteria for vessel determination and vessel–grid intersections, allowing for consistency between images, which may be untrue for human operators.

From our experience, we have found the placement of the binary threshold to be the most sensitive factor for producing a reliable final digital image for counting. We have shown that our series of processing steps (**Fig. 1A–F**) produces a single-pixel width-line rendering of the corresponding microvascular network, which retains the essential features for density determination. Our digital-image processing technique confers several advantages over manual counting. After development of this automated technique, we have been able to reduce the analysis time for each image from approx 15 min/image to 30 s/image. Not only does this method decrease the number of hours spent, but allows more sections to be analyzed, increasing the statistical reliability of our results.

When possible, the general orientation of the network should be aligned at an angle (20–45°) relative to the vertical grid lines for consistency and to maximize vessel–grid intersections. Previous studies have shown that for these longitudinal tissue sections, averaging will effectively negate any network orientation variability effects and not produce statistical anomalies ***(3)***.

References

1. Greene, A. S. (1998) Microvascular remodeling in hypertension: a role for the renin-angiotensin aldosterone system. *Curr. Concepts Hypertens.* **2,** 5.
2. Hansen-Smith, F. M., Watson, L., Lu, D. Y., and Goldstein, I. (1988). *Griffonia simplicifolia* I: fluorescent tracer for microcirculatory vessel in nonperfused thin muscles and sectioned muscle. *Microvasc. Res*. **36,** 199–215.
3. Rieder, M. J., O'Drobinak, D. M., and Greene, A. S. (1995) A computerized method for determination of microvascular density. *Microvasc. Res*. **49,** 180–189.
4. Schmid-Schoenbein, G. W., Zweifach, B. W., and Kovalcheck, S. (1977) The application of stereological principles to morphometry of the microcirculation in different tissues. *Microvasc. Res.* **14,** 303–317.

5. Underwood, E. E. (1970) *Quantitative Stereology*. Addison-Wesley, Reading, MA.
6. Greene, A. S., Lombard, J. H., Cowley , A. W. Jr., and Hansen-Smith, F. M. (1990) Microvessel changes in hypertension measured by *Griffonia simplicifolia* I Lectin. *Hypertension* **15,** 779–783.
7. Norrby, K., Jakobsson, A., and Sorbo, J. (1990) Quantitative angiogenesis in spreads of intact rat mesenteric windows. *Microvasc. Res.* **39,** 341–348.
8. Le Noble, F. A., Hekking, J. W., Van Straaten, H. W., Slaaf, D. W., and Strukyer Boudier, H. A. (1991) Angiotensin II stimulates angiogenesis in the chorio-allantoic membrane of the chick embryo. *Euro. J. Pharmacol.* **195,** 305,306.
9. Inoué, S. (1986) *Video Microscopy*, Plenum, New York.
10. Image-1 Function Guide, Version 4.0, Universal Imaging Corporation.

34

Functional Studies of the Cerebral Circulation

Julian H. Lombard

1. Introduction

Angiotensin II (Ang II) is an endogenous peptide that has a wide spectrum of physiological functions, including the regulation of hemodynamics and blood volume ***(1)***; growth, hypertrophy, and remodeling in the cardiovascular system ***(1,2)***; regulation of microvessel density ***(3,4)***, and modulation of vascular tone ***(3,5)***. Ang II is widely known as a potent vasoconstrictor, but a number of studies have demonstrated that it can have vasodilator effects as well ***(3,5)***. The recent identification of distinct AT_1 and AT_2 angiotensin receptor subtypes raises additional questions regarding the actions of Ang II on the vasculature, particularly in regard to the role of these receptors in overall cardiovascular regulation ***(1,2)***.

The role of Ang II in regulating vascular tone and blood flow in the cerebral circulation is not clear, because Ang II has been reported to have both constrictor ***(5–9)*** and dilator ***(9–11)*** effects on cerebral blood vessels. In peripheral blood vessels, there is evidence that the AT_1 receptor mediates vasoconstriction whereas the AT_2 receptor mediates vasodilation ***(4,6)***. However, the role of specific Ang II-receptor subtypes in regulating active tone in the cerebral circulation is less clear. For example, both the AT_1 and the AT_2 receptor have been proposed to contribute to angiotensin induced dilation in the cerebral circulation ***(11)***.

Studies of the regulation of active tone in arterioles and resistance arteries are aided considerably by approaches that allow the study of isolated blood vessels or the direct observation of vessels *in situ*. Both of these approaches have been employed to investigate vascular control in the cerebral circulation. Techniques employing isolated resistance arteries provide insight into the regulation of vascular tone in the absence of neural, humoral, and parenchymal cell

From: *Methods in Molecular Medicine, vol. 51: Angiotensin Protocols*
Edited by: D. H. Wang © Humana Press Inc., Totowa, NJ

influences. Isolated vessel studies also allow the investigator to evaluate the role of endothelial influences in modulating vessel function by determining resting tone and the response of the vessel to vasoactive stimuli before and after removal of the endothelium. In contrast, studies of the *in situ* microcirculation allow vascular control mechanisms to be investigated in the presence of normal neural, humoral and parenchymal cell influences.

Studies of isolated resistance arteries utilize either a wire myograph, which allows direct measurement of active and passive force in isolated vessels ***(12)***, or a vessel chamber that enables arteries to be cannulated with micropipets in order to bathe them with physiological salt solution (PSS) and to maintain them at intravascular pressure levels that approximate those encountered in vivo ***(13,14)***. A major advantage of the cannulated vessel preparation is that it allows a normal distribution of distending forces to be maintained in the vessel. Because cerebral vessels and many other arteries exhibit myogenic depolarization of the vascular smooth muscle cells as pressure in the vessel is elevated ***(15)***, transmembrane potentials of the smooth-muscle cells in vessels maintained at normal perfusion pressures are closer to the normal in vivo values than those in unpressurized vessels. This can substantially affect the sensitivity of the vessels to vasoactive stimuli, because smooth muscle transmembrane potential in cannulated vessels is closer to the steep portion of the membrane potential-active force relationship than it is in nonpressurized vessels. As a result, small changes in smooth muscle transmembrane potential in response to vasoactive agonists can be accompanied by large changes in contractile force ***(16)***, resulting in a substantial increase in the sensitivity of the pressurized vessels to vasoactive agonists relative to that of unpressurized vessels ***(17)***. Another advantage of cannulated, perfused-vessel studies is that they allow the inside and outside of the vessel to be perfused and superfused with PSS supplied from separate reservoirs. This allows the composition and gas concentrations of the perfusion and superfusion solutions to be controlled independently ***(18,19)***. The ability to independently control the composition of the perfusion and superfusion solutions is particularly useful for the selective application of drugs to the lumen or to the outside of the vessel.

In situ studies of the cerebral microcirculation can be accomplished utilizing either an open or a closed cranial window preparation to directly visualize microvessels on the surface of the brain. Techniques for preparing a cranial window are summarized below and are described in detail elsewhere ***(20–23)***. In the open cranial-window preparation, a hole is drilled through the skull, the dura is peeled back, and the preparation is superfused with artificial cerebrospinal fluid. In the closed cranial-window preparation, the skull is opened, the dura is reflected, and a chamber with inlet and outlet ports for perfusion, a port for measurement of intracranial pressure, and a clear window or cover glass is

installed. An alternative version of the closed cranial window is to thin the skull to a point where the underlying vessels can be observed without penetrating the bone ***(23)***. The latter preparation allows vessel diameters to be measured directly and blood flow to be assessed via laser-Doppler flowmetry, without penetrating the skull.

2. Materials

2.1. Isolated Blood Vessel Studies

1. Vessel chamber for microscopy studies: The main item of specialized equipment required for the study of isolated resistance arteries is a vessel chamber consisting of a tissue bath that contains inflow and outflow micropipets to allow cannulation and perfusion of the vessel. **(Fig. 1)**. This is generally purchased commercially (Living Systems Inc., Burlington, VT), but can be fabricated in house as well. The chamber is mounted on a standard microscope stage, which allows X-Y positioning of the vessel for viewing. The vessel chamber is heated with a circulating water bath and is supplied with PSS from two separate reservoirs that supply the superfusion solution and the luminal perfusate **(Fig. 2)** (*see* **Note 1**). The isolated vessels are viewed through a microscope and vessel diameters are measured via television microscopy.

   Microscopes used for studies of cannulated resistance arteries range from a standard inverted microscope to a high-power dissecting microscope equipped with a camera tube. Video microscopy is performed with a standard monochrome video camera linked to a monitor. Depending upon the microscope used for the studies, illumination can be achieved either with a standard illuminator or a fiberoptic light source and substage mirror. Vessel diameters are generally measured directly with a video micrometer, although they can be also measured off line from calibrated video tapes. A slide micrometer is used to calibrate the video micrometer and to provide a calibration for the off line measurements of vessel diameter. Diameter measurements for the initial studies of cannulated resistance arteries in our laboratory were performed with a Colorado Video Analyzer (Colorado Video, Inc., Boulder, CO) modified with specially fabricated circuitry to generate a pair of moveable reference lines. However, a variety of specialized video micrometers, (e.g., a For-A IV-550 Video Microscaler; For A, Company, Limited, Tokyo, Japan), are now available to provide quick and accurate measurements of vessel diameter without the need to construct special electronic circuitry.
2. Electrophysiological studies: If electrophysiological studies are to be conducted, an antivibration table, e.g., a Micro-G shock table (Technical Manufacturing Corp., Peabody, MA) and a Faraday cage with electrical grounding are essential, in order to maintain impalements and to prevent electrical interference (*see* **Note 2**). Membrane potentials are measured with glass microelectrodes filled with 3 *M* KCl and a high-impedance amplifier, e.g., Dagan Cell Explorer (Dagan Corporation, Minneapolis, MN) connected to an oscilloscope or a computer-operated data acquisition system (CODAS), (DATAQ instruments, Akron, OH). A detailed

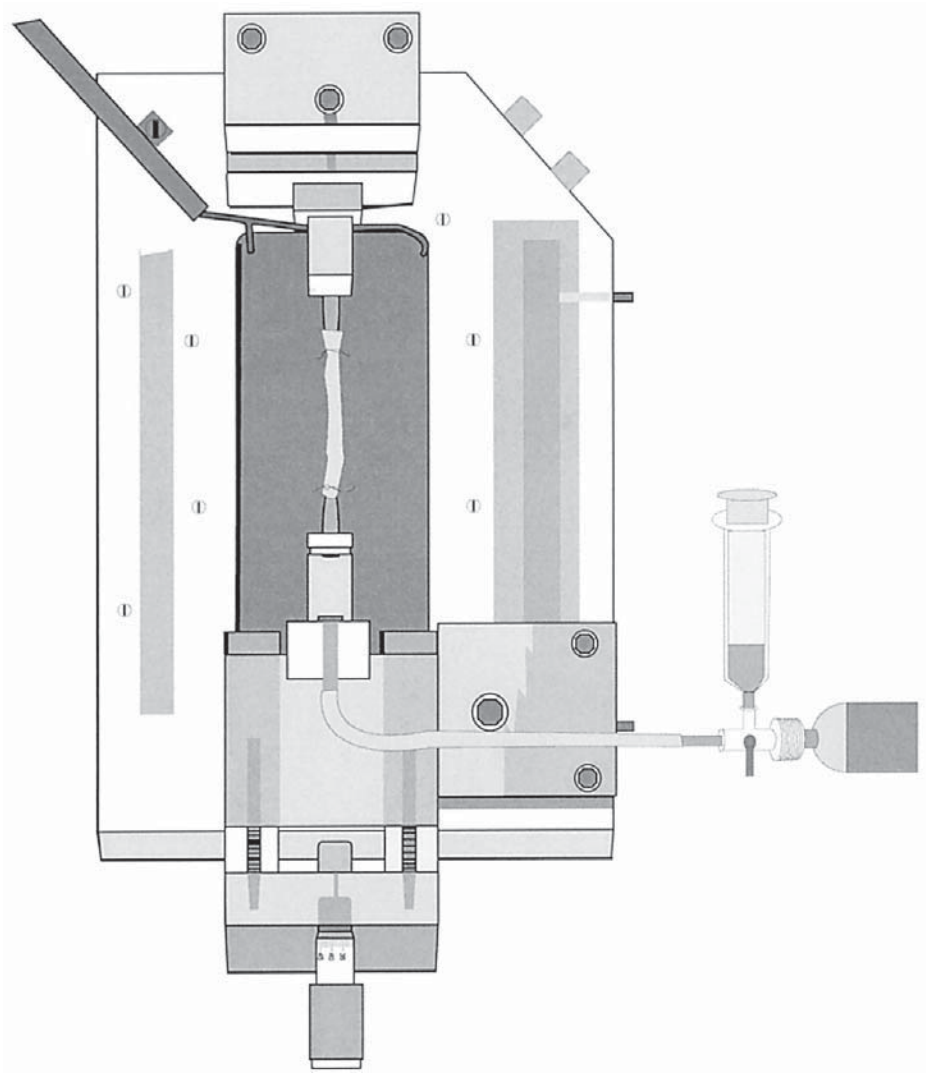

Fig. 1. Chamber for the study of isolated, perfused resistance arteries (top view). Tissue bath with cannulated vessel is in the center of the illustration. Inflow pipet and micrometer for adjusting the length of the vessel segment are toward the bottom of the illustration. Outflow for tissue bath (connected to peristaltic pump to remove superfusion solution from the bath) is at the upper left of the illustration. The syringe connected to the inflow transducer is used to inject an air bolus for endothelial removal. The air bolus perfuses the vessel lumen and exits via tubing connected to the outflow pipet (not shown). See text for details.

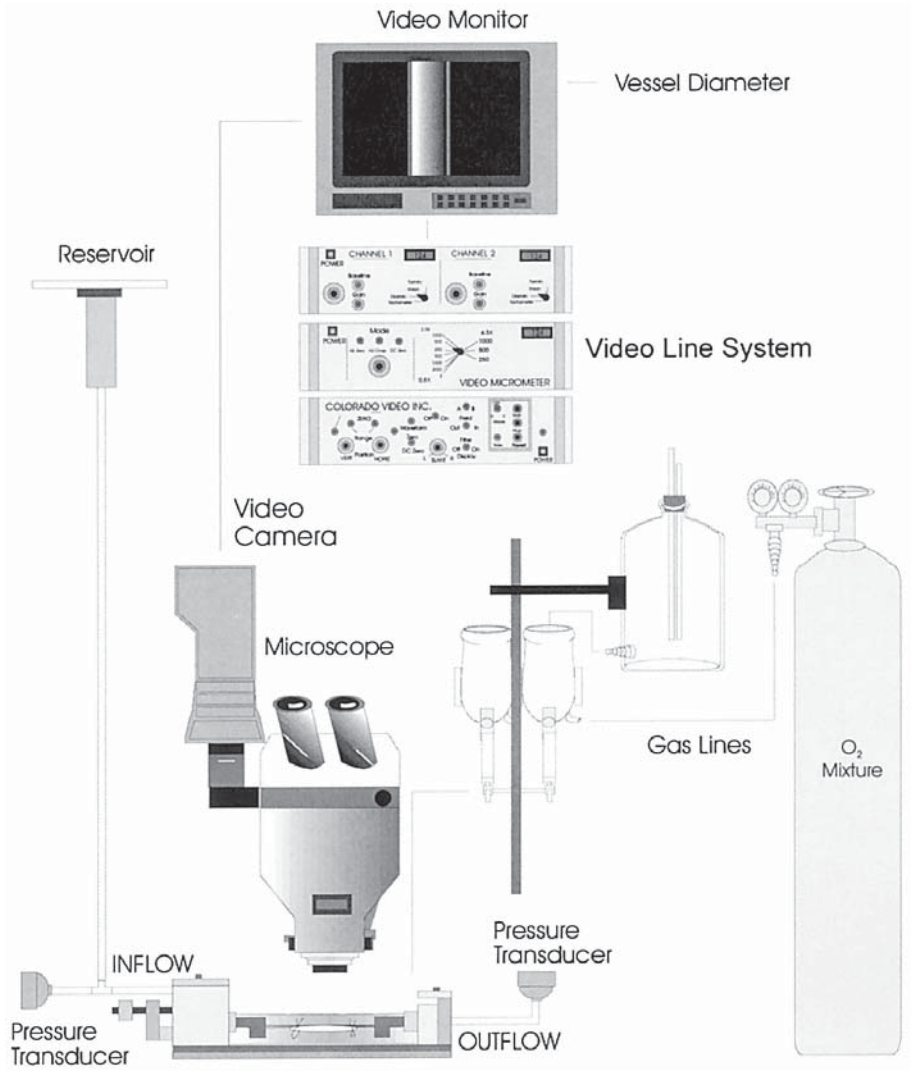

Fig. 2. Simplified diagram of experimental apparatus required for studies of isolated, perfused resistance arteries. See text for details.

description of electrophysiological approaches to study isolated or *in situ* vessels has been published previously ***(24)***.

3. Mounting pipets for studies of isolated, perfused vessels: Micropipets for cannulating isolated resistance arteries are pulled from capillary flint glass, (2.0 mm outer diameter × 1.0 mm inner diameter, 100 mm length) using a vertical pipet

puller, such as a DK Instruments Model 700C (David Kopf, Instruments, Tujunga, CA). The pipets commonly have a right angle bend produced by heating the shaft of the pipet in a flame and bending the glass. The shafts of the pipets protrude from the vessel chamber allowing them to be easily attached to the perfusion reservoir and outflow via appropriately sized tubing, whereas the tips of the pipets extend into the center of the chamber where they are accessible for vessel cannulation.

The diameters of the micropipet tips are fashioned to be only slightly less the internal diameter of the artery, in order to minimize pipet resistance upstream and downstream from the vessel. To achieve the desired tip diameter (usually about 100 μm outer diameter), the tip of the micropipet is broken using curved forceps under a dissecting scope equipped with an eyepiece micrometer. The tip is polished by brushing and rolling it in one direction against fine sandpaper. Using the flame from an alcohol lamp, the untapered end of the pipet is heat polished, in order to keep it from piercing the connecting tubing. When both pipets are mounted in the chamber, the tips are brought close together using the microscope. The microscope is focused on one pipet and the other is moved up or down (or laterally) until both are in focus, indicating that they are aligned.

4. Ties for mounting isolated perfused vessels and tying side branches: Vessels are tied onto the mounting pipets with 10–0 monofilament nylon suture (Look, Inc., Norwell, MA, or Ashaway Line and Twine, Ashaway, NJ). Attachment of the vessels is greatly facilitated by pretying the sutures to form a loop that can be pulled tight around the vessel. Ties for securing the vessel to the pipet are constructed by grasping the suture 2–3 cm from the free end and tying double loops with fine forceps (*see* **Note 3**). During this process, the loop should not be pulled to a diameter that is less than the shank of the micropipets in the chamber. The ties are snipped from the free end of the suture material, and the process is repeated as needed. Two or three of the pretied sutures are looped around the shanks of the inflow and outflow pipets, prior to cannulating the vessel. When the artery is drawn over the pipet, one of the ties is moved over the vessel and tightened.

   After the vessel is secured to the pipets, the side branches are tied off with smaller sutures, to prevent leaks and to allow intravascular pressure to be maintained. To tie side-branches, a single strand obtained from a piece of multifilament silk is used because the 10–0 nylon suture used to tie the vessels to the micropipets is too thick. A 1-cm length of 6–0 multifilament (or other size multifilament) suture is cut and the multifilament bundle is pushed and rolled with the handle of a pair of forceps in order to loosen it. Single strands from the multifilament bundle are carefully teased out under a dissecting microscope and single-loop ties are constructed from the individual strands.
5. Physiological salt solution (PSS): PSS for studies of isolated and *in situ* vessels are designed to maintain normal physiological function by simulating the composition of the extracellular fluid. Physiological salt solutions can be prepared either by dissolving the constituents into distilled water individually, or by using concentrated stock solutions, which are added to the distilled water. When con-

centrated stock solutions are used, any constituents that cannot be stored in the stock solution (e.g., NaH_2PO_2 and glucose) are added separately after the stock solutions are diluted.

To make 20X physiological salt solution, the required amounts of solutes are dissolved in 2 L of distilled water. The 20X salt stock consists of the following ingredients: 278.0 g NaC1; 14 g KCl; 11.52 g $MgSO_4 \cdot 7H_2O$; and 9.4 g $CaCl_2 \cdot 2H_2O$. The 20X buffer stock solution consists of 80.8 g of $NaHCO_3$ and 0.4 g of ethylenediaminetetraacetic acid (EDTA). To make 2 L of the working PSS solution: 100 mL of 20X salt stock, 1800 mL of distilled water; and 100 mL of 20X buffer stock are mixed. In order to prevent precipitation, 1800 mL of deionized water is added to the 20X salt stock, and the buffer stock is added to the diluted salt stock. After the stock solutions have been diluted, 0.28 g of $NaHa_2PO_4$ and 1.98 g of glucose are added to the PSS and dissolved by stirring. The final working solution has the following constituents: 119 m*M* NaC1; 4.7 m*M* KCl; 1.17 m*M* $MgSO_4 \cdot 7H_2O$, 1.6 m*M* $CaCl_2 \cdot 2H_2O$; 1.18 m*M* NaH_2PO_4; 24 m*M* $NaHCO_3$; 0.03 m*M* EDTA; and 5.5 m*M* glucose.

Bicarbonate-buffered PSS must be equilibrated with a CO_2-containing gas mixture prior to and during the course of the experiment because the pH of the solution is too alkaline unless the solution is bubbled with CO_2. Initial equilibration of the PSS is performed in a beaker or flask using a gas dispersion tube connected to a cylinder containing the appropriate concentration of CO_2 and O_2, with the balance N_2. For our studies, the best control of pH is achieved with a 7% CO_2 gas mixture. The O_2 concentration of the gas equilibration mixture should be 14–21% O_2. The 14% O_2 gas equilibration mixture maintains a PO_2 of approx 100 mmHg, which is close to arterial PO_2. The 21% O_2 gas equilibration allows PO_2 to be maintained at atmospheric PO_2 (approx 140 mmHg), which is higher than arterial PO_2. The rationale for the use of 21% O_2 solution is that this PO_2 provides a "buffer" for any diffusion limitation of O_2 to the center of the vessel. However, the overall wall thickness in isolated-resistance arteries (20–30 μm) is substantially less than that calculated to produce diffusion limitation of O_2 to the center of the vessel ***(25)***. As a result, O_2 concentrations that produce PO_2s closer to arterial PO_2 are well tolerated by the vessels.

The superfusion solution is prewarmed and gas equilibrated in a standard pharmacology organ bath connected to a temperature-controlled circulating water bath (e.g., Haake Circulator, Haake Buchler Instruments, Inc., Saddle Brook, NJ). Flow of the superfusion solution out of the tissue bath is aided with a peristaltic pump (e.g., Ismatec, Cole-Parmer). In most of the cannulated vessel stations in our laboratory, temperature in the vessel chamber (37°C) and in the superfusion solution reservoir are controlled with separate temperature-controlled circulating water baths, because prewarming of the superfusate reservoir allows the temperature of the tissue bath to be controlled more easily. Pressures at the inflow and outflow pipets are monitored with standard pressure transducers connected to a two-channel amplifier that can be monitored with a chart recorder or CODAS (DATAQ Instruments, Akron, OH).

To maintain the appropriate pH, PCO_2, and PO_2 in the tissue bath, the PSS is continuously bubbled with the appropriate gas mixture in the pharmacology organ bath that serves as the superfusion solution reservoir. Gas concentrations in the tissue bath are also controlled by continuous equilibration of the PSS with the appropriate gas mixtures via a small air stone placed in the tissue bath itself. We have found the latter step to be critically important for maintaining the appropriate pH and gas concentrations in the tissue bath. To facilitate gas equilibration in the tissue bath, the chamber is covered with glass microscope slides or with Parafilm (American National Can; Menasha, WI) between measurements. This also protects the microscope objective from being splashed with PSS, if an inverted microscope is not being used. When the system is set up, it is important to measure the pH, PCO_2, and PO_2 of the PSS in the tissue bath. These should be in the following ranges: pH: 7.35–7.4, PCO_2: 35–45 mmHg, and PO_2: 100–140 mmHg.

The PSS that perfuses the lumen of the vessel is supplied from a separate reservoir. The perfusate can either be delivered by gravity from a 60 cm^3 plastic or glass syringe, or from a glass syringe mounted in a small volume infusion pump. The reservoir or perfusion pump is connected to the inflow pipet by teflon tubing, to prevent gas equilibration with the atmosphere. In the gravity feed system, the PSS in the open reservoir is continuously equilibrated with the appropriate gas mixture using an air stone in the reservoir itself. If the perfusate is delivered from a syringe pump, the PSS is preequilibrated with the appropriate gas mixture prior to drawing it into the glass syringe that will serve as the reservoir. Because of the large surface area-to-volume ratio of the micropipet in the tissue bath, temperature equilibration of the perfusion solution occurs rapidly, and no additional steps are required to prewarm the solution in the perfusate reservoir.

6. Angiotensin solutions and receptor blockers: Ang II has a formula weight of 1046 g/*M*. To make a 10^{-3} *M* stock solution, 26.15 mg of Ang II are dissolved in 25 mL of distilled H_2O. Ang II is light sensitive, and should be stored in the dark. The standard blocker of the Ang AT_1 receptor is losartan, which has a formula weight of 461.0. To make a 10^{-3} *M* stock solution, 11.5 mg of losartan are dissolved in 25 mL of deionized water. The standard blocker of the angiotensin AT_2 receptor is PD 123319, which has a formula weight of 754.7. The drug comes in powder form, and should be stored in a desiccator at room temperature. To make a 10^{-3} *M* stock solution of PD123319, 18.9 mg of the compound are dissolved in 25 mL of deionized water. The concentration of the angiotensin-receptor blockers should be tenfold higher than the highest concentration of Ang II to be used. For example, if Ang II is to be used in a concentration range of 10^{-11} *M* to 10^{-7}*M*, losartan, or PD 123319 should be prepared at 10^{-6} *M*.

2.2. Cranial Window Studies

1. Animal preparation: A variety of materials are required to prepare an animal for cranial window studies. For rats, these include a stereotaxic apparatus (e.g., Model 900; David Kopf Instruments, Tujunga CA), rodent ventilator (e.g., Model 683, Harvard Apparatus; South Natick, MA), blood gas analyzer (e.g., AVL

model 995, AVL Scientific, Roswell, GA), chart recorder or CODAS system, blood pressure transducer, and assorted cannulas. As discussed below, anesthesia can be maintained with a variety of anesthetics, including pentobarbital ***(22,26)***, urethane ***(23)***, or halothane ***(27)***, and the animals can be premedicated with 0.54 mg/kg, ip atropine sulfate ***(23)*** to minimize respiratory secretions.

2. Installation of cranial window: Materials required for the installation of the cranial window itself include a slow speed dental drill (Rhino XP; Midwest Dental, Des Plaines, IL). and bits for opening the skull; bone wax and an electrocautery or soldering iron to control bleeding; and the cranial window, which can be fabricated in house according to published descriptions ***(20,22)***.
3. Artificial cerebral spinal fluid: To study the *in situ* cerebral circulation, the brain is bathed in artificial cerebral spinal fluid (ACSF), which has the following composition: 2.9 m*M* KCl, 38 m*M* $MgCl_2$, 1.99 m*M* $CaCl_2$, 19 m*M* $NaHCO_3$, 6.63 m*M* urea, and 3.69 m*M* glucose ***(26)***. The solution should be warmed to 37°C and equilibrated with a CO_2-containing gas mixture. Previous studies in our laboratory ***(28)*** and others ***(22,26)*** have employed 6%–8% CO_2, with O_2 concentrations ranging from 6%–21% O_2 and the balance N_2. Regardless of the composition of the ACSF and the gas equilibration mixture, it is especially important to verify that the solution has the proper pH (7.35–7.4) ***(11,21)*** as it flows over the tissue.
4. Measurement of vessel diameters, and assessment of cerebral blood flow: Many studies of the regulation of the *in situ* cerebral circulation use measurements of vessel diameters to evaluate the control of microvessel tone. Direct observation of the cerebral circulation can be accomplished with any suitable microscope equipped for television microscopy. Vessel diameters can either be measured on line with a video micrometer or off line from video tapes. Changes in blood flow also can be evaluated in open or closed cranial window preparations with a laser-Doppler flowmeter ***(23)***. The main limitation of laser-Doppler flowmetry is that this technique does not provide an absolute measurement of blood flow, although it does provide an easy and rapid evaluation of relative changes in blood flow occurring in response to vasoactive stimuli ***(23)***.

3. Methods

3.1. Cannulated Cerebral Artery Preparation

3.1.1. Isolation of Vessels

1. The first step in isolating cerebral blood vessels is to remove the brain. This is accomplished by deeply anesthetizing the animal and decapitating it. The skin above the skull is cut with a scalpel and peeled back to expose the underlying bone. The skull is opened by placing the tips of a pair of rongeurs through the foramen magnum and breaking away the bone toward the top of the skull until the brain is exposed. After the bone is cleared from the top of the skull, the skull is turned upsidedown so that the brain is hanging from the cranial nerves, which can be easily severed with a scalpel blade.

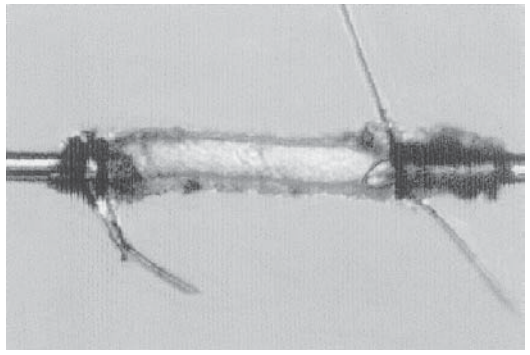

Fig. 3. Cannulated resistance artery mounted on micropipets. (Courtesy of Dr. Kathryn Gauthier.)

2. After the brain is removed from the cranium, it is placed in PSS in a small Petri dish lined with a silicone rubber. This allows the brain to be pinned to the bottom of the dissecting dish to prevent movement while the vessels of interest are removed.
3. The vessels most commonly used for isolated, perfused cerebral artery preparations are the middle cerebral artery and the posterior cerebral artery. The basilar artery can also be isolated and studied, although this vessel has a large number of branches, which must be tied off to maintain a constant intravascular pressure.
4. Some investigators ***(29)*** have studied isolated intraparenchymal vessels, which are much smaller than the middle cerebral, posterior cerebral, or basilar arteries. Preparation of these vessels is much more difficult, and requires techniques that are similar to those employed for microperfusion of renal tubules ***(30)***.

3.1.2. Mounting Vessels

1. Prior to mounting the vessel, the measuring equipment is calibrated and the PSS is warmed and equilibrated with the appropriate gas mixture. The pipets and the tubing lines from the perfusion and superfusion solution reservoirs are filled with gas equilibrated PSS.
2. When these preparations are complete, the artery is cannulated at both ends with micropipets which have tip sizes that are only slightly smaller than the lumen of the vessel, in order to minimize pipet resistance across the vessel **(Fig. 3)**.
3. To cannulate the vessel, the inflow of perfusate is turned off, and 2–3 premade 10–0 ties are slipped around the shank of the inflow pipet well away from the point where the vessel will be mounted. The ends of the loops are pulled to snug the ties against the pipet, but the sutures are not tied tightly.
4. A pair of fine-tine forceps is used to carefully grasp the inflow end of vessel, holding it only at the edge of the tissue (*see* **Note 4**). Because of the orientation of endothelial cells in the blood vessel, the artery should be oriented so that it is perfused in the same direction as blood had flowed in vivo. The artery is slipped onto the inflow pipet, a 10–0 tie is positioned over vessel,

and the ends of the suture are pulled to tighten it around the vessel. A second 10-0 tie is recommended, and in some cases, a second knot on top of the double loop is necessary.

5. Once the vessel is mounted and secured on the inflow pipet, the perfusate flow is started at a low pressure. The pipets are moved closer together and the mounting procedure is repeated with the outflow pipet. It is generally helpful to have the perfusate flowing while mounting the outflow end of the vessel.
6. After the outflow end of the vessel is cannulated, the artery is extended to approximate its *in situ* length, using the micrometer attached to the pipet holder in the vessel chamber.
7. The outflow tubing is clamped, and any side branches are tied off.
8. After cannulation, the vessel is checked for leaks by verifying that pressure in the artery does not fall when the vessel is sealed off by closing the stopcocks connected to the tubing supplying the inflow and outflow pipets.

3.1.3. Endothelial Removal

1. To determine if the response of the artery to vasoactive agonists such as Ang II is modulated by endothelium-derived vasoactive factors, the endothelium can be removed from the artery. This is usually achieved utilizing the air perfusion technique described in **Subheading 2.6.** However, the endothelium can also be removed by mechanical methods such as scraping with a human hair ***(31)*** or by drawing the vessel over the inflow pipet ***(32)*** (*see* **Note 5**).
2. In intact arteries, the integrity of the endothelium is verified by demonstrating that the vessel dilates in response to acetylcholine (ACh). To perform this test of endothelial integrity, 10^{-3} *M* ACh stock is added to the tissue bath, in order to achieve a final bath concentration of 1 μ*M* ACh. The presence of a functional endothelium is verified by the occurrence of a vasodilation in response to ACh.
3. Ten minutes are allowed to wash out the ACh, and the endothelium is then removed by perfusing the lumen of the vessel with a 2–5 mL bolus of air (**Fig. 1**). During the air perfusion procedure, it is very important to not allow the pressure in the vessel to rise above 60–80 mmHg, as exposure to higher pressures can damage the vessel. The total duration of exposure of the vessel lumen to air is 2–10 min, depending on the time it takes to inject the air bolus at the proper pressure.
4. After the vessel is perfused with air, the lumen of the vessel is perfused with PSS for 30 min, and the success of the endothelial removal is tested by evaluating the response to acetylcholine. If a dilation still occurs in response to ACh, the air perfusion can be repeated until the acetylcholine induced dilation is abolished.
5. The major problem encountered with endothelial removal is the occurrence of damage to the vessel. Therefore, it is important to demonstrate that resting tone and the response of the vessel to endothelium independent agonists are not impaired following removal of the endothelium.
6. A crucial test of vessel viability for all experiments is the demonstration that the vessel has resting tone, as evidenced by the occurrence of a large dilation in response to an endothelium independent dilator such as sodium nitroprusside or to Ca^{2+}-free solution at the end of the study. The viability of the vessel can also

be verified by testing the response of the vessel to a vasoconstrictor agonist, e.g., 10^{-7} *M* serotonin. Any vessel that does not exhibit resting tone, or does not contract in response to the vasoconstrictor agonist should not used in the study.

3.1.4. Running Experimental Protocols

1. Studies of the response of perfused vessels to vasoactive compounds such as Ang II require the introduction of the agents into the tissue bath (superfusion) or into the luminal perfusate. Delivery of drugs via the superfusion solution can be accomplished by supplying PSS with the appropriate concentration of the agent from a separate superfusion solution reservoir.
2. To visualize the entry of superfusion solution into the vessel chamber, it is helpful to allow an air bubble to enter the tubing that leads from the reservoir.
3. Once the new solution is flowing into the vessel chamber, exchange of the solution can be aided by alternately withdrawing PSS from the vessel chamber (down to a level slightly above the vessel) and replacing it with the new solution.
4. Once the solution is exchanged, the air stone is returned to the vessel chamber and the vessel is equilibrated with the drug before measurements are made.
5. If the drug to be added is expensive or in short supply, it can be added directly to the vessel chamber while briefly interrupting the flow of superfusate from the reservoir. In order to add the appropriate amount of the stock solution to the chamber, it is necessary to know the volume of the tissue bath.
6. Alternatively, the new solution can be made up in a predetermined volume of warmed, gassed PSS. This can be quickly added to the chamber by turning off the superfusate flow, quickly withdrawing all of the PSS in the tissue bath using a length of tubing connected to a large syringe, and pouring the new solution into the vessel chamber.
7. After the new solution is added, the air stone should be placed back into the chamber, and a brief equilibration period (5–10 min) allowed before measurements are performed.
8. If agents are added to the vessel lumen, the solution perfusing the vessel needs to be changed. The new perfusate should be equilibrated with the appropriate gas mixture in a separate syringe equipped with a stopcock.
9. After the perfusate is equilibrated, the outflow line from the vessel is clamped, and the stopcock leading from the primary reservoir is turned off.
10. The teflon delivery tubing is detached from the syringe that serves as the primary reservoir and is attached to the reservoir containing the new perfusate.
11. The stopcock supplying the inflow pressure transducer is opened in order to visualize the entry of solution into the tubing upstream from the pipet.
12. Prior to initiating the flow of the new perfusate, an air bubble is allowed to enter the tubing. This permits the flow of the new solution to be followed visually until it reaches the stopcock supplying the inflow pipet.
13. The solution is allowed to flow out of the stopcock, and the tubing connected to the inflow pipet is briefly disconnected to clear the air from the line.
14. After the air has exited, the tubing is reattached to the inflow pipet, making sure that there are no bubbles in the line.

15. The clamp on the outflow tubing is opened, and the new perfusate enters the vessel in 3–5 min.
16. Measurements are made after an appropriate equilibration period following the entry of the perfusate into the vessel.

3.2. Cranial Window Studies

1. To prepare an animal for cranial window studies, it is anesthetized, maintained on a warming pad, and placed in a stereotaxic apparatus, while temperature is monitored with a rectal thermistor and telethermometer.
2. A variety of anesthetics can be used. For rats, these include 50-60 mg/kg pentobarbital, ip ***(22,28)***, 1.2 g/kg urethane ip in a 20% solution ***(23)***, and volatile anesthetics such as 1% halothane ***(27)***. Supplemental anesthetic regimens include injection of 6.5 mg/kg pentobarbital iv every 2 h ***(22)***, 2.5 mg/kg pentobarbital, ip at hourly intervals or when arterial blood pressure increases in response to a noxious stimulus such as a toe pinch or tail pinch ***(26)***, ip injection of 0.24 g/kg of urethane when blood pressure increases in response to a noxious stimulus ***(23)***, and continuous administration and monitoring of a volatile anesthetic such as halothane ***(27)***.
3. Prior to placing the animal in the stereotaxic apparatus, an artery is cannulated with polyethylene tubing for arterial pressure measurement and to allow sampling for arterial blood gas measurements. A vein also may be cannulated for infusion of supplemental anesthetic, depending on the anesthetic regimen used.
4. The trachea is cannulated, and the animal is ventilated with either room air ***(23,33)*** or 30% O_2 ***(22,26)***, using a rodent ventilator. Frequency and tidal volume are adjusted until normal arterial blood gas concentrations are obtained, as described by Gerrits et al. ***(23)***. To achieve normal arterial PO_2 (approx 100 mmHg), PCO_2 (30–38 mmHg), and pH (approx 7.4) for rats weighing between 275–350 g and breathing room air, tidal volume should be set at 2.0–2.5 mL and ventilation frequency at 75–85 breaths per minute.
5. To facilitate ventilation, the respiratory muscles can be paralyzed with a neuromuscular blocker such as gallamine (80 mg/kg, ip) ***(26)***. If this is done, it is essential to continue to administer the appropriate dose of supplemental anesthetic, since the neuromuscular blocker will prevent any muscular movement or withdrawal reflexes that are customarily used to identify the point at which supplemental anesthetic needs to be administered in acute studies. If neuromuscular blockers are used, supplemental anesthesia is administered at regular levels, and the depth of anesthesia should be monitored by testing for a rise in arterial blood pressure in response to a noxious stimulus such as pinching the tail or a toe. All procedures employing systemic infusion of neuromuscular blockers should be reviewed by the institutional veterinarian.
6. After the initial surgical preparation of the animal, the cranial window is installed. The open cranial window for acute studies is prepared by carefully drilling through the parietal portion of the skull, using a slow-speed dental drill (*see* **Note 6**).

7. After the skull is opened, the dura is lifted using a needle, a pair of fine forceps, or a specialized tool (dura hook), and is cut open with ophthalmic scissors.
8. The dura is reflected over the bone, and the surface of the brain is bathed with ACSF equilibrated with an appropriate gas mixture, as described above.
9. A major problem that is encountered in open cranial window preparations is the maintenance of an appropriate pH, PCO_2 and PO_2, if the ACSF is stagnant ***(21)***. This can affect both the resting diameter of cerebral vessels, and the sensitivity of the vessels to vasoactive stimuli. This problem is also encountered if the pial surface is covered with mineral oil ***(21)***. Therefore, PO_2, PCO_2, and pH in an open cranial window preparation should be controlled by continually superfusing the area with ACSF having an appropriate, PO_2, PCO_2, and pH.
10. A variety of approaches are used for closed cranial-window studies. In our laboratory ***(28)***, a 5-mm burr hole is opened in the parietal bone and a stainless-steel frame containing a glass cranial window with ports for perfusion inlet, perfusion outlet, and intracranial pressure measurement is installed.
11. After the chamber is installed, the surface of the brain is superfused at 1 mL/min with ACSF equilibrated with the appropriate concentrations of O_2 and CO_2 while intracranial pressure is maintained at 5–10 mmHg by adjusting the height of the outflow.
12. Another closed window preparation ***(22)*** employs a quartz window attached to a plastic frame that allows continual perfusion with ACSF with a very small space between the cortical surface and the cranial window.
13. Another variation of the closed cranial window preparation ***(23)*** employs a dental drill to progressively thin the skull to a point to where the underlying vasculature is visible and flow can be evaluated via laser–Doppler techniques without penetrating the skull. This preparation, which maintains an intact dura, can be perfused with ACSF via a small (approx 600 μm) polyethylene catheter fashioned from drawn PE-10 tubing that is inserted through a small burr hole and a small slit in the dura at the edge of the cerebral window ***(34)***. Drainage of excess fluid in this preparation is accomplished through a burr hole and a small slit in the dura on the opposite side of the cranial window. Procedures for the thinned skull cranial window preparation have recently been described in detail by Gerrits et al. ***(23)***.

4. Notes

1. Maintenance of vessel viability and normal vascular reactivity requires scrupulous attention to cleanliness of the vessel chamber and the tubing connections. The tubing and connections should be inspected daily, since the tubing carrying PSS is a potential site of contamination. All tubing carrying PSS should be thoroughly cleaned and changed frequently.

   To clean the setup at the end of the day, 2–3 mL of 0.1 *M* HC1 should be flushed through the pipets and any tubing that carries PSS. The tubing and pipets should then be rinsed with 5–6 mL of deionized water. After the deionized water rinse, air should be pushed through the tubing to dry the lines. With the gas still

flowing, the organ bath that serves as the perfusate reservoir should be emptied of PSS and filled with 0.1 *M* HC1. The inside of the reservoir and the rim should be thoroughly wiped down with the 0.1 *M* HCl, and the reservoir should then be rinsed three times by completely filling it with deionized water and emptying it. After the last of the water is drained, the gas equilibration frit in the bottom of the reservoir should be dried with a cotton swab. The gas cylinder should be turned off at the main valve and allowed to empty through the frit. The perfusate syringe and teflon tubing delivery line(s) should be rinsed with 70% ethanol and allowed to air-dry. Alcohol should not be allowed to contact the plastic surfaces of the chamber, because it causes cracking and could eventually lead to a leak in the chamber. Any leak that allows water from the circulating heater to enter the tissue bath will adversely affect vessel viability and eliminate the normal responses of the artery to vasoactive stimuli. This is a rare occurrence, but it is difficult to detect and requires immediate attention. To determine whether water from the heater circuit is entering the tissue bath, the bath heater should be run for several hours while the tissue bath is dry. Appearance of fluid in the tissue bath will indicate that there is a leak in the bath that is allowing water from the heater circuit to enter the bath. Any leaks between the heater circuit and the tissue bath need to be repaired before further studies are conducted.

2. Electrical connections should be periodically checked for integrity, and loose or frayed cords and damaged leads should be repaired or replaced.
3. Pretying of the suture loops is facilitated by holding the main suture with the sticky strip of a "Post-it Note" (3M Corporation, St. Paul, MN) that is taped to a microscope slide. This holds one end of the suture steady while ties are being constructed at the free end of the suture. The sticky portion of a Post-it Note is also handy for holding the multifilament suture, while obtaining single filaments to be used in tying side branches of the vessel.
4. To maintain normal resting tone and to obtain good responses to vasoactive stimuli, it is extremely important to avoid stretching or traumatizing the vessel in any way during the dissection and mounting procedure. When the artery needs to be transferred, it should always be held by the adventitial tissue, and not by the center of the vessel.
5. Mechanical removal of the endothelium from isolated resistance arteries is technically difficult, because it requires great care to avoid damaging the vessel. Damage to the vessel is indicated by loss of resting tone, loss of the myogenic response to transmural pressure elevation, and loss of the vessel's ability to contract in response to vasoconstrictor agonists. In the vast majority of vessels, results obtained following air perfusion and mechanical removal of the endothelium are identical. However, we have demonstrated that air perfusion causes canine renal arteries to constrict and attenuates myogenic responses in these vessels, even though resting tone and vasoconstrictor responses to norepinephrine are maintained ***(32)***. This suggests that any potential differences in endothelial removal procedures should be tested by comparing myogenic responses to transmural pressure elevation before and after the different endothelial removal procedures

when new vessel types are studied. However, in the case of cerebral arteries, vessel responses are identical following air perfusion and mechanical removal of the endothelium.

6. Two of the major problems that may be encountered in preparing cranial windows are bleeding and heating of the brain while drilling. Bleeding can be controlled by utilizing bone wax, and an electrocautery or a soldering iron to cauterize any vessels that are bleeding ***(23)***. Heating of the brain can be minimized by using an air cooled drill, by proceeding cautiously, and by periodically bathing the area with saline to cool it. Another major problem that can be encountered in the excised dura preparation is swelling of the brain, which can affect systemic blood pressure, respiration, and vascular reactivity. Swelling of the brain can be prevented by shortening the surgical time, and maintaining a constant intracranial pressure.

Acknowledgments

Special thanks to Donna Bizub, who prepared the laboratory operations manual that formed the basis for many portions of the chapter; to Kathryn Gauthier, Yanping Liu, and Tianjian Huang for their helpful suggestions and assistance in preparing the illustrations for the chapter; and to Ron Gerrits, Yanping Liu, and Antal Hudetz for their helpful suggestions on the sections of the chapter dealing with cranial window preparations. Additional thanks to Luellen Lougee and Janet DeBruin for their help in preparing the illustrations for the chapter. The studies in which many of the techniques described in this chapter were developed and refined were supported by NIH grants #HL-37374 and #HL-29587.

References

1. Horiuchi, M., Akishita, M., and Dzau, V. J. (1999) Recent progress in angiotensin II type 2 receptor research in the cardiovascular system. *Hypertension* **33,** 613–621.
2. Matsubara, H. (1998) Pathophysiological role of angiotensin II type 2 receptor in cardiovascular and renal diseases. *Circ. Res.* **83,** 1182–1191.
3. Munzenmaier, D. H. and Greene, A. S. (1996) Opposing actions of angiotensin II on microvascular growth and arterial blood pressure. *Hypertension* **27,** 760–765.
4. Hernandez, I., Cowley, A. W., Jr., Lombard, J. H., and Greene, A. S. (1992) Salt intake and angiotensin II alter microvessel density in the cremaster muscle of normal rats. *Am. J. Physiol.* **263,** H664–H667.
5. Scheuer, D. A. and Perrone, M. H. (1993) Angiotensin type 2 receptors mediate depressor phase of biphasic pressure response to angiotensin. *Am. J. Physiol.* **264,** R917–R923.
6. Mayhan, W. G., Amundsen, S. M., Faraci, F. M., and Heistad, D. D. (1988) Responses of cerebral arteries after ischemia and reperfusion in cats. *Am. J. Physiol.* **255,** H879–H884.
7. Edvinsson, L., Hardebo, J. E., and Owman, C. (1979) Effects of angiotensin II on cerebral blood vessels. *Acta Physiol. Scand.* **105,** 381–383.

8. Wei, E. P., Kontos, H. A., and Patterson J. L., Jr. (1978) Vasoconstrictor effect of angiotensin on pial arteries. *Stroke* **9,** 487–489.
9. Naveri, L. (1995) The role of angiotensin receptor subtypes in cerebrovascular regulation in the rat. *Acta Physiol. Scand.* **155 Suppl. 630,** 1–48.
10. Haberl, R. L., Anneser, F., Villringer, A., and Einhaupl, K. M. (1990) Angiotensin II induces endothelium-dependent vasodilation of rat cerebral arterioles. *Am. J. Physiol.* **258,** H1840–H1846.
11. Haberl, R. L. (1994) Role of angiotensin receptor subtypes in the response of rabbit brain arterioles to angiotensin. *Stroke* **25,** 1476–1479.
12. Mulvany, M. J. and Halpern, W. (1976) Mechanical properties of vascular smooth muscle cells in situ. *Nature* **260,** 617–619.
13. Halpern, W., Osol, G., and Coy, G. S. (1984) Mechanical behavior of pressurized in vitro prearteriolar vessels determined with a video system. *Ann. Biomed. Eng.* **12,** 463–479.
14. Halpern, W. and Osol, G. (1985) Influence of transmural pressure on myogenic responses of isolated cerebral arteries of the rat. *Ann. Biomed. Eng.* **13,** 287–293.
15. Harder, D. R. (1984) Pressure-dependent membrane depolarization in cat middle cerebral artery. *Circ. Res.* **55,** 197–202.
16. Hermsmeyer, K., Trapani, A., and Abel, P. W. (1981) Membrane potential-dependent tension in vascular muscle, in *Vasodilatation* (Vanhoutte, P. M. and Leusen, I., eds.), Raven, New York, pp. 273–284.
17. Lombard, J. H., Eskinder, H., Kauser, K., Osborn, J. L., and Harder, D. R. (1990) Enhanced norepinephrine sensitivity in renal arteries at elevated transmural pressure. *Am. J. Physiol.* **259,** H29–H33.
18. Fredricks, K. T., Liu, Y., and Lombard, J. H. (1994) Response of extraparenchymal resistance arteries of rat skeletal muscle to reduced PO_2. *Am. J. Physiol.* **267,** H706–H715.
19. Fredricks, K. T., Liu, Y., Rusch, N. J., and Lombard, J. H. (1994) Role of endothelium and arterial K^+ channels in mediating hypoxic dilation of middle cerebral arteries. *Am. J. Physiol.* **267,** H580–H586.
20. Levasseur, J. E., Wei, E. P., Raper, A. J., Kontos, H. A., and Patterson, J. L., Jr. (1975) Detailed description of a cranial window technique for acute and chronic experiments. *Stroke* **6,** 308–317.
21. Navari, R. M., Wei, E. P., Kontos, H. A., and Patterson, J. L., Jr. (1978) Comparison of the open skull and cranial window preparations in the study of the cerebral microcirculation. *Microvasc. Res.* **16,** 304–315.
22. Hudetz, A. G., Feher, G., Weigle, C. G. M., Knuese, D. E., and Kampine, J. P. (1995) Video microscopy of cerebrocortical capillary flow: response to hypotension and intracranial hypertension. *Am. J. Physiol.* **268,** H2202–H2210.
23. Gerrits, R. J., Stein, E. A., and Greene, A. S. (1998) Laser-Doppler flowmetry utilizing a thinned skull cranial window preparation and automated stimulation. *Brain Res. Protocols* **3,** 14–21.

24. Lombard, J. H., Stekiel, W. J., and Harder, D. R. (1986) Membrane potentials in vascular smooth muscle of microvessels, in *Microcirculatory Technology* (Baker, C. H. and Nastuk, W. L., eds.), Academic Press, Orlando FL, pp. 299–315.
25. Pittman, R. N. and Duling, B. R. (1973) Oxygen sensitivity of vascular smooth muscle. 1. In vitro studies. *Microvasc. Res.* **6,** 202–211.
26. Alkayed, N. J., Birks, E. K., Hudetz, A. G., Roman, R. J., Henderson, L., and Harder, D. R. (1996) Inhibition of brain P-450 arachidonic acid epoxygenase decreases baseline cerebral blood flow. *Am. J. Physiol.* **271,** H1541–H1546.
27. Okamoto, H., Hudetz, A. G., Roman, R. J., Bosnjak, Z. J., and Kampine, J. P. (1997) Neuronal NOS-derived NO plays permissive role in cerebral blood flow response to hypercapnia. *Am. J. Physiol.* **272,** H559–H566.
28. Liu, Y., Rusch, N. J., and Lombard, J. H. (1999) Loss of endothelium and receptor-mediated dilation in pial arterioles of rats fed a short-term high salt diet. *Hypertension* **33,** 686–688.
29. Ngai, A. C. and Winn, H. R. (1995) Modulation of cerebral arteriolar diameter by intraluminal flow and pressure. *Circ. Res.* **77,** 832–840.
30. Duling, B. R., Gore, R. W., Dacey, R. G., and Damon, D. N. (1981) Methods for isolation, cannulation, and in vitro study of single microvessels. *Am. J. Physiol.* **241,** H108–H116.
31. Osol, G., Cipolla, M., and Knutson, S. (1989) A new method for mechanically denuding the endothelium of small (50–150 μm) arteries with a human hair. *Blood Vessels* **26,** 320–324.
32. Liu, Y., Harder, D. R., and Lombard, J. H. (1994) Myogenic activation of canine small renal arteries after nonchemical removal of the endothelium. *Am. J. Physiol.* **267,** H302–H307.
33. Hudetz, A. G., Roman, R. J., and Harder, D. R. (1992) Spontaneous flow oscillations in the cerebral cortex during acute changes in mean arterial pressure. *J.Cereb. Blood Flow Metab.* **12,** 491–499.
34. Liu, Y., Hudetz, A. G., Knaus, H.-G. and Rusch, N. J. (1998) Increased expression of Ca^{2+} -sensitive K^+ channels in the cerebral microcirculation of genetically hypertensive rats: Evidence for their protection from cerebral vasospasm. *Circ. Res.* **82,** 729– 737.